Unisexual Reproduction in filamentous Ascomycete Fungi, with particular reference to *Huntiella moniliformis*

By
Andrea Melissa Wilson

Submitted in partial fulfilment of the requirements for the degree
Philosophiae Doctor

In the Faculty of Natural and Agricultural Sciences
Department of Biochemistry, Genetics & Microbiology
University of Pretoria
Pretoria

23 August 2019

Primary Supervisor:
Prof. Brenda D. Wingfield

Co-Supervisors:
Prof. Michael J. Wingfield
Dr Magriet van der Nest
Dr P. Markus Wilken

DECLARATION

I, Ms AM Wilson, hereby declare that the dissertation which I hereby submit for the degree *Philosophiae Doctor* at the University of Pretoria, is my own work and has not previously been submitted by me for a degree at this or any other tertiary institution.

_____ _____

Signature Date

To those who have inspired me along this journey.

"If I have seen further, it is by standing on the shoulders of giants" ~ Isaac Newton

Also, to Shayleigh ♥

CONTENTS

ACKNOWLEDGEMENTS

Brenda, my primary supervisor and my primary role model, words alone cannot express the gratitude I have for the role you have played in my life, scientific development and, of course, this thesis. I could not have asked for a better supervisor and could not imagine having completed this degree under the leadership of anyone else. I only hope that I can live up to the standard you have set as a supervisor when I have students of my own one day. Thank you for teaching me the importance of grit, for encouraging me and for understanding my needs as a student, especially when I became a rather needy student towards the end! Your patience, encouragement and excitement added immensely to my ability to complete this thesis. Thank you for giving me the space and time to do the research I love, to keep asking the sexy questions and to "just sequence the genome [or transcriptome]".

To the rest of my committee, M^3, thank you for the roles you each played in the research that made this thesis possible. **Mike**, the microbiologist on this committee, thank you for sharing your phenomenal knowledge and experience with me during the course of my post-graduate career. I am extremely grateful for the interest you have consistently shown in my work and the support you have provided- both professionally and personally. **Markus**, thank you for helping me make this thesis a reality and for your belief in me from the very beginning of my scientific career. Thank you for being one of the few people with whom I can discuss the nitty gritty details of our research into the fascinating world of fungal sex. **Magriet**, thank you for always checking up on me, especially when things weren't going right. Thank you also for reminding me about the importance of my work and giving me the motivation to finish it.

I would like to acknowledge a variety of institutes and institutions for the financial support I have received during this degree. I want to thank the Forestry and Agricultural Biotechnology Institute (**FABI**), the Tree Protection Cooperative Programme (**TPCP**), the Centre of Excellence in Tree Healthy Biotechnology (**CTHB**), and the National Research Foundation (**NRF**) for supporting me during my studies. Additionally, I would like to thank the University of Pretoria (**UP**) and the **NRF** for funding my two research visits to the USA via the Study Abroad and Grantholder-linked travel bursaries, respectively. I also received significant financial support from the Department of Science and Technology (**DST**) and **Loreal-UNSECO** via the Women in Science Awards and the PhD Fellowship programmes. I'd also like to acknowledge the **Oppenheimer Memorial Trust**, **Genes** journal and **WhiteSci** for providing the financial support I needed to attend a number of international conferences during my PhD.

After joining FABI as a mentorship student in 2011, I have come into contact with a variety of incredible people. I owe a great deal of my success to the wonderful working environment that is provided at FABI, both in terms of the infrastructure and the people. I am indebted to my fellow FABIans; the students, researchers and PIs, as well as the administrative and technical staff. I'd also like to say a huge thank you to the mentorship students that helped

me along my research journey- Ms **Storme de Scally**, Ms **Dore Joubert** and Ms **Carla Buitendag**. To my FABI friends: **Ariska**, **Darryl**, **Claudette**, **Nicole**, **Leandri**, and **Benedicta**, thank you for being my family at work and making my research journey somehow funnier and more exciting, and for sharing in the difficult but rewarding work that is research. I'd also like to say a special thank you to Prof **Irene Barnes**, my work study supervisor. Thank you for giving me the opportunity to work outside of my research field, for trusting me with some of your more interesting projects and for your constant support over the years. You are one of my women-in-science role models and I am so grateful to have had the opportunity to work closely with you.

During my PhD, I was fortunate to have spent a total of four months at Pennsylvania State University. I had the most phenomenal experiences during the time I spent in the USA, many of which helped immensely towards the completion of my final research chapter. I'd like to thank a number of my friends and colleagues at PSU. For being my point of contact and happily giving me space to work, I thank Prof **David Geiser**. To Prof **Yinong Yang**, Prof **Seogchan Kang** and Mr **Matthew Wheatley**, thank you for the invaluable assistance and knowledge you provided to me. To Dr **Chris Smyth**, Ms **Clara Miller**, Ms **Emma Wallace**, and Ms **Terry Torres Cruz**, thank you for being incredible friends and familiar faces and making sure my time in your lab wasn't too stressful! And lastly, to Prof **Carolee Bull**, thank you for being my unofficial tour guide and for your passion for science and life- a passion which is contagious. #WeAre!

I could not have finished this degree without the incredible group of people I am privileged to call my support base. My family, and the friends that have become family, have seen me through this journey and made the difficult path towards the completion of this PhD a much happier and rewarding experience. In particular, to **Danielle**, who is not only an amazing friend (and now my Maid of Honour!), but also an incredible role model and women in science. Thank you for your constant support and motivation, for being a shoulder to cry on and for all the champagne to celebrate with.

I often speak of the incredible female role models I have in my life that have shown me what women can achieve. My first, and most important female role model, was and still is my **Mom**. She has shown me that hard work and perseverance always pay off and that things are not worth doing if not done right. Thank you, Mom, for being the most phenomenal mother a daughter could ask for. Thank you for supporting me through all my years of studying, for listening to me complain when things weren't working and for celebrating with me when things did (even if you weren't always sure what I was talking about). Thank you for being someone I can aspire to be like and for setting an incredible example. Then there's my **Dad**, who has consistently believed in me and my abilities and encouraged me to achieve my best. Thank you for always being so excited for me when new opportunities come my way and always wanting to discuss what my future holds. Thank you for being the kind of dad a

daughter can look up to and for being proud of my every achievement- no matter how small. To both **my parents**- thank you for the many sacrifices you had to make along the way to make sure I got what I needed and had the opportunity to reach for my dreams. None of this would have been possible without the two of you and your incredible selflessness. Together, We'll Never Walk Alone.

To my little big sisterling, **Natasha**, who has seen me through the best and the worst of this degree and still somehow managed to put up with me and love me. I am so proud of you and the young woman you have become. You consistently give your best at everything you start and have always been a huge inspiration to me. Thank you for your unwavering love and support. Thank you for the 5 minute chats, 5 hour conversations and the 5 million quotes from all our favourite shows. Thanks for seeing me through "a little bit of a rough patch, the whole [4 years] actually" - Michael Scott.

To my newfound family, those whose surnames are all **de Jager**, I want to thank you all for your love and support from the moment I met each of you. Thank you for accepting me into your family and including me as one of your own. Ek kan nie wag om amptelik deel van jou familie te word nie!

Of course, this list would not be complete without one last thank you to my soon-to-be husband: **Deon**. I'm not entirely sure where to even begin except to say thank you for everything. From the endless cups of tea, to the in-depth conversations about my research and yours. Thank you for being the most incredible source of motivation and support. Thank you for your endless patience and comfort, and for understanding me like no one else does. I cannot wait to see what our future holds, where our science will take us and what exciting opportunities we'll come across! #DNA

PREFACE

The research conducted as part of this thesis focused on the genetic pathways that underlie sexual reproduction in various filamentous ascomycete fungi, with a particular focus on the wood-infecting saprobes; *Huntiella omanensis* and *Huntiella moniliformis*. While *H. omanensis* requires a suitable mating partner in order to reproduce sexually, *H. moniliformis* undergoes unisexual reproduction. Thus, various genomic and transcriptomic comparisons between the two species were used to understand the differences between the pathways that are involved in the two sexual strategies, especially those that make unisexual reproduction unique. This was extended to comparisons between other pairs of closely related unisexual and heterothallic fungi that are unrelated to the *Huntiella* species. Consequently, the overall aim of the independent studies presented in this thesis was to further our understanding regarding the genes involved in unisexual reproduction in filamentous ascomycetes.

The first chapter of this thesis is a **Literature Review** that was published in the journal Genes *10(5): 330* in 2019. The review provides a comprehensive overview of the genes that enable sexual reproduction in a variety of filamentous ascomycetes. Sexual reproduction is a complex process that relies on the regulation of hundreds of genes. Each of the gene-encoded products subsequently interact in a variety of ways to ensure the correct tissues are produced during the conversion of vegetative tissue into sexually competent tissue. This review focused on genes that have been functionally characterized in a number of model and non-model species; and grouped these genes into those that enabled protoascomatal development, those involved in ascomatal maturation, those that were essential for the production of the ascus and those that ensured ascospores were produced.

Research Chapter One is a research article that was published in PLOS One *13(3): e0192517* in 2018. The study used a comparative transcriptomics approach to elucidate the underlying genetic pathways that allow for unisexuality in *H. moniliformis*. To achieve this, the gene expression profiles of vegetatively growing isolates of *H. moniliformis* were compared to those from sexually reproducing cultures. This data was then combined with similar data from the heterothallic *H. omanensis*. Conclusions were subsequently drawn from these comparisons, allowing for the elucidation of genes that potentially play an important role in unisexual reproduction.

Research Chapter Two utilized a combination of previously conducted research as well as publicly available genomic and transcriptomic data to compare three unisexual filamentous ascomycetes, *Neurospora africana*, *H. moniliformis* and *Thermoascus aurantiacus* with closely related heterothallic species. By comparing the gene content of the *MAT* locus as well as the expression of genes such as the *MAT* genes and the mating pheromone genes, it was possible

to identify a shared genetic mechanism that putatively enables unisexual reproduction in filamentous fungi.

Research Chapter Three describes the initial steps of the functional characterization of a novel *MAT* gene from *H. omanensis*. This was achieved via the development of a transformation and genome editing protocol for use in *Huntiella* species. This particular *MAT* gene was hypothesized to play an integral role in sexual reproduction in the first research chapter of this thesis. Using the newly developed genome editing system, it was possible to demonstrate that the gene is essential for sexual reproduction, most likely via the maturation of the developing ascoma.

Three additional research outputs were indirectly produced during the completion of my PhD studies and have been included as supplementary chapters in this thesis. **Supplementary Chapter 1** is a species description for a novel *Huntiella* species. The new species was named *H. abstrusa* in reference to the fact that its identity has been "obscured" as it was mistakenly confused with *H. moniliformis* when it was first collected. **Supplementary Chapter 2** is a genome announcement for *H. bhutanensis*, a heterothallic species that is known to be closely associated with the bark beetle, *Ips schmutzenhofer*i. **Supplementary Chapter 3** is a species description of a further nine *Huntiella* species from southern China.

Research conducted during the course of the PhD for which this thesis is presented was performed by myself, Miss AM Wilson, at the Forestry and Agricultural Biotechnology Institute (FABI) at the University of Pretoria (UP). This research was conducted under the supervision of Professors Brenda and Michael Wingfield as well as Doctors Markus Wilken and Magriet van der Nest. Cultures used for the study were provided by the culture collection of FABI (Culture collection of Michael Wingfield- CMW). Financial support for the research conducted was provided by a PhD bursary I received from the NRF, the DST/NRF SARChI chair in Fungal Genomics held by Prof BD Wingfield as well as the DST/NRF Centre of Excellence in Tree Health Biotechnology. Student travel opportunities were afforded to me by UP and the Department of Science and Technology. Infrastructure was provided by UP, and supported by the companies that belong to South African Forestry as well as the Tree Health Protection Co-Operative Programme.

This thesis was written as four independent studies, two of which have been published in internationally recognized, peer-reviewed journals. Thus, the duplication of information, in, for example, the introductory sections and references was unavoidable. The literature review chapter has been formatted according to the requisites of the journal Genes and the first research chapter is formatted following the guidelines of PLOS One. For consistency purposes, the remaining two research chapters have been formatted in a manner similar to that of the literature review.

SUMMARY (ENGLISH)

Many filamentous ascomycete fungi are capable of sexual reproduction, though the exact mechanisms they use can differ from species to species. Those that require a compatible partner are termed heterothallic, while those that can sexually reproduce in isolation are termed homothallic. The major aim of this thesis was to further our understanding of a unique type of sexual reproduction known as unisexuality. While unisexual species harbour genes typically associated with heterothallic species, they are capable of independent sexual reproduction. Utilizing a variety of bioinformatic and molecular tools, I was able to show that unisexual reproduction is likely derived from heterothallism. I also propose that this transition is possible with a few small changes to the *MAT* genes and pheromone response pathway. In all three of the unisexual filamentous ascomycete fungi I investigated, mutations in the secondary *MAT* genes resulted in significant gene truncations or the deletion of functional domains- leading to non-functional proteins. Furthermore, these species also exhibited atypical pheromone response pathways. Given that similar changes are seen in three unisexual species from unrelated genera, I suggest that the mechanism that enables unisexual reproduction is highly conserved. Using a CRISPR-Cas9-based genome editing system, I was able to take the first steps towards experimentally mimicking unisexual behaviour in a heterothallic species, by the truncation of a secondary *MAT* gene in *H. omanensis*. Future research will thus focus on disruption of the pheromone response pathway in this species.

OPSOMMING (AFRIKAANS)

Filamentagtige fungus spesies is in staat om seksueel voort te plant, maar die presiese meganisme wat hulle gebruik verskil tussen spesies. Dié spesies wat ‘n teenoorgestelde en versoenbare vennoot benodig word na as heterotallies verwys, terwyl dié wat in isolasie seksueel kan voortplant, homotallies genoem word. Die hoofdoel van hierdie tesis was om eenslagtigheid, ‘n unieke wyse van seksuele voortplanting, beter te verstaan. Alhoewel eenslagtige fungus spesies tipies die gene het wat geassosieër word met die heterotalliese voortplantingswyse, kan hulle onafhanklik van ‘n teenoorgestelde vennoot voort plant. Deur van ‘n verskeidenheid bioinformatiese en molekulêre metodes gebruik te maak, het ek gewys dat eenslagtigheid waarskynlik ‘n afgeleide vorm van heterotalliese voortplanting is. Ek stel ook voor dat hierdie oorgang moontlik is met ‘n paar klein veranderinge aan die *MAT* gene en die feromoon-reaksieweg. In al drie eenslagtige, filamentagtige spesies wat ek bestudeer het, het mutasies in die sekondêre *MAT* gene gelei na beduidende geenverkortings of die verwydering van funksionele dele vanuit die gene, wat nie-funksionele proteïene tot gevolg gehad het. Hierdie spesies het ook atipiese feromoon-reaksieweë vertoon. Gegewe dat die drie eenslagtige spesies van onverwante genusse soortgelyke geenveranderinge gehad het, stel ek voor dat die meganisme wat eenslagtige voortplanting moontlik maak hoogs gekonserveerd moet wees. Deur van ‘n CRISPR-Cas9-gebaseerde genoom-redigeringsintrument gebruik te maak, het ek die eerste stappe geneem om eenslagtige voortplanting eksperimenteel na te boots in ‘n heterotalliese spesie, deur ‘n sekondêre *MAT* geen in *H. omanensis* te verkort. Toekomstige navorsing sal daarop fokus om die feromoon-reaksieweg in hierdie spesie te ontwrig.

SCIENTIFIC OUTPUTS DIRECTLY OR INDIRECTLY EMERGING FROM THIS THESIS

1. JOURNAL PUBLICATIONS

Wilson, A.M., M.A. van der Nest, P.M. Wilken, M.J. Wingfield and B.D Wingfield (2019)
It's All in the Genes: The Regulatory Pathways of Sexual Reproduction in Filamentous Ascomycetes. Genes 10(5): 330.

Liu, F., G. Li, J. Roux, I. Barnes, **A.M. Wilson**, M.J. Wingfield and S. Chen (2018)
Nine novel species of *Huntiella* from southern China with three distinct mating strategies and variable levels of pathogenicity. Mycologia 110(6): 1145-1171.

Marin-Felix, Y., M. Hernandez-Restrepo, M.J. Wingfield, A. Akulov, A.J. Carnegie, R. Cheewangkoon, D. Gramaje, J.Z. Groenewald, V. Guarnaccia, F. Halleen, L. Lombard, J. Luangsaard, S. Marincowitz, A. Moslemi, L. Mostert, W. Quaedvlieg, R.K. Schumacher, C.F.J. Spies, R. Thangavel, P.W.J. Taylor, **A.M. Wilson**, B.D. Wingfield, A.R. Wood, and P.W. Crous (2018)
Genera of phytopathogenic fungi: GOPHY 2. Studies in Mycology 92: 47 – 133.

Wilson, A.M., M.A. van der Nest, P.M. Wilken, M.J. Wingfield and B.D Wingfield (2018)
Pheromone expression reveals putative mechanism of unisexuality in a saprobic ascomycete fungus. PLOS One 13(3): e0192517

Wingfield, B.D., T.A. Duong, A. Hammerbacher, M.A. van der Nest, **A.M. Wilson**, R. Chang, Z.W. de Beer, E.T. Steenkamp, P.M. Wilken, K. Naidoo, and M.J. Wingfield (2016)
Draft genome sequences for *Ceratocystis fagacearum*, *C. harringtonii*, *Grosmannia penicillata*, and *Huntiella bhutanensis*. IMA Fungus 7(2):317-323

2. CONFERENCE ATTENDANCE

A.M. Wilson, P.M. Wilken, M.A. van der Nest, M.J. Wingfield and B.D. Wingfield (2018) Pheromone expression in the unisexual fungus, *Huntiella moniliformis* (poster presentation). International Congress of Plant Pathology, 29 July – 3 August, Hynes Convention Center, Boston, USA

A.M. Wilson, P.M. Wilken, M.A. van der Nest, M.J. Wingfield and B.D. Wingfield (2018) Characterization of *MAT1-2-7*: a novel MAT gene in the wood-infecting fungus *Huntiella omanensis* (poster presentation). International Congress of Plant Pathology, 29 July – 3 August, Hynes Convention Center, Boston, USA

A.M. Wilson, P.M. Wilken, M.A. van der Nest, M.J. Wingfield and B.D. Wingfield (2018) Characterization of *MAT1-2-7*; a novel mating gene in *Huntiella omanensis* (oral presentation). South African Society of Microbiology Conference, 4 – 7 April, Misty Hills Hotel & Conference Venue, Johannesburg, South Africa

A.M. Wilson, P.M. Wilken, M.A. van der Nest, M.J. Wingfield and B.D. Wingfield (2017) Unpacking the Molecular Mechanism behind Unisexual Reproduction in *Huntiella moniliformis* (poster presentation). Life Sciences Symposium, 18 – 19 May Pennsylvania State University, State College, USA

A.M. Wilson, P.M. Wilken, M.A. van der Nest, M.J. Wingfield and B.D. Wingfield (2017) Unpacking the Molecular Mechanism behind Unisexual Reproduction in *Huntiella moniliformis* (oral & poster presentations). Fungal Genetics Conference, 14 – 19 March, Asilomar Conference Grounds, Pacific Grove, USA

A.M. Wilson, P.M. Wilken, M.A. van der Nest, M.J. Wingfield and B.D. Wingfield (2016) Unpacking Unisexual Reproduction in *Huntiella moniliformis* (oral presentation). South African Genetics Society/South African Society of Bioinformatics Congress, 20 – 23 September, Durban, South Africa

LITERATURE REVIEW

Published as:
Wilson AM, van der Nest MA, Wilken PM, Wingfield MJ & Wingfield BD. **2019**.
It's All in the Genes: The Regulatory Pathways of Sexual Reproduction in Filamentous Ascomycetes
Genes, 10(5): 330

genes

MDPI

Review

It's All in the Genes: The Regulatory Pathways of Sexual Reproduction in Filamentous Ascomycetes

Andi M. Wilson *, P. Markus Wilken, Magriet A. van der Nest, Michael J. Wingfield and Brenda D. Wingfield

Department of Biochemistry, Genetics and Microbiology, Forestry and Agricultural Biotechnology Institute (FABI), Faculty of Natural and Agricultural Sciences, University of Pretoria, Pretoria 0083, South Africa; markus.wilken@fabi.up.ac.za (P.M.W.); magriet.vandernest@fabi.up.ac.za (M.A.v.d.N.); mike.wingfield@fabi.up.ac.za (M.J.W.); brenda.wingfield@fabi.up.ac.za (B.D.W.)

* Correspondence: andi.wilson@fabi.up.ac.za; Tel.: +27-12-420-3939

Received: 11 March 2019; Accepted: 24 April 2019; Published: 30 April 2019

Abstract: Sexual reproduction in filamentous ascomycete fungi results in the production of highly specialized sexual tissues, which arise from relatively simple, vegetative mycelia. This conversion takes place after the recognition of and response to a variety of exogenous and endogenous cues, and relies on very strictly regulated gene, protein, and metabolite pathways. This makes studying sexual development in fungi an interesting tool in which to study gene–gene, gene–protein, and protein–metabolite interactions. This review provides an overview of some of the most important genes involved in this process; from those involved in the conversion of mycelia into sexually-competent tissue, to those involved in the development of the ascomata, the asci, and ultimately, the ascospores.

Keywords: sexual reproduction; fungi; filamentous ascomycetes; gene expression; regulatory networks; functional characterisation

1. Introduction

Fungi represent the most diverse of the eukaryotic kingdoms, with more than 100,000 species described to date [1]. While there is some disagreement regarding the actual number of fungal species present globally, this value is generally accepted to be in the millions [2,3]. Such a rich diversity has led to an incredible variety of life cycles as well as a high level of reproductive plasticity. As such, fungal species exhibit some of the most interesting mechanisms of propagation, both sexual and asexual [4].

Sexual reproduction in filamentous ascomycetes (Figure 1) is initiated upon the recognition of a variety of factors that cause the conversion of vegetative mycelia into sexually-competent tissue (reviewed in [5]). This is followed by gamete fertilization, and the production of a dikaryotic cell and the protoascomata, which mature into fully developed fruiting structures, known as ascomata. These structures harbour the sac-shaped asci that produce and protect the eight internal ascospores [6,7]. The production of these highly specialized sexual tissue types is a morphological outcome that relies upon the initiation and control of gene, protein, and secondary metabolite networks [8]. These networks interact with one another to ensure the correct spatiotemporal expression of gene products, which enables the process of sexual reproduction to take place under the most suitable environmental conditions.

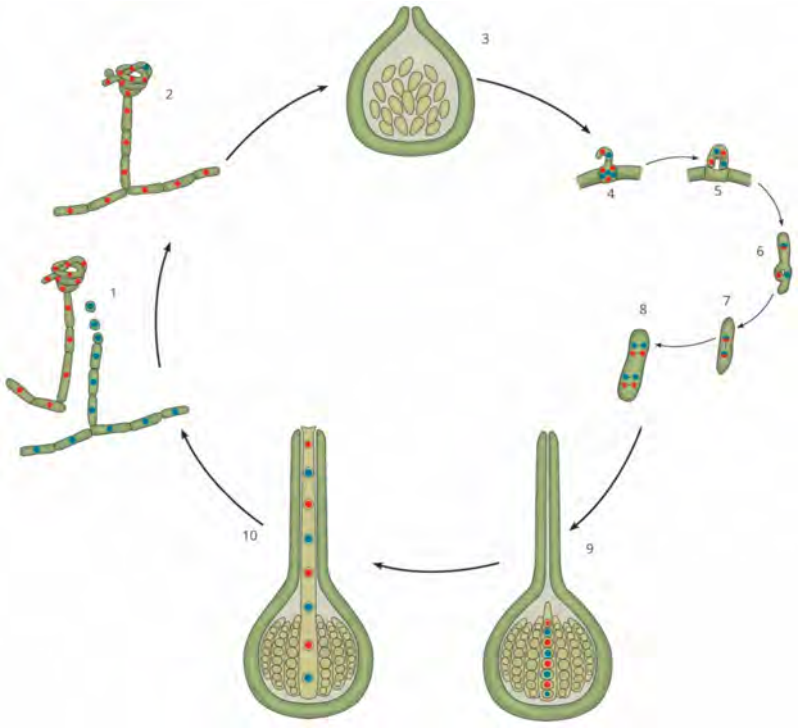

Figure 1. Generalized sexual cycle of filamentous ascomycetes. Mycelial strands (1) recognize a variety of signals before being converted into sexually competent tissue. One such signal is the recognition of a suitable mating partner. One partner produces the female structure, an ascogonium (indicated by the structure with red nuclei), while the second partner produces fertilizing spermatia (indicated by the single cells with blue nuclei). Gamete fertilization (2) occurs when the spermatia physically interact with the ascogonium. This is followed by the production of the protoascomata (3). Stages (4) to (8) occur within the immature ascomata and the developing asci. This includes the development of a crozier, nuclear migration, karyogamy, meiosis, and mitosis. This entire process culminates in a fully mature ascoma (9), which can release ascospores (10). These spores will then germinate and begin the cycle again.

In this review, we consider the many genes that play pivotal roles during the process of sexual reproduction in filamentous ascomycete fungi. To this end, three broadly divided sections are presented. These cover the major morphological changes that occur during protoascomatal development, ascus formation, and ascospore production.

2. Protoascomatal Development

The conversion of vegetative mycelia into sexually-competent, ascomatal-forming tissue is the first step in sexual reproduction. This relies on the recognition of various endogenous and exogenous cues, each of which uniquely contributes to whether sexual structures are produced.

2.1. The Mating Type Genes

The master regulators of sex in most fungi are the mating type, or *MAT*, genes. These genes, harboured at the *MAT* locus, encode proteins that typically possess DNA binding domains [9]. The *MAT* proteins act as transcription factors that regulate the expression of genes related to sex, such as those involved in mate recognition, cellular differentiation, and meiosis [10,11]. It is the *MAT* genes that determine the mating strategies employed by a fungal species, as sexual reproduction typically requires the expression of *MAT1-1* and *MAT1-2* genes (Figure 2). In heterothallic fungi, individuals possess either the *MAT1-1* or *MAT1-2* genes, which confer the MAT1-1 and MAT1-2 mating types, respectively. This system requires opposite partners to physically interact in order to produce sexual offspring.

In contrast, homothallic species typically possess both types of genes [12] and are thus able to sexually reproduce in complete isolate or with any other individual of the same species [4,13,14]. Until Turgeon and Yoder [15] proposed a revised naming system in 2000, *MAT* gene nomenclature was species-specific, making comparisons of gene content and function difficult. Thus, for the sake of this review, genes are referred to by the names that fulfil the requirements of the universal nomenclature system (Table 1), as revised and updated in 2017 by Wilken et al. [16].

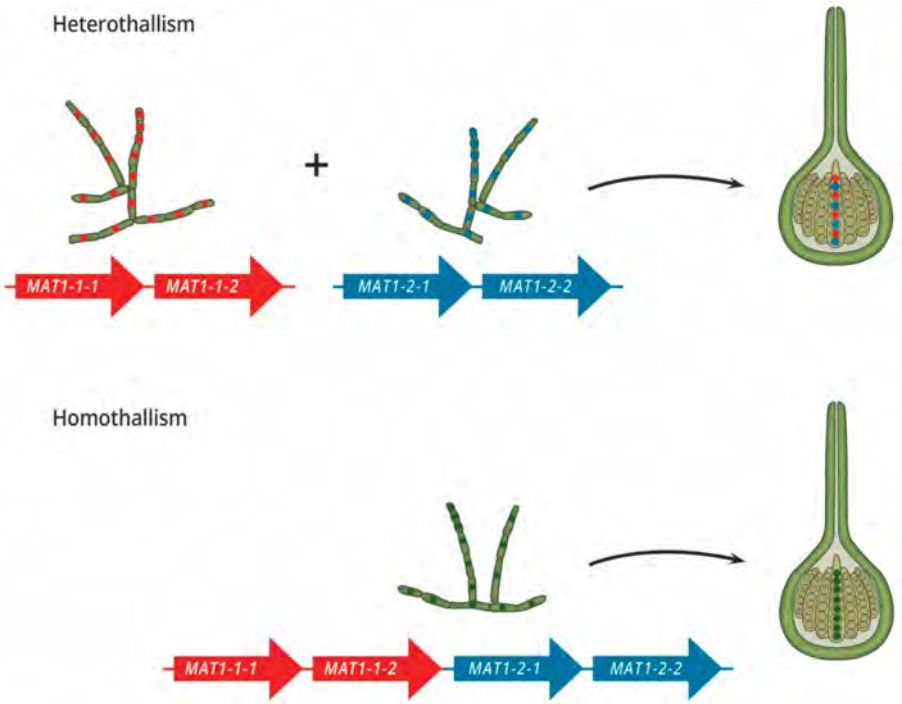

Figure 2. The sexual strategies of filamentous ascomycetes. Heterothallism: Two isolates of an opposite mating type need to physically interact in order to produce sexual structures. These mating types are genetically determined by genes at the *MAT* locus, either encoding the *MAT1-1* genes (red) or the *MAT1-2* genes (blue). These genes confer the MAT1-1 and MAT1-2 mating identities, respectively. Homothallism: Sexual reproduction can either occur within a single isolate that expresses both the *MAT1-1* and *MAT1-2* genes (as illustrated) or between any two individuals of the same species.

In *Podospora anserina*, the sexual cycle is controlled by a variety of proteins that regulate the *MAT* genes. One of the most prominent *MAT*-regulating proteins is encoded by *pro1*, a gene that is very well characterized in a number of model fungi [17–20]. In *P. anserina*, this protein regulates similar pathways to those of other fungal species, but also plays an integral role in sexual reproduction [21]. *Pro1* acts as a positive regulator upstream of a high mobility group (HMG) box protein named PaHMG8, which itself positively regulates the expression of both *MAT1-1-1* and *MAT1-2-1* [21,22]. In addition to PaHMG8, two other HMG box proteins, PaHMG5 and PaHMG6, are also responsible for the tight regulation of the two *MAT* genes and their transcription networks [22]. Transcription factors that possess the HMG box domain are involved in a multitude of biological processes, with a particular importance in pathways associated with sexual reproduction in fungi [23].

Table 1. The gene name equivalents of the *MAT*, pheromone, and pheromone receptor genes.

Species	Sexual Strategy	*MAT1-1* Idiomorph	Universal Name	*MAT1-1* Genes	α-Factor Pheromone	α-Factor Receptor	*MAT1-2* Idiomorph	Universal Name	*MAT1-2* Genes	a-Factor Pheromone	a-Factor Receptor
Cryphonectria parasitica	Heterothallic	MAT1-1	*MAT1-1-1* *MAT1-1-2* *MAT1-1-3*	*MAT1-1-1* *MAT1-1-2* *MAT1-1-3*	*Mf1/1*	-	MAT1-2	*MAT1-2-1*	*MAT1-2-1*	*Mf2/1* *Mf2/2*	-
Magnaporthe grisea	Heterothallic	MAT1-1 [a]	*MAT1-1-1*	*MAT1-1*	*MF2-1*	*ste3*-like	MAT1-2 [a]	*MAT1-2-1*	*MAT1-2*	*MF1-1*	*ste2-like*
Neurospora crassa	Heterothallic	mat A	*MAT1-1-1* *MAT1-1-2* *MAT1-1-3*	*matA-1* *matA-2* *matA-3*	*ccg4*	*pre2*	mat a	*MAT1-2-1* *MAT1-2-2*	*mata-1* *mata-2*	*mfa-1*	*pre1*
Trichoderma reesei	Heterothallic	MAT1-1	*MAT1-1-1* *MAT1-1-2* *MAT1-1-3*	*mat1-1-1* *mat1-1-2* *mat1-1-3*	*ppg1* [c]	*pre2*	MAT1-2	*MAT1-2-1*	*mat1-2-1*	*hpp1* [c]	*pre1*
Podospora anserina	Pseudo-homothallic	mat-	*MAT1-1-1* *MAT1-1-2* *MAT1-1-3*	*FMR1* *SMR1* *SMR2*	*mfm*	*pre2*	mat+	*MAT1-2-1*	*FPR1*	*mfp*	*pre1*
Sordaria macrospora	Homothallic [b]	mat A	*MAT1-1-1* *MAT1-1-2* *MAT1-1-3*	*SmtA-1* *SmtA-2* *SmtA-3*	*ppg1*	*pre2*	mat a	*MAT1-2-1*	*Smta-1*	*ppg2*	*pre1*
Aspergillus nidulans	Homothallic [b]	MAT-1	*MAT1-1-1*	*MAT1-1*	*ppgA*	*preB*	MAT-2	*MAT1-2-1*	*MAT2-1*	-	*preA*
Fusarium graminearum	Homothallic [b]	MAT1-1	*MAT1-1-1* *MAT1-1-2*	*MAT1-1-1* *MAT1-1-2*	*ppg1*	*pre2*	MAT1-2	*MAT1-2-1*	*MAT1-2-1*	*ppg2*	*pre1*

[a] Prior to the revised nomenclature of mating type genes, the *MAT* loci of *Magnaporthe* spp. were arbitrarily named Mat1-2 and Mat1-1. While these names have since been changed to comply with the naming system, the pheromone gene names still reflect the original *MAT* gene names. [b] In homothallic fungi, the mating type genes are all found within a single genome. Thus, it is not necessary to classify the locus as *MAT1-1* or *MAT1-2*. However, these species do still harbour *MAT* genes with homology to those found in heterothallic species. [c] *T. reesei* harbours the **h**-type pheromone in place of the **a**-factor pheromone found in many other species. Furthermore, the two pheromones of *T. reesei* are not expressed in a mating-type dependant manner. This is covered in the section regarding pheromones.

Transcriptional control of the mating genes in *Trichoderma reesei* is achieved by a complex of proteins that respond to the availability of light [24,25]. In this species, two photoreceptors are encoded by the *blr1* and *blr2* genes, while a third regulatory protein is encoded by the *env1* gene [26–28]. Together, these three proteins regulate sexual reproduction in a mating-type dependent manner, by controlling the expression of *MAT1-2-1* [25]. The deletion of *env1* has a more pronounced effect on sexual reproduction than that of either of the photoreceptors, suggesting that BLR1 and BLR2 exert their effect via ENV1. Expression of *MAT1-2-1* is also controlled by VEL1, yet another protein involved in light-dependent sexual development in *T. reesei* [24].

The two primary *MAT* genes, *MAT1-1-1* and *MAT1-2-1*, have been functionally characterized in a variety of heterothallic and homothallic species. Unsurprisingly, both genes are typically essential for successful sexual reproduction, though their exact functions may differ from species to species. In *P. anserina*, *Aspergillus nidulans*, and *Neurospora crassa*, both genes are essential for fertilization and thus, while both female and male structures are often still produced in strains where either *MAT* gene has been deleted, further ascomatal development never takes place [11,29–31]. In addition to its role in fertilization, the *P. anserina MAT1-1-1* gene is also essential for ascospore production [29]. In *Fusarium graminearum*, both genes are essential and the deletion of either results in mycelia that is unable to form even immature sexual structures [32]. In *Penicillium chrysogenum*, the *MAT1-1-1* gene is not involved in the development of the ascoma, however, Δ*MAT1-1-1* strains do not produce ascospores and this gene is consequently essential for sexual reproduction [33]. The *P. chrysogenums MAT1-2-1*, however, has a much earlier role in sexual development as Δ*MAT1-2-1* strains do not form sexual structures, even in the presence of a suitable mating partner [34]. In contrast, *MAT1-1-1* is dispensable for sexual reproduction in *Sordaria macrospora*, while *MAT1-2-1* remains essential [35].

In addition to the primary *MAT* genes, other secondary genes have also been described from the *MAT* loci. Currently, six other *MAT1-1* genes (*MAT1-1-2* to *MAT1-1-7*) and 10 other *MAT1-2* genes (*MAT1-2-2* to *MAT1-2-11*) are known from various fungi (as reviewed in [16]). Although these genes often have no known functional domains and are not typically conserved beyond genus or family boundaries [12], a number of them have been at least partially characterized.

The secondary *MAT1-1* genes that have been shown to be essential to sexual reproduction include the *MAT1-1-2* genes of *S. macrospora* [10], *F. graminearum* [36], and *P. anserina* [37], as well as the *MAT1-1-5* genes of *Sclerotinia sclerotiorum* [38] and *Botrytis cinerea* [39]. Deletion of any of these genes results in the complete inability to produce sexual ascospores. While the exact function of the *S. macrospora* and *S. sclerotiorum* genes remain unknown, the *P. anserina MAT1-1-2* gene is directly responsible for ascus production, nuclear recognition, and cellular division [37,40]. The *F. graminearum MAT1-1-2* and the *B. cinerea MAT1-1-5* are both specifically involved in the development of the maturing protoascomata. Consequently, while mutant strains of both species produce immature sexual structures, asci-bearing ascomata never develop [36,39]. The *P. anserina MAT1-1-3* gene, although not essential for sexual reproduction, helps to determine the nuclear identity in sexually reproducing cultures [37]. Thus, this gene, in conjunction with *MAT1-1-1*, is responsible for nuclear recognition early in the sexual process, when the protoascoma is developing [37,41].

In addition to these *MAT1-1* genes, a variety of secondary *MAT1-2* gene are also essential for sexual reproduction. These include the *MAT1-2-4* genes of *S. sclerotiorum* [38] and *A. fumigatus* [42] as well as the *MAT1-2-10* gene of *B. cinerea* [39]. Interestingly, despite being homologs, the *MAT1-2-4* of *S. sclerotiorum* is important for ascomatal development [38], while the *A. fumigatus MAT1-2-4* gene appears to play a more global role in sexual reproduction by directly affecting the expression of a variety of different sex-related genes [42]. Lastly, the *B. cinerea MAT1-2-10* plays an important role in ascomatal development, with deletion strains unable to produce asci-harbouring fruiting bodies [39].

2.2. Important Signalling Pathways

One of the major protein complexes that control sexual development in fungi is the COP9 signalosome (CSN). This complex of proteins is involved in a huge diversity of processes because

it plays an integral role in post-translational processes, including protein ubiquitination and phosphorylation [43]. In the most typical cases, the complex harbours up to eight individual subunits. One such example is encountered in *A. nidulans*, where genes *CsnA* through to *CsnH* are encoded by the genome [44]. The importance of this signalling pathway in sexual development is supported by the fact that mutant strains lacking the *CsnA*, *CsnB*, *CsnD*, and *CsnE* genes are unable to produce protoascomatal structures, despite initiating sexual development [44,45]. The deletion of a single *Csn* gene can affect the assembly of the entire signalosome, explaining the disrupted sexual development seen even in single gene knockouts [45].

The second important protein complex that is involved in sexual reproduction is known as STRIPAK, the striatin-interacting phosphatase and kinase complex (reviewed in [46]). This complex was first discovered in humans [47] and homologous complexes have since been identified in a huge variety of eukaryotic organisms, including *Drosophila melanogaster* [48]. The STRIPAK complex has been fairly well characterized in *S. macrospora*, where it is known to influence the production of the ascomata [49–51]. Three of the core proteins of this complex, PRO11, MOB3, and PRO22, have been studied in *S. macrospora* and are all essential for sexual reproduction.

The first of the STRIPAK genes to be characterized was *pro11*, which encodes a protein homologous to the mammalian striatin [51]. This gene is up-regulated during sexual reproduction [49], but is only involved in this process once the protoascomata have formed. Thus, while Δ*pro11* mutants are sterile, ascogonia and immature ascomata are produced [51]. PRO11 interacts with a second protein, encoded by the *mob3* gene [49]. MOB3 is a phocein protein and like PRO11, is also up-regulated during sexual reproduction in *S. macrospora*. It is thus not surprising that Δ*mob3* mutants are also sterile. However, the phenotypic disruption seen in *mob3* deletion mutants is more severe than that of Δ*pro11* mutants, as they are unable to produce any sexual tissues [49]. The third protein, PRO22, interacts directly with PRO11 in the STRIPAK complex, and is involved in sexual development [50]. In Δ*pro22* mutants, immature sexual tissue is formed, but does not develop further than the protoascomatal stage, which is similar to the Δ*pro11* mutants [50,51].

2.3. Nutrient Requirements for the Induction of Sexual Reproduction

One of the most important sex-regulating factors that fungi are able to recognize and respond to is nutrient availability. Before sexual reproduction can occur, vegetative mycelia need to acquire nutrients that will support the energetically-intense process of sexual reproduction [52]. Nutrient availability is one of the environmental factors that influences the expression of the *MAT* genes [46]. In *P. anserina*, it is hypothesized that nutrient starvation activates *pro1*, which in turn regulates *PaHMG8*. As previously discussed, *PaHMG8* positively influences the expression of both *MAT1-1-1* and *MAT1-2-1*, thereby acting as an intermediate between nutrient availability signalling and the onset of sexual reproduction [21,53]. While the nutrient requirements for sexual reproduction differ amongst species, a few nutrients are essential to most. These are treated individually in the sections that follow.

2.3.1. Sugars

Glucose and other sugars are the primary energy source for most living cells, including those of microorganisms [54]. Given that sexual reproduction is an energy-intensive process, carbon availability plays a significant role in its initiation. To this end, genes putatively encoding sugar-sensing proteins have been discovered in the genomes of many different fungi.

In *A. nidulans*, two of these proteins, *gprD* and *gprH*, have been partially characterized. The former shows significant similarity to the *Saccharomyces cerevisiae gpr1* [55] and the *Schizosaccharomyces pombe git3* [56] genes, both of which encode sugar sensing proteins. The latter, *gprH*, has been shown to recognize and respond to exogenous glucose levels [57]. Additionally, Δ*gprH* strains of *A. nidulans* undergo sexual reproduction without proper induction, while Δ*gprD* mutants display sexual reproduction under prohibitive conditions [57,58]. Furthermore, both mutants also show an increase in the expression of the mating pheromone receptors [57]. Taken collectively, these results

indicate that the regulation of sex due to carbon availability is the result of a combined response by *gprD* and *gprH* [57].

The A. nidulans gprH in particular responds to periods of low carbon availability, in turn activating the cAMP-PKA (cyclic AMP- protein kinase A) pathway, an intracellular signalling pathway that ultimately initiates the transcriptional changes associated with the inhibition of sex [57]. During short-term starvation, *nosA*, a positive regulator of sex, is repressed [18,57]. This protein's repression in turn activates a related protein, *rosA*, a negative regulator of sex [19,57]. Sexual reproduction is thus precluded until the stress associated with carbon starvation is alleviated.

2.3.2. Amino Acids

Amino acids are crucial nutrients that determine whether sexual reproduction will take place (Figure 3). In *A. nidulans*, sensing and responding to exogenously available amino acids is achieved via the cross-pathway regulatory network (CPRN). This pathway integrates the amino acid biosynthesis pathways with other important cellular processes, such as sexual reproduction and virulence. The two major genes involved in this pathway are *cpcA* and *cpcB*, the cross-pathway control genes. While *cpcA* responds to amino acid deficiencies, *cpcB* recognizes exogenous amino acid availability [59].

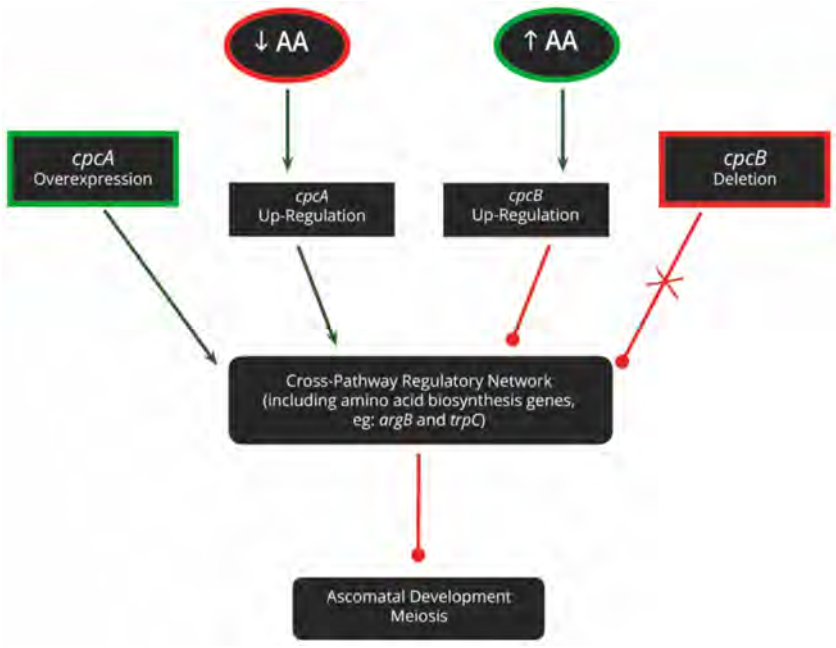

Figure 3. The involvement of the cross-pathway regulatory network (CPRN) during sexual reproduction in *A. nidulans*. In the absence of amino acids, *cpcA* is up-regulated, thereby activating the CPRN. This pathway subsequently inhibits the onset of sexual reproduction. In contrast, when amino acids are available, *cpcB* is up-regulated and the CPRN is inhibited. This results in sexual development. Either the overexpression of *cpcA* or the deletion of *cpcB* can activate the CPRN, by simulating amino acid deficiency, and thus also inhibit sexual reproduction. Shapes with green outlines indicate conditions under which sexual reproduction is directly or indirectly activated. Those with red outlines indicate conditions which directly or indirectly repress sexual reproduction. Green arrows indicate activation of a particular pathway, while red lines terminating in circles indicate repression.

The CPRN has been experimentally elucidated by generating a variety of mutants, including *cpcA* over-expression, *cpcB* deletion, and amino acid auxotrophic mutants. Both the *cpcA* and *cpcB* mutants experience amino acid starvation, regardless of the actual amino acid availability and consequently, sexual reproduction cannot take place [59,60]. These phenotypes can also not be rescued by the exogenous provision of amino acids, given their inability to recognize that amino acids are indeed available. In contrast, the phenotype of Δ*trpA-D* auxotrophic mutants, which are unable to produce

their own tryptophan and are thus sterile, can be rescued in the presence of an exogenous amino acid source [61,62]. Furthermore, Δ*argB* auxotrophic mutants are also sterile and produce only immature ascomata [63]. This phenotype can, however, not be rescued by an exogenous arginine supply, indicating that *argB* may play a greater role in sexual reproduction than simply aiding in the production of arginine.

2.3.3. Calcium

As an essential element for most living organisms, calcium plays a variety of biological roles in the lives of many eukaryotes, especially during signal transduction [64,65]. To ensure consistent calcium availability, fungi utilize two different calcium uptake systems. The high-affinity calcium uptake system (HACS) functions when there are low levels of exogenous calcium and active uptake is required [66,67]. This system is discussed in more detail in the section dealing with ascospore discharge (see below). In contrast, the low-affinity calcium uptake system (LACS) is utilized when exogenous levels of calcium are high and active uptake is not necessary. This system is comprised of at least FIG1, a transmembrane calcium channel [68].

The LACS gene, *fig1*, has been extensively studied with regards to its role during sexual reproduction in *F. graminearum* [69,70], *A. nidulans* [71], and *N. crassa* [69]. Interestingly, while the importance of the gene is obvious in all three species, its actual function depends on the sexual strategy being employed by the species. For example, in both *F. graminearum* and *A. nidulans*, *fig1* is essential for the production of ascomata during homothallic mating [69–71]. However, *fig1* is completely dispensable in *A. nidulans* when an isolate undergoes outcrossing [71]. In contrast, the gene is important for heterothallic mating in *N. crassa*, particularly in MAT1-2 isolates, where Δ*fig1* mutants are female sterile. Interestingly, this mutant phenotype is not seen in Δ*fig1* MAT1-1 isolates, indicating a mating-type specific interaction [69].

2.4. Other Environmental Triggers

Once the critical nutrient and energy requirements have been met in the vegetative mycelium, a variety of other signals are needed to successfully initiate sexual reproduction.

2.4.1. Light

Light can act as either a positive or negative regulator of sexual reproduction, depending on the species and the wavelength [72]. In order to respond to light-based signals, fungi express a variety of light-sensing molecules, which range from small peptides to giant protein complexes. This allows for the recognition of wavelengths across the visible light spectrum, from near-ultraviolet to red [72]. Two of the primary photo-recognition systems in fungi, the white collar system and the velvet complex system, have been intensively studied in *N. crassa* and *A. nidulans*, respectively.

In *N. crassa*, the blue light response relies on the recognition of blue light by WC-1, a white collar protein, which harbours the light-recognizing LOV (light oxygen voltage sensing) domain [73]. The WC-1 protein also harbours PAS (Per-Arnt-Sim) domains, which allows dimerization with both itself and a second white collar protein, WC-2 [74,75]. Additionally, both proteins possess zinc finger DNA binding motifs, which bind to the promoters of various light-inducible genes [75,76]. Thus, these domains allow the two proteins to form the entire signal transduction pathway associated with blue light illumination in *N. crassa*, from light recognition to transcriptional regulation.

Blue light enhances the production and development of ascomata in *N. crassa*. Thus, although not essential for protoascomatal production, illumination significantly increases sexual competency and the number of protoascomata produced [77]. Furthermore, upon fertilization and subsequent development, the ascomatal necks orient themselves towards the source of the blue light illumination [78], a form of phototropism that may act to enhance spore dispersal. Thus, while Δ*wc1/2* mutants are not sexually defective, they produce far fewer protoascomata, most of which are unable to orient their necks correctly [77,78].

Light has a more direct effect on the sexual cycle of *A. nidulans* than that of *N. crassa* (Figure 4), with sexual reproduction being entirely precluded in the presence of light [79]. Furthermore, light sensing and its signal transduction pathway is more complex in *A. nidulans*, involving many proteins that form a variety of multi-peptide complexes [80,81]. The majority of these complexes are made up of the velvet proteins, which form different dimers and trimers during the *A. nidulans* life cycle, each of which elicits a unique response [81–84].

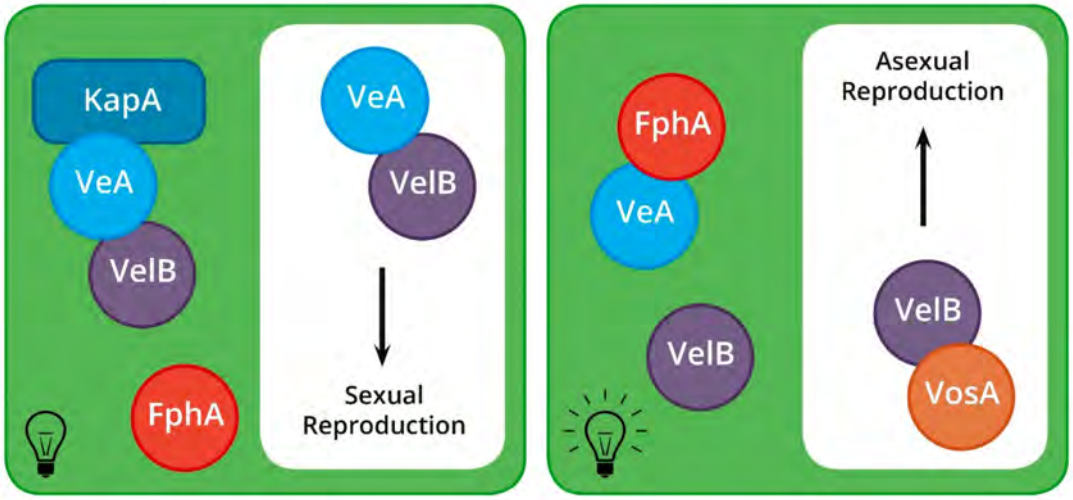

Figure 4. Sexual reproduction and light sensing in *A. nidulans*. Darkness: VeA and VelB interact with the importin protein, KapA. This allows their transport into the nucleus where they regulate gene expression and initiate sexual development. Light: FphA, the red light sensor, interacts with VeA, putatively inhibiting its interaction with KapA and VelB. This prevents the transport of VeA into the nucleus. Instead, VelB interacts with other proteins, activating asexual reproduction.

The first velvet gene, *veA*, is constitutively expressed in *A. nidulans* and displays a major up-regulation during sexual reproduction [82]. The gene is essential for mating, and, if overexpressed, leads to the production of ascomata under normally restrictive conditions [82]. A second velvet protein, VelB, which interacts with VeA in the cytoplasm, is also essential for sexual reproduction [81]. The VeA–VelB dimer interacts with a KapA importin protein during periods of darkness to bring about sexual reproduction [83]. The COP9 signalosome discussed above has also been shown to play an important role in regulating the recognition of light in *A. nidulans*. It is thought that this protein complex may be involved in the same pathway as *veA*, given that Δ*csnD* mutants are unable to respond to light [45].

During periods of red light illumination, the light sensing phytochrome, FphA, is activated and binds to VeA, thereby preventing its transport into the nucleus [85,86]. Thus, Δ*fphA* strains are sexually competent even in the presence of light. However, Δ*fphA* mutants also produce significantly fewer ascomata than wild type isolates when grown in the dark [85]. This, in addition to the fact that FphA possesses kinase activity, indicates that the protein is most likely involved in additional functions not linked to light-sensing during sexual reproduction.

2.4.2. Reactive Oxygen Species

Reactive oxygen species (ROS) are produced as by-products of aerobic respiration [87]. These radicals are known to cause damage to various cellular components, and thus most organisms express antioxidant systems for protection. The production of ROS is, however, increasingly being recognized as an important regulator of cellular processes, especially in cell differentiation and development [87,88].

In *A. nidulans*, genes involved in both ROS neutralization and production play integral roles in sexual development [89,90]. One such gene, *cpeA*, encodes a catalase-peroxidase that converts hydrogen peroxide into water. While *cpeA* is not expressed in vegetative mycelia, its expression

dramatically increases during the onset of sexual reproduction [89]. It is hypothesized that *cpeA* is expressed as a mechanism to prevent ROS-induced damage to the developing fruiting structures. *A. nidulans* also expresses the ROS-producing enzyme NADPH oxidase [90]. This protein, encoded by *noxA*, produces superoxide molecules and is up-regulated in cultures induced to undergo sexual reproduction. The importance of ROS production in sexual reproduction has been illustrated by Δ*noxA* mutants, which are unable to undergo homothallic mating, with sexual reproduction being blocked before protoascomata formation [90]. Interestingly, this knockout does not affect outcrossing, provided that the wild type partner can produce its own *noxA* and thus superoxide. It is thought that the ROS is responsible for signalling during cell differentiation prior to sexual reproduction and can be utilized by both interacting partners, regardless of which isolate produces it [90].

N. crassa expresses two NADPH oxidases that are essential for sexual reproduction. The first, *nox-1*, is a homolog of the *A. nidulans noxA* and is also significantly up-regulated during sexual development [91]. NOX-1 is specifically required for female fertility, and while Δ*nox-1* strains are sexually incompetent if used as the female partner, these strains are able to fertilize wild type female structures [91]. *N. crassa* also expresses the *nox-2* gene, which, in contrast to *nox-1*, is highly expressed in asexual cells and prior to ascomatal development. This gene plays an important role in ascospore germination, despite the fact that Δ*nox-2* strains produce normal sexual spores [91]. Although its exact role in germination is not understood, it is reasonable to speculate that the ROS produced by NOX-2 may be involved in a signalling pathway that initiates ascospore germination.

NADPH oxidases are also important regulators of sexual reproduction in *P. anserina*, both in early ascomatal production and later during ascus development and ascospore germination [53]. There are two NADPH oxidase encoding genes in the *P. anserina* genome, *nox1* and *nox2*. The two proteins are responsible for superoxide and peroxide secretion, a process which co-localizes with the developing protoascomata of sexually-competent isolates [53]. It is thought that *nox1* is responsible for a type of ROS-mediated signalling, which induces cell wall degradation of the surrounding cells and provides nutrients to the developing ascomata [53]. It is consequently not surprising that in Δ*nox1* mutants, the number and size of protoascomata is greatly reduced. Furthermore, those that are fertilized take much longer to reach maturity than wild type protoascomata [53]. Given that a constant supply of fresh nutrients can rescue the mutant phenotype, the sexual defect is likely due to nutrient starvation.

2.4.3. Pheromones

Pheromones are a broad class of chemical signals that are involved in the mating of species as diverse as mammals [92], insects [93], and reptiles [94]. These biologically active compounds are secreted into the environment and are recognized by an individual of the same species, but different gender, sex, or mating type [95]. Fungi utilize sex pheromones in the form of diffusible peptides that allow for mate recognition and attraction (extensively reviewed by [96,97]).

Genes encoding mating pheromones have been found in the genomes of many ascomycete fungi, including *Cryphonectria parasitica* [98], *Magnaporthe grisea* [99], *N. crassa* [100], *P. anserina* [101], and various *Fusarium* species [102]. As with the MAT genes, however, these genes have been given species-specific names. These genes mostly fall into one of two categories; those with similarity to the pheromone expressed by *S. cerevisiae* **a**-cells and those to the pheromone expressed by *S. cerevisiae* **α**-cells. For the purpose of this review, these pheromones will thus be termed the **a**- and **α**-factor pheromones, respectively (Table 1).

In many filamentous fungi, the **a**-factor and the **α**-factor pheromone genes are transcriptionally controlled by the *MAT* genes. Consequently, in heterothallic species, they are expressed in a mating-type dependent manner (Figure 5). In such species, the *MAT1-1-1* gene controls the expression of the **α**-factor, while the *MAT1-2-1* gene is responsible for **a**-factor expression. As a direct result, MAT1-1 individuals express only the **α**-factor and MAT1-2 individuals express only the **a**-factor [98–100,103]. Homothallic species, which typically possess both the *MAT1-1-1* and *MAT1-2-1* genes, are often able to express both pheromones [104,105].

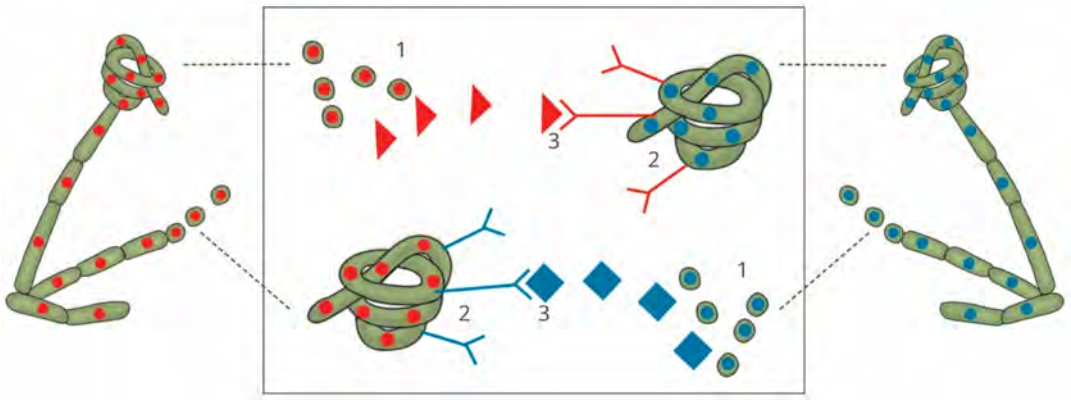

Figure 5. Pheromone signalling in heterothallic filamentous ascomycetes. (1) Pheromones are expressed, with spermatia of MAT1-1 isolates expressing the **α**-factor and spermatia of MAT1-2 isolates expressing the **a**-factor pheromone. (2) The ascogonia of these isolates also express the pheromone receptors, which recognize the pheromones. (3) Recognition of the pheromones by their receptors results in a variety of physiological changes, including growth towards the suitable partner as well as the transcriptional regulation of sex-related genes.

Given that the pheromones are typically expressed by the male cells, either spermatia or conidia, it is not surprising that both pheromones play an essential role in the male fertility of *P. anserina* and *N. crassa* [101,106]. Deleting either of the factors results in isolates that cannot fertilize female isolates and are thus male sterile. Interestingly, while a complete knockout of the **a**-factor does not affect female fertility in *N. crassa*, disruption of the 3′ non-coding region greatly reduces protoascomatal production [107]. Additionally, the **α**-factor is also essential for male fertility in *C. parasitica* [108]. In contrast, the *C. parasitica* **a**-factor has been implicated in female fertility, where **a**-factor knockout strains produce only empty ascomata, but fully functional male structures [108,109]. Thus, while clearly important for the sexual process, the actual function of the pheromones differs slightly from species to species.

A third type of pheromone has been identified in certain heterothallic *Fusarium* species, as well as in the heterothallic *T. reesei* [102,110]. This pheromone harbours a number of repeating units as well as the terminal CaaX domain, and thus has characteristics of both the **α**- and **a**-factors, respectively. This hybrid pheromone has thus been termed the **h**-type factor [110]. Given its genomic location, it is thought that the gene encoding this factor assumed the function of the **a**-factor pheromone after the loss of the original **a**-factor-encoding gene. Furthermore, a typical **α**-factor pheromone gene has been found in the genomes of the species harbouring this **h**-type factor [102,110]. This illustrates the presence of a pheromone response pathway that, at least partially, resembles the typical **α**/**a** system. It is surprising, however, that the **α**-factor and **h**-type pheromones are not expressed in a mating-type dependant manner as seen in typically heterothallic species [110].

In order to recognise these pheromones, the female structures of these fungi express receptors that are able to specifically recognize each pheromone (Figure 5) [95]. These receptors belong to the class of seven transmembrane G-protein coupled receptors, which, when activated, initiate an MAP kinase signal transduction pathway (reviewed by [111]). Recognition of the pheromone by the receptor therefore initiates a transduction pathway, which in turn activates a variety of networks that lead to sexual reproduction. The pheromone receptors are also important regulators of pheromone expression and female fertility in *N. crassa*. Thus, the deletion of the **a**-factor receptor results in a decrease in **α**-factor expression in a MAT1-1 background [112] and deletion of the **α**-factor receptor results in the down-regulation of the **a**-factor in a MAT1-2 background [113]. Protoascomata are still produced by these mutants, indicating at least a partial activation of the female fertility pathway. However, these mutants are not able to recognize, grow towards, or fuse with fertilizing spores from a male isolate, thereby precluding successful fertilization and thus sexual reproduction [112,113].

The *F. graminearum* **α**-factor receptor also plays a role in female fertility [104]. Although it is not essential for sexual reproduction, female fertility is significantly reduced in gene deletion strains. Contrastingly, deletion of the **a**-factor receptor results in no observable sexual defects [104]. Given that *F. graminearum* is homothallic, it is perhaps not entirely surprising that a system with the primary function of mate seeking is no longer essential for sexual reproduction. This, however, is not true for all homothallic species, where expression of the pheromones and their receptors is indeed essential for the production of sexual spores [114–116].

Despite their apparent primary role in mate recognition, pheromones are hypothesized to play a role in some of the downstream processes associated with sexual reproduction [97,113]. This is substantiated by the fact that pheromone expression is not limited to heterothallic species, but is an important sex-promoting pathway in some homothallic species. Furthermore, the expression of pheromone pathway genes is not limited to the initiation of sexual reproduction and instead often continues throughout the entire process. Genes encoding both the pheromones and their receptors have been identified in the homothallic species, *S. macrospora* [105,115] and *F. graminearum* [104,117]. The genes encoding the **α**-factor pheromone as well as both the pheromone receptors have also been found in *A. nidulans* [118]. These genes are expressed and functional, despite the absence of mate seeking behaviour and are thus likely to have been co-opted into other functions.

In *F. graminearum*, the **α**-factor pheromone and its receptor are not essential for self-fertility, but single deletion mutants produce far fewer mature ascomata than wildtype isolates [104]. This indicates that this pheromone/receptor pair plays a role in ascomatal production or development. Unexpectedly, deletion of the **α**-factor gene also enhanced outcrossing events, indicating that **α**-factor expression may promote selfing, rather than outcrossing as in other species. This effect, however, is abolished if its receptor is also deleted [104].

Both pheromone receptor genes play an important role in homothallic mating in *A. nidulans* [116]. Deletion of either receptor results in a significant decrease in fertility, with mutants producing small ascomata that house a limited number of ascospores. Deletion of both the receptors results in an even more severe phenotype, where mutants are unable to produce ascomata at all [116]. Similar to *F. graminearum*, however, the disruption of either or both receptors does not affect outcrossing [116]. These genes are thus only important for selfing and play no role in outcrossing in this species.

In some species, pheromone expression has been proposed to facilitate post-fertilization events, particularly before karyogamy and meiosis in both homothallic and heterothallic species [119]. In *N. crassa*, the pheromones as well as their receptors are required for the production of the ascospores [107,113]. For example, forced mating interactions between a wild type isolate and an **a**-factor mutant result in the production of ascomata harbouring very few ascospores, while forced matings between mutants results in completely barren ascomata. Additionally, deletion of both a pheromone and its receptor in *N. crassa* results in protoascomata that never mature. Similarly, the deletion of the **α**-factor pheromone in *C. parasitica* results in the production of mature, but barren, ascomata [108,109]. Taken together, these results illustrate a role for both the pheromones and their response pathway in post-fertilization events, such as ascomatal, ascal, and ascospore development.

A combination of the above mentioned environmental and physiological factors ultimately lead to asexual reproduction, sexual development, or simply the continuation of vegetative growth. If all the requirements are met and sexual reproduction can take place, an immature fruiting body will form and develop into an ascoma. Subsequently, the asci can begin to form within the mature sexual structure.

3. Ascus Production

One of the defining characteristics of ascomycete fungi is the ascus, a sac-like structure in which the ascospores are produced and housed [6]. The wall of the ascus is unique compared to all other tissues formed by fungi, different even from others formed during sexual reproduction [120]. As such, there are a number of genes that are expressed almost exclusively by the ascus [121], ensuring that the most appropriate environment is created for the developing ascospores.

In *F. graminearum*, *amd1* is one such gene and is essential for the correct development of the ascus [120,122]. The gene encodes a transmembrane protein, which localizes to the ascus membrane and possesses a domain associated with transmembrane transport [122]. While the AMD1 protein has no apparent function in the production of normal ascomata, Δ*amd1* strains are unable to produce stable ascus walls. Consequently, the wall degrades before the ascospores are ready for discharge, prompting their germination within the ascomata, and precluding effective dispersal [120–122]. Interestingly, the deletion of *amd1* results in the differential expression of many genes, including the up-regulation in membrane transport and the down-regulation of genes involved in cell-wall synthesis and cell-wall integrity [122]. This suggests that *amd1* is a master regulator of ascus wall synthesis and ensures cell wall integrity. This may be achieved by minimising cross-membrane transport and allowing the generation of turgor pressure in the ascus.

Ascus development genes have also been described from *N. crassa*, with functions mostly linked to gene regulation [123,124]. The ASD4 GATA DNA binding protein [123], the SMS-2 meiotic silencing Argonaute protein [125], and the STC1-like RNAi and chromatin remodelling protein [126] are all involved in regulating the production of the ascus. While ASD4 likely acts as a transcription factor, the other two proteins are intimately involved in the RNA silencing pathway [125,126]. The genes encoding these proteins are essential for this process, which is evident from the fact that mutant strains of *asd4*, *sms-2*, or *stc1*-like produce only empty ascomata that are incapable of forming asci. This extreme phenotype is thought to be due to the deregulation of the entire ascus development pathway, given the important role each protein plays in regulation [123,125,126].

In addition to its role in ascomatal development, ROS metabolism is also essential for ascus production in *P. anserina* [127]. The *car1* gene, now known as *pex2*, which encodes a peroxisomal assembly factor, ensures that peroxisomes are formed in abundance during asci maturation as well as ascospore delineation [127,128]. These peroxisomes play an important role in ensuring the sexual tissue is supplied with sufficient nutrients during sexual development [129]. In *pex2* mutants, these peroxisomes are not produced and the isolate is unable to undergo nuclear fusion prior to meiosis [127], precluding the development of the ascus. It is currently unclear whether this gene is essential for karyogamy itself, or whether it is involved in a process just upstream of nuclear fusion [129].

4. Ascospore Production

The production of ascospores represents the final step in sexual reproduction. If this process has been successful, these newly-produced spores will be discharged into the environment, where they germinate and initiate a new life cycle.

4.1. Meiosis and Ascospore Production

Ascosporegenesis is, by definition, dependant on a successful meiotic division cycle. There are a number of genes that have been identified in both *A. nidulans* and *N. crassa* that specifically ensure that prophase I, the first phase of meiosis, can begin. In *A. nidulans*, the deletion of either the *tubB* [130] or *grrA* [131] gene results in mutants that are able to produce asci-housing ascomata, but that cannot initiate meiosis. The similar phenotypes are particularly noteworthy given the different role each of these genes plays—while *tubB* encodes the structural α-tubulin protein, an important component in the microtubule assembly toolbox [130], *grrA* encodes a substrate adaptor protein that plays a role in the protein ubiquitylation and degradation pathway [131]. Similarly, deletion of either of the meiotic silencing genes, *sad1* and *sad2* of *N. crassa*, results in an almost identical phenotype, with mature fruiting bodies harbouring intact asci that are also unable to undergo meiosis [132,133].

Upon the completion of a successful cycle of meiosis, the developing ascospores must undergo further maturation, including partitioning and delineation within the ascus. In *N. crassa*, this process is at least partially regulated by *asd-1*, which encodes a rhamnogalacturonase that is expressed predominantly during mating [134]. In Δ*asd-1* mutants, the eight nuclei formed during meiosis remain diffuse and do not delineate into individual spores, leading to the sterility of the mutants [134].

The maturation process depends on the expression of the cAMP-PKA pathway as well as correct calcium signalling in *F. graminearum*. Given the importance of both these pathways in signal transduction, it is not surprising that the proteins associated with these pathways are essential for sexual reproduction. CPK1, a catalytic subunit of the PKA, ensures the transition of an immature spore into a single-celled ascospore harbouring only one nucleus [135]. Additionally, the deletion of *mid1*, a component of the HACS (discussed below), results in abnormal ascospores that are two-celled and septate, with fragile cell walls [136].

4.2. Ascospore Discharge

Fungal spores tend not to be motile and thus many diverse and elegant mechanisms of propagule dissemination have evolved across the Kingdom. A common mechanism of dissemination includes the forcible discharge of ascospores into their environment. This typically involves a build-up of turgor pressure, followed by the swift release of the ascospores [137].

As discussed earlier in this review, calcium is an essential mineral required for sexual reproduction in certain filamentous fungi. While LACS was discussed in terms of ascomatal formation, HACS is important for the forcible discharge of ascospores in *F. graminearum* [70,136,137]. This supports the multi-phase importance for calcium during sexual reproduction, where this element is required during the initiation of sexual development as well as in the final stages of sexual reproduction.

The HACS is made up of two ion channels, *MID1*, a mechanosensitive protein [136], and *CCH1*, an L-type protein [137]. Mutant *F. graminearum* strains of both these genes are defective in their ability to discharge ascospores [70,136,137], with the mutant phenotypes being partially rescued by the provision of exogenous calcium. This potentially activates the LACS, allowing for calcium transport via another pathway. Interestingly, despite this obvious phenotype in *F. graminearum*, the *N. crassa mid1* homolog is dispensable for ascospore discharge and *mid1* deletion strains display no other sexual defects [138]. This provides an elegant example of how protein similarity, at the sequence or structure level, is not always a good predictor of shared function.

Ascospore release in *F. graminearum* also relies on the expression of a kinase gene, *kin1* [139]. This gene encodes a member of a kinase protein family that typically harbours proteins involved in both cell-polarity and microtubule transport [139,140]. The kinase localizes to the septal pores in the newly produced ascospores and subsequently to their germ tubes [139]. In knockout studies, Δ*kin1* strains lack the ability to release the spores, despite having produced fully matured ascomata and asci [139]. Furthermore, the absence of *kin1* also interferes with the inhibition of ascospore germination prior to release. This results in the premature germination of the unreleased ascospores [139], similar to the phenotype previously discussed for Δ*amd1* strains of the same species.

It is worth noting that not all ascomycetes forcibly discharge their spores. For example, in some species, including *Magnaporthe salvinii* [141] and those belonging to the polyphyletic grouping of the ophiostomatoid fungi [142], the asci deliquesce before the spores are discharged, thus leaving them free within the ascoma. Typically, these spores are then exuded in a slimy matrix from a pore, sometimes found at the tips of the ascomatal necks. Such fungi consequently rely on a variety of dissemination means, other than forcible discharge. In species of *Graphium, Dipodascus*, and *Ceratocystis*, for example, these exudates are typically sticky and can be picked up by insects, which then act as dispersal agents [143].

5. Conclusions

Sexual reproduction in fungi provides a complex, diverse, and intriguing system to study tissue differentiation in eukaryotes. Many fungi provide simple, easy to use models, often with very well-characterized life cycles. Given that sexual reproduction relies upon the recognition and response to a variety of endogenous and exogenous cues, this system can be used to model protein–protein, metabolite–protein, and protein–DNA interactions. Furthermore, signal transduction events as well

as fine-scale and global changes in the transcriptome and proteome can be tracked in response to environmental changes.

Despite the intensive research that has already been committed to understanding the genes that play a role in fungal sexual reproduction, there are many important and intriguing questions that remain to be answered. Even in the best studied model organisms, certain aspects of sexual reproduction remain uncharacterized. This is partly due to the fact that many of the genes involved in sexual reproduction show pleiotropic effects when modified. For example, if they play a role early in sexual reproduction, this can preclude opportunities to understand how they function in later stages of the process as well. Furthermore, determining the role of genes in a single species does not necessarily imply that they have similar functions in other species, regardless of how closely related the species or how similar the gene sequence. Future research will thus likely be focused on identifying the downstream targets of the MAT transcription factors in different species. This will further elucidate the genetic pathways that underlie the different sexual strategies and identify the genes that ensure opposite mating type nuclei can be recognized as such.

The growing availability of next generation sequencing methods is facilitating increasingly rapid progress in many aspects of biological research. Genomics has, for example, allowed for the identification of genes involved in sexual reproduction in species previously thought to be asexual. Likewise, transcriptomics has enabled the elucidation of genes and pathways that are specifically expressed during sexual reproduction. In the future, we are likely to witness an increase in research that combines these technologies with classical functional characterization. This will be true not only for model species, but also for those fungi that are less well-known.

Author Contributions: Conceptualization, A.M.W. and B.D.W.; writing—original draft preparation, A.M.W., writing—review and editing, P.M.W., M.A.v.d.N., M.J.W. and B.D.W.; visualization, A.M.W., supervision, P.M.W., M.A.v.d.N., M.J.W. and B.D.W.

Funding: This research was funded by the National Research Foundation (NRF) of South Africa, grant number 116448.

Acknowledgments: We would like to thank Emma Steenkamp for her helpful review of this manuscript during its preparation. We would also like to thank Glenda Brits of the Department of Education Innovation at the University of Pretoria for producing the figures used in this review. We are also especially grateful to the anonymous reviewers for their careful reading of this manuscript and for their many insightful comments and suggestions that led to the significant improvement of this publication.

Conflicts of Interest: The authors declare no conflict of interest.

References

1. Hawksworth, D.L.; Luecking, R. Fungal Diversity Revisited: 2.2 to 3.8 Million Species. *Microbiol. Spectr.* **2017**, *5*. [CrossRef]
2. Blackwell, M. The Fungi: 1, 2, 3 … 5.1 Million Species? *Am. J. Bot.* **2011**, *98*, 426–438. [CrossRef] [PubMed]
3. Hawksworth, D. Global Species Numbers of Fungi: Are Tropical Studies and Molecular Approaches Contributing to a More Robust Estimate? *Biodivers. Conserv.* **2012**, *21*, 2425–2433. [CrossRef]
4. Billiard, S.; Lopez Villavicencio, M.; Hood, M.; Giraud, T. Sex, Outcrossing and Mating Types: Unsolved Questions in Fungi and Beyond. *J. Evol. Biol.* **2012**, *25*, 1020–1038. [CrossRef]
5. Ni, M.; Feretzaki, M.; Sun, S.; Wang, X.; Heitman, J. Sex in Fungi. *Annu. Rev. Genet.* **2011**, *45*, 405–430. [CrossRef] [PubMed]
6. James, T.Y.; Kauff, F.; Schoch, C.L.; Matheny, P.B.; Hofstetter, V.; Cox, C.J.; Celio, G.; Gueidan, C.; Fraker, E.; Miadlikowska, J. Reconstructing the Early Evolution of Fungi using a Six-Gene Phylogeny. *Nature* **2006**, *443*, 818–822. [CrossRef] [PubMed]
7. Stajich, J.E.; Berbee, M.L.; Blackwell, M.; Hibbett, D.S.; James, T.Y.; Spatafora, J.W.; Taylor, J.W. The Fungi. *Curr. Biol.* **2009**, *19*, R840–R845. [CrossRef] [PubMed]
8. Dyer, P.S. Sexual Reproduction and the Significance of *MAT* in the Aspergilli. In *Sex in Fungi: Molecular Determination and Evolutionary Implications*; Heitman, J., Kronstad, J.W., Taylor, J.W., Casselton, L.A., Eds.; American Society of Microbiology Press: Washington, DC, USA, 2007; pp. 123–142.

9. Dyer, P.; Inderbitzin, P.; Debuchy, R. Mating-Type Structure, Function, Regulation and Evolution in the Pezizomycotina. In *Growth, Differentiation and Sexuality. The Mycota*; Wendland, J., Ed.; Springer: Cham, Switzerland, 2016; Volume 1, pp. 351–385.
10. Klix, V.; Nowrousian, M.; Ringelberg, C.; Loros, J.; Dunlap, J.; Pöggeler, S. Functional Characterization of *MAT1-1*-Specific Mating-Type Genes in the Homothallic Ascomycete *Sordaria macrospora* provides New Insights into Essential and Nonessential Sexual Regulators. *Eukaryot. Cell* **2010**, *9*, 894–905. [CrossRef] [PubMed]
11. Ferreira, A.V.-B.; An, Z.; Metzenberg, R.L.; Glass, N.L. Characterization of *matA-2*, *matA-3* and Δ*matA* Mating-Type Mutants of *Neurospora crassa*. *Genetics* **1998**, *148*, 1069–1079. [PubMed]
12. Butler, G. The Evolution of *MAT*: The Ascomycetes. In *Sex in Fungi: Molecular Determination and Evolutionary Implications*; Heitman, J.K., Taylor, J.W., Casselton, L.A., Eds.; American Society of Microbiology Press: Washington, DC, USA, 2007; pp. 3–18.
13. Blakeslee, A.F. Sexual Reproduction in the Mucorineae. *Proc. Am. Acad. Arts Sci.* **1904**, *40*, 205–319. [CrossRef]
14. Lin, X.; Heitman, J. Mechanisms of Homothallism in Fungi and Transitions between Heterothallism and Homothallism. In *Sex in Fungi: Molecular Determination and Evolutionary Implications*; Heitman, J., Kronstad, J.W., Taylor, J.W., Casselton, L.A., Eds.; American Society of Microbiology Press: Washington, DC, USA, 2007; pp. 35–57.
15. Turgeon, B.G.; Yoder, O. Proposed Nomenclature for Mating Type Genes of Filamentous Ascomycetes. *Fungal Genet. Biol.* **2000**, *31*, 1–5. [CrossRef]
16. Wilken, P.M.; Steenkamp, E.T.; Wingfield, M.J.; De Beer, Z.W.; Wingfield, B.D. Which *MAT* gene? Pezizomycotina (Ascomycota) Mating-Type Gene Nomenclature Reconsidered. *Fungal Biol. Rev.* **2017**, *31*, 199–211. [CrossRef]
17. Colot, H.V.; Park, G.; Turner, G.E.; Ringelberg, C.; Crew, C.M.; Litvinkova, L.; Weiss, R.L.; Borkovich, K.A.; Dunlap, J.C. A High-Throughput Gene Knockout Procedure for *Neurospora* reveals Functions for Multiple Transcription Factors. *Proc. Natl. Acad. Sci. USA* **2006**, *103*, 10352–10357. [CrossRef]
18. Vienken, K.; Fischer, R. The Zn(II)2Cys6 Putative Transcription Factor *nosA* controls Fruiting Body Formation in *Aspergillus nidulans*. *Mol. Microbiol.* **2006**, *61*, 544–554. [CrossRef] [PubMed]
19. Vienken, K.; Scherer, M.; Fischer, R. The Zn(II)2Cys6 Putative *Aspergillus nidulans* Transcription Factor RosA (Repressor of Sexual Development) Inhibits Sexual Development Under Low-Carbon Conditions and in Submersed Culture. *Genetics* **2005**, *169*, 619–630. [CrossRef] [PubMed]
20. Sun, Q.; Choi, G.H.; Nuss, D.L. Hypovirus-Responsive Transcription Factor Gene *pro1* of the Chestnut Blight Fungus *Cryphonectria parasitica* is required for Female Fertility, Asexual Spore Development, and Stable Maintenance of Hypovirus Infection. *Eukaryot. Cell* **2009**, *8*, 262–270. [CrossRef] [PubMed]
21. Gautier, V.; Tong, L.; Nguyen, T.-S.; Debuchy, R.; Silar, P. *PaPro1* and *IDC4*, Two Genes controlling Stationary Phase, Sexual Development and Cell Degeneration in *Podospora anserina*. *J. Fungi* **2018**, *4*, 85. [CrossRef] [PubMed]
22. Benkhali, J.A.; Coppin, E.; Brun, S.; Peraza-Reyes, L.; Martin, T.; Dixelius, C.; Lazar, N.; Van Tilbeurgh, H.; Debuchy, R. A Network of HMG-Box Transcription Factors regulates Sexual Cycle in the Fungus *Podospora anserina*. *Plos Genet.* **2013**, *9*, e1003642. [CrossRef]
23. Koopman, P. HMG Domain Superfamily of DNA-bending Proteins: HMG, UBF, TCF, LEF, SOX, SRY and Related Proteins. *e LS* **2001**. [CrossRef]
24. Bazafkan, H.; Dattenböck, C.; Böhmdorfer, S.; Tisch, D.; Stappler, E.; Schmoll, M. Mating Type-Dependent Partner Sensing as Mediated by VEL1 in *Trichoderma reesei*. *Mol. Microbiol.* **2015**, *96*, 1103–1118. [CrossRef]
25. Seibel, C.; Tisch, D.; Kubicek, C.P.; Schmoll, M. ENVOY is a Major Determinant in Regulation of Sexual Development in *Hypocrea jecorina* (*Trichoderma reesei*). *Eukaryot. Cell* **2012**, *11*, 885–895. [CrossRef]
26. Castellanos, F.; Schmoll, M.; Martínez, P.; Tisch, D.; Kubicek, C.P.; Herrera-Estrella, A.; Esquivel-Naranjo, E.U. Crucial Factors of the Light Perception Machinery and their Impact on Growth and Cellulase Gene Transcription in *Trichoderma reesei*. *Fungal Genet. Biol.* **2010**, *47*, 468–476. [CrossRef]
27. Schmoll, M.; Esquivel-Naranjo, E.U.; Herrera-Estrella, A. *Trichoderma* in the Light of Day—Physiology and Development. *Fungal Genet. Biol.* **2010**, *47*, 909–916. [CrossRef] [PubMed]

28. Schmoll, M.; Franchi, L.; Kubicek, C.P. ENVOY, a PAS/LOV Domain Protein of *Hypocrea jecorina* (Anamorph *Trichoderma reesei*), modulates Cellulase Gene Transcription in Response to Light. *Eukaryot. Cell* **2005**, *4*, 1998–2007. [CrossRef]
29. Debuchy, R.; Coppin, E. The Mating Types of *Podospora anserina*: Functional Analysis and Sequence of the Fertilization Domains. *Mol. Gen. Genet.* **1992**, *233*, 113–121. [CrossRef] [PubMed]
30. Paoletti, M.; Seymour, F.A.; Alcocer, M.J.; Kaur, N.; Calvo, A.M.; Archer, D.B.; Dyer, P.S. Mating Type and the Genetic Basis of Self-Fertility in the Model Fungus *Aspergillus nidulans*. *Curr. Biol.* **2007**, *17*, 1384–1389. [CrossRef] [PubMed]
31. Staben, C.; Yanofsky, C. *Neurospora crassa* a Mating-Type Region. *Proc. Natl. Acad. Sci. USA* **1990**, *87*, 4917–4921. [CrossRef]
32. Lee, J.; Lee, T.; Lee, Y.W.; Yun, S.H.; Turgeon, B.G. Shifting Fungal Reproductive Mode by Manipulation of Mating Type Genes: Obligatory Heterothallism of *Gibberella zeae*. *Mol. Microbiol.* **2003**, *50*, 145–152. [CrossRef] [PubMed]
33. Böhm, J.; Hoff, B.; O'Gorman, C.M.; Wolfers, S.; Klix, V.; Binger, D.; Zadra, I.; Kürnsteiner, H.; Pöggeler, S.; Dyer, P.S. Sexual Reproduction and Mating-Type–Mediated Strain Development in the Penicillin-Producing Fungus *Penicillium chrysogenum*. *Proc. Natl. Acad. Sci. USA* **2013**, *110*, 1476–1481. [CrossRef] [PubMed]
34. Böhm, J.; Dahlmann, T.A.; Gümüşer, H.; Kück, U. A MAT1–2 Wild-Type Strain from *Penicillium chrysogenum*: Functional Mating-Type Locus Characterization, Genome Sequencing and Mating with an Industrial Penicillin-Producing Strain. *Mol. Microbiol.* **2015**, *95*, 859–874. [CrossRef] [PubMed]
35. Pöggeler, S.; Nowrousian, M.; Ringelberg, C.; Loros, J.; Dunlap, J.; Kück, U. Microarray and Real-Time PCR Analyses Reveal Mating Type-Dependent Gene Expression in a Homothallic Fungus. *Mol. Genet. Genom.* **2006**, *275*, 492–503. [CrossRef] [PubMed]
36. Kim, H.-K.; Cho, E.J.; Lee, S.; Lee, Y.-S.; Yun, S.-H. Functional Analyses of Individual Mating-Type Transcripts at *MAT* Loci in *Fusarium graminearum* and *Fusarium asiaticum*. *FEMS Microbiol. Lett.* **2012**, *337*, 89–96. [CrossRef]
37. Arnaise, S.; Debuchy, R.; Picard, M. What is a *Bona Fide* Mating-Type Gene? Internuclear Complementation of *mat* Mutants in *Podospora anserina*. *Mol. Gen. Genet.* **1997**, *256*, 169–178. [CrossRef]
38. Doughan, B.; Rollins, J.A. Characterization of *MAT* Gene Functions in the Life Cycle of *Sclerotinia sclerotiorum* Reveals a Lineage-Specific *MAT* Gene Functioning in Apothecium Morphogenesis. *Fungal Biol.* **2016**, *120*, 1105–1117. [CrossRef]
39. Rodenburg, S.Y.; Terhem, R.B.; Veloso, J.; Stassen, J.H.; van Kan, J.A. Functional Analysis of Mating Type Genes and Transcriptome Analysis during Fruiting Body Development of *Botrytis cinerea*. *mBio* **2018**, *9*, e01939-17. [CrossRef]
40. Arnaise, S.; Zickler, D.; Le Bilcot, S.; Poisier, C.; Debuchy, R. Mutations in Mating-Type Genes of the Heterothallic Fungus *Podospora anserina* lead to Self-Fertility. *Genetics* **2001**, *159*, 545–556. [PubMed]
41. Zickler, D.; Arnaise, S.; Coppin, E.; Debuchy, R.; Picard, M. Altered Mating-Type Identity in the Fungus *Podospora anserina* leads to Selfish Nuclei, Uniparental Progeny, and Haploid Meiosis. *Genetics* **1995**, *140*, 493–503. [PubMed]
42. Yu, Y.; Amich, J.; Will, C.; Eagle, C.E.; Dyer, P.S.; Krappmann, S. The Novel *Aspergillus fumigatus MAT1-2-4* Mating-Type Gene is Required for Mating and Cleistothecia Formation. *Fungal Genet. Biol.* **2017**, *108*, 1–12. [CrossRef]
43. Braus, G.H.; Irniger, S.; Bayram, Ö. Fungal Development and the COP9 Signalosome. *Curr. Opin. Microbiol.* **2010**, *13*, 672–676. [CrossRef] [PubMed]
44. Busch, S.; Schwier, E.U.; Nahlik, K.; Bayram, Ö.; Helmstaedt, K.; Draht, O.W.; Krappmann, S.; Valerius, O.; Lipscomb, W.N.; Braus, G.H. An Eight-Subunit COP9 Signalosome with an Intact JAMM Motif is required for Fungal Fruit Body Formation. *Proc. Natl. Acad. Sci. USA* **2007**, *104*, 8089–8094. [CrossRef]
45. Busch, S.; Eckert, S.E.; Krappmann, S.; Braus, G.H. The COP9 Signalosome is an Essential Regulator of Development in the Filamentous Fungus *Aspergillus nidulans*. *Mol. Microbiol.* **2003**, *49*, 717–730. [CrossRef]
46. Teichert, I.; Nowrousian, M.; Pöggeler, S.; Kück, U. The Filamentous Fungus *Sordaria macrospora* as a Genetic Model to Study Fruiting Body Development. *Adv. Genet.* **2014**, *87*, 199–244.
47. Hwang, J.; Pallas, D.C. STRIPAK Complexes: Structure, Biological Function, and Involvement in Human Diseases. *Int. J. Biochem. Cell Biol.* **2014**, *47*, 118–148. [CrossRef] [PubMed]

48. Ribeiro, P.S.; Josué, F.; Wepf, A.; Wehr, M.C.; Rinner, O.; Kelly, G.; Tapon, N.; Gstaiger, M. Combined Functional Genomic and Proteomic Approaches identify a PP2A Complex as a Negative Regulator of Hippo Signaling. *Mol. Cell* **2010**, *39*, 521–534. [CrossRef]
49. Bernhards, Y.; Pöggeler, S. The Phocein Homologue SmMOB3 is Essential for Vegetative Cell Fusion and Sexual Development in the Filamentous Ascomycete *Sordaria macrospora*. *Curr. Genet.* **2011**, *57*, 133–149. [CrossRef] [PubMed]
50. Bloemendal, S.; Bernhards, Y.; Bartho, K.; Dettmann, A.; Voigt, O.; Teichert, I.; Seiler, S.; Wolters, D.A.; Pöggeler, S.; Kück, U. A Homologue of the Human STRIPAK Complex controls Sexual Development in Fungi. *Mol. Microbiol.* **2012**, *84*, 310–323. [CrossRef] [PubMed]
51. Pöggeler, S.; Kück, U. A WD40 Repeat Protein regulates Fungal Cell Differentiation and can be replaced Functionally by the Mammalian Homologue Striatin. *Eukaryot. Cell* **2004**, *3*, 232–240. [CrossRef] [PubMed]
52. Han, K.H.; Lee, D.B.; Kim, J.H.; Kim, M.S.; Han, K.Y.; Kim, W.S.; Park, Y.S.; Kim, H.B.; Han, D.M. Environmental Factors Affecting Development of *Aspergillus nidulans*. *J. Microbiol.* **2003**, *41*, 34–40.
53. Malagnac, F.; Lalucque, H.; Lepère, G.; Silar, P. Two NADPH Oxidase Isoforms are required for Sexual Reproduction and Ascospore Germination in the Filamentous Fungus *Podospora anserina*. *Fungal Genet. Biol.* **2004**, *41*, 982–997. [CrossRef]
54. Johnston, M. Feasting, Fasting and Fermenting: Glucose Sensing in Yeast and Other Cells. *Trends Genet.* **1999**, *15*, 29–33. [CrossRef]
55. Kraakman, L.; Lemaire, K.; Ma, P.; Teunissen, A.W.; Donaton, M.C.; Van Dijck, P.; Winderickx, J.; De Winde, J.H.; Thevelein, J.M. A *Saccharomyces cerevisiae* G-Protein Coupled Receptor, *Gpr1*, is specifically Required for Glucose Activation of the cAMP Pathway during the Transition to Growth on Glucose. *Mol. Microbiol.* **1999**, *32*, 1002–1012. [CrossRef]
56. Welton, R.M.; Hoffman, C.S. Glucose Monitoring in Fission Yeast via the *gpa2* Gα, the *git5* Gβ and the *git3* Putative Glucose Receptor. *Genetics* **2000**, *156*, 513–521.
57. Brown, N.A.; dos Reis, T.F.; Ries, L.N.A.; Caldana, C.; Mah, J.H.; Yu, J.H.; Macdonald, J.M.; Goldman, G.H. G-Protein Coupled Receptor-Mediated Nutrient Sensing and Developmental Control in *Aspergillus nidulans*. *Mol. Microbiol.* **2015**, *98*, 420–439. [CrossRef] [PubMed]
58. Han, K.H.; Seo, J.A.; Yu, J.H. A Putative G-Protein Coupled Receptor Negatively Controls Sexual Development in *Aspergillus nidulans*. *Mol. Microbiol.* **2004**, *51*, 1333–1345. [CrossRef]
59. Hoffmann, B.; Wanke, C.; LaPaglia, S.K.; Braus, G.H. c-Jun and RACK1 Homologues Regulate a Control Point for Sexual Development in *Aspergillus nidulans*. *Mol. Microbiol.* **2000**, *37*, 28–41. [CrossRef] [PubMed]
60. Kong, Q.; Wang, L.; Liu, Z.; Kwon, N.J.; Kim, S.C.; Yu, J.H. Gβ-Like CpcB Plays a Crucial Role for Growth and Development of *Aspergillus nidulans* and *Aspergillus fumigatus*. *PLoS ONE* **2013**, *8*, e70355. [CrossRef] [PubMed]
61. Eckert, S.E.; Hoffmann, B.; Wanke, C.; Braus, G.H. Sexual Development of *Aspergillus nidulans* in Tryptophan Auxotrophic Strains. *Arch. Microbiol.* **1999**, *172*, 157–166. [CrossRef] [PubMed]
62. Käfer, E. The Anthranilate Synthetase Enzyme Complex and the Trifunctional *trpC* gene of *Aspergillus*. *Can. J. Genet. Cytol.* **1977**, *19*, 723–738. [CrossRef]
63. Serlupi-Crescenzi, O.; Kurtz, M.B.; Champe, S.P. Developmental Defects Resulting from Arginine Auxotrophy in *Aspergillus nidulans*. *Microbiology* **1983**, *129*, 3535–3544. [CrossRef]
64. Berridge, M.J.; Lipp, P.; Bootman, M.D. The Versatility and Universality of Calcium Signalling. *Nat. Rev. Mol. Cell Biol.* **2000**, *1*, 11. [CrossRef]
65. Sanders, D.; Pelloux, J.; Brownlee, C.; Harper, J.F. Calcium at the Crossroads of Signaling. *Plant Cell* **2002**, *14*, S401–S417. [CrossRef] [PubMed]
66. Fischer, M.; Schnell, N.; Chattaway, J.; Davies, P.; Dixon, G.; Sanders, D. The *Saccharomyces cerevisiae cch1* Gene is Involved in Calcium Influx and Mating. *FEBS Lett.* **1997**, *419*, 259–262. [CrossRef]
67. Iida, H.; Nakamura, H.; Ono, T.; Okumura, M.S.; Anraku, Y. *mid1*, A Novel *Saccharomyces cerevisiae* Gene Encoding a Plasma Membrane Protein, is Required for Ca2+ Influx and Mating. *Mol. Cell. Biol.* **1994**, *14*, 8259–8271. [CrossRef]
68. Muller, E.M.; Mackin, N.A.; Erdman, S.E.; Cunningham, K.W. FIG1p Facilitates Ca^{2+} Influx and Cell Fusion during Mating of *Saccharomyces cerevisiae*. *J. Biol. Chem.* **2003**, *40*, 38461–38469. [CrossRef]
69. Cavinder, B.; Trail, F. Role of *fig1*, a Component of the Low-Affinity Calcium Uptake System, in Growth and Sexual Development of Filamentous Fungi. *Eukaryot. Cell* **2012**, *11*, 978–988. [CrossRef] [PubMed]

70. Kim, H.S.; Kim, J.E.; Son, H.; Frailey, D.; Cirino, R.; Lee, Y.W.; Duncan, R.; Czymmek, K.J.; Kang, S. Roles of Three *Fusarium graminearum* Membrane Ca^{2+} Channels in the Formation of Ca^{2+} Signatures, Growth, Development, Pathogenicity and Mycotoxin Production. *Fungal Genet. Biol.* **2018**, *111*, 30–46. [CrossRef]
71. Zhang, S.; Zheng, H.; Long, N.; Carbó, N.; Chen, P.; Aguilar, P.S.; Lu, L. *FigA*, A Putative Homolog of Low-Affinity Calcium System Member *Fig1* in *Saccharomyces cerevisiae*, is Involved in Growth and Asexual and Sexual Development in *Aspergillus nidulans*. *Eukaryot. Cell* **2014**, *13*, 295–303. [CrossRef]
72. Rodriguez-Romero, J.; Hedtke, M.; Kastner, C.; Müller, S.; Fischer, R. Fungi, Hidden in Soil or Up in the Air: Light makes a Difference. *Annu. Rev. Microbiol.* **2010**, *64*, 585–610. [CrossRef]
73. He, Q.; Cheng, P.; Yang, Y.; Wang, L.; Gardner, K.H.; Liu, Y. White Collar-1, A DNA Binding Transcription Factor and a Light Sensor. *Science* **2002**, *297*, 840–843. [CrossRef]
74. Ballario, P.; Talora, C.; Galli, D.; Linden, H.; Macino, G. Roles in Dimerization and Blue Light Photoresponse of the PAS and LOV Domains of *Neurospora crassa* White Collar Proteins. *Mol. Microbiol.* **1998**, *29*, 719–729. [CrossRef]
75. Linden, H.; Macino, G. White Collar 2, A Partner in Blue-Light Signal Transduction, Controlling Expression of Light–Regulated Genes in *Neurospora crassa*. *Embo J.* **1997**, *16*, 98–109.
76. Ballario, P.; Vittorioso, P.; Magrelli, A.; Talora, C.; Cabibbo, A.; Macino, G. White Collar-1, A Central Regulator of Blue Light Responses in *Neurospora*, is a Zinc Finger Protein. *EMBO J.* **1996**, *15*, 1650–1657. [CrossRef] [PubMed]
77. Innocenti, F.D.; Pohl, U.; Russo, V. Photoinduction of Protoperithecia in *Neurospora crassa* by Blue Light. *Photochem. Photobiol.* **1983**, *37*, 49–51. [CrossRef]
78. Harding, R.W.; Melles, S. Genetic Analysis of Phototropism of *Neurospora crassa* Perithecial Beaks using White Collar and Albino Mutants. *Plant Physiol.* **1983**, *72*, 996–1000. [CrossRef]
79. Mooney, J.L.; Yager, L.N. Light is Required for Conidiation in *Aspergillus nidulans*. *Genes Dev.* **1990**, *4*, 1473–1482. [CrossRef]
80. Bayram, Ö.; Braus, G.H. Coordination of Secondary Metabolism and Development in Fungi: The Velvet Family of Regulatory Proteins. *FEMS Microbiol. Rev.* **2012**, *36*, 1–24. [CrossRef] [PubMed]
81. Bayram, Ö.; Krappmann, S.; Ni, M.; Bok, J.W.; Helmstaedt, K.; Valerius, O.; Braus-Stromeyer, S.; Kwon, N.J.; Keller, N.P.; Yu, J.H. VelB/VeA/LaeA Complex Coordinates Light Signal with Fungal Development and Secondary Metabolism. *Science* **2008**, *320*, 1504–1506. [CrossRef] [PubMed]
82. Kim, H.S.; Han, K.Y.; Kim, K.J.; Han, D.M.; Jahng, K.Y.; Chae, K.S. The *veA* Gene Activates Sexual Development in *Aspergillus nidulans*. *Fungal Genet. Biol.* **2002**, *37*, 72–80. [CrossRef]
83. Stinnett, S.M.; Espeso, E.A.; Cobeño, L.; Araújo-Bazán, L.; Calvo, A.M. *Aspergillus nidulans* VeA Subcellular Localization is Dependent on the Importin α Carrier and on Light. *Mol. Microbiol.* **2007**, *63*, 242–255. [CrossRef] [PubMed]
84. Ni, M.; Yu, J.H. A Novel Regulator Couples Sporogenesis and Trehalose Biogenesis in *Aspergillus nidulans*. *PLoS ONE* **2007**, *2*, e970. [CrossRef]
85. Blumenstein, A.; Vienken, K.; Tasler, R.; Purschwitz, J.; Veith, D.; Frankenberg-Dinkel, N.; Fischer, R. The *Aspergillus nidulans* Phytochrome FphA Represses Sexual Development in Red Light. *Curr. Biol.* **2005**, *15*, 1833–1838. [CrossRef]
86. Purschwitz, J.; Müller, S.; Fischer, R. Mapping the Interaction Sites of *Aspergillus nidulans* Phytochrome FphA with the Global Regulator VeA and the White Collar Protein LreB. *Mol. Genet. Genom.* **2009**, *281*, 35–42. [CrossRef]
87. Aguirre, J.; Ríos-Momberg, M.; Hewitt, D.; Hansberg, W. Reactive Oxygen Species and Development in Microbial Eukaryotes. *Trends Microbiol.* **2005**, *13*, 111–118. [CrossRef] [PubMed]
88. Takemoto, D.; Tanaka, A.; Scott, B. NADPH Oxidases in Fungi: Diverse Roles of Reactive Oxygen Species in Fungal Cellular Differentiation. *Fungal Genet. Biol.* **2007**, *44*, 1065–1076. [PubMed]
89. Scherer, M.; Wei, H.; Liese, R.; Fischer, R. *Aspergillus nidulans* Catalase-Peroxidase Gene (*cpeA*) is Transcriptionally Induced during Sexual Development through the Transcription Factor *StuA*. *Eukaryot. Cell* **2002**, *1*, 725–735.
90. Lara-Ortíz, T.; Riveros-Rosas, H.; Aguirre, J. Reactive Oxygen Species generated by Microbial NADPH Oxidase *NoxA* regulate Sexual Development in *Aspergillus nidulans*. *Mol. Microbiol.* **2003**, *50*, 1241–1255.

91. Cano-Domínguez, N.; Álvarez-Delfín, K.; Hansberg, W.; Aguirre, J. NADPH Oxidases NOX-1 and NOX-2 require the Regulatory Subunit NOR-1 to control Cell Differentiation and Growth in *Neurospora crassa*. *Eukaryot. Cell* **2008**, *7*, 1352–1361. [CrossRef]
92. Stowers, L.; Liberles, S.D. State-Dependent Responses to Sex Pheromones in Mouse. *Curr. Opin. Neurobiol.* **2016**, *38*, 74–79. [PubMed]
93. Raabe, M. Insect Reproduction: Regulation of Successive Steps. *Adv. Insect Physiol.* **1987**, *19*, 29–154.
94. Houck, L.D. Pheromone Communication in Amphibians and Reptiles. *Annu. Rev. Physiol.* **2009**, *71*, 161–176. [PubMed]
95. Karlson, P.; Luscher, M. 'Pheromones': A New Term for a Class of Biologically Active Substances. *Nature* **1959**, *183*, 55–56. [CrossRef]
96. Bölker, M.; Kahmann, R. Sexual Pheromones and Mating Responses in Fungi. *Plant Cell* **1993**, *5*, 1461. [CrossRef] [PubMed]
97. Jones, S.K.; Bennett, R.J. Fungal Mating Pheromones: Choreographing the Dating Game. *Fungal Genet. Biol.* **2011**, *48*, 668–676. [CrossRef]
98. Zhang, L.; Baasiri, R.A.; Van Alfen, N.K. Viral Repression of Fungal Pheromone Precursor Gene Expression. *Mol. Cell. Biol.* **1998**, *18*, 953–959. [CrossRef]
99. Shen, W.-C.; Bobrowicz, P.; Ebbole, D.J. Isolation of Pheromone Precursor Genes of *Magnaporthe grisea*. *Fungal Genet. Biol.* **1999**, *27*, 253–263. [CrossRef]
100. Bobrowicz, P.; Pawlak, R.; Correa, A.; Bell-Pedersen, D.; Ebbole, D.J. The *Neurospora crassa* Pheromone Precursor Genes are Regulated by the Mating Type Locus and the Circadian Clock. *Mol. Microbiol.* **2002**, *45*, 795–804. [CrossRef] [PubMed]
101. Coppin, E.; de Renty, C.; Debuchy, R. The Function of the Coding Sequences for the Putative Pheromone Precursors in *Podospora anserina* is Restricted to Fertilization. *Eukaryot. Cell* **2004**, *4*, 407–420. [CrossRef] [PubMed]
102. Martin, S.H.; Wingfield, B.D.; Wingfield, M.J.; Steenkamp, E.T. Causes and Consequences of Variability in Peptide Mating Pheromones of Ascomycete Fungi. *Mol. Biol. Evol.* **2011**, *28*, 1987–2003. [CrossRef] [PubMed]
103. Wilson, A.M.; van der Nest, M.A.; Wilken, P.M.; Wingfield, M.J.; Wingfield, B.D. Pheromone Expression reveals Putative Mechanism of Unisexuality in a Saprobic Ascomycete Fungus. *PLoS ONE* **2018**, *13*, e0192517. [CrossRef] [PubMed]
104. Lee, J.; Leslie, J.F.; Bowden, R.L. Expression and Function of Sex Pheromones and Receptors in the Homothallic Ascomycete *Gibberella zeae*. *Eukaryot. Cell* **2008**, *7*, 1211–1221. [CrossRef]
105. Pöggeler, S. Two Pheromone Precursor Genes are Transcriptionally Expressed in the Homothallic Ascomycete *Sordaria macrospora*. *Curr. Genet.* **2000**, *37*, 403–411. [CrossRef] [PubMed]
106. Kim, H.; Borkovich, K.A. Pheromones are Essential for Male Fertility and Sufficient to Direct Chemotropic Polarized Growth of Trichogynes during Mating in *Neurospora crassa*. *Eukaryot. Cell* **2006**, *5*, 544–554. [CrossRef]
107. Kim, H.; Metzenberg, R.L.; Nelson, M.A. Multiple Functions of *mfa-1*, a Putative Pheromone Precursor Gene of *Neurospora crassa*. *Eukaryot. Cell* **2002**, *1*, 987–999. [CrossRef] [PubMed]
108. Turina, M.; Prodi, A.; Van Alfen, N.K. Role of the *mf1-1* Pheromone Precursor Gene of the Filamentous Ascomycete *Cryphonectria parasitica*. *Fungal Genet. Biol.* **2003**, *40*, 242–251. [CrossRef]
109. Zhang, L.; Churchill, A.; Kazmierczak, P.; Kim, D.H.; Van Alfen, N. Hypovirulence-Associated Traits Induced by a Mycovirus of *Cryphonectria parasitica* are Mimicked by Targeted Inactivation of a Host Gene. *Mol. Cell. Biol.* **1993**, *13*, 7782–7792. [CrossRef] [PubMed]
110. Schmoll, M.; Seibel, C.; Tisch, D.; Dorrer, M.; Kubicek, C.P. A Novel Class of Peptide Pheromone Precursors in Ascomycetous Fungi. *Mol. Microbiol.* **2010**, *77*, 1483–1501. [CrossRef]
111. Xue, C.; Hsueh, Y.P.; Heitman, J. Magnificent Seven: Roles of G Protein-Coupled Receptors in Extracellular Sensing in Fungi. *FEMS Microbiol. Rev.* **2008**, *32*, 1010–1032. [CrossRef] [PubMed]
112. Kim, H.; Borkovich, K.A. A Pheromone Receptor Gene, *pre-1*, is Essential for Mating Type-Specific Directional Growth and Fusion of Trichogynes and Female Fertility in *Neurospora crassa*. *Mol. Microbiol.* **2004**, *52*, 1781–1798. [CrossRef]
113. Kim, H.; Wright, S.J.; Park, G.; Ouyang, S.; Krystofova, S.; Borkovich, K.A. Roles for Receptors, Pheromones, G Proteins and Mating Type Genes During Sexual Reproduction in *Neurospora crassa*. *Genetics* **2012**, *190*, 1389–1404. [CrossRef]

114. Pöggeler, S.; Kück, U. Comparative Analysis of the Mating-Type Loci from *Neurospora crassa* and *Sordaria macrospora*: Identification of Novel Transcribed ORFs. *Mol. Gen. Genet.* **2000**, *263*, 292–301. [CrossRef] [PubMed]
115. Pöggeler, S.; Kück, U. Identification of Transcriptionally Expressed Pheromone Receptor Genes in Filamentous Ascomycetes. *Gene* **2001**, *280*, 9–17. [CrossRef]
116. Seo, J.A.; Han, K.H.; Yu, J.H. The *gprA* and *gprB* Genes Encode Putative G Protein-Coupled Receptors Required for Self-Fertilization in *Aspergillus nidulans*. *Mol. Microbiol.* **2004**, *53*, 1611–1623. [CrossRef] [PubMed]
117. Seo, J.A.; Han, K.H.; Yu, J.H. Multiple Roles of a Heterotrimeric G-Protein γ-Subunit in Governing Growth and Development of *Aspergillus nidulans*. *Genetics* **2005**, *171*, 81–89. [CrossRef] [PubMed]
118. Dyer, P.S.; Paoletti, M.; Archer, D.B. Genomics Reveals Sexual Secrets of *Aspergillus*. *Microbiology* **2003**, *149*, 2301–2303. [CrossRef]
119. Coppin, E.; Debuchy, R.; Arnaise, S.; Picard, M. Mating Types and Sexual Development in Filamentous Ascomycetes. *Microbiol. Mol. Biol. Rev.* **1997**, *61*, 411–428. [PubMed]
120. Son, H.; Lee, J.; Lee, Y.-W. A Novel Gene, *gea1*, is Required for Ascus Cell-Wall Development in the Ascomycete Fungus *Fusarium graminearum*. *Microbiology* **2013**, *159*, 1077–1085. [CrossRef] [PubMed]
121. Lee, J.; Park, C.; Kim, J.C.; Kim, J.E.; Lee, Y.W. Identification and Functional Characterization of Genes Involved in the Sexual Reproduction of the Ascomycete Fungus *Gibberella zeae*. *Biochem. Biophys. Res. Commun.* **2010**, *401*, 48–52. [CrossRef]
122. Cao, S.; He, Y.; Hao, C.; Xu, Y.; Zhang, H.; Wang, C.; Liu, H.; Xu, J.-R. RNA Editing of the *amd1* Gene is Important for Ascus Maturation and Ascospore Discharge in *Fusarium graminearum*. *Sci. Rep.* **2017**, *7*, 4617. [CrossRef]
123. Feng, B.; Haas, H.; Marzluf, G.A. ASD4, A New GATA factor of *Neurospora crassa*, Displays Sequence-Specific DNA Binding and Functions in Ascus and Ascospore Development. *Biochemistry* **2000**, *39*, 11065–11073. [CrossRef]
124. Wang, Z.; Lopez-Giraldez, F.; Lehr, N.; Farré, M.; Common, R.; Trail, F.; Townsend, J.P. Global Gene Expression and Focused Knockout Analysis reveals Genes Associated with Fungal Fruiting Body Development in *Neurospora crassa*. *Eukaryot. Cell* **2014**, *13*, 154–169. [CrossRef]
125. Lee, D.W.; Pratt, R.J.; McLaughlin, M.; Aramayo, R. An Argonaute-Like Protein is Required for Meiotic Silencing. *Genetics* **2003**, *164*, 821–828. [PubMed]
126. Bayne, E.H.; White, S.A.; Kagansky, A.; Bijos, D.A.; Sanchez-Pulido, L.; Hoe, K.L.; Kim, D.U.; Park, H.O.; Ponting, C.P.; Rappsilber, J. STC1: A Critical Link between RNAi and Chromatin Modification required for Heterochromatin Integrity. *Cell* **2010**, *140*, 666–677. [CrossRef]
127. Berteaux-Lecellier, V.; Picard, M.; Thompson-Coffe, C.; Zickler, D.; Panvier-Adoutte, A.; Simonet, J.M. A Nonmammalian Homolog of the PAF1 Gene (*Zellweger syndrome*) Discovered as a Gene Involved in Caryogamy in the Fungus *Podospora anserina*. *Cell* **1995**, *81*, 1043–1051. [CrossRef]
128. Boisnard, S.; Zickler, D.; Picard, M.; Berteaux-Lecellier, V. Overexpression of a Human and a Fungal ABC Transporter similarly Suppresses the Differentiation Defects of a Fungal Peroxisomal Mutant but Introduces Pleiotropic Cellular Effects. *Mol. Microbiol.* **2003**, *49*, 1287–1296. [CrossRef] [PubMed]
129. Peraza Reyes, L.; Berteaux-Lecellier, V. Peroxisomes and Sexual Development in Fungi. *Front. Physiol.* **2013**, *4*, 244. [CrossRef] [PubMed]
130. Kirk, K.; Morris, N. The *tubB* α-Tubulin Gene is Essential for Sexual Development in *Aspergillus nidulans*. *Genes Dev.* **1991**, *5*, 2014–2023. [CrossRef]
131. Krappmann, S.; Jung, N.; Medic, B.; Busch, S.; Prade, R.A.; Braus, G.H. The *Aspergillus nidulans* F-Box Protein GrrA links SCF Activity to Meiosis. *Mol. Microbiol.* **2006**, *61*, 76–88. [CrossRef]
132. Shiu, P.K.; Raju, N.B.; Zickler, D.; Metzenberg, R.L. Meiotic Silencing by Unpaired DNA. *Cell* **2001**, *107*, 905–916. [CrossRef]
133. Shiu, P.K.; Zickler, D.; Raju, N.B.; Ruprich-Robert, G.; Metzenberg, R.L. SAD-2 is Required for Meiotic Silencing by Unpaired DNA and Perinuclear Localization of SAD-1 RNA-Directed RNA Polymerase. *Proc. Natl. Acad. Sci. USA* **2006**, *103*, 2243–2248. [CrossRef] [PubMed]
134. Nelson, M.A.; Merino, S.T.; Metzenberg, R.L. A Putative Rhamnogalacturonase Required for Sexual Development of *Neurospora crassa*. *Genetics* **1997**, *146*, 531–540.

135. Hu, S.; Zhou, X.; Gu, X.; Cao, S.; Wang, C.; Xu, J.R. The cAMP-PKA Pathway Regulates Growth, Sexual and Asexual Differentiation, and Pathogenesis in *Fusarium graminearum*. *Mol. Plant Microbe Interact.* **2014**, *27*, 557–566. [CrossRef] [PubMed]
136. Cavinder, B.; Hamam, A.; Lew, R.R.; Trail, F. *Mid1*, a Mechanosensitive Calcium Ion Channel, affects Growth, Development, and Ascospore discharge in the Filamentous Fungus *Gibberella zeae*. *Eukaryot. Cell* **2011**, *10*, 832–841. [CrossRef]
137. Hallen, H.E.; Trail, F. The L-Type Calcium Ion Channel *cch1* affects Ascospore Discharge and Mycelial Growth in the Filamentous Fungus *Gibberella zeae* (Anamorph *Fusarium graminearum*). *Eukaryot. Cell* **2008**, *7*, 415–424. [CrossRef] [PubMed]
138. Lew, R.R.; Abbas, Z.; Anderca, M.I.; Free, S.J. Phenotype of a Mechanosensitive Channel Mutant, *mid-1*, in a Filamentous Fungus, *Neurospora crassa*. *Eukaryot. Cell* **2008**, *7*, 647–655. [CrossRef]
139. Luo, Y.; Zhang, H.; Qi, L.; Zhang, S.; Zhou, X.; Zhang, Y.; Xu, J.R. FgKin1 Kinase Localizes to the Septal Pore and plays a Role in Hyphal Growth, Ascospore Germination, Pathogenesis, and Localization of Tub1 β-Tubulins in *Fusarium graminearum*. *New Phytol.* **2014**, *204*, 943–954. [CrossRef]
140. Tassan, J.P.; Le Goff, X. An Overview of the KIN1/PAR-1/MARK Kinase Family. *Biol. Cell* **2004**, *96*, 193–199. [CrossRef] [PubMed]
141. Krause, R.A.; Webster, R. The Morphology, Taxonomy, and Sexuality of the Rice Stem Rot Fungus, *Magnaporthe salvinii* (*Leptosphaeria salvinii*). *Mycologia* **1972**, *64*, 103–114. [CrossRef]
142. Spatafora, J.W.; Blackwell, M. The Polyphyletic Origins of Ophiostomatoid Fungi. *Mycol. Res.* **1994**, *98*, 1–9. [CrossRef]
143. Ingold, C. The Stalked Spore-Drop. *New Phytol.* **1961**, *60*, 181–183. [CrossRef]

RESEARCH CHAPTER 1

Published as:
Wilson AM, van der Nest MA, Wilken PM, Wingfield MJ & Wingfield BD. **2018**. Pheromone expression reveals putative mechanism of unisexuality in a saprobic ascomycete fungus.
PLOS One, 13(3): e0192517

PLOS ONE | UNIVERSITEIT VAN PRETORIA UNIVERSITY OF PRETORIA YUNIBESITHI YA PRETORIA

RESEARCH ARTICLE

Pheromone expression reveals putative mechanism of unisexuality in a saprobic ascomycete fungus

Andi M. Wilson*, Magriet A. van der Nest, P. Markus Wilken, Michael J. Wingfield, Brenda D. Wingfield

Department of Genetics, Forestry and Agricultural Biotechnology Institute, University of Pretoria, Pretoria, South Africa

* Andi.wilson@fabi.up.ac.za

OPEN ACCESS

Citation: Wilson AM, van der Nest MA, Wilken PM, Wingfield MJ, Wingfield BD (2018) Pheromone expression reveals putative mechanism of unisexuality in a saprobic ascomycete fungus. PLoS ONE 13(3): e0192517. https://doi.org/10.1371/journal.pone.0192517

Editor: Sung-Hwan Yun, Soonchunhyang University, REPUBLIC OF KOREA

Received: October 18, 2017

Accepted: January 24, 2018

Published: March 5, 2018

Data Availability Statement: Data are available on the NCBI SRA database under the following accession number: SRP108437. All cultures are available from the Culture Collection of Michael Wingfield (CMW) at the Forestry & Agricultural Biotechnology Institute (FABI) at the University of Pretoria (UP) and at the Westerdijk Fungal Biodiversity Institute, The Netherlands.

Funding: This project was financed by the University of Pretoria and the Department of Science and Technology (DST)/National Research

Abstract

Homothallism (self-fertility) describes a wide variety of sexual strategies that enable a fungus to reproduce in the absence of a mating partner. Unisexual reproduction, a form of homothallism, is a process whereby a fungus can progress through sexual reproduction in the absence of mating genes previously considered essential for self-fertility. In this study, we consider the molecular mechanisms that allow for this unique sexual behaviour in the saprotrophic ascomycete; *Huntiella moniliformis*. These molecular mechanisms are also compared to the underlying mechanisms that control sex in *Huntiella omanensis*, a closely related, but self-sterile, species. The main finding was that *H. omanensis* displayed mating-type dependent expression of the **a**- and **α**-pheromones. This was in contrast to *H. moniliformis* where both pheromones were co-expressed during vegetative growth and sexual development. Furthermore, *H. moniliformis* also expressed the receptors of both pheromones. Consequently, this fungus is likely able to recognize and respond to the endogenously produced pheromones, allowing for self-fertility in the absence of other key mating genes. Overall, these results are concomitant with those reported for other unisexual species, but represent the first detailed study considering the unisexual behaviour of a filamentous fungus.

Introduction

Sexual reproduction in fungi commonly requires an interaction between strains that carry different genetic information at the mating type locus [1]. This region, known as the *MAT1* locus in ascomycetes, harbours genes that represent either the *MAT1-1* or the *MAT1-2* idiomorph [2]. The *MAT1-1-1* gene defines the *MAT1-1* idiomorph, but can co-exist at this locus with other genes such as *MAT1-1-2* and *MAT1-1-3*. Similarly, the *MAT1-2* idiomorph is defined by the *MAT1-2-1* gene, though other genes can also be present [2]. These genes typically encode proteins with DNA binding domains and are known to regulate the global gene expression patterns associated with sexual reproduction [3].

Foundation (NRF) Centre of Excellence in Tree Health Biotechnology (CTHB). This work is based on the research supported in part by a number of grants from the National Research Foundation of South Africa (including Grant specific unique reference number, UID 83924). This research was also funded in part by Prof Brenda Wingfield's SARCHi grant. The grant holders acknowledge that opinions, findings, conclusions and/or recommendations expressed in any publication generated by the NRF supported research are that of the author(s), and that the NRF accepts no liability whatsoever in this regard. The funders had no role in study design, data collection and analysis, decision to publish, or preparation of the manuscript.

Competing interests: The authors have declared that no competing interests exist.

While isolates that possess either the *MAT1-1* or *MAT1-2* idiomorph are termed heterothallic and are self-sterile, other fungi are able to sexually reproduce even in the absence of a partner [4]. This sexual strategy, homothallism, enables self-fertility and is most commonly achieved by expressing both the *MAT1-1-1* and *MAT1-2-1* genes in a single cell, as seen in *Gibberella zeae* [5] and *Aspergillus nidulans* [6]. Other molecular mechanisms enabling self-fertility have also evolved, including unisexuality [7, 8]. Unisexual reproduction occurs in individuals that would typically be described as heterothallic but are able to progress through the sexual cycle in the absence of a mating partner. These individuals possess genes only associated with one of the two *MAT* idiomorphs and thus undergo sexual reproduction in the absence of genes that are usually considered essential for sex. To date, unisexuality has been described in only five species, including the human pathogens, *Cryptococcus neoformans* and *Candida albicans* [9±13].

Fungi typically depend on protein-based sexual pheromones to attract potential mating partners and as such, pheromones are usually expressed in a mating type-dependent manner [14, 15]. Despite their obvious role in the heterothallic system, pheromones are also expressed in many homothallic species, including *A. nidulans* [16], *Sordaria macrospora* [17] and *G. zeae* [18]. This has been illustrated where the *G. zeae* **α**-factor pheromone has been knocked out and actually enhances facultative outcrossing in female isolates. [18] Likewise, self-fertility is abolished in strains of *S. macrospora* where the pheromone receptors have been deleted [19]. This indicates that these molecules influence sexual reproduction in a multitude of mechanisms that include, but are not limited to, partner attraction.

Pheromone expression has been intimately linked to the unisexual abilities of both *Ca. albicans* and *Cr. neoformans* [9, 11]. Unisexual reproduction in *Ca. albicans* relies on the inactivation of the *Bar1* protease, an enzyme usually required for the proteolytic breakdown of the endogenously produced **α**-factor pheromone. Upon *Bar1* inactivation, the pheromone is not broken down and the cell thus recognizes it as a signal that a compatible mating partner is present. This leads to self-mating of **a** cells which is dependent on the activation of the **α**-factor receptor [9]. In contrast, **α** cells of *Cr. neoformans* do not produce endogenous **a**-factor pheromone, but rely on the presence of a few or distant **a** cells to produce the pheromone which in turn enhances the fusion of **α** cells and enables same sex mating [11].

The primary subject of this study, *Huntiella moniliformis*, is a haploid filamentous ascomycete that reproduces unisexually [13]. This is despite the fact that other species in the genus, including *H. omanensis*, are heterothallic and require a partner for mating [13]. Since very little is known regarding the genes involved in sexual reproduction in these species, having two closely related species that undergo such vastly different sexual strategies provides an opportunity to further explore this complicated process. Furthermore, no research has been conducted on the unisexual pathway in any filamentous fungus, despite a very in depth understanding of the pathway in *Ca. albicans* [9, 20±22] and *Cr. neoformans*, both of which are yeasts [11, 23±28].

The main objective of this study was to elucidate the underlying molecular pathway associated with unisexual reproduction in *H. moniliformis*. Using a comparative transcriptomics approach, we sought to identify differences in gene expression between the vegetative and sexual stages of growth in *H. omanensis* and *H. moniliformis*. Ultimately, this comparison revealed key gene expression differences between heterothallic and unisexual species that we believe contribute, at least partly, to the unique sexual behaviour seen in *H. moniliformis*.

Methods and materials

Cultures

Isolates of *H. moniliformis* and *H. omanensis* previously used in the study of Wilson *et al.* [13] were used. For *H. moniliformis*, two distinct forms of isolate CMW36919 (CBS 144008)

were used. One of these was sexually-competent, producing abundant ascomata and ascospores, while the other maintained a strictly vegetative growth form. For *H. omanensis*, three different isolates were used. Isolate CMW11056 (CBS 118113) is a mixed mating-type culture (MAT1xMAT2) representing the sexually reproducing isolate type. The vegetative isolates (CMW44450, CBS 143823 and CMW44442, CBS 143822), represent MAT1 and MAT2 isolates, respectively. The two vegetative cultures were isolated as single ascospore progeny from the mixed mating-type culture CMW11056 [13].

Cultures were grown and maintained on 2% malt extract agar plates (20 $g.L^{-1}$ malt extract (Biolab, Merck, South Africa) and 20 $g.L^{-1}$ agar (Biolab, Merck, South Africa) supplemented with thiamine hydrochloride (100 $mg.L^{-1}$, SIGMA, Steinheim, Germany) and streptomycin sulphate salt (150 $mg.L^{-1}$, SIGMA, Steinheim, Germany). These are forthwith referred to as MEA-ST plates. The cultures were maintained at room temperature for the duration of the study. All cultures used in this study are preserved in the culture collection (CMW) of the Forestry and Agricultural Biotechnology Institute (FABI), University of Pretoria, South Africa and at the Westerdijk Fungal Biodiversity Institute, The Netherlands.

RNA extraction and sequencing

Total RNA was extracted from 5±7 day-old cultures. This time period ensured that cultures did not reach the stationery phase, but gave enough time for sexual reproduction to take place. Nine MEA-ST plates were used per culture, allowing for three biological and three technical replicates. Mycelium was harvested from the vegetatively growing *H. moniliformis* isolate as well as the MAT1 and MAT2 *H. omanensis* isolates. A mixture of mycelium, ascomata and ascospores was harvested from the sexually reproducing *H. moniliformis* (unisexual) and *H. omanensis* (heterosexual) cultures.

The harvested tissue was flash frozen in liquid nitrogen and ground to a fine powder using a mortar and pestle. RNA extractions were performed using the RNeasy® Mini Kit (Qiagen, Limburg, The Netherlands) following the manufacturer's protocols with the following modifications: the RLC buffer was used as the extraction buffer and the optional on-column DNase 1 digestion was included. The integrity of the total RNA was assessed by 2% (w/v) agarose gel electrophoresis at 120V for 25 min and the concentration was estimated using an ND 1000 Spectrophotometer (ThermoScientific, Waltham, USA). The RNA was further subjected to quality testing using the Experion™ automated electrophoresis system (BioRad Laboratories, California, USA) at the ACGT Microarray Facility (University of Pretoria, South Africa). Dynabead®-based mRNA enrichment (ThermoFisher Scientific, Carlsbad, USA), cDNA synthesis and library preparation were performed at the Central Analytical Facilities (CAF) at the University of Stellenbosch (South Africa). The RNA sequencing was completed at the same facility using the Ion Proton Platform and PI™ Chip system.

RNA-seq analysis

CLC Genomics Workbench V7.5 (CLC bio, Aarhus, Denmark) was used to filter out raw reads with a Phred quality score of below 20 ($Q \leq 0.01$) and a read length of more than 300 bp. Up to two terminal ambiguous nucleotides were trimmed from the remaining reads. To remove any reads representing the rRNA fraction of the total RNA, the filtered and/or trimmed reads were mapped to a species-specific contig harbouring only the rRNA sequences using the RNA Seq (Legacy) tool in CLC Genomics Workbench. To ensure optimal mapping, a minimum length fraction of 0.5 and a minimum similarity fraction of 0.8 were used. Reads that had not mapped to the rRNA contigs were then used in further analyses.

Gene prediction and annotation was conducted on the draft genomes assemblies of *H. moniliformis* (accession JMSH01000000, [29]) and *H. omanensis* (accession JSUI00000000, [30]) using Web AUGUSTUS with the *Fusarium graminearum* gene models [31, 32]. These gene models were used because *F. graminearum* is the *Huntiella* species' closest relative for which gene models are available in the AUGUSTUS library. To detect differential expression of these predicted genes, the non-rRNA reads from each isolate type were mapped onto the species-appropriate gene annotations. Read mapping was conducted using the same length and similarity fractions as for the rRNA mapping. Intra-specific gene expression level comparisons were conducted using CLC Genomics Workbench following the method proposed by Mortazavi *et al.* [33].

For the accurate comparisons of gene expression across samples, a two-step normalization of the expression values was conducted. Firstly, RPKM values were used to represent relative expression. RPKM (Reads Per Kilobase of exon model per Million mapped reads) corrects for differences in expression levels between genes of different lengths and allows for accurate intra- and inter-sample comparisons [33]. Quantile normalization (CQN) was subsequently performed on the RPKM values in order to account for the expected technical variation specifically found in RNA-Seq data [34]. Baggerley's Z test [35] was used to test for expression differences across comparable samples, using the normalized RPKM values. To further minimize measurement errors, a corrected p-value was used to test for statistical significance. In this case, the p-value was corrected using the Benjamini-Hochberg false discovery rate (FDR) method to adjust for multiple test correction [36].

Genes displaying a 2-fold change in expression at an FDR-corrected p-value of 0.05 and lower were considered as significantly DE. When detecting expression level changes for the *MAT* genes in *H. omanensis*, a different approach was employed because the sexually reproducing culture is likely made up of approximately half MAT1 material and half MAT2 material. For example, if the expression of the *MAT1-1-1* gene has the same RPKM value in both the vegetative and sexually reproducing cultures, there would have been a 2-fold expression increase in the sexually reproducing isolates. This is because the MAT1 individual expressing the gene would represent only ~50% of the culture used for RNA extraction. The same was also true for the *MAT1-1-2* gene and for the *MAT1-2-1* and *MAT1-2-7* genes in MAT2 individuals. Consequently, we considered genes displaying equal RPKM values as being significantly DE.

Functional annotation

BLAST2GO [37] was used to assign Gene Ontology (GO) terms, InterPro identities and KEGG enzyme codes to all the genes predicted using Web AUGUSTUS. BLAST2GO also assesses GO term enrichment of one set of genes with respect to another and was used to determine whether any GO terms were enriched in the highly expressed and DE gene lists with respect to the complete list of genes from the genome. This enrichment was confirmed statistically using the Fishers Exact Test (FET) in the same program, with a p-value of 0.05 or less indicating significant enrichment. REViGO was then used to condense the enriched GO terms by removing redundant descriptions using the ᵃsmall, 0.5 allowed similarityᵒ setting. The REViGO output was then visualized using Tableau V10.1.

Genes known to be involved in sexual reproduction in other ascomycete fungi were investigated for their presence and possible DE in the two *Huntiella* species (Table 1). These included the *MAT* genes already known to be present at the *MAT* loci of the two species [13], as well as other sex-related genes from *Saccharomyces cerevisiae* [38, 39] and *Aspergillus* species [40]. The **a**- and **α**-factor pheromone genes identified based on homology to previously described

Table 1. Genes implicated in sexual reproduction in ascomycete fungi.

Gene	Function	Species	Genbank Accession Number / NCBI Gene ID	Found in *Huntiella moniliformis*	Regulation in sexually reproducing Isolate	Found in *Huntiella omanensis*	Regulation in sexually reproducing Isolate
Mating Type Genes							
MAT1-1-1	Primary mating type gene (alpha box)	*Huntiella omanensis*	KU950304	X	N/A	√	↑
MAT1-1-2	Secondary mating type gene		KU950305	X	N/A	√	-
MAT1-2-1	Primary mating type gene (HMG box)		KU950302	√	↑	√	↑
MAT1-2-7	Secondary mating type gene		KU950303	√ (Truncated)	-	√	-
Pheromone Signalling Pathway							
a-Factor Pheromone	Mating pheromone	*See text*	N/A	√	↓	√	-
α-Factor Pheromone	Mating pheromone			√	↑	√	↑
PreA (ste3)	a-Factor Pheromone Receptor	*Trichoderma gamsii*	29986161	√	-	√	-
PreB (ste2)	α-Factor Pheromone Receptor		29985002	√	-	√	↓
KEX1	Carboxypeptidase alpha-factor processor	*Saccharomyces cerevisiae*	852670	√	-	√	-
KEX2	Endoprotease alpha-factor processor		855483	√	-	√	-
mpkB	Mitogen-activated protein kinase	*Aspergillus clavatus*	4700387	√	↑	√	-
sfaD	G protein (Beta subunit)		4706342	√	-	√	-
STE12	Transcriptional activator, homeodomain protein	*Saccharomyces cerevisiae*	856484	√	-	√	-
STE13	Dipeptidyl aminopeptidase alpha-factor processor		854394	√	-	√	-
STE20	Serine/threonine protein kinase, MKKKK		856382	√	↑	√	-
STE24	Pheromone processor		853581	√	-	√	-
steC	Serine/threonine protein kinase, MKKK	*Aspergillus clavatus*	4706802	√	-	√	-
CDC24	Polarity establishment & maintenance and bud formation	*Saccharomyces cerevisiae*	851190	√	-	√	-

Symbols:

X: Gene was not identified in the genome assembly

√: Gene was identified in the genome assembly

↑: Gene was up-regulated in the sexually reproducing isolate

↓: Gene was down-regulated in the sexually reproducing isolate

-: Gene showed no differential expression

https://doi.org/10.1371/journal.pone.0192517.t001

Ascomycete pheromone proteins [41] were also included. In order to identify these genes in the genomes of the two *Huntiella* species, gene sequences were downloaded from the NCBI Gene Database (www.ncbi.nlm.nih.gov/gene) and used as queries in local BLASTn and tBLASTx searches against the draft genome assemblies using CLC Genomics Workbench.

Results

RNA-seq statistics

High quality RNA (RQI > 9) was extracted from each of the cultures used in this study (S1 Table). Sequencing of the individual samples produced an average of ~19 million reads per library for the *H. moniliformis* samples and an average of ~21 million reads per library for the *H. omanensis* samples (S2 Table). The raw RNA-seq reads used for this study are available on the NCBI SRA database under the following accession number: SRP108437. Quality filtering and trimming of the sequence reads retained 99.9% and 99.7% of the *H. moniliformis* and *H. omanensis* reads, respectively. Once reads mapping to the rRNA contigs of the two species had been discarded, an average of more than 14 million reads per library remained for use in the subsequent analyses (S2 Table).

Of the remaining non-rRNA reads, an average of 71% and 62% mapped to the respective *H. moniliformis* and *H. omanensis* genomes (S2 Table). Unmapped reads were most likely the result of sequencing errors, reads from repetitive or unassembled genome regions [42] and/or the presence of poly(A) sequences [43]. The percentage of reads mapped to the two *Huntiella* draft genomes was similar to reports from other eukaryotic RNA mapping projects: in *S. cerevisiae*, approximately 56% reads mapped to the assembled genome [44], 69% in *Heterobasidion* species [45], about 50% in human [46], and 60% in cattle [43].

Detection of gene expression

Of the predicted 6 864 genes in the 25 Mb *H. moniliformis* genome, 6 636 (97%) were expressed across both isolate types. In the 31 Mb genome of *H. omanensis*, 7 923 (94%) of the total 8 394 predicted genes were expressed across the three isolate types. A gene was considered expressed if three or more unique gene reads mapped to its annotation [47] and a normalized RPKM value of at least 0.1 was observed [48]. The majority of the expressed genes in both species were expressed by all isolates (Fig 1).

The sexually reproducing isolates of both species exhibited the highest number of uniquely expressed genes (Fig 1). Of the genes expressed in the vegetative *H. moniliformis* isolate, 156 were highly expressed (RPKM > 1 000, S3 Table) with 117 being unique to this isolate. The highly expressed genes were enriched for biological processes such as primary metabolism, macromolecule metabolism and biosynthesis (Fig 2, S4 Table). In the sexually reproducing isolate, 85 genes were highly expressed (S3 Table), with only 46 being unique to this isolate type. The highly expressed genes were enriched for processes such as cell wall organization, protein kinase C signalling, generation of energy and developmental processes (Fig 2, S4 Table). In the two vegetative isolates of *H. omanensis*, 107 genes were highly expressed, including 60 genes that were unique to the vegetative isolate type (S5 Table). These highly expressed genes were enriched for processes including glucose and carbohydrate metabolism, translational elongation and developmental processes (Fig 2, S6 Table). This is in contrast to the 74 highly expressed genes (S5 Table) in the sexually reproducing culture that included only 24 unique genes. These genes were enriched for carbohydrate catabolism, response to stress/stimulus and sexual reproduction (Fig 2, S6 Table).

Differentially expressed genes

Of the total gene complement of *H. moniliformis*, 41% of the genes were differentially expressed between vegetative and sexually reproducing isolates (Fig 3A, S7 Table). In contrast, only 24% of the total *H. omanensis* gene complement was differentially expressed in the same comparison (Fig 3B, S8 Table). In *H. moniliformis*, approximately half of the DE genes were

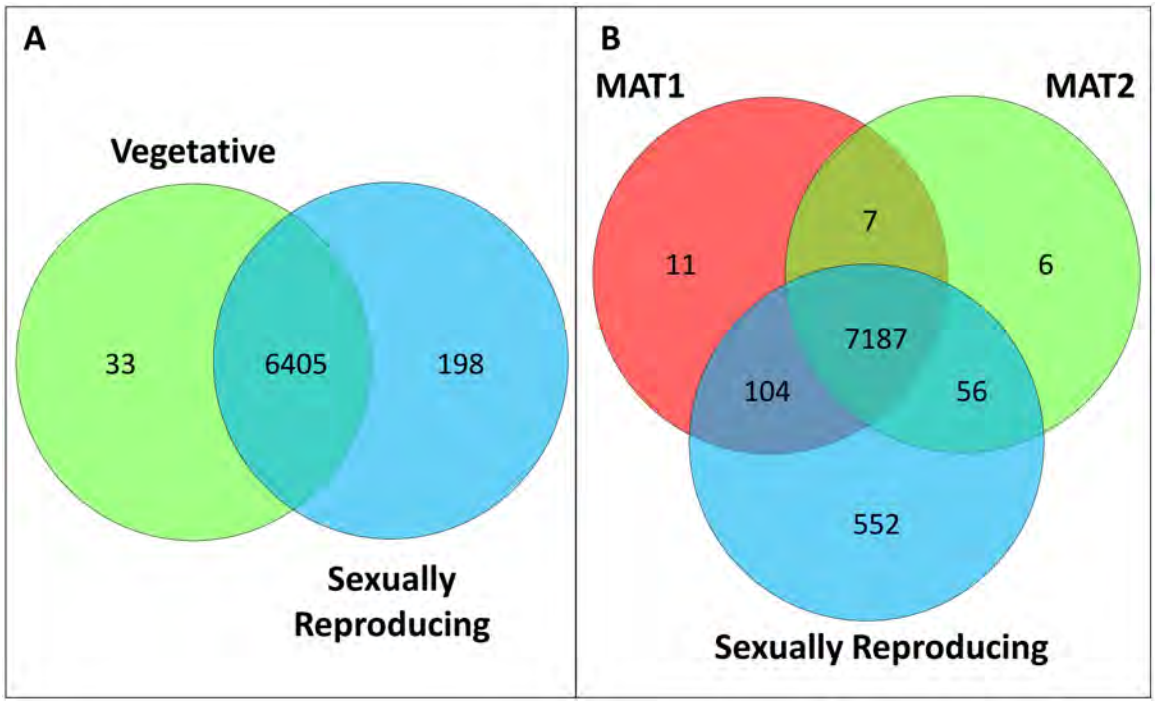

Fig 1. Genes expressed by vegetative and sexually reproducing isolate types of the two *Huntiella* species. A: The *H. moniliformis* draft genome has 6 864 predicted ORFs and expressed 97% of these during the course of this study. **B**: Similarly, the *H. omanensis* draft genome has 8 394 predicted ORFs, 94% of which were expressed.

https://doi.org/10.1371/journal.pone.0192517.g001

up-regulated in the vegetative isolate and were enriched for housekeeping functions such as transcription and translation as well as RNA processing and protein transport (S9 Table). The remaining genes were up-regulated in the sexually reproducing isolates and were enriched for cell communication, signalling and signal transduction as well as carbohydrate metabolism (S9 Table). In contrast, the majority of DE genes across the *H. omanensis* comparisons were up-regulated in the vegetative isolates. These genes included those involved in general housekeeping processes such as carbohydrate transport and metabolism, hyphal growth and cell wall biogenesis. The remaining genes were up-regulated in the sexually reproducing isolate and included those involved in the termination of G-protein coupled receptor signalling pathways, carbon utilization and microtubule organization.

Expression of the *MAT* genes

The *MAT* genes of the *Huntiella* species (Table 1) were identified in a previous study [13]. In *H. omanensis*, the primary *MAT* genes (*MAT1-1-1* and *MAT1-2-1*) were up-regulated in the sexually reproducing culture, while *MAT1-1-2* showed no evidence of differential expression. *MAT1-2-7* also showed a general pattern of up-regulation during sexual reproduction, but high intra-sample variation rendered this result insignificant. This gene was discovered using bioinformatics analyses in a previous study [13] and has no similarity to any other known proteins. Given that six other genes had already been described at the *MAT1-2* idiomorphs in a variety of other ascomycetes, this gene was named *MAT1-2-7*. This gene has recently been reported in *Knoxdaviesia* species [49]. Its association with the *MAT* locus in *H. omanensis* and the increase in its expression during sexual reproduction suggests that it has some unknown

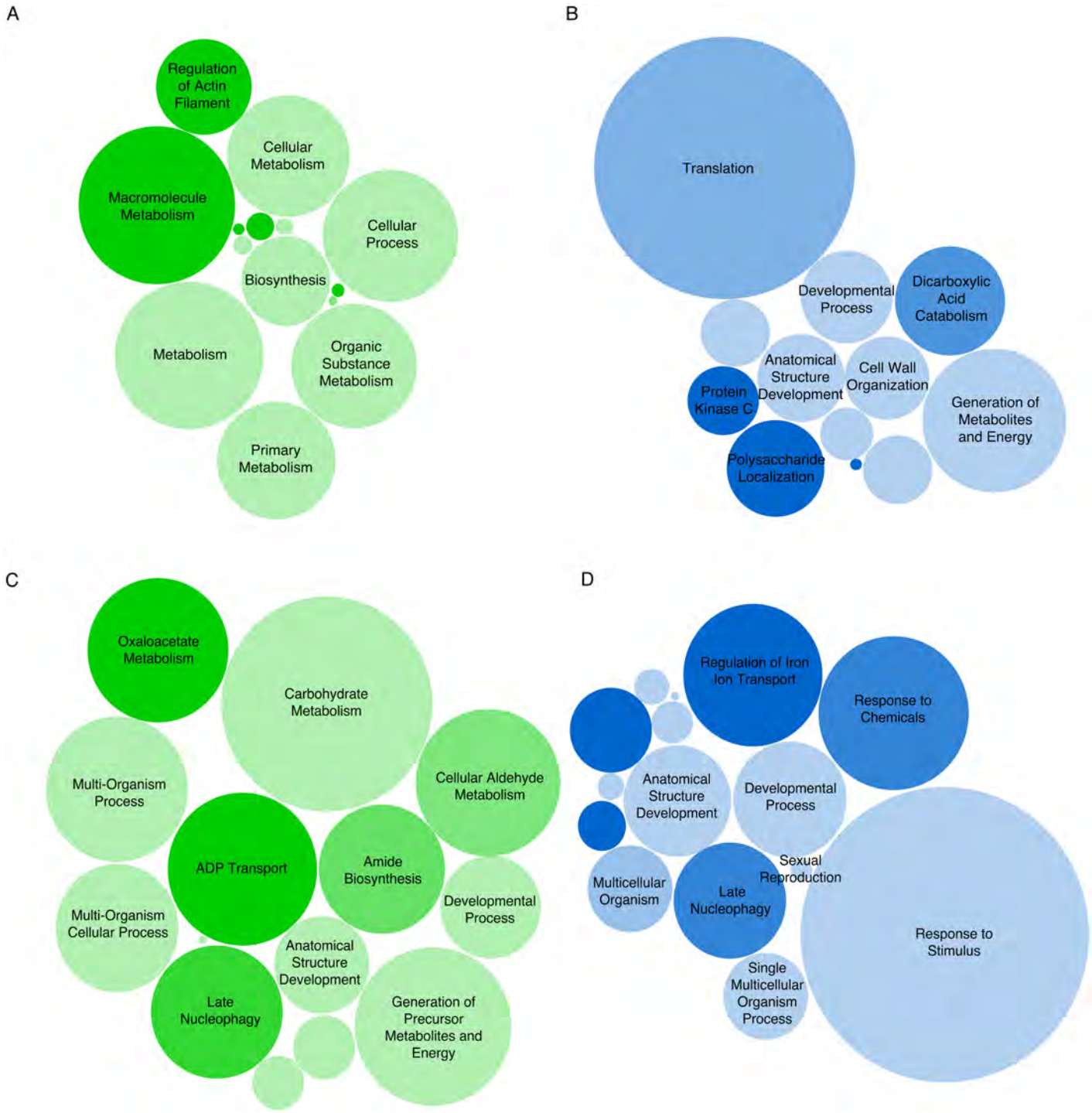

Fig 2. Biological process GO term enrichment in highly expressed gene sets. A: Vegetative and **B**: sexually reproducing cultures of *H. moniliformis*. **C**: Vegetative and **D**: sexually reproducing cultures of *H. omanensis*. The size of the circles is proportional to the relative number of GO terms associated with each process biological process. The shading intensity represents the significance of the enrichment: **A**: p-values range from 3.7×10^{-67} to 0.05, **B**: p-value range from 2.2×10^{-7} to 0.05, **C**: p-values range from 1.3×10^{-9} to 0.05 and **D**: p-values range from 1.7×10^{-6} to 0.05.

https://doi.org/10.1371/journal.pone.0192517.g002

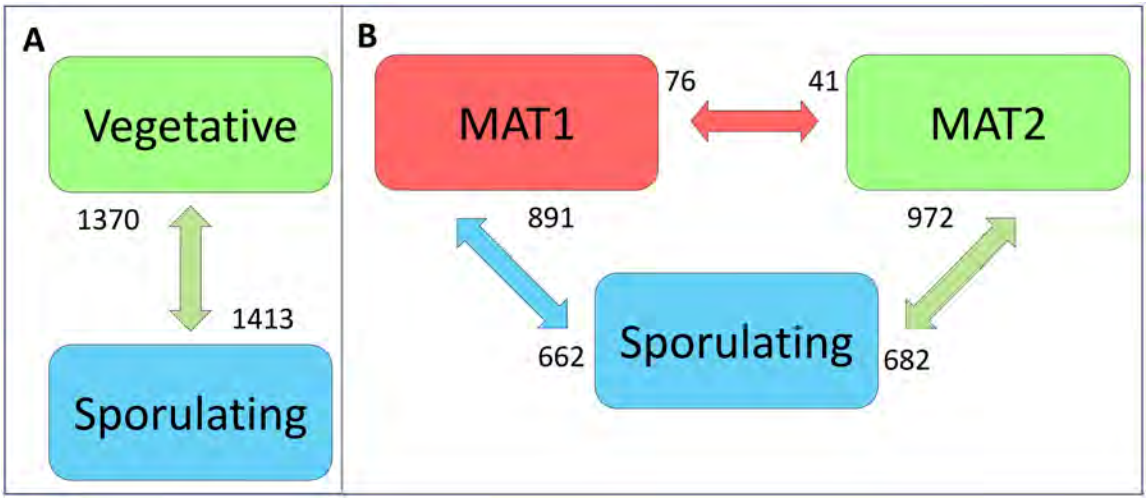

Fig 3. The number of genes differentially expressed in each isolate type comparison. A: In *H. moniliformis*, a similar number of genes were up-regulated in the vegetative and sexually reproducing isolates. **B**: In *H. omanensis*, many more genes were up-regulated in the MAT1 and MAT2 vegetative isolates than in the sexually reproducing isolate. The numbers above and below each isolate type box represent the number of genes that were up-regulated in that isolate in the particular comparison illustrated by the arrows.

https://doi.org/10.1371/journal.pone.0192517.g003

function during sexual reproduction. The *H. moniliformis MAT1-2-1* gene did not show a significant increase in expression during sexual reproduction. The truncated *H. moniliformis MAT1-2-7* gene was not expressed in either the vegetative or sexually reproducing cultures. This gene possesses a premature stop codon in *H. moniliformis* and it has been proposed that it would produce a non-functional gene product of only 48 aa in length [13].

Expression of the pheromone response pathway

Many of the genes involved in the pheromone cascade were identified in the genomes of the two *Huntiella* species (Table 1). These included the **a**- and **α**-factor pheromones, the two **α**-pheromone processing factors, both pheromone receptors as well as several genes that play a role in the G-protein-coupled signal transduction pathway. The pheromone genes in *H. omanensis* were expressed in a mating-type dependent manner, with MAT1 individuals expressing the **α**-factor pheromone and MAT2 individuals expressing the **a**-factor pheromone. This was in contrast to the expression patterns of the pheromones in *H. moniliformis* (Fig 4), where no mating-type dependent expression was observed. The MAT2 individual expressed both the **α**-factor and **a**-factor pheromones at appreciable levels. The remaining genes were all expressed in *H. omanensis* and *H. moniliformis* in all isolate types.

There was some evidence to suggest that the pheromone receptor genes in *H. omanensis* exhibited mating-type dependent expression. The expression data indicated that the **α**-factor pheromone receptor was expressed solely by the MAT2 individual. The **a**-factor pheromone receptor was expressed almost exclusively by the MAT1 isolate, but was still expressed by the MAT2 isolate, albeit at much lower levels. This expression pattern did not extend to *H. moniliformis*. Rather, both receptor genes were expressed at a low, constitutive level in both the vegetative and sexually reproducing cultures.

The only genes that were differentially expressed in this pathway in *H. omanensis* were the **α**-factor pheromone (up-regulated) and its receptor (down-regulated). Again, *H. moniliformis* exhibited a different pattern and while the **a**-factor pheromone showed a decrease in

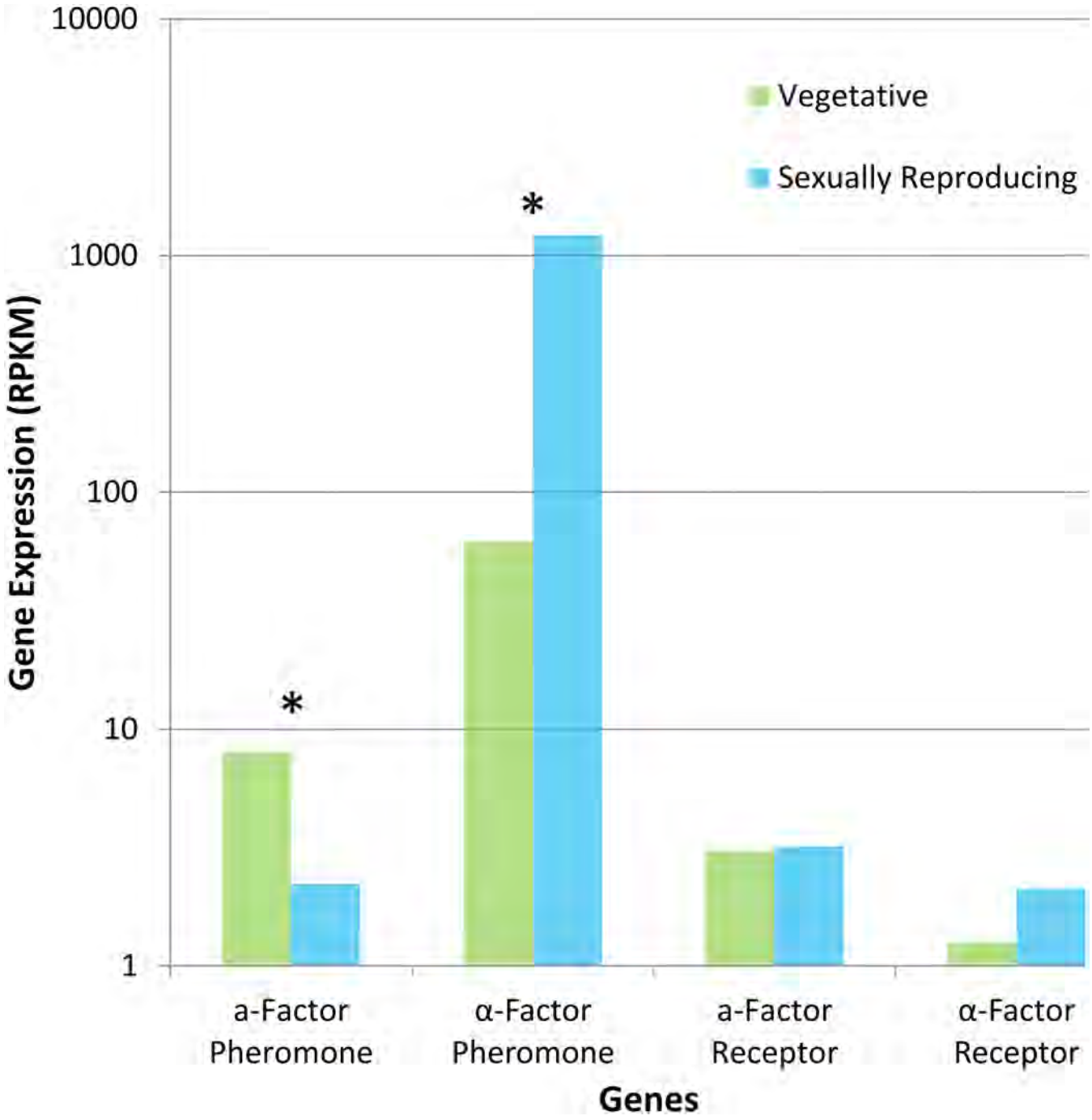

Fig 4. Differential expression of pheromone factor and receptor genes in *H. moniliformis*. Both pheromone factor genes showed differential expression, with the **a**-factor showing a significant decrease in expression in the sexually reproducing isolate while the **α**-factor showed a significant increase. The pheromone receptors showed no evidence of differential gene expression and seem to be expressed constitutively throughout the lifecycle. A logarithmic scale is used for the Y-axis. * indicates that there is a significant difference between two bars (2-fold change at FDR-corrected p-value < 0.05).

https://doi.org/10.1371/journal.pone.0192517.g004

expression in the sexually reproducing culture, the expression of the **α**-factor pheromone increased by almost 20-fold ($p<0.001$). Additionally, the *mpkB*, *ste20* and *ste23* genes (all involved in the signal transduction section of the response pheromone pathway) were also up-regulated in the sexually reproducing *H. moniliformis* culture.

Discussion

Unisexual reproduction enables the production of sexual spores in fungi that usually require an opposite mating partner. To date, unisexuality has been observed in only five species; four ascomycetes and one basidiomycete. Although three of these species are filamentous fungi, the underlying molecular mechanisms enabling this form of self-fertility have only been characterized in the two yeast species. We compared the gene expression changes associated with unisexual reproduction in the filamentous ascomycete *H. moniliformis* to similar changes associated with heterothallic mating in a closely related species. The results showed that there are significant differences in the pheromone production in these two species.

A comparative transcriptomics approach revealed that changes in the expression of the pheromone precursor genes in the heterothallic *H. omanensis* were very similar to the general expression profiles in self-sterile model fungi such as *N. crassa*. Although individual isolates of *N. crassa* possess genes for both the **α**- and **a**-factor pheromones, they are expressed in a mating-type specific manner [50]. Thus, mat A (= MAT1) individuals express only the **α**-factor pheromone, while mat a (= MAT2) individuals express only the **a**-factor pheromone. Sexual reproduction is then initiated only in the presence of a mating partner of the opposite mating-type, despite the fact that both partners express both pheromone receptor genes [51]. Our results showed that pheromone expression in *H. omanensis* also follows this pattern. Interestingly, there was also some evidence of mating-type dependent receptor expression, a profile not observed in *N. crassa* or other heterothallic species [51].

The expression pattern of the pheromones in *H. moniliformis* provides a putative molecular mechanism that enables the species to reproduce unisexually. These genes exhibit neither the same mating-type dependent expression nor the differential expression seen in *H. omanensis*. However, they do display expression profiles similar to other homothallic species such as *S. macrospora* [17] and thus, both pheromones are expressed by a single isolate. It is important to recognize that species exhibiting primary homothallism, such as *S. macrospora*, possess both *MAT1-1* and *MAT1-2* genes, and thus, despite these genes being under mating-type control, both pheromones can be expressed. In contrast, *H. moniliformis* is able to achieve this expression profile, while harbouring only the *MAT1-2-1* gene.

Pheromone expression is only part of the sexual activation pathway. This is because pheromones can only elicit their intended response if recognized by the appropriate pheromone receptor. In our study, both receptors were expressed at appreciable levels by both fungal species studied. This indicates that the pheromone response pathway is being utilized. In *H. omanensis*, the **α**-factor receptor showed down-regulation in the sexually reproducing isolate, while the *H. omanensis* **a**-factor receptor as well as both receptors in *H. moniliformis* showed no evidence of differential expression. This result indicates that differential expression of the receptors is not important to sexual reproduction in these species and that constitutive expression is sufficient. This could also indicate that differential expression of the pheromones themselves controls the activation of sexual reproduction, irrespective of whether it is a heterothallic or homothallic interaction.

The results of this study have also provided the first experimental validation for the expression of the *MAT1-2* idiomorph-associated gene, *MAT1-2-7*. This gene was previously detected using *de novo* gene prediction software [13] and is thought to produce a full-length protein of 155 aa in *H. omanensis*. Its position upstream of the archetypical *MAT1-2-1* gene in MAT2 isolates coupled with its absence in the MAT1 isolates highlighted the role that it might play in mating. In the present study, *MAT1-2-7* had no detectable expression level in vegetatively growing isolates, but was shown to be expressed in sexually reproducing cultures. This expression pattern, in addition to its idiomorphic position, strongly supports a role for the *MAT1-2-7*

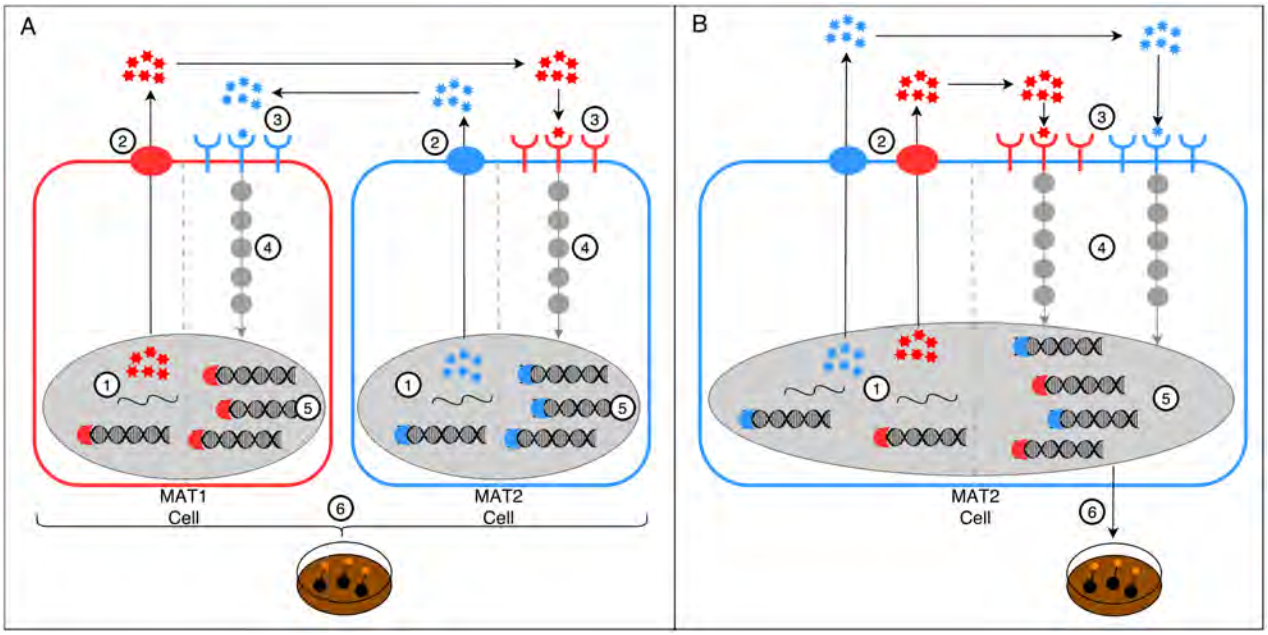

Fig 5. The proposed model for unisexual reproduction in *H. moniliformis* via the mating-type independent pheromone expression. **A**: The pheromone system in *H. omanensis*: MAT1 individuals express the **α**-factor pheromone and MAT2 individuals express the **a**-factor pheromone (1). These pheromones are secreted (2) and recognized by the pheromone receptors of a suitable mating partner (3). This recognition activates the pheromone transduction pathway, a MAP kinase cascade (4). Assuming other sex-favouring environmental conditions are met, this cascade alters gene expression patterns within the cells (5) and allows for the conversion of vegetative mycelia into sexually-competent tissue (6). **B**: The proposed pheromone system in *H. moniliformis*. The two species systems likely work in a very similar manner, except that *H. moniliformis* is able to express, secrete and recognize both the **α**- and **a**-factor pheromones (1, 2 & 3). Once the MAP kinase cascade has been activated (4), the genetic and physiological changes are likely very similar to those in *H. omanensis* (5 & 6).

https://doi.org/10.1371/journal.pone.0192517.g005

gene in sexual reproduction. Because it is truncated in *H. moniliformis*, we believe it is likely that this gene plays a role in the inhibition of self-fertility.

H. omanensis was included in this study because it represents a typical heterothallic species. It was consequently able to provide a basis for comparison of gene expression changes that occur during a sexual interaction in *Huntiella* species. This was especially important due to the unavailability of MAT1 *H. moniliformis* isolates. Thus, following the model proposed for *H. omanensis*, expression of the **a**-factor pheromone in *H. moniliformis* is either directly or indirectly influenced by genes present at the *MAT1-2* idiomorph. This same model would suggest that the **α**-factor pheromone should be controlled by genes at the *MAT1-1* idiomorph. However, *H. moniliformis* MAT2 individuals also express this gene. Taken collectively, these results suggest that MAT2 individuals of *H. moniliformis* have been able to overcome the mating-type dependent expression of the pheromones that would otherwise prevent homothallic behaviour in typically heterothallic species (Fig 5).

A modification of the typical heterothallic pheromone expression pattern represents the most likely molecular mechanism that underlies unisexual reproduction in *H. moniliformis*. Although, the genetic elements that govern this system remain unknown, they would likely have enabled a transition from typical heterothallism to unisexual reproduction via a change in the control of pheromone expression. Comparisons between the expression patterns of the pheromone genes as well as the genic content of the *MAT1-2* loci in the two *Huntiella* species provides a basis for some speculation regarding the origin of mating-type independent pheromone expression observed in *H. moniliformis*. In this case, it is plausible that the pheromone expression patterns of the unisexual species could be attributed to the truncation of *MAT1-2-7*

gene. This hypothesis rests on the assumption that a fully functional MAT1-2-7 protein acts as a repressor of the **α**-factor pheromone in MAT2 individuals, with its absence in MAT1 individuals allowing for expression of this pheromone. The genes of the *MAT* locus have been shown to be essential for pheromone expression in *N. crassa* [50], *S. macrospora* [52] and *C. neoformans* [25] and provides a precedent for the direct involvement of the MAT proteins in the pheromone system. In fact, a recent study has shown that the inactivation of the Mat2 gene in *C. neoformans* disables the pheromone pathway and preferentially enables unisexual behaviour over bisexual mating [24].

The hypothesis that the truncated *MAT1-2-7* gene is responsible for the unisexual behaviour of *H. moniliformis* is further supported by mutation studies performed on the heterothallic *P. anserina* [53]. Here, disruptions in a number of the *MAT* genes resulted in self-fertility. Importantly, it has been shown that the wild type mat+ genes (= *MAT1-2*) are not only required for the activation of mat+ functions, but also for the repression of *mat-* (= *MAT1-1*) fertilization functions. Thus, when there is a mutation in the mat+ gene, FPR1, the repression of fertilization is lifted and the mutant is rendered self-fertile. We suggest that this could be similar to what occurs in *H. omanensis*, where a full length *MAT1-2-7* gene represses the **α**-factor pheromone, rendering the MAT2 isolates self-sterile. However, in *H. moniliformis*, the *MAT1-2-7* gene is truncated, the repression of the **α**-factor pheromone does not occur and mating-type independent expression is possible. This in turn leads to self-activation, self-fertility and culminates in unisexual reproduction.

The results of this study suggest that the mating-type independent expression of the **a**- and **α**-factor pheromones is responsible for the unique ability of the MAT2 individuals of *H. moniliformis* to complete a sexual cycle in the absence of a MAT1 mating partner. As presented above, the role of pheromone expression in unisexuality has been previously investigated in both *Ca. albicans* and *Cr. neoformans* [9, 20, 23±26]. The results presented here are most similar to observations for *Ca. albicans*, and we hypothesize that endogenous production of both the **a**- and **α**-factor pheromones by a single MAT2 individual is sufficient to initiate the sexual cycle in *H. moniliformis*. We believe that this is the most probable explanation for the data presented here but acknowledge that other plausible hypotheses may also exist.

The unisexual pathway exhibited by *H. moniliformis* was originally assumed to be a sexual process. This was partly due to the similarity of the reproductive structures and spores found in *H. moniliformis* and the heterothallic *H. omanensis* [13]. The apparent importance of pheromone expression in the unisexual pathway of *H. moniliformis* further substantiates this assumption. However, it is worth noting that another spore-producing process, known as haploid fruiting, also enables spore production in single mating type isolates. Although similar to unisexuality in that way, this process is not necessarily linked to sexual reproduction or the formation of a diploid state [54±56]. It may even require different environmental conditions to those necessary for sexual reproduction [57]. Haploid fruiting can be induced in *Schizophyllum commune* when the mycelium is physically damaged [55] or when a fruiting-inducing chemical is present in the environment [54]. While this raises an alternative hypothesis for the process through which *H. moniliformis* produces progeny, the currently available data supports a sexual process.

This study utilized a transcriptomics approach that has some inherent limitations. The most important is that conclusions drawn from the data assume that gene expression is directly correlated with the production of a functional protein product. In addition, pheromones are often expressed as pre-pheromone proteins that require post-translational modification. Therefore, future studies will include the functional characterization of the two pheromone genes as well as the *MAT1-2-7* gene in order to enhance our understanding of the

role these genes play in unisexuality. Furthermore, studies utilizing synthetic pheromones will be conducted in an attempt to initiate unisexual behaviour in *H. omanensis*.

Supporting information

S1 Table. Quality and concentration of total RNA extractions from vegetative and sexually reproducing cultures of *H. omanensis* and *H. moniliformis*.
(XLSX)

S2 Table. RNA sequencing and genome mapping statistics.
(XLSX)

S3 Table. Genes highly expressed in vegetative and sexually reproducing cultures of *H. moniliformis*.
(XLSX)

S4 Table. FET enriched GO terms associated with the genes highly expressed in vegetative and sexually reproducing cultures of *H. moniliformis*.
(XLSX)

S5 Table. Genes highly expressed in vegetative and sexually reproducing cultures of *H. omanensis*.
(XLSX)

S6 Table. FET enriched GO terms associated with the genes highly expressed in vegetative and sexually reproducing cultures of *H. omanensis*.
(XLSX)

S7 Table. Genes differentially expressed in vegetative and sexually reproducing cultures of *H. moniliformis*.
(XLSX)

S8 Table. Genes differentially expressed in vegetative and sexually reproducing cultures of *H. omanensis*.
(XLSX)

S9 Table. FET enriched GO terms associated with the genes up-regulated in vegetative and sexually reproducing cultures of *H. moniliformis*.
(XLSX)

S10 Table. FET enriched GO terms associated with the genes grouped in cluster A and B of the DE genes of *H. omanensis*.
(XLSX)

Author Contributions

Conceptualization: Andi M. Wilson, Magriet A. van der Nest, P. Markus Wilken.

Data curation: Andi M. Wilson.

Formal analysis: Andi M. Wilson.

Funding acquisition: Michael J. Wingfield, Brenda D. Wingfield.

Investigation: Andi M. Wilson.

Methodology: Andi M. Wilson.

Project administration: Andi M. Wilson.

Resources: Brenda D. Wingfield.

Software: Brenda D. Wingfield.

Supervision: Magriet A. van der Nest, P. Markus Wilken, Michael J. Wingfield, Brenda D. Wingfield.

Validation: Andi M. Wilson.

Visualization: Andi M. Wilson.

Writing ± original draft: Andi M. Wilson.

Writing ± review & editing: Andi M. Wilson, Magriet A. van der Nest, P. Markus Wilken, Michael J. Wingfield, Brenda D. Wingfield.

References

1. Coppin E, Debuchy R, Arnaise S, Picard M. Mating Types and Sexual Development in Filamentous Ascomycetes. Microbiology and Molecular Biology Reviews. 1997; 61(4):411±28. PMID: 9409146
2. Turgeon BG, Yoder O. Proposed Nomenclature for Mating Type Genes of Filamentous Ascomycetes. Fungal Genetics and Biology. 2000; 31(1):1±5. https://doi.org/10.1006/fgbi.2000.1227 PMID: 11118130
3. Kronstad JW, Staben C. Mating Type in Filamentous Fungi. Annual Review of Genetics. 1997; 31:245± 76. https://doi.org/10.1146/annurev.genet.31.1.245 PMID: 9442896
4. Lin X, Heitman J. Mechanisms of Homothallism in Fungi and Transitions between Heterothallism and Homothallism. In: Heitman J, Kronstad JW, Taylor JW, Casselton LA, editors. Sex in Fungi: Molecular Determination and Evolutionary Implications. Washington, D.C.: ASM Press; 2007. p. 35±57.
5. Bowden RL, Leslie JF. Sexual Recombination in *Gibberella zeae*. Phytopathology. 1999; 89(2):182±8. https://doi.org/10.1094/PHYTO.1999.89.2.182 PMID: 18944794
6. Pontecorvo G, Roper J, Hemmons LM, MacDonald K, Bufton A. The Genetics of *Aspergillus nidulans*. Advances in Genetics. 1953; (5):141±238. PMID: 13040135
7. Roach K, Feretzaki M, Sun S, Heitman J. Unisexual Reproduction. Advances in Genetics. 2014; 85:255±305. https://doi.org/10.1016/B978-0-12-800271-1.00005-6 PMID: 24880737
8. Wilson AM, Wilken PM, van der Nest MA, Steenkamp ET, Wingfield MJ, Wingfield BD. Homothallism: An Umbrella Term for describing Diverse Sexual Behaviours. IMA Fungus. 2015; 6(1):207. https://doi.org/10.5598/imafungus.2015.06.01.13 PMID: 26203424
9. Alby K, Schaefer D, Bennett RJ. Homothallic and Heterothallic Mating in the Opportunistic Pathogen *Candida albicans*. Nature. 2009; 460(7257):890±3. https://doi.org/10.1038/nature08252 PMID: 19675652
10. Glass NL, Smith ML. Structure and Function of a Mating-Type Gene from the Homothallic Species *Neurospora africana*. Molecular and General Genetics 1994; 244(4):401±9. PMID: 8078466
11. Lin X, Hull CM, Heitman J. Sexual Reproduction between Partners of the Same Mating Type in *Cryptococcus neoformans*. Nature. 2005; 434(7036):1017±21. https://doi.org/10.1038/nature03448 PMID: 15846346
12. Schuerg T, Gabriel R, Baecker N, Baker SE, Singer SW. *Thermoascus aurantiacus* is an Intriguing Host for the Industrial Production of Cellulases. Current Biotechnology. 2017; 6(2):89±97.
13. Wilson A, Godlonton T, van der Nest M, Wilken P, Wingfield M, Wingfield B. Unisexual Reproduction in *Huntiella moniliformis*. Fungal Genetics and Biology. 2015; 80:1±9. https://doi.org/10.1016/j.fgb.2015.04.008 PMID: 25910452
14. Coppin E, de Renty C, Debuchy R. The Function of the Coding Sequences for the Putative Pheromone Precursors in *Podospora anserina* is Restricted to Fertilization. Eukaryotic Cell. 2005; 4(2):407±20. https://doi.org/10.1128/EC.4.2.407-420.2005 PMID: 15701803
15. Shen W-C, Bobrowicz P, Ebbole DJ. Isolation of Pheromone Precursor Genes of *Magnaporthe grisea*. Fungal Genetics and Biology. 1999; 27(2):253±63.
16. Paoletti M, Seymour FA, Alcocer MJ, Kaur N, Calvo AM, Archer DB, et al. Mating Type and the Genetic Basis of Self-Fertility in the Model Fungus *Aspergillus nidulans*. Current Biology. 2007; 17(16):1384±9. https://doi.org/10.1016/j.cub.2007.07.012 PMID: 17669651

17. Pöggeler S. Two Pheromone Precursor Genes are Transcriptionally Expressed in the Homothallic Ascomycete *Sordaria macrospora*. Current Genetics. 2000; 37(6):403±11. PMID: 10905431

18. Lee J, Leslie JF, Bowden RL. Expression and Function of Sex Pheromones and Receptors in the Homothallic Ascomycete *Gibberella zeae*. Eukaryotic Cell. 2008; 7(7):1211±21. https://doi.org/10.1128/EC.00272-07 PMID: 18503004

19. Klix V, Nowrousian M, Ringelberg C, Loros J, Dunlap J, Pöggeler S. Functional Characterization of *MAT1-1*-Specific Mating-Type Genes in the Homothallic Ascomycete *Sordaria macrospora* provides New Insights into Essential and Nonessential Sexual Regulators. Eukaryotic Cell. 2010; 9(6):894±905. https://doi.org/10.1128/EC.00019-10 PMID: 20435701

20. Alby K, Bennett RJ. Interspecies Pheromone Signaling Promotes Biofilm Formation and Same-Sex Mating in *Candida albicans*. Proceedings of the National Academy of Sciences. 2011; 108(6):2510±5.

21. Bennett RJ, Johnson AD. Completion of a Parasexual Cycle in *Candida albicans* by Induced Chromosome Loss in Tetraploid Strains. The EMBO Journal. 2003; 22(10):2505±15. https://doi.org/10.1093/emboj/cdg235 PMID: 12743044

22. Schaefer D, Côté P, Whiteway M, Bennett RJ. Barrier Activity in *Candida albicans* Mediates Pheromone Degradation and Promotes Mating. Eukaryotic Cell. 2007; 6(6):907±18. https://doi.org/10.1128/EC.00090-07 PMID: 17416895

23. Feretzaki M, Heitman J. Genetic Circuits that govern Bisexual and Unisexual Reproduction in *Cryptococcus neoformans*. PLoS Genetics. 2013; 9(8):e1003688. https://doi.org/10.1371/journal.pgen.1003688 PMID: 23966871

24. Gyawali R, Zhao Y, Lin J, Fan Y, Xu X, Upadhyay S, et al. Pheromone Independent Unisexual Development in *Cryptococcus neoformans*. PLoS Genetics. 2017; 13(5):e1006772. https://doi.org/10.1371/journal.pgen.1006772 PMID: 28467481

25. Lin X, Jackson JC, Feretzaki M, Xue C, Heitman J. Transcription Factors Mat2 and Znf2 Operate Cellular Circuits Orchestrating Opposite-and Same-Sex Mating in *Cryptococcus neoformans*. PLoS Genetics. 2010; 6(5):e1000953. https://doi.org/10.1371/journal.pgen.1000953 PMID: 20485569

26. Ni M, Feretzaki M, Li W, Floyd-Averette A, Mieczkowski P, Dietrich FS, et al. Unisexual and Heterosexual Meiotic Reproduction Generate Aneuploidy and Phenotypic Diversity *de novo* in the Yeast *Cryptococcus neoformans*. PLoS Biology. 2013; 11(9):e1001653. https://doi.org/10.1371/journal.pbio.1001653 PMID: 24058295

27. Wang P, Perfect JR, Heitman J. The G-protein β subunit GPB1 is required for Mating and Haploid Fruiting in *Cryptococcus neoformans*. Molecular and Cellular Biology. 2000; 20(1):352±62. PMID: 10594037

28. Wickes BL, Mayorga ME, Edman U, Edman JC. Dimorphism and Haploid Fruiting in *Cryptococcus neoformans*: Association with the α Mating Type. Proceedings of the National Academy of Sciences. 1996; 93(14):7327±31.

29. van der Nest MA, Bihon W, De Vos L, Naidoo K, Roodt D, Rubagotti E, et al. Draft Genome Sequences of *Diplodia sapinea*, *Ceratocystis manginecans*, and *Ceratocystis moniliformis*. IMA Fungus. 2014; 5 (1):135±40. https://doi.org/10.5598/imafungus.2014.05.01.13 PMID: 25083413

30. Van der Nest MA, Wilken PM, Naidoo K, Roodt D, Crouch JA, Demers JE, et al. *Draft Genome* Sequences of *Amanita jacksonii*, *Ceratocystis albifundus*, *Fusarium circinatum*, *Huntiella omanensis*, *Leptographium procerum*, *Rutstroemia sydowiana* and *Sclerotinia echinophila*. IMA Fungus. 2014; 5:473±85.

31. Stanke M, Steinkamp R, Waack S, Morgenstern B. AUGUSTUS: A Web Server for Gene Finding in Eukaryotes. Nucleic Acids Research. 2004; 32(2):W309±W12.

32. Stanke M, Waak S. Gene Prediction with a Hidden-Markov Model and a New Intron Submodel. Bioinformatics. 2003; 19:ii215±ii25. PMID: 14534192

33. Mortazavi A, Williams BA, McCue K, Schaeffer L, Wold B. Mapping and Quantifying Mammalian Transcriptomes by RNA-Seq. Nature methods. 2008; 5(7):621±8. https://doi.org/10.1038/nmeth.1226 PMID: 18516045

34. Hansen KD, Irizarry RA, Zhijin W. Removing Technical Variability in RNA-Seq Data using Conditional Quantile Normalization. Biostatistics. 2012; 13(2):204±16. https://doi.org/10.1093/biostatistics/kxr054 PMID: 22285995

35. Baggerly KA, Deng L, Morris JS, Aldaz CM. Differential Expression in SAGE: Accounting for Normal Between-Library Variation. Bioinformatics. 2003; 19(12):1477±83. PMID: 12912827

36. Benjamini Y, Hochberg Y. Controlling the False Discovery Rate: A Practical and Powerful Approach to Multiple Testing. Journal of the Royal Statistical Society. 1995; 57(1):289±300.

37. Conesa A, Götz S, García-Gómez JM, Terol J, Talón M, Robles M. Blast2GO: A Universal Tool for Annotation, Visualization and Analysis in Functional Genomics Research. Bioinformatics. 2005; 21 (18):3674±6. https://doi.org/10.1093/bioinformatics/bti610 PMID: 16081474

38. Mitchell AP. Control of Meiotic Gene Expression in *Saccharomyces cerevisiae*. Microbiological Reviews. 1994; 58(1):56±70. PMID: 8177171

39. Spellman PT, Sherlock G, Zhang MQ, Iyer VR, Anders K, Eisen MB, et al. Comprehensive Identification of Cell CycleÐRe gulated Genes of the Yeast *Saccharomyces cerevisiae* by Microarray Hybridization. Molecular Biology of the Cell. 1998; 9(12):3273±97. PMID: 9843569

40. Fedorova ND, Khaldi N, Joardar VS, Maiti R, Amedeo P, Anderson MJ, et al. Genomic Islands in the Pathogenic Filamentous Fungus *Aspergillus fumigatus*. PLoS Genetics. 2008; 4(4):e1000046. https://doi.org/10.1371/journal.pgen.1000046 PMID: 18404212

41. Martin SH, Wingfield BD, Wingfield MJ, Steenkamp ET. Causes and Consequences of Variability in Peptide Mating Pheromones of Ascomycete Fungi. Molecular Biology and Evolution. 2011; 28 (7):1987±2003. https://doi.org/10.1093/molbev/msr022 PMID: 21252281

42. Marioni JC, Mason CE, Mane SM, Stephens M, Gilad Y. RNA-Seq: An Assessment of Technical Reproducibility and Comparison with Gene Expression Arrays. Genome Research. 2008; 18(9):1509±17. https://doi.org/10.1101/gr.079558.108 PMID: 18550803

43. Huang W, Khatib H. Comparison of Transcriptomic Landscapes of Bovine Embryos using RNA-Seq. BMC Genomics. 2010; 11(1):711.

44. Nagalakshmi U, Wang Z, Waern K, Shou C, Raha D, Gerstein M, et al. The Transcriptional Landscape of the Yeast Genome defined by RNA Sequencing. Science. 2008; 320(5881):1344±9. https://doi.org/10.1126/science.1158441 PMID: 18451266

45. Van der Nest MA, Olson Å, Karlsson M, Lind M, Dalman K, Brandström-Durling M, et al. Gene Expression Associated with Intersterility in *Heterobasidion*. Fungal Genetics and Biology. 2014; 73:104±19. https://doi.org/10.1016/j.fgb.2014.10.008 PMID: 25459536

46. Sultan M, Schulz MH, Richard H, Magen A, Klingenhoff A, Scherf M, et al. A Global View of Gene Activity and Alternative Splicing by Deep Sequencing of the Human Transcriptome. Science. 2008; 321 (5891):956±60. https://doi.org/10.1126/science.1160342 PMID: 18599741

47. Wickramasinghe S, Rincon G, Islas-Trejo A, Medrano JF. Transcriptional Profiling of Bovine Milk using RNA Sequencing. BMC Genomics. 2012; 13(1):45.

48. Ramsköld D, Luo S, Wang Y-C, Li R, Deng Q, Faridani OR, et al. Full-Length mRNA-Seq from Single-Cell Levels of RNA and Individual Circulating Tumor Cells. Nature Biotechnology. 2012; 30(8):777±82. https://doi.org/10.1038/nbt.2282 PMID: 22820318

49. Aylward J, Steenkamp ET, Dreyer LL, Roets F, Wingfield MJ, Wingfield BD. Genetic Basis for High Population Diversity in Protea-Associated *Knoxdaviesia*. Fungal Genetics and Biology. 2016; 96:47±57. https://doi.org/10.1016/j.fgb.2016.10.002 PMID: 27720822

50. Bobrowicz P, Pawlak R, Correa A, Bell-Pedersen D, Ebbole DJ. The *Neurospora crassa* Pheromone Precursor Genes are Regulated by the Mating Type Locus and the Circadian Clock. Molecular Microbiology. 2002; 45(3):795±804. PMID: 12139624

51. Poggeler S, Kück U. Identification of Transcriptionally Expressed Pheromone Receptor Genes in Filamentous Ascomycetes. Gene. 2001; 280(1):9±17.

52. Poggeler S, Nowrousian M, Ringelberg C, Loros J, Dunlap J, Kück U. Microarray and Real-Time PCR Analyses Reveal Mating Type-Dependent Gene Expression in a Homothallic Fungus. Molecular Genetics and Genomics. 2006; 275(5):492±503. https://doi.org/10.1007/s00438-006-0107-y PMID: 16482473

53. Arnaise S, Zickler D, Le Bilcot S, Poisier C, Debuchy R. Mutations in Mating-Type Genes of the Heterothallic Fungus *Podospora anserina* lead to Self-Fertility. Genetics. 2001; 159(2):545±56. PMID: 11606532

54. Leonard TJ, Dick S. Chemical Induction of Haploid Fruiting Bodies in *Schizophyllum commune*. Proceedings of the National Academy of Sciences. 1968; 59(3):745±51.

55. Leonard TJ, Dick S. Induction of Haploid Fruiting by Mechanical Injury in *Schizophyllum commune*. Mycologia. 1973; 65(4):809±22.

56. Leslie JF, Leonard TJ. Three Independent Genetic Systems that Control Initiation of a Fungal Fruiting Body. Molecular and General Genetics. 1979; 171(3):257±60.

57. Raper JR, Krongelb GS. Genetic and Environmental Aspects of Fruiting in *Schizophyllum commune* Fr. Mycologia. 1958; 50(5):707±40.

RESEARCH CHAPTER 2

Convergent evolution: Shared genetic mutations in distantly-related unisexual filamentous ascomycetes

Andi M. Wilson[1*], Raphael Gabriel[2], Steven Singer[2], Timo Schuerg[2], P. Markus Wilken[1], Magriet A. van der Nest[1,3], Michael J. Wingfield[1] & Brenda D. Wingfield[1]

[1] Department of Biochemistry, Genetics and Microbiology, Forestry and Agricultural Biotechnology Institute (FABI), Faculty of Natural and Agricultural Sciences, University of Pretoria, Hatfield Campus Pretoria, 0083, South Africa

[2] Biological Systems and Engineering Division, Lawrence Berkeley National Laboratory, Berkeley, CA, 94720, USA

[3] Biotechnology Platform, Agricultural Research Council (ARC), Onderstepoort Campus, Pretoria, 0110, South Africa

ABSTRACT

Sexual reproduction in fungi typically requires the expression of two genes, *MAT1-1-1* and *MAT1-2-1*. Fungi can express both genes in a single isolate and engage in homothallism- the ability to sexually reproduce in isolation. Alternatively, a single isolate could harbour only one of these two genes and will thus require a complementary mating partner carrying the other gene in order to engage in sexual reproduction via heterothallic mating. To date, species from only five genera have been shown to undergo unisexual reproduction, which entails sexual recombination in the absence of one of these typically essential genes. This critical review compares genetic, genomic and transcriptomic data from three filamentous ascomycete fungi that have been described as unisexual and identifies shared genetic changes that may be associated with their ability to sexually reproduce in this unique manner. We show that these shared changes include significant mutations to their secondary *MAT* genes, as well as interesting differences in their pheromone response pathways compared to their heterothallic relatives. This shared mechanism is particularly notable given that the three species are accommodated in different genera, thus illustrating that a similar transition to unisexuality has occurred independently in their lineages.

1. INTRODUCTION

Sexual reproduction in fungi usually occurs either between two isolates of opposite mating type that each harbour a different set of mating type (*MAT*) genes (heterothallism) or within a single isolate that harbours all the necessary *MAT* genes (homothallism) (1,2). In ascomycetous fungi, these *MAT* genes are classified as either of the *MAT1-1* or *MAT1-2* type, which confer the MAT1-1 and MAT1-2 mating identities, respectively. These genes encode transcription factors that control a variety of sex-related genes, including those involved in meiosis and the pheromone response pathway (3). The MAT1-1-1 protein, for example, controls the expression of the α-factor mating pheromone, while the MAT1-2-1 protein controls the expression of the **a**-factor mating pheromone. Isolates of opposite mating type are thus able to recognize and respond to suitable mating partners (4–7). Homothallic species that harbour both *MAT* genes are usually able to express both pheromones (8,9), suggesting a role for the pheromones in other processes in addition to mate recognition (10,11).

In addition to the typical forms of heterothallism and homothallism as described above, there exists a unique form of homothallism known as unisexual reproduction. This strategy enables independent sexual reproduction in an isolate harbouring what would typically be considered a heterothallic genotype (12). Therefore, the defining characteristic of unisexuality is that these isolates, despite expressing only a single mating type, are capable of sexual recombination when cultured in isolation (13–16). The discovery of unisexuality overturned the paradigmatic view that sexual reproduction in fungi is dependent on the expression of the two primary *MAT* genes, *MAT1-1-1* and *MAT1-2-1* (12).

The two best defined unisexual cycles are those of the basidiomycetous yeast, *Cryptococcus neoformans* and the ascomycetous yeast, *Candida albicans*. *Cr. neoformans* has a well-defined heterothallic cycle where isolates of the α and **a** mating types interact to produce sexual structures (17). However, cultures representing a single mating type are able to engage in unisexual behaviour when certain environmental conditions are met (15,18). Although this process was originally thought to be asexual and therefore mitotic in nature (19), it has been shown to involve strictly sexual processes such as meiosis and genome diploidization (20,21). This was later confirmed with the observation that non-isogenic α-strains of *Cr. neoformans*

could utilize meiosis, a hallmark of sexual reproduction, as a means to facilitate genetic recombination (15). This further supported unisexual reproduction as a truly sexual process.

In order for isolates of *Cr. neoformans* to sexually reproduce, a single cell must convert from haploid to diploid phase (22). During unisexual reproduction, this can occur via one of two mechanisms: endoreplication (15), when a single cell simply duplicates its own genome; or cell fusion, when two cells of either mating type fuse and undergo karyogamy (22) (Figure 1). The frequency at which either of these mechanisms occurs can be enhanced by the presence of pheromones in the environment. A small number of **a** cells expressing **a**-factor pheromone, for example, can initiate unisexual reproduction between two cells of the α mating type (15,21,23). Similarly, matings between two **a** cells are induced in the presence of α-cells.

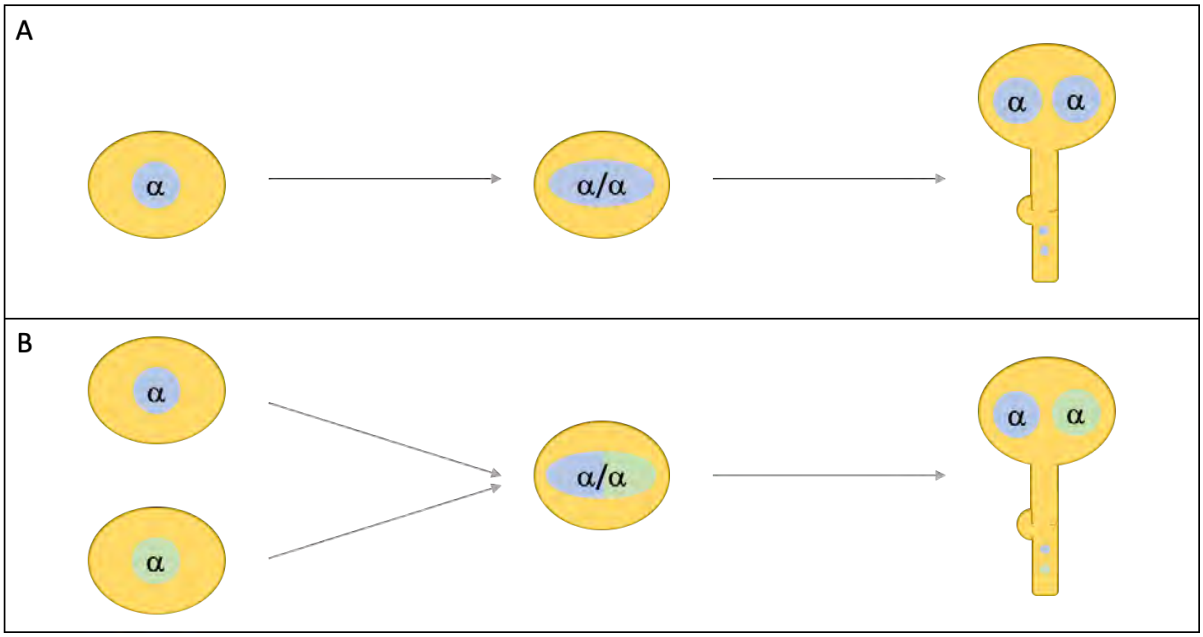

Figure 1: The two mechanisms of unisexuality in *Cryptococcus neoformans*. A) A genome of a single cell of either mating type can undergo endoreplication and thereby form a diploid cell which can consequently undergo sexual reproduction via the unisexual pathway. B) Two non-isogenic cells of the same mating type can fuse, thereby forming a diploid cell which can then unisexually reproduce. Both of these mechanisms are enhanced in the presence of pheromone peptides expressed by a cell of the opposite mating type.

Pheromone expression is also an important factor in the unisexual cycle of *Ca. albicans*. During heterothallic mating, **a** cells express both the **a**-factor as well as the α-factor pheromone (24,25). These cells also express a Bar1 protease which degrades the α-factor, ensuring that **a** cells secrete only the **a**-factor pheromone and maintain their cell identity (26). However, some *Ca. albicans* **a** cells have mutations in the *Bar1* gene that renders the protein non-functional (14). In these isolates, the α-factor can thus be expressed and secreted and is then recognized by the same cell in which it was expressed. This initiates the mating pathway via the autocrine pathway and results in unisexual reproduction (Figure 2A). A second manner by which unisexual reproduction can be achieved in *Ca. albicans* relies on the presence of α cells in a population dominated by **a** cells and is termed the paracrine pathway (14,27). The secretion of the α-factor by α cells initiates the sexual pathway in the **a** cells, rendering these cells sexually competent. Due to the high number of **a** cells in the population, the sexually competent cells are then likely to fuse with other **a** cells and complete the sexual cycle (Figure 2B), similar to the unisexual cycle of *Cr. neoformans*.

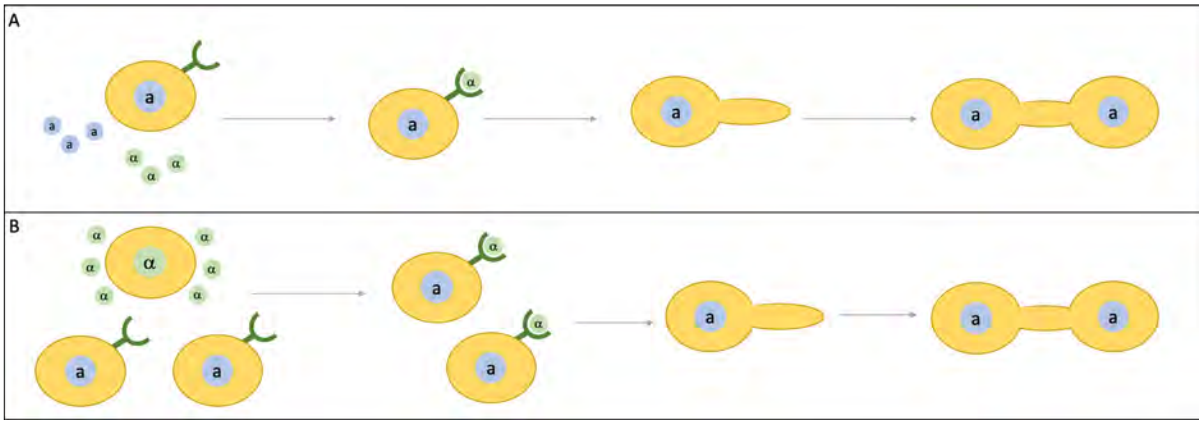

Figure 2: The two mechanisms of unisexuality in *Candida albicans*. A) Autocrine mode: a single cell of the **a**-mating type expresses both pheromones in the absence of a functional Bar1 protease. This cell can then respond to its endogenously produced α-factor and produce sexual structures. B) Paracrine mode: an α-cell expresses the α-factor which binds to the receptors of **a**-cells in the environment and stimulates sexual reproduction between two cells of the **a**-mating type.

Unisexuality has been described in only three genera of filamentous ascomycetes. The first of these was *Neurospora*, where MAT1-1 isolates of *N. africana*, *N. galapagosensis, N. dodgei* and *N. lineolata* have all been shown to reproduce unisexually (28,29). MAT1-2 isolates of two *Huntiella* species, *H. moniliformis* and *H. fecunda* were subsequently described as unisexual (13,30). Most recently, *Thermoascus aurantiacus* was shown to undergo a unisexual cycle despite possessing only the *MAT1-1* genes (16). In contrast to the unisexual yeasts, *Cr. neoformans* and *Ca. albicans*, the unisexual cycles of these filamentous fungi have not been investigated in great detail and the genetic mechanisms underlying this capability remain to be discovered.

This critical review considers the common genetic mechanisms that may enable unisexuality in this group of distantly related filamentous ascomycetes. For this purpose, we investigated previously published genetic, genomic and transcriptomic data regarding the *MAT* loci and pheromone response pathways in a variety of unisexual species as well as their heterothallic relatives. In cases where such data had not previously been published, we utilized publicly available NGS data to run additional analyses, which are detailed in the supplementary data. We hypothesize that unisexuality is derived from a heterothallic state via the mutation of genes involved in the initiation phase of sexual reproduction. We thus present data which shows that unisexual species harbour significantly altered secondary *MAT* genes and exhibit major changes to their pheromone expression profiles when compared to their heterothallic relatives. Together, these differences result in the unique unisexual strategy exhibited by these three unrelated species.

2. UNISEXUAL FILAMENTOUS ASCOMYCETES

Publicly available genome and transcriptome data for three unisexual species from different genera were obtained from either the National Centre for Biotechnology Information (NCBI) or the Joint Genomes Institute (JGI) (Table S1 & S2). For comparative purposes, genome and transcriptome data of a closely related, heterothallic species that shared the same mating type were also obtained from these sources. Based on the available datasets, comparisons were drawn between *N. africana* and a MAT1-1 isolate of *N. crassa* as well as *H. moniliformis* and a MAT1-2 isolate of *H. omanensis.* For *T. aurantiacus*, the closest relative of this species

for which NGS data is available was a MAT1-1 isolate of *Byssochlamys spectabilis*, a heterothallic species from a related genus.

Heterothallic *Neurospora* species such as *N. crassa*, have well-characterised *MAT* idiomorphs. MAT1-1 isolates harbour three *MAT* genes, *matA-1* (*MAT1-1-1*), *matA-2* (*MAT1-1-2*) and *matA-3* (*MAT1-1-3*) (31). These proteins each possess the typical conserved functional domains; the α-box, the MAT1-1-2 superfamily domain, and the HMG box domain, respectively. Isolates with the *MAT1-2* idiomorph harbour only a single *MAT* gene, *mata-1* (*MAT1-2-1*) that also encodes a protein with the HMG box domain (32). The *MAT* idiomorphs are associated with genes normally found near the *MAT* loci of other ascomycetes (Figure 3), including an AP endonuclease (*APN2*) and the cytoskeleton assembly control protein (*SLA2*). The unisexual *N. africana* harbours the same *MAT1-1* genes, although the *MAT* locus structure is markedly different (Figure 3). An inversion of approximately 70 kb has rearranged this locus and relocated the *MAT1-1-2* and *MAT1-1-3* genes. Thus, while the *MAT1-1-1* gene remains associated with the *SLA2* gene as in *N. crassa*, the other two genes are associated with *APN2* at a different genomic location.

Heterothallic *Huntiella* species also have well-defined *MAT* idiomorphs, conferring the two alternate mating types (13). In *H. omanensis*, for example, isolates with the *MAT1-1* idiomorph express the *MAT1-1-1* and *MAT1-1-2* genes. MAT1-2 isolates also harbour two genes at their *MAT1-2* idiomorph, the primary *MAT* gene, *MAT1-2-1*, possessing the conserved HMG box domain, as well as a secondary *MAT* gene, *MAT1-2-7*, which possesses no recognizable conserved domains (13). All studied isolates of the unisexual *H. moniliformis* harbour only the *MAT1-2* idiomorph and its respective genes. The *MAT* loci of both species are associated with the *SLA2* and *APC* genes (Figure 4).

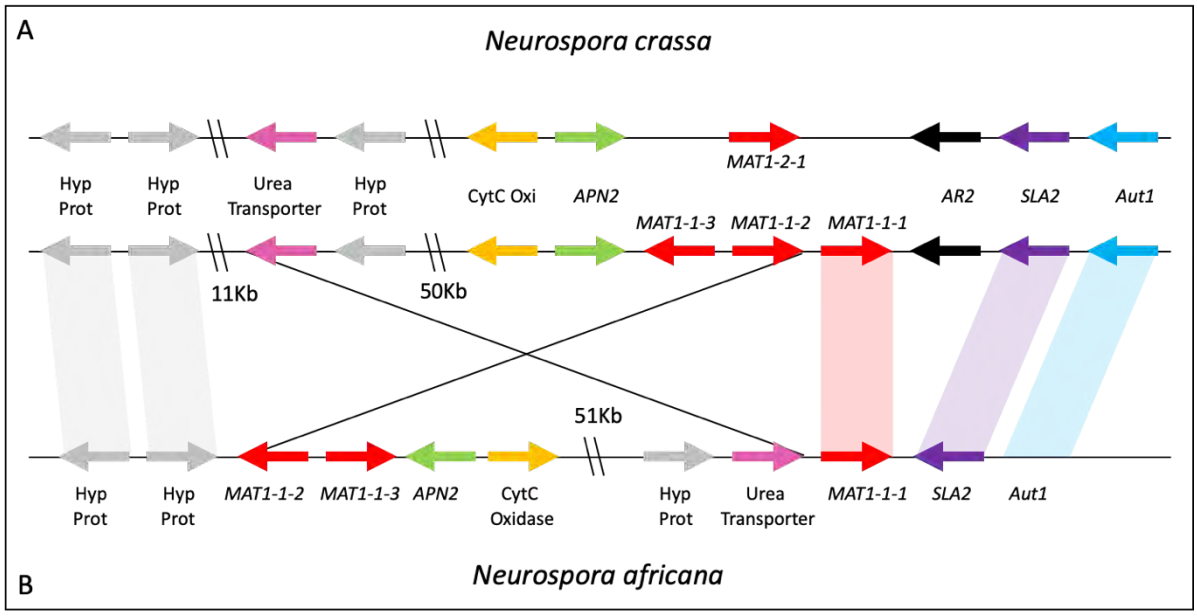

Figure 3: The *MAT* loci of *Neurospora crassa* and *N. africana*. A) The two *MAT* idiomorphs of *N. crassa*. The top region represents the *MAT1-2* idiomorph, while the bottom represents the *MAT1-1* idiomorph. B) The *MAT1-1* idiomorph of *N. africana*, illustrating the inversion that separates the *MAT1-1* idiomorph in this species.

Key: Hyp Prot: Hypothetical protein (grey), CytC Oxi: Cytochrome C Oxidase (yellow), APN2: AP endonuclease (green), AR2: nucleotide binding protein, SLA2: cytoskeleton assembly control protein (purple), Aut1: autophagy gene (blue).

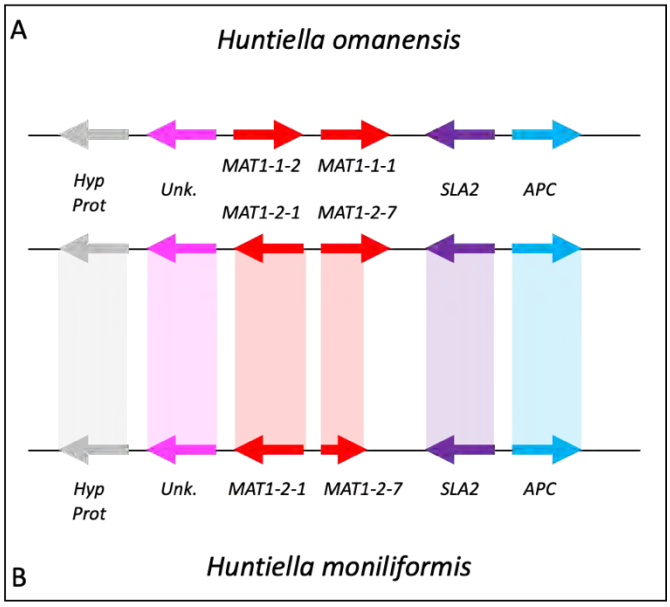

Figure 4: The *MAT* loci of *Huntiella omanensis* and *H. moniliformis*. A) The two *MAT* idiomorphs of *H. omanensis*. The top region represents the *MAT1-1* idiomorph, while the bottom represents the *MAT1-2* idiomorph. B) The *MAT1-2* idiomorph of *H. moniliformis*, illustrating the gene content and locus structure conservation between the two species.

Key: Hyp Prot: Hypothetical protein (grey), Unk.: Unknown protein (pink), SLA2: cytoskeleton assembly control protein (purple), APC: anaphase promoting complex (blue).

MAT1-1 isolates of the heterothallic *B. spectabilis* harbour the *MAT1-1-1* gene as well as a secondary *MAT* gene (Figure 5) (33). This gene shows similarity to the *MAT1-1-4* gene of *Trichophyton verrucosum*, which was renamed *MAT1-1-9* in a recent update of *MAT* gene nomenclature (34). The *MAT* locus of *B. spectabilis* is also associated with the *SLA2* gene, as well as a PH domain protein and a cytochrome C oxidase gene. Similarly, MAT1-1 isolates of the unisexual *T. aurantiacus* harbour both the *MAT1-1-1* and *MAT1-1-9* genes, which are associated with homologs of the *B. spectabilis* flanking genes (Figure 5).

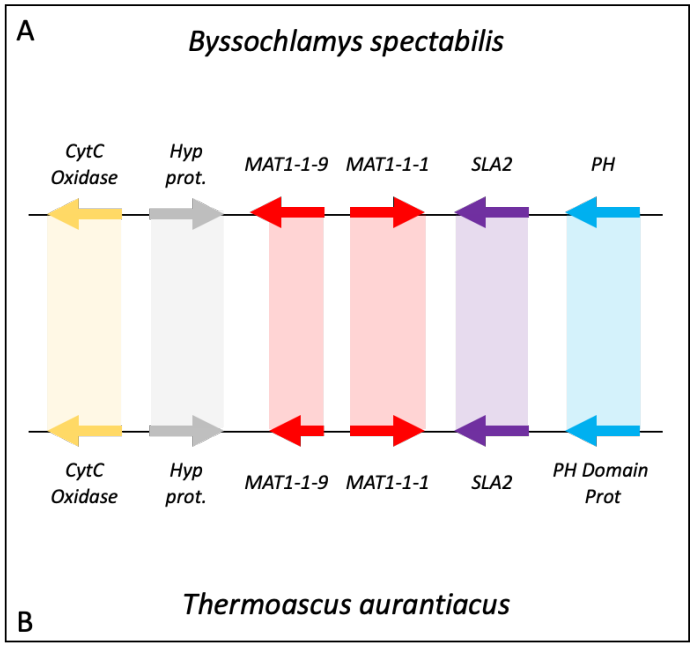

Figure 5: The *MAT* loci of *Byssochlamys spectabilis* and *Thermoascus aurantiacus.* A) The *MAT1-1* idiomorph of *B. spectabilis.* B) The *MAT1-1* idiomorph of *T. aurantiacus*, illustrating the gene content and locus structure conservation between the two species. **Key:** CytC Oxdiase: CytochromeC oxidase (yellow), Hyp Prot: Hypothetical protein (grey), SLA2: cytoskeleton assembly control protein (purple), PH: PH domain protein (blue).

3. MUTATIONS IN A SECONDARY *MAT* GENE

The genes present at the *MAT* loci of the three unisexual species considered in this study are largely comparable to those of their heterothallic relatives. This is particularly true for the primary *MAT* genes, *MAT1-1-1* in the *Neurospora*, *Thermoascus and Byssochlamys* species, as well as *MAT1-2-1* in the two *Huntiella* species (Figure 6). In each case, the unisexual species and their heterothallic relatives harbour the same primary *MAT* genes, that are of similar length and show high levels of sequence identity at both the nucleotide and amino acid level. These genes also encode proteins that possess the relevant protein domains.

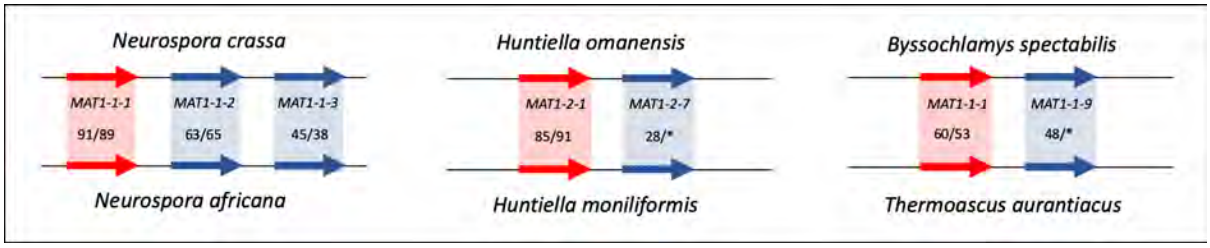

Figure 6: Nucleotide and amino acid sequence conservation of the various *MAT* genes and their encoded proteins. The primary *MAT* genes are indicated in red and show high levels of percentage identity at both the nucleotide (the number indicated before the forward slash) and the amino acid (the number indicated after the forward slash) level. In contrast, the secondary *MAT* genes, indicated in blue, show much lower levels of identity. The * indicates that the protein of the unisexual species was significantly truncated and thus could not accurately be compared to that of the heterothallic species

The high degree of conservation found in the primary *MAT* genes does not extend to the secondary *MAT* genes of these species. In all three cases, there have been significant changes to the secondary *MAT* genes, including both partial deletion and truncation events. The exception here is the *MAT1-1-2* gene of *N. africana* which, while shorter than that of *N. crassa*, is still expressed and encodes a protein harbouring the relevant conserved domain (Figure 7). In *N. crassa*, the *MAT1-1-3* gene is characterized by four exons which are interrupted by three introns (Figure 8). The functional domain, an HMG box, spans the third intron and is thus encoded by sequence from both exons three and four. In contrast, a deletion of a significant region of the *N. africana MAT1-1-3*, including the majority of the third exon and third intron, produces a protein that does not possess the HMG box (Figure 8). It is thus reasonable to speculate that this gene no longer serves the function that is has in *N. crassa*.

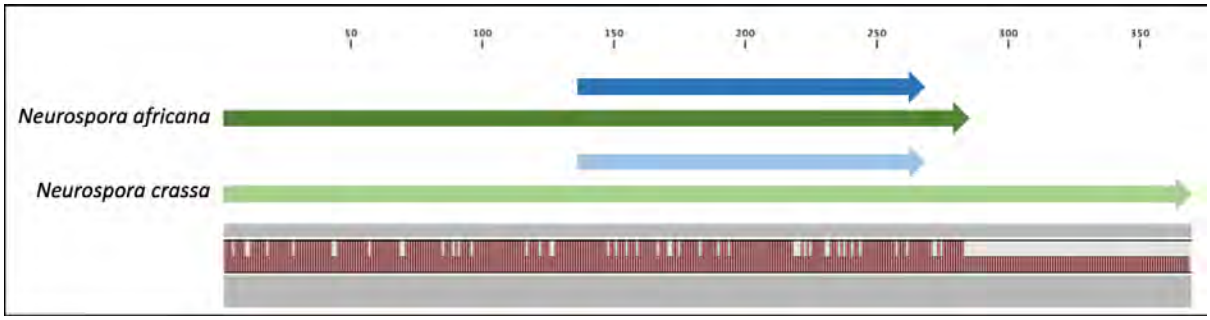

Figure 7: Truncation in the *Neurospora africana MAT1-1-2* gene does not affect the functional domain of the MAT1-1-2 protein. A protein alignment between the MAT1-1-2 proteins of *N. africana* (top, dark green) and *N. crassa* (bottom, light green) shows that the *N. africana* protein is much shorter than that of *N. crassa*. The functional protein domains (dark and light blue), however, are of similar length and position.

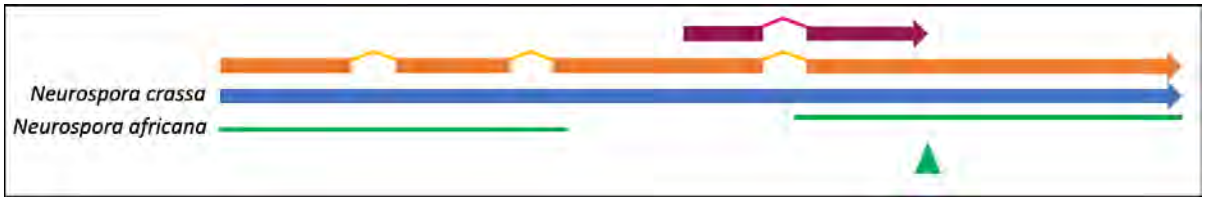

Figure 8: A deletion in the *Neurospora africana MAT1-1-3* results in the deletion of the HMG box functional domain. The blue bar represents the sequence of the *MAT1-1-3* gene from *N. crassa*, while the orange connected bars represent the coding sequence of the gene, interrupted by three introns. The maroon bar represents the HMG functional domain which is also interrupted by an intron. The green represents the regions within the *N. africana* genome where significant similarity to the *N. crassa MAT1-1-3* gene was found. While the 5' and 3' regions of the *N. crassa* gene show significant similarity to that of *N. africana*, large parts of the third exon and intron, have been entirely deleted in *N. africana*. This results in the deletion of a significant part of the functional domain as well as the inclusion of a premature in frame stop codon shortly after the second intron in *N. africana* (indicated by the green arrow). Together, this likely renders the protein non-functional.

In the cases of both *H. moniliformis* and *T. aurantiacus*, the introduction of premature stop codons has significantly truncated their respective secondary *MAT* genes. This stop codon shortens the *H. moniliformis MAT1-2-7* gene to less than a third of the length the *H. omanensis* homolog (13). Furthermore, while expressed during sexual development in *H. omanensis*, expression of this gene cannot be detected in vegetative or sexual tissues of *H. moniliformis* (6). The *MAT1-1-9* genes of *T. aurantiacus* and *B. spectabilis* present an

interesting case. *De novo* predictions of these genes produce similar gene models, which are comparable in both length and gene structure. However, the available RNA sequence data from *T. aurantiacus* does not support the gene model for this species. Instead, mapping the RNA data to the genomic region harbouring the *MAT1-1-9* gene in *T. aurantiacus* supports a gene model with fewer introns than originally predicted (Figure 9). The exclusion of these introns introduces a premature stop codon which significantly shortens the protein coding region to only 51 nt. As neither the *MAT1-2-7* nor the *MAT1-1-9* proteins harbour recognizable conserved domains, it is difficult to assess the effect of these truncations on the functional regions of the proteins. However, it is reasonable to assume that the significantly shortened length of each protein would render them non-functional.

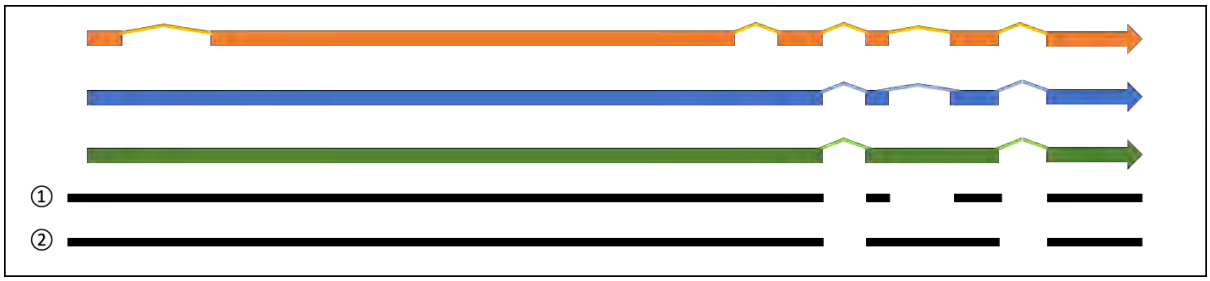

Figure 9: Predicted and supported gene models of the *T. aurantiacus MAT1-1-9* gene. The predicted gene model by Fgenesh is indicated in orange, and harbours a total of five introns which interrupt six exons. Indicated in blue and green are the two alternate models supported by the RNA seq data. Neither model supports the first or second introns, and instead suggests alternative splicing which results in one of two splice variants. The RNA mapped consensus sequences are indicated by the black bars, with ① supporting a total of four exons, and ② supporting only three exons. However, in both splice variants, the first intron is removed, thereby introducing a premature stop codon. This gene consequently encodes a truncated protein.

4. ALTERATIONS TO THE PHEROMONE RESPONSE PATHWAY

While the pheromone expression patterns of the heterothallic species considered here closely follow those reported from other heterothallic species (5,6), pheromone expression in the three unisexual species is unusual for isolates of a single mating type. Under this paradigm, the MAT1-1 isolates of both *N. africana* and *T. aurantiacus* and the MAT1-2 isolate of *H. moniliformis* should only express the α-factor and the **a**-factor pheromones,

respectively. However, both *N. africana* and *H. moniliformis* (6) express both pheromone factors as well as their cognate receptors. This suggests that a single isolate of either species is able to recognize itself, or another isolate of the same mating type, as a suitable mating partner, thus allowing for sexual reproduction in the absence of an opposite mating type partner.

The pheromone expression profile of *T. aurantiacus* also exhibits some interesting deviations from that observed in other homothallic or unisexual species. The α-factor pheromone gene from *B. spectabilis* were identified in this study. To do this, a microsynteny approach was used, exploiting the synteny between the α-factor pheromone gene and its flanking regions in *Aspergillus nidulans* and *B. spectabilis* (Figure 10). The predicted *B. spectabilis* α-factor pheromone gene produce putative proteins with the structural characteristics typical of the ascomycete α-factor pheromone (Figure 11). This synteny-based approach also resulted in the identification of a significantly truncated α-factor pheromone gene in the genome of *T. aurantiacus* (Figure 10). This shortened gene would produce a protein of only 17 aa and does not harbour the mature pheromone sequence (Figure 12).

In addition to the absence of a functional α-factor pheromone gene in *T. aurantiacus*, a gene encoding the **a**-factor pheromone could not be found in the genomes of either *T. aurantiacus* or that of *B. spectabilis*. These species reside within the Eurotiomycetes, a fungal class which also accommodates the model species *A. nidulans*. The **a**-factor pheromone has not been identified in any studied Eurotiomycetes species, despite thorough genomic investigations (35,36). In future, techniques such as comparative transcriptomics may be useful to identify this elusive gene. The identification of this gene will help shed light on the role of the pheromone response pathway in many homothallic species and particularly in this unisexual species.

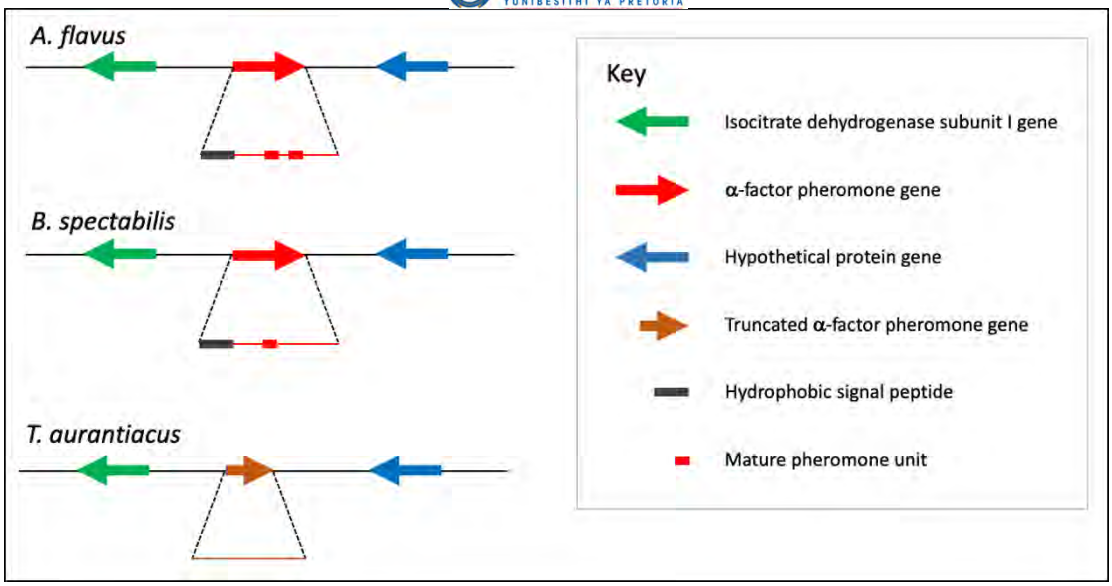

Figure 10: Identification of the *Byssochlamys spectabilis*, *Thermoascus aurantiacus* α-factor pheromone genes. A microsynteny approach was used to identify the α-factor genes in *B. spectabilis* and *T. crustaceus* using the *A. flavus* α-factor gene and its flanking genes. By identifying the α-factor gene flanking genes in *B. spectabilis* and T. aurantiacus, it was possible to manually annotate the intergenic region and identify the full-length α-factor gene in *B. spectabilis*. Only a truncated version of this gene could be identified in the *T. aurantiacus* genome.

Species	Pheromone Structure	Pheromone Sequence
N. crassa	---■-■-■-■-■---	■ QWCRIHGQSCW
N. africana	---■-■-■-■----	■ QWCRIHGQSCW ■ QWCRIRGQSCW
H. omanensis	---■-■-■-■-■-■-■-■---	■ DSNGGLPGELL ■ NSNAGLPGELL ■ YSNAGLPGELL
H. moniliformis	---■-■-■-■-■-■---	■ DANGGLPGELF ■ DAWGGLPGELF
B. spectabilis	---■---	■ WCRRPGQPC

Figure 11: The structure of the unprocessed α-factor pheromone proteins. Each species shows a slightly different pheromone protein structure, with *H. omanensis* harbouring the most individual repeats of the mature α-factor (eight), while *B. spectabilis* and *T. crustaceus* only harbour one each. *N. crassa* harbours only identical repeats, while *N. africana* and the *Huntiella* species have repeats of different sequence.

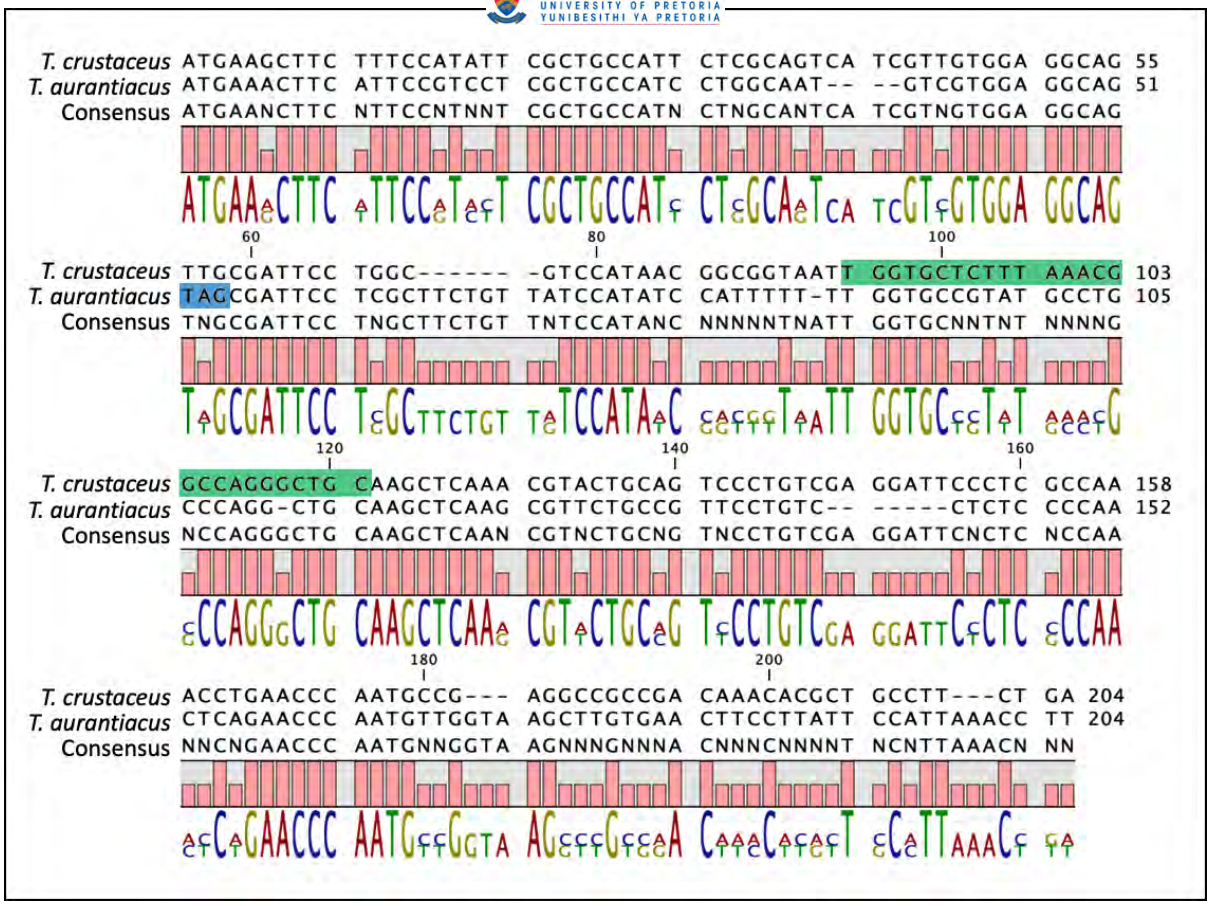

Figure 12: Comparison of the α-factor pheromone encoding regions in *Thermoascus crustaceus* and *T. aurantiacus*. The green bar identifies the area in this gene that encodes for the mature pheromone repeat in *T. crustaceus.* However, before the sequence that would encode this mature repeat in *T. aurantiacus*, an in frame stop codon (indicated by the blue bar) is present and precludes the translation of the full-length pheromone factor.

The pheromone receptors also play an integral role in the pheromone response pathway and have been shown to be important for sexual reproduction in a variety of heterothallic and homothallism species alike (8,11,37,38). Genes encoding the receptors for both pheromones can be found in the genomes of all seven species considered in this study. Both receptors from the *Neurospora* species, the *Huntiella* species and *T. crustaceus* as well as the **a**-factor receptor from *T. aurantiacus* harbour the recognizable protein domains associated with these receptors. They also possess the typical seven transmembrane domain structure required for receptor function (Figure 13). The *T. aurantiacus* α-factor receptor deviates from this conserved structure and possesses only three transmembrane domains (Figure 13). Thus, the pheromone response pathway appears to have been significantly altered in the unisexual *T. aurantiacus*.

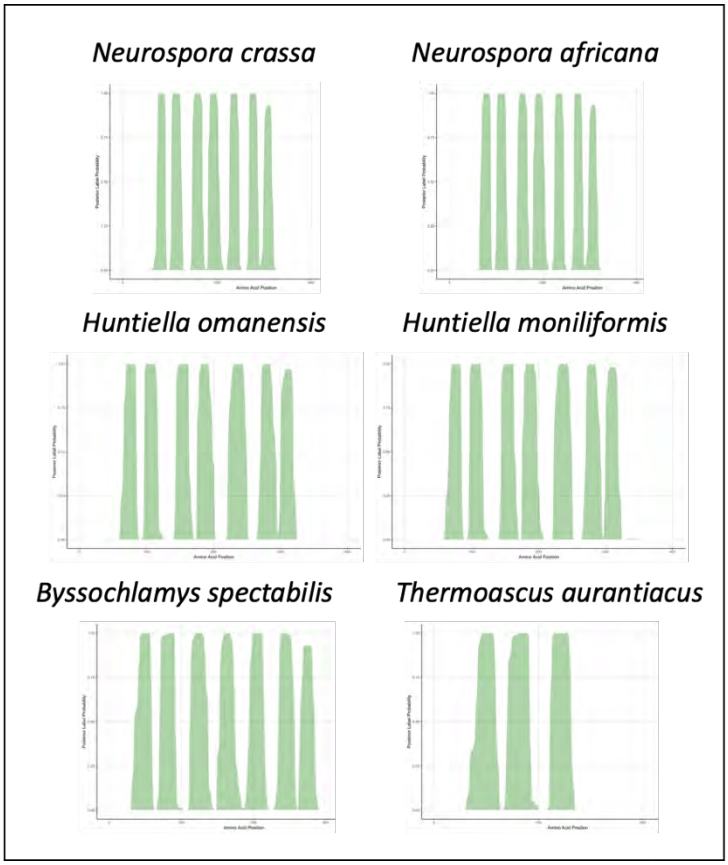

Figure 13: Transmembrane domains of the α-factor pheromone receptor proteins. In the *Neurospora* and *Huntiella* species as well as in *T. crustaceus*, seven transmembrane domains exist in the α-factor pheromone receptor, as expected from these proteins. In contrast, the *T. aurantiacus* receptor possesses only three transmembrane domains and may thus be non-functional.

The x-axis represents the length of the protein, while the y-axis represents the posterior label probability, a measure of the likelihood that a region of the protein is hydrophobic.

5. THE TRANSITION TO UNISEXUALITY

A long-held debate in the field of fungal biology concerns the ancestral sexual strategy of fungi (39,40). It is thought, for example, that homothallism is the ancestral state for species of *Aspergillus* (41), *Sclerotinia* and *Botrytis* (42), and that transitions towards heterothallism have taken place during their evolutionary trajectory. In contrast, the ancestral strategy for fungi belonging to the genera *Neurospora* (43) and *Cochliobolus* (44) is thought to be heterothallism, with various independent transitions towards homothallism having taken place. The ancestral state for all fungi continues to be debated, especially given that there is empirical evidence to support both reproductive strategies as the ancestral state.

Transitioning between homothallism and heterothallism has occurred frequently across the fungal Kingdom (40). It is thought that these shifts are predominantly the result of changes in the selective pressures of the environment (45). Harsh environmental conditions that demand the generation of high genetic diversity and environmentally-resistant spores, for example, may lead to the transition towards heterothallism in an attempt to enhance

outcrossing and increase genetic diversity (46). In contrast, given that the major costs associated with sexual reproduction (such as mate seeking and recognition) are absent in homothallic species, environments where the probability of encountering a mate is limited might select for some form of homothallic behaviour (47).

In this review, we posit that unisexuality has its origins in heterothallism. This is certainly possible for *Cr. neoformans*, the most extensively investigated of the unisexual species (48). While this yeast has a well-characterized heterothallic cycle (17), the vast majority of naturally-occurring isolates collected are of the α mating type (49). Given that both **a** and α cells are capable of unisexual reproduction (18), the unequal mating type ratio is most likely not the result of a fitness advantage conferred to the unisexually-reproducing α cells. Rather, it appears more likely that unisexuality evolved as a mechanism to ensure sexual outcrossing in a population dominated by a single mating type. In this case, the heterothallic lifestyle represents the ancestral state, while unisexuality (and thus homothallism) is likely a derived state. A similar transition may have occurred in the unisexual species investigated in this study. For example, all isolates of *H. moniliformis* that have been collected to date are of the MAT1-2 mating type (13), suggesting either a dominance of this mating type in nature or the extinction of the MAT1-1 mating type. A similar case is found in naturally occurring isolates of *N. africana*, where only isolates harbouring the *MAT1-1* genes have been collected (29). Thus, while the uneven mating type ratio could be attributed to unisexual reproduction, unisexuality could also have evolved in response to this mating type inequality.

We suggest that the transition from heterothallism to unisexuality is the result of relatively minor changes to the genes that control the initiation of sexual reproduction: the *MAT* genes and the pheromone response pathway genes. It has been shown in several species that the genes and pathway involved in sexual reproduction in heterothallic species are similar to those involved in homothallic mating (20,50,51). In fact, homothallic species such as *A. nidulans*, *F. graminearum* and *Sordaria macrospora*, retain the pheromone response pathway, a pathway that is primarily involved in partner attraction and recognition (8,9,35). This form of conservation strongly suggests that, while the sexual processes in homothallic and heterothallic mating differ in the initiation phase, the downstream pathways and networks remain the same (41). This further adds to the ease with which a species can

transition between the two mating strategies, as small changes to the initiation processes should be sufficient.

6. CONCLUSION

Unisexual reproduction remains an understudied sexual strategy in the filamentous fungi. Given the importance of sexual reproduction to the evolutionary longevity and survival of species, unisexual reproduction may have evolved as a mechanism to ensure genetic recombination under environmental conditions typically not conducive for typical sexual reproduction. We have provided evidence in this review to suggest that the transition from heterothallism to unisexuality can occur via relatively minor mutations in a certain set of genes and thus may represent a fairly common occurrence. Because the difference between primary homothallism and unisexuality is strictly based on the *MAT* locus structure and gene content, the increased availability of whole genome sequencing coupled with classical fungal physiology, will likely reveal an increased number of unisexual species, both in the ascomycetes and the basidiomycetes.

7. ACKNOWLEDGEMENTS

This project was financed by the University of Pretoria, the Department of Science and Technology (DST)/National Research Foundation (NRF) Centre of Excellence in Tree Health Biotechnology and the Genomics Research Institute (University of Pretoria Institutional Research Theme). This work is based on the research supported in part by a number of grants from the National Research Foundation of South Africa. The Grant holders acknowledge that opinions, findings and conclusions or recommendations expressed in any publication generated by the NRF supported research are that of the author(s), and that the NRF accepts no liability whatsoever in this regard.

8. REFERENCES

1. Ni M, Feretzaki M, Sun S, Wang X, Heitman J. Sex in fungi. Annu Rev Genet. 2011;45(1):405–30.
2. Blakeslee AF. Sexual reproduction in the Mucorineae. Proc Am Acad Arts Sci. 1904;40(4):205–319.
3. Kronstad JW, Staben C. Mating type in filamentous fungi. Annu Rev Genet. 1997;31(1):245–76.
4. Shen WC, Bobrowicz P, Ebbole DJ. Isolation of pheromone precursor genes of *Magnaporthe grisea*. Fungal Genet Biol. 1999;27(2–3):253–63.
5. Bobrowicz P, Pawlak R, Correa A, Bell-Pedersen D, Ebbole DJ. The *Neurospora crassa* pheromone precursor genes are regulated by the mating type locus and the circadian clock. Mol Microbiol. 2002;45(3):795–804.
6. Wilson AM, van der Nest MA, Wilken PM, Wingfield MJ, Wingfield BD. Pheromone expression reveals putative mechanism of unisexuality in a saprobic ascomycete fungus. PLoS One. 2018;13(3):e0192517.
7. Zhang L, Baasiri RA, Van Alfen NK. Viral repression of fungal pheromone precursor gene expression. Mol Cell Biol. 1998;18(2):953–9.
8. Lee J, Leslie JF, Bowden RL. Expression and function of sex pheromones and receptors in the homothallic ascomycete *Gibberella zeae*. Eukaryot Cell. 2008;7(7):1211–21.
9. Pöggeler S. Two pheromone precursor genes are transcriptionally expressed in the homothallic ascomycete *Sordaria macrospora*. Curr Genet. 2000;37(6):403–11.
10. Jones SK, Bennett RJ. Fungal mating pheromones: Choreographing the dating game. Fungal Genet Biol [Internet]. 2011;48(7):668–76. Available from: http://dx.doi.org/10.1016/j.fgb.2011.04.001
11. Kim H, Wright SJ, Park G, Ouyang S, Krystofova S, Borkovich KA. Roles for receptors, pheromones, G proteins, and mating type genes during sexual reproduction in *Neurospora crassa*. Genetics. 2012;190(4):1389–404.
12. Roach KC, Feretzaki M, Sun S, Heitman J. Unisexual reproduction. In: Friedmann T, Dunlap JC, Goodwin SF, editors. Advances in Genetics. 85th ed. Waltham: Academic Press; 2014. p. 255–305.
13. Wilson AM, Godlonton T, van der Nest MA, Wilken PM, Wingfield MJ, Wingfield BD.

Unisexual reproduction in *Huntiella moniliformis*. Fungal Genet Biol. 2015;80:1–9.

14. Alby K, Schaefer D, Bennett RJ. Homothallic and heterothallic mating in the opportunistic pathogen *Candida albicans*. Nature. 2009;460(7257):890–3.
15. Lin X, Hull CM, Heitman J. Sexual reproduction between partners of the same mating type in *Cryptococcus neoformans*. Nature. 2005;434(7036):1017–21.
16. Schuerg T, Gabriel R, Baecker N, Baker SE, Singer SW. *Thermoascus aurantiacus* is an intriguing host for the industrial production of cellulases. Curr Biotechnol. 2016;6(2):89–97.
17. Kwon-chung KJ. Morphogenesis of *Filobasidiella neoformans*, the sexual state of *Cryptococcus neoformans*. Mycologia. 1976;68(4):821–33.
18. Tscharke RL, Lazera M, Chang YC, Wickes BL, Kwon-Chung KJ. Haploid fruiting in *Cryptococcus neoformans* is not mating type α-specific. Fungal Genet Biol. 2003;39(3):230–7.
19. Wickes BL, Mayorga ME, Edman U, Edman JC. Dimorphism and haploid fruiting in *Cryptococcus neoformans*: Association with the α-mating type. Microbiology [Internet]. 1996;93(14):7327–31. Available from: http://www.ncbi.nlm.nih.gov/pubmed/8692992%0Ahttp://www.pubmedcentral.nih.gov/articlerender.fcgi?artid=PMC38983
20. Lin X, Jackson JC, Feretzaki M, Xue C, Heitman J. Transcription factors Mat2 and Znf2 operate cellular circuits orchestrating opposite- and same-sex mating in *Cryptococcus neoformans*. PLoS Genet. 2010;6(5):30.
21. Wang P, Perfect JR, Heitman J. The G-Protein beta subunit GPB1 is required for mating and haploid fruiting in *Cryptococcus neoformans*. Mol Cell Biol. 2000;20(1):352–62.
22. Cerikçioğlu N. Mating types, sexual reproduction and ploidy in fungi: Effects on virulence. Mikrobiyol Bul. 2009;43(3):507–13.
23. Hull CM, Davidson RC, Heitman J. Cell identity and sexual development in *Cryptococcus neoformans* are controlled by the mating-type-specific homeodomain protein SXI1α. Genes Dev. 2002;16(23):3046–60.
24. Bennett RJ, Johnson AD. Completion of a parasexual cycle in *Candida albicans* by induced chromosome loss in tetraploid strains. EMBO J. 2003;22(10):2505–15.
25. Dignard D, El-Naggar AL, Logue ME, Butler G, Whiteway M. Identification and characterization of MFAl, the gene encoding *Candida albicans* a-factor pheromone.

Eukaryot Cell. 2007;6(3):487–94.

26. Schaefer D, Côte P, Whiteway M, Bennett RJ. Barrier activity in *Candida albicans* mediates pheromone degradation and promotes mating. Eukaryot Cell. 2007;6(6):907–18.
27. Alby K, Bennett RJ. Interspecies pheromone signaling promotes biofilm formation and same-sex mating in *Candida albicans*. Proc Natl Acad Sci. 2011;108(6):2510–5.
28. Glass NL, Metzenberg RL, Raju NB. Homothallic Sordariaceae from nature: The absence of strains containing only the a mating type sequence. Exp Mycol. 1990;14(3):274–89.
29. Glass NL, Smith ML. Structure and function of a mating-type gene from the homothallic species *Neurospora africana*. Mol Gen Genet. 1994;244(4):401–9.
30. Liu FF, Li GQ, Roux J, Barnes I, Wilson AM, Wingfield MJ, et al. Nine novel species of *Huntiella* from southern China with three distinct mating strategies and variable levels of pathogenicity. Mycologia [Internet]. 2018;110(6):1145–71. Available from: https://doi.org/10.1080/00275514.2018.1515450
31. Glass NL, Grotelueschen J, Metzenberg RL. *Neurospora crassa* A mating-type region. Proc Natl Acad Sci. 1990;87(13):4912–6.
32. Staben C, Yanofsky C. *Neurospora crassa* a mating-type region. Genetics. 1990;87(July):4917–21.
33. Houbraken J, Varga J, Rico-Munoz E, Johnson S, Samson RA. Sexual reproduction as the cause of heat resistance in the food spoilage fungus Byssochlamys spectabilis (anamorph Paecilomyces variotii). Appl Environ Microbiol. 2008;74(5):1613–9.
34. Wilken PM, Steenkamp ET, Wingfield MJ, de Beer ZW, Wingfield BD. Which *MAT* gene? Pezizomycotina (Ascomycota) mating-type gene nomenclature reconsidered. Fungal Biol Rev [Internet]. 2017;31(4):199–211. Available from: http://dx.doi.org/10.1016/j.fbr.2017.05.003
35. Dyer PS, Paoletti M, Archer DB. Genomics reveals sexual secrets of *Aspergillus*. Microbiology. 2003;149(9):2301–3.
36. Pöggeler S. Genomic evidence for mating abilities in the asexual pathogen *Aspergillus fumigatus*. Curr Genet. 2002;42(3):153–60.
37. Kim H, Borkovich KA. A pheromone receptor gene, *pre-1*, is essential for mating type-specific directional growth and fusion of trichogynes and female fertility in *Neurospora crassa*. Mol Microbiol. 2004;52(6):1781–98.

38. Seo JA, Han KH, Yu JH. The gprA and gprB genes encode putative G protein-coupled receptors required for self-fertilization in *Aspergillus nidulans*. Mol Microbiol. 2004;53(6):1611–23.

39. Billiard S, López-Villavicencio M, Hood ME, Giraud T. Sex, outcrossing and mating types: Unsolved questions in fungi and beyond. J Evol Biol. 2012;25(6):1020–38.

40. Lin X, Heitman J. Mechanisms of homothallism in fungi and transitions between heterothallism and homothallism. In: Heitman J, Kronstad JW, Taylor JW, Casselton LA, editors. Sex in Fungi. ASM Press, Washington D.C.; 2007. p. 35–57.

41. Galagan JE, Calvo SE, Cuomo C, Ma LJ, Wortman JR, Batzoglou S, et al. Sequencing of *Aspergillus nidulans* and comparative analysis with *A. fumigatus* and *A. oryzae*. Nature. 2005;438(7071):1105–15.

42. Amselem J, Cuomo CA, van Kan JAL, Viaud M, Benito EP, Couloux A, et al. Genomic analysis of the necrotrophic fungal pathogens *Sclerotinia sclerotiorum* and *Botrytis cinerea*. PLoS Genet. 2011;7(8):e1002230.

43. Gioti A, Mushegian AA, Strandberg R, Stajich JE, Johannesson H. Unidirectional evolutionary transitions in fungal mating systems and the role of transposable elements. Mol Biol Evol. 2012;29(10):3215–26.

44. Yun S-H, Berbee ML, Yoder OC, Turgeon BG. Evolution of the fungal self-fertile reproductive life style from self-sterile ancestors. Proc Natl Acad Sci. 1999;96(10):5592–7.

45. Lee SC, Ni M, Li W, Shertz C, Heitman J. The evolution of sex: A perspective from the fungal kingdom. Microbiol Mol Biol Rev. 2010;74(2):298–340.

46. Heitman J. Sexual reproduction and the evolution of microbial pathogens. Curr Biol. 2006;16:R711–25.

47. Billiard S, López-Villavicencio M, Devier B, Hood ME, Fairhead C, Giraud T. Having sex, yes, but with whom? Inferences from fungi on the evolution of anisogamy and mating types. Biol Rev. 2011;86(2):421–42.

48. Wang L, Lin X. Mechanisms of unisexual mating in *Cryptococcus neoformans*. Fungal Genet Biol [Internet]. 2011;48(7):651–60. Available from: http://dx.doi.org/10.1016/j.fgb.2011.02.001

49. Kwon-Chung KJ, Bennett JE. Distribution of α and a mating types of *Cryptococcus neoformans* among natural and clinical isolates. Am J Epidemiol. 1978;108(4):337–40.

50. Beatty NP, Smith ML, Louise Glass N. Molecular characterization of mating-type loci in selected homothallic species of *Neurospora*, *Gelasinospora* and *Anixiella*. Mycol Res [Internet]. 1994;98(11):1309–16. Available from: http://dx.doi.org/10.1016/S0953-7562(09)80304-3

51. Ferreira AVB, An Z, Metzenberg RL, Glass NL. Characterization of *mat A-2*, *mat A-3* and *ΔmatA* mating-type mutants of *Neurospora crassa*. Genetics. 1998;148(3):1069–79.

52. Stanke M, Waack S. Gene prediction with a hidden Markov model and a new intron submodel. Bioinformatics. 2003;19(SUPPL. 2):215–25.

53. Salamov AA, Solovyev V V. *Ab initio* gene finding in *Drosophila* genomic DNA. Genome Res. 2000;10:516–22.

54. Galagan JE, Calvo SE, Borkovich KA, Selker EU, Read ND, Jaffe D, et al. The genome sequence of the filamentous fungus *Neurospora crassa*. Nature. 2003;422:859–68.

55. Gioti A, Stajich JE, Johannesson H. *Neurospora* and the dead-end hypothesis: Genomic consequences of selfing in the model genus. Evolution (N Y). 2013;67(12):3600–16.

56. van der Nest MA, Beirn LA, Crouch JA, Demers JE, de Beer ZW, De Vos L, et al. Draft genomes of *Amanita jacksonii*, *Ceratocystis albifundus*, *Fusarium circinatum*, *Huntiella omanensis*, *Leptographium procerum*, *Rutstroemia sydowiana*, and *Sclerotinia echinophila*. IMA Fungus. 2014;5(2):472–85.

57. Van Der Nest MA, Bihon W, De Vos L, Naidoo K, Roodt D, Rubagotti E, et al. Draft genome sequences of *Diplodia sapinea, Ceratocystis manginecans*, and *Ceratocystis moniliformis*. IMA Fungus. 2014;5(1):135–40.

58. Prefecture K. Draft genome sequence of the formaldehyde-resistant fungus *Byssochlamys spectabilis* No. 5 (Anamorph *Paecilomyces variotii* No. 5) (NBRC109023). Microbiol Resour Announements. 2014;2(1):e001162-13.

59. Singer SW. Genome assembly of *Thermoascus aurantiacus*. Jt Genomes Inst.

60. Yin G, Hua SST, Pennerman KK, Yu J, Bu L, Sayre RT, et al. Genome sequence and comparative analyses of atoxigenic *Aspergillus flavus* WRRL 1519. Mycologia [Internet]. 2018;110(3):482–93. Available from: https://doi.org/10.1080/00275514.2018.1468201

61. Wang Z, Lopez-giraldez F, Lehr N, Common R, Trail F, Townsend JP. Global gene expression and focused knockout analysis reveals genes associated with fungal fruiting body development in *Neurospora crassa*. 2014;13(1):154–69.

62. Schuerg T, Prahl JP, Gabriel R, Harth S, Tachea F, Chen CS, et al. Xylose induces cellulase production in *Thermoascus aurantiacus*. Biotechnol Biofuels. 2017;10(1):1–11.

63. Mcclendon SD, Batth T, Petzold CJ, Adams PD, Simmons BA, Singer SW. *Thermoascus aurantiacus* is a promising source of enzymes for biomass deconstruction under thermophilic conditions. Biotechnol Biofuels. 2012;5(54):1–9.

64. Marchler-bauer A, Derbyshire MK, Gonzales NR, Lu S, Chitsaz F, Geer LY, et al. CDD: NCBI' s conserved domain database. Nucleic Acids Res. 2015;43:D222-226.

65. Gasteiger E, Hoogland C, Gattiker A, Duvaud S, Wilkins MR, Appel RD, et al. Protein identification and analysis tools on the ExPASy Server. In: Walker J, editor. The Proteomics Protocols Handbook. Totowa, NJ: Springer: Humana Press Inc.; 2005. p. 571–608.

66. Krogh A, Sonnhammer ELL, Ka L. Advantages of combined transmembrane topology and signal peptide prediction — the Phobius web server. Nucleic Acids Res. 2007;35:W429–32.

67. Wickham H. A Layered grammar of graphics. J Comput Graph Stat. 2010;19(1):3–28.

68. Wilkinson L, Anand A, Grossman R. Graph-Theoretic Scagnostics. Proc EEE Symp Inf Vis [Internet]. 2005;1(1):21. Available from: http://ieeexplore.ieee.org/lpdocs/epic03/wrapper.htm?arnumber=1575779

9. SUPPORTING INFORMATION

9.1 Genome assemblies and annotation

All of the genome assemblies used in this study are publicly available from either the National Centre for Biotechnology Information (NCBI) or the Joint Genomes Institute (JGI) (Table S1).

All eight genomes were subjected to gene annotation using the web-based gene annotator AUGUSTUS (52). For both *Neurospora* genomes, the *N. crassa* species-specific gene model parameters were used. The *Fusarium graminearum* parameters were used for both *Huntiella* genomes, while the *B. spectabilis, T. aurantiacus* and *A. flavus* genomes were annotated using *Aspergillus nidulans* specific parameters. These species specific parameters were chosen based on the closest relative that could be found in the AUGUSTUS gene model parameter library. In addition to these genome-wide annotations, the contigs on which the target genes (*MAT*, pheromone and pheromone receptor genes) were identified were also subjected to Fgenesh annotation (53). The RNA sequence mapping described below was also used to confirm or correct the predicted gene models.

Table S1: The genome assemblies used in this study

Species	Source	Accession Number	Reference
Neurospora crassa OR74A	NCBI	AABX00000000.3	(54)
Neurospora africana FGSC1740	NCBI	CAPO000000000.2	(55)
Huntiella omanensis CMW 11056	NCBI	JSUI00000000.1	(56)
Huntiella moniliformis CMW 10134	NCBI	JMSH00000000.1	(57)
Byssochlamys spectabilis NBRC 109023	NCBI	RCHW00000000.1	(58)

Thermoascus aurantiacus ATCC 26904	JGI	405671	(59)
Aspergillus flavus NRRL3357	NCBI	AAIH00000000.2	(60)

9.2 RNA-seq data

The majority of the RNA sequence data used in this study was obtained as raw reads from the Sequence Read Archive (SRA) and Gene Expression omnibus (GEO) databases of the NCBI (Table S2).

Table S2: RNA sequencing data used in this study

Species	Accession Number	Reference
Neurospora crassa FGSC4200 & FGSC2489	GSE41484	(61)
Neurospora africana FGSC1740	ERS213531	European Bioinformatics Institute
Huntiella omanensis CMW 11056	SRP108437	(6)
Huntiella moniliformis CMW 369191	SRP108437	(6)
Byssochlamys spectabilis CBS 101075	SRP138004	Joint Genomes Institute

9.2.1 RNA-seq data for *Thermoascus aurantiacus*

T. aurantiacus ATCC 26904 was grown in a modified glucose-preculture medium as previously described (62). Accordingly, ascospores from 7-day-old potato dextrose agar plates were harvested and 1 x 10^6 spores per ml were used to inoculate glucose pre-cultures (2% glucose [w/v], McClendon, pH = 5.25, 0.8% soy meal peptone [w/v]). 50 mL pre-cultures were incubated for 48 h in 250 mL Erlenmeyer flasks at 50 °C and 180 rpm. These cultures were filtered under vacuum, using a Buchner funnel and Whatman paper #1, each washed with 100 mL defined McClendon's medium without

peptone (McClendon's salts pH = 5.25, 0.25 mM ammonia nitrate) (63) and shifted to four new flasks containing the same medium and either 2% beechwood xylan (Megazyme) or no carbon source. All cultures were grown under constant incandescent light for 48 hours in a rotary shaker at 50 °C and 180 rpm. From these shift cultures, samples were taken 1, 4, 6 and 8 hours after shifting. The sampling procedure involved taking an aliquot of 8 ml culture and vacuum filtering and washing it on a Whatman paper with immediate freezing in liquid nitrogen. Total nucleic acids were extracted through grinding with a mortar and pestle in liquid nitrogen and resuspension in TRIzol® Reagent (Thermo Fisher Scientific). RNA was isolated with Phenol:Chloroform:Isoamyl Alcohol, ethanol precipitation and subsequent DNAseI treatment. RNA quantity was determined on a Qubit (Thermo Fisher Scientific) and RIN values were determined using a Bioanalyzer (Agilent RNA 6000 Nano). Samples of suitable quality (RIN values > 8) from all time points of xylan and no carbon cultures were taken for cDNA synthesis and library construction with the TruSeq® Stranded Total RNA Library Kit (Illumina®). For this study, only one biological replicate for each condition and time point was sequenced on a MiSeq (Illumina®).

9.3 Gene identification

a. *MAT* genes

The *MAT* gene reference sequences for *N. crassa*, *N. africana*, *H. omanensis*, *H. moniliformis* and *B. spectabilis* were downloaded from NCBI (Table S3). These sequences were used as BLASTn queries against their respective genomes in order to identify the *MAT* loci. In order to identify the *T. aurantiacus MAT1-1-1* gene, the MAT1-1-1 protein sequence from *B. spectabilis* was used in a tBLASTn search against the *T. aurantiacus* genome. The identified *MAT* genes were translated into putative proteins products and subjected to functional domain annotation using the NCBI Conserved Domain Search (64).

Table S3: The gene and protein sequences used in various BLAST searches

Species	Gene	Accession Number/Gene ID
Neurospora crassa	*matA-1*	3880391
	matA-2	3880488
	matA-3	3880489
	pre1	3872329
	pre2	3875871
Neurospora africana	*matA-1*	HE600066.1
	matA-2	HE600066.1
	matA-3	HE600066.1
Huntiella omanensis	*MAT1-2-1*	KU950302.1
	MAT1-2-7	KU950303.1
Huntiella moniliformis	*MAT1-2-1*	KU950299.1
	MAT1-2-7	KU950298.1
Byssochlamys spectabilis	*MAT1-1-1*[a]	GAD92179.1
Aspergillus flavus	*ppgA* (pheromone)	7919755
	preA (pheromone receptor)	7912518
	preB (pheromone receptor)	7914252

[a] Protein sequence

b. Pheromone genes

α-factor pheromone

Genes encoding the α-factor pheromone had been previously identified in the genomes of the two *Neurospora* (5) and *Huntiella* (6) species. Identification of these genes in the *B. spectabilis* and *T. aurantiacus* genomes was achieved using a microsynteny approach based on the location of the α-factor pheromone gene in the *Aspergillus flavus* genome (Table S3). The proteins encoded by the genes directly flanking the *A. flavus* α-factor gene were used in local tBLASTn searches against the genomes of *B. spectabilis* and *T. aurantiacus*. The region between the identified flanking genes in *B. spectabilis* and *T. aurantiacus* was subjected to Fgenesh (53) and manual annotation in order to identify the pheromone gene.

The predicted α-factor pheromone genes were translated and analysed using the hydrophobicity and signal peptide predicting software programs, ExPASy ProtScale (65) and Phobius (66). Hydrophobicity was measured using the Kyte & Doolittle measure, with a window size of 9, a relative weight of window edges compared to window centres of 100%, a linear weight variation model and no scale normalization. Probability outputs from both programs were used to generate plots using the *ggplot2* package in R (67,68). Additionally, the Kex2 processing sites were identified in each gene and the potential mature α-factor repeats were annotated.

***a**-factor pheromone*

The **a**-factor pheromone genes have been previously identified in both the genomes of the *Neurospora* (5) and *Huntiella* (6) species considered in this study. No **a**-factor pheromone has been identified in the genomes of any other Eurotiomycetes species and thorough tBLASTn searches using all the a-factor pheromone sequences from (35,36) yielded no significant results. A method similar to the microsynteny-based approach used above also failed to produce usable results. Instead, all of the predicted coding sequences in the *B. spectabilis* and *T. aurantiacus* genomes were translated into putative protein products. These proteins were then filtered for those harbouring the terminal CaaX domain. These proteins were then screened to identify proteins with other similarities to previously identified **a**-factor pheromones.

c. Pheromone receptor genes

Both pheromone receptor genes, *pre1* (**a**-factor receptor) and *pre2* (α-factor receptor) had previously been identified in *N. crassa* (54). These two genes were identified in the *N. africana* genome using the *N. crassa* sequences as local BLASTn queries (Table S3). Both receptors had also previously been discovered in the genomes of *H. omanensis* and *H. moniliformis* (6). In order to identify these genes in the *B. spectabilis* and *T. aurantiacus* genomes, the *A. flavus preA* (**a**-factor receptor) and *preB* (α-factor receptor) genes as well as their translated proteins were used in local BLASTn and tBLASTn searches, respectively (Table S3). The **a**- and α-factor receptor genes from each of the seven species were

translated and subjected to functional domain discovery using the NCBI Conserved Domain Search (64) to confirm their identity. These proteins were also subjected to hydrophobicity analysis using Phobius (66) in order to identify putative transmembrane domains.

9.4 Gene, protein and functional domain comparisons

All nucleotide and amino acid comparisons were conducted using the *Create Alignment* and *Create Pairwise Comparison* functions in CLC MainWorkbench V8.1 (CLC bio, Aarhus, Denmark). The gene, protein and functional domain alignments were conducted using the default settings, which includes gap open and gap extension costs of 50 and the "Very accurate (slow)" alignment setting. Pairwise comparisons were also conducted using the default settings and included gap, differences, distance, percent identity and identity comparisons.

9.5 RNA-seq mapping

Expression analysis was conducted using CLC Genomics Workbench V7.5 (CLC bio, Aarhus, Denmark). The raw data were filtered to retain only reads with a Phred score of at least 20 ($Q \geq 0.01$). The filtered reads were then mapped to the contigs harbouring the various genes of interest using the NGS Core Tool *Map Reads to Reference*. No masking was included and the mapping settings were maintained at default. To ensure maximum mapping, the minimum length fraction and minimum similarity fraction values were set at 0.5 and 0.8, respectively. These relatively lenient mapping parameters ensured that reads spanning introns could successfully be mapped. This also ensured that successful mapping occurred despite the genome and transcriptomes originating from different isolates, as is the case for the majority of the species considered here. The resulting gene mappings were used to: 1) confirm or correct the gene models predicted by the various gene annotation programmes and, 2) determine whether the various genes of interest are expressed in the two different sexual systems.

RESEARCH CHAPTER 3

The novel *H. omanensis* mating gene, *MAT1-2-7*, is essential for ascomatal maturation

Andi M. Wilson[1], P. Markus Wilken[1], Magriet A. van der Nest[1,2], Michael J. Wingfield[1] & Brenda D. Wingfield[1]

[1] Department of Biochemistry, Genetics and Microbiology, Forestry and Agricultural Biotechnology Institute (FABI), Faculty of Natural and Agricultural Sciences, University of Pretoria, Hatfield Campus Pretoria, 0083, South Africa

[2] Biotechnology Platform, Agricultural Research Council (ARC), Onderstepoort Campus, Pretoria, 0110, South Africa

ABSTRACT

Sexual reproduction is a highly conserved feature of the Eukaryotes, yet sexual compatibility is determined by a wide variety of mechanisms. In ascomycete fungi, sexual development is controlled by genes at the mating type (*MAT*) locus that confer either MAT1-1 or MAT1-2 mating identity. Although the locus harbours, at minimum, a single gene, the *MAT* loci of certain species, including *Huntiella omanensis*, encode for two or more genes. The *MAT1-2* idiomorph of *H. omanensis* is made up of *MAT1-2-1*, a primary *MAT* gene that is highly conserved in the Pezizomycotina and possesses the HMG-box domain. This domain is a well-characterized DNA binding motif associated with transcription regulation. The idiomorph also harbours a novel secondary *MAT* gene, named *MAT1-2-7*, with no recognizable functional domain. In this study, we developed a transformation and genome editing system to characterize the *MAT1-2-7* gene with respect to its function in mating. We have shown that *MAT1-2-7* is essential for sexual reproduction and that isolates carrying the disrupted *MAT1-2-7* gene are incapable of ascomatal maturation. *MAT1-2-7* was also shown to influence the vegetative radial growth rate of *H. omanensis*, illustrating the pleiotropic effects associated with *MAT* genes.

1. INTRODUCTION

Sexual reproduction in ascomycetes is controlled almost entirely by genes present at the mating type (*MAT*) locus. At minimum, this includes the primary *MAT* genes, *MAT1-1-1* and *MAT1-2-1* [1,2]. However, other secondary genes can also be present, often in a lineage-specific manner. As the nomenclature suggests, the *MAT1-1-1* gene is the defining feature of the *MAT1-1* idiomorph, while the same is true of the *MAT1-2-1* gene at the *MAT1-2* idiomorph [3]. In heterothallic, or self-sterile, fungi, a single individual can be assigned a mating type based on the genic content of its *MAT* locus, with the *MAT1-1* idiomorph conferring the MAT1-1 mating type and the *MAT1-2* idiomorph conferring the MAT1-2 mating type [1].

At present, there is no clear definition of a *MAT* gene. This is in part due to the limited number of functional studies on these genes, particularly in non-model species, but also the fairly extensive variation in the genic content of the *MAT* locus [2]. Some authors have classified a *bona fide* MAT protein as one that allows for internuclear recognition and that is functional only when expressed from the *MAT* locus [4]. This definition is highly restrictive as it relies on the functional characterization of these genes as well as the ability to precisely track the expression and location of the protein during sexual reproduction. It also does not consider the many other processes involved in sexual reproduction that are not linked to recognition but remain essential for the production of recombinant offspring. Other authors define the *MAT* locus simply as a location in the genome responsible for mating, and thus a *MAT* gene is a gene that resides within this locus [3,5]. This definition does not rely on functional characterization and is thus more relevant in non-model fungi where gene characterization has not yet been possible.

The locus-specific definition for a mating gene has led to the description of many *MAT* genes (as recently reviewed [5]). Of these, the *MAT1-1-1* and *MAT1-2-1* genes fulfil an essential role in the mating process and are found in almost all studied species [6–8]. They are thus considered the primary mating genes. In comparison, the secondary *MAT* genes are not as well-conserved and often do not have recognizable conserved domains [5]. These genes have been named numerically in the order of their discovery in various species [3]. Thus, for

example, *Cryphonectria parasitica* harbours the *MAT1-1-2* and *MAT1-1-3* genes at the *MAT1-1* idiomorph [9]; while the *MAT1-2-2* and *MAT1-2-9* genes are harboured in the *MAT1-2* idiomorphs of *Neurospora crassa* [10] and *Fusarium fujikuroi* [5,11], respectively.

Functional characterization of the *MAT* genes in diverse fungal species has predominantly focused on *MAT1-1-1* and *MAT1-2-1*, and in some cases, has even concentrated specifically on their functional domains. These genes have been shown to be essential for sexual reproduction in model and non-model species alike [6–8,12]. The precise functions of *MAT1-1-1* and *MAT1-2-1* are also fairly well-conserved, with both primary genes often playing important roles during the initiation of sexual reproduction. However, while these genes are well-characterized, similar research is lacking with respect to the secondary *MAT* genes. The few examples that do exist include the *Fusarium graminearum MAT1-1-2* and the *Botrytis cinerea MAT1-1-5*, both of which are important for the maturation of the ascomata [13,14]. In addition to their role in mating, *MAT* genes can also influence other important non-mating factors, such as pathogenicity, growth and vegetative incompatibility [15,16].

Huntiella omanensis, a member of the Ceratocystidaceae [17], has recently been the topic of genomic and transcriptomic studies with respect to its sexual development [18,19]. MAT1-1 isolates of this fungus possess the *MAT1-1-1* and *MAT1-1-2* genes, while the MAT1-2 isolates harbour the *MAT1-2-1* and *MAT1-2-7* genes [18]. *MAT1-1-1*, *MAT1-1-2* and *MAT1-2-1* all encode proteins that are comparable to those encoded by this locus in other species and they each possess the expected functional domains associated with these proteins. In contrast, *MAT1-2-7* was first detected *in silico* and showed no similarity to any other known genes. It also encoded a protein with no recognizable functional domains [18]. Later the gene was found to be expressed during sexual reproduction despite undetectable expression levels during the vegetative growth phase [19]. Its position within the *MAT* locus combined with its expression pattern thus suggested that this gene might have a role in the sexual process.

Huntiella moniliformis, a close relative of *H. omanensis*, possesses a significantly truncated and likely non-functional version of the *MAT1-2-7* gene [18]. Interestingly, this species also

undergoes unisexual reproduction, unlike the many heterothallic species found in this genus [18]. It has thus been hypothesized that *MAT1-2-7* plays a role in the regulation of sexual reproduction in these species and that its truncation in *H. moniliformis* leads, at least in part, to the homothallic behaviour observed in this species [19]. However, *H. moniliformis* also exhibits an interesting pheromone expression pattern, with a single isolate capable of producing both mating pheromones. This is unlike *H. omanensis*, which, similar to many heterothallic species, expresses the pheromones in a mating-type dependent manner [19]. It is not known whether the truncation of the *MAT1-2-7* gene, the indiscriminate pheromone expression or a combination of both has led to unisexual reproduction.

The aim of this study was to characterize the *H. omanensis MAT1-2-7* gene with respect to its involvement in mating. This was achieved by developing a protoplast-based transformation and CRISPR-Cas9 genome editing protocol for use in the first successful genetic modification of any species within the genus *Huntiella*. The *H. omanensis MAT1-2-7* gene was confirmed as an essential mating gene that plays an important role in ascomatal maturation.

2. METHODS AND MATERIALS

2.1 Strains and culture conditions

Four wild type isolates of *H. omanensis* were used in this study, two MAT1 isolates (CMW 44436 and CMW 44437) and two MAT2 isolates (CMW 44439 and CMW 44442). Additionally, two independent *MAT1-2-7* mutant strains were derived from the CMW 44442 MAT2 isolate (as detailed below). These isolates have been named *ΔMAT127-H1* (CMW 54810) and *ΔMAT127-H4* (CMW 54811). Unless otherwise stated, the isolates were cultured and maintained on 2% malt extract agar, supplemented with 100 $mg.L^{-1}$ thiamine hydrochloride and 150 $mg.L^{-1}$ streptomycin sulphate salt (Sigma, St Louis, USA) and is referred to as MEA-ST. The cultures were maintained at 22 °C in a standard light-dark cycle. These cultures have been preserved in the culture collection (CMW) of the Forestry and Agricultural Biotechnology Institute (FABI) at the University of Pretoria in South Africa.

2.2 sgRNA design, synthesis and transcription

The single guide RNA (sgRNA) is an RNA molecule that allows the Cas9 protein to recognize the genomic region of interest and allows for DNA cleavage at a targeted region [20]. It is comprised of a 20 bp region called the protospacer which corresponds to the genomic location to be targeted and a longer scaffold region that physically binds to the Cas9 protein. Together, the sgRNA and Cas9 protein form the ribonucleoprotein (RNP) which is capable of creating targeted dsDNA breaks [21]. The sgRNA used to target the *H. omanensis MAT1-2-7* gene (Figure 1) was designed to adhere to the following parameters, 1) the 20 nt protospacer was found directly upstream of a 5' NGG 3' protospacer adjacent motif (PAM), a motif which is specifically targeted by the *Streptococcus pyogenes* Cas9 enzyme used below, 2) the protospacer together with the PAM sequence showed no significant similarity to any other regions of the *H. omanensis* genome, 3) the combined sgRNA construct passed a number of RNA folding restrictions, 4) the protospacer targeted the 5' region of the gene near the point targeted for the introduction of the in frame stop codon.

These parameters were satisfied by annotating each of the 5' NGG 3' sequences in the *MAT1-2-7* gene and filtering through the potential sgRNA constructs. Each of the PAM sequences and the adjacent 20 nt, representing the potential protospacer, were used in local BLASTn searches against the *H. omanensis* genome to detect any potential off-target effects. Those that passed these initial control steps were subjected to RNA folding analysis using the RNAfold webserver [22], with default settings. In order for sgRNA molecules to efficiently target the correct region of the genome and bind the Cas9 enzyme, constructs needed to have similarly structured minimal free energy and centroid secondary structures; each made up of three stem loops and five rings. The secondary structures should also have high base pairing probabilities throughout the structure, with the exception of the 5' terminal region where the protospacer is located. The sgRNA that passed all of these requirements and that targeted the most 5' region of the gene was selected for use.

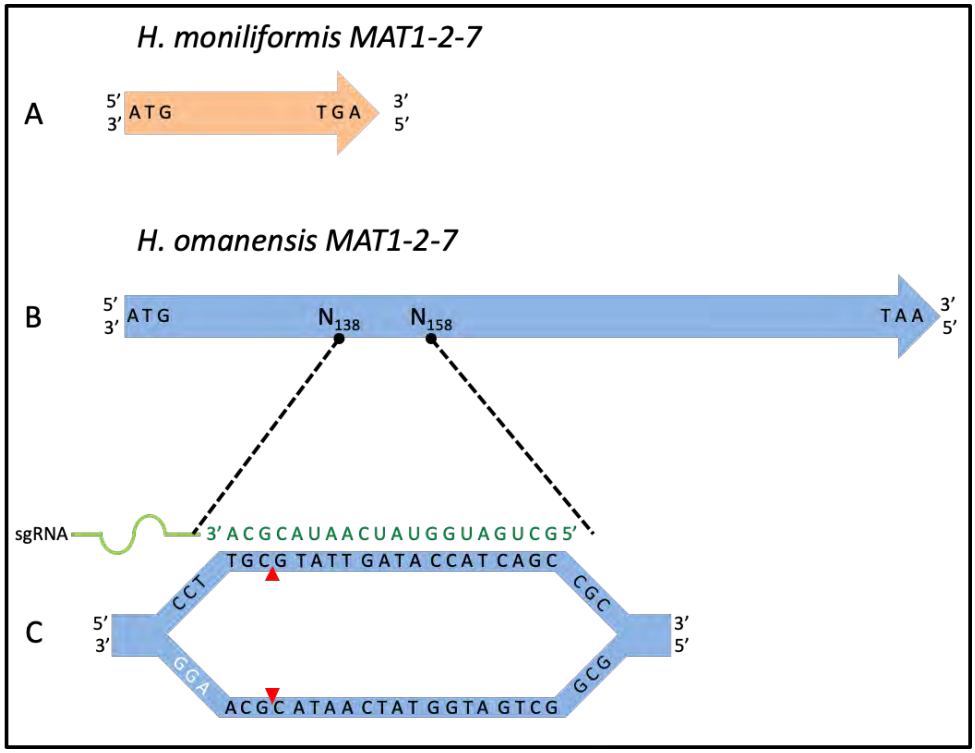

Figure 1: The design of the sgRNA. The sgRNA was designed in such a way to ensure that the knockout of the *H. omanensis MAT1-2-7* gene resulted in gene truncation similar to that seen in *H. moniliformis*. The designed sgRNA targets the N_{138} to N_{158} region of the *H. omanensis MAT1-2-7* gene as it is in this region that the premature stop codon is found in the *H. moniliformis MAT1-2-7*. **A)** The *H. moniliformis MAT1-2-7* gene is only 147 nt in length and thus less than a third of **B)** the *H. omanensis MAT1-2-7* gene, which is 468 nt in length. **C)** Illustration of the sgRNA target region. The scaffold of the sgRNA is indicated in light green with the protospacer sequence indicated by the adjacent green nucleotides. The PAM sequence is indicated as white text on the bottom strand. The predicted Cas9 cut site is indicated by the red arrows.

The full-length sgRNA was synthesized by Twist Biosciences (San Francisco, USA) as a dsDNA molecule. This construct was then amplified using primers targeting the protospacer and scaffold sequence. The forward primer was designed to include a 5' overhang harbouring a T7 promoter (Figure S1). The construct was amplified using Phusion High-Fidelity DNA polymerase (ThermoFisher Scientific, Waltham, USA) following the manufacturer's instructions (Table S1). The resulting DNA products were visualized on a 2% SeaKem® LE agarose gel (Lonza, Rockland, USA) stained with GelRed™ (Biotium, Fremont, USA) and electrophoresed at 100V for 20 min. PCR products were purified using a 6.66% G-50 Sephadex solution (Sigma, St Louis, USA) and Centri-Sep spin columns (Princeton Separations, Freehold, USA), using the manufacturer's instructions. The cleaned products were cycle-sequenced using a BigDye Terminator Cycle Sequencing Kit v3.1 (Life Technologies, Carlsbad, USA) (Table S2).

The construct was subsequently transcribed using the HiScribe™ T7 Quick High Yield RNA synthesis kit (New England Biolabs, Ipswich, USA) in accordance with the manufacturer's instructions. This entailed incubating approximately 1μg of target DNA together with the T7 RNA polymerase at 37°C for 16 hours. The transcribed sgRNA was then visualized as above.

2.3 *In vitro* testing of sgRNA

The cleavage ability of the designed and synthesized sgRNA was tested *in vitro*. This entailed incubating a PCR product which included the target region together with the RNP complex. The PCR product was produced using FastStart Taq DNA Polymerase (Roche, Basel, Switzerland) and primers targeting an 872 bp region of the *MAT1-2-7* gene (Figure S2 and Table S3). Successful and targeted Cas9-mediated cleavage of this PCR product would yield two DNA products 737 and 135 bp in length (Figure S2).

The RNP was produced using the sgRNA synthesized and transcribed as described above as well as the EnGen® Spy Cas9 NSL protein (New England Biolabs, Ipswich, USA) following the manufacturer's instructions (Figure S1). In short, a solution of 30nM sgRNA, 30nM Cas9 protein, 10X NEBuffer 3.1 and ddH_2O was prepared and incubated at 25°C for 10 min. The target DNA was added to a final concentration of 3 nM and the solution was incubated for a further 15 min at 37°C. In order to stop the reaction, 3 μg of Proteinase K (Sigma, St Louis, USA) and 2 μg of RNase A (Roche, Basel, Switzerland) were subsequently added. The reaction was incubated at room temperature for 10 min. The resulting DNA products were visualized as above.

2.4 dDNA design

Upon Cas9-induced cleavage, the cell will attempt to repair the cut, by either using non-homologous end joining or homology directed repair [23]. In the latter case, a construct harbouring a sequence of interest can be provided in the form of a donor DNA (dDNA). This allows for the introduction of foreign DNA directly into the region being cut. The dDNA includes the sequence to be introduced flanked by arms that are

homologous to the region being targeted by the sgRNA. In this study, the dDNA was made up of homologous arms flanking the *BclI* restriction site (5' TGA TCA 3') and a hygromycin B resistance cassette (Figure 2). The dDNA was designed to ensure the stop codon encoded by the BclI site (TGA) was in frame with the coding region of the *MAT1-2-7* gene, thereby introducing a premature stop codon. The position of this stop codon was also designed to be at the same position as the premature stop codon found in the *H. moniliformis MAT1-2-7* and thus allowed the *H. omanensis MAT1-2-7* to be truncated in a manner similar to that of *H. moniliformis*. The introduction of the hygromycin resistance cassette allowed for the selection of successfully transformed isolates.

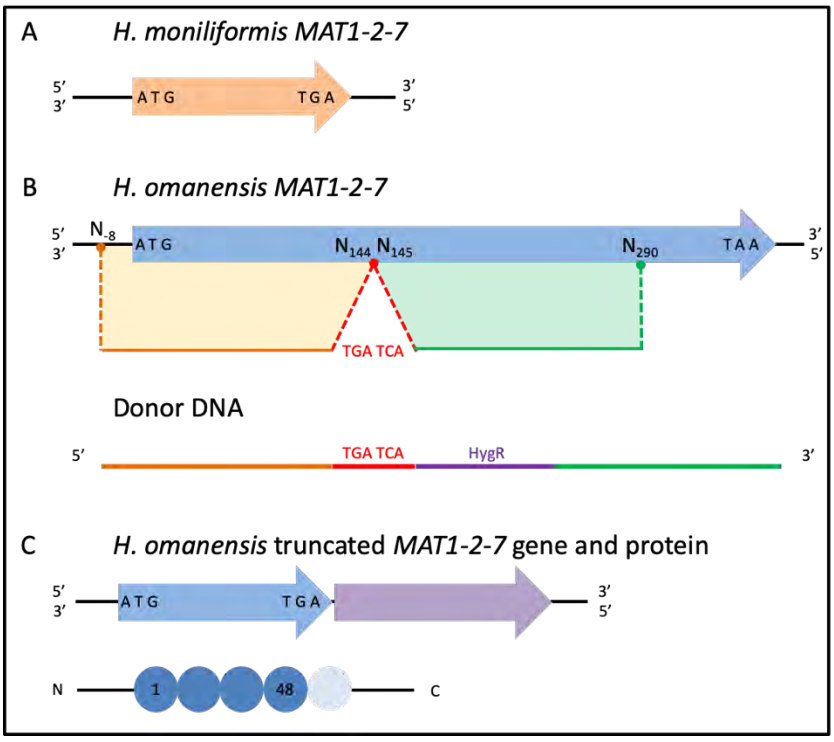

Figure 2: Designing the donor DNA. The dDNA, similar to the sgRNA, was designed to ensure that the knockout of the *H. omanensis MAT1-2-7* gene resulted in gene truncation similar to that seen in *H. moniliformis*. **A)** The premature stop codon (TGA) found in the *H. moniliformis MAT1-2-7* gene is at nucleotide positions N_{145} – N_{147} and codon position C_{49}. **B)** The donor DNA has been designed to including the *BslI* restriction enzyme (RE) cut site (red) and the hygromycin B resistance cassette (purple), flanked by regions of homology (orange and green) to the genomic region harbouring the *MAT1-2-7*. The RE site was designed to occur in frame with the *MAT1-2-7* coding sequence and thus introduces the stop codon, TGA, leading to the premature termination of translation. **C)** After Cas9-mediated cutting and homologous recombination of the dDNA, the *H. omanensis MAT1-2-7* gene possessed a premature stop codon which would result in the translation of a 48 aa protein. The gene models are not drawn to scale.

Originally, the dDNA was designed to be inserted into a plasmid harbouring an independent hygromycin resistance cassette and thus a dDNA molecule consisting of only the *MAT1-2-7*-homologous flanking regions and the *BclI* restriction site was synthesized by Twist Biosciences (San Francisco, USA) as a dsDNA molecule. The full length dDNA also harbouring the hygromycin B resistance cassette was thus assembled using a step-wise, overhang PCR approach (Figure S3, Tables S4 – S9). This entailed amplifying the 5' and 3' regions of the synthesized construct using primers with overhangs homologous to the sequence of the hygromycin B resistance cassette. The entire hygromycin B resistance cassette was amplified in a single reaction from the pcb1004 plasmid [24]. These resultant PCR products were then used in a single amplification reaction to produce the single, full-length dDNA construct. Each of the intermediate and final PCR products were visualized, purified and sequenced as above.

2.5 Protoplast extractions

A protoplast extraction protocol was optimized for use in *Huntiella* species using a combination of the *Magnaporthe oryzae* and other filamentous ascomycete protoplast extraction protocols [25,26] with a number of species-specific alterations. A mycelial plug was inoculated in 200ml of 2% (w/v) malt extract broth and allowed to grow for between 24 and 48 hours with shaking at 100 rpm at 25 °C. To harvest conidia, the resulting liquid culture was filtered through a single layer of Miracloth® (Merck, New Jersey, USA) and centrifuged at 4000 rpm for 10 mins at 4 °C in an Eppendorf 5810 R centrifuge. The pellet was resuspended in 200ml of 1% (w/v) malt extract broth and allowed to grow for up to 12 hours as above. The resulting germlings and young mycelial strands were harvested by centrifugation at 4000 rpm for 10 mins at 4°C, followed by resuspension in 1M sorbitol (Sigma, St Louis, USA). This solution was either used immediately in enzymatic degradation reactions or stored at -80°C.

The germlings and young mycelia were subjected to enzymatic degradation by *Trichoderma harzianum* lysing enzymes (Sigma, St Louis, USA). The enzyme concentrations, final volumes and incubation times are summarized in Table 1. In general, 1 ml germling/mycelia solution was added to 9 ml enzyme solution and

incubated at 25 °C with shaking at 80 rpm. The resultant protoplast suspension was filtered through Miracloth® and then centrifuged at 3000 rpm for 10 mins. The protoplast pellet was carefully resuspended in 300ul STC buffer (20% sucrose, 50mM Tris-HCl pH 8.00 and 50mM $CaCl_2$). Protoplasts were either used immediately in transformation experiments or stored at -80 °C.

Table 1: Degradation of the germling/mycelia solution with lysing enzymes from *Trichoderma harzianum*

Reaction	Enzyme Concentration	Degradation Time
A	1.250 μg.ml^{-1}	3 hours
B	1.875 μg.ml^{-1}	3 hours
C	2.500 μg.ml^{-1}	2.5 hours
D	3.750 μg.ml^{-1}	2.5 hours
E	4.375 μg.ml^{-1}	2 hours
F	5.000 μg.ml^{-1}	2 hours

2.6 Transformations

A single transformation reaction consisted of protoplasts, sgRNA-Cas9 RNPs and the dDNA construct. The RNP was assembled as detailed above and in accordance with manufacturer's suggestions, using 3 μM solutions of each reagent. These were combined with the 1X Cas9 reaction buffer to a total volume of 12.5 μl. This solution was incubated at room temperature for 10 min.

Approximately 5 x 10^6 protoplasts, a single volume of the RNP solution and 6 μg of the dDNA construct were co-incubated on ice for 20 mins. Subsequently, a freshly prepared 30% PTC (polyethylene glycol 8000 in STC buffer) solution was slowly dripped onto the protoplast solution, creating a hydrophobic layer above the cells. This solution was incubated for a further 20 min at room temperature. An osmotic control medium (OCM- 0.3% yeast extract, 20% sucrose, 0.3% cas-amino acids) was added to the protoplast solution and incubated with shaking at 80 rpm over night at

room temperature. The solution was divided into five Petri dishes and covered with OCMA medium (OCM + 1% agar) supplemented with 30 ug.ml^{-1} hygromycin B from *Streptomyces hygroscopicus* (Sigma, St Louis, USA). Once set, this medium was covered with a layer of OCMA medium supplemented with 40 ug.ml^{-1} hygromycin B. Single isolates that were able to grow through the top layer of medium were transferred to MEA supplemented with 50 ug.ml^{-1} hygromycin B (MEA-50).

2.7 Confirmation of transformants and stability of the insert

Isolates that were capable of growth on MEA-50 were subjected to single hyphal tip isolations and transferred to MEA-ST. DNA was extracted from these isolates after five days of growth as described in previous studies [18]. Extracted DNA was subjected to PCR amplification using primers targeting the 5' and 3' integration regions as well as the entire length of the integrated dDNA construct (Figure S4). These reactions were conducted using LongAmp® Taq (New England Biolabs, Ipswich, USA) according to the manufacturer's instructions (Table S10). PCR products were visualized, purified and sequenced as above.

To ensure that the dDNA had integrated only at a single site in the genome, DNA from the two mutant isolates was subjected to Southern blot analysis. Genomic DNA (30µg per isolate per enzyme) was digested using HindIII and EcoRI (ThermoScientific, Waltham, USA), in individual reactions and in accordance with the manufacturer's instructions. Digestions were conducted at 37 °C for 16 hours and were inactivated by incubation at 80 °C (HindIII) and 65 °C (EcoRI) for 20 mins. The digested gDNA fragments were subsequently separated on a 0.75% agarose gel and electrophoresed for 90 mins at 80V in 1x TAE buffer. The subsequent DNA transfer from the gel onto a nylon membrane was conducted as previously described [27]. The membrane was then subjected to probe hybridization and visualization as per the manufacturer's manual [28]. In short, a DIG-labelled probe was synthesized using a PCR-approach and DIG-labelled dNTPs (Sigma, St Louis, USA, Table S11). The probe was designed to target a short, 336 bp region of the hygromycin resistance cassette. Once the probe was hybridized to the membrane, the membrane was treated with a 1:5000 solution of anti-digoxigenin-AP (Sigma, St Louis, USA). This was followed by incubation in a 1:5

NBT/BCIP colour substrate solution (Sigma, St Louis, USA). The colour precipitation reaction was allowed to develop for 2.5 hrs, before the membrane was neutralized and washed with double distilled water.

In order to test the stability of the integration of the hygromycin cassette, the knockout strains were alternatively transferred media supplemented with hygromycin B to media without antibiotic supplementation (Figure S5). This was conducted three times and each isolate was allowed to grow for three days at 25 °C before being transferred to fresh media.

2.8 Phenotypic analysis of the wild type and mutant strains

2.8.1 Mating tests

The ability of each knockout strain to produce ascomata was assessed and compared with that of the wild type isolates. Two media types were used to induce ascomatal development: MEA-ST as detailed above as well as 2% potato dextrose agar supplemented with 100 $mg.L^{-1}$ thiamine hydrochloride and 150 $mg.L^{-1}$ streptomycin sulphate salt (PDA-ST). Plates for mating tests were set up by co-incubating two isolates on a single plate, approximately 2cm apart. The plates were not wrapped closed with parafilm, which is the standard procedure when culturing these fungi. Each of the six isolates used in this study were crossed with each other, thereby producing a total of 15 potential mating combinations (Table S12). Additionally, all isolates were also cultured in isolation to assess whether they were able to undergo unisexual reproduction. The cultures were incubated at 20 °C for a total of 21 days and were visually inspected for ascomatal production and maturation as well as ascospore exudation every 24-36 hours. Where mature ascomata and ascospores were produced, single ascospore masses were inoculated onto fresh MEA-ST plates and assessed for the production of ascomata, and thus the fertility of these spore masses, after seven days.

2.8.2 Conidial production

The efficiency of isolates to produce conidia (asexual spores) was assessed for each knockout strain and the four wild type strains. This made it possible to determine

whether the *MAT1-2-7* disruption had any effect on number of conidia produced in five-day-old cultures. To achieve this, 8 mm diameter mycelium-covered agar plugs were excised from cultures, submerged in water and agitated. The displaced conidia were counted using a haemocytometer (Marienfeld, Harsewinkel, Germany). Three independently growing cultures of each isolate were used and a total of three agar plugs were used per culture (Figure S6). The average number of conidia produced by the mutant strains was compared with that of the conidia produced by the MAT1-1 and MAT1-2 wild type isolates using a two-tailed, independent t-test in Excel.

2.8.3 Growth rate

The growth rate of each knockout strain and all four wild type strains was assessed to determine whether the disruption of the *MAT1-2-7* gene had any effect on vegetative growth. This was achieved by excising 5 mm diameter mycelium-covered agar plugs and inoculating these onto sterile MEA-ST plates. Five plates of each isolate were used, and these cultures were grown for three days at 20 °C. Two measurements of colony diameter were taken perpendicular to each other at 60 hours post inoculation. The two measurements were averaged to produce a mean diameter of growth. The growth of each of the mutant strains was compared with that of the growth of the wild type isolates of both mating type using a two-tailed, independent t-test in Excel.

2.9 RNA extraction, cDNA synthesis and RT-PCR

RNA was extracted from five day-old, vegetatively-growing isolates including the two mutant strains as well as a MAT1 isolate (CMW 44436) and a MAT2 isolate (CMW 44442). RNA was also extracted from a five-day old MAT1-1 (CMW 44436) x Δ *MAT127-H4* cross that produced protoascomata. These cultures were grown on MEA-ST overlaid with cellophane to allow for easy tissue harvesting. A total of three biological and three technical repeats were used, translating to nine MEA-ST plates of fungal tissue per isolate type.

Harvested tissue was flash frozen in liquid nitrogen and, using a sterile mortar and pestle, was ground into a fine powder. Total RNA was extracted using the RNeasy® Mini Kit (Qiagen, Limburg, The Netherlands) following the manufacturer's protocols.

The RLC extraction buffer was used and the optional on-column DNase1 treatment was conducted. Gel electrophoresis (2% agarose gel, 120V, 25 min) was used to assess the integrity of the recovered RNA. The concentration of the RNA was estimated using an ND 1000 spectrophotometer (ThermoScientific, Waltham, USA).

The RNA was converted to cDNA using the RevertAid H Minus First Strand cDNA Synthesis Kit with oligo(dT)18 primers (ThermoScientific, Waltham, USA) to select for mRNA transcripts. In this synthesis reaction, 1 µg of total RNA, 0.5 mM primers and RNase-free water to a final volume of 5µl were combined and incubated for 5 minutes at 70°C, followed by incubation on ice for at least 5 minutes. This 5 µl reaction was then added to a solution containing 1X reaction buffer, $MgCl_2$ to a final concentration of 8mM, total dNTPs to a final concentration of 1 mM, 160 units of reverse transcriptase and RNase-free water to a final volume of 15 µl. The final 20 µl reaction was then incubated at 25°C for 5 minutes, 42°C for 1 hour and 70°C for 15 minutes. The resulting cDNA was diluted (1:20, 1:50, 1:100, 1:500, 1:1 000, 1:10 000, 1:100 000, 1:1 000 000 and 1:10 000 000) and subjected to PCR amplification using primers that targeted the two pheromone genes, the two pheromone receptors and *MAT1-2-1* (Figure S7, Table S13). The dilution series of cDNA allowed for a semi-quantitative measurement of each of the genes' expression. Where possible, these primers were designed to flank introns to ensure that potential gDNA contamination could be identified if present. PCR products were visualized and purified as above. The PCR products were also sequenced as described above to precisely confirm the predicted intron/exon boundaries and to determine if alternatively spliced transcripts of these genes were present.

3. RESULTS

3.1. sgRNA_2 successfully cleaves the *MAT1-2-7* target sequence *in vitro*

A total of 13 potential sgRNA molecules were predicted from the *H. omanensis MAT1-2-7* gene (Table 2). A single construct, sgRNA_7, showed significant similarity to another region in the *H. omanensis* genome and was thus not considered in further analyses. Of the remaining 12 potential sgRNA molecules, four passed the RNA folding

parameters, showing similar minimal free energy and centroid structures, with high binding probabilities. Finally, sgRNA_2 was chosen for further *in vitro* testing given that it targeted the most 5' region of the gene of the remaining sgRNA constructs (Figure 3).

The sgRNA_2 could support the efficient cleavage of the PCR product harbouring the target sequence. Gel electrophoresis revealed a significant length difference between the full-length PCR product (above 800 bp) and the cleaved product (above 700 bp). This sgRNA was thus used for the *in vivo* genome editing experiments.

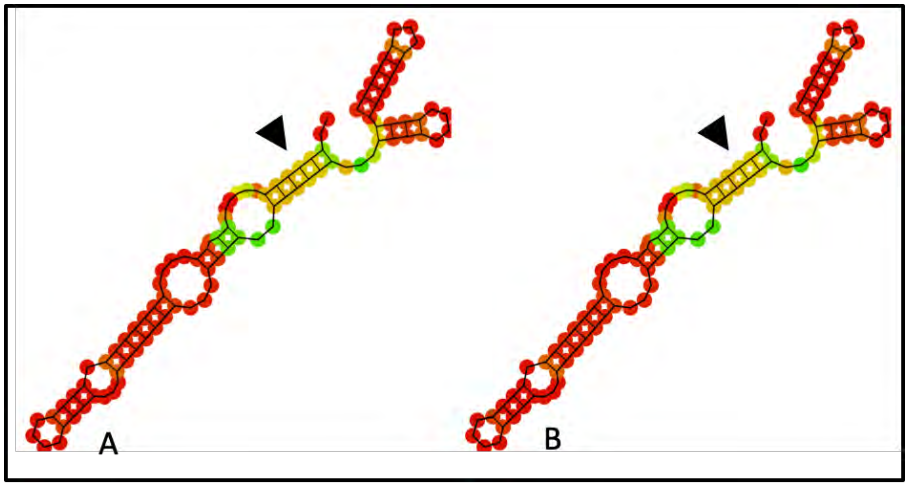

Figure 3: The secondary structures of sgRNA_2. A) The minimal free energy structure. **B)** The centroid structure. In both cases, high binding probabilities are indicated by red and dark orange coloured nucleotides, while lower probabilities are indicated in light orange, yellow and green. Both structures also have three stem loop structures, with five ring structures in the major step loop. The black arrows indicate the region encoding the protospacer with lower secondary structure binding probabilities.

Table 2: The identified protospacer regions of the sgRNA molecules and their target positions in the *H. omanensis MAT1-2-7* gene

Name	Strand	Position	Protospacer and PAM Sequences [a]	Reason for exclusion
sgRNA_1	-	126 – 148	TCAATACGCAAGGATGGATGAGG	Folding
sgRNA_2	-	136 – 158	GCTGATGGTATCAATACGCAAGG	Chosen
sgRNA_3	-	158 – 180	GATGACGTCGAGCAAAGAGGCGG	Folding
sgRNA_4	-	161 – 183	GGGGATGACGTCGAGCAAAGAGG	Position
sgRNA_5	-	183 – 205	AGTTCTGGAGATATCGATTTGGG	Folding
sgRNA_6	-	198 – 220	GTGGCTGTTGGAAGCAGTTCTGG	Folding
sgRNA_7	-	210 – 232	TTGTAAAGGGCGGTGGCTGTTGG	Specificity
sgRNA_8	-	237 – 259	GTTTCTTGAACAGAAGGGGGAGG	Folding
sgRNA_9	+	271 – 293	AAAGGCTTTATGGGGATTTCCGG	Position
sgRNA_10	-	290 – 312	GTATCGGTACATGTATCGACCGG	Folding
sgRNA_11	-	335 – 357	ATCTTCTGGGAGATCAAGCATGG	Position
sgRNA_12	+	342 – 364	TGATCTCCCAGAAGATGCAGTGG	Folding
sgRNA_13	+	353 – 375	AAGATGCAGTGGCATTGCATGGG	Folding

[a] The sequence of the protospacer is indicated in black text, the PAM sequence is indicated in red text and the scaffold sequence is not indicated. All sequences are written in a 5' to 3' orientation.

3.2. Two knockout strains were isolated, *ΔMAT127-H1* and *ΔMAT127-H4*

A total of 26 isolates were capable of growing through the OCMA medium supplemented with 40 ug.ml^{-1} hygromycin B. After transfer to MEA-50, 17 were capable of sustained growth and were thus considered successful transformants. PCR amplification and sequencing of the 5' and 3' integration sites showed that the dDNA had successfully integrated into the target region of two independent strains. Both integration events had resulted in the successful truncation of the *MAT1-2-7* gene (Figure 4). These mutant strains, named *ΔMAT127-H1* and *ΔMAT127-H4,* showed exactly the same gene disruption pattern, harbouring the premature stop codon as well as the hygromycin resistance cassette at the region expected. In both cases, the stop codon was introduced at nucleotide position 145 of the gene. Thus, if expressed,

the gene would produce a protein product of only 48 aa, which is likely to be non-functional. Both isolates also showed stable integration of the hygromycin resistance cassette, as observed by the alternated transfers of these isolates from antibiotic-supplemented to unsupplemented media (Figure 5). Southern blot analysis confirmed the homologous integration of the hygromycin resistance cassette at a single region in the genome as well as the absence of heterologous integration of the cassette at other locations (Figure 5). Phenotypic analyses on both mutant strains showed very similar phenotypes.

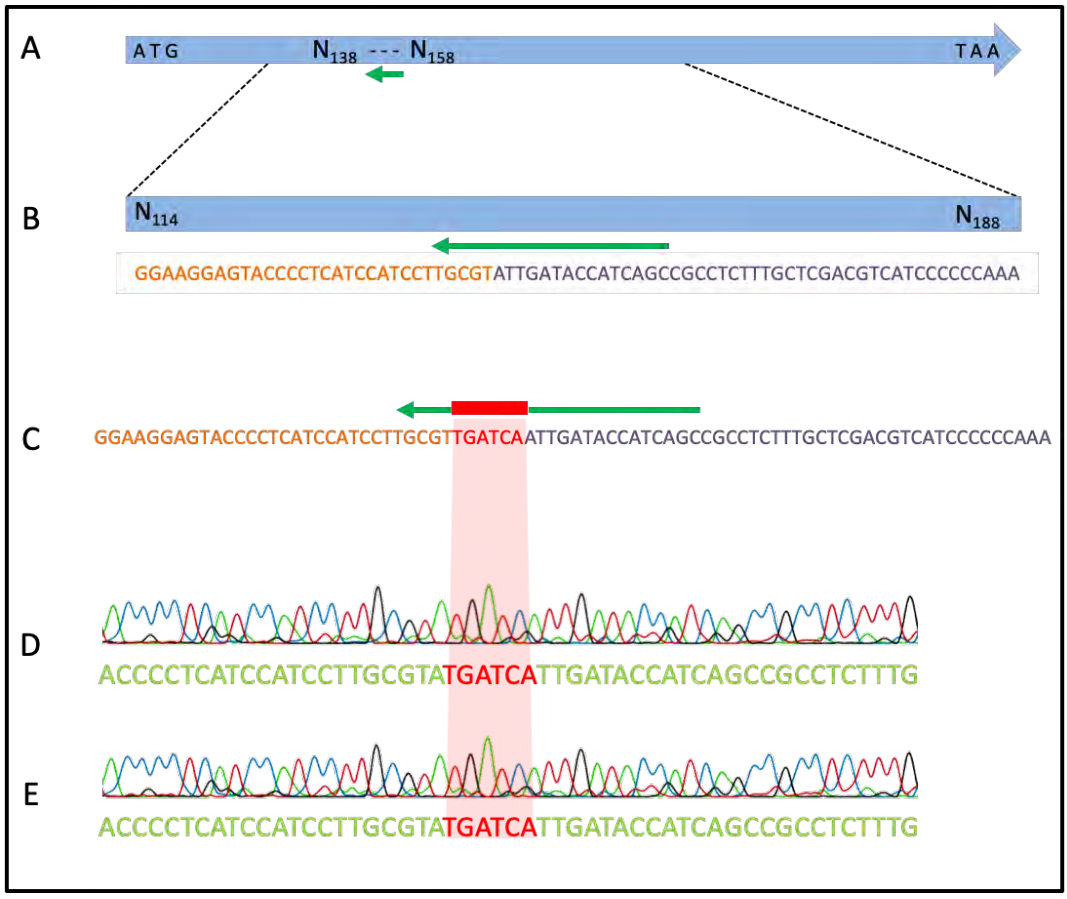

Figure 4: The successful integration of the BclI restriction enzyme site, including the TGA stop codon, into the *MAT1-2* idiomorph of *H. omanensis*. A) The full length *H. omanensis MAT1-2-7* gene, with the sgRNA target site indicated by the green arrow between nucleotides 138 and 158. **B)** A magnified schematic of the sgRNA target site within the *H. omanensis MAT1-2-7* gene. **C)** A magnified schematic of a region of the dDNA showing the BclI RE site flanked by arms homologous to the *MAT1-2* locus of *H. omanensis*. **D)** and **E)** Sanger sequence chromatogram indicating the successful integration of the BclI RE site into the *MAT1-2-7* gene of isolates *ΔMAT127-H1* and *ΔMAT127-H4,* respectively.

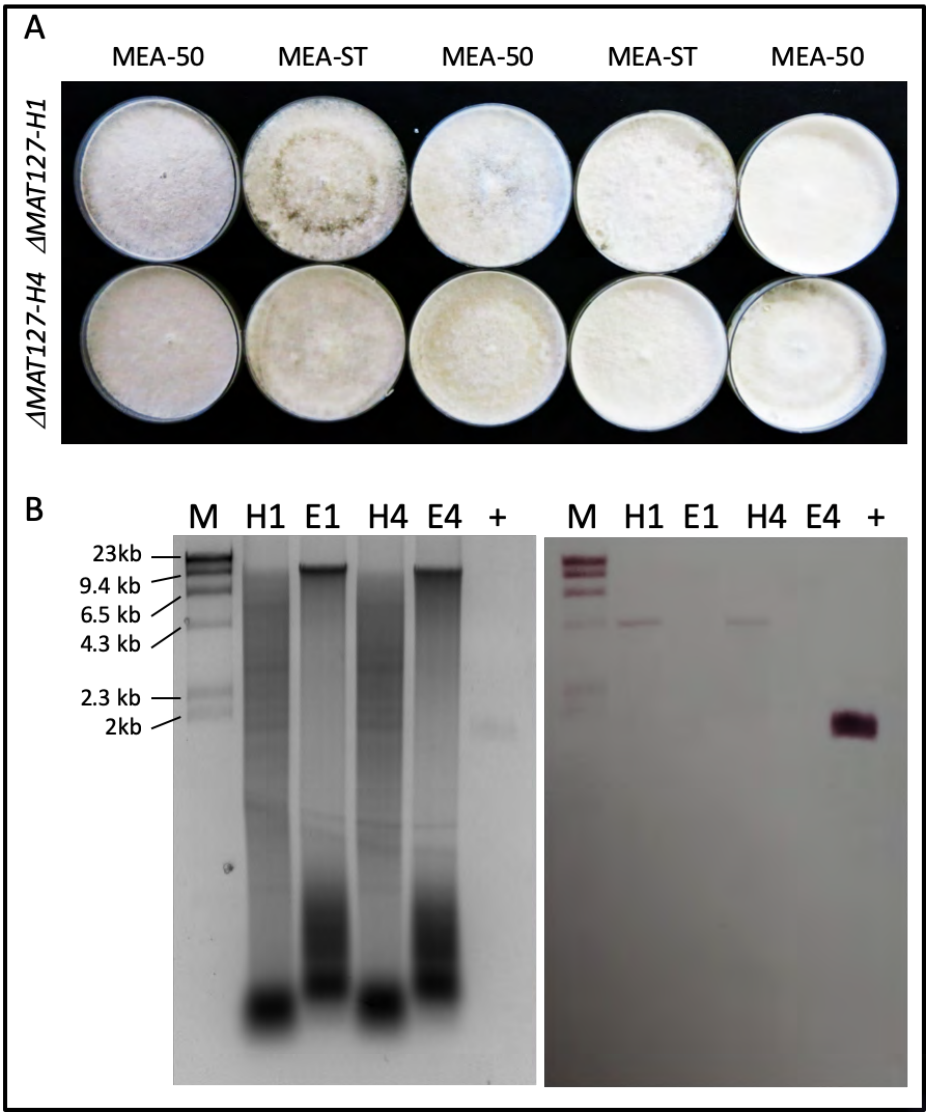

Figure 5: Integration stability and copy number of the hygromycin resistance cassette. A) The two mutant isolates, *ΔMAT127-H1* and *ΔMAT127-H4,* were alternatively transferred between hygromycin B supplemented media (MEA-50) and unsupplemented media (MEA-ST) to assess the stability of the hygromycin resistance cassette's integration in the *H. omanensis* genome. Sustained growth was observed on MEA-50 plates, subsequent to growth on MEA-ST plates, indicating that the cassette has been successfully integrated. **B)** In both mutant isolates, the hygromycin cassette was integrated only once into the genome. Lefthand panel: The digested gDNA from both mutant isolates on a 0.75% agarose gel. Righthand panel: The digested gDNA from both mutant isolates after being transferred to the nylon membrane and hybridized with the DIG-labelled probe.
M: DIG-labeled DNA marker, H1: *ΔMAT127-H1* DNA digested with HindIII, E1: *ΔMAT127-H1* digested with EcoRI, H4: *ΔMAT127-H4* digested with HindIII, E4: *ΔMAT127-H4* digested with EcoRI, +: positive control, PCR product of the entire hygromycin cassette.

3.3. *MAT1-2-7* disruption does not affect *MAT1-2-1* expression in *H. omanensis*

The *MAT* locus of many fungal species exhibits significant positional effects [4]. Thus, any disruption to the *MAT* locus may have unexpected effects on the other genes present within this region and may lead to unintentional phenotypic effects. In an effort to ensure that the disruption of the *H. omanensis MAT1-2-7* did not affect *MAT1-2-1*, we assessed the expression of the *MAT1-2-1* gene via RT-PCR. The expression of *MAT1-2-1* was detected in vegetatively growing isolates of both mutant isolates as well the wild type MAT1-2 isolate- CMW 44442 (Figure 6). The cDNA sequence for the mutant isolates was identical to that of the wild type MAT1-2 isolate. In all three isolates, the RNA had been fully processed and had undergone splicing to remove both introns. This indicated that the *MAT1-2-1* gene is expressed normally in the mutant strains and that any subsequent phenotypic differences were the result of *MAT1-2-7* disruption and not generalized *MAT* locus interference.

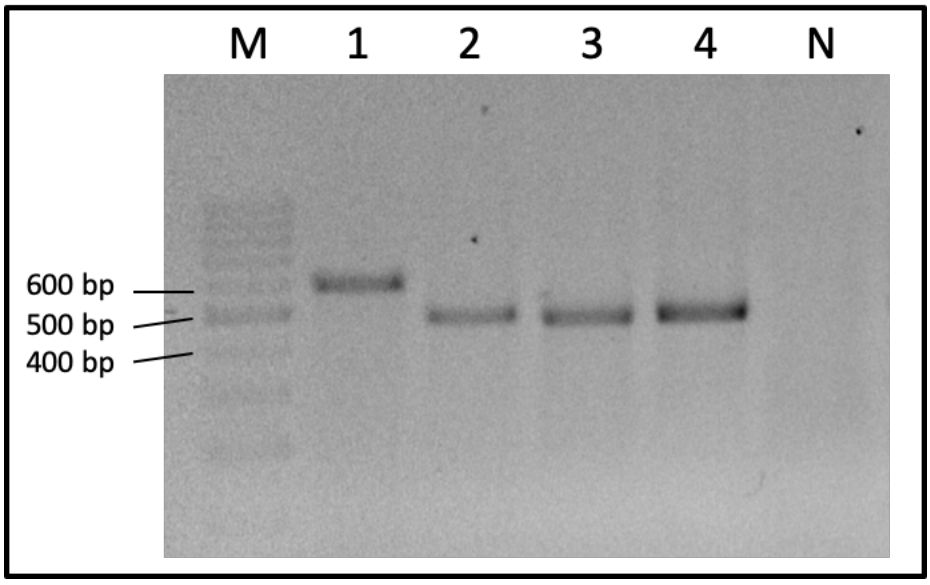

Figure 6: Expression and splicing of the *H. omanensis* *MAT1-2-1*. The *MAT1-2-1* gene of *H. omanensis* has a single intron of 53 nt which is spliced out after transcription. Lane 1 shows a *MAT1-2-1* PCR product derived from the gDNA of a MAT1-2 wildtype isolate (CMW 44442). Lanes 2 – 4 show the *MAT1-2-1* PCR products produced from the cDNA of a MAT1-2 wild type isolate (CMW 44442), and cDNA from the two mutant isolates, *ΔMAT127-H1* (CMW 54810) and *ΔMAT127-H4* (CMW 54811). The mutant isolates express the *MAT1-2-1* gene as expected and also correctly splice out the intron before translation- suggesting that the *MAT1-2-1* gene is unaffected by the disruption of the *MAT1-2-7* gene. Lanes M and N show the 100 bp molecular marker and negative control, respectively.

3.4. *MAT1-2-7* is essential for ascomatal development and maturation

Ascomatal development in *Huntiella* species (Figure S8) commences with the production of small, light-coloured, round protoascomata. This is followed by the emergence of a dark, beak-like structure from the young ascomatal base, which develops into an extended neck. During this process, the ascomatal base also darkens. Once mature, a sticky mass of ascospores is exuded from the tip of the neck.

In the crosses between MAT1-1 and MAT1-2 wild type isolates, mature ascomata were produced within 66 hours of co-inoculation and incubation at 20°C (Figure 7). The ascomata consisted of dark, globose bases with extended necks (Figure 8). A number of protoascomata were also seen at this stage in varying degrees of development; from light-coloured ascomatal bases with small beaks to darker bases with more pronounced immature necks. However, the majority of the ascomata were mature at this point. After approximately 90 hours, the ascomata began to exude ascospore masses from the tips of their necks. Ascospore masses that were transferred to sterile plates were capable of producing sexually-competent cultures within seven days (Figure 8).

At 66 hours post co-inoculation, matings between a wild type MAT1-1 partner and either of the two mutant MAT1-2 partners had produced only immature protoascomata (Figure 7). The majority of the ascomatal bases were light-coloured and only a few had begun to produce the dark, beak-like structures (Figure 8). A similar phenotype was observed at 90 hours, with very little maturation of the immature ascomata. After 114 hours, the majority of the bases had darkened but the beaks had not developed into extended necks. By 21 days post-inoculation, the protoascomata had not matured beyond young, beaked structures, with the exception of the occasional structure with a short neck. No ascospores were produced by these protoascomata. When broken open, even the most mature of the protoascomata were devoid of any spore contents (Figure 8).

We conducted a variety of control crosses between the two MAT1 isolates, the two MAT2 isolates and the two mutant isolates. We also paired each of the mutant

isolates with each of the MAT2 isolates. Additionally, each of the six isolates were cultured in isolation. In all of these cases, no sexual development was observed.

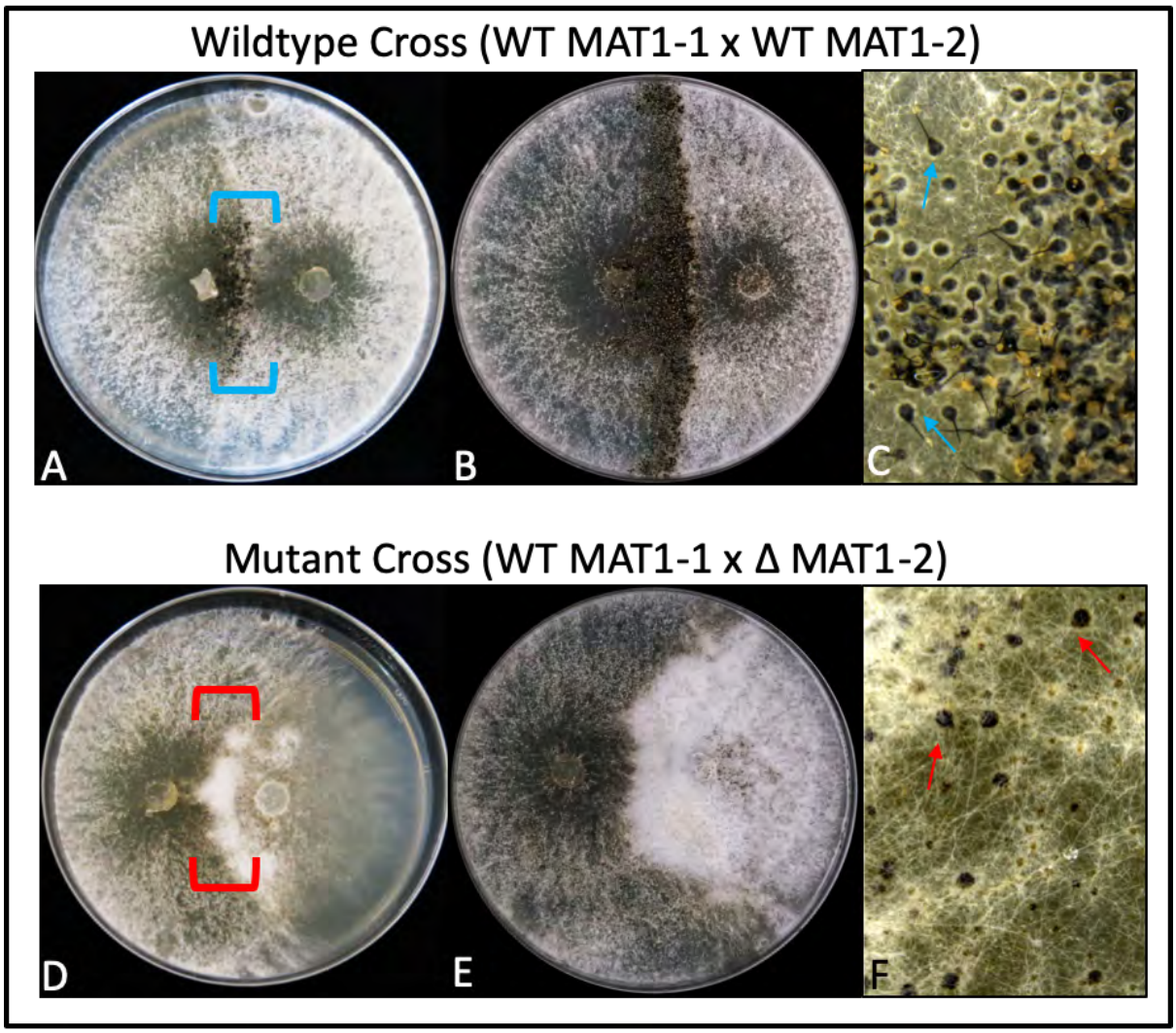

Figure 7: Sexual development in matings between wildtype isolates (top panel) and between a MAT1-1 wildtype isolate and a MAT1-2 mutant isolate (bottom panel). A) and **D):** Sexual development at 66 hours in the wildtype and mutant crosses, respectively. In the wildtype cross, mature ascomata can be observed at the zone of interaction (indicated in blue), while only immature protoascomata have been formed in the mutant cross (indicated in red). **B)** and **E)** Sexual development at 90 hours in the wildtype and mutant crosses, respectively. The wildtype crosses had produced ascospore masses which have exuded from the tips of the ascomatal necks, while the mutant cross had only formed slightly matured protoascomata, most with small darkened beaks. **C)** and **F)** The most mature sexual structures produced by the wildtype and mutant crosses, respectively. The wildtype crosses produced fully mature, ascospore-bearing ascomata (particularly clear examples indicated by the blue arrows), while the mutant crosses produced only dark and slightly beaked protoascomata (particularly clear examples indicated by the red arrows).

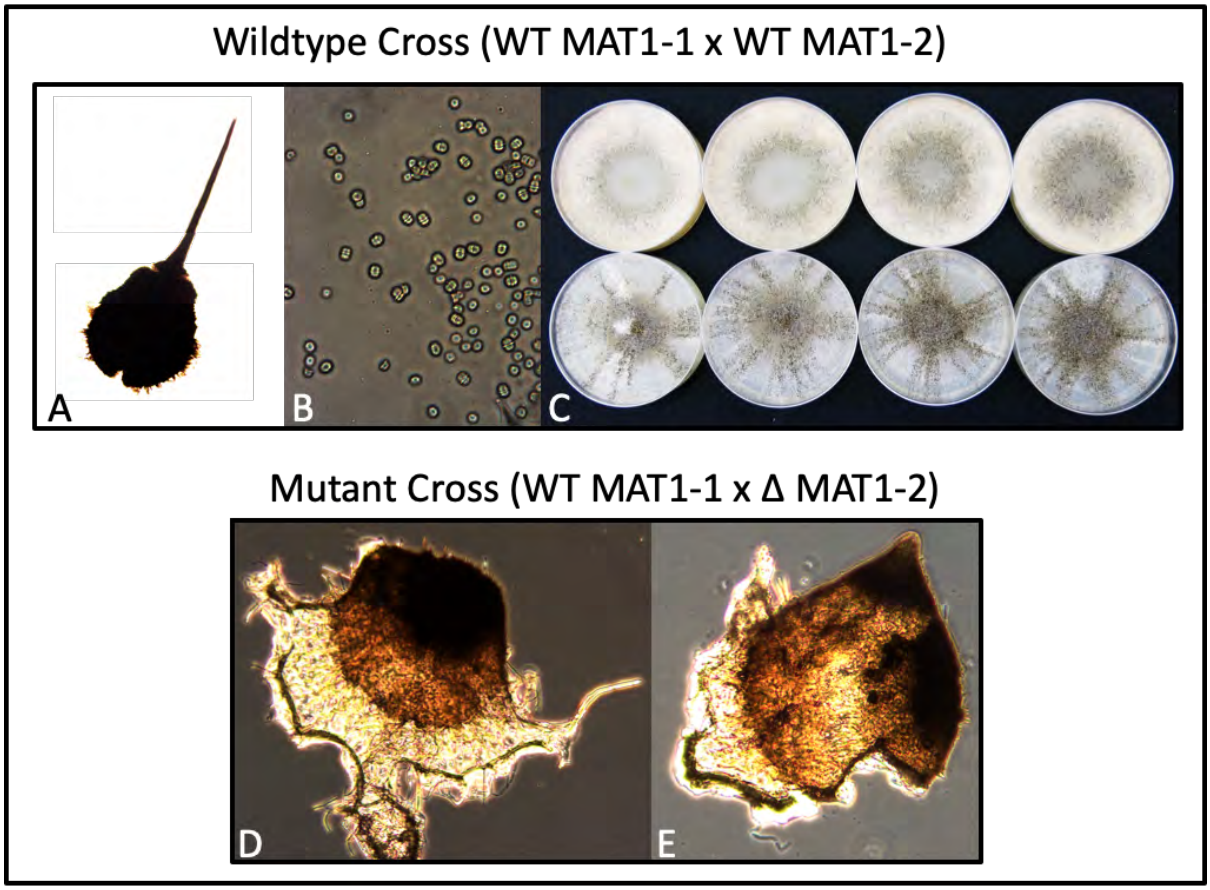

Figure 8: Sexual development in matings between wildtype isolates (top panel) and between a MAT1-1 wildtype isolate and a MAT1-2 mutant isolate (bottom panel). A) A mature ascomata, a dark globose base and an extended neck. The hat-shaped ascospores, pictured in **B)** exuded from the pore found at the top of the neck. **C)** The sexually competent cultures produced by transferring ascospore masses from the wildtype cross onto sterile plates. **D)** A young protoascomata beginning to darken. **E)** The most mature sexual structure formed in the mutant cross: a maturing protoascomata exhibiting the beak-like structure which, in wildtype crosses, would have extended into the neck.

3.5. Pheromone expression is altered in the mutant isolate

In *H. omanensis*, as is the case with other heterothallic species, MAT1-1 isolates almost exclusively express the α-pheromone and there is little to no expression of the **a**-pheromone. In contrast, MAT1-2 isolates express the **a**-pheromone, with little to no expression of the α-pheromone [19]. The semi-quantitative PCR approach used in this study showed that the **a**-pheromone is expressed at high levels in the MAT1-2 wild type isolate, with detection of the **a**-pheromone mRNA transcript possible even in a 1:1 000 000 dilution. In contrast, the **a**-pheromone was expressed at lower levels in both the mutants, where transcripts were not detected at dilutions higher than 1:1 000 and 1:100 000 in the *ΔMAT127-H1* and *ΔMAT127-H4* isolates, respectively (Figure

9). This suggested that the **a**-pheromone gene product is positively controlled by the MAT1-2-7 protein in *H. omanensis*. Thus, in the absence of a functional MAT1-2-7 gene product, there is less **a**-pheromone expression.

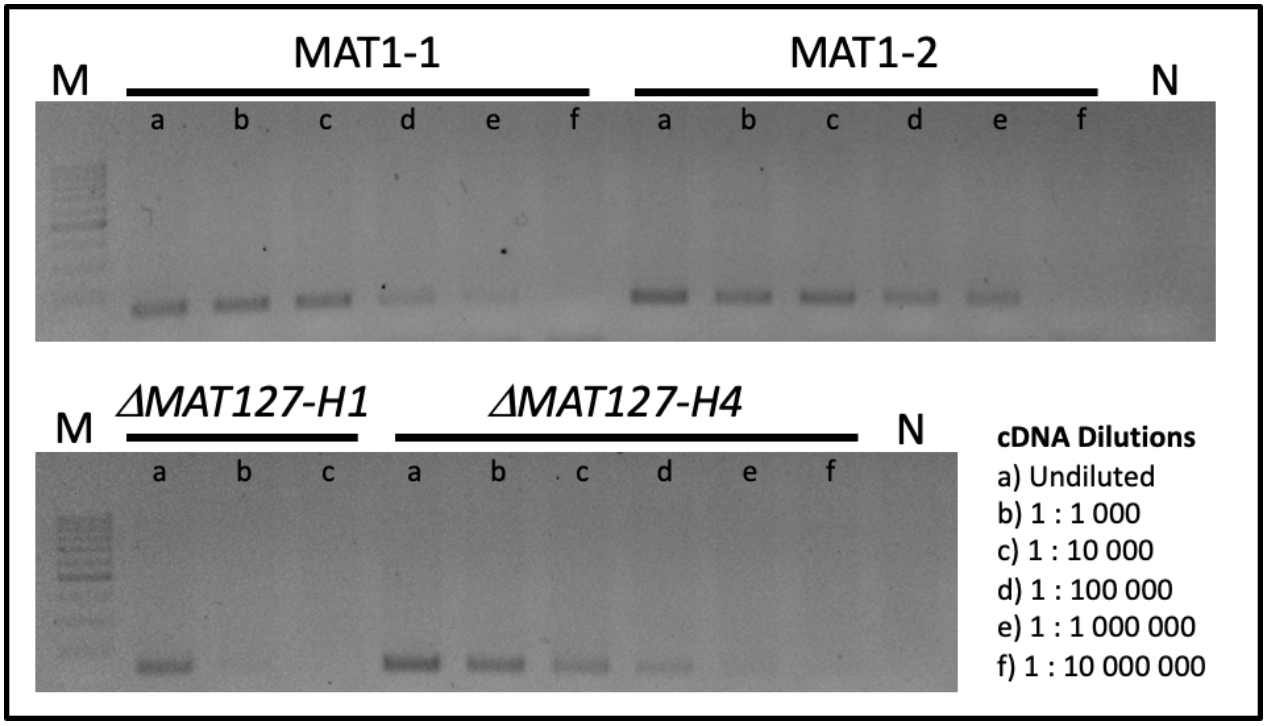

Figure 9: Expression of the a-pheromone. Transcripts of the **a**-pheromone receptor were detectable in MAT1-1 and MAT1-2 wild type isolates as well as the two mutant isolates. The semi-quantitative approach used in this study shows that the MAT1-1 isolate expresses the **a**-pheromone at lower level, with transcripts becoming undetectable at dilutions higher than 1: 1 000 000, while the pheromone transcript is still detectable at this dilution in the MAT1-2 isolate. Both mutant isolates, *ΔMAT127-H1* and *ΔMAT127-H4,* express the **a**-pheromone at much lower levels than the wild type isolates, with expression becoming undetectable at dilutions higher than 1: 10 000 and 1: 1 000 000, respectively. Lanes M and N show the 100 bp molecular marker and negative control, respectively.

As expected, expression of the α-pheromone was detected in the wild type MAT1-1 isolate. In contrast, the expression of this gene was undetectable in the wild type MAT1-2 isolate (Figure 10). The expression of this pheromone could also not be detected in the *ΔMAT127-H4* isolate. It was, however, possible to detect α-pheromone expression in the *ΔMAT127-H1* isolate. This indicated that while the

disruption of the *MAT1-2-7* gene resulted in the negative regulation of the **a**-pheromone, it also up-regulated the α-pheromone, particularly in the *ΔMAT127-H1* isolate.

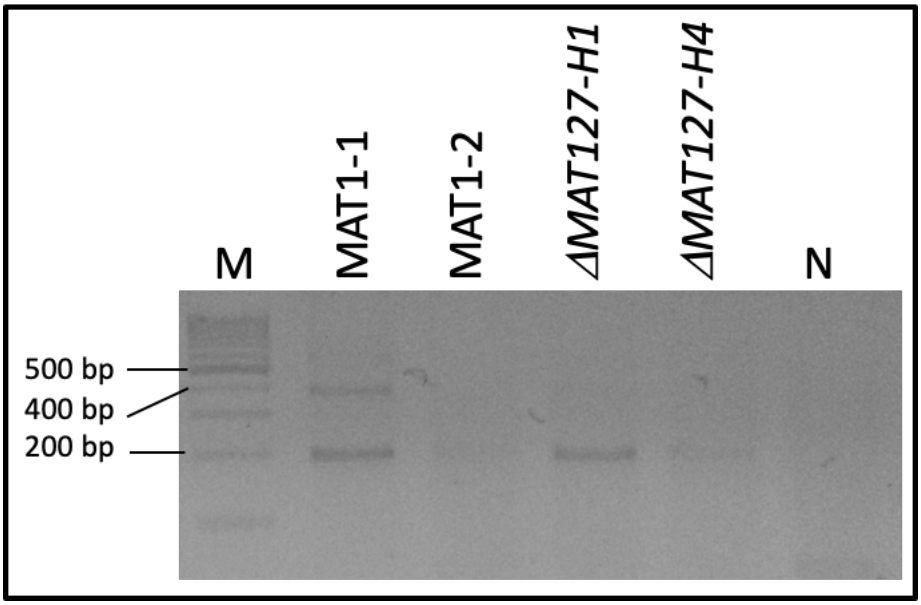

Figure 10: Expression of the α-pheromone. Transcripts of the α-pheromone were detectable in the wild type MAT1-1 isolate but were not detected in the wild type MAT1-2 isolate, as expected. Interestingly, while the *ΔMAT127-H4* mutant showed no evidence of the α-pheromone expression, the α-pheromone was expressed at detectable levels in the *ΔMAT127-H1* mutant. The larger band in the MAT1-1 lane is the result of non-specific binding due to the repetitive nature of the α-pheromone gene sequence. Lanes M and N show the 100 bp molecular marker and negative control, respectively.

3.6. The pheromone receptors are alternatively spliced in *H. omanensis*

Different splice variants of the α- and **a**-pheromone receptors were expressed by isolates of both mating type (Figure 11). In MAT1 isolates, the α-pheromone receptor was expressed with its intron unspliced, yielding a protein harbouring a premature stop codon and one that encodes only six of the seven transmembrane domains that characterize this type of receptor. It is unlikely that this form of the receptor protein would be functional, as the even number of transmembrane domains would preclude the existence of both intra- and extracellular domains. These MAT1 isolates also express the **a**-pheromone receptor, but in this case, the receptor's mRNA transcript is correctly spliced and thus produces a fully functional, seven-transmembrane domain

protein. The reciprocal was true for MAT2 isolates, which produced a correctly spliced and presumably functional α-pheromone receptor with all seven transmembrane domains, while the transcript of the **a**-pheromone receptor remained unspliced. This transcript would be translated into a protein harbouring only five transmembrane domains and was probably non-functional. The mutant isolates both expressed the pheromone receptors in the same manner as the wild type MAT2 isolate.

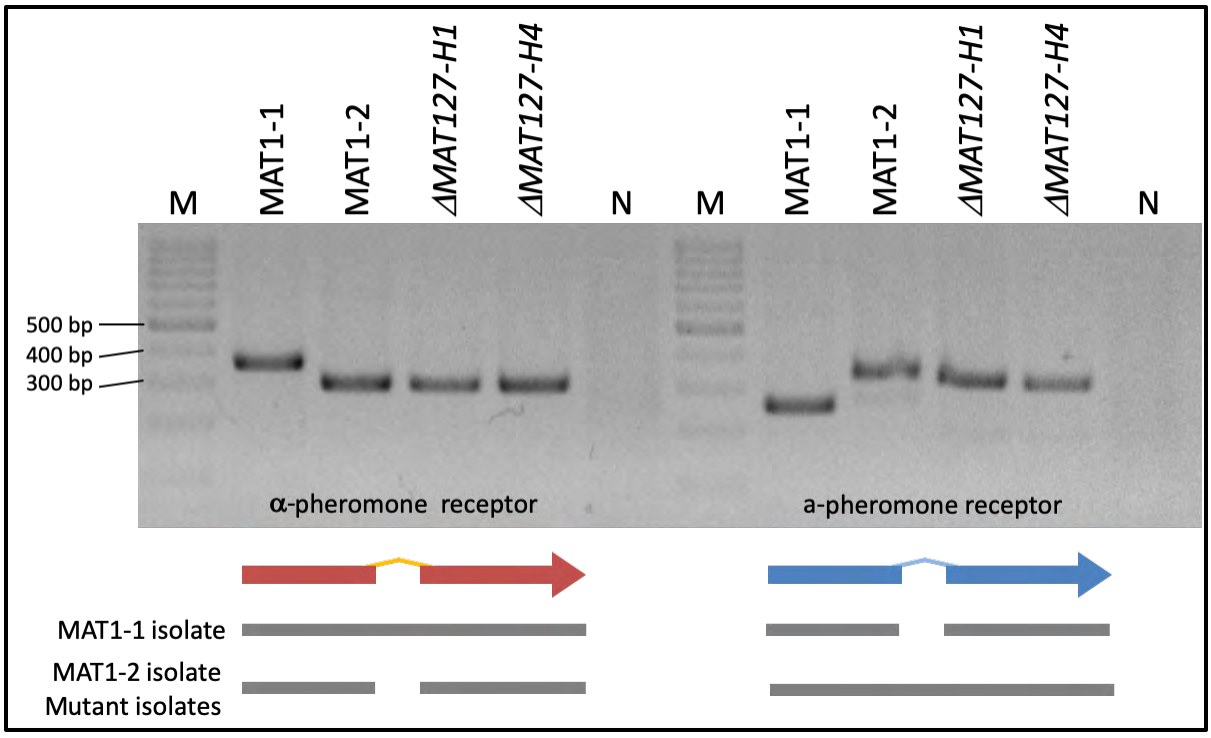

Figure 11: Mating-type dependant alternative splicing of the pheromone receptors. The two pheromone receptors are spliced differently in the two mating types. In MAT1-1 isolates, the α-pheromone receptor mRNA transcript remains unspliced and likely results in a non-functional protein that is incapable of recognizing the α-pheromone. In contrast, the MAT1-1 isolates express a splice **a**-pheromone receptor transcript which, when translated, will produce a functional, seven transmembrane domain protein. The opposite is true for the MAT1-2 isolates, where the α-pheromone receptor transcript is correctly spliced, while the **a**-pheromone receptor remains unspliced, producing a non-functional receptor protein. In both cases, the two mutant isolates produce transcripts identical to that of the wild type MAT1-2 isolates, indicating that the *MAT1-2-7* disruption does not affect the expression or splicing of the pheromone receptor proteins. Lanes M and N show the 100 bp molecular marker and negative control, respectively.

3.7. *MAT1-2-7* truncation does not lead to unisexuality in *H. omanensis*

The in frame stop codon introduced into the *H. omanensis MAT1-2-7* gene closely mimicked that of the *H. moniliformis MAT1-2-7* gene, where the truncation is thought, in part, to be responsible for the unisexual phenotype observed in this species. However, *MAT1-2-7* disruption in *H. omanensis* did not result in this phenotype. Neither of the two mutant isolates were capable of protoascomatal development when cultured in isolation, which is the defining characteristic of unisexual reproduction in filamentous ascomycetes. Furthermore, crosses between the mutant isolates and the MAT1-2 did not result in the production of either protoascomata or ascomata.

3.8. Conidiation is not affected by *MAT1-2-7* truncation

The number of conidia produced by each of the wild type isolates was comparable with that of both mutant strains, and was fairly variable, even between isolates of the same mating type. The average conidial production by MAT1 isolates was 1.23 E+05 spores per mycelial plug, the average by MAT2 isolates was 2.03 E+5 spores per mycelial plug and the average by the mutant strains was 2.33 E+05 spores per mycelial plug (Table 3, Table S14). Thus, it is unlikely that *MAT1-2-7* is significantly involved in any process related to conidial development in *H. omanensis*.

Table 3: The disruption of the *MAT1-2-7* gene does not affect the number of conidia produced. The p-values indicated below are the results from a two-tailed, independent t-test.

Isolate	Average conidia per agar block	*p-value*
		ΔMAT127
MAT1	1.23 E+05	0.061
MAT2	2.03 E+05	0.676
ΔMAT127	2.33 E+05	-

3.9. *MAT1-2-7* is involved in vegetative growth

The average radial growth rate of the mutant isolates was significantly slower than that of the wild type isolates of both mating types (Figure 11, Table 4, Table S15). By the 60 hour time point, all four wild type isolates grew to an average diameter of up to 59 mm, while both mutants strains had average diameters of up to 41 mm in the same period. The culture morphology of the mutants was also different to that of the wild type. While wild type isolates of both mating types formed aerial hyphae with a "fluffy" phenotype, both mutants produced much smoother mycelia that was submerged within the agar (Figure 12).

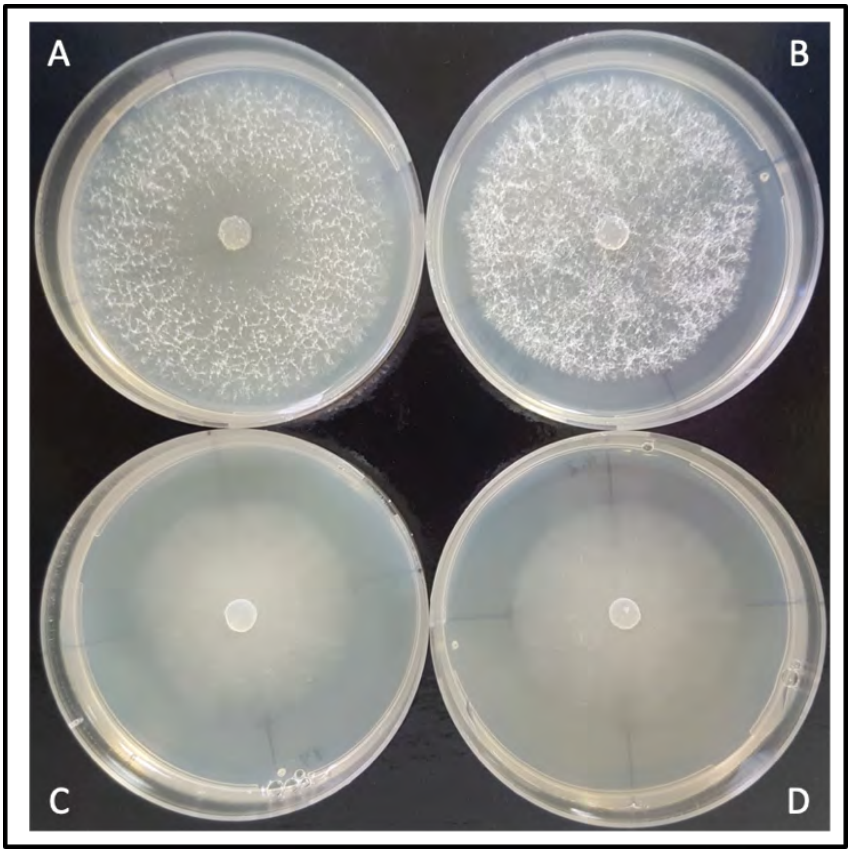

Figure 12: ***MAT1-2-7*** **truncation leads to a decrease in growth rate and difference in culture morphology. A)** and **B)** Wildtype isolates CMW 44442 and CMW 44439, respectively. **C)** and **D)** Mutant isolates *ΔMAT127-H1* and *ΔMAT127-H4,* respectively. These isolates show a maximum growth of up to 41 mm in 60 hours, compared to the wild type maximum of 59 mm in the same time period. Additionally, while the wildtype isolates produce aerial mycelia, the mutant isolates both produce much smoother, submerged mycelia.

Table 4: The mutant isolates both grew significantly slower than the wild type isolates of both mating types. The p-values indicated below are the results from a two-tailed, independent t-test.

Isolate	Average growth in 60 hours (mm)	*p-value*	
		ΔMAT127-H1	***ΔMAT127-H4***
MAT1 (CMW 44436)	56.2	1.3 E-09	5.8 E-10
MAT1 (CMW 44437)	57.7	6.1 E-11	1.3 E-11
MAT2 (CMW 44439)	57.0	1.9 E-10	5.5 E-11
MAT2 (CMW 44442)	51.8	3.7 E-07	2.21 E-7
***ΔMAT127-H1* (CMW 54810)**	40.1	-	0.42
***ΔMAT127-H4* (CMW 54811)**	39.8	0.42	-

4. DISCUSSION

The development of an efficient and effective transformation and genome editing protocol for use in *Huntiella* species has been a valuable addition to the molecular toolkit available for these species. This protocol will finally allow for the functional characterization of genes involved in many biological processes, such as sexual reproduction, growth and host-specificity. Furthermore, it will likely be possible to extend the methods used here to some of the other economically relevant species that reside in the Ceratocystidaceae. In this study, this technique was used to functionally characterize the novel *H. omanensis* mating gene, *MAT1-2-7,* with regards to its role in sexual reproduction. We disrupted the gene by introducing an in frame stop codon at a position that mimicked the truncation seen in the *H. moniliformis MAT1-2-7* gene. We were thus able to show that *MAT1-2-7* is a true mating gene that is essential for sexual reproduction. Furthermore, we also showed that it exhibited pleiotropic effects by influencing radial growth rate in this fungus.

This study showed that *MAT1-2-7* was essential for ascomatal maturation in *H. omanensis*, a process that has been closely linked with the secondary *MAT* genes of other ascomycete species as well [4,13,29]. Crosses between wild type MAT1-1 and MAT1-2 isolates of *H. omanensis* produced mature, ascospore-exuding ascomata within four days of co-incubation

[18]. Transfer of the ascospore masses could produce sexually reproducing cultures within a further seven days. However, crosses between a wild type MAT1-1 isolate of *H. omanensis* and either of the two *ΔMAT1-2-7* mutant isolates produced only protoascomata at the zone of interaction. The development of these structures was delayed compared to that of the wild type crosses, and they never developed to maturity. Furthermore, no ascospores were produced in these sexual structures, suggesting that the production of sexual spores is entirely precluded in these mutant isolates, even in the presence of a wild type mating partner.

Given that protoascomatal maturation occurs fairly early during the process of mating, it appears that the *H. omanensis MAT1-2-7* is important during the initial phases of sexual reproduction. Interestingly, the *H. omanensis MAT1-2-7* truncation resulted in a phenotype comparable to that of other species in which secondary *MAT* genes had also been disturbed. The disruption of the *Podospora anserina MAT1-1-2* [4,30], the *Fusarium graminearum MAT1-1-2* and *MAT1-1-3* [13], the *Sordaria macrospora MAT1-1-2* [31], the *Botrytis MAT1-1-5* and *MAT1-2-10* [14] and *Aspergillus fumigatus MAT1-2-4* [29], resulted in the production of immature protoascomata that never develop or fully mature, but barren, ascomata. These results support the notion that a finer control of sexual reproduction has been achieved by the acquisition of secondary *MAT* genes [29]. Thus, instead of being responsible for sexual initiation, as is the role of the primary *MAT* genes [13,14], they are instead important for further development.

In ascomycete fungi, one of the direct targets of the MAT transcription factors is the pheromone response pathway [32–34]. In particular, the pheromone genes are typically transcriptionally controlled by the proteins encoded by the *MAT* locus. It is thus likely that the underlying mechanism by which *MAT1-2-7* disruption affects ascomatal development is via the pheromone response pathway. This is supported by the fact that both of the *ΔMAT1-2-7* mutants showed a decrease in the expression of the **a**-pheromone, the mating pheromone usually expressed by MAT2 isolates. Furthermore, one of the two mutants was able to express the α-pheromone, suggesting that the normal mating-type dependent regulation of the pheromones in *H. omanensis* [19] has been affected by the *MAT1-2-7* knockout. In other filamentous ascomycete fungi, such as *P. anserina* [35] and *N. crassa*

[36], the expression of the mating pheromones is closely linked with male fertility. In these species, the downregulation or complete knockout of the pheromone-encoding genes results in isolates that are female fertile, but unable to produce the male cells that are capable of fertilizing the female structures of an opposite mating type. Given the downregulation of the **a**-pheromone in the MAT1-2 isolates harbouring the disrupted *MAT1-2-7* gene, it is likely that the maturation of protoascomata is precluded by an inability of the MAT1-2 isolate to fertilize the female structures of the MAT1-1 partner.

Significant differences are apparent in the phenotypes of the artificially introduced and naturally occurring *MAT1-2-7* truncations, as seen in *H. omanensis* and *H. moniliformis*, respectively. In *H. moniliforms*, sexual reproduction is not precluded, and instead, MAT1-2 isolates of this species are capable of sexual reproduction even in the absence of a MAT1-1 mating partner [18,19]. In contrast, the truncation in *H. omanensis* leads to a complete halt in ascomatal development even in the presence of a wild type mating partner. This suggests that while the disruption of the *MAT1-2-7* gene in *H. moniliformis* may have played a role in the evolution towards unisexuality, this change alone was not sufficient to shift its reproductive strategy. In fact, the indiscriminate expression of both pheromone types in *H. moniliformis* has also been hypothesized to play a role in the ability of this species to unisexually reproduce [19]. Interestingly, one of the two *H. omanensis* mutant strains was capable of expressing both the **a**- and α-pheromone types and yet was incapable of unisexual reproduction. This suggests that there are other, yet to be investigated, genes that are also involved in the unisexual pathway or that the isolate is unable to recognize the endogenously produced pheromones.

A final factor that could contribute to the lack of unisexual reproduction in the two mutant *H. omanensis* isolates is the mating-type specific alternative splicing of the pheromone receptor genes. In most ascomycete species, both MAT1-1 and MAT1-2 isolates express both pheromone receptors and thus mating specificity is mediated solely by the mating-type dependent expression of the pheromones [37]. In this study, we showed that *H. omanensis* isolates express both receptors but only produce functional versions of the receptor with which they will recognize an opposite mating partner. Thus, MAT2 isolates, which express the **a**-pheromone and recognize the α-pheromone, only express a functional

α-pheromone receptor. This was also true of the two mutant isolates. Thus, although the mutants do express the **a**-pheromone, they are unable to produce a functional **a**-pheromone receptor with which to recognize and respond to the pheromone. Of course, one of the mutant isolates was capable of α-pheromone expression and also a functional version of the α-pheromone receptor. It is thus possible that unisexual reproduction relies on the expression and recognition of both pheromones.

Despite being primarily involved in mating, certain *MAT* genes can exhibit pleiotropic effects, affecting processes such as growth [16], virulence [16] and vegetative incompatibility [15]. While the truncation of *MAT1-2-7* did not have a detectable effect on the conidial production in *H. omanensis*, vegetative growth was significantly affected in both of the *ΔMAT1-2-7* mutant isolates. While wild type *H. omanensis* isolates of both mating type grow rapidly and produce aerial mycelia, the mutant strains grew submerged within the agar and more slowly. A similar phenotype is seen in *Ceratocystis albifundus*, where deletion of *MAT1-2-1* during mating type switching has a direct effect on the growth of these isolates [16]. It may not be surprising that sexual reproduction and vegetative growth were linked, as both are intimately linked to secondary metabolism and the regulation of the associated biochemical pathways [38]. The underlying mechanism of these pleiotropic effects remains unknown and will need to be investigated in the future.

This study is the first to successfully genetically manipulate any species of *Huntiella*, providing a convenient system with which to functionally characterize the novel *MAT1-2-7* gene. Genetic manipulation was achieved by developing a protoplast-based transformation protocol established on those established in other filamentous fungi [25,26]. This was combined with a fairly novel use of the CRISPR-Cas9 genome editing system in fungi, whereby the sgRNA and a purified Cas9 enzyme were combined *in vivo* to form the RNP before being used for transformation *in vitro*. This method allowed us to overcome certain challenges associated with the classical plasmid-based CRISPR-Cas9 system [39,40], such as sufficient Cas9 expression and potentially random genomic integration. A similar technique was recently used in *F. oxysporum* [39] and *Mucor circinelloides* [40] and we thus propose

that this method will allow for successful gene characterization in other non-model species for which the molecular toolkit is still limited.

5. CONCLUSION

This study is the first to report the successful genetic manipulation of any species of *Huntiella*. It thus represents a valuable addition to molecular toolkit that is available to thoroughly investigate the biology of these species. This study focused on ascertaining the function of *MAT1-2-7* in the sexual cycle of *H. omanensis*, but the functions of genes involved in other biological processes like asexual reproduction, growth and host-specificity can now be better interrogated and underlying genetic mechanisms can be elucidated. Furthermore, this protocol can be used as a base from which species-specific protocol optimization can be conducted, allowing for the development of a similar protocol in the other, economically important species residing in the Ceratocystidaceae.

6. ACKNOWLEDGEMENTS

This project was financed by the University of Pretoria, the Department of Science and Technology (DST)/National Research Foundation (NRF) Centre of Excellence in Tree Health Biotechnology (CTHB). The grant holders acknowledge that opinions, findings and conclusions or recommendations expressed in this piece of work are that of the researchers and that the funding bodies accept no liability whatsoever in this regard. We would also like to thank Mr Matthew Weatley and Prof Yinong Yang, both of whom provided invaluable insight into the CRISPR-Cas9-based genome editing system developed in this study. Further experimental support was received from both Dr Tuan Duong and Ms Mmatshepho Phasha. We would like to thank Prof Cobus Visagie for producing a number of the photographic and micrographic images utilized in this study.

7. REFERENCES

1. Dyer PS, Inderbitzin P, Debuchy R. **2016.** Mating-type structure, function, regulation and evolution in the Pezizomycotina. Growth, Differentiation and Sexuality. 3rd ed. Springer International Publishing; pp. 351–385.
2. Debuchy R, Berteaux-Lecellier V, Silar P. **2010.** Mating systems and sexual

morphogenesis in ascomycetes. In: Borkovich KA, Ebbole DJ, editors. Cellular and molecular biology of filamentous fungi. ASM Press, Washington D.C.; pp. 501–535.

3. Turgeon BG, Yoder OC. **2000**. Proposed nomenclature for mating type genes of filamentous ascomycetes. Fungal Genetics and Biology. 31: 1–5.
4. Arnaise S, Debuchy R, Picard M. **1997**. What is a *bona fide* mating-type gene? Internuclear complementation of mat mutants in *Podospora anserina*. Molecular and General Genetics. 256: 169–178.
5. Wilken PM, Steenkamp ET, Wingfield MJ, de Beer ZW, Wingfield BD. **2017**. Which *MAT* gene? Pezizomycotina (Ascomycota) mating-type gene nomenclature reconsidered. Fungal Biology Reviews. 31: 199–211.
6. Paoletti M, Seymour FA, Alcocer MJC, Kaur N, Calvo AM, Archer DB, et al. **2007**. Mating type and the genetic basis of self-fertility in the model fungus *Aspergillus nidulans*. Current Biology. 17: 1384–1389.
7. Staben C, Yanofsky C. **1990**. *Neurospora crassa* a mating-type region. Genetics. 87: 4917–4921.
8. Debuchy R, Coppin E. **1992**. The mating types of *Podospora anserina*: Functional analysis and sequence of the fertilization domains. Molecular & General Genetics. 233: 113–121.
9. McGuire IC, Marra RE, Turgeon BG, Milgroom MG. **2001**. Analysis of mating-type genes in the chestnut blight fungus, *Cryphonectria parasitica*. Fungal Genetics and Biology. 34: 131–144.
10. Pöggeler S, Kück U. **2000**. Comparative analysis of the mating-type loci from *Neurospora crassa* and *Sordaria macrospora*: Identification of novel transcribed ORFs. Molecular and General Genetics. 263: 292–301.
11. Martin SH, Wingfield BD, Wingfield MJ, Steenkamp ET. **2011**. Structure and evolution of the *Fusarium* mating type locus: New insights from the *Gibberella fujikuroi* complex. Fungal Genetics and Biology. Elsevier Inc.; 48: 731–740.
12. Ferreira AVB, An Z, Metzenberg RL, Glass NL. **1998**. Characterization of *mat A-2*, *mat A-3* and *ΔmatA* mating-type mutants of *Neurospora crassa*. Genetics. 148: 1069–1079.
13. Kim HK, Cho EJ, Lee S, Lee YS, Yun SH. **2012**. Functional analyses of individual mating-type transcripts at *MAT* loci in *Fusarium graminearum* and *Fusarium asiaticum*. FEMS

Microbiology Letters. 337: 89–96.

14. Rodenburg SYA, Terhem RB, Veloso J, Stassen JHM, van Kan JAL. **2018**. Functional analysis of mating type genes and transcriptome analysis during fruiting body development of *Botrytis cinerea*. mBio. 9: 1–19.
15. Newmeyer D, Branch Howe H, Galeazzi D. **1973**. A search for complexity at the mating-type locus of *Neurospora crassa*. Canadian Journal of Genetics and Cytology. 15: 577–585.
16. Lee DH, Roux J, Wingfield BD, Wingfield MJ. **2015**. Variation in growth rates and aggressiveness of naturally occurring self-fertile and self-sterile isolates of the wilt pathogen *Ceratocystis albifundus*. Plant Pathology. 64: 1103–1109.
17. de Beer ZW, Duong TA, Barnes I, Wingfield BD, Wingfield MJ. **2014**. Redefining *Ceratocystis* and allied genera. Studies in Mycology. 79: 187–219.
18. Wilson AM, Godlonton T, van der Nest MA, Wilken PM, Wingfield MJ, Wingfield BD. **2015**. Unisexual reproduction in *Huntiella moniliformis*. Fungal Genetics and Biology. 80: 1–9.
19. Wilson AM, van der Nest MA, Wilken PM, Wingfield MJ, Wingfield BD. **2018**. Pheromone expression reveals putative mechanism of unisexuality in a saprobic ascomycete fungus. PLoS ONE. 13: e0192517.
20. Jinek M, Chylinski K, Fonfara I, Hauer M, Doudna JA, Charpentier E. **2012**. A programmable dual-RNA-guided DNA endonuclease in adaptive bacterial immunity. Science. 337: 816–822.
21. Gasiunas G, Barrangou R, Horvath P, Siksnys V. **2012**. Cas9–crRNA ribonucleoprotein complex mediates specific DNA cleavage for adaptive immunity in bacteria. Proceedings of the National Academy of Sciences. 109: 2579–2586.
22. Gruber AR, Lorenz R, Bernhart SH, Neubo R, Hofacker IL. **2008**. The Vienna RNA websuite. Nucleic Acids Research. 36: W70–W74.
23. Ran FA, Hsu PD, Wright J, Agarwala V, Scott DA, Zhang F. **2013**. Genome engineering using the CRISPR-Cas9 system. Cell. 8: 2281–2308.
24. Carroll AM, Sweigard JA, Valent B. **1994**. Improved vectors for selecting resistance to hygromycin. Fungal Genetics Reports. 41: 41–44.
25. Leung H, Lehtinen U, Karjalainen R, Skinner D, Tooley P, Leong S, et al. **1990**. Transformation of the rest blast fungus *Magnaporte grisea* to hygromycin B

resistance. Current Genetics. 17: 409–411.

26. Chung K-R, Lee M-H. **2015.** Split-marker-mediated transformation and targeted gene disruption in filamentous fungi. In: van den Berg MA, Maruthachalam K, editors. Genetic Transformation Systems in Fungi. Cham: Springer International Publishing; pp. 175–180.
27. Sambrook J, Green M. **2012.** Molecular cloning: A laboratory manual. 4th ed. Cold Spring Harbor Laboratory Press;
28. Eisel D, Seth O, Grunewald-Janho S, Krunchen D, Ruger B. **2008.** DIG application manual: For filter hybridization. Roche Diagnostics;
29. Yu Y, Amich J, Will C, Eagle CE, Dyer PS, Krappmann S. **2017**. The novel *Aspergillus fumigatus MAT1-2-4* mating-type gene is required for mating and cleistothecia formation. Fungal Genetics and Biology. Elsevier; 108: 1–12.
30. Arnaise S, Zickler D, Le Bilcot S, Poisier C, Debuchy R. **2001**. Mutations in mating-type genes of the heterothallic fungus *Podospora anserina* lead to self-fertility. Genetics. 159: 545–556.
31. Klix V, Nowrousian M, Ringelberg C, Loros JJ, Dunlap JC, Pöggeler S. **2010**. Functional characterization of *MAT1-1*-specific mating-type genes in the homothallic ascomycete *Sordaria macrospora* provides new insights into essential and nonessential sexual regulators. Eukaryotic Cell. 9: 894–905.
32. Bobrowicz P, Pawlak R, Correa A, Bell-Pedersen D, Ebbole DJ. **2002**. The *Neurospora crassa* pheromone precursor genes are regulated by the mating type locus and the circadian clock. Molecular Microbiology. 45: 795–804.
33. Shen WC, Bobrowicz P, Ebbole DJ. **1999**. Isolation of pheromone precursor genes of *Magnaporthe grisea*. Fungal Genetics and Biology. 27: 253–263.
34. Zhang L, Baasiri RA, Van Alfen NK. **1998**. Viral repression of fungal pheromone precursor gene expression. Molecular and Cellular Biology. 18: 953–959.
35. Coppin E, de Renty C, Debuchy R. **2004**. The function of the coding sequences for the putative pheromone precursors in *Podospora anserina* is restricted to fertilization. Eukaryotic Cell. 4: 407–420.
36. Kim H, Borkovich KA. **2006**. Pheromones are essential for male fertility and sufficient to direct chemotropic polarized growth of trichogynes during mating in *Neurospora crassa*. Eukaryotic Cell. 5: 544–554.

37. Pöggeler S, Kück U. **2001**. Identification of transcriptionally expressed pheromone receptor genes in filamentous ascomycetes. Gene. 280: 9–17.

38. Calvo AM, Wilson RA, Bok JW, Keller NP. **2002**. Relationship between secondary metabolism and fungal development. Microbiology and Molecular Biology Reviews. 66: 447–459.

39. Wang Q, Cobine PA, Coleman JJ. **2018**. Efficient genome editing in Fusarium oxysporum based on CRISPR/Cas9 ribonucleoprotein complexes. Fungal Genetics and Biology. 117: 21–29.

40. Nagy G, Szebenyi C, Csernetics Á, Vaz AG, Judit E, Vágvölgyi C, et al. **2017**. Development of a plasmid free CRISPR-Cas9 system for the genetic modification of *Mucor circinelloides*. Scientific Reports. 7: 1–10.

SUPPLEMENTARY TABLES

Table S1: PCR protocol used to amplify the sgRNA targeting the *MAT1-2-7* gene

Reagent	Final Concentration	Volume
ddH_2O	-	Up to 20 µl
Forward Primer	0.5 µM	1 µl
Reverse Primer	0.5 µM	1 µl
Phusion DNA Polymerase Mastermix	0.02 $U.\mu l^{-1}$	10 µl
Template DNA	10 ng	1 µl

Primer	Sequence [a]
T7_gRNA2_F	TAATACGACTCACTATAGGGGCTGATGGTATCAATACGCA
Scaff_gRNA_R	GCACCGACTCGGTGCCACTT

[a] Red text indicates the region of the primer coding for the T7 promoter.

Initial denaturation	98 °C	01:00	
Denaturation	98 °C	00:10	X 30
Annealing	55 °C	01:00	
Extension	72 °C	00:30	
Final Extension	72 °C	10:00	

Table S2: Sanger sequencing protocols used in this study

Reagent	Final Concentration	Volume
ddH_2O	-	Up to 10 ul
Sequencing Buffer	1X	1 ul
Primer	0.5 µM	0.5 ul
BigDye	-	2 ul
PCR Product	Variable	2.5 ul

Initial denaturation	96 °C	02:00	
Denaturation	96 °C	00:10	X 25
Annealing	50 °C	00:05	
Extension	60 °C	04:00	

Table S3: PCR protocols used to amplify the product used in the *in vitro* gRNA tests

Reagent	Final Concentration	Volume
ddH_2O	-	Up to 25 µl
10 X PCR Buffer	1 X	2.5 µl
$MgCl_2$	0.5 mM	0.5 µl
dNTPS	200 µM each	0.5 µl
Forward Primer	0.2 µM	0.5 µl
Reverse Primer	0.2 µM	0.5 µl
FastStart Taq DNA Polymerase	1 U	0.2 µl
Template DNA	10 ng	1 µl

Primer	Sequence
AF	GTCAGCCCTAAACCTTGAAAT
O127R	GAAATCCCCATAAAGCCT

Initial denaturation	95 °C	04:00	
Denaturation	95 °C	00:30	X 15
Annealing	55 °C	00:30	
Extension	72 °C	01:00	
Denaturation	95 °C	00:30	X 25
Annealing	55 °C	00:30 + 5s/cycle	
Extension	72 °C	01:00	
Final Extension	72 °C	10:00	

Table S4: PCR protocols used to amplify the 5' region of the dDNA.

Reagent	Final Concentration	Volume
ddH_2O	-	Up to 20 µl
Forward Primer	0.5 µM	1 µl
Reverse Primer	0.5 µM	1 µl
Phusion DNA Polymerase Mastermix	0.02 $U.\mu l^{-1}$	10 µl
Template DNA	10 ng	1 µl

Primer	Sequence
dDNA_F	TGGCGTAATGGACATTGA
dDNA_HR	TTCAGCATCTTTTACTTTCACCAGCGTTGGAGATATCGATTTGGGGG

Initial denaturation	98 °C	01:00	
Denaturation	98 °C	00:10	X 30
Annealing	55 °C	01:00	
Extension	72 °C	00:30	
Final Extension	72 °C	10:00	

Table S5: PCR protocols used to amplify the 3' region of the dDNA.

Reagent	Final Concentration	Volume
ddH_2O	-	Up to 20 µl
Forward Primer	0.5 µM	1 µl
Reverse Primer	0.5 µM	1 µl
Phusion DNA Polymerase Mastermix	0.02 $U.\mu l^{-1}$	10 µl
Template DNA	10 ng	1 µl

Primer	Sequence
dDNA_HF	ACTTATTCAGGCGTAGCAACCAGGCGTCCACCGCCCTTTACAATG
dDNA_R	GAAATCCCCATAAAGCCT

Initial denaturation	95 °C	01:00	
Denaturation	95 °C	00:20	X 13
Annealing	53 °C	01:00	
Extension	72 °C	01:00	
Denaturation	95 °C	00:20	
Annealing	52 °C	01:00	
Extension	72 °C	01:00	
Denaturation	95 °C	00:20	
Annealing	51 °C	01:00	
Extension	72 °C	01:00	
Denaturation	95 °C	00:20	
Annealing	50 °C	01:00	
Extension	72 °C	01:00	
Final Extension	72 °C	10:00	

Table S6: PCR protocols used to amplify the hygromycin resistance cassette of the dDNA.

Reagent	Final Concentration	Volume
ddH_2O	-	Up to 20 µl
Forward Primer	0.5 µM	1 µl
Reverse Primer	0.5 µM	1 µl
Phusion DNA Polymerase Mastermix	0.02 $U.\mu l^{-1}$	10 µl
Template DNA	10 ng	1 µl

Primer	Sequence
HygF	AACGCTGGTGAAAGTAAAAGATGCTGAA
HygR	ACGCCTGGTTGCTACGCCTGAATAAGT

Initial denaturation	98 °C	01:00	
Denaturation	98 °C	00:10	X 30
Annealing	62 °C	01:00	
Extension	72 °C	03:00	
Final Extension	72 °C	10:00	

Table S7: PCR protocols used to combine the 5' region the dDNA with the hygromycin resistance cassette

Reagent	Final Concentration	Volume
ddH_2O	-	Up to 25 µl
Forward Primer	0.5 µM	1 µl
Reverse Primer	0.5 µM	1 µl
LongAmp Taq 2 X Mastermix	1 X	12.5 µl
Template DNA 1	5 ng	1 µl
Template DNA 2	5 ng	1 µl

Primer	Sequence
dDNA_F	TGGCGTAATGGACATTGA
HygR	ACGCCTGGTTGCTACGCCTGAATAAGT

Initial denaturation	94 °C	00:30	
Denaturation	94 °C	00:30	X 30
Annealing	50 °C	00:30	
Extension	65 °C	02:00	
Final Extension	65 °C	10:00	

Table S8: PCR protocols used to combine the 3' region the dDNA with the hygromycin resistance cassette

Reagent	Final Concentration	Volume
ddH_2O	-	Up to 20 µl
Forward Primer	0.5 µM	1 µl
Reverse Primer	0.5 µM	1 µl
Phusion DNA Polymerase Mastermix	0.02 $U.\mu l^{-1}$	10 µl
Template DNA 1	5 ng	1 µl
Template DNA 2	5 ng	1 µl

Primer	Sequence
HygF	AACGCTGGTGAAAGTAAAAGATGCTGAA
dDNA_R	GAAATCCCCATAAAGCCT

Initial denaturation	98 °C	01:00	
Denaturation	98 °C	00:30	X 30
Annealing	50 °C	00:30	
Extension	72 °C	02:00	
Final Extension	72 °C	10:00	

Table S9: PCR protocols used to assemble the full-length dDNA

Reagent	Final Concentration	Volume
ddH_2O	-	Up to 25 µl
LongAmp Taq 2 X Mastermix	1 X	12.5 µl
DMSO	-	1 µl
Template DNA 1	5 ng	1 µl
Template DNA 2	5 ng	1 µl

Initial denaturation	94 °C	01:00	
Denaturation	94 °C	01:00	X 30
Annealing	50 °C	01:00	
Extension	65 °C	02:30	
Final Extension	65 °C	10:00	

Table S10: PCR protocols used to confirm integration of the dDNA into the genome of *H. omanensis.*

Reagent	Final Concentration	Volume
ddH_2O	-	Up to 25 µl
Forward Primer	0.5 µM	1 µl
Reverse Primer	0.5 µM	1 µl
LongAmp Taq 2 X Mastermix	1 X	12.5 µl
Template DNA	10 ng	1 µl

Primer	Sequence
AF	GTCAGCCCTAAACCTTGAAAT
BR	ATTTTTGGTTAAGTTGGGCGG
ygF	GATGTAGGAGGGCGTGGATATGTCCT
HyR	GTATTGACCGATTCCTTGCGGTCCGAA

Initial denaturation	94 °C	05:00	
Denaturation	94 °C	00:30	X 30
Annealing	55 °C	00:30	
Extension	65 °C	[a]	
Final Extension	65 °C	10:00	

[a] AF + BR: 04:00, AF + HyR: 02:00, ygF + BR: 03:00

Table S11: DIG-labeled probe synthesis

Reagent	Final Concentration	Volume
ddH_2O	-	17.13 µl
Buffer, with $MgCl_2$	1X	5X
DIG mix	-	2.5 µl
Forward Primer	0.3 µM	0.75 µl
Reverse Primer	0.3 µM	0.75 µl
High fidelity enzyme	-	0.37 µl
Template DNA	10 ng	1 µl

Primer	Sequence
ygF	GATGTAGGAGGGCGTGGATATGTCCT
hyR	GTATTGACCGATTCCTTGCGGTCCGAA

Initial denaturation	94 °C	05:00	
Denaturation	94 °C	00:30	X 40
Annealing	66 °C	00:30	
Extension	72 °C	00:30	
Final Extension	72 °C	10:00	

Table S12: Mating tests performed

	Combination	Partner 1	Partner 2
A x B	WT MAT1 x WT MAT1	CMW 44436	CMW 44437
A x C	WT MAT1 x WT MAT2	CMW 44436	CMW 44439
A x D	WT MAT1 x WT MAT2	CMW 44436	CMW 44442
A x E	WT MAT1 x Δ MAT2	CMW 44436	CMW 54810
A x F	WT MAT1 x Δ MAT2	CMW 44436	CMW 54811
B x C	WT MAT1 x WT MAT2	CMW 44437	CMW 44439
B x D	WT MAT1 x WT MAT2	CMW 44437	CMW 44442
B x E	WT MAT1 x Δ MAT2	CMW 44437	CMW 54810
B x F	WT MAT1 x Δ MAT2	CMW 44437	CMW 54811
C x D	WT MAT2 x WT MAT2	CMW 44439	CMW 44442
C x E	WT MAT2 x Δ MAT2	CMW 44439	CMW 54810
C x F	WT MAT2 x Δ MAT2	CMW 44439	CMW 54811
D x E	WT MAT2 x Δ MAT2	CMW 44442	CMW 54810
D x F	WT MAT2 x Δ MAT2	CMW 44442	CMW 54811
E x F	Δ MAT2 x Δ MAT2	CMW 54810	CMW 54811

Table S13: RT-PCRs of *MAT1-2-1*, the two pheromones and the two pheromone receptors

Reagent	Final Concentration	Volume
ddH_2O	-	Up to 25 µl
10 X PCR Buffer	1 X	2.5 µl
$MgCl_2$	0.5 mM	0.5 µl
dNTPS	200 µM each	0.5 µl
Forward Primer	0.5 µM	0.5 µl
Reverse Primer	0.5 µM	0.5 µl
FastStart Taq DNA Polymerase	1 U	0.2 µl
Template DNA	10 ng	1 µl

Primer	Sequence	
B121F	ATTGCTGGCTGATTTCACG	*MAT1-2-1*
BM121R	TAGTCTGGGTGGGTGTTC	
OαF2	TTCTCTACCATCCTGGCT	α pheromone
OαR2	AGTTTTCCAAGAAGTGGC	
OaF	CAAGAACACCACCACCTCCA	a pheromone
OaR	AACACCGCGCATGACAGT	
Oste2F	TGACGCCGATGGAGATTT	α pheromone receptor
Oste2R	CATTGTCTTGTTGGTTGCTG	
Oste3F	CTTATCAAATCTCGCTGCCT	a pheromone receptor
Oste3R	ATGACGAGACGACGACGA	

Initial denaturation	95 °C	04:00	
Denaturation	95 °C	00:30	X 15

Annealing	[a]	00:30	
Extension	72 °C	01:00	
Denaturation	95 °C	00:30	
Annealing	[a]	00:30 + 5s/cycle	X 25
Extension	72 °C	01:00	
Final Extension	72 °C	10:00	

[a] B121F & BM121R: 56 °C, OαF2 & OαR2: 60°C, OaF & OaR: 62°C, Oste2F & Oste2R: 56 °C, Oste3F & Oste3R; 56°C.

Table S14: Average conidia per mycelial-covered plug

	Plate 1	**Plate 2**	**Plate 3**	**Average**
MAT1-1 (CMW44436)	1.25 E+05	8.75 E+04	7.00 E+04	9.42 E+04
MAT1-1 (CMW44437)	1.60 E+05	1.55 E+05	1.40 E+05	1.52 E+05
MAT1-2 (CMW44439)	1.70 E+05	5.25 E+04	1.53 E+05	1.25 E+05
MAT1-2 (CMW 44442)	1.63 E+05	2.88 E+05	3.93 E+05	2.81 E+05
ΔMAT127-H1 (CMW 54810)	1.23 E+05	1.05 E+05	1.60 E+05	1.92 E+05
ΔMAT127-H4 (CMW 54811)	2.63 E+05	3.65 E+05	3.83 E+05	3.37 E+05

Table S15: Growth measurements at 60 hours post-inoculation

		Repeats				
	Measurement	1	2	3	4	5
MAT1-1 (CMW44436)	**1**	55	55	56	57	58
	2	56	56	55	57	57
	Average	**55.5**	**55.5**	**55.5**	**57**	**57.5**
MAT1-1 (CMW44437)	**1**	58	57	59	57	57
	2	57	59	58	58	57
	Average	**57.5**	**58**	**58.5**	**57.5**	**57**
MAT1-2 (CMW44439)	**1**	58	56	58	55	57
	2	57	56	57	58	58
	Average	**57.5**	**56**	**57.5**	**56.5**	**57.5**
MAT1-2 (CMW 44442)	**1**	54	51	50	52	53
	2	54	52	49	52	51
	Average	**54**	**51.5**	**49.5**	**52**	**52**
ΔMAT127-H1 (CMW 54810)	**1**	38	40	41	40	41
	2	41	39	41	41	39
	Average	**39.5**	**39.5**	**41**	**40.5**	**40**
ΔMAT127-H4 (CMW 54811)	**1**	39	40	41	41	40
	2	40	39	39	40	39
	Average	**39.5**	**39.5**	**40**	**40.5**	**39.5**

SUPPLEMENTARY FIGURES

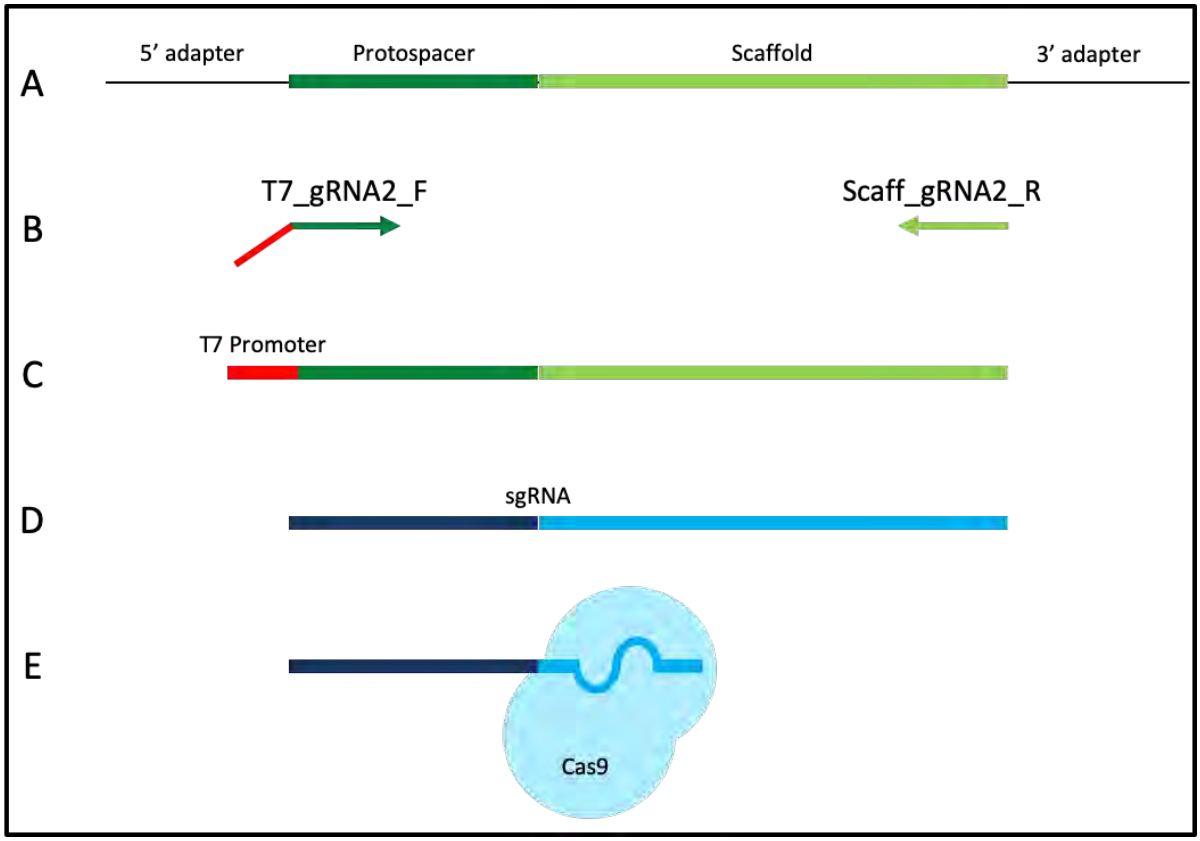

Figure S1: The synthesis, amplification and transcription of the sgRNA and assembly of the RNP. **A)** Once designed, the sgRNA molecule sequence was synthesized by Twist Biosciences (San Francisco, USA) as a dsDNA molecule and included adapters flanking the sgRNA sequence. **B)** The sgRNA sequence was amplified using primers targeting only the sgRNA region, with the forward primer also harbouring the sequence for the T7 promoter. **C)** The resulting PCR product harboured a T7 promoter region, the protospacer as well as the scaffold sequence. **D)** Transcription of the PCR product was performed to produce the full length sgRNA as a ssRNA molecule. **E)** The sgRNA was combined with the Cas9 enzyme to produce the ribonucleoprotein (RNP) which was then used for *in vitro* and *in vivo* cleavage of the target region.

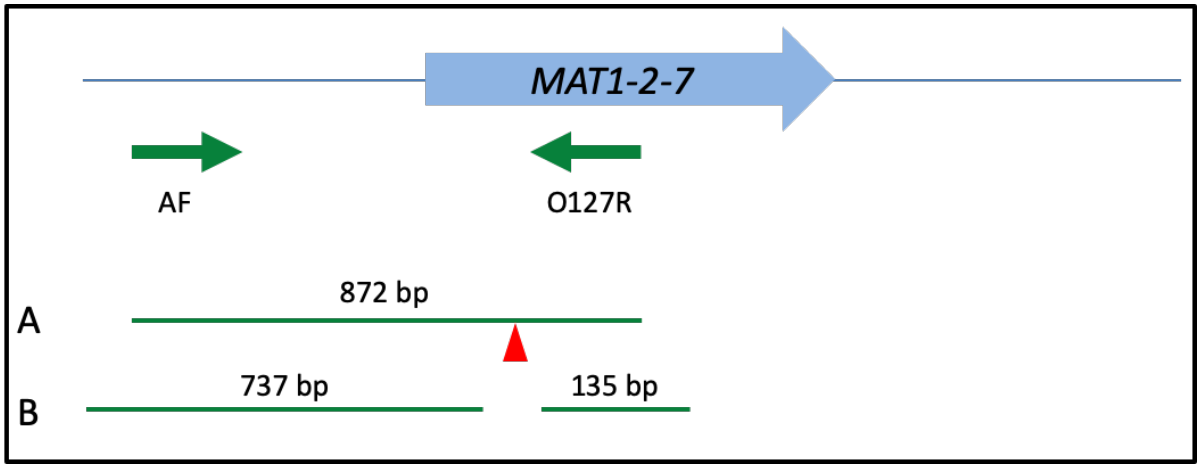

Figure S2: ***in vitro*** **gRNA test.** Primers targeting the genomic region harbouring the 5' terminus of the *MAT1-2-7* gene were used to produce the A) fragment harbouring the gRNA_2 target region. When successfully cut by the RNP, the resulting two DNA molecule are B) 737 and 135 bp in length.

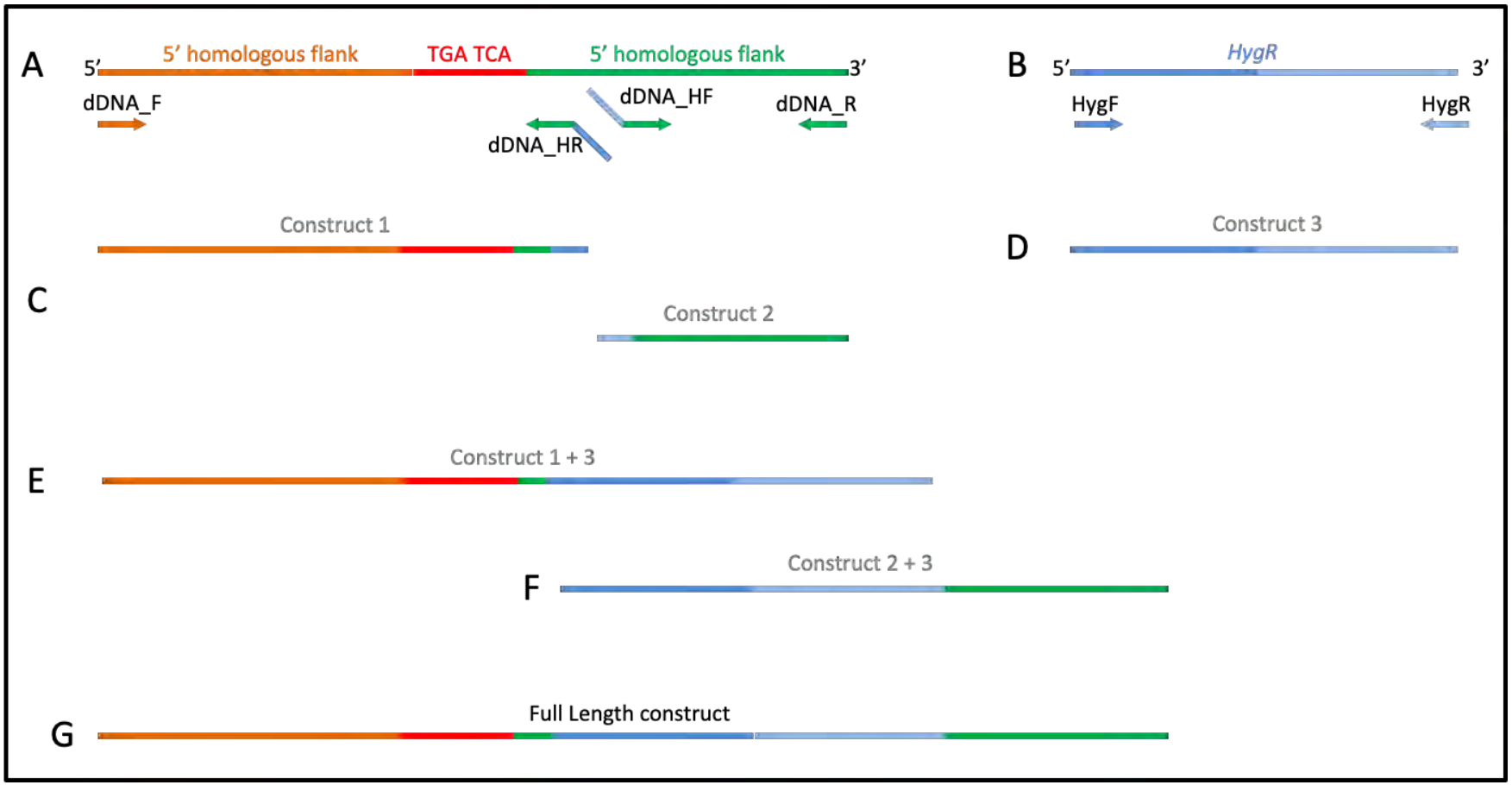

Figure S3: The synthesis, amplification and assembly of the dDNA construct. The full-length dDNA construct consists of sequence from **A)** the Twist BioScience-synthesized pre-dDNA as well as **B)** the hygromycin B resistance cassette. **C)** The 5' and 3' regions of the pre-dDNA were amplified using primers with overhangs homologous to the terminal regions of the hygromycin resistance cassette to produce constructs 1 and 2. **D)** The hygromycin resistance cassette was amplified with primers targeting the entire region to produce construct 3. **E)** Constructs 1 and 3 were combined to form a construct harbouring the 5' homologous flank, the BclI restriction site and the hygromycin resistance cassette. **F)** Constructs 2 and 3 were combined to form a construct harbouring the 3' homologous flank and the hygromycin resistance cassette. **G)** The preceding two constructs were combined into a single, full-length construct.

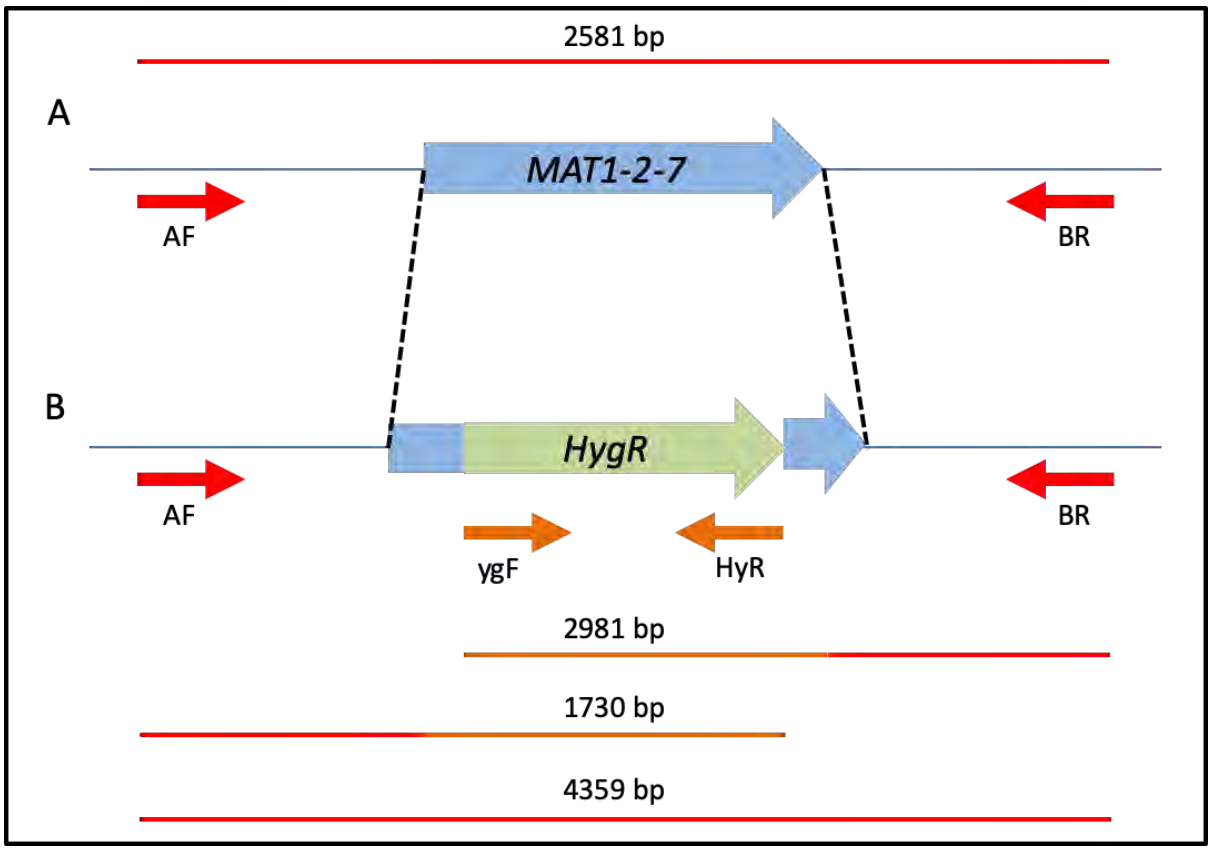

Figure S4: PCRs confirming the integration of the dDNA into the target region. A) In the wildtype isolate, the primers AF and BR can successfully produce a PCR product of approximately 2500bp. The same primer combination produces a much longer fragment of more than 4000bp in **B)** the mutant strains. Additionally, primers targeting the 5' and 3' integration regions only produce PCR products in the mutant strains, providing fragments of 1730 and 2981bp, respectively.

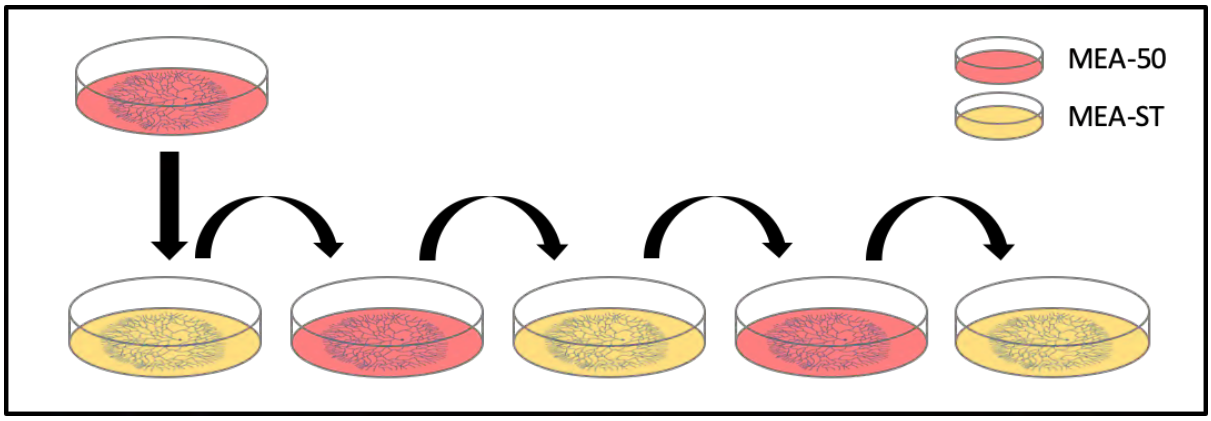

Figure S5: Assessing the stability of the integration of the hygromycin resistance cassette and the disruption of the *MAT1-2-7* gene. Confirmed knockout strains were transferred from MEA-50 media to MEA-ST media and back again three times to whether these strains would maintain the hygromycin resistance cassette when cultured in the absence of antibiotic.

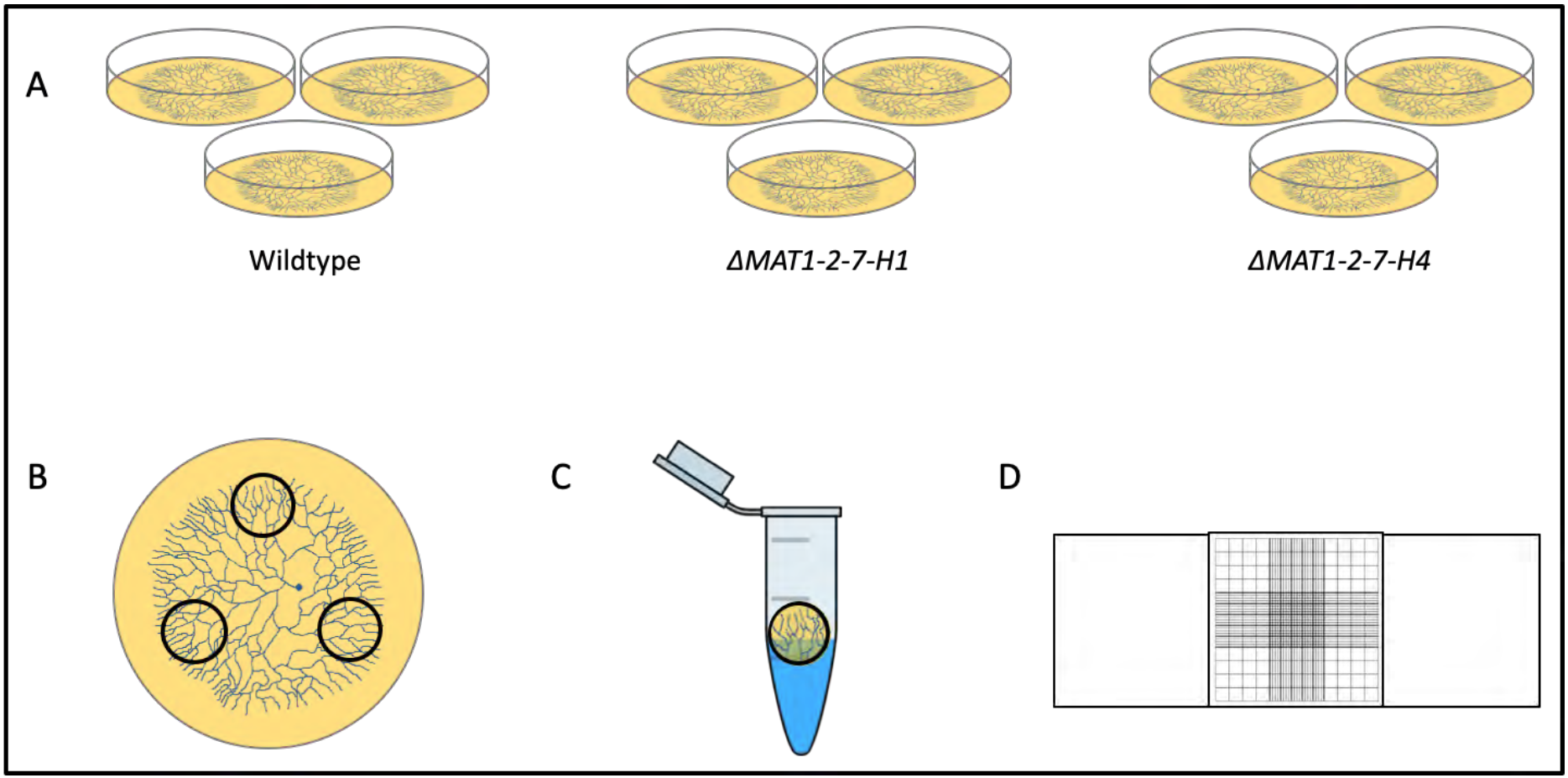

Figure S6: Assessing the asexual capabilities of the knockout strains compared to that of the wildtype isolate. A) The three isolate types that were used to assess the effect of the knockout of *MAT1-2-7* on the production of conidia. Three independently growing cultures of each isolate type were used. **B)** Three mycelium-covered agar plugs of approximately 8 mm in diameter were excised from each culture and **C)** submerged and agitated in water. **D)** The resulting solutions of conidia were then diluted and counted using a haemocytometer.

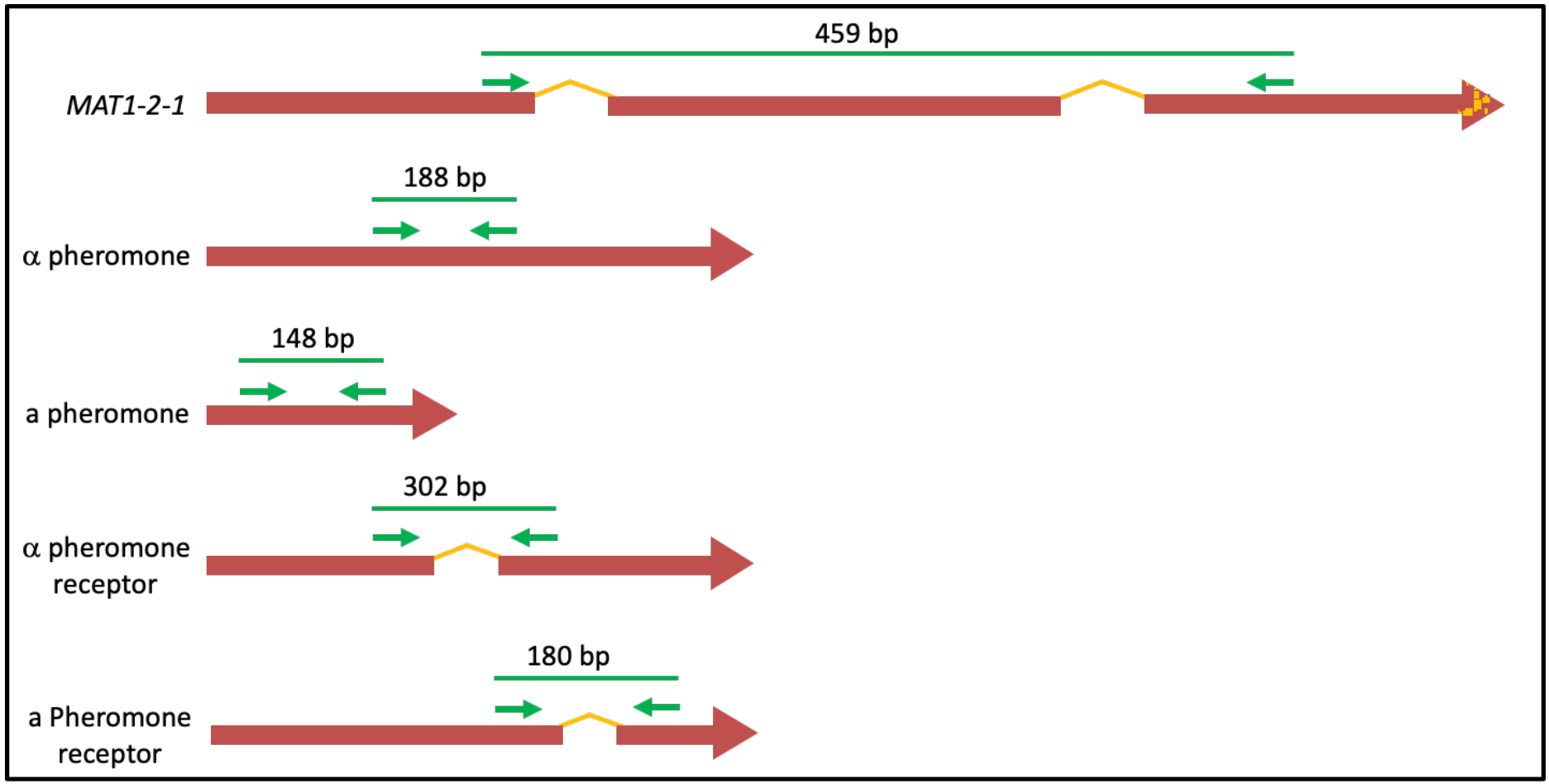

Figure S7: RT-PCR primers targeting the *MAT* and pheromone genes. The *MAT1-2-1,* α pheromone receptor and a pheromone receptor primers were designed to flank these genes' introns so that gDNA contamination could be identified if it was present. In each case, the number indicated above the green line is the length of the PCR product produced from a cDNA template and thus does not include the intronic sequence.

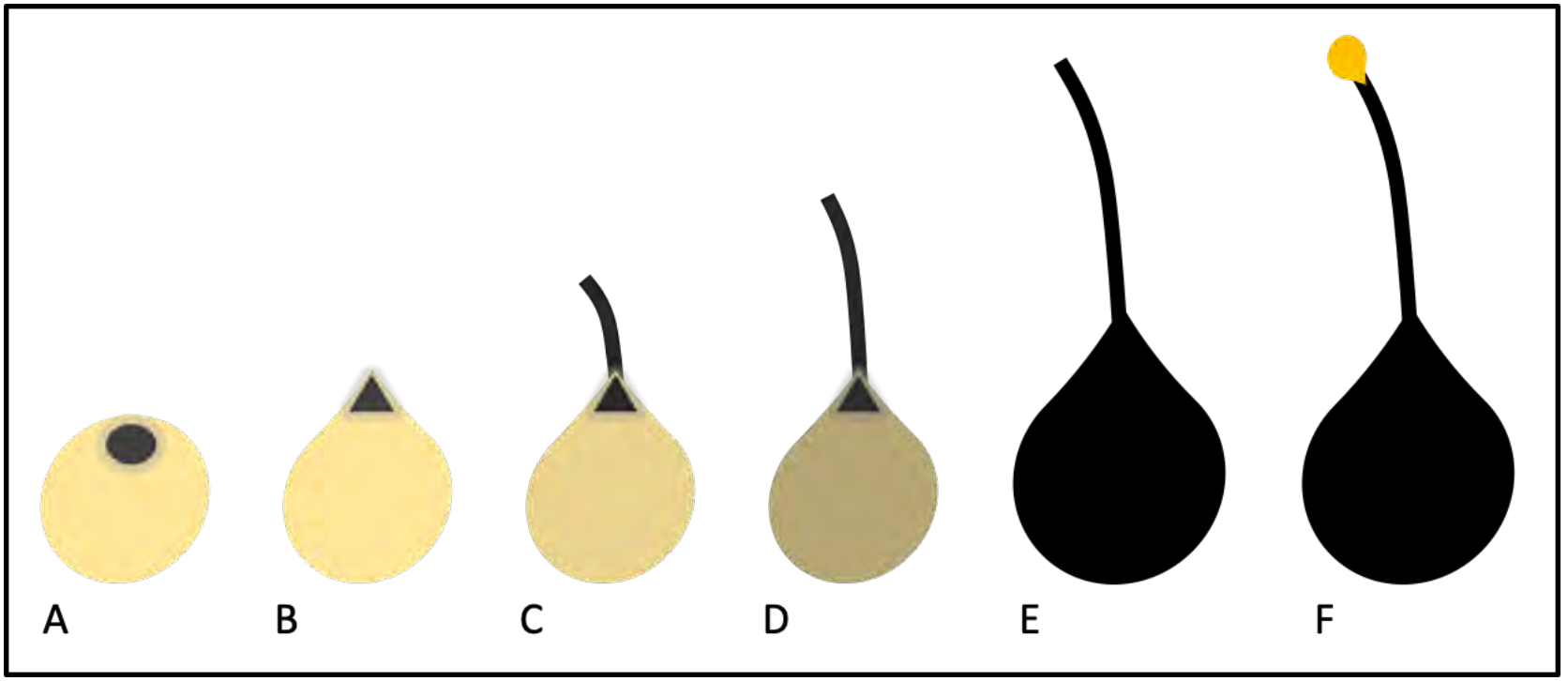

Figure S8: A schematic illustrating the sexual development of *Huntiella* species. A) Sexual reproduction begins with the production of the production of light-coloured, round protoascomata. This is followed by **B)** the emergence of a dark, beak-like structure from the young ascomatal base, which develops into **C)** an extended neck. **D)** During this process, the ascomatal base also darkens. **E)** Once mature, **F)** a sticky mass of ascospores is exuded from the tip of the neck.

CONCLUDING REMARKS

CONCLUDING REMARKS

Sexual reproduction is a complex process that involves hundreds of genes and gene products, their correct spatiotemporal expression and intricate interactions between each another. This process is further complicated in fungi due to the existence of many distinct mechanisms of sexual reproduction; including heterothallism, primary homothallism, pseudohomothallism, mating-type switching and unisexual reproduction. Although heterothallism and primary homothallism are relatively well-characterized, the other three systems are somewhat more complicated, not as thoroughly researched, and are thus less well-understood. The focus of this thesis was to address the knowledge gap that exists in our collective understanding of unisexuality in fungi.

To date, only a few fungal species have been described as unisexual, including two yeast species of significance to the human health sector. The first is *Cryptococcus neoformans*, a basidiomycetous yeast which is an opportunistic pathogen of immune-compromised patients [1]. The second, *Candida albicans*, is an ascomycetous yeast and causes common fungal infections such as thrush [2]. Given the importance of these two yeasts in clinical settings, it is perhaps unsurprising that almost everything we know regarding the unisexual reproductive pathway is based on these two species. Three genera of filamentous ascomycetes are also known to include unisexual species; *Neurospora* [3,4], *Huntiella* [5,6] and *Thermoascus* [7]. With the exception of their description as unisexual, no further research had been conducted regarding the reproductive strategies of these species.

The aim of the research presented in this thesis was to enhance our understanding of this unique sexual strategy in filamentous ascomycete fungi. This was achieved by utilizing a variety of bioinformatic tools and developing a number of molecular protocols to investigate the underlying genetic pathways associated with unisexual reproduction. The primary focus of the research in this thesis involved the comparison between the unisexual *H. moniliformis* and the heterothallic *H. omanensis*. It was subsequently possible to compare the results generated from this *Huntiella*-based research with data from two other genera, *Neurospora* and *Thermoascus*. I was able to show that similar genetic, genomic and transcriptomic differences can be found between other pairs of unisexual and heterothallic relatives, such

as major alterations to the mating type genes as well as the expression of the mating pheromones. This supports the notion that unisexual reproduction in filamentous ascomycetes is the result of a common set of changes in two or more genes in heterothallic species. These changes appear to be sufficient to confer the ability to sexually reproduce independently.

One of the major challenges that we faced during the course of conducting this research was the lack of protocols for transformation and genome editing in species of *Huntiella*. The need for such a system became particularly important when the major hypothesis derived from the first research chapter was that the truncation of a single gene could potentially allow for the transition from heterothallism to unisexuality. To experimentally test this hypothesis, we needed to disrupt this gene in a heterothallic species. Thus, one of the outcomes of this thesis was the development of a transformation system for use in *Huntiella* species. While gene disruption and functional characterization are fairly routine procedures in many model species, transferring this technology to non-model species is not trivial and requires a great deal of species-specific optimization.

The first genetic manipulation system that I attempted was the classical homology-based split marker approach combined with a protoplast-dependent transformation protocol. The development of an efficient protoplast extraction protocol was fairly straightforward given that a variety of pre-existing protocols were available from a number of other filamentous ascomycete fungi. So too was the non-targeted transformation of foreign DNA into these protoplasts. However, despite numerous attempts, targeted disruption of the *MAT* locus using the split marker approach was not possible. In more than 80 independent cases of successful transformation and genomic integration, the antibiotic resistance cassette was randomly integrated elsewhere in the genome and did not disrupt the *MAT* locus. This was perhaps not entirely surprising as this technique relies strongly on efficient homologous recombination (HR). Unlike in yeasts such as *Saccharomyces cerevisiae*, where HR is highly efficient, the non-homologous end joining (NHEJ) pathway is often the preferred DNA repair mechanism in filamentous fungi [8–10]. This pathway leads to the heterologous integration of almost all exogenous DNA. Thus, the efficiency of homologous integration can become unsuitable for the high-throughput development of mutant strains in filamentous fungi.

The next technique that I used was thus a system that would enable more targeted genome disruption. The obvious answer was to use the fairly recently described CRISPR-Cas9 genome editing system, which boasts efficiency, technical ease and, most importantly, accuracy. I had the opportunity to work with Prof Yinong Yang from Pennsylvania State University, who has experience using the CRISPR-Cas9 technology in filamentous fungi. I was thus able to use a plasmid developed in his research group to undertake the next round of experiments. This particular plasmid (pX330-U6-Chimeric) encodes a codon-optimized *Cas9* gene, a cassette for expressing the single-guide RNA (sgRNA) as well as a gene conferring hygromycin resistance. In order to use this plasmid, however, I needed to ensure that the promoter expressing the *Cas9* gene would enable sufficient expression of the gene in *H. omanensis*. This was tested using a different plasmid which expresses a green fluorescent protein (GFP) under the control of the same promoter. Despite successful transformation of this plasmid into *H. omanensis* protoplasts, fluorescence was never detected, indicating that either the promoter was not suitable for use in *H. omanensis* or that for currently unknown reasons GFP is not expressed or is non-fluorescent in this species. This was especially surprising given the fact that the a similar plasmid had been used to efficiently express GFP in *Ceratocystis albifundus*, a member of a closely related genus [11].

To address the GFP problem, I designed plasmids harbouring the GFP gene under the control of two *Huntiella*-specific promoters. Highly expressed, housekeeping genes were identified from the RNA-seq data produced in the first research chapter of this thesis. Promoters for these genes were predicted using the genome and transcriptome sequence data. Of these, the upstream promoter elements of the glyceraldehyde 3-phosphate dehydrogenase (GADPH) and elongation factor (EF) genes were chosen. I assembled two independent plasmids, each harbouring the GFP gene under control of one of the two promoters, together with ampicillin and hygromycin resistance cassettes as selective markers for use in bacteria and fungi, respectively. Again, however, despite successful transformation with the newly developed plasmids, fluorescence was not detected. This led me to believe that GFP is not transcribed, nor translated or, alternatively, is degraded in *H. omanensis*. This was entirely unexpected and, given the importance of GFP as a marker in fungal transformations, deserves further investigation.

As a consequence of the difficulties associated with *in vivo Cas9* expression, the next step was to use purified Cas9 enzyme and an *in vitro* transcribed sgRNA to form the ribonucleoprotein (RNP) with which to transform the protoplasts. This technique had recently been developed in *Fusarium oxysporum* [12] and was used for stable and efficient gene disruption. This plasmid-independent technique worked the first time it was attempted and two mutant isolates that possessed the targeted gene disruption were produced.

The challenging nature of developing a successful knockout protocol in non-model species has undoubtedly affected the efficiency with which functional characterization research can be conducted. The success with the CRISPR-Cas9 system has provided a relatively easy-to-use system that allows for the targeted introduction of precise mutations. It would be misleading, however, to assume that this system will work seamlessly across the Ceratocystidaceae, or within other fungal families. A great deal of protocol optimization is typically needed to establish transformation protocols in non-model species. Furthermore, while the sgRNA-Cas9 RNP-based protocol is a plasmid-independent system, it is dependent on the development of a technique with which to produce protoplasts. This is further complicated by the fact that the methodologies and enzymes needed for producing protoplasts are not standardized across all fungi, even in closely-related species.

Despite, or perhaps because of, the abovementioned difficulties, one of the most exciting outcomes of the research presented in this thesis is the development of an efficient and effective genome editing protocol for use in species of the *Huntiella* genus. This protocol will, in the future, be optimized for use in species of other genera residing in the family Ceratocystidaceae and has the potential to be used for functional characterization of genes involved in mating, pathogenicity and host-specificity. Importantly, the method described in this thesis does not require the *Cas9* gene to be introduced and expressed in each species of interest. This will hopefully reduce the complexity of transferring the technology to other species. A case in point is the fact that while GFP is used extensively in other filamentous ascomycetes, it was not possible to express GFP in *H. omanensis*, illustrating the usefulness of a protein-based system.

During the course of this research, other *Huntiella*-specific data has been developed that can be used in future research. In this thesis, I produced RNA-seq data from the transcriptomes of two species- *H. omanensis* and *H. moniliformis*. Not included in this thesis, but indirectly derived from it, are the genomes of two further species, *H. bhutanensis* and a newly described species, *H. abstrusa.* Also produced was RNA-seq data for the latter species. This data can be utilized for a variety of different applications, including fully annotating the currently available *Huntiella* genomes. Furthermore, we can also use this data to investigate other biological aspects of these species, including, for example, their saprobic nature, especially when compared to the predominantly pathogenic species that reside in other genera of the family the Ceratocystidaceae.

This thesis has contributed significantly to knowledge regarding unisexual reproduction in filamentous species. This will enable more focused research into the mechanisms that underlie unisexuality, similar to what has been done in the two yeast species, *Cr. neoformans* and *Ca. albicans*. It is clear that mating pheromones play a central role in unisexuality in filamentous species. It is also apparent that, at least in *H. omanensis*, disruption of the *MAT* locus alone is insufficient to enable unisexual behaviour. The pheromone response pathway may thus play an independent and important role in this transition as well. Furthermore, the pheromone response pathway involves a variety of proteins, in addition to the pheromones, and thus the genes that encode these proteins also provide intriguing targets for further investigation.

In the two unisexual yeasts, sexual reproduction typically occurs between two cells of the same mating type. These can either be between cells derived from a single mother cell, or between two non-isogenic cells. It is still not clear what precisely is happening during unisexual reproduction in a single isolate of a filamentous fungus. While it is clear that a single isolate of *H. moniliformis* can produce ascomata, it is not known if two non-isogenic isolates can also recombine sexually. This represents an important next step in understanding unisexuality in *H. moniliformis*. If we are able to induce unisexual behaviour in *H. omanensis*, this could be tested in this species as well. Additionally, since no MAT1-1 isolates of *H. moniliformis* have been found, it has been impossible to assess the relationship between unisexual and heterothallic mating within a single species. Development of unisexual MAT1-

2 *H. omanensis* isolates would allow us to understand whether unisexuality and heterothallism can be maintained by single isolates and whether a particular sexual strategy is preferred under different environmental conditions. This kind of research could also be attempted in *N. africana* and *T. aurantiacus*, however, given the development of the transformation and genome editing protocols for *H. omanensis*, this genus remains the more attractive option.

Research from the second research chapter of this thesis addresses the fact that unisexual species have been described from three disparate fungal genera. It is thus a trait that has arisen independently at least three times. Given the selective advantages of sexual recombination, it is likely that unisexuality is far more widespread than has currently been documented. This potential under-documentation is exacerbated by the difficulties associated with describing a species as unisexual. Phenotypically, unisexual species are indistinguishable from other homothallic species in that a single isolate is capable of sexual reproduction. Genetically, however, unisexual species harbour very distinct *MAT* loci. The ever-increasing availability of genome data from non-model species is allowing for the identification of unisexual species by enabling the annotation and description of the genes at the *MAT* locus. It is thus likely that species currently known to be homothallic and thought to reproduce via primary homothallism may later be reclassified as unisexual once data regarding their genomes and *MAT* loci become available.

The implications of unisexuality, especially if it becomes more commonly described, are far-reaching. This is particularly true for the fields of human, animal and plant pathology, where it will change how we respond to the introduction of pathogens into novel environments. When a new pathogen is identified, researchers typically investigate whether the introduction included isolates of both mating types or only a single mating type. In the event of the existence of both mating types, it is assumed that sexual reproduction can take place, which has been shown to cause an increase in genetic variation and virulence, thereby worsening the potential effects the pathogen has on its host [13]. This situation demands a more intense response to the pathogen. For example, the introduction of both mating types makes it essential to breed for host resistance to more than one genotype of the pathogen and to continually monitor for the emergence of pathogen resistance as a consequence of continued

genetic recombination. In contrast, if only a single mating type is identified, the response will be different, as sexual reproduction and the associated risks of a sexually recombining population are presumed to be absent. Breeding for resistance to a single genotype may be possible and genetic resistance to the pathogen in the host is likely to be maintained over many years. This, however, will not be true in the case of unisexual species, where isolates of a single mating type can recombine. Understanding the nature of single mating type introductions of pathogens is thus important and they should be treated with more caution [14].

The unisexual cycle is also capable of producing the ascospores which are often hardier than conidia and enable the fungus to spread further and remain viable for longer. In *Cr. neoformans*, particularly, unisexual reproduction produces the spores that act as the infectious propagules, making unisexuality an important process in the clinical setting [15,16]. In *Huntiella* species and other ophiostomatoid plant pathogens, it is the sexual spores, in the form of ascospore masses, that are transmitted from tree to tree via insect dispersal [17,18]. This, implicates unisexual reproduction in the ability of *H. moniliformis* to spread from host to host, given that the chance of a MAT1-2 isolate of *H. moniliformis* finding a MAT1-1 partner to mate with is potentially zero.

Although model species provide valuable information regarding the life cycles, sexual strategies and other important biological processes in fungi, it is within the non-model species that we find interesting deviations from the norm. These differences often provide us with a more comprehensive understanding of these processes and what is possible from a biological standpoint. The discovery of unisexuality, for example, showed us that genes that were historically thought to be essential, can in fact be dispensable under certain circumstances. The development of a more complete molecular toolbox for studying these species is beginning to allow for the in-depth analysis of many different fungi, and eventually, will enable a far more comprehensive understanding of the species that reside in the Fungal Kingdom, and within the greater Eukaryotic lineage.

REFERENCES

1. Lin X, Hull CM, Heitman J. **2005**. Sexual reproduction between partners of the same mating type in *Cryptococcus neoformans*. Nature. 434: 1017–1021.
2. Alby K, Schaefer D, Bennett RJ. **2009**. Homothallic and heterothallic mating in the opportunistic pathogen *Candida albicans*. Nature. 460: 890–893.
3. Glass NL, Smith ML. **1994**. Structure and function of a mating-type gene from the homothallic species *Neurospora africana*. Molecular & General Genetics. 244: 401–409.
4. Glass NL, Metzenberg RL, Raju NB. **1990**. Homothallic Sordariaceae from nature: The absence of strains containing only the a mating type sequence. Experimental Mycology. 14: 274–289.
5. Wilson AM, Godlonton T, van der Nest MA, Wilken PM, Wingfield MJ, Wingfield BD. **2015**. Unisexual reproduction in *Huntiella moniliformis*. Fungal Genetics and Biology. 80: 1–9.
6. Liu FF, Li GQ, Roux J, Barnes I, Wilson AM, Wingfield MJ, et al. **2018**. Nine novel species of *Huntiella* from southern China with three distinct mating strategies and variable levels of pathogenicity. Mycologia. 110: 1145–1171.
7. Schuerg T, Gabriel R, Baecker N, Baker SE, Singer SW. **2016**. *Thermoascus aurantiacus* is an intriguing host for the industrial production of cellulases. Current Biotechnology. 6: 89–97.
8. Wagner J, Rodriguez FJ, Kele J, Sousa K, Rawal N, Pasolli HA, et al. **2004**. Highly efficient gene replacements in *Neurospora* strains deficient for nonhomologous end-joining. Proceedings of the National Academy of Sciences. 101: 12248–12253.
9. Pöggeler S, Kück U. **2006**. Highly efficient generation of signal transduction knockout mutants using a fungal strain deficient in the mammalian *ku70* ortholog. Gene. 378: 1–10.
10. Nayak T, Szewczyk E, Oakley CE, Osmani A, Ukil L, Murray SL, et al. **2006**. A versatile and efficient gene-targeting system for *Aspergillus nidulans*. Genetics. 172: 1557–1566.
11. Sayari M, Nest MA Van Der, Steenkamp ET, Adegeye OO, Marincowitz S. **2019**. Agrobacterium-mediated transformation of *Ceratocystis albifundus*. Microbiological

Research. Elsevier; 226: 55–64.

12. Wang Q, Cobine PA, Coleman JJ. **2018**. Efficient genome editing in Fusarium oxysporum based on CRISPR/Cas9 ribonucleoprotein complexes. Fungal Genetics and Biology. 117: 21–29.
13. Groenewald M, Barnes I, Bradshaw RE, Brown A V, Dale A, Groenewald JZ, et al. **2007**. Characterization and distribution of mating type genes in the Dothistroma needle blight pathogens. Phytopathology. 97: 825–834.
14. Feretzaki M, Heitman J. **2013**. Unisexual reproduction drives evolution of Eukaryotic microbial pathogens. PLoS Pathogens. 9: e1003674.
15. Fraser JA, Giles SS, Wenink EC, Geunes-Boyer SG, Wright JR, Diezmann S, et al. **2005**. Same-sex mating and the origin of the Vancouver Island *Cryptococcus gattii* outbreak. Nature. 437: 1360–1364.
16. Velagapudi R, Hsueh Y, Geunes-boyer S, Wright JR, Heitman J. **2009**. Spores as infectious propagules of *Cryptococcus neoformans*. Infection and Immunity. 77: 4345–4355.
17. INGOLD CT. **2006**. The stalked spore-drop. New Phytologist. 60: 181–183.
18. Malloch D, Blackwell M. **1993.** Dispersal biology of the ophiostomatoid fungi. In: Wingfield M, Seifert K, Webber J, editors. Ceratocystes and Ophiostoma: taxonomy, ecology and pathogenicity. St. Paul, MN: APS Press; pp. 195–206.

SUPPLEMENTARY CHAPTERS

doi:10.5598/imafungus.2016.07.02.11

IMA FUNGUS · 7(2): 317–323 (2016)

ARTICLE

IMA Genome-F 7

Draft genome sequences for *Ceratocystis fagacearum, C. harringtonii, Grosmannia penicillata,* and *Huntiella bhutanensis*

Brenda D. Wingfield[1], Tuan A. Duong[1], Almuth Hammerbacher[2], Magriet A. van der Nest[1], Andi Wilson[1], Runlei Chang[2], Z. Wilhelm de Beer[2], Emma T. Steenkamp[2], P. Markus Wilken[1], Kershney Naidoo[1], and Michael J. Wingfield[2]

[1]Department of Genetics, Forestry and Agricultural Biotechnology Institute (FABI), University of Pretoria, Pretoria, South Africa; corresponding author e-mail: Brenda.Wingfield@up.ac.za

[2]Department of Microbiology and Plant Pathology, Forestry and Agricultural Biotechnology Institute (FABI), University of Pretoria, Pretoria, South Africa

Abstract: Draft genomes for the fungi *Ceratocystis fagacearum, C. harringtonii, Grosmannia penicillata,* and *Huntiella bhutanensis* are presented. *Ceratocystis fagacearum* is a major causal agent of vascular wilt of oaks and other trees in the family *Fagaceae*. *Ceratocystis harringtonii,* previously known as *C. populicola,* causes disease in *Populus* species in the USA and Canada. *Grosmannia penicillata* is the causal agent of bluestain of sapwood on various conifers, including *Picea* spp. and *Pinus* spp. in Europe. *Huntiella bhutanensis* is a fungus in *Ceratocystidaceae* and known only in association with the bark beetle *Ips schmutzenhorferi* that infests *Picea spinulosa* in Bhutan. The availability of these genomes will facilitate further studies on these fungi.

Key words:
bluestain fungi
entomogenous fungi
Ips
Populus
tree diseases
vascular wilt

Article info: Submitted: 1 September 2016; Accepted: 6 November 2016; Published: 29 November 2016.

IMA Genome-F 7A

Draft genome sequence for the oak pathogen *Ceratocystis fagacearum*

Ceratocystis fagacearum (*Microascales*; *Ceratocystidaceae*) is a wilt pathogen of oak (*Quercus* spp.) and other *Fagaceae* in the eastern and north-central US (Henry *et al.* 1944, Billings 2000, Juzwik *et al.* 2004). Based on ecological and phylogenetic data, however, *C. fagacearum* falls outside of the genus *Ceratocystis* sensu stricto as defined by De Beer *et al.* (2014). Its taxonomic position as a discrete genus is currently being established (De Beer, unpublished).

Ceratocystis fagacearum causes a damaging and important vascular wilt disease known as oak wilt (Appel 1995). Infection occurs in spring through wounds commonly made during pruning operations. Trees die rapidly and the pathogen can pass from one tree to another via root grafts resulting in rows or patches of dying trees. As the trees die, pressure pads develop under the bark to expose spore-bearing mats where *C. fagacearum* produces a fruity odour attractive to insects (Lin & Phelan 1992, Cease & Juzwik 2001). These include sap-feeding nitidulid beetles that can transfer the pathogen to freshly made wounds on trees, thereby resulting in new infections (Cease & Juzwik 2001, Juzwik *et al.* 2004).

The aim of this study was to sequence the genome of *C. fagacearum*. The data are thus intended to compliment the previously established genome resources for species in the Ceratocystidaceae (Wilken *et al.* 2013, van der Nest *et al.* 2014a, b, Wingfield *et al.* 2015a, b, Belbahri 2015, Wingfield *et al.* 2016), particularly in order to draw comparisons between them.

SEQUENCED STRAIN

USA: *Iowa*: West Des Moines, isol. *Quercus rubra,* Jan. 1991, *S. Seegmueller* (CMW 2656, CBS 138363, PREM 61535 - dried culture).

NUCLEOTIDE SEQUENCE ACCESSION NUMBER

The *Ceratocystis fagacearum* isolate CMW 2656 Whole Genome Shotgun project has been deposited in GenBank under the accession number MKGJ00000000.

MATERIALS AND METHODS

Ceratocystis fagacearum isolate CMW 2656 is obtainable from the culture collection (CMW) of the Forestry and Agricultural Biotechnology Institute (FABI), University of Pretoria, South Africa and the CBS-KNAW Fungal

Biodiversity Centre (CBS), Utrecht, The Netherlands. The fungus was grown at 25 °C on 2 % malt extract agar (MEA: 20 % w/v, Biolab, Midrand, South Africa) supplemented with 100 µg/L thiamine. Total genomic DNA was isolated using a phenol-chloroform method as described by Roux *et al.* (2004) and sequenced on the Genomics Analyzer IIx platform (Illumina) at the Genome Centre (University of California at Davis, CA). Two libraries (one with 350-bp and one with 600-bp paired-end inserts) were generated according to standard Illumina protocols and produced sequences with read lengths of approximately 100 bases. Reads with a limit of 0.05 and below were quality controlled and trimmed using CLC Genomics Workbench v. 7.5.1 (CLCBio, Aarhus). This software was also used to produce a draft genome assembly using the *de novo* assembly function under default settings. The assemblies were subsequently scaffolded using SSPACE v. 2.0 (Boetzer *et al.* 2011) and gaps filled using GapFiller v. 2.2.1 (Boetzer & Pirovano 2012). The online version of the *de novo* prediction software AUGUSTUS was employed to predict the putative open reading frames (ORFs) using *Fusarium graminearum* gene models (Stanke *et al.* 2004). Genome completeness was assessed with the Benchmarking Universal Single-Copy Orthologs (BUSCO v. 1.1b1) tool (Simão *et al.* 2015).

RESULTS AND DISCUSSION

The draft nuclear genome of *C. fagacearum* had an estimated size of 26 736 264 bases with 123x coverage. The assembly included 1257 contigs larger than 500 bases with an N50 value of 42 305 bases and an average GC content of 46.9 %. AUGUSTUS predicted 6703 ORFs, which correlated with an average gene density of 251 ORFs/Mb. This assembly had a high degree of completeness with a BUSCO score of 96 %, of which 1321 were Complete Single-Copy BUSCOs, 61 were Complete Duplicated BUSCOs, 47 were Fragmented BUSCOs, and only nine were missing BUSCO orthologs out of the 1438 BUSCO groups searched (Simao *et al*. 2015).

Comparison of these genome statistics revealed no striking differences between the genome of *C. fagacearum* and those determined in previous studies (Wilken *et al.* 2013, van der Nest *et al.* 2014a, b, Wingfield *et al.* 2015a, b, 2016, Belbahri 2015). This is despite its unique ecology and taxonomic position (de Beer *et al.* 2014). Future genome-based analyses will undoubtedly improve our understanding of the molecular and evolutionary processes underlying the biology of this pathogen.

Authors: **M.A. van der Nest, P.M. Wilken, E.T. Steenkamp, A. Wilson, K. Naidoo, Al. Hammerbacher, M.J. Wingfield, and B.D. Wingfield**
**Contact*: Magriet.vanderNest@fabi.up.ac.za*

IMA Genome-F 7B

Draft genome sequence of the poplar pathogen *Ceratocystis harringtonii*

The genome of black cottonwood (*Populus trichocarpa*) has been sequenced and is available for study, which has resulted in it becoming an important model tree for woody plant research (Tuskan *et al.* 2006). This tree species is well known for its resistance to fungal infection, and to date only a few pathogens are known to infect it (Royle & Ostry 1995). Fungal species currently causing severe disease on plantation-grown poplar include rust diseases caused by species of *Melampsora* (e. g. Newcombe *et al.* 2000) and leaf spots caused by *Marssonia* spp. (e.g. Erickson *et al.* 2004). In order to gain increased understanding of the adaptations allowing pathogens to infect poplar, the genome of the European poplar rust fungus, *Melampsora larici-populina*, was sequenced. This provided a powerful tool for studies in molecular plant-pathogen interactions in the phyllosphere of a perennial host (Duplessis *et al.* 2011). In contrast, little is known regarding stem-infecting pathogens in poplar, and particularly which resistance mechanisms exist to provide such extensive protection against fungal infection of its woody tissues. Furthermore, knowledge pertaining to strategies that pathogens employ to overcome this resistance has not been well documented.

Ceratocystis harringtonii resides in *Ceratocystidaceae* (de Beer *et al.* 2013a, b), and was previously treated as *C. populicola* (Johnson *et al.* 2005). It causes target-shaped cankers on infected trunks and rooted cuttings (Wood & French 1963, Johnson *et al.* 2005). Furthermore, it is one of the few pathogens known to breach the effective defence barriers in poplar stems. This fungus occurs throughout the natural range of *Populus* species in the USA and Canada, as well as in hybrid poplar plantations in Poland (Gremmen & de Kam 1977). The pathogen is most aggressive on the North American poplar species *P. trichocarpa*, *P. balsamifera,* and *P. tremuloides,* while the European *P. nigra* is known to be almost entirely resistant to infection (Johnson *et al.* 2005). One mechanism by which *C. harringtonii* elicits host defences is by the production of cerato-populin, a pathogen-associated molecular pattern protein. This toxin is similar to the well-characterized ceratoplatanin and cerato-ulmin, which are known in *C. platani* and *Ophiostoma novo-ulmi*, respectively (Comparini *et al.* 2009, Lombardi *et al.* 2013, Martellini *et al.* 2013).

In order to extend our knowledge on plant-pathogen interactions in woody hosts and to understand the basis of resistance against fungal stem infection in poplar, the genome of *C. harringtonii* was sequenced. This genome sequence will provide a powerful tool to interrogate the mechanisms by which plant pathogens infect woody stems and cause canker disease in a highly resistant tree species.

SEQUENCED STRAIN

Poland: isol. ex hybrid poplar *Populus maximowiczii* x *P. laurifolia* x *P. nigra* 'Italica' (*P.* x*berolinensis*), 1977, *J.*

Gremmen (culture CBS 110.78 = CMW 14789 (ex-epitype); PREM 61533- dried culture).

NUCLEOTIDE SEQUENCE ASSESSION NUMBER

This Whole Genome Shotgun project of the *Ceratocystis harringtonii* genome has been deposited at DDBJ/EMBL/GenBank under accession number MKGM00000000; this is the first version described here.

MATERIALS AND METHODS

Total genomic DNA was isolated from the mycelium of a single-spore culture of isolate *C. harringtonii* CMW 14789 grown on 2 % malt extract agar (MEA: 2 % w/v, Biolab, Midrand, South Africa) supplemented with 100 µg/L thiamine for 10 d using the method of Barnes *et al.* (2001). The Genomics analyzer IIx platform (Illumina) at the Genome Centre (University of California at Davis, CA) was used for sequencing the genome. Two 350-bp and three 600-bp paired-end libraries were made using standard Illumina protocols. Sequence data was assessed for quality, trimmed and assembled with the software package CLC Genomics (CLCBio, Aarhus, Denmark) using default settings. Poor quality reads (limit of 0.05) and/or terminal nucleotides were discarded. The contigs were assembled into scaffolds using SSPACE v.2.0 (Boetzer *et al.* 2011) and gaps were filled using GapFiller v. 2.2.1 (Boetzer & Pirovano 2012). The genome assembly was verified and completeness assessed using the Benchmarking Universal Single-Copy Orthologs (BUSCO) software (Simão *et al.* 2015). Contigs smaller than 500 bp were removed from the final dataset.

RESULTS AND DISCUSSION

Sequencing of five *C. harringtonii* DNA libraries yielded a total of 31 057 034 paired-end reads with an average length of 101 bases. After trimming, 30 972 782 reads were recovered with an average length of 96 bases. The estimated size of the assembled draft genome was 26 Mb with a coverage of 110x. The genome had a mean GC content of 48.8 % and a N50 contig size of 66 kb. A total of 920 contigs were assembled of which 813 were larger than 500 bases (excluding the mitochondrial genome sequence data). BUSCO analysis revealed that out of 1438 possible BUSCO groups searched 1327 were single-copy, while 67 were duplicated and six were fragmented or missing. Analysis using AUGUSTUS (Stanke *et al.* 2006) revealed 6627 putative open reading frames.

Genome sizes differ widely among *Sordariomycetes*, for example the *Fusarium graminearum* and *Trichoderma reesii* genomes have approximate sizes of 36 Mb and 34 Mb, respectively (Martinez *et al.* 2008, King *et al.* 2015), while the genome of *Ceratocystiopsis minuta* is only 21 Mb in size (Wingfield *et al.* 2016). The estimated genome size of *C. harringtonii* (26 Mb) is marginally smaller than the genomes reported for other closely related members of *Ceratocystidaceae* (28 – 32 Mb; Wingfield *et al.* 2016, Wilken *et al.* 2013, van der Nest *et al.* 2014). Despite the smaller genome size, the *C. harringtonii* genome contains similar numbers of predicted ORF's as other sequenced species of *Ceratocystis* (Wilken *et al.* 2013, van der Nest *et al.* 2014, Wingfield *et al.* 2016).

The *C. harringonii* draft genome will be an important resource in studies of plant/pathogen interactions in woody tissues. This is especially true because this fungus is one of only a few reported pathogens that can overcome the defence mechanisms in the stem tissues of the model tree, *P. trichocarpa.* Furthermore, with growing numbers of genomes available for species in *Ceratocystisticaceae*, the *C. harringtonii* genome will also be used for comparative genomic studies and those considering the mechanisms of host specialization in this fascinating group of plant pathogens.

Authors: **A. Hammerbacher*, P.M. Wilken, M.A. van der Nest, A. Wilson, K. Naidoo, M.J. Wingfield, and B.D. Wingfield**
**Contact*: almuth.hammerbacher@fabi.up.ac.za

IMA Genome-F 7C

Draft genome sequence of *Grosmannia penicillata*

The asexual morph of *Grosmannia penicillata* was first described as *Leptographium penicillatum* (Grosmann 1931), the causal agent of blue stain of sapwood surrounding the galleries of the spruce bark beetle, *Ips typographus*. The sexual morph was discovered soon afterwards and described as *Ceratostomella penicillata* (Grosmann 1932), but Goidánich (1936) considered the species to be distinct from other *Ceratostomella* spp. and introduced a new generic name, *Grosmannia*, with *G. penicillata* as type species. Subsequently, *Grosmannia* was treated as a synonym of *Ophiostoma* (Siemaszko 1939, Arx 1952, Jacobs & Wingfield 2001) and *Ceratocystis* (Bakshi 1951, Hunt 1956, Upadhyay 1981) until Zipfel *et al.* (2006) re-instated the name to accommodate the sexual morphs of *Leptographium* spp. After the implementation of the one fungus one name principles (Hawksworth 2011), *Leptographium*, as the older generic name, currently has preference over *Grosmannia* (de Beer & Wingfield 2013). However, the type species of the two genera, *L. lundbergii* and *G. penicillata*, group in distinct lineages of which the generic status needs reconsideration (de Beer & Wingfield 2013). For the interim, the lineage that includes *G. penicillata* and 17 other *Leptographium* and *Grosmannia* species, are referred to as the *G. penicillata* species complex in *Leptographium s. lat.* (Six *et al*., 2011, Linnakoski *et al*. 2012, de Beer & Wingfield 2013).

Grosmannia penicillata occurs on various conifers including *Picea* and *Pinus* spp. in Europe (Jacobs & Wingfield 2001). It is vectored by various scolytine bark beetle species (*Coleoptera; Curculionidae; Scolytinae*) but most importantly, by the aggressive tree-killing bark beetle *Ips typographus* (Jacobs & Wingfield 2001, Linnakoski *et al.* 2012). Inoculation

studies have indicated that *G. penicillata* is not pathogenic to its hosts (Jankowiak *et al.* 2009, Repe *et al.* 2015). This is unlike *Endoconidiophora polonica,* as defined by de Beer *et al*. (2014), that is a common associate of *I. typographus* and is able to kill trees in inoculation tests (Horntvedt *et al.* 1983, Repe *et al.* 2015).

In this study, we determined the genome sequence of *G. penicillata*. The primary intention was to provide basal genomic data to enable further studies on the taxonomy and evolutionary relationships of this species and other genera and species in the *Ophiostomatales*.

SEQUENCED STRAIN

Norway: *Akershus*: Ås, isol. *Picea abies*, Jan. 1980, *H. Solheim* (culture CMW 2644 = CBS 116008; PREM 61536 – dried culture)

NUCLEOTIDE SEQUENCE ACCESSION NUMBER

The genomic sequence of *Grosmannia penicillata* (CMW 2644, CBS 116008) has been deposited at DDBJ/EMBL/GenBank under the accession number MLJV00000000. The version described in this paper is version MLJV01000000.

MATERIALS AND METHODS

Grosmannia penicillata isolate CMW 2644 was obtained from the culture collection (CMW) of the Forestry and Agricultural Biotechnology Institute (FABI), the University of Pretoria, South Africa. Genomic DNA was extracted from the freeze-dried mycelium using the method described by Duong *et al.* (2013). Two pair-end libraries (350 bp and 530 bp average insert size) were prepared and sequenced using the Illumina HiSeq 2000 platform with 100 bp read length. Obtained reads were subjected to quality and adapters trimming using Trimmomatic v. 0.36 (Bolger *et al.* 2014). The genome was assembled using the program SPAdes v. 3.9 (Bankevich *et al.* 2012). The scaffolds obtained from SPAdes were subjected to further scaffolding with SSPACE-standard v. 3.0 (Boetzer *et al.* 2011). Assembly gaps were filled with GapFiller V1-10 (Boetzer & Pirovano 2012). The completeness of the assembly was assessed with the Benchmarking Universal Single-Copy Orthologs (BUSCO v. 1.1b1) program using the fungal dataset (Simão *et al.* 2015). The number of protein coding genes was determined using Augustus v 3.2.2 (Stanke *et al.* 2006).

RESULTS AND DISCUSSION

Over 11 million read pairs and 1.4 million single reads were obtained after the quality trimming. *De-novo* assembly using SPAdes resulted in 293 scaffolds which were larger than 500 bp. The number of final scaffolds was reduced to 199 after scaffolding with SSPACE and filling gaps with GapFiller. The current assembly has an N50 of 316 Kb and size of 26.33 Mb, with an overall GC content of 58.73 %. When compared with other species of *Leptographium s. lat.* for which whole genome data are available, *G. penicillata* has a similar genome size to that of *Leptographium lundbergii* (26.6 Mb) (Wingfield *et al.* 2015), and slightly smaller than those of *G. clavigera* (29.8 Mb) (DiGuistini *et al.* 2011) and *L. procerum* (28.6 Mb) (van der Nest *et al.* 2014).

The assembly included 94.6 % complete, 4.2 % fragmented, and 1.2 % missing, BUSCOs. Augustus predicted a total of 8713 protein coding genes, of which 6718 are multi-exon and 1995 are single-exon genes. As the type species of *Grosmannia*, the genome sequence of *G. penicillata* will be a valuable resource to study the taxonomic relationships between species in the genus. The data will also be useful in comparisons between genera in *Ophiostomatales* where questions relating to their ecology and evolutionary biology are of particular interest.

Authors: **T.A. Duong*, M.J. Wingfield, Z.W. de Beer, R. Chang, and B.D. Wingfield**
**Contact*: Tuan.Duong@fabi.up.ac.za

IMA Genome-F 7D

Draft genome sequence for the bark beetle-associated fungus *Huntiella bhutanensis*

Huntiella bhutanensis (*Ascomycota; Microascales*) is a filamentous fungus in *Ceratocystidaceae*. The species was previously accommodated in *Ceratocystis* as *C. bhutanensis* (van Wyk *et al.* 2004). However, a recent taxonomic review of this and related genera led to the re-circumscription of these fungi into distinct genera based on morphological, ecological and molecular characteristics (de Beer *et al.* 2014). Thus, *H. bhutanensis,* along with other cosmopolitan saprobes such as *Huntiella omanensis* and *H. moniliformis,* were assigned to the genus *Huntiella* (de Beer *et al.* 2014).

Huntiella bhutanensis was first isolated from adults of the bark beetle *Ips schmutzenhoferi* (*Coleoptora*; *Curculionidae*; *Scolytinae*) or their galleries found on *Picea spinulosa* in Bhutan (van Wyk *et al.* 2004). This was only the second report of any ophiostomatoid fungi from this country and represented the first species of *Ceratocystidaceae* to be reported in this locality (van Wyk *et al.* 2004). Despite its close relationship with the bark beetle, and unlike many other bark beetle-associates in the *Ceratocystidaceae*, *H. bhutanensis* is not considered a primary pathogen and in inoculation studies, it gave rise to only small necrotic lesions on *P. spinulosa* trees (Kirisits *et al.* 2012).

The non-pathogenic nature of *H. bhutanensis* is consistent with other *Huntiella* species that are weak pathogens or saprobes (de Beer *et al.* 2014). It also shares many morphological characteristics with other *Huntiella* species, such as globose ascomatal bases, extended ascomatal necks, and hat-shaped ascospores (van Wyk *et al.* 2004). It is unusual amongst species in the genus in that it is able to grow at 4°C (van Wyk *et al.* 2004) and it gives off a

putrid odour unlike the sweet smelling odours typical of other *Huntiella* species (van Wyk *et al.* 2004).

The aim of this study was to produce a good quality draft genome assembly for *H. bhutanensis* for use in future comparative genomics studies, both between species and genera in *Ceratocystidaceae*. Genome sequences are already publically available for *H. moniliformis* (van der Nest *et al.* 2014a) and *H. omanensis* (van der Nest *et al.* 2014b) and thus the availability of this genome assembly will aid in the elucidation and comparison of ecological strategies, sexual cycles, and other key life-style aspects of and between these species.

SEQUENCED STRAINS

Bhutan: isol. *Picea spinulosa*, July 2001, *M. J. Wingfield* (CMW 8217, CBS 114289, PREM 57807- dried culture).

NUCLEOTIDE SEQUENCE ACCESSION NUMBER

The *Huntiella bhutanensis* isolate CMW 8217 Whole Genome Shotgun project has been deposited at DDBJ/ENA/GenBank under the MJMS00000000. The version described in this paper is version MJMS01000000.

MATERIALS AND METHODS

Huntiella bhutanensis isolate CMW 8217 is preserved in the culture collection (CMW) of the Forestry and Agricultural Biotechnology Institute (FABI) at the University of Pretoria, South Africa. It can also be requested from the CBS-KNAW Fungal Biodiversity Centre (CBS), Utrecht, The Netherlands. Genomic DNA was isolated using the method of Barnes *et al.* (2001) and sequenced using the Genomics Analyzer IIx, Illumina platform at the UC Davis Genome Centre, University of California, Davis (CA). Paired-end libraries of both 350-bp and 600-bp insert sizes were prepared and sequenced following Illumina protocol. Quality trimming of the reads obtained was conducted using CLC Genomics Workbench v. 7.5.1 (CLCBio, Aarhus). This same program was used to assemble a draft genome sequence using the *de novo* assembly function, with default settings. Thereafter, SSPACE v. 2.0 (Boetzer *et al.* 2011) was used to scaffold the assemblies, and gaps created during this process were filled using GapFiller v. 2.2.1 (Boetzer & Pirovano 2012). The web-based *de novo* gene prediction software AUGUSTUS was used to predict the number of putative open reading frames (ORFs) in this assembly using the gene models of *Fusarium graminearum* (Stanke *et al.* 2004). Genome completeness was assessed with the Benchmarking Universal Single-Copy Orthologs (BUSCO v. 1.22) tool (Simão *et al.* 2015) using the fungal dataset.

RESULTS AND DISCUSSION

Sequencing of the *Huntiella bhutanensis* libraries yielded 35 886 298 raw reads with an average length of 101 bases. Trimming and quality control left 35 822 293 reads with an average length of 96 bases. The assembled nuclear genome of *H. bhutanensis* had a size of 26.77 Mb with an average coverage of 126X. This assembly had 448 scaffolds larger than 500 bases, an N50 value of 201 808 bases and an approximate GC content of 47.9 %. Web AUGUSTUS predicted 7 261 ORFs. This corresponded to an average gene density of 279 ORFs/Mb. The BUSCO analysis for this assembly also indicated a high level of completeness. Out of the 1438 fungal BUSCO groups searched, the genome contained 1315 (91.4 %) complete single copy BUSCOs, 62 (4.3 %) complete duplicated BUSCOs, 52 (3.6 %) fragmented BUSCOs and only nine (< 1 %) missing BUSCO orthologs.

The genome of *H. bhutanensis* is about 5 Mb smaller than that of its phylogenetically-close relative *H. omanensis* and possesses 1 134 fewer genes (van der Nest *et al.* 2014b). However, the genome assemblies of *H. bhutanensis* and *H. moniliformis* are more similar, at 25.4 Mb and 26.7 Mb with 6832 and 7261 ORFs, respectively (van der Nest *et al.* 2014a). The genome sequence of *H. bhutanensis* will serve as an essential resource in future genome comparisons between species of this genus and will aid in the characterization of their lifestyles, sexual cycles, and other key aspects of their biology.

Authors: **A. Wilson*, M.A. van der Nest, P.M. Wilken, K. Naidoo, M.J. Wingfield, and B.D. Wingfield**
**Contact*: Andi.Wilson@fabi.up.ac.za

ACKNOWLEDGEMENTS

This work was co-funded by the Genomics Research Institute (University of Pretoria), the University of Pretoria Research Development Programme, the DST/NRF Center of Excellence in Tree Health Biotechnology (FABI, University of Pretoria), and the National Research Foundation (NRF) (Grant number 87332). Sequencing the genomes of *Ceratocystis fagacearum, C. harringtonii, Huntiella bhutanensis* was made possible through the Improving Academics Qualifications (IAQ) grant from the NRF.

REFERENCES

Appel DN (1995) The oak wilt enigma: perspectives from the Texas epidemic. *Annual Review of Phytopathology* **33**: 103–118.

Appel DN, Kurdyla T, Lewis R (1990) Nitidulids as vectors of the oak wilt fungus and other *Ceratocystis* spp. in Texas. *European Journal of Forest Pathology* **20**: 412–417.

Arx JA von (1952) Ueber die Ascomycetengattungen *Ceratostomella* Sacc., *Ophiostoma* Syd. und *Rostrella* Zimmermann. *Antonie van Leeuwenhoek* **18**: 201–213.

Bakshi, BK (1951) Studies on four species of *Ceratocystis*, with a discussion on fungi causing sap-stain in Britain. *Mycological Papers* **35**: 1–16.

Bankevich A, Nurk S, Antipov D, Gurevich AA, Dvorkin M, *et al.* (2012) SPAdes: a new genome assembly algorithm and its

applications to single-cell sequencing. *Journal of Computational Biology* **19**: 455–477.

Barnes I, Gaur A, Burgess T, Roux J, Wingfield BD, Wingfield MJ (2001) Microsatellite markers reflect intra-specific relationships between isolates of the vascular wilt pathogen *Ceratocystis fimbriata*. *Molecular Plant Pathology* **2**: 319–25.

Belbahri L (2015) Genome sequence of *Ceratocystis platani*, a major pathogen of plane trees. http://www.ncbi.nlm.nih.gov/nuccore/814603118.

Billings RF (2000) State forest health problems: a survey of state foresters. *Journal of Forestry* **98**: 20–25.

Boetzer M, Henkel CV, Jansen HJ, Butler D, Pirovano W (2011) Scaffolding pre-assembled contigs using SSPACE. *Bioinformatics* **27**: 578–579.

Boetzer M, Pirovano W (2012) Toward almost closed genomes with GapFiller. *Genome Biology* **13**: R56.

Bolger AM, Lohse M, Usadel B (2014) Trimmomatic: a flexible trimmer for Illumina sequence data. *Bioinformatics*. **30**: 2114–2120.

Cease KR, Juzwik J (2001) Predominant nitidulid species (*Coleoptera*: *Nitidulidae*) associated with spring oak wilt mats in Minnesota. *Canadian Journal of Forest Research* **31**: 635–643.

Comparini C, Carresi L, Pagni E, Sbrana F, Sebastiani F, *et al*. (2009) New proteins orthologous to cerato-platanin in various *Ceratocystis* species and the purification and characterization of cerato-populin from *Ceratocystis populicola*. *Applied Microbiology and Biotechnology* **84**: 309–322.

de Beer ZW, Duong TA, Barnes I, Wingfield BD, Wingfield MJ (2014) Redefining *Ceratocystis* and allied genera. *Studies in Mycology* **79**: 187–219.

de Beer ZW, Wingfield MJ (2013) Emerging lineages in the *Ophiostomatales*, In: *The Ophiostomatoid Fungi: expanding frontiers* (Seifert KA, de Beer ZW, Wingfield MJ eds): 21–46. [CBS Biodiversity Series no. 12.] Utrecht: CBS-KNAW Fungal Biodiversity Centre.

DiGuistini S, Wang Y, Liao NY, Taylor G, Tanguay P, *et al.* (2011) Genome and transcriptome analyses of the mountain pine beetle-fungal symbiont *Grosmannia clavigera*, a lodgepole pine pathogen. *Proceedings of the National Academy of Sciences, USA*. **108**: 2504–2509.

Duong TA, de Beer ZW, Wingfield BD, Wingfield MJ (2013) Characterization of the mating-type genes in *Leptographium procerum* and *Leptographium profanum*. *Fungal Biology*. **117**: 411–421.

Duplessis S, Cuomo CA, Lin YC, Aerts A, Tisserant E, *et al*. (2011) Obligate biotrophy features unraveled by the genomic analysis of rust fungi. *Proceedings of the National Academy of Sciences, USA* **108**: 9166–9171.

Erickson JE, Stanosz GR, Kruger EL (2004) Photosynthetic consequences of *Marssonina* leaf spot differ between two poplar hybrids. *New Phytologist* **161**: 577–583.

Goidànich G (1936) II genere di Ascomiceti '*Grosmannia*' G. Goid. *Bollettino della Stazione di Patología Vegetale di Roma* **16**: 26–40.

Gremmen J, Kam, MD (1977) *Ceratocystis fimbriata*, a fungus associated with poplar canker in Poland. *European Journal of Forest Pathology* **7**: 44–47.

Grosmann H (1931) Beitrage zur Kenntnis der Lebensgemeinschaft zwischen Borkenkäfern und Pilzen. *Zeitschrift für Parasitenkunde* **3**: 56–102.

Grosmann H (1932) Über die systematischen Beziehungen der Gattung *Leptographium* Lagerberg et Melin zur Gattung *Ceratostomella* Sacc. *Nova Hedwigia* **72**: 183–194.

Hawksworth DL (2011) A new dawn for the naming of fungi: impacts of decisions made in Melbourne in July 2011 on the future publication and regulation of fungal names. *MycoKeys* **1**: 7–20; *IMA Fungus* **2**: 155–162.

Henry BW, Moses CS, Richards CA, Riker AJ (1944) Oak wilt: Its significance, symptoms and cause. *Phytopathology* **34**: 636–647.

Horntvedt, R, Christiansen, E, Solheim, H, Wang, S (1983) Artificial inoculation with *Ips typographus*-associated blue-stain fungi can kill healthy Norway spruce trees. *Meddelelser fra Norsk Institutt for Skogforskning* **38**: 1–20.

Hunt J (1956) Taxonomy of the genus *Ceratocystis*. *Lloydia* **19**: 1–58.

Jacobs K, Wingfield MJ (2001) *Leptographium species: tree pathogens, insect associates and agents of blue-stain.* St Paul, MN: American Phytopathological Society Press.

Jankowiak R, Rossa R, Bilański P (2009) A preliminary study on the pathogenicity of three blue-stain fungi associated with *Tetropium* spp. to Norway spruce in Poland. *Forest Research Papers* **70**: 69–75.

Johnson JA, Harrington TC, Engelbrecht CJB (2005) Phylogeny and taxonomy of the North American clade of the *Ceratocystis fimbriata* complex. *Mycologia* **97**: 1067–1092.

Juzwik J, Skalbeck TC, Neuman MF (2004) Sap beetle species (*Coleoptera*: *Nitidulidae*) visiting fresh wounds on healthy oaks during spring in Minnesota. *Forest Science* **50**: 757–764.

King R, Urban M, Hammond-Kosack MC, Hassani-Pak K, Hammond-Kosack KE (2015) The completed genome sequence of the pathogenic ascomycete fungus *Fusarium graminearum*. *BMC Genomics* **16**: 544.

Kirisits T, Konrad H, Wingfield MJ (2012) Ophiostomatoid fungi associated with the Eastern Himalayan spruce bark beetle (*Ips schmutzenhoferi*) in Bhutan: species assemblage and phytopathogenicity. *Journal of Agricultural Extension and Rural Development* **4:** 266–268.

Lin H, Phelan PL (1992) Comparison of volatiles from beetle-transmitted *Ceratocystis fagacearum* and four non-insect-dependent fungi. *Journal of Chemical Ecology* **18**: 1623–1632.

Linnakoski R, de Beer ZW, Duong TA, Niemelä P, Pappinen A, Wingfield MJ (2012) *Grosmannia* and *Leptographium* spp. associated with conifer-infesting bark beetles in Finland and Russia, including *Leptographium taigense* sp. nov. *Antonie van Leeuwenhoek* **102**: 375–399.

Lombardi L, Faoro F, Luti S, Baccelli I, Martellini F, *et al*. (2013) Differential timing of defense-related responses induced by cerato-platanin and cerato-populin, two non-catalytic fungal elicitors. *Physiologia Plantarum* **149**: 408–421.

Martellini F, Faoro F, Carresi L, Pantera B, Baccelli I, *et al*. (2013) Cerato-populin and cerato-platanin, two non-catalytic proteins from phytopathogenic fungi, interact with hydrophobic inanimate surfaces and leaves. *Molecular Biotechnology* **55**: 27–42.

Martinez D, Berka RM, Henrissat B, Saloheimo M, Arvas M, *et al*. (2008) Genome sequencing and analysis of the biomass-degrading fungus *Trichoderma reesei* (syn. *Hypocrea jecorina*). *Nature Biotechnology* **26**: 553–560.

Mayers CG, McNew DL, Harrington TC, Roeper RA, Fraedrich SW, Biedermann PH, Castrillo LA, Reed SE (2015) Three genera in the *Ceratocystidaceae* are the respective symbionts of three independent lineages of ambrosia beetles with large, complex

mycangia. *Fungal Biology* **119**: 1075–1092.

Newcombe G, Stirling B, McDonald S, Bradshaw HD (2000) *Melampsora ×columbiana*, a natural hybrid of *M. medusae* and *M. occidentalis*. *Mycological Research* **104**: 261–274.

Repe A, Bojović S, Jurc M (2015) Pathogenicity of ophiostomatoid fungi on *Picea abies* in Slovenia. *Forest Pathology*. **45**: 290–297.

Roux J, van Wyk M, Hatting H, Wingfield MJ (2004) *Ceratocystis* species infecting stem wounds on *Eucalyptus grandis* in South Africa. *Plant Pathology* **53**: 414–421.

Royle DJ, Ostry M (1995) Disease and pest control in the bioenergy crops poplar and willow. *Biomass and Bioenergy* **9**: 69–79.

Siemaszko, W (1939) Zespoly grzybów towarzyszących kornikom polskim. *Planta Polonica* **7**: 1–54.

Simão FA, Waterhouse RM, Ioannidis P, Kriventseva EV, Zdobnov EM (2015) BUSCO: assessing genome assembly and annotation completeness with single-copy orthologs. *Bioinformatics* **31**: 3210–3212.

Six D, de Beer Z, Duong T, Carroll A, Wingfield M (2011) Fungal associates of the lodgepole pine beetle, *Dendroctonus murrayanae*. *Antonie van Leeuwenhoek* **100**: 231–244.

Stanke M, Steinkamp R, Waack S, Morgenstern B (2004) AUGUSTUS: A web server for gene finding in Eukaryotes. *Nucleic Acids Research* **32**: W309–W312.

Tuskan GA, Difazio S, Jansson S, Bohlmann J, Grigoriev I, *et al*. (2006) The genome of black cottonwood, *Populus trichocarpa* (Torr. & Gray). *Science* **313**: 1596–1604.

Upadhyay HP (1981) *A monograph of Ceratocystis and Ceratocystiopsis.* Athens, GA: University of Georgia Press.

van der Nest MA, Beirn LA, Crouch JA, Demers JE, de Beer ZW, *et al.* (2014b) IMA Genome-F 3: Draft genomes of *Amanita jacksonii*, *Ceratocystis albifundus*, *Fusarium circinatum*, *Huntiella omanensis*, *Leptographium procerum*, *Rutstroemia sydowiana*, and *Sclerotinia echinophila*. *IMA Fungus* **5**: 473–486.

van der Nest MA, Bihon W, De Vos L, Naidoo K, Roodt D, *et al.* (2014a) IMA Genome-F 2: *Ceratocystis manginecans*, *Ceratocystis moniliformis*, *Diplodia sapinea*: Draft genome sequences of *Diplodia sapinea*, *Ceratocystis manginecans*, and *Ceratocystis moniliformis*. *IMA Fungus* **5**: 135–140.

van Wyk M, Roux J, Barnes I, Wingfield BD, Chhetri DB *et al.* (2004) *Ceratocystis bhutanensis* sp. nov., associated with the bark beetle *Ips schmutzenhoferi* on *Picea spinulosa* in Bhutan. *Studies in Mycology* **50**: 365–379.

Wilken PM, Steenkamp ET, Wingfield MJ, de Beer ZW, Wingfield BD (2013) IMA Genome-F 1: *Ceratocystis fimbriata*: draft nuclear genome sequence for the plant pathogen, *Ceratocystis fimbriata*. *IMA Fungus* **4**: 357–358.

Wingfield BD, Ades PK, Al-Naemi FA, Beirn LA, Bihon W, *et al.* (2015a) IMA Genome- F 4: Draft genome sequences of *Chrysoporthe austroafricana*, *Diplodia scrobiculata*, *Fusarium nygamai*, *Leptographium lundbergii*, *Limonomyces culmigenus*, *Stagonosporopsis tanaceti*, and *Thielaviopsis punctulata*. *IMA Fungus* **6**: 233–248.

Wingfield BD, Barnes I, de Beer ZW, de Vos L, Duong TA, *et al.* (2015b) IMA Genome-F 5: Draft genome sequences of *Ceratocystis eucalypticola*, *Chrysoporthe cubensis*, *C. deuterocubensis*, *Davidsoniella virescens*, *Fusarium temperatum*, *Graphilbum fragrans*, *Penicillium nordicum*, and *Thielaviopsis musarum*. *IMA Fungus* **6**: 493–506.

Wingfield BD, Ambler JM, Coetzee M, de Beer ZW, Duong TA, *et al*. (2016) Draft genome sequences of *Armillaria fuscipes*, *Ceratocystiopsis minuta*, *Ceratocystis adiposa*, *Endoconidiophora laricicola*, *E. polonica* and *Penicillium freii* DAOMC 242723. *IMA Fungus* **30**: 217–227.

Wood FA, French DW (1963) *Ceratocystis fimbriata*, the cause of a stem canker of quaking aspen. *Forest Science* **9**: 232–235.

Zipfel RD, de Beer ZW, Jacobs K, Wingfield BD, Wingfield MJ (2006) Multi-gene phylogenies define *Ceratocystiopsis* and *Grosmannia* distinct from *Ophiostoma*. *Studies in Mycology* **55**: 75–97.

available online at www.studiesinmycology.org

STUDIES IN MYCOLOGY 92: 47–133 (2019).

Genera of phytopathogenic fungi: GOPHY 2

Y. Marin-Felix[1,2*], M. Hernández-Restrepo[1], M.J. Wingfield[2], A. Akulov[3], A.J. Carnegie[4], R. Cheewangkoon[5], D. Gramaje[6], J.Z. Groenewald[1], V. Guarnaccia[1], F. Halleen[7,8], L. Lombard[1], J. Luangsa-ard[9], S. Marincowitz[2], A. Moslemi[10], L. Mostert[7], W. Quaedvlieg[11], R.K. Schumacher[12], C.F.J. Spies[7,8], R. Thangavel[13], P.W.J. Taylor[10], A.M. Wilson[2], B.D. Wingfield[2], A.R. Wood[14], and P.W. Crous[1,2,15*]

[1]*Westerdijk Fungal Biodiversity Institute, P.O. Box 85167, 3508 AD Utrecht, The Netherlands;* [2]*Department of Biochemistry, Genetics and Microbiology, Forestry and Agricultural Biotechnology Institute (FABI), University of Pretoria, P. Bag X20, Pretoria 0028, Pretoria, 0002, South Africa;* [3]*V.N. Karasin National University of Kharkiv, Svobody sq. 4, Kharkiv 61077, Ukraine;* [4]*Forest Science, NSW Department of Primary Industries, Locked Bag 5123, Parramatta, New South Wales 2124, Australia;* [5]*Department of Plant Pathology, Faculty of Agriculture, Chiang Mai University, Chiang Mai 50200, Thailand;* [6]*Instituto de Ciencias de la Vid y del Vino, Consejo Superior de Investigaciones Científicas, Universidad de la Rioja, Gobierno de La Rioja, 26071 Logroño, La Rioja, Spain;* [7]*Department of Plant Pathology, University of Stellenbosch, Private Bag X1, Matieland 7602, South Africa;* [8]*Plant Protection Division, ARC Infruitec-Nietvoorbij, Private Bag X5026, Stellenbosch 7599, South Africa;* [9]*Microbe Interaction and Ecology Laboratory, Biodiversity and Biotechnological Resource Research Unit (BBR), BIOTEC, NSTDA 113, Thailand Science Park Phahonyothin Rd., Khlong Nueng, Khlong Luang, Pathum Thani 12120, Thailand;* [10]*Faculty of Veterinary and Agricultural Sciences, University of Melbourne 3010, Melbourne, Victoria, Australia;* [11]*Naktuinbouw, Sotaweg 22, 2371 GD Roelofarendsveen, the Netherlands;* [12]*Hölderlinstraße 25, 15517 Fürstenwalde/Spree, Germany;* [13]*Plant Health and Environment Laboratory, Ministry for Primary Industries, P.O. Box 2095, Auckland 1140, New Zealand;* [14]*ARC – Plant Protection Research Institute, Private Bag X5017, Stellenbosch 7599, South Africa;* [15]*Wageningen University and Research Centre (WUR), Laboratory of Phytopathology, Droevendaalsesteeg 1, 6708 PB Wageningen, The Netherlands*

**Correspondence*: Y. Marin-Felix, y.marin@westerdijkinstitute.nl; P.W. Crous, p.crous@westerdijkinstitute.nl

Abstract: This paper represents the second contribution in the Genera of Phytopathogenic Fungi (GOPHY) series. The series provides morphological descriptions and information regarding the pathology, distribution, hosts and disease symptoms for the treated genera. In addition, primary and secondary DNA barcodes for the currently accepted species are included. This second paper in the GOPHY series treats 20 genera of phytopathogenic fungi and their relatives including: *Allantophomopsiella, Apoharknessia, Cylindrocladiella, Diaporthe, Dichotomophthora, Gaeumannomyces, Harknessia, Huntiella, Macgarvieomyces, Metulocladosporiella, Microdochium, Oculimacula, Paraphoma, Phaeoacremonium, Phyllosticta, Proxypiricularia, Pyricularia, Stenocarpella*, *Utrechtiana* and *Wojnowiciella*. This study includes the new genus *Pyriculariomyces*, 20 new species, five new combinations, and six typifications for older names.

Key words: DNA barcodes, Fungal systematics, 26 new taxa, Six new typifications.

Taxonomic novelties: New genera: *Pyriculariomyces* Y. Marín, M.J. Wingf. & Crous; **New species:** *Apoharknessia eucalypti* Crous & M.J. Wingf., *Cylindrocladiella addiensis* L. Lombard & Crous, *Cylindrocladiella nauliensis* L. Lombard & Crous, *Diaporthe heterophyllae* Guarnaccia & Crous, *Diaporthe racemosae* A.R. Wood, Guarnaccia & Crous, *Dichotomophthora basellae* Hern.-Restr., Cheew. & Crous, *Dichotomophthora brunnea* Hern.-Restr. & Crous, *Harknessia bourbonica* Crous & M.J. Wingf., *Harknessia corymbiae* Crous & A.J. Carnegie, *Harknessia cupressi* Crous & R.K. Schumach., *Harknessia pilularis* Crous & A.J. Carnegie, *Huntiella abstrusa* A.M. Wilson, Marinc., M.J. Wingf., *Metulocladosporiella chiangmaiensis* Y. Marín, Cheew. & Crous, *Metulocladosporiella malaysiana* Y. Marín & Crous, *Metulocladosporiella musigena* Y. Marín, Cheew. & Crous, *Metulocladosporiella samutensis* Y. Marín, Luangsa-ard & Crous, *Microdochium novae-zelandiae* Hern.-Restr., Thangavel & Crous, *Phaeoacremonium pravum* C.F.J. Spies, L. Mostert & Halleen, *Phyllosticta iridigena* Y. Marín & Crous, *Phyllosticta persooniae* Y. Marín & Crous; **New combinations:** *Macgarvieomyces luzulae* (Ondřej) Y. Marín, Akulov & Crous, *Pyriculariomyces asari* (Crous & M.J. Wingf.) Y. Marín, M.J. Wingf. & Crous, *Utrechtiana arundinacea* (Corda) Crous, Quaedvl. & Y. Marín, *Utrechtiana constantinescui* (Melnik & Shabunin) Crous & Y. Marín; **New status and combination:** *Oculimacula acuformis* (Nirenberg) Y. Marín & Crous; **Typification: Epitypification:** *Helminthosporium arundinaceum* Corda, *Phomopsis pseudotsugae* M. Wilson, *Pyricularia luzulae* Ondřej, *Pyricularia zingiberis* Y. Nishik; **Lectotypification:** *Phomopsis pseudotsugae* M. Wilson, *Pyricularia zingiberis* Y. Nishik.

Available online 1 May 2018; https://doi.org/10.1016/j.simyco.2018.04.002.

INTRODUCTION

The series, Genera of Phytopathogenic Fungi (GOPHY), was launched by Marin-Felix *et al.* (2017) to provide a stable platform for the taxonomy of phytopathogenic fungi. The common denominator of the genera included in this series is their association with plant diseases. The authors recognise that many species treated are not well-known plant pathogens or where Koch's postulates have not been proven for them. The focus of the series is mainly to resolve generic and species concepts of the fungi studied. This is particulary important because many taxa have been shown to represent species complexes, or to be accommodated in genera that are poly- or paraphyletic (Crous *et al.* 2015b). The series links to a larger initiative known as the "The Genera of Fungi project" (www.GeneraOfFungi.org, Crous *et al.* 2014a, 2015a, Giraldo *et al.* 2017), which aims to revise the generic names of all currently accepted fungi (Kirk *et al.* 2013). Some of the main problems are that for many genera and species type material has not been designated or/and that the vast majority of these taxa were described before the DNA phylogenetic era (Hibbett *et al.* 2011) and thus lack DNA barcodes (Schoch *et al.* 2012). Another important aim of this project is to secure the application of names by generating DNA barcodes of type species of genera and type specimens of species. In those cases where no type material has been preserved, taxa need to be recollected, epi- or neotypes designated,

Peer review under responsibility of Westerdijk Fungal Biodiversity Institute.

and registered in MycoBank to ensure traceability of the nomenclatural act (Robert *et al.* 2013). The ultimate objective is to move to a single scientific name for fungi (Crous *et al.* 2015b) for which sexual-asexual links have been resolved.

For each paper in the GOPHY series, morphological descriptions and information regarding the pathology, distribution, hosts and disease symptoms are provided for the treated genera. In addition, this information is linked to primary and secondary DNA barcodes of the currently accepted species in each genus. These DNA barcodes are critically important because of problems relating to generic delimitation and species identification based solely on morphology. A clear example is the delimitation of the genera *Bipolaris* and *Curvularia*, treated in the first paper of the GOPHY series (Marin-Felix *et al.* 2017). These two genera share many morphological similarities, and intermediate conidial characters (Manamgoda *et al.* 2012). Species delimitation in both genera based on morphology alone is of limited value because many species have overlapping characters (Sivanesan 1987, Madrid *et al.* 2014, Manamgoda *et al.* 2014). Some genera include species that do not produce reproductive structures and their identification must rely on DNA data. For some phytopathogenic genera, the DNA barcodes for species delimitation have been established in previous studies, but for the vast majority, these data remain unavailable.

Mycologists wishing to contribute to future issues in the GOPHY series are encouraged to contact Pedro Crous (p.crous@westerdijkinstitute.nl) before submitting their contributions. This will ensure there is no overlap with activities arising from other research groups. Preference will be given to genera that include novel DNA data and/or novel species, combinations or typifications. The generic contributions, apart from being published in this series of papers, will also be placed in the database displayed on www.plantpathogen.org.

MATERIAL AND METHODS

Isolates and morphological analysis

Descriptions of the new taxa and typifications are based on cultures obtained from the collection at the Westerdijk Fungal Biodiversity Institute in Utrecht, The Netherlands (CBS), the working collection of P.W. Crous (CPC), housed at the Westerdijk Fungal Biodiversity Institute, and the culture collection (CMW) of the Forestry and Agricultual Biotechnology Institute (FABI), at the University of Pretoria, South Africa. For fresh collections, we followed the procedures previously described in Crous *et al.* (1991a). Colonies were transferred to different media, i.e. cherry decoction agar (CHA), carnation leaf agar (CLA), cornmeal agar (CMA), 2 % malt extract agar (MEA), 2 % potato dextrose agar (PDA), synthetic nutrient-poor agar (SNA), oatmeal agar (OA), water agar (WA) (Crous *et al.* 2009), autoclaved pieces of grapevine canes placed on water agar (grapevine water agar; GWA), pine needle agar (PNA; Smith *et al.* 1996), or malt extract peptone agar (MPA; Speakman 1984), and incubated at different conditions depending on the taxon to induce sporulation. Requirements of media and conditions of incubations are specified in each genus. Reference strains and specimens are maintained at the CBS, CMW and CPC.

Vegetative and reproductive structures were mounted in 100 % lactic acid either directly from specimens or from colonies sporulating on MEA, PDA, PNA, OA or SNA. For cultural characterisation, isolates were grown and incubated on different culture media and temperatures as stipulated for each genus. Colour notations were rated according to the colour charts of Rayner (1970). Taxonomic novelties were deposited in MycoBank (www.MycoBank.org; Crous *et al.* 2004a).

DNA isolation, amplification and analyses

Fungal DNA was extracted and purified directly from the colonies or host material as specified for each genus. Primers and protocols for the amplification and sequencing of gene loci, and software used for phylogenetic analyses can be found in the bibliography related to the phylogeny presented for each respective genus. Phylogenetic analyses consisted of Maximum-Likelihood (ML), Bayesian Inference (BI), and Maximum Parsimony (MP). The ML and the BI were carried out using methods described by Hernández-Restrepo *et al.* (2016b), and the MP using those described by Crous *et al.* (2006b). Sequence data generated in this study were deposited in GenBank and the alignments and trees in TreeBASE (http://www.treebase.org).

RESULTS

Allantophomopsiella Crous, IMA Fungus 5: 180. 2014. Fig. 1.

Classification: *Leotiomycetes, Leotiomycetidae, Phacidiales, Phacidiaceae.*

Type species: *Allantophomopsiella pseudotsugae* (M. Wilson) Crous., basionym: *Phomopsis pseudotsugae* M. Wilson. Lectotype designated here: material deposited in Royal Botanic Garden Edinburgh, E00414771. Epitype and ex-epitype strain designated here: CBS H-23354, CBS 320.53.

DNA barcodes (genus): ITS, LSU.

DNA barcodes (species): ITS, *rpb2.* Table 1.

Conidiomata up to 600 µm diam, pycnidial, immersed, becoming erumpent, irregularly multilocular, dark brown, ostiolate; *conidiomatal wall* composed of 3–4 layers of dark brown cells, *textura angularis*. *Conidiophores* arising from inner layer of conidioma, branched, septate, at times reduced to conidiogenous cells. *Conidiogenous cells* integrated or discrete, ampulliform to subcylindrical or lageniform, hyaline, smooth with minute periclinal thickening at apex. *Conidia* inequilaterally fusiform or naviculate, hyaline, smooth, aseptate, guttulate, bearing mucoid apical appendages, flabelliform to irregular in shape. *Sexual morph* unknown (adapted from Crous *et al.* 2014b).

Culture characteristics: Colonies spreading, flat with sparse aerial mycelium and feathery margins. On PDA surface olivaceous grey, reverse iron-grey. On OA surface olivaceous grey with patches of iron-grey.

Optimal media and cultivation conditions: PNA at 25 °C under continuous near-ultraviolet light to promote sporulation.

Distribution: North America and Europe.

Hosts: Conifers (*Pinaceae*).

Disease symptoms: Canker and dieback.

Notes: This genus was recently introduced by Crous *et al.* (2014b) to accommodate *A. pseudotsugae*, a pathogen of conifers that was found to be very damaging, especially after

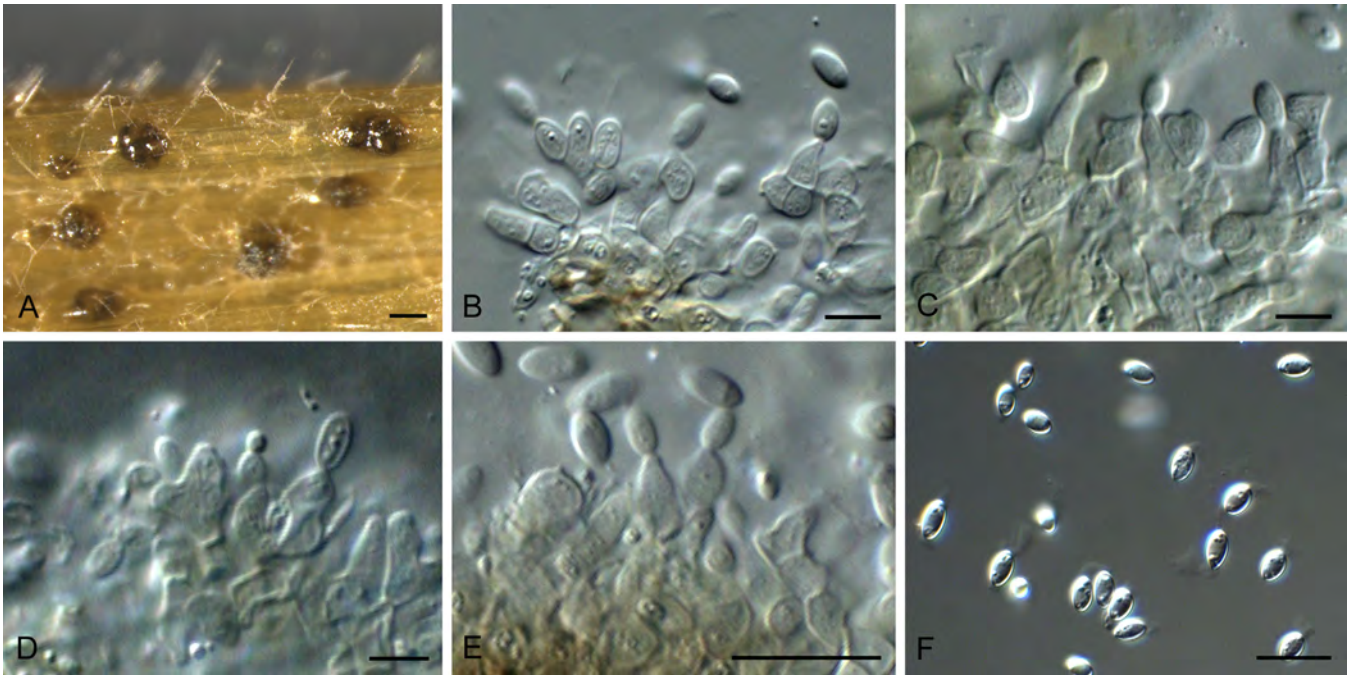

Fig. 1. *Allantophomopsiella pseudotsugae* (CBS 841.91). **A.** Conidiomata forming on autoclaved barley leaves. **B–E.** Conidiogenous cells giving rise to conidia. **F.** Conidia. Scale bars: A = 300 µm; others = 10 µm. Pictures taken from Crous *et al.* (2014b).

Table 1. DNA barcodes of accepted *Allantophomopsiella* sp.

Species	Isolate[1]	GenBank accession numbers[2]		Reference
		ITS	*rpb2*	
Allantophomopsiella pseudotsugae	CBS 320.53^{ET}	KJ663825	KJ663905	Crous *et al.* (2014b)

[1] CBS: Westerdijk Fungal Biodiversity Institute, Utrecht, the Netherlands. ^{ET} indicates ex-epitype strain.
[2] ITS: internal transcribed spacers and intervening 5.8S nrDNA; *rpb2*: partial RNA polymerase II second largest subunit gene.

wounding during tree dormancy (Roll Hansen 1992). In a study considering the pathogenicity of this fungus on *Pinus sylvestris* associated with pruning wounds, it was observed that *Allantophomopsis pseudotsugae* occurred commonly in slash of pine trees wounded during the autumn (Uotila 1990).

Allantophomopsiella is morphologically related to the phytopathogenic genera *Apostrasseria* and *Allantophomopsis*. However, it can be easily differentiated from both genera by the lack of percurrent proliferation on its conidiogenous cells, and by the production of inequilaterally fusiform or naviculate conidia.

References: Uotila 1990 (pathogenicity); Crous *et al.* 2014b (morphology and phylogeny).

Allantophomopsiella pseudotsugae (M. Wilson) Crous, IMA Fungus 5: 180. 2014. Fig. 1.
Basionym: *Phomopsis pseudotsugae* M. Wilson, Transactions of the Royal Scottish Arboricultural Society 34: 147. 1920.
Synonyms: *Phacidiella coniferarum* G.G. Hahn, Mycologia 49: 227. 1957.
Phacidium coniferarum (G.G. Hahn) DiCosmo, *et al.*, Canad. J. Bot. 61: 37. 1983.
Allantophomopsis pseudotsugae (M. Wilson) Nag Raj, Coelomycetous anamorphs with appendage-bearing conidia: 116. 1993.
Additional synonyms are provided in Nag Raj (1993).

Materials examined: **UK**, Scotland, Murthly, on *Pseudotsuga menziesii* (*Pinaceae*), Apr. 1920, M. Wilson (**lectotype of *Phomopsis pseudotsugae* designated here**: MBT379803, material deposited in Royal Botanic Garden Edinburgh, E00414771). **Norway**, Førde in Sunnfjord, shoot of *Pseudotsuga menziesii* (*Pinaceae*), Apr. 1948, H. Robak (**epitype of *Phomopsis pseudotsugae* designated here** CBS H-23354, MBT379804, culture ex-epitype CBS 320.53).

Notes: *Allantophomopsis pseudotsugae* was introduced by Wilson (1920) as *Phomopsis pseudotsugae* to accommodate a fungus that infects *Pseudotsuga menziesii* in Scotland. Type material was not specified when it was described, but the author deposited original material used for the Royal Botanic Garden Edinburgh. This material with the barcode number E00414771, which appears to be syntype material of the species, is selected here as lectotype. To fix the use of the name, the strain CBS 320.53 is designated here as ex-epitype. This strain was collected in Norway, occurring on the type host (Wilson 1920), and fits well with the description of the species recently provided by Crous *et al.* (2014b).

Authors: Y. Marin-Felix & P.W. Crous

Apoharknessia Crous & S.J. Lee, Stud. Mycol. 50: 239. 2004. Fig. 2.

Classification: *Sordariomycetes*, *Diaporthomycetidae*, *Diaporthales*, *Apoharknessiaceae*.

Type species: *Apoharknessia insueta* (B. Sutton) Crous & S.J. Lee, basionym: *Harknessia insueta* B. Sutton. Holotype of *H. insueta*: IMI 22697. Epitype and ex-epitype strain designated by Lee *et al.* (2004): CBS H-9913, CBS 111377 = STE-U 1451.

DNA barcodes (genus): ITS, LSU.

DNA barcodes (species): ITS, *cal*, *tub2*. Table 2.

Conidiomata pycnidial, separate to gregarious, subepidermal, becoming erumpent, stromatic, amphigenous, depressed

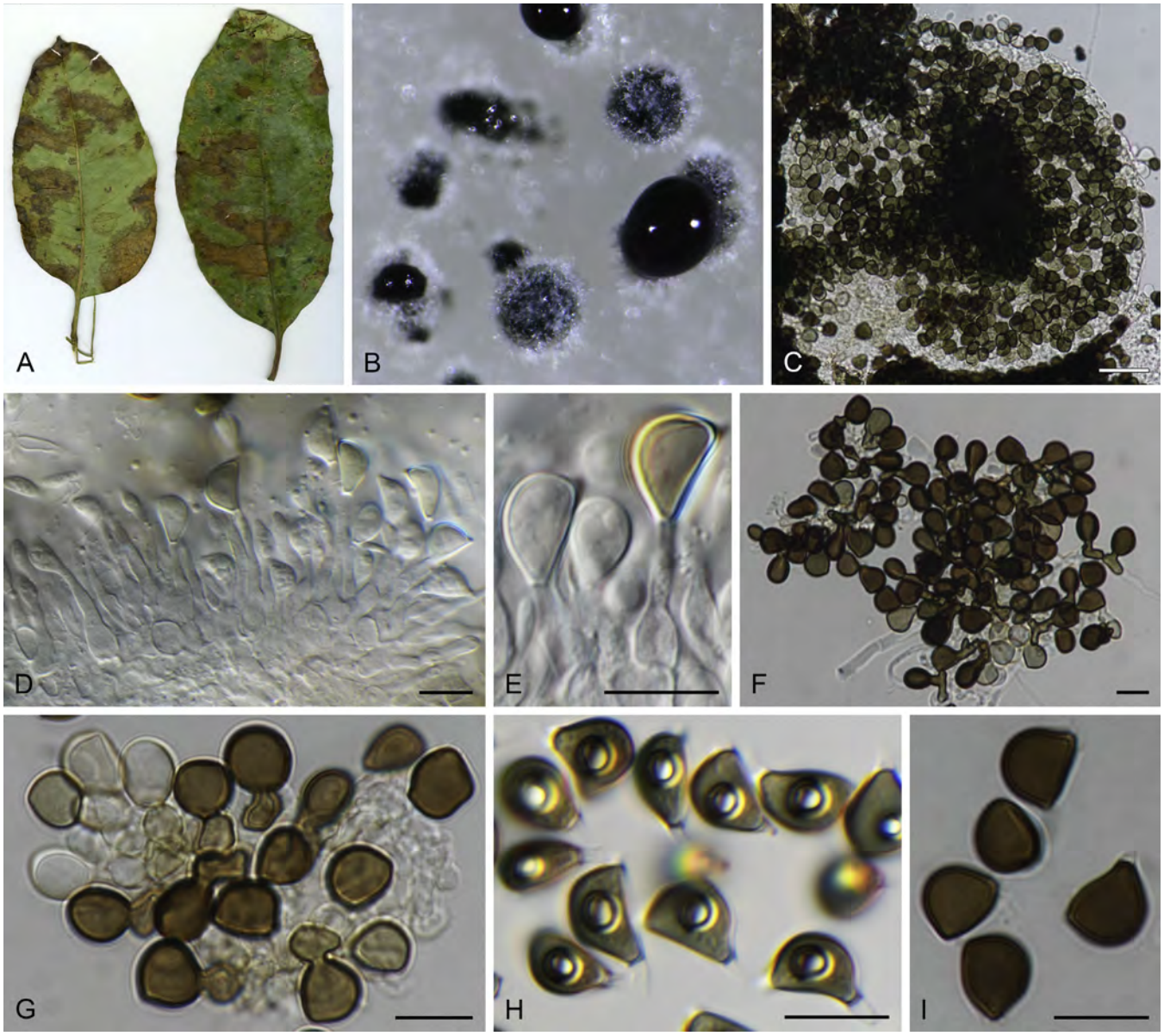

Fig. 2. *Apoharknessia* spp. **A.** Disease symptoms of *Apoharknessia eucalyptorum* on *Eucalyptus pellita*. **B, C.** Conidiomata. **B.** *Apoharknessia eucalyptorum* (ex-type CBS 142519). **C.** *Apoharknessia insueta* (ex-type CBS 111377). **D–G.** Conidiogenous cells and conidia. **D, E.** *Apoharknessia eucalyptorum* (ex-type CBS 142519). **F, G.** *Apoharknessia insueta* (ex-type CBS 111377). **H, I.** Conidia. **H.** *Apoharknessia eucalyptorum* (ex-type CBS 142519). **I.** *Apoharknessia insueta* (ex-type CBS 111377). Scale bars: C = 25 µm; others = 10 µm. Picture B taken from Crous *et al.* (2017a).

Table 2. DNA barcodes of accepted *Apoharknessia* spp.

Species	Isolates[1]	GenBank accession numbers[2]			References
		ITS	*cal*	*tub2*	
Apoharknessia eucalypti	CBS 142518^{T}	MG934432	MG934510	MG934505	Present study
Ap. eucalyptorum	CBS 142519^{T}	KY979752	KY979867	KY979919	Crous *et al.* (2017a)
Ap. insueta	CBS 111377^{ET}	JQ706083	MG934511	MG934506	Crous *et al.* (2012c), present study

[1] CBS: Westerdijk Fungal Biodiversity Institute, Utrecht, the Netherlands. ^{T} and ^{ET} indicate ex-type and ex-epitype strains.
[2] ITS: internal transcribed spacers and intervening 5.8S nrDNA; *cal*: partial calmodulin gene; *tub2*: partial β-tubulin gene.

globose or subglobose to irregular, unilocular, glabrous; *opening* irregularly, with yellowish, furfuraceous cells, lacking a definite ostiole; *conidiomatal wall* of *textura angularis*. *Conidiophores* reduced to conidiogenous cells lining cavity. *Conidiogenous cells* lageniform to ampulliform or ampulliform to subcylindrical, hyaline, smooth, in mucilage, percurrently proliferating once or twice near apex. *Conidia* broadly ellipsoidal to obovoid or obliquely gibbose, apex obtusely rounded, aseptate, non-apiculate, medium brown or brown, with or without a longitudinal hyaline band on flat surface, thick-walled, smooth, with or without striations along length of conidia, with prominent central guttule; *basal appendage* absent or hyaline, tubular, smooth, thin-walled, devoid of cytoplasm; *apical appendage* absent or hyaline, conical or tubular, short, smooth, thin-walled, devoid of cytoplasm. *Sexual morph* unknown.

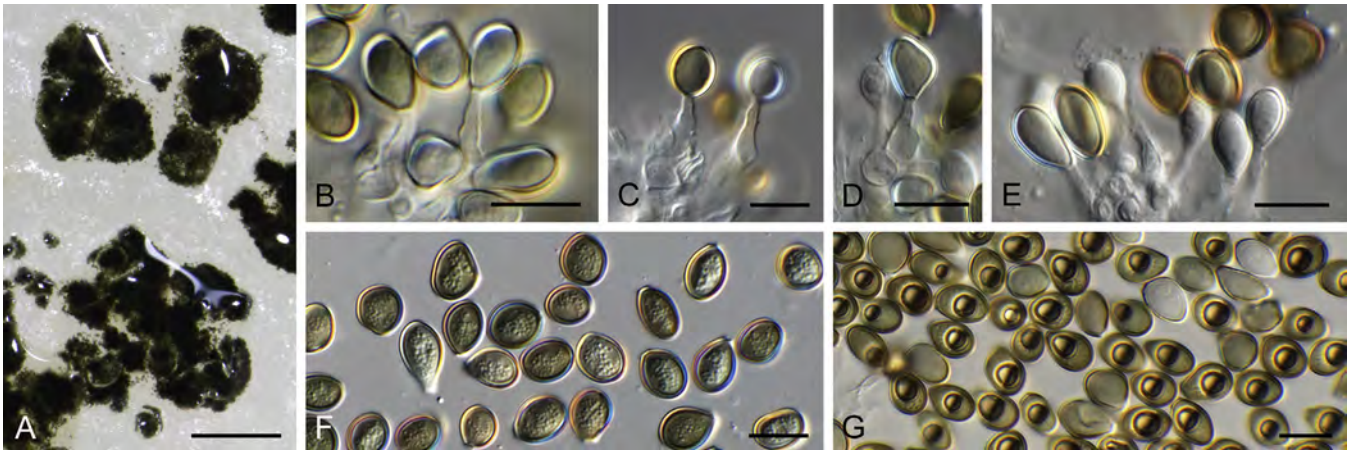

Fig. 3. *Apoharknessia eucalypti* (ex-type CBS 142518). **A.** Conidiomata sporulating on SNA. **B–E.** Conidiogenous cells and conidia. **F, G.** Conidia. Scale bars: A = 250 µm, B–G = 10 µm.

Culture characteristics: Colonies flat on MEA, PDA and OA, with sparse or moderate aerial mycelium, smooth, lobate margins, fast sporulating. On MEA surface greenish black or olivaceous black in centre, dirty white in outer region; reverse olivaceous grey in centre, dirty white in outer region.

Optimal media and cultivation conditions: MEA, PDA and OA under continuous near-ultraviolet light at 25 °C to promote sporulation.

Distribution: Brazil, Colombia, Cuba, Malaysia and Mauritius.

Hosts: *Eucalyptus* (*Myrtaceae*).

Disease symptoms: Leaf spots.

Notes: The genus *Apoharknessia* was established by Lee *et al.* (2004) for *Ap. insueta*, a presumed foliar pathogen of eucalypts in Brazil, Colombia, Cuba and Mauritius. The genus included two species following the description of *Ap. eucalyptorum* to accommodate a presumed endophyte of *Eucalyptus pellita* isolated from collections made in Malaysia (Crous *et al.* 2017a).

Apoharknessia is distinguished from *Harknessia* by having an apical appendage on its conidia, and cultures that lack fluffy aerial mycelium and sporulate abundantly on the aerial hyphae. Cultures of *Harknessia s. str.* are slow to sporulate, and tend to form abundant pycnidial conidiomata in culture (Lee *et al.* 2004).

Recently, the family *Apoharknessiaceae* was introduced based on a phylogenetic study of the members of the *Diaporthales*, in order to accommodate *Apoharknessia*, designated as the type genus of the family, together with *Lasmenia*, which is also a genus associated with plant disease (Senanayake *et al.* 2017).

References: Lee *et al.* 2004 (morphology and phylogeny); Crous *et al.* 2012c, 2017a, Senanayake *et al.* 2017 (phylogeny).

Apoharknessia eucalypti Crous & M.J. Wingf., **sp. nov.** MycoBank MB820945. Fig. 3.

Etymology: Name refers to *Eucalyptus*, the host genus from which this fungus was collected.

Foliicolous, isolated from leaves incubated in moist chambers (presumed endophytic). *Conidiomata* up to 250 µm diam, pycnidial, solitary to gregarious, subepidermal, becoming erumpent, stromatic, amphigenous, depressed globose; *opening* irregularly, with yellowish, furfuraceous cells; *conidiomatal wall* of *textura angularis*. *Conidiophores* reduced to conidiogenous cells lining cavity. *Conidiogenous cells* 8–12 × 3–5 µm, ampulliform to subcylindrical, hyaline, smooth, in mucilage, percurrently proliferating once or twice near apex. *Conidia* (7–)8–10(–11) × (5–)6(–7) µm, broadly ellipsoid to obovoid, apex obtusely rounded, aseptate, non-apiculate, medium brown, thick-walled, smooth, striations along length of conidium body, with prominent central guttule. *Basal appendage* absent or 0–2 µm long, 2 µm diam, hyaline, tubular, smooth, thin-walled, devoid of cytoplasm.

Culture characteristics: Colonies on MEA, PDA and OA, with moderate aerial mycelium and smooth, lobate margins, reaching 60 mm diam after 2 wk at 25 °C. On MEA surface greenish black in middle, dirty white in outer region; reverse olivaceous grey in centre, dirty white in outer region. On PDA surface and reverse olivaceous grey in centre, dirty white in outer region. On OA surface greenish black in middle, outer region dirty white.

Material examined: **Malaysia**, Sabah, isolated from leaves of *Eucalyptus pellita* (*Myrtaceae*), May 2015, M.J. Wingfield (**holotype** CBS H-23081, culture ex-type CPC 27550 = CBS 142518).

Notes: *Apoharknessia eucalypti* is an odd member of the genus in that its conidia generally lack an apical appendage. The latter was observed on one or two conidia, irrespective of the media used for cultivation. The ITS sequence of *Ap. eucalypti* is only 92 % similar to that of *Ap. insueta* [GenBank JQ706083; Identities = 569/618 (92 %), 33 gaps (5 %)] and 97 % similar to that of *Ap. eucalyptorum* [GenBank KY979752; Identities = 604/621 (97 %), 5 gaps (0 %)].

Authors: P.W. Crous, Y. Marin-Felix, J.Z. Groenewald & M.J. Wingfield

Cylindrocladiella Boesew., Canad. J. Bot. 60: 2289. 1982. Fig. 4.
Synonym: *Nectricladiella* Crous & C.L. Schoch, Stud. Mycol. 45: 54. 2000.

Classification: *Sordariomycetes*, *Hypocreomycetidae*, *Hypocreales*, *Nectriaceae*.

Type species: *Cylindrocladiella parva* (P.J. Anderson) Boesew., basionym: *Cylindrocladium parvum* P.J. Anderson. Representative strain: CBS 114524 = ATCC 28272.

DNA barcodes (*genus*): LSU, ITS.

DNA barcodes (*species*): *his3*, *tef1*, *tub2*. Table 3. Fig. 5.

Ascomata perithecial, superficial, solitary, basal stroma absent, globose to obpyriform, collapsing laterally when dry, smooth, with

Fig. 4. *Cylindrocladiella* spp. **A–D.** Conidiophores of *Cylindrocladiella* spp. on infected alfalfa seeds **A–B.** *Cylindrocladiella* spp. sporulating on the seed coat of *Medicago sativa*. **C.** Root rot of *M. sativa* seedling. **D.** *Cylindrocladiella* spp. on carnation leaf. **E–AA.** Asexual morph. **E–I.** Penicillate conidiophores. **E.** *Cylindrocladiella longistipitata* (ex-type CBS 116075). **F.** *Cylindrocladiella kurandica* (ex-type CBS 129577). **G.** *Cylindrocladiella lanceolata* (ex-type CBS 129566). **H.** *Cylindrocladiella pseudoparva* (ex-type CBS 129560). **I.** *Cylindrocladiella nederlandica* (ex-type CBS 152.91). **J–N.** Penicillate conidiogenous apparatus. **J.** *Cylindrocladiella hawaiiensis* (ex-type CBS 129569). **K.** *Cylindrocladiella australiensis* (ex-type CBS 129567). **L.** *Cylindrocladiella natalensis* (ex-type CBS 114943). **M.** *Cylindrocladiella cymbiformis* (ex-type CBS 129553). **N.** *Cylindrocladiella ellipsoidea* (ex-type CBS 129573). **O–S.** Subverticillate conidiophores. **O.** *Cylindrocladiella australiensis* (ex-type CBS 129567). **P.** *Cylindrocladiella longiphialidica* (ex-type CBS 129557). **Q.** *Cylindrocladiella pseudohawaiiensis* (ex-type CBS 210.94). **R, S.** *Cylindrocladiella natalensis* (ex-type CBS 114943). **T–Y.** Terminal vesicles of stipe extensions. **T.** *Cylindrocladiella hawaiiensis* (ex-type CBS 129569). **U.** *Cylindrocladiella stellenboschensis* (ex-type CBS 110668). **V.** *Cylindrocladiella cymbiformis* (ex-type CBS 129553). **W.** *Cylindrocladiella variabilis* (ex-type CBS 129561). **X.** *Cylindrocladiella lanceolata* (ex-type CBS 129566). **Y.** *Cylindrocladiella kurandica* (ex-type CBS 129577). **Z, AA.** Conidia. **Z.** *Cylindrocladiella natalensis* (ex-type CBS 114943). **AA.** *Cylindrocladiella brevistipitata* (ex-type CBS 142783). Scale bars: E–I, O = 50 µm; J–N, P–AA = 10 µm.

Table 3. DNA barcodes of accepted *Cylindrocladiella* spp.

Species	Isolates[1]	GenBank accession numbers[2]					References
		ITS	LSU	*his3*	*tef1*	*tub2*	
Cylindrocladiella addiensis	CBS 143794^T	MH111383	–	–	MH111393	MH111388	Present study
	CBS 143793	MH111385	–	–	MH111395	MH111390	Present study
	CBS 143795	MH111384	–	–	MH111394	MH111389	Present study
C. australiensis	CBS 129567^T	JN100624	JN099222	JN098932	JN099060	JN098747	Lombard *et al.* (2012)
C. brevistipitata	CBS 142786^T	–	–	–	MF444940	MF444926	Lombard *et al.* (2017)
C. camelliae	IMI 346845	AF220952	JN099249	AY793509	JN099087	AY793471	Van Coller *et al.* (2005), Lombard *et al.* (2012)
C. clavata	CBS 129564^T	JN099095	JN099135	JN098858	JN098974	JN098752	Lombard *et al.* (2012)
C. cymbiformis	CBS 129553^T	JN099103	JN099143	JN098866	JN098988	JN098753	Lombard *et al.* (2012)
C. elegans	CBS 338.92^T	AY793444	JN099201	AY793512	JN099039	AY793474	van Coller *et al.* (2005), Lombard *et al.* (2012)
C. ellipsoidea	CBS 129573^T	JN099094	JN099134	JN098857	JN098973	JN098757	Lombard *et al.* (2012)
C. hahajimaensis	MAFF 238172^T	JN687561	–	–	JN687562	–	Inderbitzin *et al.* (2012)
C. hawaiiensis	CBS 129569^T	JN100621	JN099219	JN098929	JN099057	JN098761	Lombard *et al.* (2012)
C. horticola	CBS 142784^T	MF444911	–	–	MF444938	MF444924	Lombard *et al.* (2017)
C. humicola	CBS 142779^T	MF444906	–	–	MF444933	MF444919	Lombard *et al.* (2017)
C. infestans	CBS 111795^T	AF220955	JN099199	AY793513	JN099037	AF320190	Schoch *et al.* (2000), Crous *et al.* (2001), van Coller *et al.* (2005), Lombard *et al.* (2012)
C. kurandica	CBS 129577^T	JN100646	JN099245	JN098953	JN099083	JN098765	Lombard *et al.* (2012)
C. lageniformis	CBS 340.92^T	AF220959	JN099165	AY793520	JN099003	AY793481	Schoch *et al.* (2000), van Coller *et al.* (2005), Lombard *et al.* (2012)
C. lanceolata	CBS 129566^T	JN099099	JN099139	JN098862	JN098978	JN098789	Lombard *et al.* (2012)
C. lateralis	CBS 142788^T	MF444914	–	–	MF444942	MF444928	Lombard *et al.* (2017)
C. longiphialidica	CBS 129557^T	JN100585	JN099264	JN098851	JN098966	JN098790	Lombard *et al.* (2012)
C. longistipitata	CBS 116075^T	AF220958	JN099155	AY793546	JN098993	AY793506	Schoch *et al.* (2000), van Coller *et al.* (2005), Lombard *et al.* (2012)
C. microcylindrica	CBS 111794^T	AY793452	JN099203	AY793523	JN099041	AY793483	van Coller *et al.* (2005), Lombard *et al.* (2012)
C. natalensis	CBS 114943^T	JN100588	JN099178	JN098895	JN099016	JN098794	Lombard *et al.* (2012)
C. nederlandica	CBS 152.91^T	JN100603	JN099195	JN098910	JN099033	JN098800	Lombard *et al.* (2012)
C. novazelandica	CBS 486.77^T	AF220963	JN099212	AY793525	JN099050	AY793485	Schoch *et al.* (2000), van Coller *et al.* (2005), Lombard *et al.* (2012)
C. nauliensis	CBS 143792^T	MH111387	–	–	MH111397	MH111392	Present study
	CBS 143791	MH111386	–	–	MH111396	MH111391	Present study
C. parva	CBS 114524	AF220964	JN099171	AY793526	JN099009	AY793486	Schoch *et al.* (2000), van Coller *et al.* (2005), Lombard *et al.* (2012)
C. peruviana	IMUR 1843^T	AF220966	JN099266	AY793540	JN098968	AY793500	Schoch *et al.* (2000), van Coller *et al.* (2005), Lombard *et al.* (2012)
C. pseudocamelliae	CBS 129555^T	JN100577	JN099256	JN098843	JN098958	JN098814	Lombard *et al.* (2012)
C. pseudohawaiiensis	CBS 210.94^T	JN099128	JN099174	JN098890	JN099012	JN098819	Lombard *et al.* (2012)
C. pseudoinfestans	CBS 114531^T	AF220957	JN099166	AY793548	JN099004	AY793508	Schoch *et al.* (2000), van Coller *et al.* (2005), Lombard *et al.* (2012)
C. pseudoparva	CBS129560^T	JN100620	JN099218	JN098927	JN099056	JN098824	Lombard *et al.* (2012)
C. queenslandica	CBS 129574^T	JN099098	JN099098	JN098861	JN098977	JN098826	Lombard *et al.* (2012)
C. reginae	CBS 142782^T	MF444909	–	–	MF444936	MF444922	Lombard *et al.* (2017)
C. stellenboschensis	CBS 110668^T	JN100615	JN099213	JN098922	JN099051	JN098829	Lombard *et al.* (2012)
C. terrestris	CBS 142789^T	MF444915	–	–	MF444943	MF444929	Lombard *et al.* (2017)
C. thailandica	CBS 129571^T	JN100582	JN099261	JN098848	JN098963	JN098834	Lombard *et al.* (2012)
C. variabilis	CBS 129561^T	JN100643	JN099242	JN098950	JN099080	JN098719	Lombard *et al.* (2012)
C. viticola	CBS 112897^T	AY793468	JN099226	AY793544	JN099064	AY793504	van Coller *et al.* (2005), Lombard *et al.* (2012)
C. vitis	CBS 142517^T	KY979751	KY979806	–	KY979891	KY979918	Crous *et al.* (2017a)

[1] CBS: Westerdijk Fungal Biodiversity Institute, Utrecht, the Netherlands; IMI: International Mycological Institute, CABI-Bioscience, Egham, Bakeham Lane, U.K; IMUR: Institute of Mycology, University of Recife, Recife, Brazil; MAFF: Genetic Resources Centre, National Agriculture and Food Research Organization (NARO), NARO Genebank, Ibaraki, Japan. ^{T} indicates ex-type strains.

[2] ITS: internal transcribed spacers and intervening 5.8S nrDNA; LSU: 28S large subunit nrDNA; *his3*: partial histone H3 gene; *tef1*: partial translation elongation factor 1-alpha gene; *tub2*: partial β-tubulin gene.

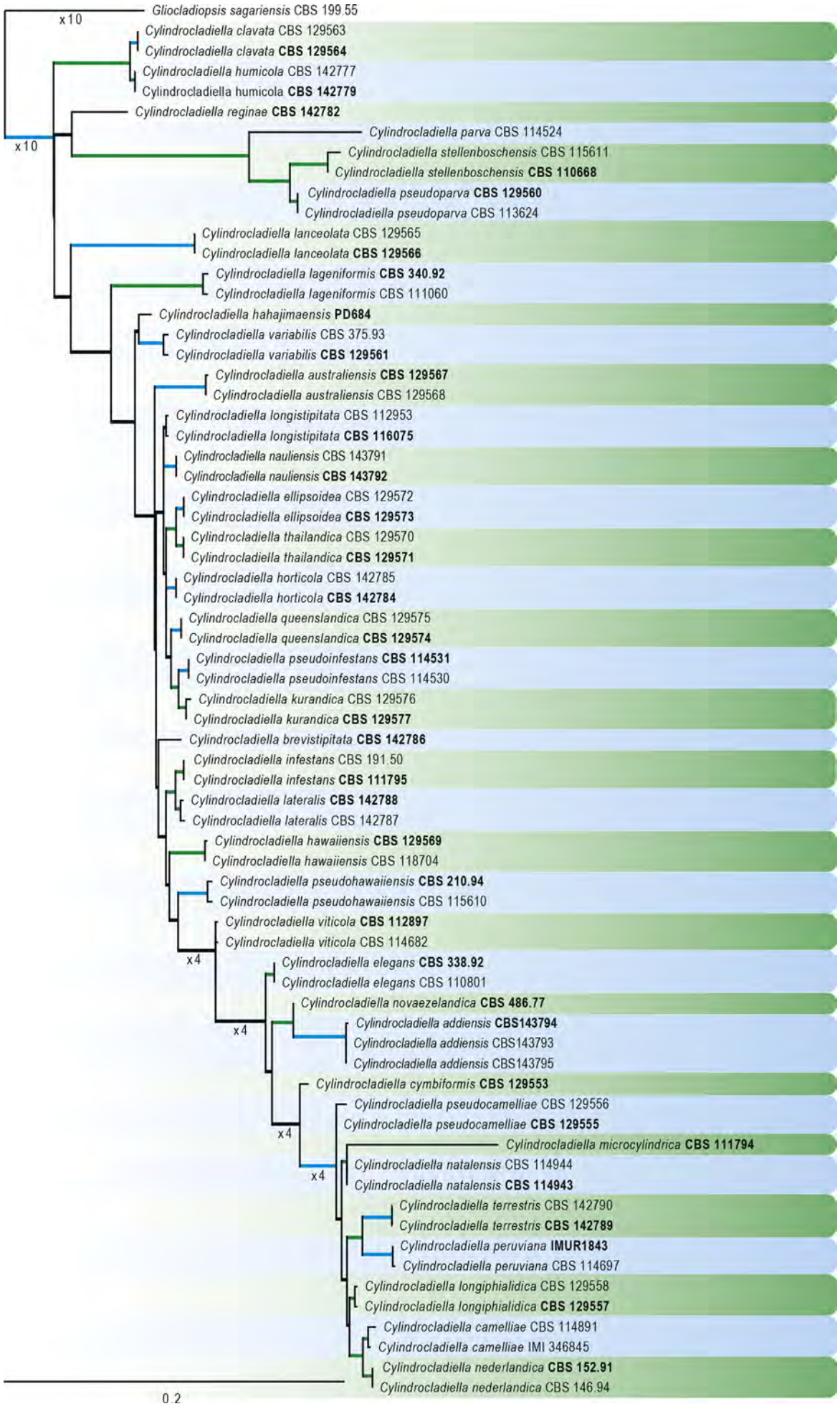
Gliocladiopsis sagariensis CBS 199.55
x10
Cylindrocladiella clavata CBS 129563
Cylindrocladiella clavata CBS 129564
Cylindrocladiella humicola CBS 142777
Cylindrocladiella humicola CBS 142779
Cylindrocladiella reginae CBS 142782
x10
Cylindrocladiella parva CBS 114524
Cylindrocladiella stellenboschensis CBS 115611
Cylindrocladiella stellenboschensis CBS 110668
Cylindrocladiella pseudoparva CBS 129560
Cylindrocladiella pseudoparva CBS 113624
Cylindrocladiella lanceolata CBS 129565
Cylindrocladiella lanceolata CBS 129566
Cylindrocladiella lageniformis CBS 340.92
Cylindrocladiella lageniformis CBS 111060
Cylindrocladiella hahajimaensis PD684
Cylindrocladiella variabilis CBS 375.93
Cylindrocladiella variabilis CBS 129561
Cylindrocladiella australiensis CBS 129567
Cylindrocladiella australiensis CBS 129568
Cylindrocladiella longistipitata CBS 112953
Cylindrocladiella longistipitata CBS 116075
Cylindrocladiella nauliensis CBS 143791
Cylindrocladiella nauliensis CBS 143792
Cylindrocladiella ellipsoidea CBS 129572
Cylindrocladiella ellipsoidea CBS 129573
Cylindrocladiella thailandica CBS 129570
Cylindrocladiella thailandica CBS 129571
Cylindrocladiella horticola CBS 142785
Cylindrocladiella horticola CBS 142784
Cylindrocladiella queenslandica CBS 129575
Cylindrocladiella queenslandica CBS 129574
Cylindrocladiella pseudoinfestans CBS 114531
Cylindrocladiella pseudoinfestans CBS 114530
Cylindrocladiella kurandica CBS 129576
Cylindrocladiella kurandica CBS 129577
Cylindrocladiella brevistipitata CBS 142786
Cylindrocladiella infestans CBS 191.50
Cylindrocladiella infestans CBS 111795
Cylindrocladiella lateralis CBS 142788
Cylindrocladiella lateralis CBS 142787
Cylindrocladiella hawaiiensis CBS 129569
Cylindrocladiella hawaiiensis CBS 118704
Cylindrocladiella pseudohawaiiensis CBS 210.94
Cylindrocladiella pseudohawaiiensis CBS 115610
Cylindrocladiella viticola CBS 112897
Cylindrocladiella viticola CBS 114682
x4
Cylindrocladiella elegans CBS 338.92
Cylindrocladiella elegans CBS 110801
Cylindrocladiella novaezelandica CBS 486.77
x4
Cylindrocladiella addiensis CBS143794
Cylindrocladiella addiensis CBS143793
Cylindrocladiella addiensis CBS143795
Cylindrocladiella cymbiformis CBS 129553
Cylindrocladiella pseudocamelliae CBS 129556
Cylindrocladiella pseudocamelliae CBS 129555
x4
Cylindrocladiella microcylindrica CBS 111794
Cylindrocladiella natalensis CBS 114944
Cylindrocladiella natalensis CBS 114943
x4
Cylindrocladiella terrestris CBS 142790
Cylindrocladiella terrestris CBS 142789
Cylindrocladiella peruviana IMUR1843
Cylindrocladiella peruviana CBS 114697
Cylindrocladiella longiphialidica CBS 129558
Cylindrocladiella longiphialidica CBS 129557
Cylindrocladiella camelliae CBS 114891
Cylindrocladiella camelliae IMI 346845
Cylindrocladiella nederlandica CBS 152.91
Cylindrocladiella nederlandica CBS 146.94
0.2

minute, brown setae arising from ascomatal wall surface, red, changing colour in KOH, ostiole consisting of clavate cells, lined with inconspicuous periphyses. *Asci* unitunicate, 8-spored, cylindrical, sessile, thin-walled, with a flattened apex, and a refractive apical apparatus. *Ascospores* uniseriate, overlapping, hyaline, ellipsoid to fusoid with obtuse ends, smooth, 1-septate. *Conidiophores* monomorphic, penicillate, or dimorphic (penicillate and subverticillate), mononematous, hyaline. *Penicillate conidiophores* consist of a stipe, a penicillate arrangement of fertile branches, a stipe extension, and a terminal vesicle. *Subverticillate conidiophores* consist of a stipe, and one or two series of phialides. *Stipe* septate, hyaline, smooth. *Stipe extensions* aseptate, straight, thick-walled, with one basal septum, terminating in a thin-walled vesicle of characteristic shape. *Conidiogenous apparatus* with primary branches 0–1-septate, secondary branches aseptate, terminating in 2–4 phialides. *Phialides* cylindrical, straight or doliiform to reniform to cymbiform, hyaline, aseptate, apex with minute periclinal thickening and collarette. *Conidia* cylindrical, rounded at both ends, straight, (0–)1(–3)-septate, frequently slightly flattened at base, held in asymmetrical clusters by hyaline slime. *Chlamydospores* brown, thick-walled, more frequently arranged in chains than clusters (adapted from Boesewinkel 1982 and Lombard *et al.* 2012).

Culture characteristics: Colonies on MEA white to pale brick when young, becoming pale brick to dark sepia when mature, fluffy, cottony, effuse to convex with papillate surface, margin entire, undulate, lobate, or fimbriate, sometimes with abundant chlamydospores forming microsclerotia within medium.

Optimal media and cultivation conditions: CLA to induce sporulation of the asexual morph at 25 °C, while for the sexual morph sterile toothpicks placed on SNA is used at 20 °C.

Distribution: Worldwide.

Hosts: Soil-borne, weak pathogen of forestry, agricultural and horticultural crops (Crous 2002, Lombard *et al.* 2012).

Disease symptoms: Leaf spots, cutting rot, stem cankers, damping-off and root rot.

Notes: Boesewinkel (1982) established the asexual genus *Cylindrocladiella*, based on *C. parva*, to accommodate several cylindrocladium-like species characterised by small (<20 µm long), 1-septate, cylindrical conidia and aseptate stipe extensions. Initially, *Cylindrocladiella* spp. were linked to the sexual genus *Nectricladiella* (Crous & Wingfield 1993, Schoch *et al.* 2000). Following the implementation of the International Code of Nomenclature for algae, fungi and plants (ICN; McNeill *et al.* 2012), Rossman *et al.* (2013) proposed that the generic name *Cylindrocladiella* be retained over *Nectricladiella*. Recently, Lombard *et al.* (2015) showed that the genus *Cylindrocladiella* formed a monophyletic group in the *Nectriaceae*, closely related to the genera *Aquanectria* and *Gliocladiopsis*. To date, 36 species of *Cylindrocladiella* have been recognised (Crous & Wingfield 1993, van Coller *et al.* 2005, Inderbitzin *et al.* 2012, Lombard *et al.* 2012, 2015, 2017; Crous *et al.* 2017a), of which two are linked to nectricladiella-like sexual morphs (Schoch *et al.* 2000, Crous 2002, Lombard *et al.* 2012, 2015). These fungi are generally soil-borne and regarded as saprobes or weak pathogens of numerous plant hosts (Crous 2002, van Coller *et al.* 2005, Scattolin & Montecchio 2007, Lombard *et al.* 2012). Disease symptoms associated with *Cylindrocladiella* infection include leaf spots and root, stem and cutting rots (Crous *et al.* 1991b, Peerally 1991, Crous & Wingfield 1993, Crous 2002, van Coller *et al.* 2005, Scattolin & Montecchio 2007, Lombard *et al.* 2012).

References: Boesewinkel 1982 (morphology and pathogenicity); Crous & Wingfield 1993 (morphology); Schoch *et al.* 2000, Lombard *et al.* 2012, 2017 (morphology and phylogeny); Crous 2002 (morphology, pathogenicity and monograph); van Coller *et al.* 2005 (morphology, pathogenicity and phylogeny).

Cylindrocladiella addiensis L. Lombard & Crous, **sp. nov.** MycoBank MB824497.

Etymology: Name refers to Addis Ababa, Ethiopia, from where this fungus was collected.

Cultures sterile. *Cylindrocladiella addiensis* differs from its closest phylogenetic neighbours, *C. elegans* and *C. noveazelandica*, by unique fixed alleles in three loci based on the alignments deposited in TreeBASE (S22340): ITS position 92(T); *tef1* positions 32(T), 80(C), 84(C), 154(indel), 155(A), 156(G), 157(indel), 199(A), 244(G), 261(G), 368(T), 398(T), 458(G/C), 466(G), 467(C), 475(T), 478(C), 483(T), 485(T), 487(T), 490(T) and 492(G); *tub2* position 174(indel).

Culture characteristics: Colonies convex, cottony, with smooth margins, cream; reverse pale luteous; chlamydospores not seen; reaching 45–65 mm after 1 wk on MEA at 24 °C in ambient light.

Materials examined: **Ethiopia**, Addis Ababa, from soil, 2010, coll. P.W. Crous, isol. L. Lombard [**holotype** CBS 143794 (maintained as metabolically inactive culture), isotype cultures CBS 143793, CBS 143795 (also maintained as metabolically inactive cultures).

Note: None of the three isolates of *C. addiensis* could be induced to sporulate on MEA, PDA, OA, SNA or SNA amended with carnation leaf pieces.

Cylindrocladiella nauliensis L. Lombard & Crous, **sp. nov.** MycoBank MB824500. Fig. 6.

Etymology: Name refers to the area Aek Nauli, Indonesia, from where this fungus was collected.

Conidiophores 35–55 × 3–6 µm, dimorphic, penicillate and subverticillate, mononematous and hyaline, comprising a stipe, a penicillate arrangement of fertile branches, a stipe extension and a terminal vesicle; *stipe* septate, hyaline, smooth; *stipe extension* 100–135 µm long, 4–5 µm wide, aseptate, straight, thick-walled with one basal septum, terminating in thin-walled, broadly clavate to ellipsoidal vesicles sometimes with papillate apex. *Penicillate conidiogenous apparatus* 10–22 × 2–4 µm, with primary branches aseptate, secondary branches 8–15 × 2–4 µm, aseptate, each terminal branch producing 2–4 phialides; *phialides* 8–13 × 2–3 µm, elongate doliiform to reniform to cymbiform, hyaline, aseptate, apex with minute periclinal thickening and collarette. *Subverticillate conidiophores* abundant, comprised of a

Fig. 5. The Maximum Likelihood (ML) consensus tree of *Cylindrocladiella* spp. inferred from the combined ITS (547 bp), *tef1* (527 bp) and *tub2* (502 bp) sequence alignment. Thickened lines indicate branches present in the ML, Maximum parsimony (MP) and Bayesian consensus trees. Branches with ML-bootstrap (BS) & MP-BS = 100 % and posterior probabilities (PP) = 1.00 are in blue. Branches with ML-BS & MP-BS ≥ 75 % and PP ≥ 0.95 are in green. The scale bar indicates 0.02 expected changes per site. The tree is rooted to *Gliocladiopsis sagariensis* CBS 199.55. Ex-type strains are indicated in **bold**. GenBank accession numbers are indicated in Table 3 and in Lombard *et al.* (2012, 2017). TreeBASE: S22340.

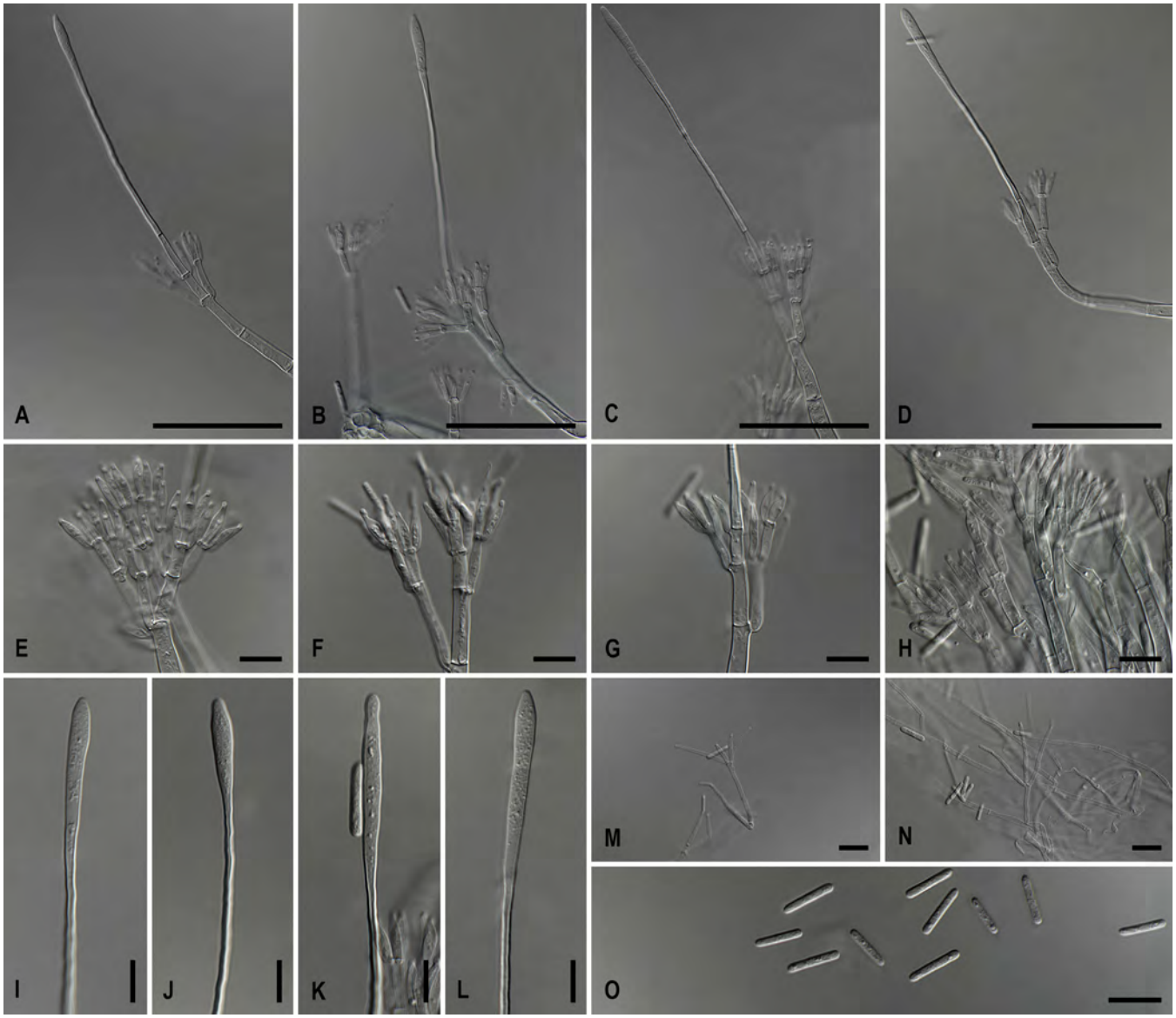

Fig. 6. *Cylindrocladiella nauliensis* (ex-type CBS 143792). **A–D.** Penicillate conidiophores. **E–H.** Penicillate conidiogenous apparatus. **I–L.** Terminal vesicles of stipe extensions. **M, N.** Subverticillate conidiophores. **O.** Conidia. Scale bars: A–D = 50 µm; E–O = 10 µm.

septate stipe and rarely primary branches terminating in 2–4 phialides; *primary branches* 25–45 × 2–4 µm, straight, hyaline, 0–1-septate; *phialides* 12–32 × 2–3 µm, cymbiform to cylindrical, hyaline, aseptate, apex with minute periclinal thickening and collarette. *Conidia* (10–)11–13(–14) × 2–3 µm (av. = 12 × 2 µm), cylindrical, rounded at both ends, straight, 1-septate, frequently slightly flattened at base, held in asymmetrical clusters by hyaline slime. *Sexual morph* unknown.

Culture characteristics: Colonies convex, cottony, with smooth margins, cream with pale luteous to brick centre; reverse pale luteous to honey with sepia centre; chlamydospores moderate throughout medium arranged in chains; reaching 60–70 mm after 1 wk on MEA at 24 °C in ambient light.

Materials examined: **Indonesia**, Sumatra Utara, Aek Nauli, from soil, May 2005, coll. M.J. Wingfield, isol. L. Lombard (**holotype** CBS H-23400, culture ex-type CBS 143792), isotype culture CBS 143791 (metabolically inactive).

Notes: *Cylindrocladiella nauliensis* is closely related to *C. longistipitata*. The stipe extensions of *C. nauliensis* (up to 135 µm long) are shorter than those of *C. longistipitata* (up to 216 µm long; Lombard *et al.* 2012). Additionally, the conidia of *C. nauliensis* are smaller [(10–)11–13(–14) × 2–3 µm (av. = 12 × 2 µm)] than those of *C. longistipitata* [(12–)14–16(–17) × 2–4 µm (av. = 15 × 3 µm); Lombard *et al.* 2012].

Authors: L. Lombard & P.W. Crous

Diaporthe Nitschke, Pyrenomyc. Germ. 2: 240. 1870. Figs 7, 8.
Synonym: *Phomopsis*, Sacc., Syll. fung. (Abellini) 2: 484. 1883.

Classification: *Sordariomycetes*, *Sordariomycetidae*, *Diaporthales*, *Diaporthaceae*.

Type species: *Diaporthe eres* Nitschke. Lectotype designated by Udayanga *et al.* (2014a): B 70 0009145. Epitype and ex-epitype strain designated by Udayanga *et al.* (2014a): BPI 892912, AR5193 = CBS 138594.

DNA barcodes (*genus*): ITS.

DNA barcodes (*species*): *cal*, *his3*, *tef1*, *tub2*. Table 4. Fig. 9.

Ascomata immersed in substrate, subglobose or irregular, solitary or clustered in groups, often erumpent through a pseudostroma mostly surrounding ascomata with more or less elongated ascomatal necks. *Pseudostroma* distinct, often delimited with dark lines. *Asci* unitunicate, 8-spored, sessile, elongate to clavate or cylindrical, loosening from ascogenous cells at an

Fig. 7. Disease symptoms associated with *Diaporthe* spp. **A, B.** *Helianthus annuus* plants affected by *Diaporthe gulyae* (courtesy Susan Thompson). **C, D.** Branch canker of *Persea americana* with associated *Diaporthe foeniculina* and *Diaporthe sterilis*. **E, F.** Phomopsis cane (courtesy Alessandro Vitale) and cane bleaching on shoot of *Vitis vinifera* caused by *Diaporthe* spp. (courtesy José Luis Ramos Sáez de Ojer). **G, H.** Decay of *Vaccinium corymbosum* caused by *Diaporthe baccae* and *Diaporthe sterilis* and artificial infection caused by inoculation of *Diaporthe sterilis*. **I.** Trunk canker with gummosis of *Citrus limon* caused by *Diaporthe limonicola* and *Diaporthe melitensis*. Pictures C, D taken from Guarnaccia *et al.* (2016); I from Guarnaccia & Crous (2017).

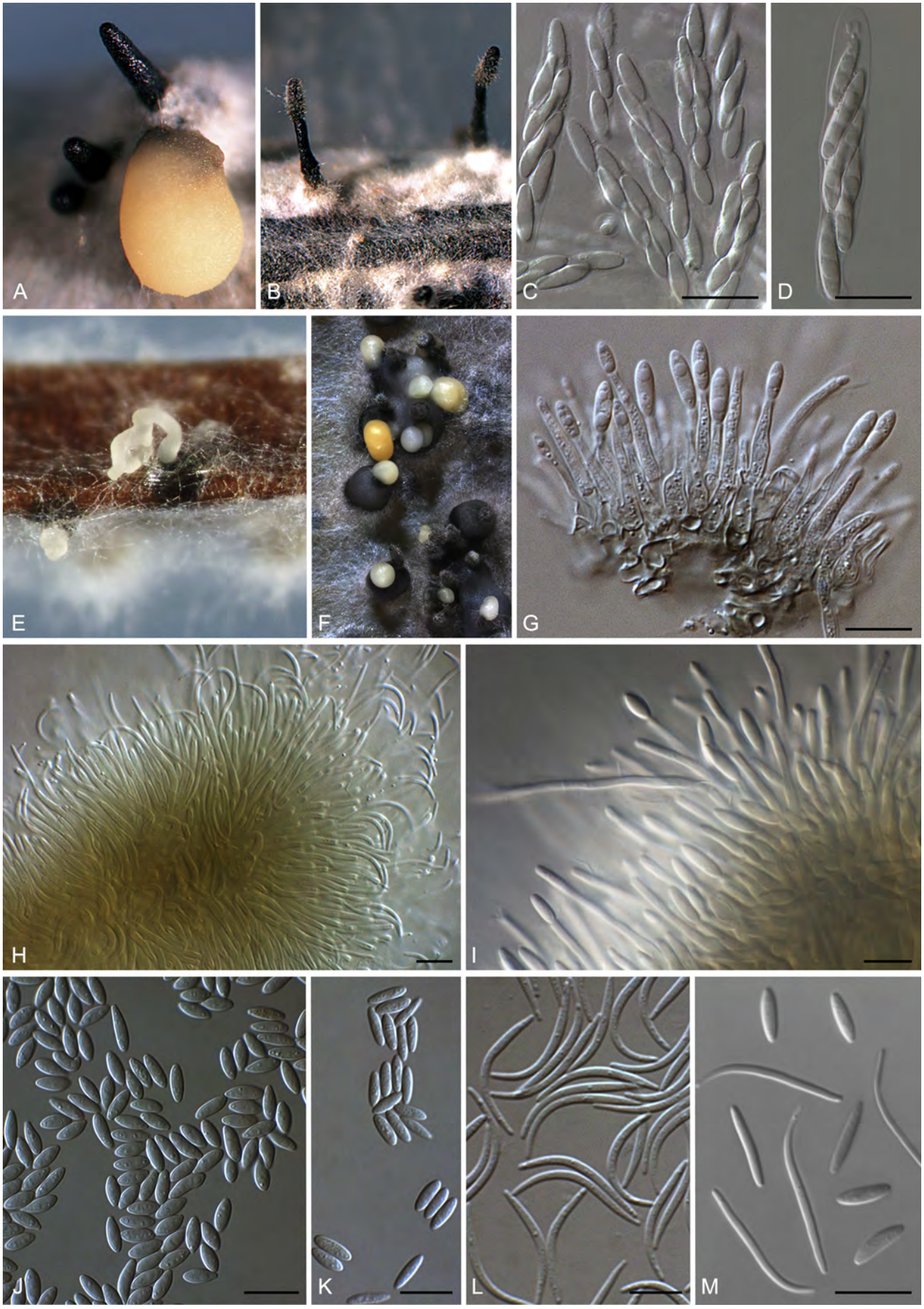

early stage and floating free in ascomata. *Ascospores* biseriate to uniseriate in ascus, fusoid, ellipsoid to cylindrical, straight, inequilateral or curved, septate, hyaline, sometimes with appendages. *Conidiomata* pycnidial, deeply embedded in culture on several media, globose to conical, eustromatic, multilocular, occasionally with ostiolate necks, scattered or aggregated, brown to black, surface covered with hyphae, cream to pale luteous or yellowish, conidial droplets or cirrus exuding from central ostioles; *conidiomatal wall* consisting of pale brown, thick walled, *textura angularis*. *Conidiophores* cylindrical to clavate, straight to sinuous, densely aggregated, branched, 0–6-septate, smooth, hyaline in upper region, pale brown at base. *Conidiogenous cells* phialidic, hyaline, cylindrical, terminal and lateral, tapering slightly towards apex. *Paraphyses* occasionally produced, intermingled among conidiophores, hyaline, smooth, 1–3-septate. *Alpha conidia* aseptate, generally hyaline, smooth, fusiform to ellipsoidal, with obtuse or acute to rounded ends, non- to multi-guttulate, but often bi-guttulate. *Beta conidia* aseptate, hyaline, filiform, smooth, straight or more often hooked, eguttulate, tapering or truncated towards ends. *Gamma conidia* rarely produced, hyaline, smooth, non- to multi-guttulate, fusiform to subcylindrical with acute or rounded apex (adapted from Gomes *et al.* 2013, Udayanga *et al.* 2014a).

Culture characteristics: Colonies on MEA, PDA and OA producing abundant compact, flattened, aerial mycelium, sometimes in rings, with an entire to irregular margin, white, cream to yellowish or pale olivaceous grey, smoke grey to grey, cottony; reverse pale brown to grey, dark green, producing brownish dots with age, with solitary or aggregated conidiomata at maturity.

Optimal media and cultivation conditions: On MEA, PDA and OA at 25 °C, or sterile pine needles placed on SNA at 25 °C under near-ultraviolet light (12 h light, 12 h dark) to induce sporulation of the asexual morph.

Distribution: Worldwide.

Hosts: On a wide range of plant families.

Disease symptoms: Root and fruit rots, dieback, stem cankers, leaf spots, leaf and pod blights, and seed decay.

Notes: The genus *Diaporthe* presently includes 213 species supported by ex-type cultures and supplementary DNA barcodes, which include endophytes, saprobes and important plant pathogenic species. Recent phylogenetic analyses of the genus *Diaporthe* grouped some of those species into complexes, such as *D. arecae*, *D. eres* and *D. sojae* (Huang *et al.* 2013, Udayanga *et al.* 2014a, 2015). Several pathology studies confirmed *Diaporthe* species to be associated with diverse suites of diseases (Fig. 7) on a broad range of economically important agricultural crops (Udayanga *et al.* 2011). More than one *Diaporthe* species is frequently reported as causative agents of the same disease (Thompson *et al.* 2011, Guarnaccia *et al.* 2016).

Although *Diaporthe* was historically considered monophyletic based on the typical phomopsis-like asexual morph, the paraphyletic nature of this genus was recently revealed (Gao *et al.* 2017, Senanayake *et al.* 2017). Most of the known species in early literature were described in relation to their host association and morphological characters. However, a single species of *Diaporthe* can be found on diverse hosts, and can co-occur on the same host or lesion in different life modes. Phylogenetic studies demonstrated that morphological characters are not always reliable for species level identification due to their variability under changing environmental conditions (Gomes *et al.* 2013). As a consequence, identification and description of species based on host association alone is no longer tenable. For accurate species delimitation, phylogenetic inference of the ITS, *cal*, *his3*, *tef1* and *tub2* or combinations of these is required.

References: Mostert *et al.* 2001, Van Niekerk *et al.* 2005, Thompson *et al.* 2011, Guarnaccia *et al.* 2016, 2018 (morphology, pathogenicity and phylogeny); Udayanga *et al.* 2011, 2014a, 2015, Gomes *et al.* 2013 (morphology and phylogeny); Dissanayake *et al.* 2017b, c, Gao *et al.* 2017 (phylogeny).

Diaporthe heterophyllae Guarnaccia & Crous, **sp. nov.** MycoBank MB823830. Fig. 10.

Etymology: Name refers to *Acacia heterophylla*, the host from which this fungus was collected.

On PNA: *Conidiomata* 250–350 µm diam, pycnidial, globose or irregular, solitary, deeply embedded in media, erumpent, dark brown to black, whitish translucent to yellow conidial drops and/or cirrus exuded from ostioles; *conidiomatal wall* consisting of 3–4 layers of medium brown *textura angularis*. *Conidiophores* 7–22 × 1.5–4 µm, hyaline, smooth, 0–1-septate, densely aggregated, cylindrical, straight. *Conidiogenous cells* 6–9 × 1–2 µm, phialidic, hyaline, terminal, cylindrical, tapered towards apex. *Paraphyses* not observed. *Alpha conidia* 6–10.5 × 2.5–4.5 µm, mean ± SD = 8.4 ± 1.1 × 3.2 ± 0.4 µm, L/W ratio = 2.6, aseptate, ovate to ellipsoidal, hyaline, multi-guttulate and acute or rounded at both ends. *Beta conidia* 17–24 × 1–2 µm, mean ± SD = 21.7 ± 1.8 × 1.5 ± 0.3 µm, L/W ratio = 14.5, hyaline, aseptate, eguttulate, filiform, curved, tapering towards both ends. *Gamma conidia* not observed.

Culture characteristics: Colonies covering medium within 10 d at 21 °C, with surface mycelium flattened, dense and felty. Colony on MEA, PDA and OA at first white, becoming cream to yellowish, flat on MEA and OA, dense, felted on PDA; reverse grey with brownish dots with age, with visible solitary conidiomata at maturity on all media.

Material examined: **France**, La Rèunion, on *Acacia heterophylla* (*Fabaceae*), 8 Mar. 2015, P.W. Crous (**holotype** CBS H-23376, culture ex-type CBS 143769 = CPC 26215).

Notes: *Diaporthe heterophyllae* is phylogenetically close but clearly differentiated from *D. eres* based on ITS, *tef1*, *tub2*, *his3* and *cal* sequence similarity (98 %, 88 %, 97 %, 95 %, and 97 %, respectively). Morphologically, *D. heterophyllae* differs from *D. eres* in its

Fig. 8. *Diaporthe* spp. **A–D.** Sexual morph. **A, B.** Ascomata. **A.** *Diaporthe ambigua* (ex-type CBS 114015). **B.** *Diaporthe aspalathi* (ex-type CBS 117169). **C, D.** Asci with ascospores. **C.** *Diaporthe ambigua* (ex-type CBS 114015). **D.** *Diaporthe aspalathi* (ex-type CBS 117169). **E–M.** Asexual morph. **E, F.** Conidiomata sporulating. **E.** *Diaporthe limonicola* (ex-type CBS 142549). **F.** *Diaporthe pseudomangiferae* (ex-type CBS 101339). **G–I.** Conidiogenous cells and conidia. **G.** *Diaporthe raonikayaporum* (ex-type CBS 133182). **H.** *Diaporthe tecomae* (CBS 100547). **I.** *Diaporthe limonicola* (ex-type CBS 142549). **J, K.** Alpha conidia. **J.** *Diaporthe cinerascens* (CBS 719.96). **K.** *Diaporthe pseudomangiferae* (ex-type CBS 101339). **L.** Beta conidia of *Diaporthe eleagni* (CBS 504.72). **M.** Alpha, beta and gamma conidia of *Diaporthe limonicola* (ex-type CBS 142549). Scale bars = 10 µm. Pictures A–D taken from Van Rensburg *et al.* (2006); F–H, J–L from Gomes *et al.* (2013); E, I, M from Guarnaccia & Crous (2017).

Table 4. DNA barcodes of accepted *Diaporthe* spp.

Species	Isolates[1]	GenBank accession numbers[2]					References
		ITS	*tub2*	*his3*	*tef1*	*cal*	
Diaporthe acaciarum	CBS 138862^T	KP004460	KP004509	KP004504	–	–	Crous *et al.* (2014b)
D. acaciigena	CBS 129521^T	KC343005	KC343973	KC343489	KC343731	KC343247	Gomes *et al.* (2013)
D. acericola	MFLUCC 17-0956^T	KY964224	KY964074	–	KY964180	KY964137	Dissanayake *et al.* (2017a)
D. acerina	CBS 137.27	KC343006	KC343974	KC343490	KC343732	KC343248	Gomes *et al.* (2013)
D. acutispora	CGMCC 3.18285^T	KX986764	KX999195	KX999235	KX999155	KX999274	Gao *et al.* (2017)
D. alleghaniensis	CBS 495.72^T	FJ889444	KC843228	KC343491	GQ250298	KC343249	Gomes *et al.* (2013)
D. alnea	CBS 146.46^T	KC343008	KC343976	KC343492	KC343734	KC343250	Gomes *et al.* (2013)
D. ambigua	CBS 114015^T	KC343010	KC343978	KC343494	KC343736	KC343252	Gomes *et al.* (2013)
D. ampelina	CBS 114016^T	AF230751	JX275452	–	GQ250351	JX197443	Gomes *et al.* (2013)
D. amygdali	CBS 126679^T	KC343022	KC343990	KC343506	KC343748	KC343264	Gomes *et al.* (2013)
D. anacardii	CBS 720.97^T	KC343024	KC343992	KC343508	KC343750	KC343266	Gomes *et al.* (2013)
D. angelicae	CBS 111592^T	KC343026	KC343994	KC343511	KC343752	KC343268	Gomes *et al.* (2013)
D. apiculatum	LC 3418^T	KP267896	KP293476	KP293550	KP267970	–	Gao *et al.* (2016)
D. aquatica	IFRDCC 3051^T	JQ797437	–	–	–	–	Hu *et al.* (2012)
D. arctii	CBS 136.25	KC343031	KC343999	KC343515	KC343757	KC343273	Gomes *et al.* (2013)
D. arecae	CBS 161.64^T	KC343032	KC344000	KC343516	KC343758	KC343274	Gomes *et al.* (2013)
D. arengae	CBS 114979^T	KC343034	KC344002	KC343518	KC343760	KC343276	Gomes *et al.* (2013)
D. aseana	MFLUCC 12-0299a^T	KT459414	KT459432	–	KT459448	KT459464	Hyde *et al.* (2016)
D. asheicola	CBS 136967^T	KJ160562	KJ160518	–	KJ160594	KJ160542	Lombard *et al.* (2014)
D. aspalathi	CBS 117169^T	KC343036	KC344004	KC343520	KC343762	KC343278	Van Rensburg *et al.* (2006)
D. australafricana	CBS 111886^T	KC343038	KC344006	KC343522	KC343764	KC343280	Gomes *et al.* (2013)
D. baccae	CBS 136972^T	KJ160565	MF418509	MF418264	KJ160597	–	Lombard *et al.* (2014)
D. batatas	CBS 122.21	KC343040	KC344008	KC343524	KC343766	KC343282	Gomes *et al.* (2013)
D. beckhausii	CBS 138.27	KC343041	KC344009	KC343525	KC343767	KC343283	Gomes *et al.* (2013)
D. beilharziae	BRIP 54792^T	JX862529	KF170921	–	JX862535	–	Thompson *et al.* (2015)
D. benedicti	CFCC 50062^T	KP208847	KP208855	KP208851	KP208853	KP208849	Fan *et al.* (2015)
D. betulae	CFCC 50469^T	KT732950	KT733020	KT732999	KT733016	KT732997	Du *et al.* (2016)
D. betulicola	CFCC 51128^T	KX024653	KX024657	KX024661	KX024655	KX024659	Du *et al.* (2016)
D. bicincta	CBS 121004^T	KC343134	KC344102	KC343618	KC343860	KC343376	Gomes *et al.* (2013)
D. biconispora	CGMCC 3.17252^T	KJ490597	KJ490418	KJ490539	KJ490476	–	Huang *et al.* (2015)
D. biguttulata	ICMP20657^T	KJ490582	KJ490403	KJ490524	KJ490461	–	Huang *et al.* (2015)
D. biguttusis	CGMCC 3.17081^T	KF576282	KF576306	–	KF576257	–	Gao *et al.* (2015)
D. bohemiae	CBS 143347^T	MG281015	MG281188	MG281361	MG281536	MG281710	Guarnaccia *et al.* (2018)
D. brasiliensis	CBS 133183^T	KC343042	KC344010	KC343526	KC343768	KC343284	Gomes *et al.* (2013)
D. caatingaensis	CBS 141542^T	KY085927	KY115600	KY115605	KY115603	KY115597	Crous *et al.* (2016a)
D. camptothecicola	CFCC 51632^T	KY203726	KY228893	KY228881	KY228887	KY228877	Yang *et al.* (2017c)
D. canthii	CBS 132533^T	JX069864	KC843230	–	KC843120	KC843174	Crous *et al.* (2012b)
D. carpini	CBS 114437	KC343044	KC344012	KC343528	KC343770	KC343286	Gomes *et al.* (2013)
D. cassines	CBS 136440^T	KF777155	–	–	KF777244	–	Crous *et al.* (2013)
D. caulivora	CBS 127268^T	KC343045	KC344013	KC343529	KC343771	KC343287	Gomes *et al.* (2013)
D. celastrina	CBS 139.27^T	KC343047	KC344015	KC343531	KC343773	KC343289	Gomes *et al.* (2013)
D. celeris	CBS 143349^T	MG281017	MG281190	MG281363	MG281538	MG281712	Guarnaccia *et al.* (2018)
D. ceratozamiae	CBS 131306^T	JQ044420	–	–	–	–	Crous *et al.* (2011b)
D. cf. *heveae* 1	CBS 852.97	KC343116	KC344084	KC343600	KC343842	KC343358	Gomes *et al.* (2013)
D. cf. *heveae* 2	CBS 681.84	KC343117	KC344085	KC343601	KC343843	KC343359	Gomes *et al.* (2013)
D. chamaeropis	CBS 454.81	KC343048	KC344016	KC343532	KC343774	KC343290	Gomes *et al.* (2013)
D. charlesworthii	BRIP 54884m^T	KJ197288	KJ197268	–	KJ197250	–	Thompson *et al.* (2015)
D. cichorii	MFLUCC 17-1023^T	KY964220	KY964104	–	KY964176	KY964133	Dissanayake *et al.* (2017a)
D. cinerascens	CBS 719.96	KC343050	KC344018	KC343534	KC343776	KC343292	Gomes *et al.* (2013)

Table 4. (Continued).

Species	Isolates[1]	GenBank accession numbers[2]					References
		ITS	*tub2*	*his3*	*tef1*	*cal*	
D. cissampeli	CBS 141331^T	KX228273	KX228384	KX228366	–	–	Crous *et al.* (2016b)
D. citri	CBS 135422^T	KC843311	KC843187	MF418281	KC843071	KC843157	Udayanga *et al.* (2014b)
D. citriasiana	CBS 134240^T	JQ954645	KC357459	MF418282	JQ954663	KC357491	Huang *et al.* (2013)
D. citrichinensis	CBS 134242^T	JQ954648	MF418524	KJ420880	JQ954666	KC357494	Huang *et al.* (2013)
D. compacta	LC3083^T	KP267854	KP293434	KP293508	KP267928	–	Gao *et al.* (2016)
D. convolvuli	CBS 124654	KC343054	KC344022	KC343538	KC343780	KC343296	Gomes *et al.* (2013)
D. crataegi	CBS 114435	KC343055	KC344023	KC343539	KC343781	KC343297	Gomes *et al.* (2013)
D. crotalariae	CBS 162.33^T	KC343056	KC344024	KC343540	KC343782	KC343298	Gomes *et al.* (2013)
D. cucurbitae	DAOM 42078^T	KM453210	KP118848	KM453212	KM453211	–	Udayanga *et al.* (2015)
D. cuppatea	CBS 117499^T	AY339322	JX275420	KC343541	AY339354	JX197414	Van Rensburg *et al.* (2006)
D. cynaroidis	CBS 122676	KC343058	KC344026	KC343542	KC343784	KC343300	Gomes *et al.* (2013)
D. cytosporella	CBS 137020^T	KC843307	KC843221	*MF418283*	KC843116	KC843141	Udayanga *et al.* (2014b)
D. decedens	CBS 109772	KC343059	KC344027	KC343543	KC343785	KC343301	Gomes *et al.* (2013)
D. detrusa	CBS 109770	KC343061	KC344029	KC343545	KC343787	KC343303	Gomes *et al.* (2013)
D. diospyricola	CBS 136552^T	KF777156	–	–	–	–	Crous *et al.* (2013)
D. discoidispora	ICMP20662^T	KJ490624	KJ490445	KJ490566	KJ490503	–	Huang *et al.* (2015)
D. dorycnii	MFLUCC 17-1015^T	KY964215	KY964099	–	KY964171	–	Dissanayake *et al.* (2017a)
D. elaeagni-glabrae	CGMCC 3.18287^T	KX986779	KX999212	KX999251	KX999171	KX999281	Gao *et al.* (2017)
D. eleagni	CBS 504.72	KC343064	KC344032	KC343548	KC343790	KC343306	Gomes *et al.* (2013)
D. ellipicola	CGMCC 3.17084^T	KF576270	KF576291	–	KF576245	–	Gao *et al.* (2015)
D. endophytica	CBS 133811^T	KC343065	KC344033	KC343549	KC343791	KC343307	Gomes *et al.* (2013)
D. eres	CBS 138594^T	KJ210529	KJ420799	KJ420850	KJ210550	KJ434999	Udayanga *et al.* (2014a)
D. eucalyptorum	CBS 132525^T	JX069862	–	–	–	–	Crous *et al.* (2012b)
D. eugeniae	CBS 444.82	KC343098	KC344066	KC343582	KC343824	KC343340	Gomes *et al.* (2013)
D. fibrosa	CBS 109751	KC343099	KC344067	KC343583	KC343825	KC343341	Gomes *et al.* (2013)
D. foeniculina	CBS 111553^T	KC343101	KC344069	KC343585	KC343827	KC343343	Gomes *et al.* (2013)
D. fraxini-angustifoliae	BRIP 54781^T	JX862528	KF170920	–	JX852534	–	Tan *et al.* (2013)
D. fusicola	CGMCC 3.17087^T	KF576281	KF576305	–	KF576256	KF576233	Gao *et al.* (2015)
D. ganjae	CBS 180.91^T	KC343112	KC344080	KC343596	KC343838	KC343354	Gomes *et al.* (2013)
D. gardeniae	CBS 288.56	KC343113	KC344081	KC343597	KC343839	KC343355	Gomes *et al.* (2013)
D. garethjonesii	MFLUCC 12-0542a^T	KT459423	KT459441	–	KT459457	KT459470	Hyde *et al.* (2016)
D. goulteri	BRIP 55657a^T	KJ197290	KJ197270	–	KJ197252	–	Thompson *et al.* (2015)
D. gulyae	BRIP 54025^T	JF431299	KJ197271	–	JN645803	–	Thompson *et al.* (2015)
D. helianthi	CBS 592.81^T	KC343115	KC344083	KC343599	KC343841	JX197454	Gomes *et al.* (2013)
D. helicis	CBS 138596^T	KJ210538	KJ420828	KJ420875	KJ210559	KJ435043	Udayanga *et al.* (2014a)
D. heterophyllae	CBS 143769^T	MG600222	MG600226	MG600220	MG600224	MG600218	Present study
D. hickoriae	CBS 145.26^T	KC343118	KC344086	KC343602	KC343844	KC343360	Gomes *et al.* (2013)
D. hispaniae	CBS 143351^T	MG281123	MG281296	MG281471	MG281644	MG281820	Guarnaccia *et al.* (2018)
D. hongkongensis	CBS 115448^T	KC343119	KC344087	KC343603	KC343845	KC343361	Gomes *et al.* (2013)
D. hordei	CBS 481.92	KC343120	KC344088	KC343604	KC343846	KC343362	Gomes *et al.* (2013)
D. hungariae	CBS 143353^T	MG281126	MG281299	MG281474	MG281647	MG281823	Guarnaccia *et al.* (2018)
D. impulsa	CBS 114434	KC343121	KC344089	KC343605	KC343847	KC343363	Gomes *et al.* (2013)
D. incompleta	CGMCC 3.18288^T	KX986794	KX999226	KX999265	KX999186	KX999289	Gao *et al.* (2017)
D. inconspicua	CBS 133813^T	KC343123	KC344091	KC343607	KC343849	KC343365	Gomes *et al.* (2013)
D. infecunda	CBS 133812^T	KC343126	KC344094	KC343610	KC343852	KC343368	Gomes *et al.* (2013)
D. infertilis	CBS 230.52^T	KC343052	KC344020	KC343536	KC343778	KC343294	Guarnaccia & Crous (2017)
D. isoberliniae	CBS 137981^T	KJ869133	KJ869245	–	–	–	Crous *et al.* (2014c)
D. juglandicola	CFCC 51134^T	KU985101	KX024634	–	KX024628	KX024616	Yang *et al.* (2017a)

(*continued on next page*)

Table 4. (Continued).

Species	Isolates[1]	GenBank accession numbers[2]					References
		ITS	*tub2*	*his3*	*tef1*	*cal*	
D. kochmanii	BRIP 54033^T	JF431295	–	–	JN645809	–	Thompson *et al.* (2011)
D. kongii	BRIP 54031^T	JF431301	KJ197272	–	JN645797	–	Thompson *et al.* (2011)
D. leucospermi	CBS 111980^T	JN712460	KY435673	KY435653	KY435632	KY435663	Crous *et al.* (2011c)
D. limonicola	CBS 142549^T	MF418422	MF418582	MF418342	MF418501	MF418256	Guarnaccia & Crous (2017)
D. litchicola	BRIP 54900^T	JX862533	KF170925	–	JX862539	–	Tan *et al.* (2013)
D. lithocarpus	CGMCC 3.15175^T	KC153104	KF576311	–	KC153095	–	Gao *et al.* (2014)
D. litoricola	MFLUCC 16-1195^T	MF190139	–	–	–	–	Senanayake *et al.* (2017)
D. longicicola	CGMCC 3.17089^T	KF576267	KF576291	–	KF576242	–	Gao *et al.* (2015)
D. longicolla	FAU 599^T	KJ590728	KJ610883	KJ659188	KJ590767	KJ612124	Udayanga *et al.* (2015)
D. longispora	CBS 194.36^T	KC343135	KC344103	KC343619	KC343861	KC343377	Gomes *et al.* (2013)
D. lonicerae	MFLUCC 17-0963^T	KY964190	KY964073	–	KY964146	KY964116	Dissanayake *et al.* (2017a)
D. lusitanicae	CBS 123212^T	KC343136	KC344104	KC343620	KC343862	KC343378	Gomes *et al.* (2013)
D. macintoshii	BRIP 55064a^T	KJ197289	KJ197269	–	KJ197251	–	Thompson *et al.* (2015)
D. mahothocarpus	CGMCC 3.15181	KC153096	–	–	KC153087	–	Gao *et al.* (2014)
D. malorum	CBS142383^T	KY435638	KY435668	KY435648	KY435627	KY435658	Santos *et al.* (2017)
D. manihotia	CBS 505.76	KC343138	KC344106	KC343622	KC343864	KC343380	Gomes *et al.* (2013)
D. maritima	DAOMC 250563^T	KU552025	KU574615	–	KU552023	–	Tanney *et al.* (2016)
D. masirevicii	BRIP 57892a^T	KJ197277	KJ197257	–	KJ197239	–	Thompson *et al.* (2015)
D. mayteni	CBS 133185^T	KC343139	KC344107	KC343623	KC343865	KC343381	Gomes *et al.* (2013)
D. maytenicola	CBS 136441^T	KF777157	KF777250	–	–	–	Crous *et al.* (2013)
D. megalospora	CBS 143.27	KC343140	KC344108	KC343624	KC343866	KC343382	Gomes *et al.* (2013)
D. melitensis	CBS 142551^T	MF418424	MF418584	MF418344	MF418503	MF418258	Guarnaccia & Crous (2017)
D. melonis	CBS 507.78^T	KC343142	KC344110	KC343626	KC343868	KC343384	Gomes *et al.* (2013)
D. middletonii	BRIP 54884e^T	KJ197286	KJ197266	–	KJ197248	–	Thompson *et al.* (2015)
D. miriciae	BRIP 54736j^T	KJ197283	KJ197263	–	KJ197245	–	Thompson *et al.* (2015)
D. momicola	MFLUCC 16-0113^T	KU557563	KU557587	–	KU557631	KU557611	Dissanayake *et al.* (2017c)
D. multigutullata	ICMP20656^T	KJ490633	KJ490454	KJ490575	KJ490512	–	Huang *et al.* (2015)
D. musigena	CBS 129519^T	KC343143	KC344111	KC343627	KC343869	KC343385	Gomes *et al.* (2013)
D. neilliae	CBS 144.27^T	KC343144	KC344112	KC343628	KC343870	KC343386	Gomes *et al.* (2013)
D. neoarctii	CBS 109490	KC343145	KC344113	KC343629	KC343871	KC343387	Gomes *et al.* (2013)
D. neoraonikayaporum	MFLUCC 14-1136^T	KU712449	KU743988	–	KU749369	KU749356	Doilom *et al.* (2017)
D. nomurai	CBS 157.29	KC343154	KC344122	KC343638	KC343880	KC343396	Gomes *et al.* (2013)
D. nothofagi	BRIP 54801^T	JX862530	KF170922	–	JX862536	–	Tan *et al.* (2013)
D. novem	CBS 127271^T	KC343157	KC344125	KC343641	KC343883	KC343399	Gomes *et al.* (2013)
D. obtusifoliae	CBS 143449^T	MG386072	–	MG386137	–	–	Crous *et al.* (2017b)
D. ocoteae	CBS 141330^T	KX228293	KX228388	–	–	–	Crous *et al.* (2016b)
D. oncostoma	CBS 589.78	KC343162	KC344130	KC343646	KC343888	KC343404	Gomes *et al.* (2013)
D. oraccinii	LC 3166^T	KP267863	KP293443	KP293517	KP267937	–	Gao *et al.* (2016)
D. ovalispora	ICMP20659^T	KJ490628	KJ490449	KJ490570	KJ490507	–	Huang *et al.* (2015)
D. ovoicicola	CGMCC 3.17092^T	KF576264	KF576288	–	KF576239	KF576222	Gao *et al.* (2015)
D. oxe	CBS 133186^T	KC343164	KC344132	KC343648	KC343890	KC343406	Gomes *et al.* (2013)
D. padi var. *padi*	CBS 114200	KC343169	KC344137	KC343653	KC343895	KC343411	Gomes *et al.* (2013)
D. paranensis	CBS 133184	KC343171	KC344139	KC343655	KC343897	KC343413	Gomes *et al.* (2013)
D. parapterocarpi	CBS 137986^T	KJ869138	KJ869248	–	–	–	Crous *et al.* (2014c)
D. pascoei	BRIP 54847^T	JX862532	KF170924	–	JX862538	–	Tan *et al.* (2013)
D. passiflorae	CBS 132527^T	JX069860	KY435674	KY435654	KY435633	KY435664	Crous *et al.* (2012b)
D. passifloricola	CBS 141329^T	KX228292	KX228387	KX228367	–	–	Crous *et al.* (2016b)
D. penetriteum	LC 3353	KP714505	KP714529	KP714493	KP714517	–	Gao *et al.* (2016)
D. perjuncta	CBS 109745^T	KC343172	KC344140	KC343656	KC343898	KC343414	Gomes *et al.* (2013)

Table 4. (Continued).

Species	Isolates[1]	GenBank accession numbers[2]					References
		ITS	*tub2*	*his3*	*tef1*	*cal*	
D. perniciosa	CBS 124030	KC343149	KC344117	KC343633	KC343875	KC343391	Gomes *et al.* (2013)
D. perseae	CBS 151.73	KC343173	KC344141	KC343657	KC343899	KC343415	Gomes *et al.* (2013)
D. pescicola	MFLUCC 16-0105^T	KU557555	KU557579	–	KU557623	KU557603	Dissanayake *et al.* (2017c)
D. phaseolorum	CBS 113425	KC343174	KC344142	KC343658	KC343900	KC343416	Gomes *et al.* (2013)
D. phragmitis	CBS 138897^T	KP004445	KP004507	KP004503	–	–	Crous *et al.* (2014b)
D. podocarpi-macrophylli	CGMCC3.18281^T	KX986774	KX999207	KX999246	KX999167	KX999278	Gao *et al.* (2017)
D. pseudomangiferae	CBS 101339^T	KC343181	KC344149	KC343665	KC343907	KC343423	Gomes *et al.* (2013)
D. pseudophoenicicola	CBS 462.69^T	KC343184	KC344152	KC343668	KC343910	KC343426	Gomes *et al.* (2013)
D. pseudotsugae	MFLU 15-3228	KY964225	KY964108	–	KY964181	KY964138	Dissanayake *et al.* (2017a)
D. psoraleae	CBS 136412^T	KF777158	KF777251	–	KF777245	–	Crous *et al.* (2013)
D. psoraleae-pinnatae	CBS 136413^T	KF777159	KF777252	–	–	–	Crous *et al.* (2013)
D. pterocarpi	MFLUCC 10-0571	JQ619899	JX275460	–	JX275416	JX197451	Udayanga *et al.* (2012)
D. pterocarpicola	MFLUCC 10-0580a	JQ619887	JX275441	–	JX275403	JX197433	Udayanga *et al.* (2012)
D. pulla	CBS 338.89^T	KC343152	KC344120	KC343636	KC343878	KC343394	Gomes *et al.* (2013)
D. pustulata	CBS 109742	KC343185	KC344153	KC343669	KC343911	KC343427	Gomes *et al.* (2013)
D. pyracanthae	CBS142384^T	KY435635	KY435666	KY435645	KY435625	KY435656	Santos *et al.* (2017)
D. racemosae	CBS 143770^T	MG600223	MG600227	MG600221	MG600225	MG600219	Present study
D. raonikayaporum	CBS 133182^T	KC343188	KC344156	KC343672	KC343914	KC343430	Gomes *et al.* (2013)
D. ravennica	MFLUCC 15-0479^T	KU900335	KX432254	–	KX365197	–	Dissanayake *et al.* (2017a)
D. rhoina	CBS 146.27	KC343189	KC344157	KC343673	KC343915	KC343431	Gomes *et al.* (2013)
D. rostrata	CFCC 50062^T	KP208847	KP208855	KP208851	KP208853	KP208849	Fan *et al.* (2015)
D. rudis	CBS 113201	KC343234	KC344202	KC343718	KC343960	KC343476	Udayanga *et al.* (2014b)
D. saccarata	CBS 116311^T	KC343190	KC344158	KC343674	KC343916	KC343432	Gomes *et al.* (2013)
D. sackstonii	BRIP 54669b^T	KJ197287	KJ197267	–	KJ197249	–	Thompson *et al.* (2015)
D. salicicola	BRIP 54825^T	JX862531	KF170923	–	JX862537	–	Tan *et al.* (2013)
D. sambucusii	CFCC 51986^T	KY852495	KY852511	KY852503	KY852507	KY852499	Yang *et al.* (2018)
D. schini	CBS 133181^T	KC343191	KC344159	KC343675	KC343917	KC343433	Gomes *et al.* (2013)
D. schisandrae	CFCC 51988^T	KY852497	KY852513	KY852505	KY852509	KY852501	Yang *et al.* (2018)
D. schoeni	MFLU 15-1279^T	KY964226	KY964109	–	KY964182	KY964139	Dissanayake *et al.* (2017a)
D. sclerotioides	CBS 296.67^T	KC343193	KC344161	KC343677	KC343919	KC343435	Gomes *et al.* (2013)
D. scobina	CBS 251.38	KC343195	KC344163	KC343679	KC343921	KC343437	Gomes *et al.* (2013)
D. sennae	CFCC 51636^T	KY203724	KY228891	–	KY228885	KY228875	Yang *et al.* (2017b)
D. sennicola	CFCC 51634^T	KY203722	KY228889	–	KY228883	KY228873	Yang *et al.* (2017b)
D. serafiniae	BRIP 55665a^T	KJ197274	KJ197254	–	KJ197236	–	Thompson *et al.* (2015)
D. siamensis	MFLUCC 10-0573a	JQ619879	JX275429	–	JX275393	–	Udayanga *et al.* (2012)
D. sojae	CBS 139282^T	KJ590719	KJ610875	KJ659208	KJ590762	KJ612116	Udayanga *et al.* (2015)
D. spartinicola	CBS 140003^T	KR611879	KR857695	KR857696	–	–	Crous *et al.* (2015c)
D. sterilis	CBS 136969^T	KJ160579	KJ160528	MF418350	KJ160611	KJ160548	Lombard *et al.* (2014)
D. stewartii	CBS 193.36	FJ889448	–	–	GQ250324	–	Santos *et al.* (2010)
D. stictica	CBS 370.54	KC343212	KC344180	KC343696	KC343938	KC343454	Gomes *et al.* (2013)
D. subclavata	ICMP20663^T	KJ490630	KJ490451	KJ490572	KJ490509	–	Huang *et al.* (2015)
D. subordinaria	CBS 101711	KC343213	KC344181	KC343697	KC343939	KC343455	Gomes *et al.* (2013)
D. taoicola	MFLUCC 16-0117^T	KU557567	KU557591	–	KU557635	–	Dissanayake *et al.* (2017c)
D. tecomae	CBS 100547	KC343215	KC344183	KC343699	KC343941	KC343457	Gomes *et al.* (2013)
D. tectonae	MFLUCC 12-0777^T	KU712430	KU743977	–	KU749359	KU749345	Doilom *et al.* (2017)
D. tectonendophytica	MFLUCC 13-0471^T	KU712439	KU743986	–	KU749367	KU749354	Doilom *et al.* (2017)
D. tectonigena	MFLUCC 12-0767^T	KU712429	KU743976	–	KU749371	KU749358	Doilom *et al.* (2017)
D. terebinthifolii	CBS 133180^T	KC343216	KC344184	KC343700	KC343942	KC343458	Gomes *et al.* (2013)

(*continued on next page*)

Table 4. (Continued).

Species	Isolates[1]	GenBank accession numbers[2]					References
		ITS	*tub2*	*his3*	*tef1*	*cal*	
D. ternstroemia	CGMCC 3.15183[T]	KC153098	–	–	KC153089	–	Gao *et al.* (2014)
D. thunbergii	MFLUCC 10-0756a	JQ619893	JX275449	–	JX275409	JX197440	Udayanga *et al.* (2012)
D. torilicola	MFLUCC 17-1051[T]	KY964212	KY964096	–	KY964168	KY964127	Dissanayake *et al.* (2017a)
D. toxica	CBS 534.93[T]	KC343220	KC344188	KC343704	KC343946	KC343462	Gomes *et al.* (2013)
D. toxicodendri	FFPRI420987	LC275192	LC275224	LC275216	LC275216	LC275200	Ando *et al.* (2017)
D. tulliensis	BRIP 62248a	KR936130	KR936132	–	KR936133	–	Crous *et al.* (2015e)
D. ueckerae	FAU 656	KJ590726	KJ610881	KJ659215	KJ590747	KJ612122	Huang *et al.* (2015)
D. undulata	CGMCC 3.18293[T]	KX986798	KX999230	KX999269	KX999190	–	Gao *et al.* (2017)
D. unshiuensis	CGMCC3.17569[T]	KJ490587	KJ490408	KJ490529	KJ490466	–	Huang *et al.* (2015)
D. vaccinii	CBS 160.32[T]	AF317578	KC344196	KC343712	GQ250326	KC343470	Gomes *et al.* (2013)
D. vangueriae	CBS 137985[T]	KJ869137	KJ869247	–	–	–	Crous *et al.* (2014c)
D. vawdreyi	BRIP 57887a	KR936126	KR936128		KR936129	–	Crous *et al.* (2015e)
D. velutina	CGMCC 3.18286[T]	KX986790	KX999223	KX999261	KX999182	–	Gao *et al.* (2017)
D. vexans	CBS 127.14	KC343229	KC344197	KC343713	KC343955	KC343471	Gomes *et al.* (2013)
D. virgiliae	CBS 138788[T]	KP247573	KP247582	–	–	–	Machingambi *et al.* (2015)
D. woodii	CBS 558.93	KC343244	KC344212	KC343728	KC343970	KC343486	Gomes *et al.* (2013)
D. woolworthii	CBS 148.27	KC343245	KC344213	KC343729	KC343971	KC343487	Gomes *et al.* (2013)
D. xishuangbanica	CGMCC 3.18282[T]	KX986783	KX999216	KX999255	KX999175	–	Gao *et al.* (2017)
D. yunnanensis	CGMCC 3.18289[T]	KX986796	KX999228	KX999267	KX999188	KX999290	Gao *et al.* (2017)

[1] BRIP: Queensland Plant Pathology Herbarium, Brisbane, Australia; CBS: Westerdijk Fungal Biodiversity Institute, Utrecht, the Netherlands; CFCC: China Forestry Culture Collection Center, Beijing, China; CGMCC: Chinese General Microbiological Culture Collection Center, Beijing, China; DAOM: Plant Research Institute, Department of Agriculture (Mycology), Ottawa, Canada; DAOMC: Canadian Collection of Fungal Cultures, Ottawa, Canada; FAU: Isolates in culture collection of Systematic Mycology and Microbiology Laboratory; FFPRI: Forestry and Forest Products Research Institute, Japan; ICMP: International Collection of Micro-organisms from Plants, Landcare Research, Private Bag 92170, Auckland, New Zealand; IFRDCC: International Fungal Research and Development Culture Collection; MFLU: Mae Fah Luang University herbarium, Thailand; MFLUCC: Mae Fah Luang University Culture Collection, Chiang Rai, Thailand; LC: Working collection of Lei Cai, housed at Institute of Microbiology, Chinese Academy of Sciences, Beijing, China. [T] indicates ex-type strains.
[2] ITS: internal transcribed spacers and intervening 5.8S nrDNA; *tub2*: partial β-tubulin gene; *his3*: partial histone H3 gene; *tef1*: partial elongation factor 1-alpha gene; *cal*: partial calmodulin gene.

longer alpha conidia (6.5–10.5 *vs.* 6–8.5 µm) and in its shorter beta conidia (17–24 *vs.* 22–28 µm) (Udayanga *et al.* 2014a).

Diaporthe racemosae A.R. Wood, Guarnaccia & Crous, **sp. nov.** MycoBank MB823831. Fig. 11.

Etymology: Name refers to *Euclea racemosa*, the host from which this fungus was collected.

On PNA: *Conidiomata* 350–600 µm diam, pycnidial, globose or irregular, solitary, deeply embedded in media, erumpent, dark brown to black, yellowish translucent to pale brown conidial drops and/or cirrus exuded from ostioles; *conidiomatal wall* consisting of 3–4 layers of pale brown *textura angularis*. *Conidiophores* 7–17 × 2–4 µm, hyaline, smooth, 0–1-septate, densely aggregated, cylindrical, straight. *Conidiogenous cells* 5.5–8 × 1–2 µm, phialidic, hyaline, terminal, subcylindrical, tapered towards apex. *Paraphyses* not observed. *Alpha conidia* 4–6.5 × 2–3 µm, mean ± SD = 5.7 ± 0.6 × 2.3 ± 0.3 µm, L/W ratio = 2.5, aseptate, ellipsoidal to subcylindrical, hyaline, non- to multi-guttulate and acute or rounded at both ends. *Beta* and *gamma conidia* not observed.

Culture characteristics: Colonies covering medium within 10 d at 21 °C, with surface mycelium flattened, dense and felty. Colony on MEA and OA at first white, becoming olivaceous to dark grey. On PDA at first white, becoming white to yellowish; reverse grey with brownish dots with age, with visible solitary conidiomata at maturity on all media.

Material examined: **South Africa**, Western Cape, Bot River, from *Euclea racemosa* (*Ebenaceae*), 29 Dec. 2014, A.R. Wood (**holotype** CBS H-23377, culture ex-type CBS 143770 = CPC 26646).

Notes: *Diaporthe racemosae* is phylogenetically close but clearly differentiated from *D. schini* based on ITS, *tef1*, *tub2*, *his3* and *cal* sequence similarity (98 %, 94 %, 98 %, 94 %, and 96 %, respectively). Moreover, *D. racemosa* produces only alpha conidia, while *D. schini* produces only beta conidia (Gomes *et al.* 2013).

Authors: V. Guarnaccia, A.R. Wood & P.W. Crous

Dichotomophthora Mehrl. & Fitzp. ex M.B. Ellis, Dematiaceous Hyphomycetes (Kew): 388. 1971. Fig. 12.
Synonyms: Dichotomophthora Mehrl. & Fitzp., Mycologia 27: 550. 1935. (nom. inval., Art. 39.1, Melbourne).
Dichotomophthora Mehrl. & Fitzp. ex P.N. Rao, Mycopath. Mycol. appl. 28: 139. 1966. (nom. inval., Art. 39.1, Melbourne).

Classification: *Dothideomycetes, Pleosporomycetidae, Pleosporales, Pleosporaceae*.

Type species: *Dichotomophthora portulacae* Mehrl. & Fitzp. ex M.B. Ellis. Type specimen and ex-paratype strain: IMI 8742, CBS 174.35.

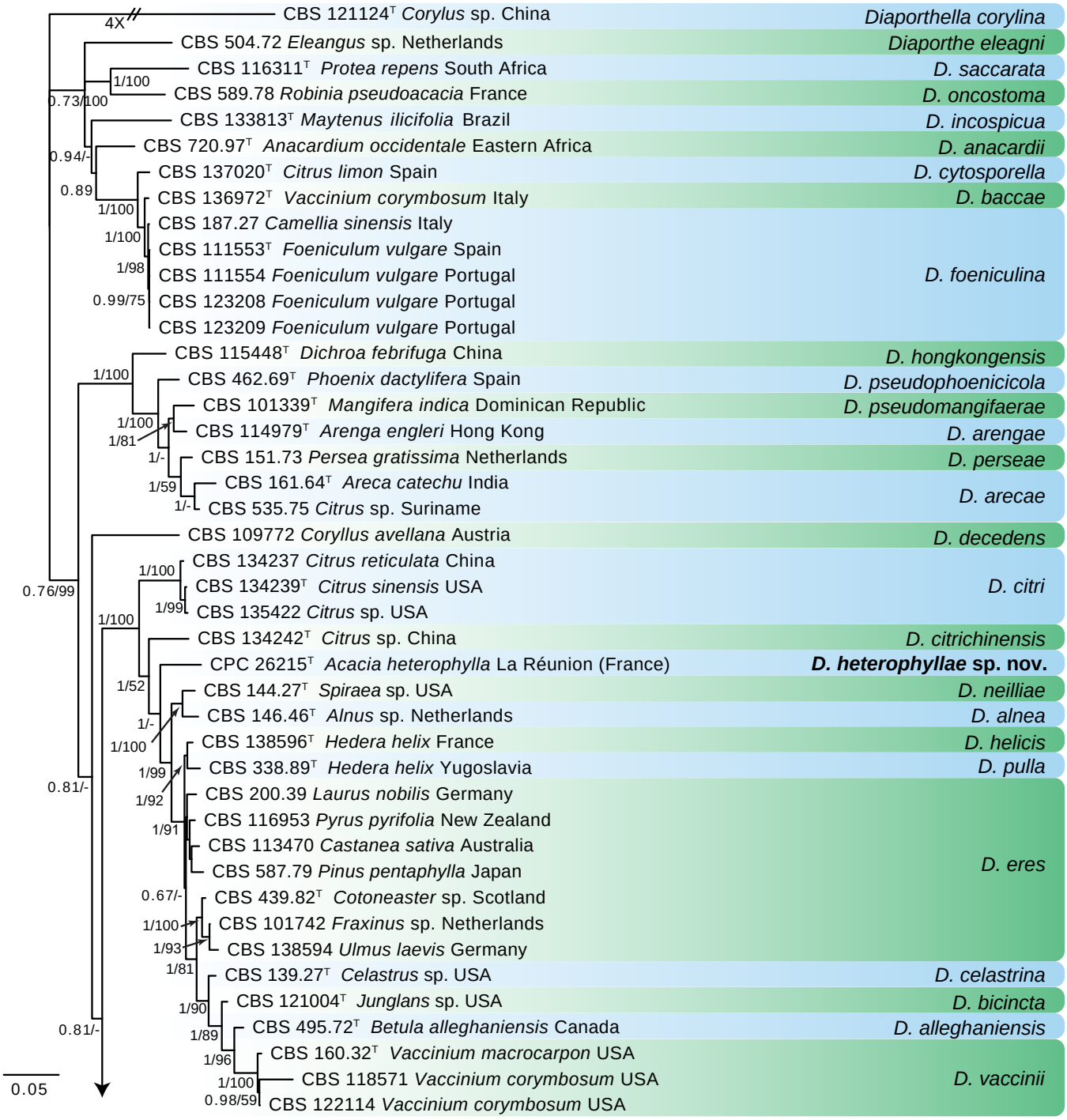

Fig. 9. Consensus phylogram of 2 052 trees resulting from a Bayesian analysis of the combined ITS (637 bp), *tub2* (833 bp), *his3* (592 bp), *tef1* (496 bp) and *cal* (817 bp) sequence alignment of *Diaporthe* spp. Bootstrap support values and Bayesian posterior probability values are indicated at the nodes. Substrate and country of origin are listed next to the strain numbers. The newly recognised species are showed in **bold**. The tree was rooted to *Diaporthella corylina* CBS 121124. T indicates ex-type strain. TreeBASE: S21865.

DNA barcodes (genus): ITS.

DNA barcodes (species): ITS, *rpb2, gpdh*. Table 5. Fig. 13.

Conidiophores macronematous, mononematous, unbranched or irregularly branched, sometimes swollen and repeatedly dichotomously or trichotomously branched or lobed at apex, forming a stipe and head; *stipe* hyaline to brown; *branches* usually short. *Conidiogenous cells* mono- or polytretic, integrated, terminal, lobed, cicatrized. *Conidia* solitary, dry, simple, ellipsoidal to cylindrical, rounded at ends, subhyaline to brown, multidistoseptate. *Microconidia* ovoid, 0–2-distoseptate. *Sclerotia* often formed in culture resembling immature perithecia, semi- or immersed in agar, subglobose, ellipsoidal, ovoid, dark brown or black. *Sexual morph* unknown (adapted from Ellis 1971).

Culture characteristics: Colonies on PDA and OA white, hazel, orange, or dark grey to olivaceous, cottony, velvety, somewhat fluffy, or flat, margin irregular, effuse; reverse centre hazel, dark brown, periphery hazel, orange to luteous. Diffusible pigment luteous to orange (produced in some strains).

Optimal media and cultivation conditions: On PDA and OA at 25 °C under near-ultraviolet light (12 h light, 12 h dark). Some strains are sterile in culture.

Distribution: Worldwide.

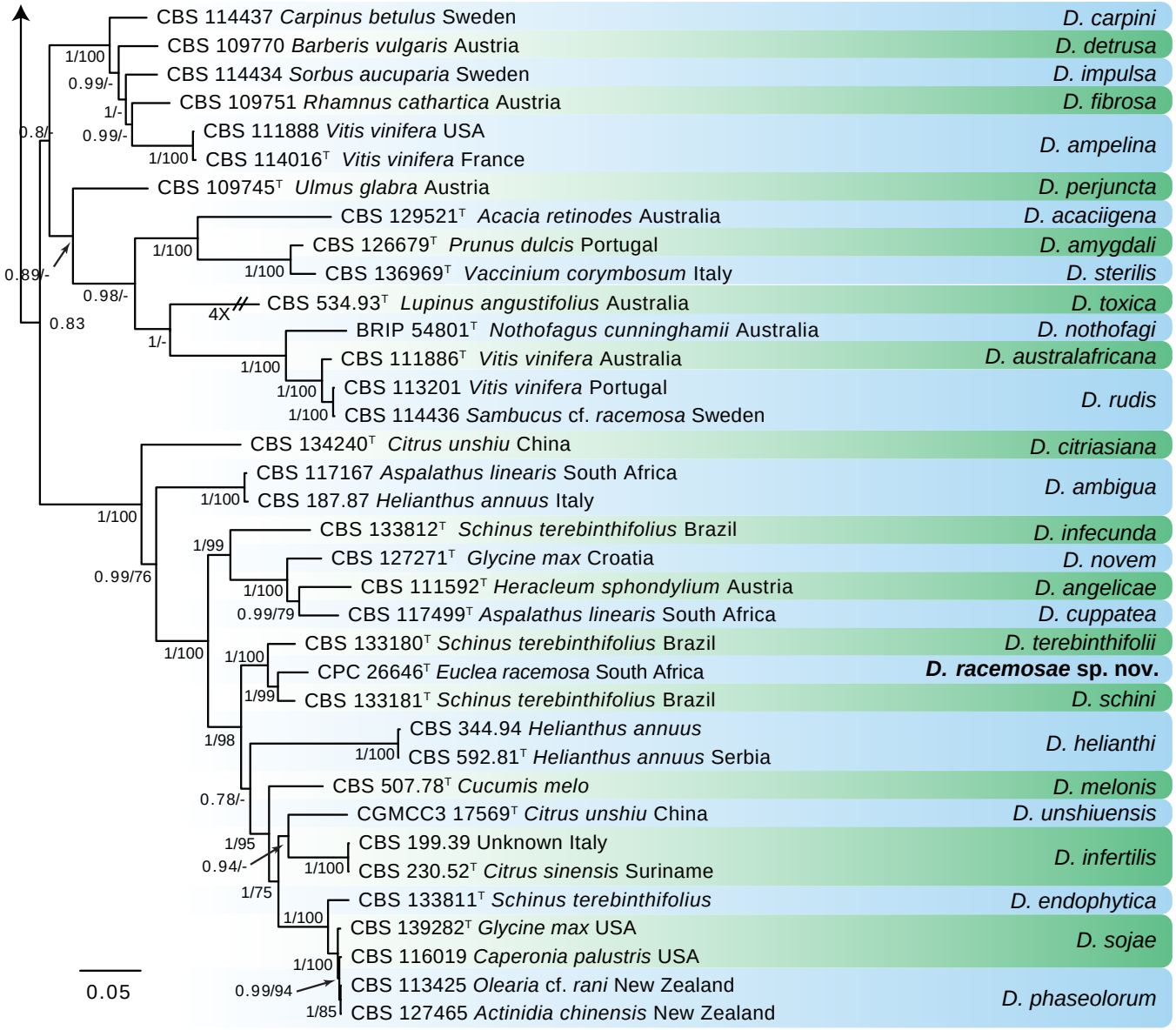

Fig. 9. (Continued).

Hosts: *Anredera* and *Basella* (*Basellaceae*), *Beta vulgaris* (*Chenopodiaceae*), *Gymnocalycium mihanovichii* var. *friedrichii* and *Myrtillocactus geometrizans* (*Cactaceae*), *Portulaca* (*Portulacaceae*), and soil.

Disease symptoms: Leaf spots, foliar abscission, stem blight, seed rot and damping-off.

Notes: *Dichotomophthora* was introduced as a monotypic genus with *Di. portulacae* isolated from *Portulaca oleracea* in Hawaii (Mehrlich & Fitzpatrick 1935). However, the publication lacked a Latin diagnosis of the fungus and the name was therefore invalid. Later, Rao (1966) provided a Latin description of *Di. portulacae* and introduced a new species, *Di. indica*, but the validation was misapplied and both names were regarded as invalid (de Hoog & van Oorschot 1983). Ellis (1971) validated the genus and the species based on the holotype specimen of *Di. portulacae* (IMI 8742). De Hoog & van Oorschot (1983) revised the taxonomy of *Dichotomophthora* and included *Di. portulacae* and *Di. lutea*. *Dichotomophthora portulacae* was restricted to species with dichotomously branched conidiophores, and conidia with 2–3 septa, 45–75 × 20–30 µm. *Dichotomophthora lutea* was introduced based on *Dactylaria lutea,* which is characterised by unbranched or irregularly branched conidiophores, and conidia with 1–5 septa, 30–115 × 10–20 µm.

Dichotomophthora species are mainly known as plant pathogens with a wide host range as well as soil-borne fungi or saprobes (Mehrlich & Fitzpatrick 1935, Routien 1957, Rao 1966, Ellis 1971, Klisiewicz 1985, Baudoin 1986, Pfeiffer *et al.* 1989, Eken 2003, Farr & Rossman 2017, Soares & Nechet 2017). However, a case of human keratitis caused by *Di. portulacae* was reported from subtropical Africa (de Hoog *et al.* 2000). Since many records of *Di. portulacae* may represent *Di. lutea* due to previous taxonomic confusion, host and distribution data need to be re-evaluated (de Hoog & van Oorschot 1983, Farr & Rossman 2017, Soares & Nechet 2017).

This is the first time that numerous isolates, including the ex-type strains of both species of *Dichotomophthora*, have been subjected to phylogenetic analyses. Our results suggest that *Dichotomophthora* belongs in the *Pleosporaceae* (*Pleosporales*), closely related to *Curvularia*. The phylogenetic analysis and subtle morphological evidence revealed two additional new species, introduced here as *Di. basellae* and *Di. brunnea*. For an

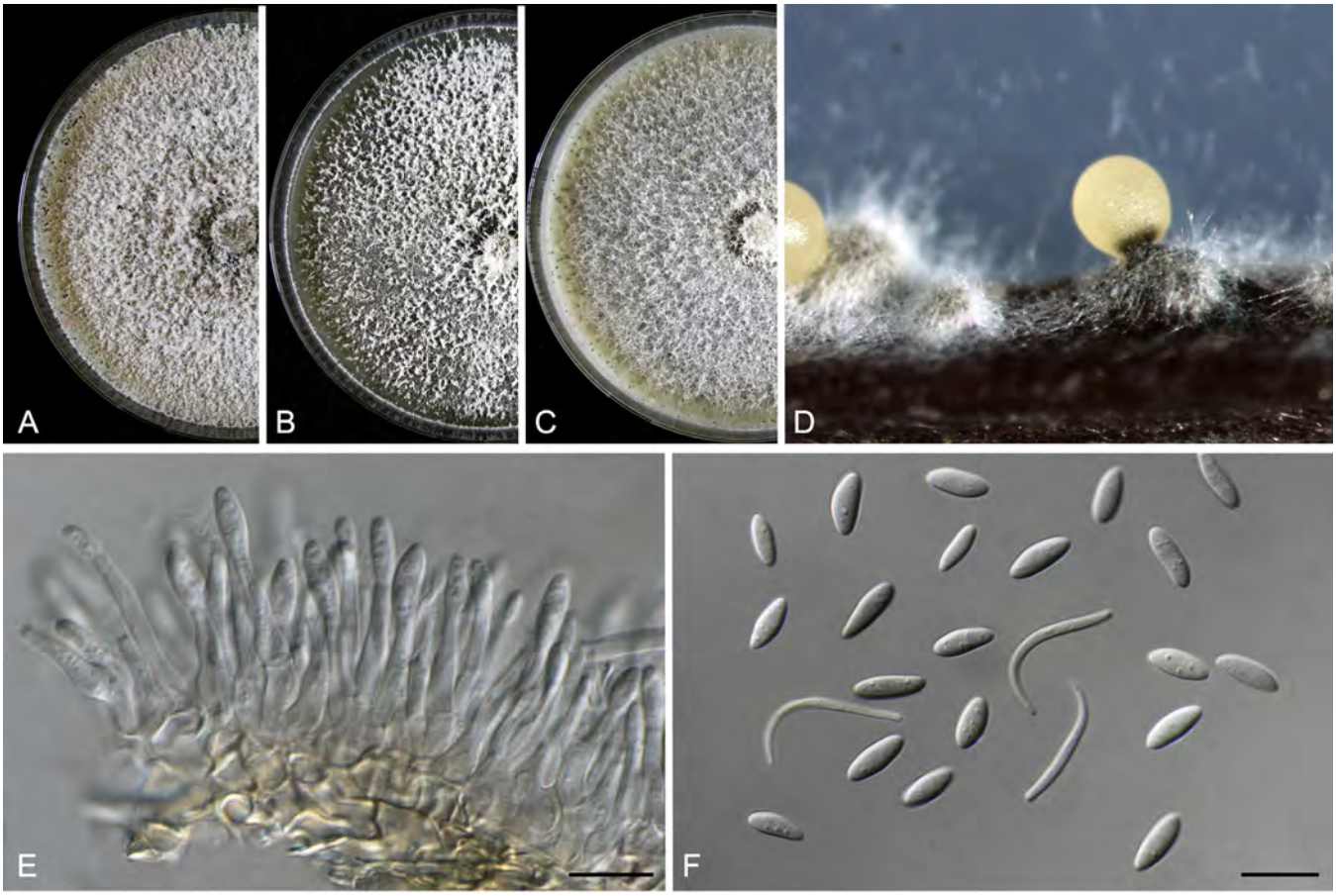

Fig. 10. *Diaporthe heterophyllae* (ex-type CBS 143769). **A–C.** Colonies on MEA, PDA and OA, respectively. **D.** Conidiomata sporulating on PNA. **E.** Conidiogenous cells and conidia. **F.** Alpha and beta conidia. Scale bars = 10 µm.

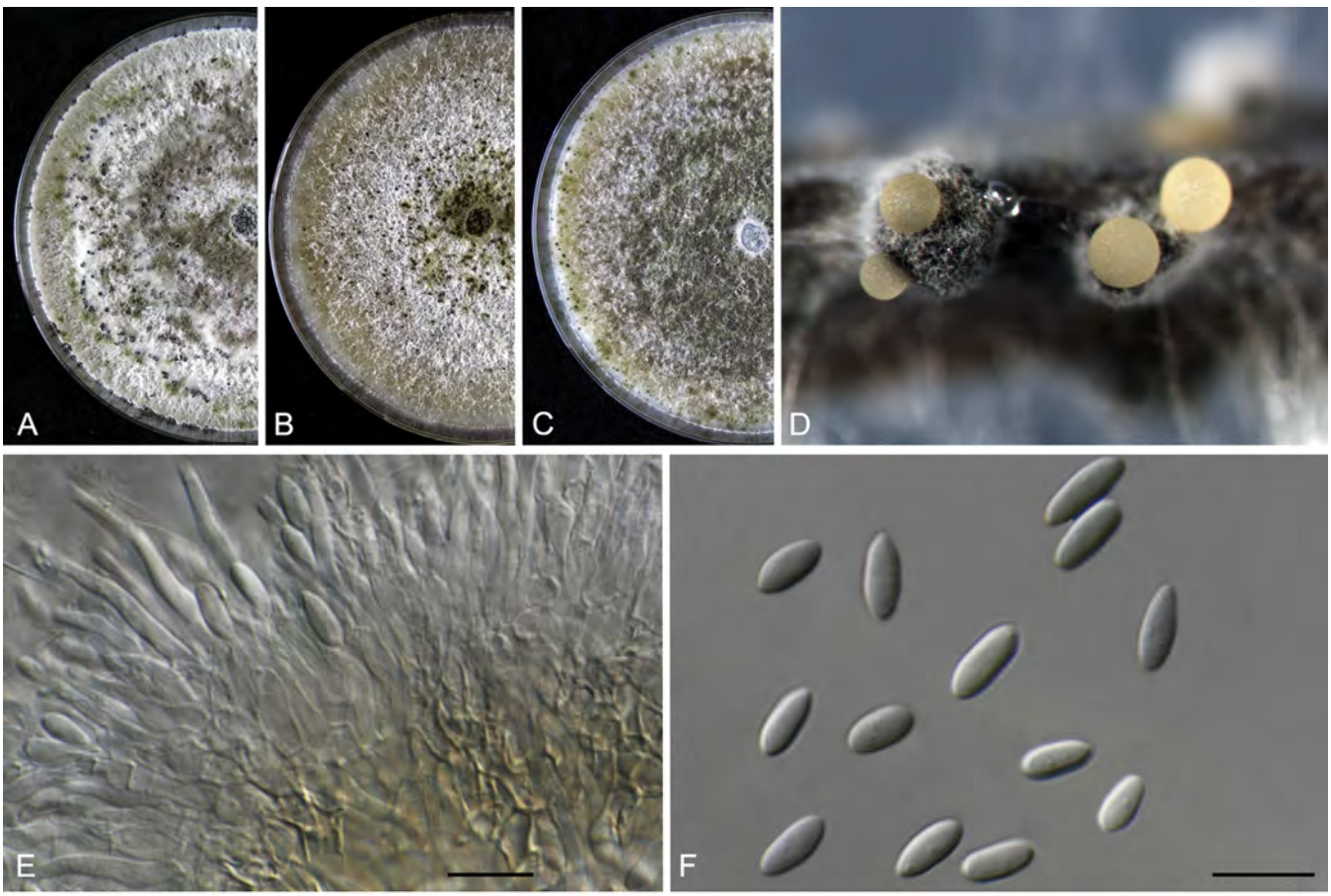

Fig. 11. *Diaporthe racemosae* (ex-type CBS 143770). **A–C.** Colonies on MEA, PDA and OA, respectively. **D.** Conidiomata sporulating on PNA. **E.** Conidiogenous cells and conidia. **F.** Alpha conidia. Scale bars = 10 µm.

Fig. 12. *Dichotomophthora lutea*. **A–E.** Colonies on PDA. **F–J.** Colonies on OA. **K.** Habit. **L–N.** Conidiophores and conidia. **O–Q.** Conidiogenous cells. **R, S.** Conidiogenous cells and conidia. **T, U.** Conidia and microconidia. **V–X.** Sclerotia. **Y.** Anastomosing conidia. (**A, F** = ex-type CBS 145.57; **B, G, K, O–T, V, Y** = CBS 584.71; **C, H** = CBS 585.71; **D, I, U** = CBS 132.81; **E, J, W, X** = CBS 518.78). Scale bars: V–X = 100 µm; L, P = 20 µm; others = 10 µm.

Table 5. DNA barcodes of accepted *Dichotomophthora* spp.

Species	Isolates[1]	GenBank accession numbers[2]			References
		ITS	*gapdh*	*rpb2*	
Dichotomophthora basellae	CPC 33016[T]	LT990654	LT990670	LT990640	Present study
Di. brunnea	CBS 149.94[T]	LT990653	LT990669	LT990639	Present study
Di. lutea	CBS 145.57[T]	LT990647	LT990663	LT990634	Present study
	CBS 584.71	LT990648	LT990664	LT990635	Present study
	CBS 585.71	LT990649	LT990665	LT990636	Present study
	CBS 518.78	LT990650	LT990666	–	Present study
	CBS 132.81	LT990651	LT990667	LT990637	Present study
Di. portulacae	CBS 174.35[PT]	LT990652	LT990668	LT990638	Present study

[1] CBS: Westerdijk Fungal Biodiversity Institute, Utrecht, the Netherlands; CPC: Culture collection of Pedro Crous, housed at the Westerdijk Fungal Biodiversity Institute. [T] and [PT] indicate ex-type and paratype strains, respectively.
[2] ITS: internal transcribed spacers and intervening 5.8S nrDNA; *gapdh*: partial glyceraldehyde-3-phosphate dehydrogenase gene; *rpb2*: partial RNA polymerase II second largest subunit gene.

accurate identification at the species level, a DNA sequence analysis is recommended, since *Dichotomophthora* species are morphologically variable in culture and on natural substrates.

References: Mehrlich & Fitzpatrick 1935, Routien 1957, Rao 1966, Ellis 1971, de Hoog & van Oorschot 1983 (taxonomy and morphology); Klisiewicz 1985, Baudoin 1986, Pfeiffer *et al.* 1989, Eken 2003, Soares & Nechet 2017 (pathogenicity).

Dichotomophthora basellae Hern.-Restr., Cheew. & Crous, **sp. nov.** MycoBank MB824604. Fig. 14.

Etymology: Name reflects the substrate from which this fungus was isolated, *Basella alba*.

Hyphae 3–7.5 µm wide, hyaline to brown, septate, smooth to verruculose. *Conidiophores* macronematous, mononematous, unbranched or irregularly branched, sometimes swollen and repeatedly dichotomously or trichotomously branched or lobed at apex, forming a stipe and head; *stipe* 970–1370 × 10–12(–14) µm, pale brown, smooth; *branches* usually short; *head* 23–65 µm wide, pale brown to brown. *Conidiogenous cells* polytretic, integrated and terminal, lobed, cicatrized, individual lobes 6–14 × 6–9.5 µm. *Conidia* 32–86 × 10–18 µm, solitary, dry, ellipsoidal to cylindrical rounded at ends, subhyaline to yellow brown, 2–5-distoseptate. *Microconidia* 11–30 × 9–13(–15) µm, obovoid to ellipsoidal, 0–2-distoseptate. *Sclerotia* 295–444 × 234–409 µm, resembling immature perithecia, semi- or immersed in agar, globose, subglobose, ellipsoidal, ovoid, dark brown or black. *Sexual morph* unknown.

Culture characteristics: Colonies at 25 °C under near-ultraviolet light (12 h light, 12 h dark), on PDA and OA reaching 45–50 mm after 1 wk, centre black, periphery luteous, velvety, flat, margin regular, effuse; reverse centre olivaceous, dark brown, periphery pale luteous. Diffusible pigment luteous.

Material examined: **Thailand**, Chiang Mai, Chiang Mai university experimental farm, on leaves of *Basella alba* (*Basellaceae*), 2010, R. Cheewangkoon (**holotype** CBS H-23383, culture ex-type CPC 33016).

Notes: *Dichotomophthora basellae* is represented by one strain isolated from leaf spots on *Basella rubra* in Thailand. This species is morphologically similar to *Di. lutea* in having multi-lobed conidiogenous cells producing pale brown conidia, and colonies that produce a luteous to orange diffusible pigment in culture. In our study, *Di. basellae* produces larger conidia than *Di. lutea* (32–86 × 10–18 µm *vs.* 14–65.5 × 7.5–13 µm). However, de Hoog & van Oorschot (1983) described larger conidia in *Di. lutea* (30–115 × 10–20 µm). Additional studies with more isolates are thus required to compare these morphological differences and substrate preferences of both species.

Dichotomophthora brunnea Hern.-Restr. & Crous, **sp. nov.** MycoBank MB824605. Fig. 15.

Etymology: From the Latin *brunnea* meaning brown, because of the brown colour of the conidia.

Hyphae 2.5–7 µm wide, hyaline to dark brown, septate, slightly constricted at septa, smooth. *Conidiophores* macronematous, mononematous, repeatedly dichotomously or irregularly branched, lobed at apex, forming a stipe and head; *stipe* 42–536 × 4.5–7.5 µm, pale brown to brown, smooth; *branches* usually short; *head* 10–28 µm wide, brown to pale brown. *Conidiogenous cells* mono- or polytretic, integrated, terminal, lobed, cicatrized, individual lobes 6.5–17 × 4–9 µm. *Conidia* 29–56.5 × 6–10 µm, solitary, dry, ellipsoidal to cylindrical rounded at ends, brown to dark brown, 2–6(–8)-distoseptate, straight or slightly curved. *Microconidia* 13–19.5 × 7–9.5 µm, obovoid to ellipsoidal, 0–1-distoseptate. *Sclerotia* not observed. *Sexual morph* unknown.

Culture characteristics: Colonies on PDA and OA at 25 °C under near-ultraviolet light (12 h light, 12 h dark), after 1 wk, reaching 90 mm, dark olivaceous, velvety, margin irregular, rhizoid (PDA) or entire (OA); reverse black. Diffusible pigment not produced.

Material examined: **Unknown country**, unknown substrate, date and collector (**holotype** CBS H-23382, culture ex-type dep. A. Arambarri LPS 325 = CBS 149.94).

Notes: *Dichotomophthora brunnea* was previously maintained as *Di. portulacae* in the CBS collection. However, the phylogenetic analysis suggests that the strain CBS 149.94 is a distinct species. Morphologically, the new species differs from *Di. basellae* and *Di. lutea* in having dark brown conidia and conidiogenous cells with 1–3 lobes (*vs.* yellowish or pale brown conidia and conidiogenous cells with usually more than three lobes). Neither pigment nor sclerotia were observed on the media tested.

Dichotomophthora lutea (Routien) de Hoog & Oorschot, Proc. Kon. Ned. Akad. Wetensch., Sect. C 86: 56. 1983. Fig. 12.
Basionym: Dactylaria lutea Routien, Mycologia 49: 191. 1957.
Synonym: *Dichotomophthora indica* Rao, Mycopath. Mycol. Appl. 28: 139. 1966. (nom. inval., Art. 35.1, Melbourne).

Hyphae 3–7.5 µm wide, hyaline to brown, septate, smooth to verruculose. *Conidiophores* macronematous, mononematous,

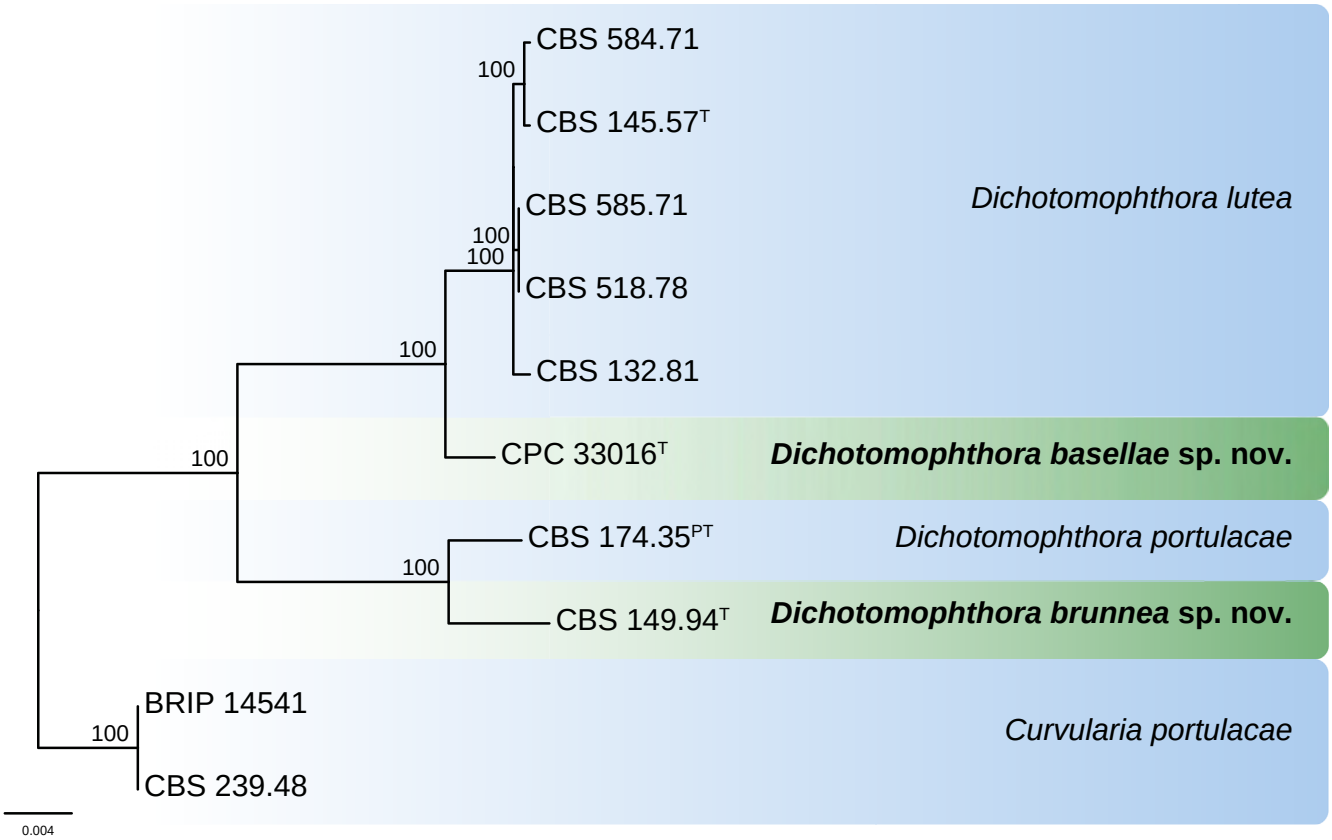

Fig. 13. RAxML phylogram obtained from the combined ITS (759 bp), LSU (880 bp), *gapdh* (594 bp) and *rpb2* (958 bp) sequence alignment of all the accepted species of *Dichotomophthora*. The tree was rooted to *Curvularia portulacae* CBS 239.48 and BRIP 14541. The novel species described in this study are shown in **bold**. RAxML bootstrap support (BS) values above 70 % are shown in the nodes. GenBank accession numbers are indicated in Table 5. ^{T} and ^{PT} indicate ex-type and ex-paratype strains, respectively. TreeBASE: S21899.

unbranched or irregularly branched, sometimes swollen and repeatedly dichotomously or trichotomously branched or lobed at apex, forming a stipe and head; *stipe* 7.5–10(–12) µm wide, hyaline to brown, smooth; *branches* usually short; *head* 16.5–62 µm wide, pale brown to brown. *Conidiogenous cells* polytretic, integrated and terminal, discrete, lobed, cicatrized, individual lobes 8–13 × 4–11 µm. *Conidia* 14–65.5 × 7.5–13 µm, solitary, dry, ellipsoidal to cylindrical rounded at ends, straight to slightly curved, subhyaline to yellow brown, 0–4-distoseptate, sometimes constricted at septa, sometimes anastomosing conidia observed. *Microconidia* 12–27 × 7–13 µm, obovoid, 0–2-distoseptate. *Sclerotia* 146–325 × 197–370 µm, present or absent, often formed in culture, resembling immature perithecia, semi- or immersed in agar, globose, subglobose, ellipsoidal or ovoid, dark brown or black. *Sexual morph* unknown.

Culture characteristics: Colonies on PDA and OA at 25 °C under near-ultraviolet light (12 h light, 12 h dark), reaching 20–80 mm after 1 wk, white, hazel, orange, or dark grey to olivaceous, cottony, velvety, somewhat fluffy, or flat, margin irregular, effuse; reverse centre hazel, dark brown, periphery hazel, orange to luteous. Diffusible pigment luteous to orange (produced in some strains).

Materials examined: **Argentina**, isolated from soil, unknown date, J.B. Routien, (culture ex-type of *Dactylaria lutea* CBS 145.57). **Cuba**, Santiago de las Vegas, on leaves of *Portulaca oleracea* (*Portulacaceae*), 9 Mar. 1980, G. Arnold, INIFAT A80/85 = CBS 132.81. **Italy**, isolated from seedbed of *Pinus radiata* (*Pinaceae*), unknown date, G. Magnani, CBS 584.71. **The Netherlands**, on leaves of *Portulaca oleracea* (*Portulacaceae*), unknown date and collector, CBS 585.71; The Hague, on leaves of *Portulaca oleracea* (*Portulacaceae*), Jul. 1978, G.H. Boerema, CBS 518.78.

Notes: In the phylogenetic tree (Fig. 13), *Di. lutea* is represented by five strains isolated from soil and leaves of *Po. oleraceae* from Argentina, Cuba, Italy and the Netherlands. This species shows morphological variation among strains, with different colour and aspect of the colonies, production or absence of diffusible pigment and sclerotia. The above description is based on CBS 584.71, CBS 585.71, CBS 518.78 and CBS 132.81. The conidia were smaller than those described by de Hoog & van Oorschot (1983) based on the ex-type strain CBS 145.57 (14–65.5 × 7.5–13 *vs*. 30–115 × 10–20 µm). Unfortunately, the ex-type strain was sterile under the culture media and conditions tested.

Dichotomophthora portulacae Mehrl. & Fitzp. ex M.B. Ellis, Dematiaceous Hyphomycetes (Kew): 388. 1971.
Synonyms: *Dichotomophthora portulacae* Mehrl. & Fitzp., Mycologia 27: 550. 1935. (nom. inval., Art. 39.1, Melbourne).
Dichotomophthora portulacae Mehrl. & Fitzp. ex P.N. Rao, Mycopath. Mycol. Appl. 28: 139. 1966. (nom. inval., Art. 38.5(a), Melbourne).

Hyphae 1.5–6 µm wide, subhyaline to pale brown, septate, slightly constricted at septa, smooth to verruculose. *Conidiophores* macronematous, mononematous, branched more or less dichotomously in apical region, forming a stipe and head; *stipe* 120–220 µm long, up to 14 µm wide at apex, reddish brown, smooth, verruculose near base, terminal branches up to 110 µm long, each ending in two slightly swollen, rounded or angular

Fig. 14. *Dichotomophthora basella* (ex-type CPC 33016). **A–C.** Disease symptoms caused by *Di. basella* in leaves of *Basella rubra*. **D.** Colony on PDA. **E.** Colony on OA. **F.** Colony overview with sclerotia and conidiophores. **G–I.** Conidiophores and conidia. **J, K.** Conidiogenous cells. **L.** Conidia. **M.** Microconidia. **N, O.** Sclerotia. Scale bars: N, O = 100 µm; H = 50 µm; others = 10 µm.

lobes. *Conidiogenous cells* mono- or polytretic, integrated and terminal, cicatrized. *Conidia* 45–75 × 20–30 µm, solitary, dry, ellipsoidal to cylindrical rounded at ends, dark reddish-brown, smooth, 2–3-distoseptate. *Sclerotia* 120–170 µm diam, often formed in culture, resembling perithecia, subglobose to globose or ovoid, dark reddish-brown. *Sexual morph* unknown (adapted from de Hoog & van Oorschot 1983).

Culture characteristics: Colonies at 25 °C under near-ultraviolet light (12 h light, 12 h dark) after 1 wk, on PDA reaching 60 mm, centre white, periphery olivaceous, cottony, margin irregular, effuse, white; reverse centre black, periphery olive. On OA reaching 45 mm, pale greenish grey, cottony, margin effuse, buff; reverse greenish olivaceous. Diffusible pigment not produced.

Material examined: **USA**, Hawaii, on *Portulaca oleracea* (*Portulacaceae*), unknown date and collector, isol. F.P. Mehrlich (ex-paratype culture CBS 174.35).

Notes: In this study *Di. portulacae* was represented only by the ex-paratype strain, which together with *Di. brunnea* (CBS 149.94) formed a subclade in *Dichotomophthora*. Both species have dark brown or reddish brown conidia and conidiogenous cells with 1–3 lobes. Nevertheless, *Di. portulacae* has shorter conidia with fewer septa, (45–75 × 20–30 µm, 2–3-distoseptate *vs*. 29–56.5 × 6–10 µm, 2–6-distoseptate).

Authors: M. Hernández-Restrepo, R. Cheewangkoon & P.W. Crous

Gaeumannomyces Arx & D.L. Olivier, Trans. Brit. Mycol. Soc. 35: 32. 1952. Fig. 16.

Fig. 15. *Dichotomophthora brunnea* (ex-type CBS 149.49). **A.** Colony on PDA. **B.** Colony on OA. **C.** Colony overview with conidiophores. **D–J.** Conidiophores, conidiogenous cells and conidia. **K.** Microconidia. **L–Q.** Conidia. Scale bars: D–G = 50 µm; H = 20 µm; others = 10 µm.

Synonyms: *Rhaphidospora* Fr., Summa veg. Scand. 2: 401. 1849.
Rhaphidophora Ces. & De Not., Sfer. Ital.: 79. 1863.

Classification: *Sordariomycetes*, *Sordariomycetidae*, *Magnaporthales*, *Magnaporthaceae*.

Type species: *Gaeumannomyces graminis* (Sacc.) Arx & D.L. Olivier, basionym: *Rhaphidophora graminis* Sacc. Representative strain: CPC 26020 = CBS 141384.

DNA barcode (genus): LSU.

DNA barcodes (species): ITS, *tef1*, *rpb1*. Table 6. Fig. 17.

Ascomata perithecial, superficial, submerged, globose, subglobose to elliptical, with a central, ostiolate, cylindrical neck, dark brown to black; *ascomatal wall* comprised of pseudoparenchymatous cells, light or brown. *Hamathecium* comprised of septate, often constricted at septa, hyaline paraphyses, widest at base and gradually narrow at apex, exceeding asci, dissolving at maturity. *Asci* numerous, unitunicate, cylindrical to elongated clavate, short stalked, with apical refractile ring, 8-spored. *Ascospores* cylindrical, slightly curved to sinuate, widest in middle, ends rounded, vacuolated, septate, septa often indistinct, hyaline to pale brown, faintly tinted yellowish in mass. *Conidiophores* branched, verticillate, indeterminate, brown, often reduced to

conidiogenous cells, hyaline to brown. *Conidiogenous cells* phialidic, solitary or in dense clusters, lageniform, cylindrical, straight or slightly curved tapering to a short cylindrical to funnel-shaped or hardly visible collarette. *Conidia* dimorphic (A) according to Wong & Walker (1975) "germinating phialidic conidia": solitary, grouped in slimy heads, ovoid to cylindrical, straight or slightly curved, tapering to an often acute base, hyaline, and/or (B) according to Wong & Walker (1975) "non-germinating phialidic conidia": solitary, arranged in heads, hyaline, falcate to lunate, usually strongly curved in a semicircle with varying degrees of curvature. *Hyphopodia* when present hyaline becoming brown when mature, simple or lobed. *Sclerotia* present or absent (adapted from Hernández-Restrepo *et al.* 2016b).

Culture characteristics: Colonies on PDA mycelium mostly submerged, dark (grey olivaceous, greyish sepia, isabelline) aerial mycelium scarce, or sometimes cottony, white; margin effuse, irregular to rhizoid. On MEA elevated, cottony to funiculose, aerial mycelium white or pale i.e. pale greenish grey, smoke grey, submerged mycelium black, margin effuse to rhizoid. Cultures of *Gaeumannomyces* vary in colour, growth rate and amount of aerial mycelium, dark hyphal strands and black sclerotia.

Optimal media and cultivation conditions: MEA and PDA incubated at 15–30 °C depending of species. Other methods described for production of perithecia include PDA with wheat seedlings (Speakman 1982) and flooded cultures in MPA (Speakman 1984).

Distribution: Worldwide.

Hosts: Mainly pathogens on grasses (*Poaceae* on *Avena*, *Hordeum*, *Oryza* & *Leersia*, *Secale*, *Sorghum*, *Triticum*, x*Triticale*, *Zea*, turf grasses, buffalo grass and other grasses) and *Cyperaceae*, but some occur on non-grass hosts as saprobes or endophytes.

Disease symptoms: Take-all, crown black sheath rot, dieback, root decline, patches of white heads after flowering, stem- and root rot.

Notes: Gaeumannomyces comprises about 20 species (Hernández-Restrepo *et al.* 2016b) that are mainly pathogenic to grasses, but some species are also regarded as saprobic or endophytic. The generic type *Gaeumannomyces graminis* included four varieties based on ascospore size, hyphopodial morphology and host preferences i.e. *G. graminis* var. *graminis*, *G. graminis* var. *avenae, G. graminis* var. *tritici* and *G. graminis* var. *maydis* (Turner 1940, Dennis 1960, Walker 1972, Yao *et al.* 1992). After a wide range of isolates were subjected to DNA sequence analyses, it was demonstrated that these established varieties and cryptic species represent different, phylogenetically supported species (Ward & Bateman 1999, Ulrich *et al.* 2000, Freeman & Ward 2004, Hernández-Restrepo *et al.* 2016b). *Gaeumannomyces tritici* and *G. avenae*, the causal agents of take-all of wheat and oat respectively, are more aggressive pathogens than *G. graminis* and other species in the genus. Species of *Gaeumannomyces* are morphologically difficult to distinguish because of their simple morphology, overlapping morphological features and considerable intraspecific variation.

References: von Arx & Olivier 1952, Deacon 1973, 1974 (taxonomy); Walker 1972, 1975, 1980, 1981 (taxonomy, morphology, pathogenicity); Asher & Shipton 1981 (biology and control); Elliott 1991, Elliott *et al.* 1993 (pathogenicity); Bateman *et al.* 1992, Augustin *et al.* 1999, Ulrich *et al.* 2000, Rachdawong *et al.* 2002 (molecular data); Freeman & Ward 2004 (review); Hernández-Restrepo *et al.* 2016b (morphology and phylogeny).

Authors: M. Hernández-Restrepo & P.W. Crous

Harknessia Cooke, Grevillea 9: 85. 1881. Fig. 18.
Synonyms: *Caudosporella* Höhn., Sber. Akad. Wiss. Wien, Math.-naturw. Kl., Abt. 1 123: 135. 1914.
Mastigonetron Kleb., Mykol. Zentbl. 4: 17. 1914.
Cymbothyrium Petr., Sydowia 1: 148. 1947.

Classification: *Sordariomycetes*, *Sordariomycetidae*, *Diaporthales*, *Harknessiaceae.*

Type species: *Harknessia eucalypti* Cooke. Representative strain: CBS 342.97.

DNA barcode (genus): LSU.

DNA barcodes (species): ITS, *cal*, *tub2.* Table 7. Fig. 19.

Ascomata perithecial, single or aggregated, immersed, brown; *necks* emergent to depressed; *ascomatal wall* of 3–5 layers of brown cells of *textura angularis*. *Paraphyses* hyaline, septate, dispersed between asci. *Asci* 8-spored, unitunicate, cylindrical to clavate, short pedicellate, with J- apical ring. *Ascospores* uni- to biseriate, ellipsoid to fusoid, hyaline, aseptate, thick-walled, guttulate, smooth-walled. *Conidiomata* erumpent, scattered, pycnidial, unilocular, globose to subglobose, brown; *conidiomatal wall* comprising 3–4 layers of brown-walled cells of *textura angularis*. *Macroconidiophores* lining cavity or limited to a basal layer in some species; usually reduced to conidiogenous cells, rarely septate and branched; commonly invested in mucus. *Macroconidiogenesis cells* ampulliform, subcylindrical or cylindrical, hyaline, proliferating percurrently. *Macroconidia* consisting of a body with a basal appendage, delimited by a septum; *conidium body* unicellular, ellipsoid to fusoid, subcylindrical, globose, broadly ventricose, broadly ellipsoid or broadly fusoid, thick-walled, smooth, brown, with or without pale and dark coloured longitudinal bands, occasionally longitudinally striate, guttulate; *basal appendages* hyaline, tubular, smooth, thin-walled, often collapsing. *Microconidiophores* absent or present, in same conidioma, reduced to microconidiogenous cells. *Microconidiogenous cells* ampulliform or subcylindrical to lageniform, hyaline, smooth, with apical periclinal thickening. *Microconidia* hyaline, smooth, aseptate, oval to ellipsoid.

Culture characteristics: Colonies spreading, fluffy, with moderate to abundant aerial mycelium, covering plate in 1 mo. On MEA surface dirty white to cream or pale luteous; reverse cream; sometimes sporulating with black conidiomata, oozing black masses. These culture characteristics also apply to the new taxa described below.

Optimal media and cultivation conditions: MEA, PDA and OA under continuous near-ultraviolet light at 25 °C to promote sporulation.

Distribution: Worldwide.

Hosts: On diverse gymnosperm and dicotyledonous hosts, especially on *Eucalyptus* (*Myrtaceae*), which is host to 27 of the currently accepted 38 species.

Disease symptoms: Associated with leaf spots, leaf tip dieback or leaf scorch and stem cankers, but pathogenicity has not been established definitively (Crous *et al.* 2012c).

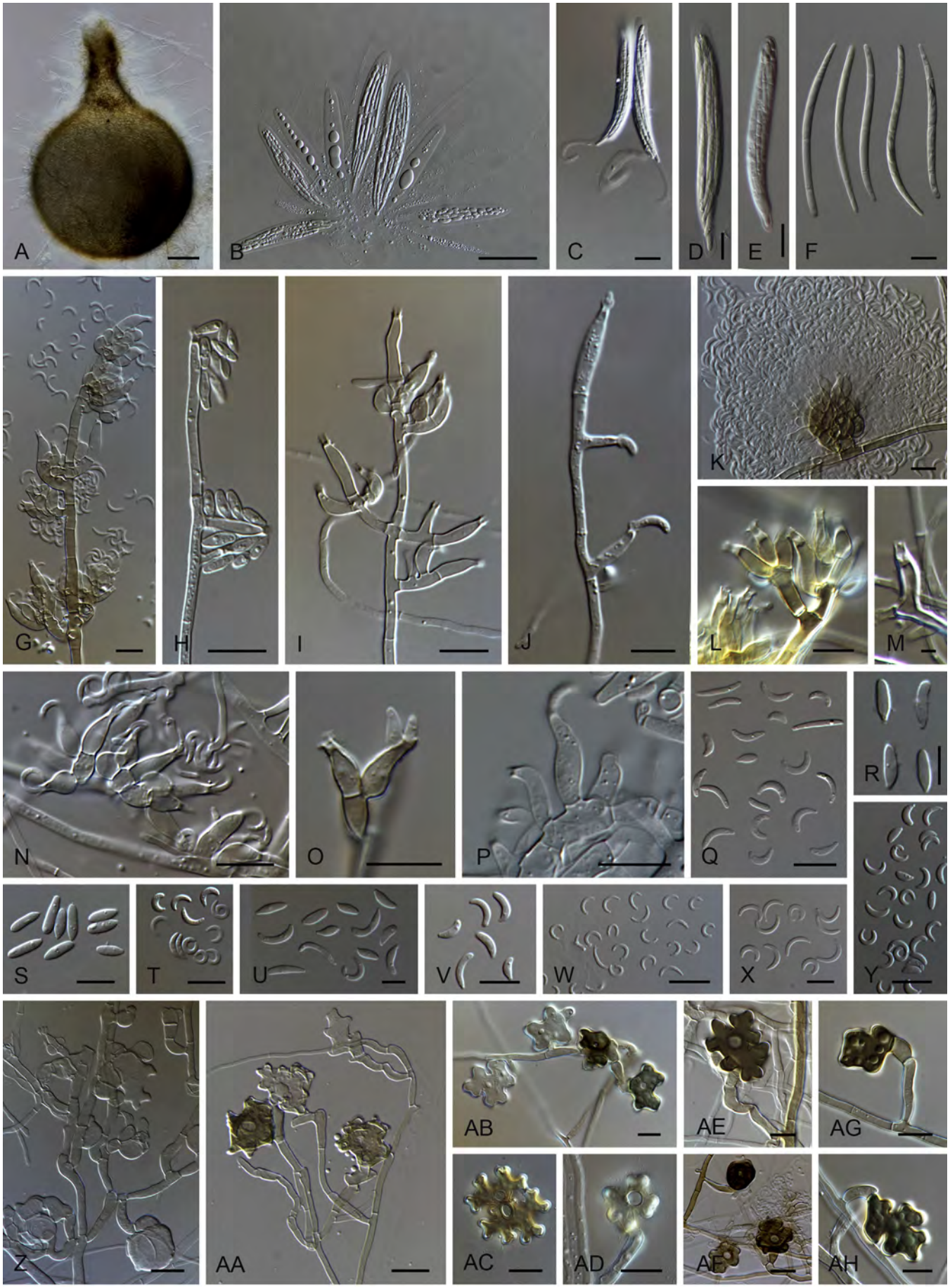

Table 6. DNA barcodes of accepted *Gaeumannomyces* spp.

Species	Isolates[1]	GenBank accession numbers[2]			References
		ITS	*rpb1*	*tef1*	
Gaeumannomyces amomi	CBS 109354^{T}	AY265318	–	KX306679	Bussaban *et al.* (2005), Hernández-Restrepo *et al.* (2016b)
G. arxii	CBS 903.73^{T}	KM484837	KM485053	KX306681	Klaubauf *et al.* (2014), Hernández-Restrepo *et al.* (2016b)
G. australiensis	CBS 141387^{T}	KX306480	KX306619	KX306683	Hernández-Restrepo *et al.* (2016b)
G. avenae	CPC 26258^{ET}	KX306486	KX306622	KX306688	Hernández-Restrepo *et al.* (2016b)
G. californicus	CBS 141377^{T}	KX306490	KX306625	KX306691	Hernández-Restrepo *et al.* (2016b)
G. ellisiorum	CBS 387.81^{T}	KM484835	KM485051	KX306692	Klaubauf *et al.* (2014), Hernández-Restrepo *et al.* (2016b)
G. floridanus	CBS 141378^{T}	KX306491	KX306626	KX306693	Hernández-Restrepo *et al.* (2016b)
G. fusiformis	CBS 141379^{T}	KX306492	KX306627	KX306694	Hernández-Restrepo *et al.* (2016b)
G. glycinicola	CPC 26057^{T}	KX306493	KX306628	KX306695	Hernández-Restrepo *et al.* (2016b)
G. graminicola	CBS 352.93^{T}	KM484834	KM485050	KX306697	Klaubauf *et al.* (2014), Hernández-Restrepo *et al.* (2016b)
G. graminis	CPC 26020	KX306498	KX306633	KX306701	Hernández-Restrepo *et al.* (2016b)
G. hyphopodioides	CBS 350.77^{T}	KX306506	KM009192	KM009204	Hernández-Restrepo *et al.* (2016b), Luo *et al.* (2014)
G. oryzicola	CBS 141390^{T}	KX306516	KX306646	KX306717	Hernández-Restrepo *et al.* (2016b)
G. oryzinus	CBS 235.32	JX134669	KM485049	JX134695	Klaubauf *et al.* (2014), Luo & Zhang (2013)
G. radicicola	CBS 296.53^{T}	KM484845	KM485061	KM009206	Klaubauf *et al.* (2014)
G. setariicola	CBS 141394^{T}	KX306524	KX306654	KX306725	Hernández-Restrepo *et al.* (2016b)
G. tritici	CBS 905.73	KM484841	KM485057	KX306731	Klaubauf *et al.* (2014), Hernández-Restrepo *et al.* (2016b)
G. walkeri	CBS 141400^{T}	KX306543	KX306670	KX306746	Hernández-Restrepo *et al.* (2016b)
G. wongoonoo	BRIP 60376^{A}	KP162137	–	–	Wong (2002)

[1] BRIP: Queensland Plant Pathology Herbarium, Brisbane, Australia; CBS: Westerdijk Fungal Biodiversity Institute, Utrecht, the Netherlands; CPC: Culture collection of Pedro Crous, housed at the Westerdijk Fungal Biodiversity Institute. $^{T, ET}$ and ^{A} indicate ex-type, ex-epitype and authentic strains, respectively.
[2] ITS: internal transcribed spacers and intervening 5.8S nrDNA; *rpb1*: partial RNA polymerase II largest subunit gene; *tef1*: partial elongation factor gene.

Notes: *Harknessia* is characterised by having stromatic to pycnidial conidiomata, and dark brown conidia with tube-shaped basal appendages, longitudinal striations, and rhexolytic secession (Crous *et al.* 2012c). Sexual morphs were initially described in *Cryptosporella* (Nag Raj & DiCosmo 1981), which was rejected in favour of the older genus *Wuestneia* (Reid & Booth 1989). However, the type species of *Wuestneia*, *Wu. aurea* (= *Wuestneia xanthostroma*), was located in the *Cryphonectriaceae* and was associated with a coelomycete asexual morph having hyaline conidia. *Wuestneia* is therefore not considered as synonym of *Harknessia*, and only species placed in the *Harknessiaceae* and linked to *Harknessia* morphs were thus transferred to *Harknessia* (Crous *et al.* 2012c).

The family *Harknessiaceae* was introduced based on LSU sequences of taxa belonging to *Diaporthales* in order to accommodate *Harknessia* (Crous *et al.* 2012c).

References: Lee *et al.* 2004 (morphology and phylogeny); Crous *et al.* 2012c (morphology and phylogeny).

Harknessia bourbonica Crous & M.J. Wingf., **sp. nov.** MycoBank MB824016. Fig. 20.

Etymology: Name refers to Île Bourbon, the original name of La Réunion Island.

Caulicolous and *foliicolous*, isolated from leaves and twigs incubated in moist chambers (presumed endophyte). *Conidiomata* up to 300 µm diam, pycnidial, separate to gregarious, subepidermal, becoming erumpent, stromatic, amphigenous, depressed globose; with irregular opening and border of yellowish, furfuraceous cells; *conidiomatal wall* of *textura angularis*. *Conidiophores* reduced to conidiogenous cells lining conidiomatal cavity. *Conidiogenous cells* 8–10 × 4–8 µm, ampulliform to subcylindrical, hyaline, smooth, invested in mucilage, percurrently proliferating once or twice near apex. *Conidia* (12–)13–14(–15) × (8–)9–10 µm *in vitro*, broadly ventricose to ellipsoid, apex subobtusely rounded, aseptate, non-apiculate, yellow-brown, thick-walled, striations in restricted areas, multi-guttulate. *Basal appendage* (5–)8–12 × 2–2.5 µm

Fig. 16. *Gaeumannomyces* spp. **A–F.** Sexual morph. **A.** Ascoma of *Gaeumannomyces oryzicola* (ex-type CBS 141390). **B.** Asci and paraphyses of *Gaeumannomyces oryzinus* (CPC 26065). **C–E.** Asci. **C, D.** *Gaeumannomyces oryzinus* (CPC 26043). **E.** *Gaeumannomyces oryzicola* (ex-type CBS 141390). **F.** Ascospores of *Gaeumannomyces oryzinus* (CBS 235.32). **G–AH.** Asexual morph. **G–P.** Conidiophores and conidiogenous cells. **G.** *Gaeumannomyces californicus* (ex-type CBS 141377). **H.** *Gaeumannomyces fusiformis* (ex-type CBS 141379). **I.** *Gaeumannomyces arxii* (CBS 903.73). **J, N.** *Gaeumannomyces walkeri* (ex-type CBS 141400). **K.** *Gaeumannomyces graminis* (CBS 141386). **L.** *Gaeumannomyces graminicola* (CBS 352.93). **M.** *Gaeumannomyces oryzicola* (ex-type CBS 141390). **O.** *Gaeumannomyces oryzinus* (CPC 26032). **P.** *Gaeumannomyces radicicola* (ex-type CBS 296.53). **Q–Y.** Conidia. **Q.** *Gaeumannomyces radicicola* (ex-type CBS 296.53). **R.** *Gaeumannomyces oryzicola* (ex-type CBS 141390). **S, T.** *Gaeumannomyces walkeri* (ex-type CBS 141400). **U.** *Gaeumannomyces oryzinus* (CPC 26067). **V.** *Gaeumannomyces ellisiorum* (ex-type CBS 387.81). **W.** *Gaeumannomyces floridanus* (ex-type CBS 141378). **X.** *Gaeumannomyces graminicola* (CPC 26036). **Y.** *Gaeumannomyces arxii* (CBS 903.73). **Z–AH.** Hyphopodia. **Z.** *Gaeumannomyces ellisiorum* (ex-type CBS 387.81). **AA, AC.** *Gaeumannomyces glycinicola* (CBS 141380). **AB.** *Gaeumannomyces floridanus* (ex-type CBS 141378). **AD.** *Gaeumannomyces graminicola* (CPC 26025). **AE.** *Gaeumannomyces californicus* (ex-type CBS 141377). **AG.** *Gaeumannomyces oryzinus* (CPC 26032). **AF.** *Gaeumannomyces hyphopodioides* (CPC 26267). **AH.** *Gaeumannomyces walkeri* (ex-type CBS 141400). Scale bars: A, B = 50 µm; C–F = 20 µm; others = 10 µm. Pictures taken from Hernández-Restrepo *et al.* (2016b).

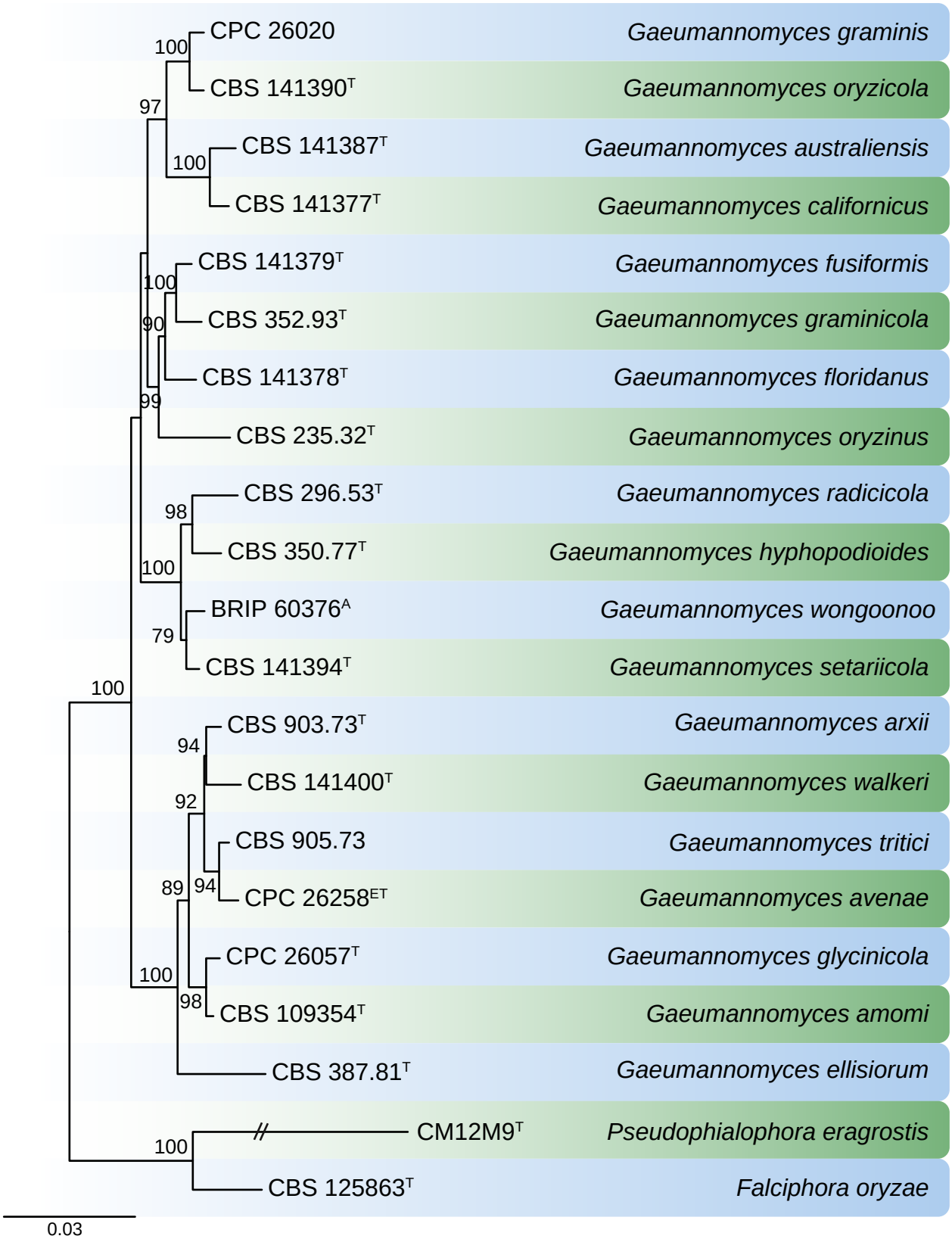

Fig. 17. RAxML phylogram obtained from the combined ITS (715 bp), LSU (881 bp), *rpb1* (617 bp) and *tef1* (427 bp) sequence alignment of all the accepted species of *Gaeumannomyces*. The tree was rooted to *Pseudophialophora eragrostis* CM12m9 and *Falciphora oryzae* CBS 125863. RAxML bootstrap support (BS) values above 70 % are shown in the nodes. GenBank accession numbers are indicated in Table 6. ^{T}, ^{ET} and ^{A} indicate ex-type, ex-epitype and authentic strains, respectively. TreeBASE: S21899.

in vitro, hyaline, tubular, smooth, thin-walled, devoid of cytoplasm. *Microconidia* not seen.

Material examined: **France**, La Réunion, 21°15'5.4"S 55°36'3.3"E, on leaf litter of *Eucalyptus robusta* (*Myrtaceae*), 8 Mar. 2015, P.W. Crous & M.J. Wingfield (**holotype** CBS H-23387, culture ex-type CBS 143913 = CPC 26533).

Notes: *Harknessia bourbonica* is related to *Ha. ravenstreetina*, which was also isolated from *Eucalyptus* leaves. The two species are distinguished in that *Ha. ravenstreetina* has longer conidia (14–20 µm) that lack striations and has shorter basal appendages (1.5–5 × 2–2.5 µm).

Harknessia corymbiae Crous & A.J. Carnegie, **sp. nov.** MycoBank MB824017. Fig. 21.

Etymology: Name refers to the host genus, *Corymbia*.

Caulicolous and *foliicolous*, isolated from leaves and twigs incubated in moist chambers (presumed endophyte). *Conidiomata* up to 250 µm diam, pycnidial, separate to gregarious, subepidermal, becoming erumpent, stromatic, amphigenous, depressed globose; with irregular opening and border of yellowish, furfuraceous cells; *conidiomatal wall* of *textura angularis*. *Conidiophores* reduced to conidiogenous cells lining conidiomatal cavity. *Conidiogenous cells* 6–10 × 4–5 µm, ampulliform to subcylindrical, hyaline, smooth, invested in mucilage, percurrently proliferating once or twice near apex. *Conidia* (23–)25–28(–30) × (8–)9 µm *in vitro*, subcylindrical, apex apiculate, aseptate, yellow-brown, thick-walled, lacking striations, granular; in lactic acid some conidia appear to have a central line of paler pigment. *Basal appendage* (50–)65–80(–100) × 3–4 µm *in vitro*, hyaline, tubular, smooth, thin-walled, devoid of cytoplasm. *Microconidia* 3–4 × 1.5–2 µm, hyaline, smooth, guttulate, aseptate, subcylindrical with obtuse ends.

Material examined: **Australia**, New South Wales, Bom Bom State Forest, on leaf litter of *Corymbia maculata* (*Myrtaceae*), 13 Mar. 2017, A.J. Carnegie (**holotype** CBS H-23388, culture ex-type CPC 33289).

Notes: *Harknessia corymbiae* was located in a distinct clade distant from the other species of the genus. The only accepted species presently known from *Corymbia* is *Ha. rhabdosphaera*. Both species were collected from Australia, but *Ha. rhabdosphaera* has smaller, striated conidia [(13–)15–17 × (13–)14–15 µm] with short basal appendages (up to 5 µm long).

Harknessia cupressi Crous & R.K. Schumach., **sp. nov.** MycoBank MB824018. Fig. 22.

Etymology: Name refers to the host genus, *Cupressus*.

Caulicolous and *foliicolous*, isolated from needles incubated in moist chambers (presumed endophyte). *Conidiomata* up to 250 µm diam, pycnidial, separate to gregarious, subepidermal, becoming erumpent, stromatic, amphigenous, depressed globose; with irregular opening and border of yellowish, furfuraceous cells; *conidiomatal wall* of *textura angularis*. *Conidiophores* reduced to conidiogenous cells lining conidiomatal cavity. *Conidiogenous cells* 5–10 × 3–5 µm, ampulliform to subcylindrical, hyaline, smooth, invested in mucilage, percurrently proliferating once or twice near apex. *Conidia* (20–)21–23(–25) × (8–)9–11(–13) µm *in vitro*, broadly ventricose, apex apiculate, aseptate, yellow-brown, thick-walled, striations in restricted areas, multi-guttulate. *Basal appendage* 2–5(–12) × 2–2.5 µm *in vitro*, hyaline, tubular, smooth, thin-walled, devoid of cytoplasm. *Microconidia* 4–7 × 3–4 µm, hyaline, smooth, aseptate, broadly ellipsoid.

Materials examined: **Spain**, Zaragoza, Carretera El Frago, on needles of *Cupressus sempervirens* (*Cupressaceae*), 7 Jan. 2016, coll. R. Blasco, det. R.K. Schumacher (**holotype** CBS H-23389, culture ex-type CBS 143914 = CPC 30192); *ibid*., CPC 30174.

Notes: *Harknessia cupressi* was located in an independent clade distant from the other species of the genus. *Harknessia cupressi* is the only species known from *Cupressus sempervirens*.

Harknessia pilularis Crous & A.J. Carnegie, **sp. nov.** MycoBank MB824020. Fig. 23.

Etymology: Name refers to *Eucalyptus pilularis*, the host species from which this fungus was isolated.

Caulicolous and *foliicolous*, isolated from leaves and twigs incubated in moist chambers (presumed endophyte). *Conidiomata* up to 250 µm diam, pycnidial, separate to gregarious, subepidermal, becoming erumpent, stromatic, amphigenous, depressed globose; with irregular opening and border of yellowish, furfuraceous cells; *conidiomatal wall* of *textura angularis*. *Conidiophores* reduced to conidiogenous cells lining conidiomatal cavity. *Conidiogenous cells* 4–7 × 2–5 µm, ampulliform to subcylindrical, hyaline, smooth, invested in mucilage, percurrently proliferating once or twice near apex. *Conidia* (13–)14–16(–20) × (8–)11–12(–13) µm *in vitro*, globose to rarely broadly ellipsoid, apex obtusely rounded, aseptate, non-apiculate, yellow-brown, thick-walled, striations covering entire conidial body, multi-guttulate. *Basal appendage* (2–)3–5 × 2–2.5 µm *in vitro*, hyaline, tubular, smooth, thin-walled, devoid of cytoplasm. *Microconidia* not seen.

Materials examined: **Australia**, New South Wales, Pine Creek State Forest, 30.405423S 152.932698E, on leaves of *Eucalyptus pilularis* (*Myrtaceae*), 23 Jan. 2017, A.J. Carnegie (**holotype** CBS H-23391, culture ex-type CPC 33218); *ibid*., CPC 33356.

Notes: *Harknessia pilularis* is related to *Ha. rhabdosphaera*, but *Ha. rhabdosphaera* produces longer conidiogenous cells (7–15 × 4–6 µm), and wider conidia (13–15 µm).

Authors: Y. Marin-Felix, A.J. Carnegie, M.J. Wingfield, R.K. Schumacher & P.W. Crous

Huntiella Z.W. de Beer, *et al.*, Stud. Mycol. 79: 211. 2014. Fig. 24.

Classification: Sordariomycetes, *Hypocreomycetidae*, *Microascales*, *Ceratocystidaceae*.

Type species: Huntiella moniliformis (Hedgc.) Z.W. de Beer, *et al.*, basionym: *Ceratostomella moniliformis* Hedgc. Holotype: BPI 595959.

DNA barcodes (genus): LSU, 60S, *mcm7*.

DNA barcodes (species): ITS, *mcm7*, *tef1*, *tub2*. Table 8. Fig. 25.

Ascomata perithecial, ellipsoidal, subglobose, globose to obpyriform or ovoid; *bases* ornamented with dark brown to black conical spines or pale brown, unbranched hyphae; *necks* long, straight or slightly curved, tapering towards apex, dark brown to black at base, becoming paler towards apex, ostiolate, with a disciform base; *hyphae* on neck hyaline, not divergent, straight or convergent. *Asci* evanescent. *Ascospores* hyaline, aseptate, in face view subglobose, in side view ellipsoidal giving an impression of a hat, with hood-like gelatinous sheath. *Conidiophores* macronematous, rarely branched, septate, occasionally reduced to conidiogenous cells. *Conidiogenous cells* hyaline, enteroblastic, mostly of two types, lageniform, producing rectangular-shaped conidia and cylindrical, producing barrel-shaped conidia. *Conidia* aseptate, majority of species have two distinct shapes: bacilliform, hyaline, or barrel-shaped or oblong to ellipsoidal, hyaline or subhyaline. *Chlamydospores* absent.

Culture characteristics: On 2 % MEA aerial mycelium abundant, colonies white, yellow green to brown, smoke grey, dark olive to black. Some species produce aromas: *Hu. bhutanensis* produces an unpleasant rotten odour, *Hu. decipiens*, *Hu. moniliformis* and *Hu. salinaria* a pleasant banana-oil aroma, *Hu. moniliformopsis* little to no distinct odour, and *Hu. omanensis* fruity aroma that turns to a fermented odour with age.

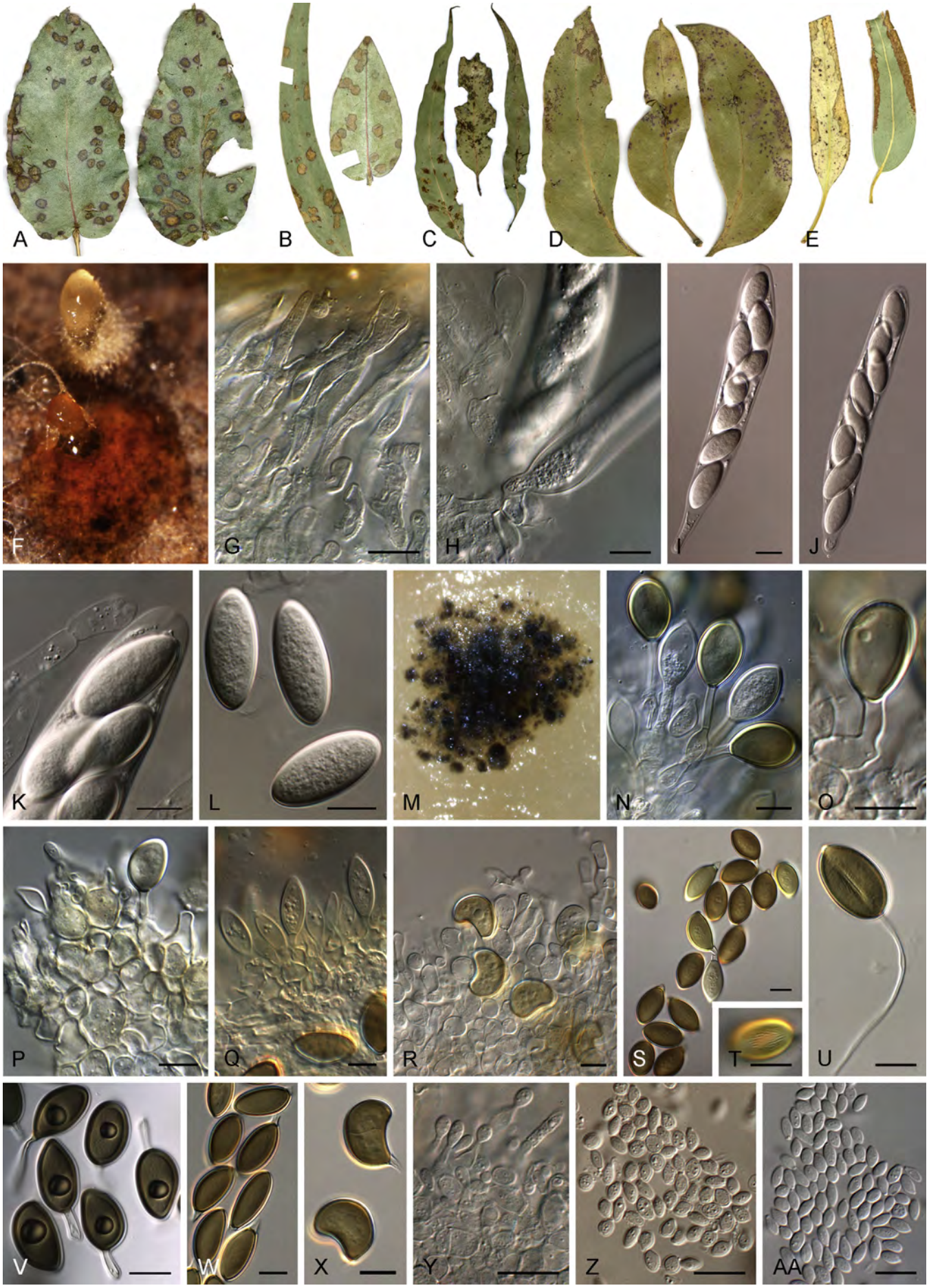

Table 7. DNA barcodes of accepted *Harknessia* spp.

Species	Isolates[1]	GenBank accession number[2]			References
		ITS	*cal*	*tub2*	
Harknessia arctostaphyli	CBS 137228^{ET}	KJ152781	–	KJ179923	Moreno-Rico *et al.* (2014)
Ha. australiensis	CBS 132119^{T}	JQ706085	JQ706171	JQ706130	Crous *et al.* (2012c)
Ha. banksiae	CBS 142539^{T}	KY979782	KY979872	KY979938	Crous *et al.* (2017a)
Ha. banksiae-repens	CBS 142541^{T}	KY979785	KY979875	KY979940	Crous *et al.* (2017a)
Ha. banksiigena	CBS 142540^{T}	KY979784	KY979874	–	Crous *et al.* (2017a)
Ha. bourbonica	CBS 143913^{T}	MG934433	MG934512	–	Present study
Ha. capensis	CBS 111829^{T}	AY720719	AY720782	AY720751	Lee *et al.* (2004)
Ha. communis	CBS 142538^{T}	KY979778	KY979868	–	Crous *et al.* (2017a)
Ha. corymbiae	CPC 33289^{T}	MG934434	MG934513	MG934507	Present study
Ha. cupressi	CBS 143914^{T}	MG934435	MG934514	–	Present study
	CPC 30174	MG934436	MG934515	–	Present study
Ha. ellipsoidea	CBS 132121^{T}	JQ706087	JQ706173	JQ706132	Crous *et al.* (2012c)
Ha. eucalypti	CBS 342.97	AY720745	AY720808	AY720777	Lee *et al.* (2004)
Ha. eucalyptorum	CBS 111115^{T}	AY720747	AY720810	AY720779	Lee *et al.* (2004)
Ha. fusiformis	CBS 110785^{T}	AY720721	AY720784	AY720753	Lee *et al.* (2004)
Ha. gibbosa	CBS 120033^{T}	EF110615	JQ706182	JQ706142	Crous *et al.* (2007), (2012c)
Ha. globispora	CBS 111578^{T}	AY720722	AY720785	AY720754	Lee *et al.* (2004)
Ha. hawaiiensis	CBS 114811	AY720723	AY720786	AY720755	Lee *et al.* (2004)
Ha. ipereniae	CBS 120030^{T}	EF110614	JQ706192	JQ706151	Crous *et al.* (2007), (2012c)
Ha. karwarrae	CBS 115648	AY720748	AY720811	AY720780	Lee *et al.* (2004)
Ha. kleinzeeina	CPC 16277^{T}	JQ706108	JQ706193	JQ706152	Crous *et al.* (2012c)
Ha. leucospermi	CBS 775.97^{T}	AY720727	AY720790	AY720759	Lee *et al.* (2004)
Ha. malayensis	CBS 142544^{T}	KY979789	KY979879	KY979941	Crous *et al.* (2017a)
Ha. molokaiensis	CBS 114877^{T}	AY720749	AY720812	AY579335	Lee *et al.* (2004), Mostert *et al.* (2005)
Ha. pellitae	CBS 142543^{T}	KY979788	KY979878	–	Crous *et al.* (2017a)
Ha. pilularis	CPC 33218^{T}	MG934438	MG934517	MG934508	Present study
	CPC 33356	MG934439	MG934518	MG934509	Present study
Ha. platyphyllae	CBS 142542^{T}	KY979787	KY979877	–	Crous *et al.* (2017a)
Ha. proteae	CBS 136426^{T}	KF777162	–	–	Crous *et al.* (2013)
Ha. protearum	CBS 112618^{T}	AY720732	AY720795	AY720764	Lee *et al.* (2004)
Ha. pseudohawaiiensis	CBS 132124^{T}	JQ706111	JQ706196	JQ706155	Crous *et al.* (2012c)
Ha. ravenstreetina	CBS 132125^{T}	JQ706112	JQ706197	JQ706156	Crous *et al.* (2012c)
Ha. renispora	CBS 153.71^{IsoT}	AY720737	AY720800	AY720769	Lee *et al.* (2004)
Ha. rhabdosphaera	CBS 122373	JQ706118	JQ706201	JQ706161	Crous *et al.* (2012c)
Ha. spermatoidea	CBS 132127^{ET}	JQ706120	JQ706203	JQ706163	Crous *et al.* (2012c)
Ha. syzygii	CBS 111124^{T}	AY720738	AY720801	AY720770	Lee *et al.* (2004)
Ha. uromycoides	CBS 110729	AY720739	AY720802	AY720771	Lee *et al.* (2004)
Ha. viterboensis	CBS 115647^{T}	AY720740	AY720803	AY720772	Lee *et al.* (2004)
Ha. weresubiae	CBS 132128^{ET}	JQ706122	JQ706205	JQ706165	Crous *et al.* (2012c)

[1] CBS: Westerdijk Fungal Biodiversity Institute, Utrecht, The Netherlands; CPC: Culture collection of Pedro Crous, housed at the Westerdijk Fungal Biodiversity Institute. ^{T}, ^{ET} and ^{IsoT} indicate ex-type, ex-epitype and ex-isotype strains, respectively.

[2] ITS: internal transcribed spacers and intervening 5.8S nrDNA; *cal*: partial calmodulin gene; *tub2*: partial β-tubulin gene.

Fig. 18. *Harknessia* spp. **A–E.** Disease symptoms on *Eucalyptus*. **A.** *Harknessia fusiformis* (CPC 13649). **B.** *Harknessia hawaiiensis* (CPC 15003). **C.** *Harknessia ravenstreetina* (ex-type CBS 132125). **D.** *Harknessia rhabdosphaera* (CPC 13593). **E.** *Harknessia globispora* (CPC 14924). **F–L.** Sexual morph of *Harknessia eucalyptorum* (CPC 12697). **F.** Ascoma with short neck, oozing ascospores. **G, H.** Paraphyses and asci. **I, J.** Asci. **K.** Paraphyses and ascal tip. **L.** Ascospores. **M–AA.** Asexual morphs. **M.** Sporulating colony on OA of *Harknessia ellipsoidea* (ex-type CBS 132121). **N–R.** Conidiogenous cells giving rise to conidia. **N, O.** *Harknessia gibbosa* (ex-type CBS 120033). **P.** *Harknessia pseudohawaiiensis* (CPC 17380). **Q.** *Harknessia ravenstreetina* (ex-type CBS 132125). **R.** *Harknessia renispora* (CPC 17163). **S–X.** Conidia. **S, T.** *Harknessia australiensis* (ex-type CBS 132119). **U.** *Harknessia kleinzeeina* (ex-type CPC 16277). **V.** *Harknessia eucalyptorum* (CPC 12697). **W.** *Harknessia ravenstreetina* (ex-type CBS 132125). **X.** *Harknessia renispora* (CPC 17163). **Y.** Microconidiogenous cells giving rise to microconidia of *Harknessia renispora* (CPC 17163). **Z, AA.** Microconidia. **Z.** *Harknessia renispora* (CPC 17163). **AA.** *Harknessia pseudohawaiiensis* (CPC 17380). Scale bars = 10 µm. Pictures taken from Crous *et al.* (2012c).

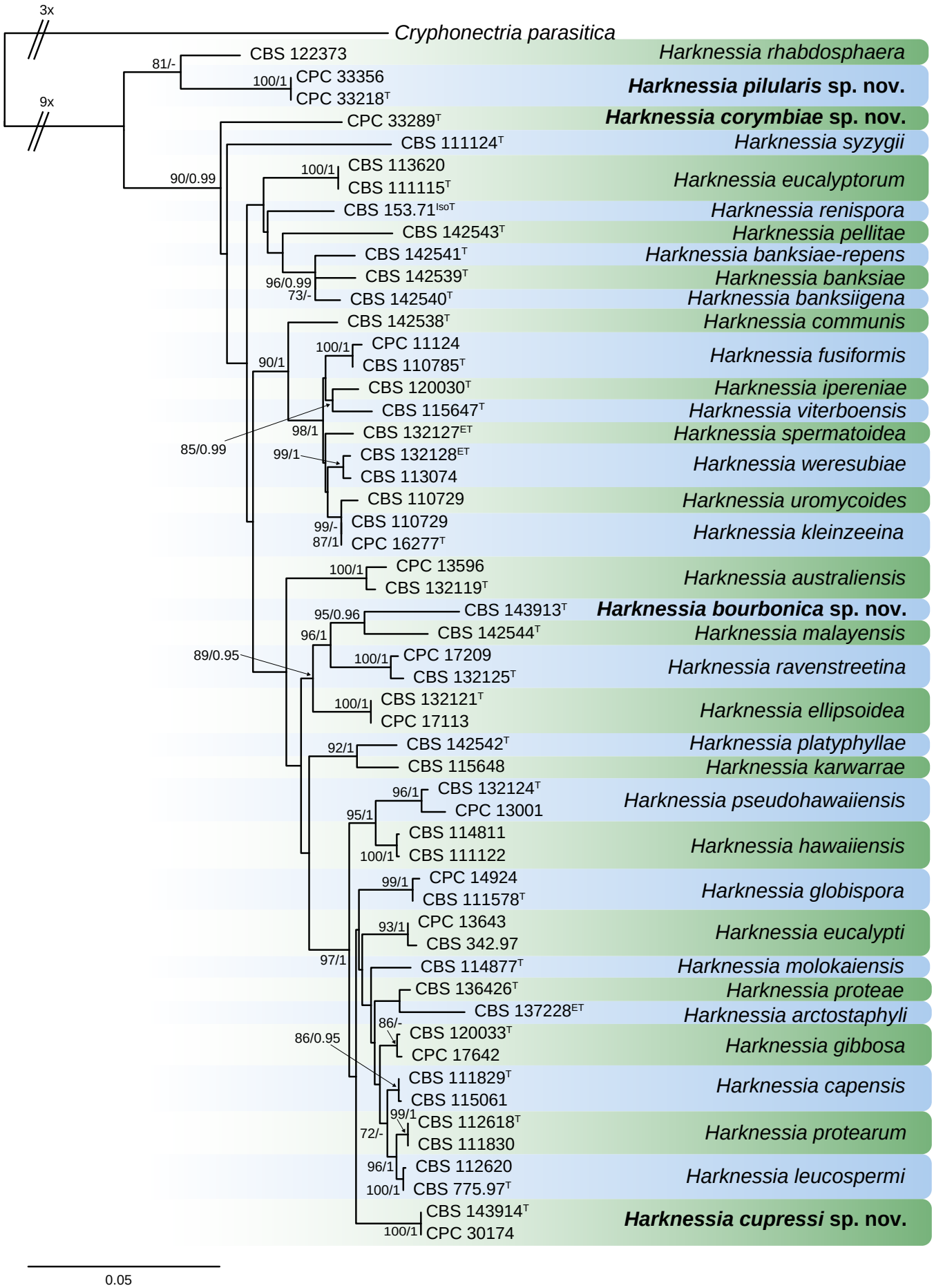

Fig. 19. RAxML phylogram obtained from the combined ITS (643 bp), *cal* (499 bp) and *tub2* (838 bp) sequence alignment of all accepted species of *Harknessia*. The tree was rooted to *Cryphonectria parasitica*. The novelties proposed in this study are indicated in **bold**. RAxML bootstrap support (BS) values above 70 % and Bayesian posterior probability scores above 0.95 are shown at the nodes. GenBank accession numbers were listed in Table 7 or in Crous *et al.* (2012c). $^{T, ET}$ and ^{IsoT} indicate ex-type, ex-epitype and ex-isotype strains, respectively. TreeBASE: S21899.

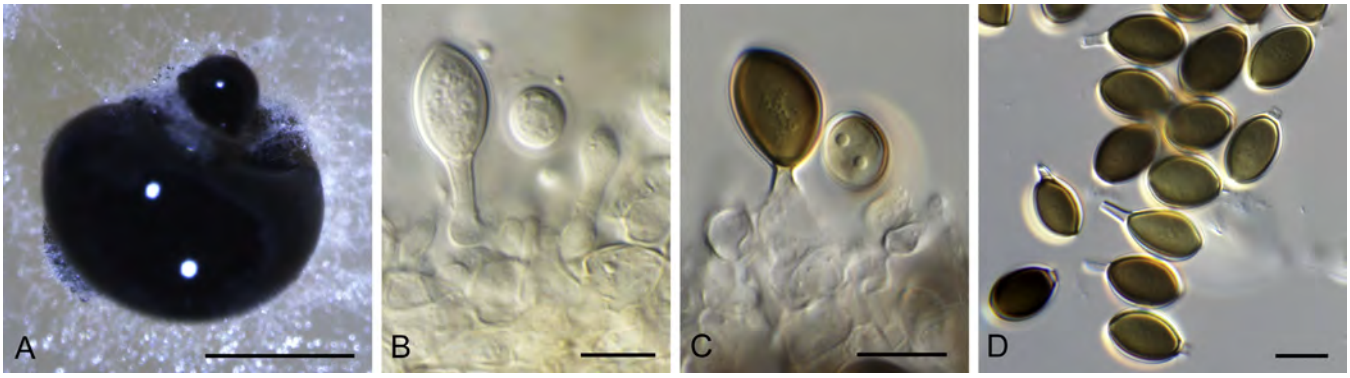

Fig. 20. *Harknessia bourbonica* (ex-type CBS 143913). **A.** Conidioma on OA. **B, C.** Conidiogenous cells giving rise to conidia. **D.** Conidia. Scale bars: A = 150 µm, B–D = 10 µm.

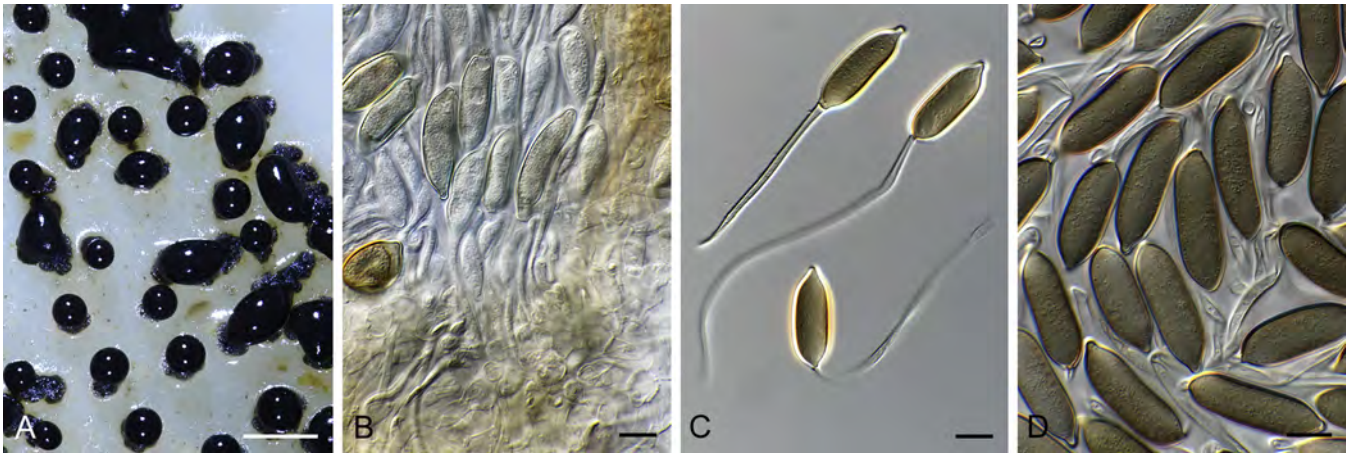

Fig. 21. *Harknessia corymbiae* (ex-type CPC 33289). **A.** Conidiomata on OA. **B.** Conidiogenous cells giving rise to conidia. **C, D.** Conidia. Scale bars: A = 250 µm, B–D = 10 µm.

Fig. 22. *Harknessia cupressi* (ex-type CBS 143914). **A.** Conidiomata on OA. **B, C.** Conidiogenous cells giving rise to conidia. **D, E.** Conidia. Scale bars: A = 250 µm, B–E = 10 µm.

Optimal media and cultivation conditions: On 2 % MEA in dark, optimum growth varies between species: *Hu. sublaevis* 20–30 °C; *Hu. bhutanensis, Hu. oblonga, Hu. ceramica* and *Hu. tribiliformis* 20–25 °C; *Hu. decipiens*, *Hu. chinaeucensis, Hu. inquinans, Hu. microbasis, Hu. salinaria* and *Hu. sumatrana* 25–30 °C; *Hu. cryptoformis, Hu. omanensis*, *Hu. savannae* and *H. tyalla* 30–35 °C.

Distribution: Australia, Bhutan, China, Ecuador, Indonesia, Malawi, Oman, South Africa and Tasmania.

Hosts: *Acacia* (*Fabaceae*), *Combretum* and *Terminalia* (*Combretaceae*), *Eucalyptus* (*Myrtaceae*), *Mangifera* (*Anacardiaceae*) associated with *Cryphalus scabricollis* (bark beetle, *Scolytinae*), *Picea* (*Pinaceae*) infested with *Ips schmutzenhoferi* (bark beetle, *Scolytinae*), *Pinus* (*Pinaceae*), *Ziziphus* (*Rhamnaceae*), and *Staphilinid* (rove beetle, *Staphylinidae*).

Disease symptoms: *Huntiella* species do not produce distinct disease symptoms on their hosts in nature. They usually infect freshly made wounds on trees and infections are often associated with nitidulid beetles (*Coleoptera*: *Nitidulidae*) and flies (*Diptera*). Pathogenicity tests using some of the species have given rise to lesions under controlled environments, but, based on the size of lesions and failure to re-isolate the fungus from

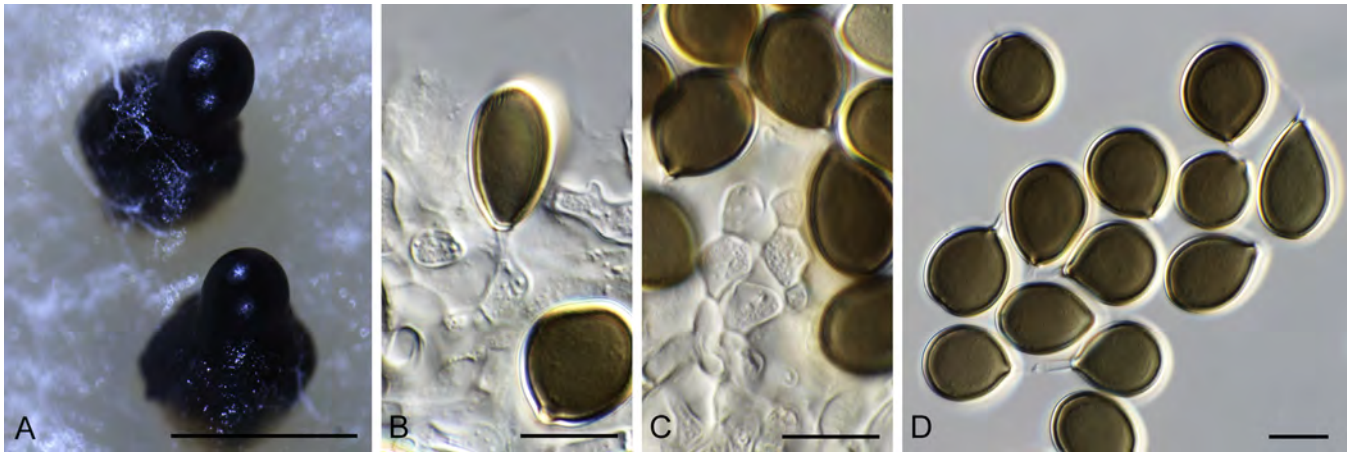

Fig. 23. *Harknessia pilularis* (ex-type CPC 33218). **A.** Conidiomata on OA. **B, C.** Conidiogenous cells giving rise to conidia. **D.** Conidia. Scale bars: A = 250 µm, B–D = 10 µm.

these lesions, they are generally considered not to be primary pathogens (Tarigan *et al.* 2010, van Wyk *et al.* 2011, de Beer *et al.* 2014).

Notes: *Huntiella* is one of nine genera in the recently erected family, *Ceratocystidaceae* (De Beer *et al.* 2014, Mayers *et al.* 2015, Nel *et al.* 2018). The genus was proposed to accommodate *Ceratocystis moniliformis* and related species that form a well-defined monophyletic lineage within the group previously treated as *Ceratocystis sensu lato* (Wingfield *et al.* 2013). *Huntiella* currently includes 17 species.

Species of *Huntiella* have several features in common, namely conical spines on their ascomatal bases, disk-like structures at the bases of the ascomatal necks, which break off easily, hat-shaped ascospores and one to two types of conidia (De Beer *et al.* 2014). Although morphological and culture characteristics overlap between the species, some species can be differentiated. These include *Hu. sublaevis* that has a limited number of spines on the ascomata (Van Wyk *et al.* 2011), and *Hu. chinaeucensis* and *Hu. microbasis* that have only rectangular-shaped conidia (Tarigan *et al.* 2010, Chen *et al.* 2013). With the exception of *Hu. ceramica* that is known only from the asexual morph, all other species have both sexual and asexual morphs. Different *Huntiella* species exhibit a variety of sexual strategies, with *Hu. omanensis* undergoing heterothallic mating while MAT2 isolates of *Hu. moniliformis* are able to reproduce unisexually (Wilson *et al.* 2015).

References: Kamgan *et al.* 2008, Heath *et al.* 2009, Tarigan *et al.* 2010, Kamgan Nkuekam *et al.* 2012, Chen *et al.* 2013, Kamgan Nkuekam *et al.* 2013 (pathogenicity); De Beer *et al.* 2013a (higher classification); De Beer *et al.* 2013b (nomenclature); Wingfield *et al.* 2013, De Beer *et al.* 2014 (generic definitions and phylogenetic relationships); Wilson *et al.* 2015 (mating strategies).

Huntiella abstrusa A.M. Wilson, Marinc., M.J. Wingf., **sp. nov.** MycoBank MB821072. Fig. 26.

Etymology: Name refers to the fact that this cryptic species was obscured by the name *Ceratocystis moniliformis* for more than a decade.

On MEA: *Ascomata* 145–315 × 130–275 µm, perithecial, embedded in media or superficial in mycelial mass, single or in groups, pale brown when young, becoming dark brown with age, ellipsoidal to subglobose; *ascomatal wall of textura epidermoidea* to *textura globulosa*, covered with short sterile hyphae, 30–105 µm long, hyaline becoming pale brown with age, mostly unbranched, flexuous, tapering towards apex, with conical spines; *necks* 595–1100 µm long, 21–71.5 µm wide near base, 11–18 µm wide near apex, dark brown, tapering towards apex, becoming easily detached from ascomatal base when pressed, with a disk-like structure near base; *hyphae* near apex 18.5–37 µm long, 1–2 µm wide near base, 0.5–1.5 µm wide, mostly straight, showing no distinct divergent nor convergent, aseptate, unbranched, hyaline, tapering towards apex. *Asci* not observed. *Ascospores* 4.5–5.5 × 3.5–6 µm (av. 5.2 × 4.6 µm) without sheath, 2–3.5 µm thick in side-view, hyaline, oblong to subglobose, clothed with gelatinous sheath, 0.5–1.5 µm thick, in side-view giving an impression of a hat. *Conidiophores* up to 80 µm long, septate, flexuous, sometimes branched, occasionally reduced to conidiogenous cells, often lightly sub-hyaline to pale brown near base. *Conidiogenous cells* hyaline, enteroblastic, in two shapes, originating from same or different hyphae; lageniform, 15.5–33 µm long, 2–4.5 µm wide at base, gradually tapering towards apex, 1–3 µm wide at apex, producing rectangular conidia; or cylindrical with wide-mouthed, 22–50 µm long, 3.5–6.5 µm wide at apex, 3–4 µm wide at base, producing barrel-shaped conidia. *Conidia* in chains, hyaline, aseptate, in two shapes, rectangular, 4–8.5 × 1.5–2.5 µm (av. 5.6 × 1.8 µm); or barrel-shaped, 5–14.5 × 4–7 µm (av. 8.1 × 5.9 µm). *Chlamydospores* absent.

Culture characteristics: On 2 % MEA optimum growth at 30 °C reaching 82.7 mm in dark in 3 d, followed by 25 °C reaching 77.3 mm, showing slow growth at 10, 15, 20, 35 °C. Cultures circular with smooth margins, aerial mycelium fluffy to velvety, moderately dense, above and below dark brown fading towards edge and with white margins.

Material examined: **Indonesia**, Riau province, Teso East, S 0°04'33.00", E 101°37'23.00", on the bark of *Eucalyptus* sp. (*Myrtaceae*), Oct. 2005, M. Tarigan (**holotype** PREM 61671, culture ex-type CBS 142243 = CMW 21092).

Notes: For more than a decade, *Hu. abstrusa* was thought to be *Ceratocystis moniliformis* (now *Hu. moniliformis*). Phylogenetic analyses of ITS, LSU, 60S, *mcm7* and *tub2* have shown that *Hu. abstrusa* is distinct from *Hu. moniliformis* and other *Huntiella* spp. It is most closely related to *Hu. inquinans*, *Hu. microbasis* and *Hu. sumatrana* from Indonesia, *Hu. chinaeucensis* from China and *Hu. bhutanensis* from Bhutan (De Beer *et al.* 2014, Van Wyk *et al.* 2004, Tarigan *et al.* 2010, Chen *et al.* 2013). Neither *Hu. abstrusa* nor any of the other *Huntiella* species are primary pathogens and

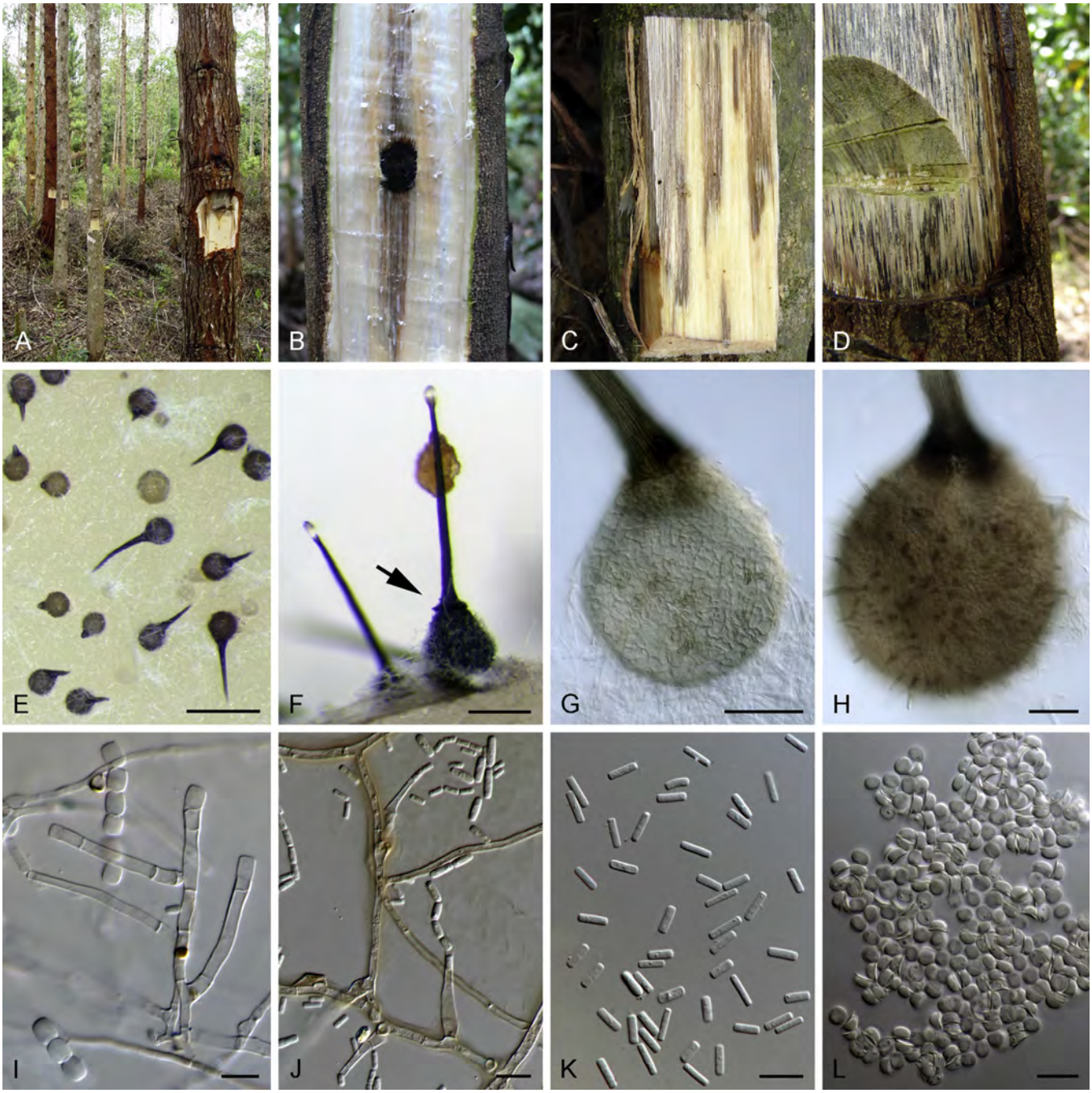

Fig. 24. *Huntiella* spp. **A–D.** Disease symptoms. **A.** *Eucalyptus* trees artificially wounded to trap *Huntiella* spp. **B.** Lesion associated with inoculation with *Huntiella sumatrana* on an *Acacia mangium* stem. **C.** Discolouration of wood associated with artificially induced wound on the stem of a *Eucalyptus* tree from which *Huntiella* spp. were isolated. **D.** Blue-stained *Eucalyptus* wood associated with *Huntiella* infection. **E–H, L.** Sexual morphs. **E.** Ascomata on 2 % MEA in various developmental stage from young (paler) to mature (darker). **F.** Mature ascomata with fresh ascospore droplets at the tip of necks and ostiolar neck with a disc-like base (arrow). **G, H.** Young ascoma showing developing of conical spines (G) and ascomatal hyphae (H). **L.** Ascospores. **I–K.** Asexual morphs. **I.** Tubular-form conidiogenous cell producing barrel-shaped conidia. **J.** Flask-shaped conidiogenous cells producing rectangular-shaped conidia. **K.** Rectangular-shaped conidia. **E, F, H, K.** *Huntiella omanensis* (CMW 11056). **G, L.** *Huntiella moniliformis* (CMW 36908). **I, J.** *Huntiella abstrusa* (CMW 21092). Scale bars: E = 500 µm; F = 250 µm; G, H = 50 µm; I–L = 10 µm.

typically infect freshly made wounds on trees. Despite only minor morphological differences between *Huntiella* species, *Hu. abstrusa* can be distinguished from the other species by its longer necks and the presence of barrel-shaped conidia. The *Hu. abstrusa* isolate examined is considered heterothallic.

Authors: A.M. Wilson, S. Marincowitz, M.J. Wingfield & B.D. Wingfield

Macgarvieomyces Klaubauf, *et al.*, Stud. Mycol. 79: 106. 2014. Fig. 27.

Classification: *Sordariomycetes, Sordariomycetidae, Magnaporthales, Pyriculariaceae*.

Type species: *Macgarvieomyces borealis* (de Hoog & Oorschot) Klaubauf, *et al.*, basionym: *Pyricularia borealis* de Hoog & Oorschot. Holotype and ex-type strain: IMI 105288, CBS 461.65.

DNA barcodes (genus): LSU, ITS.

DNA barcodes (species): ITS, *act, cal*, *rpb1*. Table 9. Fig. 28.

Mycelium consisting of smooth, hyaline, branched, septate hyphae. *Conidiophores* solitary, erect, straight or curved, mostly unbranched, medium to dark brown, smooth or finely verruculose, septate. *Conidiogenous cells* integrated, terminal, rarely intercalary, medium to dark brown, smooth or finely verruculose, forming a rachis with protruding denticles, appearing flat-tipped.

Table 8. DNA barcodes of accepted *Huntiella* spp.

Species	Isolates[1]	GenBank accession numbers[2]				References
		ITS	*tub2*	*mcm7*	*tef1*	
Huntiella abstrusa	CBS 142243^{T}	KY913291	KY913290	KY913289	–	Present study
Hu. bhutanensis	CBS 114289^{T}	AY528952 NR119506	AY528962	KM495412	AY528962[a]	Van Wyk *et al.* (2004), De Beer *et al.* (2014)
Hu. ceramica	CBS 122299^{T}	EU245022	EU244994	KM495485	EU244926[b]	Heath *et al.* (2009), De Beer *et al* (2014)
Hu. chinaeucensis	CBS 127185^{T}	JQ862729	JQ862717	KM495416	JQ862741[c]	Chen *et al.* (2013), De Beer *et al.* (2014)
Hu. cryptoformis	CBS 131279^{T}	KC691464	KC691488	–	KC691512[c]	Mbenoun *et al.* (2014)
Hu. decipiens	CBS 129736^{T}	HQ203216	HQ203233	KM495422	HQ236435[c]	Kamgan Nkuekam *et al.* (2013), De Beer *et al.* (2014)
Hu. inquinans	CBS 124388^{T}	EU588587	EU588666	KM495436	EU588674[a]	Tarigan *et al.* (2010), De Beer *et al* (2014)
Hu. microbasis	CBS 124013^{T}	EU588593	EU588672	KM495442	EU588680[a]	Tarigan *et al.* (2010); De Beer *et al.* (2014)
Hu. moniliformis	CBS 118127	FJ151422	FJ151456	KM495443	FJ151478[a]	Van Wyk *et al.* (2011), De Beer *et al.* (2014)
Hu. moniliformopsis	CBS 109441^{T}	AY528998	AY528987	KM495444	AY529008[a]	Yuan & Mohammed (2002), Van Wyk *et al.* (2004), De Beer *et al.* (2014)
Hu. oblonga	CBS 122291^{T}	EU245019	EU244991	KM495447	EU244951[b]	Heath *et al.* (2009), De Beer *et al.* (2014)
Hu. omanensis	CBS 115787	DQ074742	DQ074732	KM495449	DQ074737[a]	Al-Subhi *et al.* (2006)
Hu. salinaria	CBS 129733^{T}	HQ203213	HQ203230	KM495461	HQ236432[c]	Kamgan Nkuekam *et al.* (2013), De Beer *et al.* (2014)
Hu. savannae	CBS 121151^{T}	EF408551	EF408565	KM495462	EF408572[c]	Kamgan *et al.* (2008), De Beer *et al.* (2014)
Hu. sublaevis	CBS 122517	FJ151431	FJ151465	KM495464	FJ151486[b]	Van Wyk *et al.* (2011), De Beer *et al.* (2014)
Hu. sumatrana	CBS 124011^{PT}	EU588589	EU588668	KM495465	EU588678[a]	Tarigan *et al.* (2010), De Beer *et al.* (2014)
Hu. tribiliformis	CBS 115866^{T}	AY529003	AY529003	KM495468	AY529014[a]	Van Wyk *et al.* (2006), De Beer *et al.* (2014)
Hu. tyalla	CBS 128703^{T}	HM071900	HM071913	KM495470	HQ236452[c]	Kamgan Nkuekam *et al.* (2012), De Beer *et al.* (2014)

[1] CBS: Westerdijk Fungal Biodiversity Institute, Utrecht, the Netherlands. ^{T} and ^{PT} indicate ex-type and ex-paratype strains, respectively.
[2] ITS: internal transcribed spaces and intervening 5.8S nrDNA, *tub2*: partial β-tubulin gene, *mcm7*: mini-chromosome maintenance complex component 7, *tef1*: partial translation elongation factor 1-alpha gene. [a, b] and [c] in *tef1* column indicate the primers used in sequencing: a: Ef1-728f, ef1-986r, b: EF1f, EF1r, c:EF1f, EF2r.

Conidia solitary, narrowly obclavate to narrowly pyriform, hyaline, often becoming pale brown with age, smooth, granular, guttulate, medianly 1-septate, apex obtusely rounded; *hila* somewhat thickened, refractive or not, not or slightly darkened. *Chlamydospores* brown, ellipsoid, arranged in chains (adapted from Klaubauf *et al.* 2014).

Culture characteristics: Colonies on MEA buff to rosy buff, isabelline or pale luteous, with pale olivaceous grey central mycelium, with entire, lobate or round and hairy edge, umbonate to conical or flat to slightly raised colony with somewhat velvety or wool-like texture; reverse iron grey, ochreous and buff towards edge or pale luteous. On CMA and OA transparent, pale luteous to olivaceous or grey olivaceous, flat, smooth and velutinous surface, undulate margin. Colonies on PDA pale luteous, white with buff centre or whitish to buff with honey centre, round, flat, fringed margin; reverse white with buff centre or whitish to buff with honey centre.

Optimal media and cultivation conditions: On OA at 25 °C under dark, or autoclaved barley seeds placed on SNA at 25 °C under near-ultraviolet light (12 h light, 12 h dark).

Distribution: Europe and New Zealand.

Hosts: Primarily on *Juncus effusus* and *Luzula* spp. (*Juncaceae*), also reported on *Carex* sp. and *Kyllinga brevifolia* (*Cyperaceae*).

Disease symptoms: Leaf spots.

Notes: *Macgarvieomyces* was recently introduced to accommodate two species previously placed in *Pyricularia*. Phylogenetic analyses based on LSU, ITS, *act*, *cal* and *rpb1* demonstrated that these taxa are not congeneric with *Pyricularia s. str.* (Klaubauf *et al.* 2014). Species in this genus were isolated from *Juncaceae* in Europe and associated with leaf spots. Species have also been reported on *Cyperaceae* and New Zealand (Farr & Rossman 2017); however, these host and distribution data have not been corroborated based on DNA sequence analyses.

Reference: Klaubauf *et al.* 2014 (morphology and phylogeny).

Macgarvieomyces luzulae (Ondřej) Y. Marín, Akulov & Crous, **comb. nov.** MycoBank MB823764. Fig. 29.
Basionym: *Pyricularia luzulae* Ondřej, Česká Mykol. 42: 81. 1988.

Leaf spots up to 17 mm long, ellipsoid to fusiform, grey to pale brown at middle, dark brown at margin. On SNA: *Mycelium* with hyaline, smooth, septate, branched, 2–3 µm diam hyphae. *Conidiophores* 60–120 × 4–7 µm, erect, dark brown, unbranched, subcylindrical, straight to flexuous, thick-walled, finely verruculose, 2–3-septate. *Conidiogenous cells* 30–50 × 4–6 µm, terminal and subcylindrical, finely verruculose, dark brown, tapering toward apex with numerous denticles pointing upwards, 1–4 × 1–1.5 µm; *scars* unthickened. *Conidia* (18–)20–22(–30) × (4–)5(–6) µm, solitary, narrowly pyriform, hyaline, becoming pale brown with age, guttulate, 1(–2)-septate, apex obtusely rounded, base truncate, 2 µm diam, slightly darkened, refractive.

Culture characteristics: Colonies flat, spreading, with sparse to moderate aerial mycelium and smooth, lobate margins, covering plate after 2 wk at 25 °C. On MEA, PDA and OA surface and reverse pale luteous.

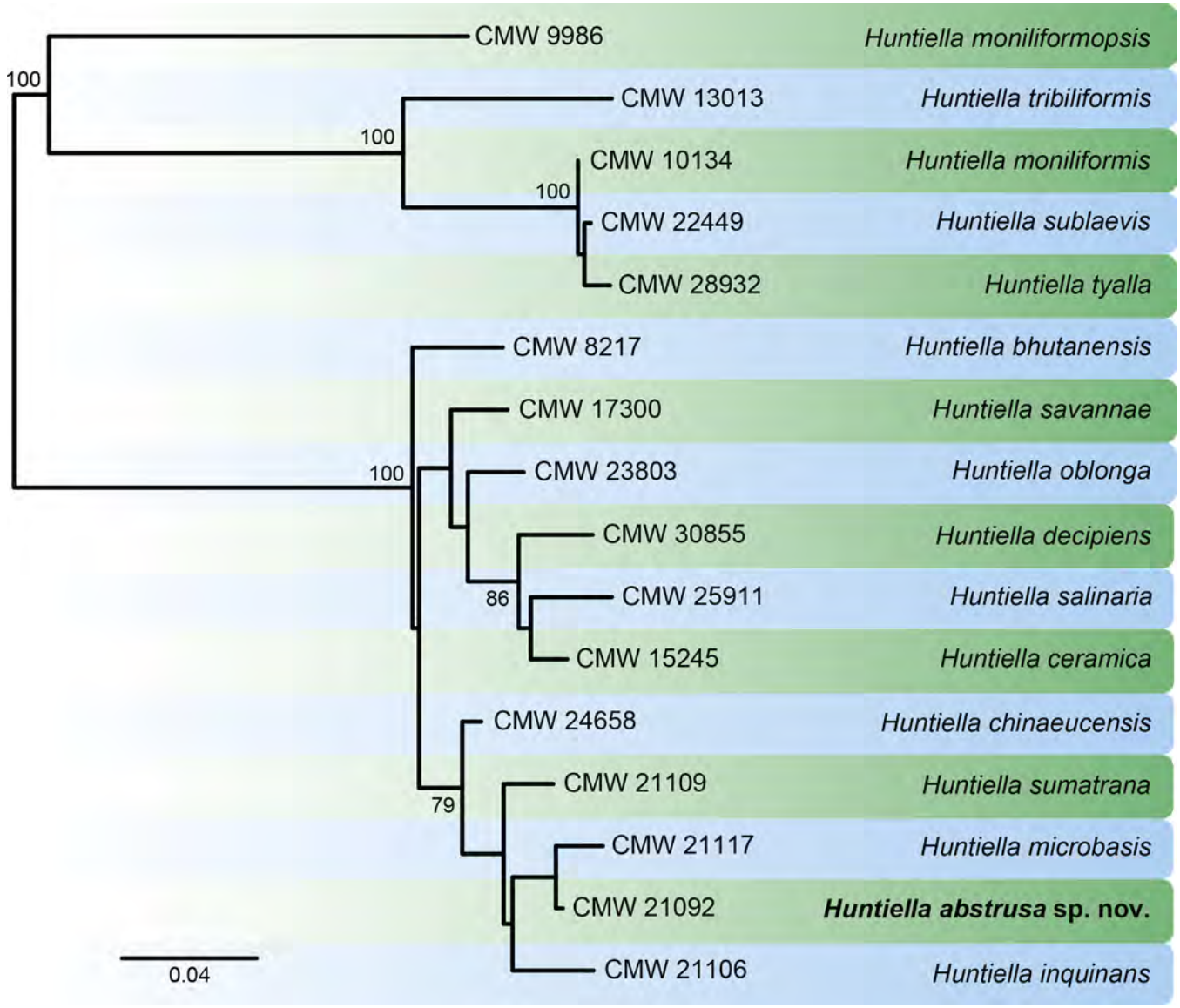

Fig. 25. A maximum likelihood (ML) phylogram constructed using the combined dataset of the 60S (370 bp), LSU (813 bp), ITS (393 bp), *mcm7* (589 bp) and *tub2* (433 bp) gene regions of *Huntiella* spp. ML analyses were performed using PhyML with Smart Model Selection Online, selecting the GTR substitution model. Bootstrap values of 70 % or more are indicated above the branches. The newly described species, *Hu. abstrusa*, is indicated in **bold**. TreeBASE: S20860.

Materials examined: **Slovakia**, on leaves of *Luzula sylvatica* (*Juncaceae*), Jul. 1984 (**holotype of *Pyricularia luzulae*** PRM 842743). **Ukraine**, on leaves of *Luzula* sp. (*Juncaceae*), 2016, A. Akulov (**epitype of *Pyricularia luzulae* designated here** MBT379806, CBS H-23355, culture ex-epitype CBS 143401 = CPC 32458); *ibid*., CWU (Myc) AS 5966 / 6437; Carpathian Biosphere reserve, on leaves of *Luzula sylvatica* (*Juncaceae*), Aug. 2016, A. Akulov, CPC 31555; *ibid*., CPC 31571.

Notes: *Pyricularia luzulae* was introduced for a fungus isolated on *Luzula sylvatica* from Slovakia (Ondřej 1988). In the original description PRM 842743 was designated as holotype, but no living culture was associated with this specimen. Therefore, a strain that closely fits the description of the protologue, and isolated from the same host in a close country to Slovakia, namely Ukraine, is designated here as epitype. The only difference observed was in the conidial size, since in the original description (*in vivo*) the conidia were larger and 1–2-septate (17.5–36 × 3.5–7.5 µm). However, the measurements of our isolate growing *in vivo* are 27.5–33 × 6.5–7.5 µm, and *in vitro* 18–30 × 4–6 µm, and conidia could become 2-septate with age.

The phylogenetic study of *Py. luzulae* revealed that it belongs to *Macgarvieomyces*. As noted above, the host of this genus is *Juncus effusus* in the same family as *Luzula* (*Juncaceae*).

Authors: Y. Marin-Felix, A. Akulov & P.W. Crous

Metulocladosporiella Crous, *et al.*, Mycol. Res. 110: 269. 2006. Fig. 30.

Classification: *Eurotiomycetes, Chaetothyriomycetidae, Chaetothyriales, Herpotrichiellaceae.*

Type species: *Metulocladosporiella musae* (E.W. Mason) Crous, *et al.*, basionym: *Cladosporium musae* E.W. Mason. Lectotype designated by Crous *et al.* (2006a): IMI 7521 (slide). Epitype and ex-epitype strain designated by Crous *et al.* (2006a): CBS H-14788, CBS 161.74 = ATCC 36973.

DNA barcodes (*genus*): LSU, ITS.

DNA barcodes (*species*): ITS, *tef1*. Table 10. Fig. 31.

Mycelium internal and external on substrate, hyphae branched, septate, hyaline, subhyaline to pale olivaceous, thin-walled. *Stromata* lacking. *Conidiophores* macronematous, mononematous, occasionally with intermixed micronematous conidiophores, solitary or in loose groups, arising from hyphae, erect, with a long, subcylindrical, simple stipe and a branched

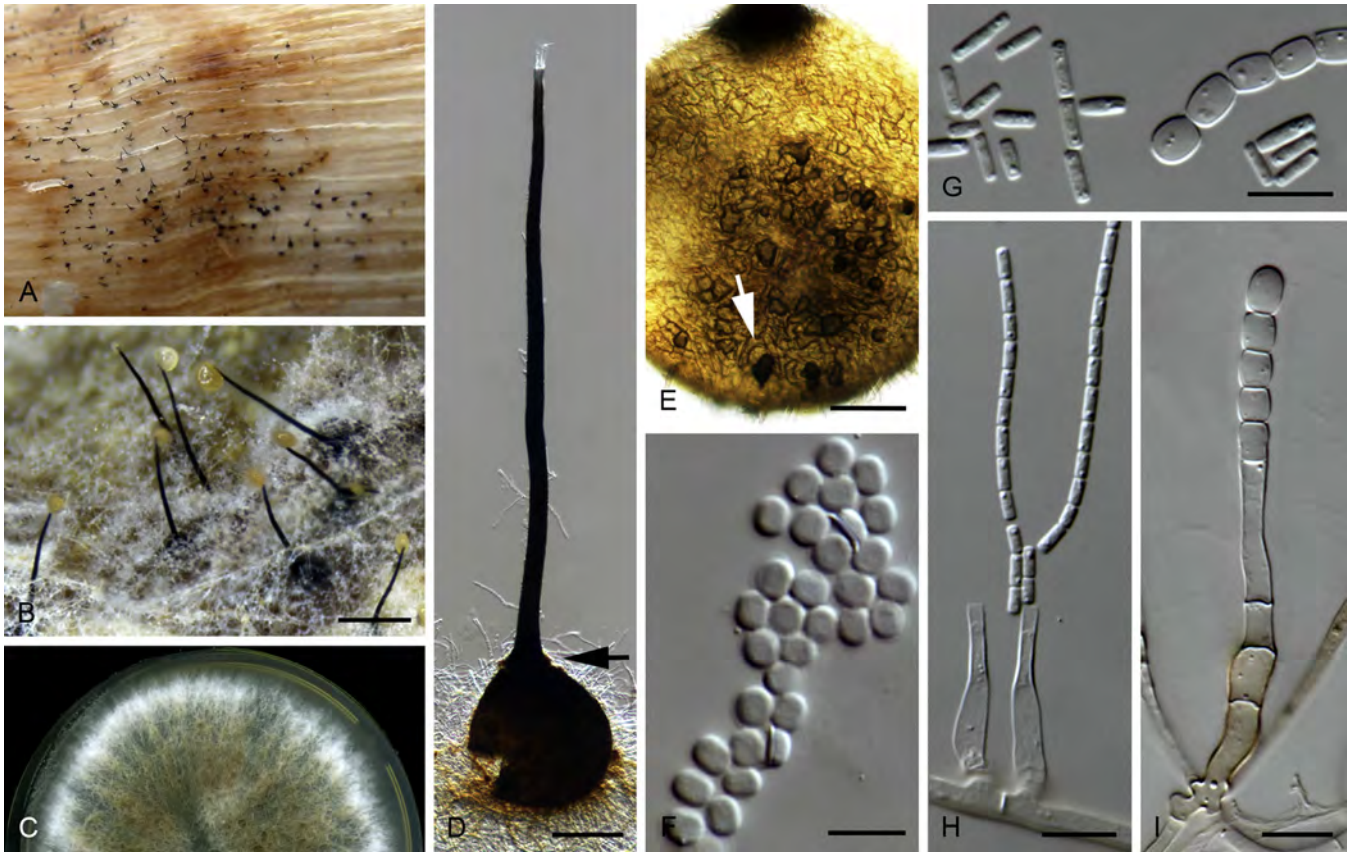

Fig. 26. *Huntiella abstrusa* (ex-type CBS 142243 = CMW 21092). **A.** Ascomata on host substrate. **B.** Ascospore droplets of cream to yellow-coloured at the tip of ascomatal neck and ascomata embedded in aerial hyphae producing asexual structures. **C.** Colony on 2 % MEA grown in the dark at 30 °C for 3 d. **D.** Mature ascoma with a disk-like base (arrow). **E.** Base of young ascoma (1 wk) with conical spines (arrow) (image taken in bright field). **F.** Ascospores. **G.** Two types of conidia: rectangular-shaped and barrel-shaped conidia. **H.** Flask-shaped conidiogenous cells and rectangular-shaped conidia. **I.** Tubular-shaped conidiogenous cell and barrel-shaped conidia. Scale bars: B = 500 µm; D = 100 µm; E = 50 µm; F–I = 10 µm.

terminal part; *stipe* septate, medium to brown, smooth or almost so, usually swollen at base; *branched part* loose to dense, metuloid, of short to long branchlets and ramoconidia, tips paler than stipes, subhyaline to pale olivaceous. *Conidiogenous cells* integrated, terminal, occasionally intercalary, polyblastic, sympodial; *conidiogenous loci* (conidial scars) subconspicuous to conspicuous, subdenticulate, truncate, unthickened to slightly thickened, and somewhat darkened-refractive. *Conidia* and *ramoconidia* in simple and branched chains, ellipsoid, ovoid, subcylindrical, or fusiform, 0–1-septate, subhyaline to pale olivaceous, thin-walled, smooth; *hila* truncate, unthickened to slightly thickened or slightly darkened-refractive; *secession* schizolytic. *Sexual morph* unknown (adapted from Crous *et al.* 2006a).

Culture characteristics: Colonies on PDA and OA under near-ultraviolet light with smooth, regular margins and sparse to moderate aerial mycelium. On PDA surface pale mouse grey to mouse grey or dirty white-grey, greyish sepia, smoke grey to grey olivaceous, or olivaceous; reverse greenish black, cinnamon to isabelline with centre fuscous black, or grey olivaceous to dark grey olivaceous or olivaceous black.

Optimal media and cultivation conditions: SNA under near-ultraviolet light at 25 °C to induce sporulation.

Distribution: Africa, America, Asia and Oceania.

Hosts: *Musa* spp. (*Musaceae*).

Disease symptoms: Leaf spots; Cladosporium speckle disease of banana.

Notes: *Metulocladosporiella* was introduced by Crous *et al.* (2006a) to accommodate two cladosporium-like species causing speckle disease on banana. *Metulocladosporiella* can be distinguished from *Cladosporium* and allied genera by the presence of apically branched, brown conidiophores with paler tips and chains of pale, smooth, often subhyaline conidia.

The phylogenetic analysis based on the ITS and LSU sequences demonstrated that *Metulocladosporiella* belongs in *Chaetothyriales*. Morphologically, the conidiogenous loci and conidial hila resemble those of *Cladophialophora*, which is another member of this order. However, *Cladophialophora* produces unbranched, micro- to semimacronematous conidiophores, and concolourous conidia. Moreover, *Cladophialophora* includes human pathogenic species (Crous *et al.* 2006a). In the present study, the recommended barcodes for species delimitation are ITS and *tef1*.

Hitherto, all species described in *Metulocladosporiella* are pathogens of banana and occur in countries where this crop is cultivated (Jones 2000, Crous *et al.* 2006a).

Reference: Crous *et al.* 2006a (morphology and phylogeny).

Metulocladosporiella chiangmaiensis Y. Marín, Cheew. & Crous, **sp. nov.** MycoBank MB824031. Fig. 32.

Etymology: Name from Chiang Mai, the province in Thailand where this fungus was collected.

Mycelium internal and external, superficial; *hyphae* 1.5–3.5 µm wide, branched, septate, occasionally slightly constricted at septa, with small swellings, hyaline, subhyaline to pale

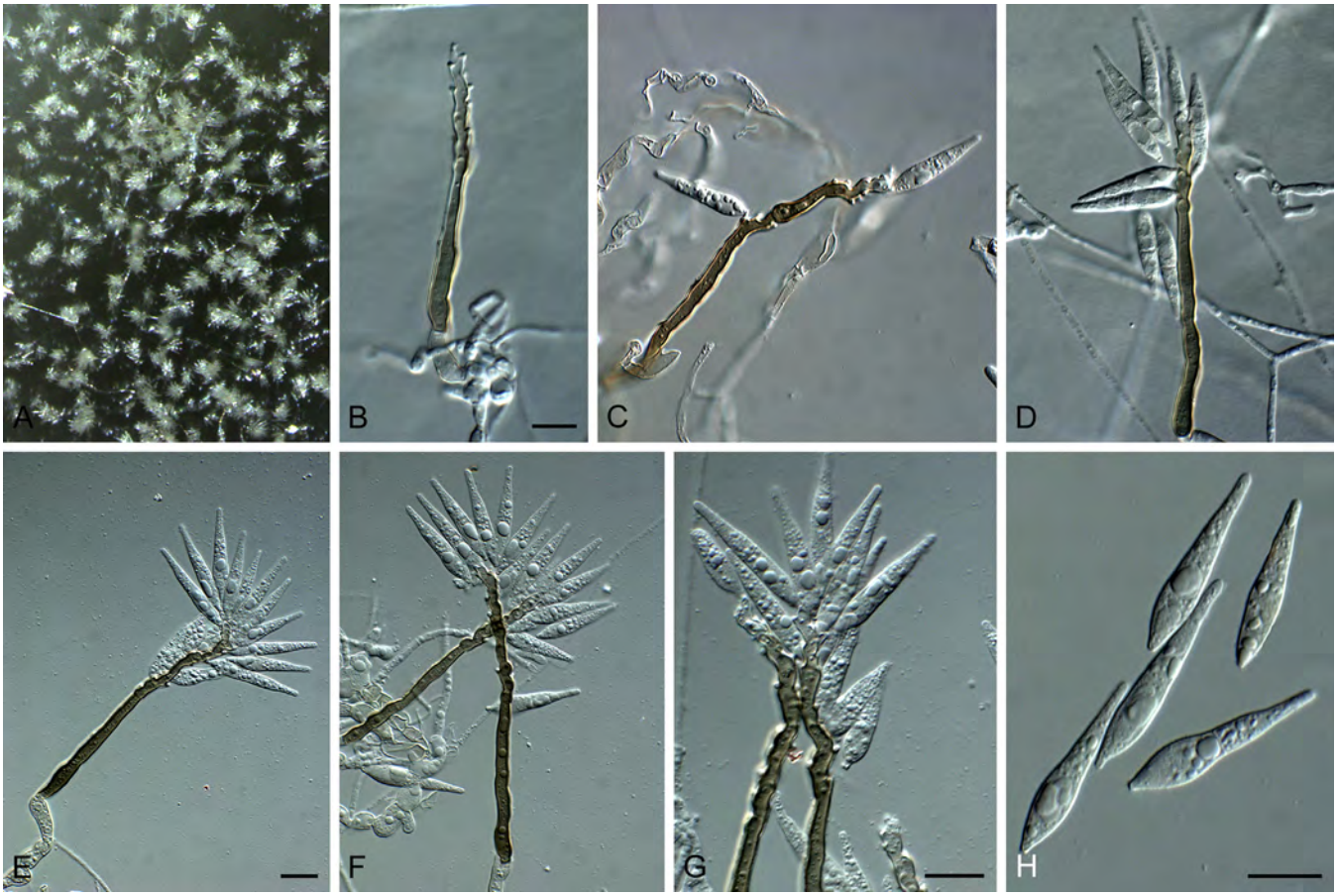

Fig. 27. A–H. *Macgarvieomyces juncicola* (CBS 610.82). **A.** Colony sporulating on OA. **B–G.** Conidiophores and conidia forming on SNA. **H.** Conidia. Scale bars = 10 µm. Pictures taken from Klaubauf *et al.* (2014).

Table 9. DNA barcodes of accepted *Macgarvieomyces* spp.

Species	Isolates[1]	GenBank accession numbers[2]				References
		ITS	*act*	*cal*	*rpb1*	
Macgarvieomyces borealis	CBS 461.65^{T}	KM484854	KM485170	KM485239	KM485070	Klaubauf *et al.* (2014)
Ma. juncicola	CBS 610.82	KM484855	KM485171	KM485240	KM485071	Klaubauf *et al.* (2014)
Ma. luzulae	CBS 143401^{ET}	MG934440	MG934463	MG934519	MG934469	Present study
	CPC 31555	MG934441	MG934464	MG934520	MG934470	Present study
	CPC 31571	MG934442	MG934465	MG934521	MG934471	Present study

[1] CBS: Westerdijk Fungal Biodiversity Institute, Utrecht, the Netherlands; CPC: Culture collection of Pedro Crous, housed at the Westerdijk Fungal Biodiversity Institute. ^{T} and ^{ET} indicate ex-type and ex-epitype strains.
[2] ITS: internal transcribed spacers and intervening 5.8S nrDNA; *act*: partial actin gene; *cal*: partial calmodulin gene; *rpb1*: partial RNA polymerase II largest subunit gene.

olivaceous, thin-walled, smooth, hyphae occasionally aggregated, forming ropes; with numerous intermixed *micronematous conidiophores*, erect from vegetative mycelium, intercalary, straight to flexuous, unbranched, subhyaline, usually with simple terminal conidial chains. *Macronematous conidiophores* 85–1050 µm long, arising from superficial hyphae, erect, solitary to loosely aggregated, composed of a subcylindrical stipe, 5.5–9.5(–10.5) µm wide, 3–18 septate, swollen or lobed at base, 8–17(–18.5) µm diam, with short, rhizoid, subhyaline to pale brown hyphae growing from base, medium to brown in lower half, paler towards apex, tips pale brown or even subhyaline, thick-walled below, thin-walled towards apex, smooth; *apex* persistently branched, branched part composed of usually fairly compact, closely arranged subcylindrical branchlets; *primary branches* (13–)17–45(–55) × 3–5.5 µm, 0(–1)-septate, giving rise to 1–3 secondary branches, or to conidiogenous cells; *secondary branches* 13–28 × 2.5–5(–5.5) µm, 0(–1)-septate, giving rise to 1–2(–3) conidiogenous cells; *conidiogenous cells* 9–17 × 3–5 µm, subcylindrical, terminal or occasionally intercalary, sympodial, polyblastic, conidiogenous loci 1–1.5(–2) µm wide, subconspicuous to conspicuous, subdenticulate, somewhat protuberant, truncate, wall unthickened to somewhat so, darkened-refractive. *Conidia* 5.5–10(–12.5) × 2.5–4 µm, in simple and branched acropetal chains, ellipsoid-ovoid, fusoid, subcylindrical, aseptate, subhyaline to pale brown, thin-walled, smooth, with 1–3(–4) hila, 1–1.5 µm diam, up to 2 µm diam at base of ramoconidia, truncate, unthickened or almost so, and somewhat darkened-refractive, secession schizolytic; *ramoconidia* 7–15(–17) × 3–4.5 µm.

Culture characteristics: Colonies on PDA reaching 25–28 mm diam after 2 wk at 25 °C, moderate aerial mycelium, velvety,

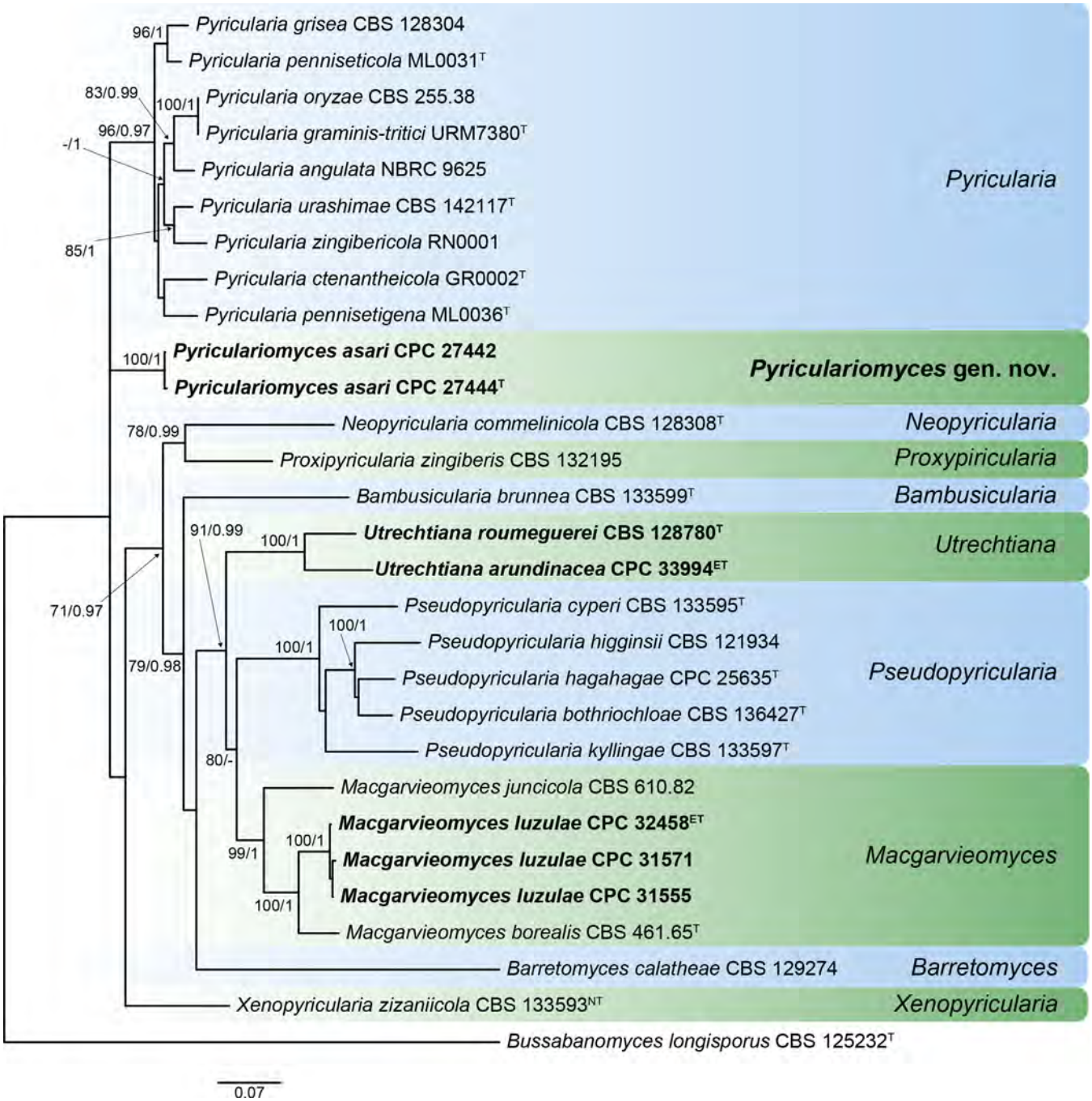

Fig. 28. RAxML phylogram obtained from the combined ITS (548 bp), *act* (375 bp), *cal* (579 bp) and *rpb1* (1011 bp) sequence alignment of members of *Pyriculariaceae*. The tree was rooted to *Bussabanomyces longisporus* CBS 125232. The novelties proposed in this study are indicated in **bold**. RAxML bootstrap support (BS) values above 70 % and Bayesian posterior probability scores above 0.95 are shown at the nodes. GenBank accession numbers were listed in Klaubauf *et al.* (2014). $^{T, ET}$ and ^{NT} indicate ex-type, ex-epitype and ex-neotype strains, respectively. TreeBASE: S21899.

umbonate; surface greyish sepia, halo surrounding centre vinaceous buff, and margins hazel; reverse cinnamon to isabelline, centre fuscous black. Colonies on OA reaching 32–35 mm diam after 2 wk at 25 °C, sparse aerial mycelium, flat except margins due to aerial mycelium; surface hazel, centre brown vinaceous, margins smoke grey; reverse livid vinaceous, centre brown vinaceous, margins pale brown vinaceous.

Material examined: **Thailand**, Chiang Mai Province, Mae Klang Luang, N 18° 32.465', E 98° 32.874', from leaves of *Musa* sp. (*Musaceae*), 6 Oct. 2008, P.W. Crous & R. Cheewangkoon (**holotype** CBS H-23393, culture ex-type CBS 143918= CPC 18646).

Notes: *Metulocladosporiella chiangmaiensis* is related to *M. musigena*. Both species are known from Thailand, and produce more micronematous conidiophores than any other species in the genus. However, *M. chiangmaiensis* produces longer macronematous conidiophores and shorter conidia than *M. musigena*, which produces conidiogenous cells directly from the apex of its macronematous conidiophores, which is not the case in *M. chiangmaiensis*.

Metulocladosporiella malaysiana Y. Marín & Crous, **sp. nov.** MycoBank MB824032. Fig. 33.

Etymology: Name refers to Malaysia, the country from where it was isolated.

Mycelium internal and external, superficial; *hyphae* 1–3.5 µm wide, branched, septate, occasionally constricted at septa, with

Fig. 29. A–I. *Macgarvieomyces luzulae* (ex-epitype CBS 143401). **A.** Disease symptoms on leaves of *Luzula sylvatica*. **B.** Colony sporulating on OA. **C–H.** Conidiophores and conidia forming on SNA. **I.** Conidia. Scale bars = 5 µm.

swellings, hyaline, subhyaline to pale brown, thin-walled, smooth, hyphae occasionally aggregated, forming ropes; occasionally with intermixed *micronematous conidiophores*, erect from vegetative mycelium, intercalary, straight to flexuous, unbranched, subhyaline, usually with simple terminal conidial chains. *Macronematous conidiophores* 57–565 µm long, arising from superficial hyphae, erect, solitary to loosely aggregated, composed of a subcylindrical stipe, 5–8 µm wide, (1–)2–11-septate, swollen or lobed at base, 7–15 µm diam, with short, rhizoid, subhyaline to pale brown hyphae growing from base, medium to brown in lower half, paler towards apex, tips pale brown or even subhyaline, thick-walled below, thin-walled towards apex, smooth; *apex* persistently branched, composed of fairly compact, closely arranged subcylindrical branchlets; *primary branches* (12–)16–44(–60) × 3.5–5.5 µm, 0–1(–2)-septate, giving rise to 1–2(–3) secondary branches, or to conidiogenous cells; *secondary branches* 11.5–26.5(–39) × 3–4.5 µm, 0(–1)-septate, giving rise to 1–2(–3) conidiogenous cells; *conidiogenous cells* 10–23 × 2.5–4.5 µm, subcylindrical, terminal or occasionally intercalary, sympodial, polyblastic, conidiogenous loci 1–2 µm wide, subconspicuous to conspicuous, subdenticulate, somewhat protuberant, truncate, wall not to slightly thickened, darkened-refractive. *Conidia* 5.5–13.5(–14.5) × (2.5–)3–4.5(–5) µm, in simple and branched acropetal chains, ellipsoid-ovoid, fusoid, subcylindrical, aseptate, subhyaline to pale brown, thin-walled, smooth, with 1–3 hila, 0.8–1.4 µm diam, up to 2 µm diam at base of ramoconidia, truncate, not to slightly thickened, and somewhat darkened-refractive, secession schizolytic; *ramoconidia* 7–13(–14) × 3–4.5(–5) µm.

Culture characteristics: Colonies on PDA reaching 23–27 mm diam after 2 wk at 25 °C, moderate aerial mycelium, giving cottony appearance, umbonate, margins fringed; surface olivaceous, mycelium smoke grey; reverse grey olivaceous to dark grey olivaceous. Colonies on OA reaching 30–34 mm diam after 2 wk at 25 °C, sparse aerial mycelium, umbonate, margins fringed; surface olivaceous, mycelium smoke grey to grey olivaceous; reverse dark grey olivaceous.

Material examined: **Malaysia**, from leaves of *Musa* sp. (*Musaceae*), 2010, M.H. Wong (**holotype** CBS H-23394, culture ex-type CBS 143919 = CPC 18131).

Notes: *Metulocladosporiella malaysiana* is related to *M. samutensis*. These can be easily distinguished based on the length of the macronematous conidiophores (57–565 in *M. malaysiana vs.* 200–1120 µm in *M. samutensis*), and the

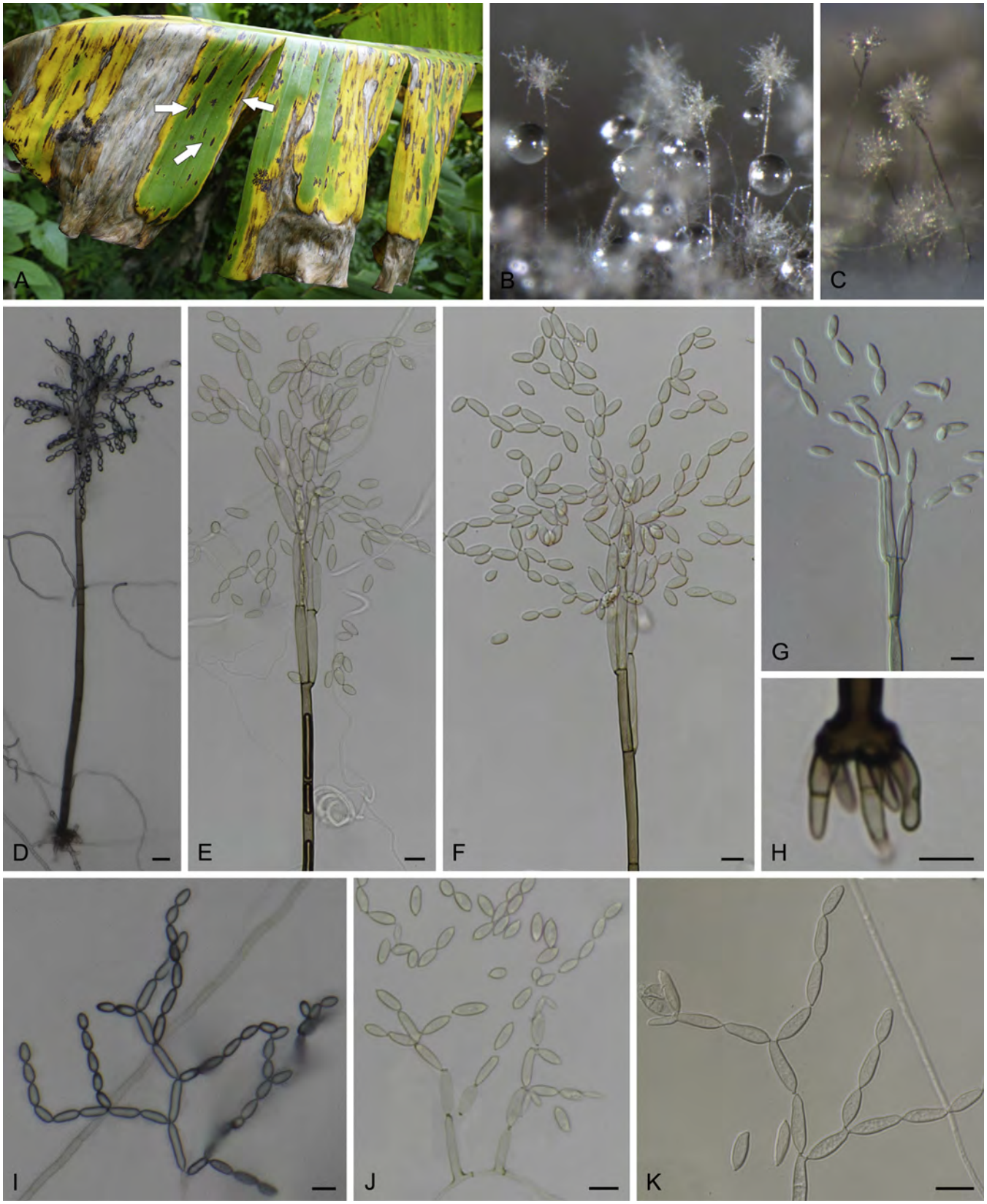

Fig. 30. *Metulocladosporiella* spp. **A.** Disease symptoms on *Musa* sp (indicated by the arrows). **B–K.** Asexual morph. **B–D.** Macronematous conidiophores. **B.** *Metulocladosporiella musicola* (CBS 121396). **C.** *Metulocladosporiella musicola* (ex-type CBS 110960). **D.** *Metulocladosporiella musae* (CPC 33937). **E–G.** Conidiogenous apparatus. **E, F.** *Metulocladosporiella musae* (CPC 33937). **G.** *Metulocladosporiella musicola* (ex-type CBS 110960). **H.** Lobed bases of macronematous conidiophore of *Metulocladosporiella musae* (CPC 33937). **I–K.** Micronematous conidiophores. **I, J.** *Metulocladosporiella musae* (CPC 33937). **K.** *Metulocladosporiella musicola* (CBS 121396). Scale bars = 10 µm.

almost total absence of secondary branches in *M. samutensis*. Moreover, *M. malaysiana* produces fewer micronematous conidiophores than the other species of *Metulocladosporiella*.

Metulocladosporiella musigena Y. Marín, Cheew. & Crous, **sp. nov.** MycoBank MB824033. Fig. 34.

Etymology: Name refers to *Musa*, the host from which it was isolated.

Mycelium internal and external, superficial; *hyphae* 1–4 µm wide, branched, septate, occasionally slightly constricted at septa, with small swellings, hyaline, subhyaline to pale

Table 10. DNA barcodes of accepted *Metulocladosporiella* spp.

Species	Isolates[1]	GenBank accession numbers[2]			References
		ITS	*cal*	*tef1*	
Metulocladosporiella chiangmaiensis	CBS 143918[T]	MG934443	MG934522	MG934476	Present study
M. malaysiana	CBS 143919[T]	MG934444	MG934523	MG934477	Present study
M. musae	CBS 161.74[ET]	DQ008137	–	MG934478	Crous *et al.* (2006a), present study
	CBS 113863	DQ008138	MG934524	MG934479	Crous *et al.* (2006a), present study
	CPC 33937	MG934445	MG934525	MG934480	Present study
M. musicola	CBS 110960[T]	DQ008127	MG934526	MG934481	Crous *et al.* (2006a), present study
	CBS 110962	MG934446	MG934527	MG934482	Crous *et al.* (2006a), present study
	CBS 110964	MG934447	MG934528	MG934483	Crous *et al.* (2006a), present study
	CBS 113860	DQ008130	MG934529	MG934484	Crous *et al.* (2006a), present study
	CBS 113861	DQ008131	MG934530	MG934485	Crous *et al.* (2006a), present study
	CBS 113862	DQ008132	MG934531	MG934486	Crous *et al.* (2006a), present study
	CBS 113864	DQ008133	MG934532	MG934487	Crous *et al.* (2006a), present study
	CBS 113865	DQ008134	MG934533	MG934488	Crous *et al.* (2006a), present study
	CBS 113873	DQ008135	MG934534	MG934489	Crous *et al.* (2006a), present study
	CPC 18124	MG934448	MG934535	MG934490	Present study
	CPC 32807	MG934449	MG934536	MG934491	Present study
	CPC 32849	MG934450	MG934537	MG934492	Present study
	CPC 32970	MG934451	MG934538	MG934493	Present study
M. musigena	CBS 143920[T]	MG934452	MG934539	MG934494	Present study
M. samutensis	CBS 143921[T]	MG934453	MG934540	MG934495	Present study

[1] CBS: Westerdijk Fungal Biodiversity Institute, Utrecht, the Netherlands; CPC: Culture collection of Pedro Crous, housed at the Westerdijk Fungal Biodiversity Institute. [T] and [ET] indicate ex-type and ex-epitype strains.
[2] ITS: internal transcribed spacers and intervening 5.8S nrDNA; *cal*: partial calmodulin gene; *tef1*: partial translation elongation factor 1-alpha gene.

olivaceous, thin-walled, smooth, hyphae occasionally aggregated, forming ropes; with a great amount of intermixed *micronematous conidiophores*, erect from vegetative mycelium, intercalary, straight to flexuous, unbranched, subhyaline, usually with simple terminal conidial chains. *Macronematous conidiophores* (115–)170–780 µm long, arising from superficial hyphae, erect, solitary to loosely aggregated, composed of a subcylindrical stipe, 4.5–7.5 µm wide, 5–14 septate, swollen or lobed at base, 7.5–14.5(–18.5) µm diam, with short, rhizoid, subhyaline to pale brown hyphae growing from base, medium to brown in lower half, paler towards apex, tips brown, pale brown or subhyaline, thick-walled below, thinner-walled towards apex, smooth; *apex* usually persistently branched, branched part composed of usually fairly compact, closely arranged subcylindrical branchlets, or sometimes giving rise directly to conidiogenous cells; *primary branches* 19–32.5(–43.5) × 3–4.5 µm, 0(–1)-septate, giving rise to 1–3 secondary branches, or to conidiogenous cells; *secondary branches* 15.5–31(–38) × 3–4.5 µm, 0(–1)-septate, giving rise to 1–3 conidiogenous cells; *conidiogenous cells* 13.5–28(–39.5) × 2.5–5 µm, subcylindrical, terminal or occasionally intercalary, sympodial, polyblastic, conidiogenous loci 1–2 µm wide, subconspicuous to conspicuous, subdenticulate, somewhat protuberant, truncate, wall unthickened to somewhat so, darkened-refractive. *Conidia* 5–15.5(–19.5) × 2–3.5 µm, in simple and branched acropetal chains, ellipsoid-ovoid, fusoid, subcylindrical, aseptate, subhyaline to pale brown, thin-walled, smooth, with 1–3(–4) hila, 0.8–1.2 µm diam, up to 1.7 µm diam at base of ramoconidia, truncate, unthickened or almost so, and somewhat darkened-refractive, secession schizolytic; *ramoconidia* 8–20.5 × 2.5–4 µm.

Culture characteristics: Colonies on PDA reaching 21–24 mm diam after 2 wk at 25 °C, moderate aerial mycelium, powdery, umbonate; surface smoke grey to grey olivaceous; reverse grey olivaceous to olivaceous black. Colonies on OA reaching 31–34 mm diam after 2 wk at 25 °C, moderate aerial mycelium, powdery, umbonate, slightly lobate; surface dark olivaceous, mycelium smoke grey to grey olivaceous; reverse dark slate blue.

Material examined: **Thailand**, Chiang Mai Province, Mae Rim District, Queen Sirikit Botanic Garden, from *Musa* sp. (*Musaceae*), 19 Jul. 2008, P.W. Crous & R. Cheewangkoon (**holotype** CBS H-23395, culture ex-type CBS 143920 = CPC 31490).

Notes: *Metulocladosporiella musigena* produces macronematous conidiophores directly producing conidiogenous cells at the apex, or composed of fairly compact branches, which are not observed in the other species of the genus. Moreover, it is characterised by the production of an excessive number of micronematous conidiophores.

Metulocladosporiella samutensis Y. Marín, Luangsa-ard & Crous, **sp. nov.** MycoBank MB824034. Fig. 35.

Etymology: Name from Samut Songkhram, the province in Thailand from where it was isolated.

Mycelium internal and external, superficial; *hyphae* 1.5–4 µm wide, branched, septate, occasionally slightly constricted at septa, with small swellings, hyaline, subhyaline to pale brown, thin-walled, smooth, hyphae occasionally aggregated, forming ropes; with intermixed *micronematous conidiophores*, erect from vegetative mycelium, intercalary, straight to flexuous, unbranched, subhyaline to pale brown, usually with simple terminal conidial chains. *Macronematous conidiophores* (200–)425–1000(–1120) µm long, arising from superficial hyphae, erect, solitary to loosely aggregated, composed of a subcylindrical stipe, 5.5–7.5(–8) µm wide, (4–)8–21(–29)-septate, swollen or lobed at base, 7–14.5(–20.5) µm diam, with short rhizoid subhyaline to pale brown hyphae growing from base, medium to brown in lower half, paler towards apex, tips pale

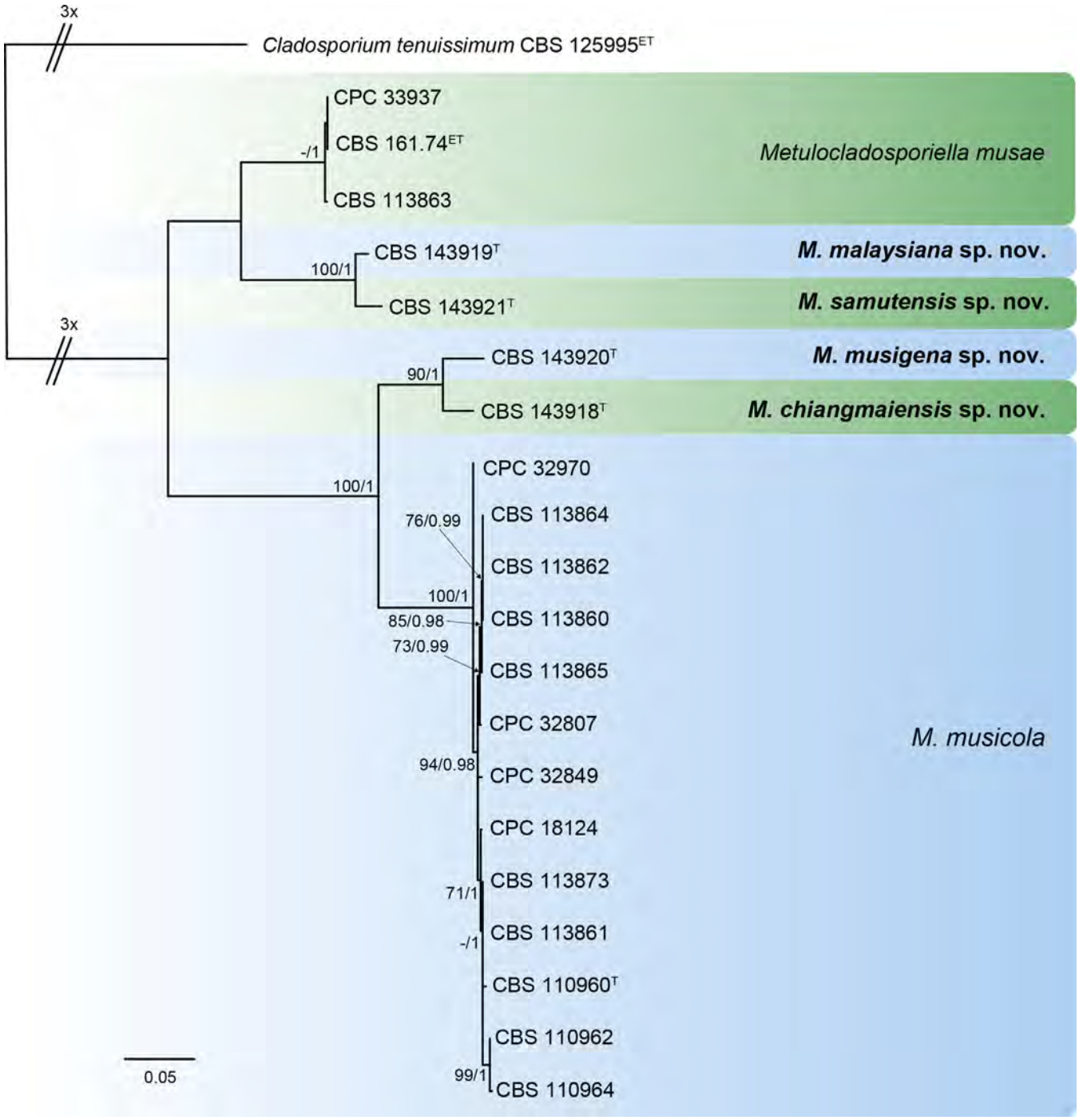

Fig. 31. RAxML phylogram obtained from the combined ITS (667 bp), *cal* (524 bp) and *tef1* (454 bp) sequence alignment of taxa belonging to *Metulocladosporiella*. The tree was rooted to *Cladosporium tenuissimum* CBS 125995ET. The novelties proposed in this study are indicated in **bold**. RAxML bootstrap support (BS) values above 70 % and Bayesian posterior probability scores above 0.95 are shown at the nodes. GenBank accession numbers are indicated in Table 10. T and ET indicate ex-type and ex-epitype strains, respectively. TreeBASE: S21899.

brown or occasionally subhyaline, thick-walled below, thinner towards apex, smooth; *apex* giving rise directly to 1–2(–3) conidiogenous cells, or branched, branched part composed of loosely arranged subcylindrical branchlets; *primary branches* 24.5–39(–44) × 3–4(–5) µm, 0–1-septate, giving rise to 1–2(–3) conidiogenous cells, or rarely 1–2 secondary branches; *conidiogenous cells* (12–)14–25(–32) × 3.5–5 µm, subcylindrical, terminal or occasionally intercalary, sympodial, polyblastic, conidiogenous loci 1–2 µm wide, subconspicuous to conspicuous, subdenticulate, somewhat protuberant, truncate, wall unthickened to somewhat so, darkened-refractive. *Conidia* 4.5–12.5(–13.5) × 3–4 µm, in simple and branched acropetal chains, ellipsoid–ovoid, fusiform, subcylindrical, aseptate, subhyaline to pale brown, thin-walled, smooth, with 1–3 hila, 1–1.5(–2) µm diam, truncate, unthickened or almost so, and somewhat darkened-refractive, secession schizolytic; *ramoconidia* 8–13.5(–15.5) × 3–5 µm.

Culture characteristics: Colonies on PDA reaching a diameter of 34–36 mm after 2 wk at 25 °C, moderate aerial mycelium, powdery because of macroconidia, margins fringed; surface smoke grey to grey olivaceous, margins olivaceous; reverse olivaceous grey. Colonies on OA reaching a diameter of 39–40 mm after 2 wk at 25 °C, moderate aerial mycelium, powdery because of macroconidia, margins fringed; surface

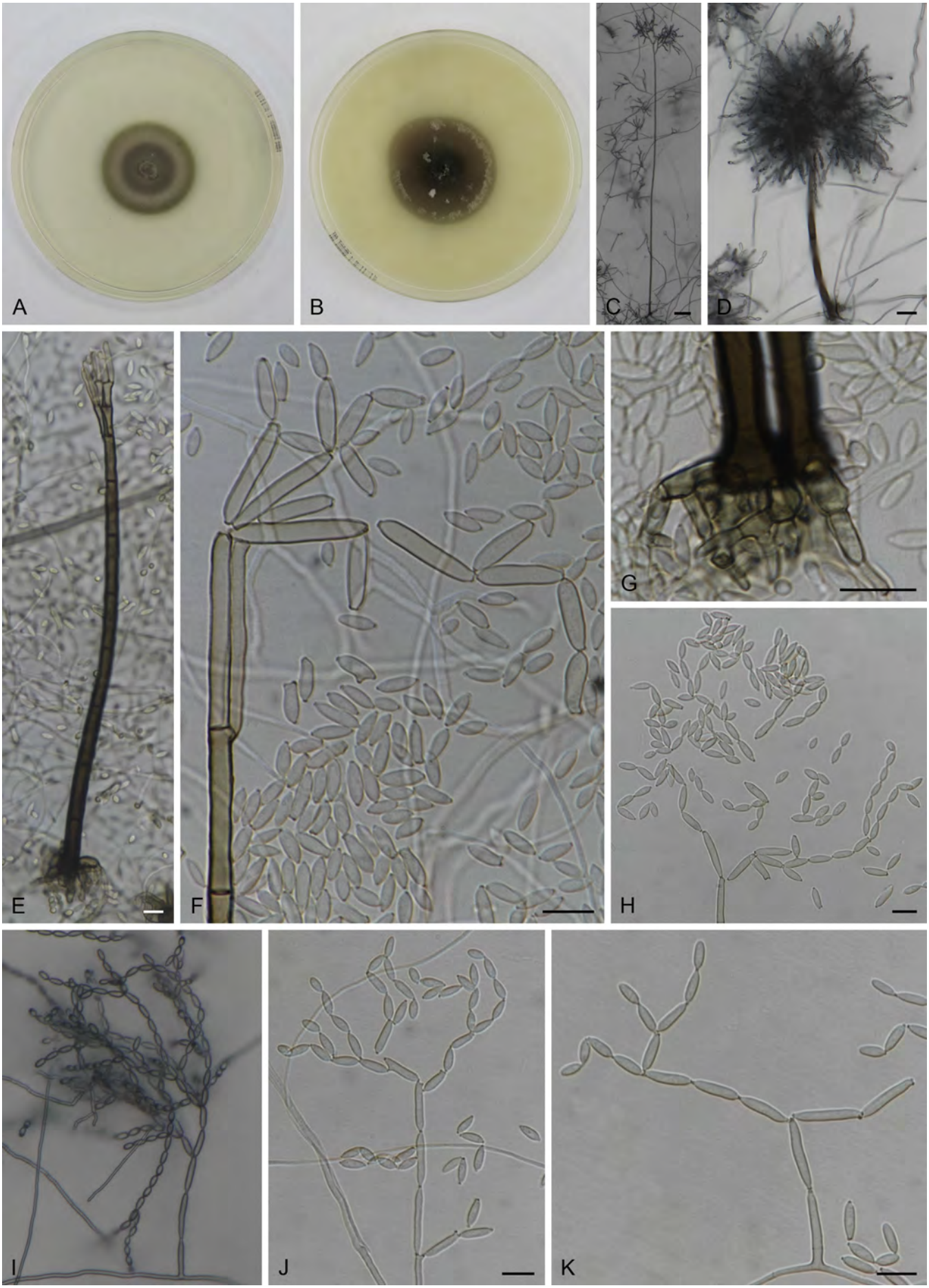

Fig. 32. *Metulocladosporiella chiangmaiensis* (ex-type CBS 143918). **A.** Colony on PDA. **B.** Colony on OA. **C–E.** Macronematous conidiophores. **F.** Conidiogenous apparatus. **G.** Lobed bases of macronematous conidiophore. **H–K.** Micronematous conidiophores. Scale bars: C = 50 µm; D = 20 µm; others = 10 µm.

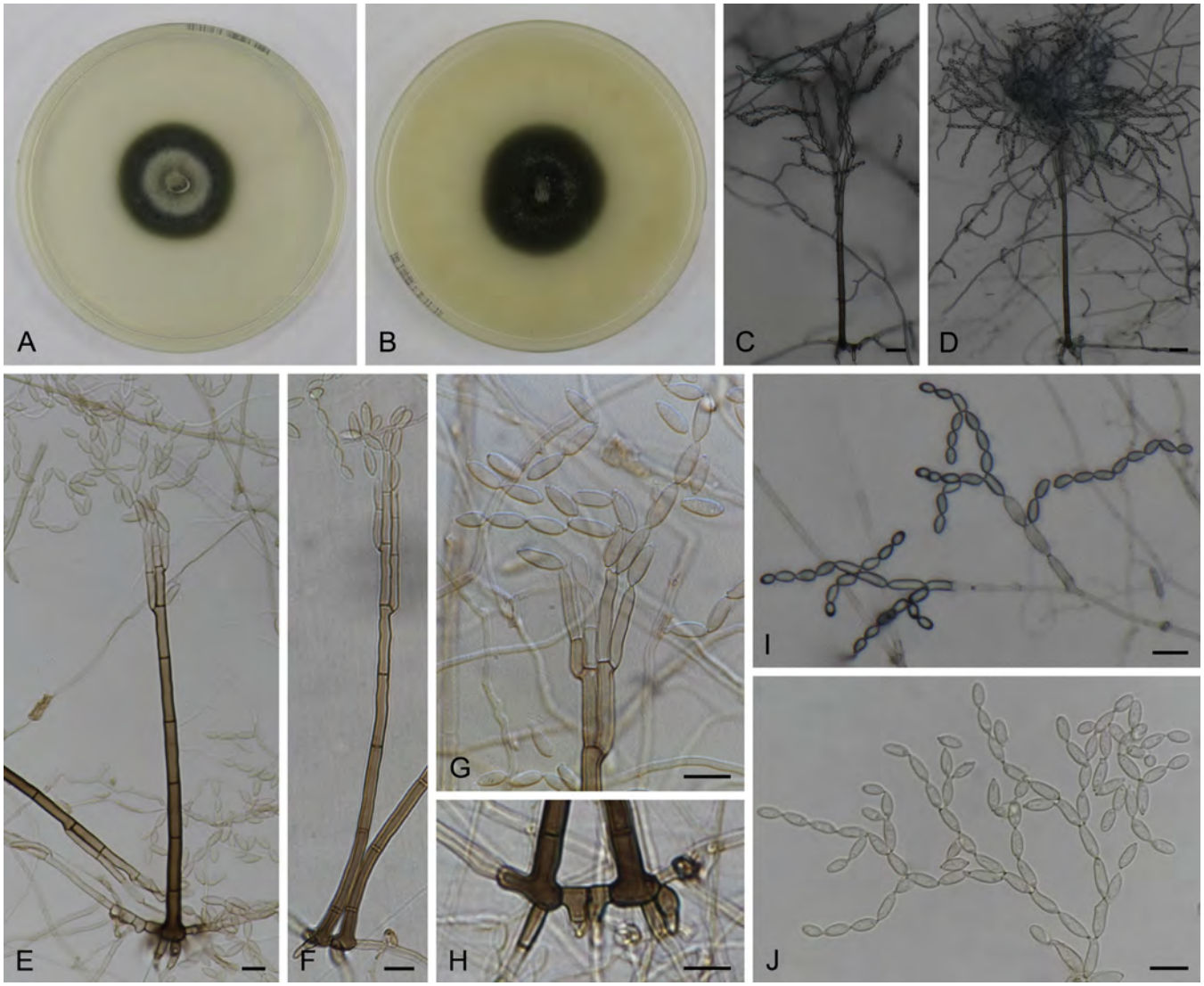

Fig. 33. *Metulocladosporiella malaysiana* (ex-type CBS 143919). **A.** Colony on PDA. **B.** Colony on OA. **C–F.** Macronematous conidiophores. **G.** Conidiogenous apparatus. **H.** Lobed bases of macronematous conidiophore. **I, J.** Micronematous conidiophores. Scale bars: C, D = 20 µm; others = 10 µm.

smoke grey to grey olivaceous, margins grey olivaceous; reverse olivaceous grey.

Material examined: **Thailand**, Samut Songkhram Province, from *Musa* sp. (*Musaceae*), 8 Jun. 2008, P.W. Crous (**holotype** CBS H-23396, culture ex-type CBS 143921 = CPC 33939).

Notes: *Metulocladosporiella samutensis* can easily be distinguished from other species of *Metulocladosporiella* by the production of conidiogenous cells directly from the apex, or loosely arranged primary branches, being almost totally absent of secondary branches.

Authors: Y. Marin-Felix, R. Cheewangkoon, J. Luangsa-ard & P.W. Crous

Microdochium Syd. & P. Syd., Ann. Mycol. 22: 267. 1924. Fig. 36.
Synonyms: *Monographella* Petr., Ann. Mycol. 22: 144. 1924.
Griphosphaerella Petr., Ann. Mycol. 25: 209. 1927.
Gloeocercospora D.C. Bain & Edgerton, Phytopathology 33: 225. 1943. (nom. inval., Art. 39.1, Melbourne).
Gloeocercospora D.C. Bain & Edgerton ex Deighton, Trans. Brit. Mycol. Soc. 57: 358. 1971.
Gerlachia W. Gams & E. Müll., Neth. J. Pl. Path. 86: 49. 1980.

Classification: *Sordariomycetes*, *Xylariomycetidae*, *Xylariales*, *Microdochiaceae*.

Type species: *Microdochium phragmitis* Syd. Holotype: K-IMI 193888. Epitype and ex-epitype strain designated by Hernández-Restrepo *et al.* (2016a): CBS H-22135, CBS 285.71.

DNA barcode (genus): LSU.

DNA barcodes (species): ITS, *rpb2*, *tub2*. Table 11. Fig. 37.

Ascomata perithecial, immersed, subepidermal, solitary or in groups, pale brown to black, globose, subglobose to oval; *ostiole* central, neck papillate and often acute, usually more distinctly pigmented than ascomatal body, filled with slightly clavate periphyses; *ascomatal wall* brown, thin-walled, thickened and darker around ostiole, in face view *textura angularis-epidermoidea*. *Hamathecium* comprising septate, filamentous, apically free, thin-walled paraphyses. *Asci* unitunicate, oblong to clavate, with 8 bi- to multiseriate ascospores, apex with an amyloid, refractive, flat, funnel-shaped ring. *Ascospores* clavate, fusoid or oblong, hyaline to brownish, straight or curved, smooth, septate. *Conidiomata* absent or present, sporodochial, epidermal or subepidermal, erumpent through stomata, or rupture of outer epidermal wall and cuticle, or by specialised egression hyphae

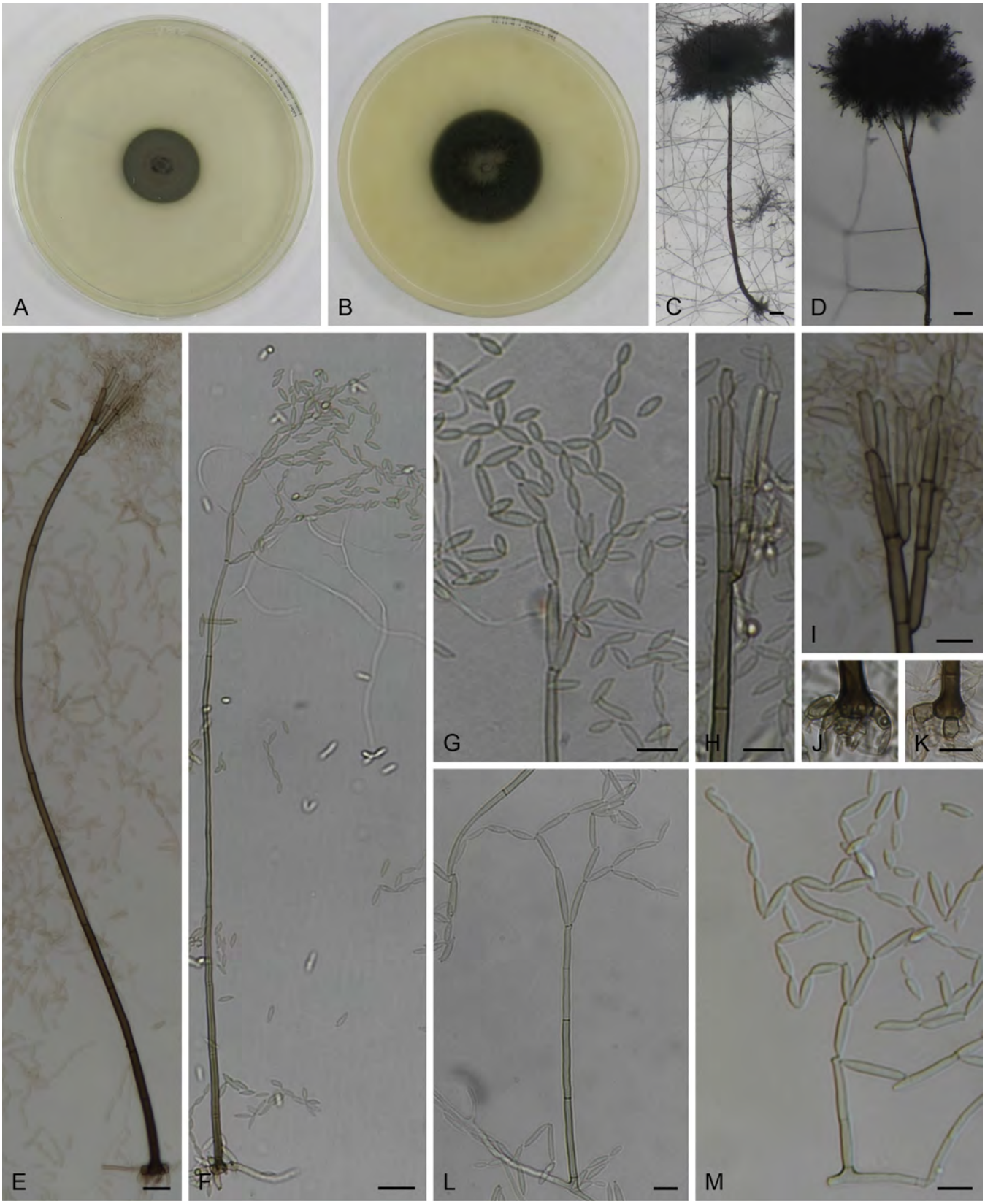

Fig. 34. *Metulocladosporiella musigena* (ex-type CBS 143920). **A.** Colony on PDA. **B.** Colony on OA. **C–F.** Macronematous conidiophores. **G–I.** Conidiogenous apparatus. **J, K.** Lobed bases of macronematous conidiophore. **L, M.** Micronematous conidiophores. Scale bars: C–F = 20 µm; G–M = 10 µm; K applies to J, K.

through outer epidermal wall, hyaline, pseudoparenchymatic, spreading after egress. *Conidiophores* more or less verticillate, often slightly differentiated, reduced to conidiogenous cells, hyaline, smooth. *Conidiogenous cells* holoblastic, discrete, hyaline, smooth, solitary or aggregated in small sporodochia. Two kinds: with sympodial proliferation, cylindrical or slightly tapering to clavate, denticulate with one or more apical denticles; or with percurrent proliferation (annellidic), subcylindrical, obpyriform, ampulliform to lageniform. *Conidia* dry or in slimy mass, unicellular or multiseptate, hyaline, smooth, lunate, falcate, fusiform, filiform, obovoid or subpyriform, straight or curved, apex rounded, base flattened. Sometimes conidia originate directly

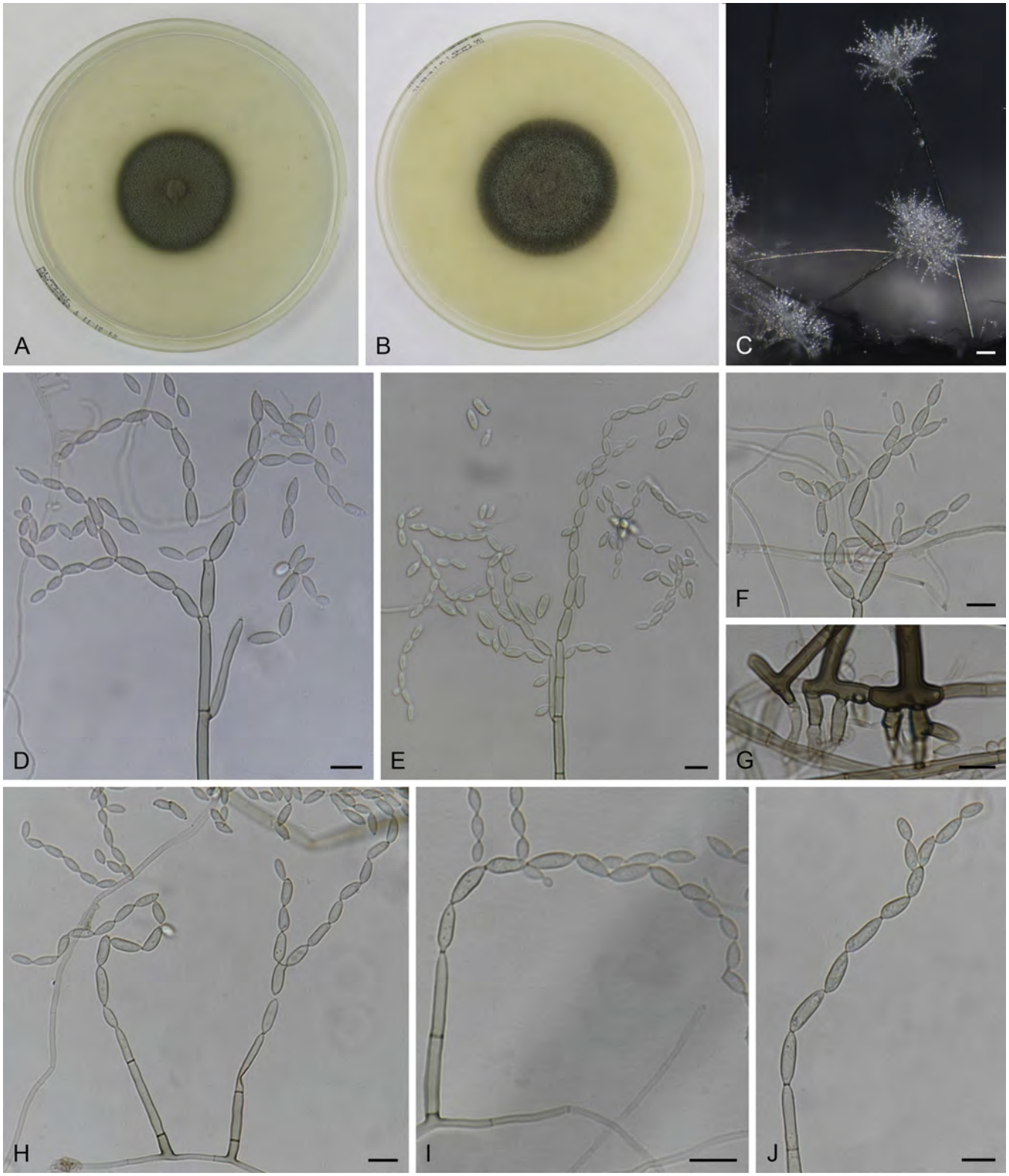

Fig. 35. *Metulocladosporiella samutensis* (ex-type CBS 143921). **A.** Colony on PDA. **B.** Colony on OA. **C.** Macronematous conidiophores. **D–F.** Conidiogenous apparatus. **G.** Lobed bases of macronematous conidiophore. **H–J.** Micronematous conidiophores. Scale bars: C = 20 µm; others = 10 µm.

from hyphae. *Chlamydospores* terminal or intercalary, solitary, in chains or grouped in clusters, brown (adapted from Hernández-Restrepo *et al.* 2016a).

Culture characteristics: Colonies on OA saffron, salmon, peach or white when young, some species grey or dark grey when mature, glabrous or with moderate amount of mycelium, cottony to floccose, margin effuse.

Optimal media and cultivation conditions: OA at 25 °C under dark conditions.

Distribution: Worldwide.

Hosts: Mainly pathogens of grasses and cereals, but some also occur on non-grass hosts as *Opuntia* (*Cactaceae*) and *Lycopodium* (*Lycopodiaceae*), may cause losses to crops including rice,

maize, wheat, barley and sorghum. Other species can be found in harvested grains.

Disease symptoms: Microdochium patch or pink snow patch, leaf scald disease, tar spot disease, root necrosis and decay of grasses, leaf spots, among others.

Notes: *Microdochium* includes plant pathogenic as well as saprobic and soil fungi (Sydow 1924, de Hoog & Hermanides-Nijhof 1977, Parkinson *et al.* 1981, Jaklitsch & Voglmayr 2012, Zhang *et al.* 2015, Hernández-Restrepo *et al.* 2016a, Crous *et al.* 2018). For many years, species of *Microdochium* were recognised as fusarium-like fungi; however, morphological and molecular data separate these genera. Conidiogenesis in *Microdochium* is not phialidic as in true *Fusarium* species and the conidia have truncate basal cells rather than "foot-cells". The sexual morphs of *Microdochium* are monographella-like, and it belongs in the *Microdochiaceae* (*Xylariales*) phylogenetically distant from true *Fusarium* in *Nectriaceae* (*Hypocreales*).

For an accurate species identification of *Microdochium* species, DNA sequence analyses are required. Among the four loci studied (i.e. LSU, ITS, *rpb2* and *tub2*), LSU is useful only for generic placement. Phylogenies based on individual gene regions of ITS, *rpb2* and *tub2*, can be used to distinguish 14 species in *Microdochium*; those phylogenies generated from *tub2* show longer distances between species and higher support values. This is more informative than ITS and *rpb2* (Hernández-Restrepo *et al.* 2016a).

References: Parkinson *et al.* 1981, Müller & Samuels 1984, Zhang *et al.* 2015 (morphology and pathogenicity); von Arx 1981, 1984, Braun 1995 (taxonomy); Hong *et al.* 2008 (pathogenicity); Hernández-Restrepo *et al.* 2016a (morphology and phylogeny).

Microdochium novae-zelandiae Hern.-Restr., Thangavel & Crous, **sp. nov.** MycoBank MB824606. Fig. 38.

Etymology: Name is derived from New Zealand, the country where this fungus was collected.

Mycelium superficial and immersed, composed of septate, branched, hyaline, smooth, 1–2.5 wide hyphae. *Conidiomata* sporodochium-like, formed in aerial mycelium or on agar surface, hyaline to pink. *Conidiophores* often reduced to conidiogenous cells. *Conidiogenous cells* 4–10 × 2–3 µm, integrated, terminal, polyblastic, proliferation sympodial, cylindrical to lageniform, hyaline, smooth; sometimes conidia formed directly on mycelium. *Conidia* 5.5–10 × 2–2.5 µm, solitary, fusoid, allantoid, lunate or slightly sigmoid, straight or curved, hyaline, smooth, 0(–1)-septate, base truncate. *Chlamydospores* not observed.

Culture characteristics: Colonies on OA reaching 45 mm diam after 1 wk at 25 °C, centre flat and rosy buff, periphery cottony and white, margins effuse; reverse rosy buff in centre.

Materials examined: **New Zealand**, Christchurch, from turf leaves (*Poaceae*), 2015, R. Thangavel (**holotype** CBS H-23384, culture ex-type CBS 143847 = CPC 29376 = ICMP 21872 = MPI T15_05208H); *ibid*., Richmond, Nelson, on spruce (*Pinaceae*), 2014, R. Thangavel (CPC 29693 = MPI T14_00277D).

Notes: *Microdochium novae-zelandiae* is known from two isolates, both of which were collected in New Zealand from different hosts belonging to the families *Pinaceae* and *Poaceae*. Based on a four-gene analysis, the new species was placed in a clade distinct from *M. bolleyi*, *M. colombiense*, *M. majus* and *M. nivale* (Fig. 37). Morphologically, *M. novae-zelandiae* has conidia similar in size to *M. bolleyi* and *M. colombiense*. However, subtle morphological differences exist in the conidial shapes of these taxa with *M. novae-zelandiae* having sigmoidal conidia. Compared with *M. phragmitis*, conidia of *M. novae-zelandiae* are smaller, mainly aseptate with variable shape [5.5–10 × 2–2.5 µm, 0(–1)-septate, fusiform, allantoid, lunate or slightly sigmoid in *M. novae-zelandiae vs*. 10–14.5 × 2–3 µm, 0–1-sepate, fusiform to navicular in *M. phragmitis*].

Authors: M. Hernández-Restrepo, R. Thangavel & P.W. Crous

Oculimacula Crous & W. Gams, Eur. J. Pl. Path. 109: 845. 2003. Fig. 39.
Synonym: *Helgardia* Crous & W. Gams, Eur. J. Pl. Path. 109: 845. 2003.

Classification: *Leotiomycetes*, *Leotiomycetidae*, *Helotiales*, *Incertae sedis*.

Type species: *Oculimacula yallundae* (Wallwork & Spooner) Crous & W. Gams = *Helgardia herpotrichoides* (Fron) Crous & W. Gams, basionym: *Cercosporella herpotrichoides* Fron. Holotype: K(M) 233697. Neotype and ex-neotype strain of *Helgardia herpotrichoides* designated by Crous *et al.* (2003): CBS H-23003, CBS 110665.

DNA barcode (genus): LSU.

DNA barcodes (species): ITS, *tef1*. Table 12. Fig. 40.

Ascomata 0.5–2.5 mm diam, apothecial, sessile, gregarious, circular to lobate, on a subiculum of white to dark brown hyphae, attached to substrate via a superficial mat of pale brown, thin hyphae. *Disk* smooth, grey with a pale grey margin, becoming emarginate and flattened to convex at maturity. *Receptacle* pale brown to grey-brown, cup-shaped. *Medullary excipulum* of multiseptate, hyaline hyphae. *Ectal excipulum* of thin-walled, dark brown, angular cells, becoming more elongated towards margin. *Paraphyses* filiform with obtuse ends, similar in length to asci. *Asci* 8-spored, unitunicate, clavate to subcylindrical or fusoid, with a short stalk, and an apical pore staining blue in Melzer's reagent. *Ascospores* bi- to multiseriate, hyaline, smooth, aseptate, fusoid to subcylindrical or clavate with rounded ends, mostly straight. *Conidiophores* fasciculate or solitary on superficial mycelium, or arising from pale brown stromata, subcylindrical to geniculate-sinuous, rarely branching, hyaline to pale olivaceous, smooth, consisting of conidiogenous cells only, or slightly differentiated with up to 2 septa. *Conidiogenous cells* integrated, proliferating sympodially at apex, with inconspicuous, dense geniculations; *conidiogenous loci* unthickened, inconspicuous, not darkened. *Conidia* solitary, hyaline, smooth, arranged in slimy packets, acicular, filiform, straight to curved, one- to multiseptate, forming smaller, secondary conidia via microcyclic conidiation (adapted from Crous *et al.* 2003).

Culture characteristics: Colonies with moderate aerial mycelium giving a cottony appearance. On PDA surface grey to olive grey, brownish-grey, pinkish-grey or greenish; reverse grey to greenish-black, greenish, brownish or creamy pink.

Optimal media and cultivation conditions: SNA under continuous near-ultraviolet light at 25 °C.

Distribution: Africa, Australasia, Europe, New Zealand and North America.

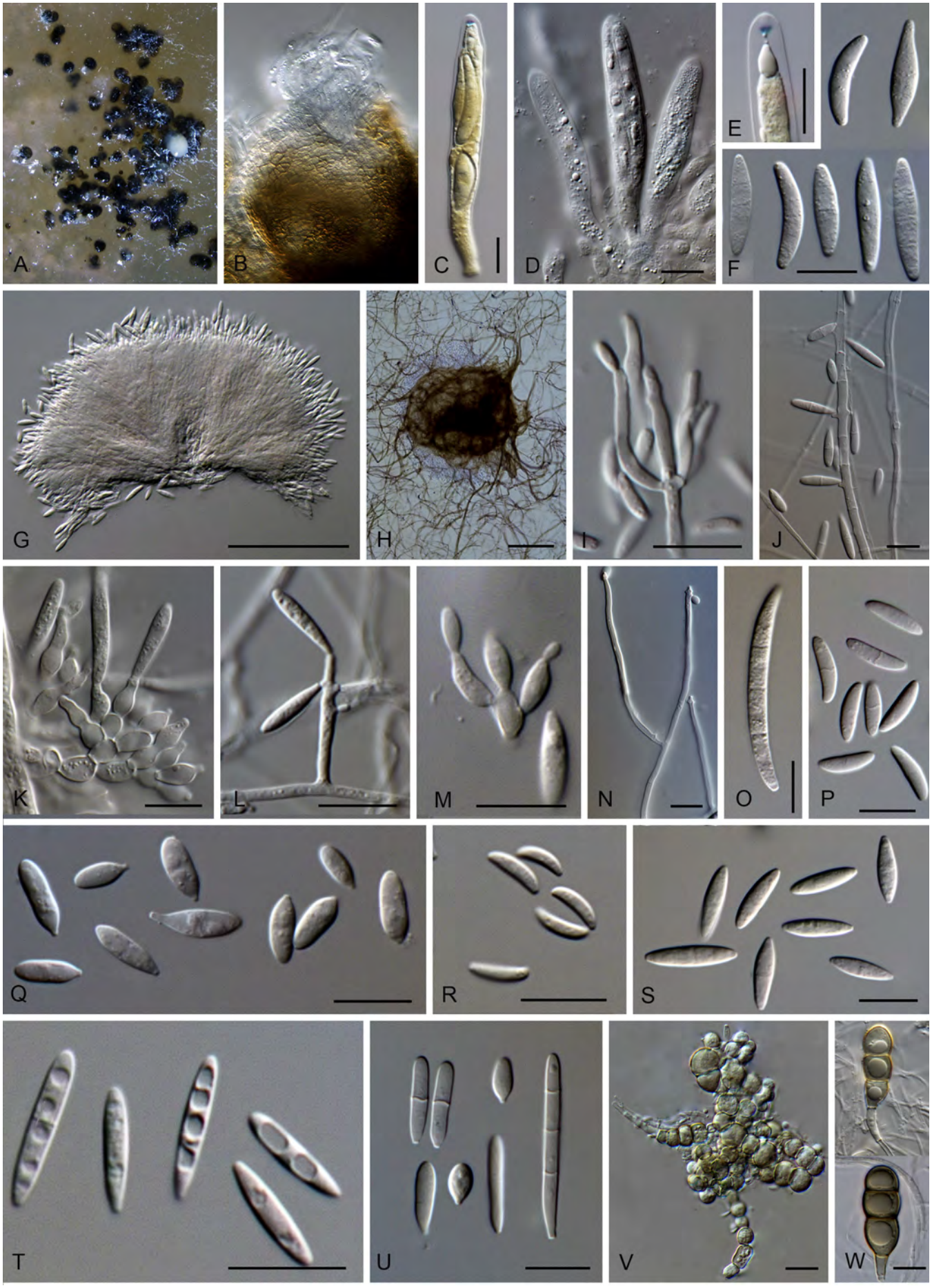

Table 11. DNA barcodes of accepted *Microdochium* spp.

Species	Isolates[1]	GenBank accession numbers[2]			References
		ITS	*rpb2*	*tub2*	
Microdochium albescens	CBS 290.79	KP859014	KP859123	KP859077	Hernández-Restrepo *et al.* (2016a)
Mi. bolleyi	CBS 540.92	KP859010	KP859119	KP859073	Hernández-Restrepo *et al.* (2016a)
	CPC 29378	LT990657	LT990643	LT990610	Present study
Mi. citrinidiscum	CBS 109067^{T}	KP859003	KP859112	KP859066	Hernández-Restrepo *et al.* (2016a)
Mi. colombiense	CBS 624.94^{T}	KP858999	KP859108	KP859062	Hernández-Restrepo *et al.* (2016a)
Mi. chrysanthemoides	CGMCC3.17929^{T}	KU746690	–	KU746781	Zhang *et al.* (2017)
Mi. fisheri	CBS 242.91^{T}	KP859015	KP859124	KP859078	Hernández-Restrepo *et al.* (2016a)
Mi. lycopodinum	CBS 122885^{T}	KP859016	KP859125	KP859079	Hernández-Restrepo *et al.* (2016a)
Mi. majus	CBS 741.79	KP859001	KP859110	KP859064	Hernández-Restrepo *et al.* (2016a)
Mi. neoqueenslandicum	CBS 108926^{T}	KP859002	KP859111	KP859065	Hernández-Restrepo *et al.* (2016a)
Mi. nivale	CBS 116205^{T}	KP859008	KP859117	KP859071	Hernández-Restrepo *et al.* (2016a)
Mi. novae-zelandiae	CBS 143847	LT990655	LT990641	LT990608	Present study
	CPC 29693	LT990656	LT990642	LT990609	Present study
Mi. phragmitis	CBS 285.71^{ET}	KP859013	KP859122	KP859076	Hernández-Restrepo *et al.* (2016a)
Mi. seminicola	CBS 139951^{T}	KP859038	KP859147	KP859101	Hernández-Restrepo *et al.* (2016a)
Mi. sorghi	CBS 691.96	KP859000	KP859109	KP859063	Hernández-Restrepo *et al.* (2016a)
Mi. tainanense	CBS 269.76^{T}	KP859009	KP859118	KP859072	Hernández-Restrepo *et al.* (2016a)
Mi. trichocladiopsis	CBS 623.77^{T}	KP858998	KP859107	KP859061	Hernández-Restrepo *et al.* (2016a)

[1] CBS: Westerdijk Fungal Biodiversity Institute, Utrecht, the Netherlands; CPC: Personal collection of Pedro Crous housed at the Westerdijk Fungal Biodiversity Institute; CGMCC: China General Microbiological Culture Collection Center. ^{T} and ^{ET} indicate ex-type and ex-epitype strains.
[2] ITS: internal transcribed spacers and intervening 5.8S nrDNA; *rpb2*: partial RNA polymerase II second largest subunit gene; *tub2*: partial β-tubulin gene.

Hosts: *Poaceae*, including *Triticum* and *Hordeum*, among others.

Disease symptoms: Eyespot lesions that girdle the stem and soften the stem-base.

Notes: *Oculimacula* encompasses four species associated with eyespot disease symptoms of cereals in the temperate regions of the world. Eyespot is an important disease of stem bases in which the infection occurs at or near the soil line, attacking chiefly the basal leaf sheaths and internodal tissues of the culms (Sprague & Fellows 1934, Lucas *et al.* 2000). The fungus sporulates in the fall and spring producing the disease, and survives the winter on diseased stubble standing or lying in the field (Sprague & Fellows 1934). Disease control relies on the use of fungicides, delayed seeding in the fall and by planting resistant cultivars (Murray 1996, Douhan *et al.* 2002).

Oculimacula was introduced by Crous *et al.* (2003) to accommodate sexual morphs previously classified in *Tapesia*, while *Helgardia* was introduced for the asexual morphs linked to *Oculimacula*. Johnston *et al.* (2014) synonymised these generic names and conserved the name *Oculimacula* because it is most commonly used by plant pathologists for the eyespot diseases of wheat and barley.

References: Sprague & Fellows 1934 (morphology and pathogenicity); Sprague 1936, Lucas *et al.* 2000 (pathogenicity); Nirenberg 1981 (morphology and pathogenicity); Crous *et al.* 2003 (morphology and phylogeny).

Oculimacula acuformis (Nirenberg) Y. Marín & Crous, **comb. et stat. nov.** MycoBank MB824638.
Basionym: *Pseudocercosporella herpotrichoides* var. *acuformis* Nirenberg, Z. PflKrankh. PflSchutz 88: 244. 1981.
Synonyms: *Ramulispora herpotrichoides* var. *acuformis* (Nirenberg) Boerema, *et al.*, Netherlands Journal of Plant Pathology, Supplement 1 98: 22. 1992.
Tapesia yallundae var. *acuformis* Boerema, *et al.*, Netherlands J. of Pl. Path., Supplement 1 98: 22. 1992. (nom. inval., Art. 40.3, Melbourne).
Ramulispora acuformis (Nirenberg) Crous, S. Afr. J. Bot. 61: 46. 1995.
Tapesia acuformis (Boerema, *et al.*) Crous, S. Afr. J. Bot. 61: 46. 1995. (nom. inval., Art. 40.3, Melbourne).
Helgardia acuformis (Nirenberg) Crous & W. Gams, Eur. J. Pl. Path. 109: 846. 2003.
Oculimacula acuformis (Boerema, *et al.*) Crous & W. Gams, Eur. J. Pl. Path. 109: 846. 2003. (nom. inval., Art. 40.3, Melbourne).

Material examined: Germany, Tübingen, from *Secale cereale* (*Poaceae*) culm base, 1978, H. Nirenberg (culture ex-type CBS 495.80).

Notes: *Oculimacula acuformis* was introduced to accommodate *Tapesia yallundae* var. *acuformis* (Crous *et al.* 2003). However,

Fig. 36. *Microdochium* spp. **A–F.** Sexual morph of *Microdochium seminicola* (ex-type CBS 139951). **A.** Colony overview. **B.** Ascomata. **C–E.** Asci. **F.** Ascospores. **G–U.** Asexual morphs. **G, H.** Sporodochium. **G.** *Microdochium phragmites* (CBS 423.78). **H.** *Microdochium lycopodinum* (CBS 109399). **I–N.** Conidiophores and conidiogenous cells. **I.** *Microdochium neoqueenslandicum* (ex-type CBS 108926). **J.** *Microdochium citrinidiscum* (ex-type CBS 109067). **K.** *Microdochium seminicola* (ex-type CBS 139951). **L.** *Microdochium phragmites* (ex-epitype CBS 285.71). **M.** *Microdochium phragmites* (CBS 423.78). **N.** *Microdochium fisheri* (ex-type CBS 242.91). **O–U.** Conidia. **O.** *Microdochium seminicola* (ex-type CBS 139951). **P.** *Microdochium lycopodinum* (CBS 109399). **Q.** *Microdochium fisheri* (ex-type CBS 242.91). **R.** *Microdochium neoqueenslandicum* (ex-type CBS 108926). **S.** *Microdochium phragmites* (CBS 423.78). **T.** *Microdochium phragmites* (ex-epitype CBS 285.71). **U.** *Microdochium citrinidiscum* (ex-type CBS 109067). **V, W.** Chlamydospores. **V.** *Microdochium bolleyi* (CPC 29379). **W.** *Microdochium trichocladiopsis* (ex-type CBS 623.77). Scale bars: H = 100 µm; G = 50 µm; others = 10 µm.

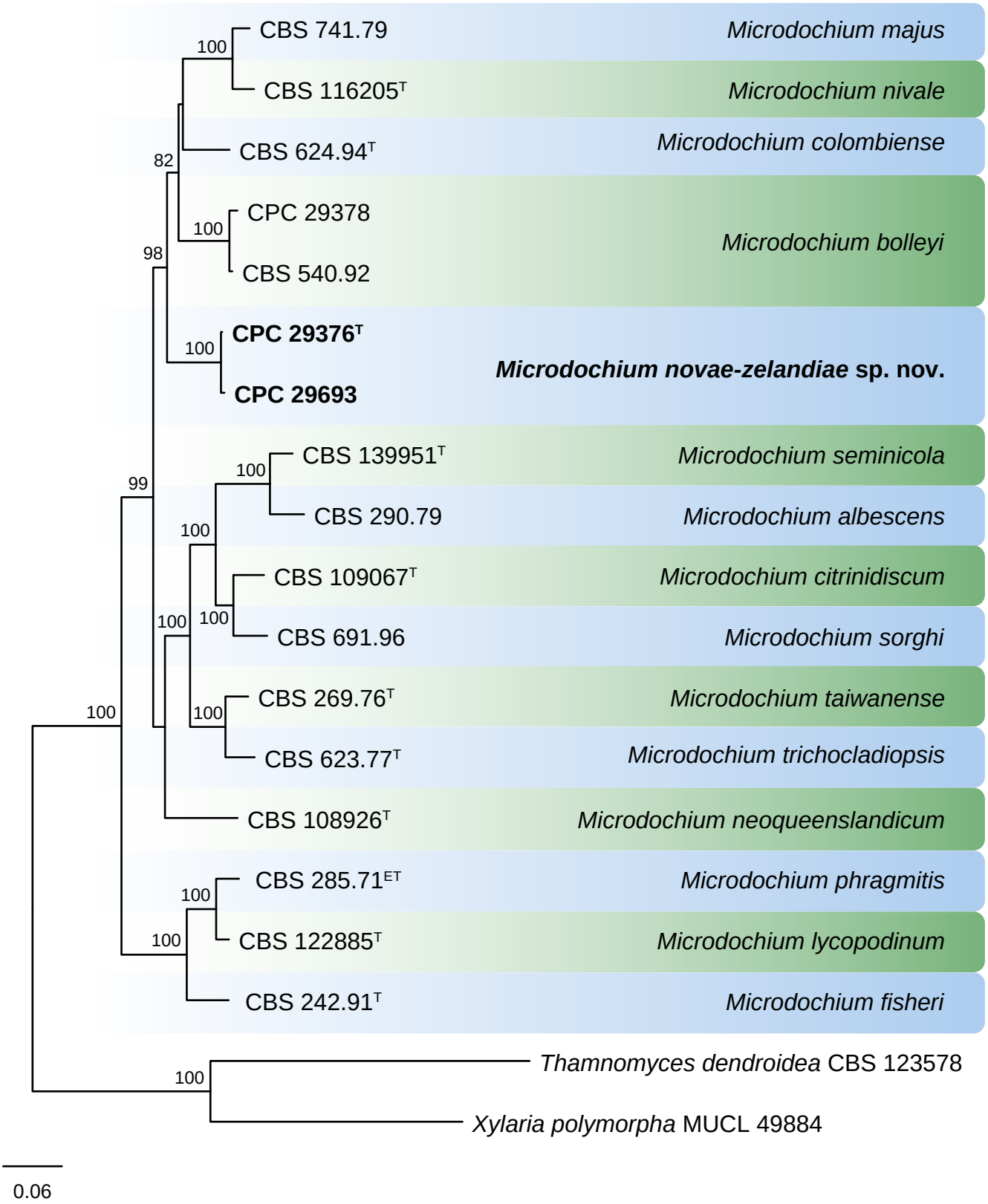

Fig. 37. RAxML phylogram obtained from the combined ITS (618 bp), LSU (838 bp), *tub2* (689 bp) and *rpb2* (858 bp) sequence alignment of all the accepted species of *Microdochium*. The tree was rooted to *Thamnomyces dendroidea* CBS 123578 and *Xylaria polymorpha* MUCL 49884. The novel species described in this study is shown in **bold**. RAxML bootstrap support (BS) values above 70 % are shown in the nodes. GenBank accession numbers are indicated in Table 11. ^{T} and ^{ET} indicate ex-type and ex-epitype strains, respectively. TreeBASE: S21899.

the combination is invalid because the basionym lacks details for the ex-type strain (Art 40.3). We have consequently proposed the new combination based on its asexual morph *Pseudocercosporella herpotrichoides* var. *acuformis*. This latter species was transferred to *Helgardia* in the same publication where *Oculimacula acuformis* was proposed and when both genera were first introduced (Crous *et al.* 2003). *Helgardia acuformis* is a synonym of *Oculimacula acuformis*.

Authors: Y. Marin-Felix, J.Z. Groenewald & P.W. Crous

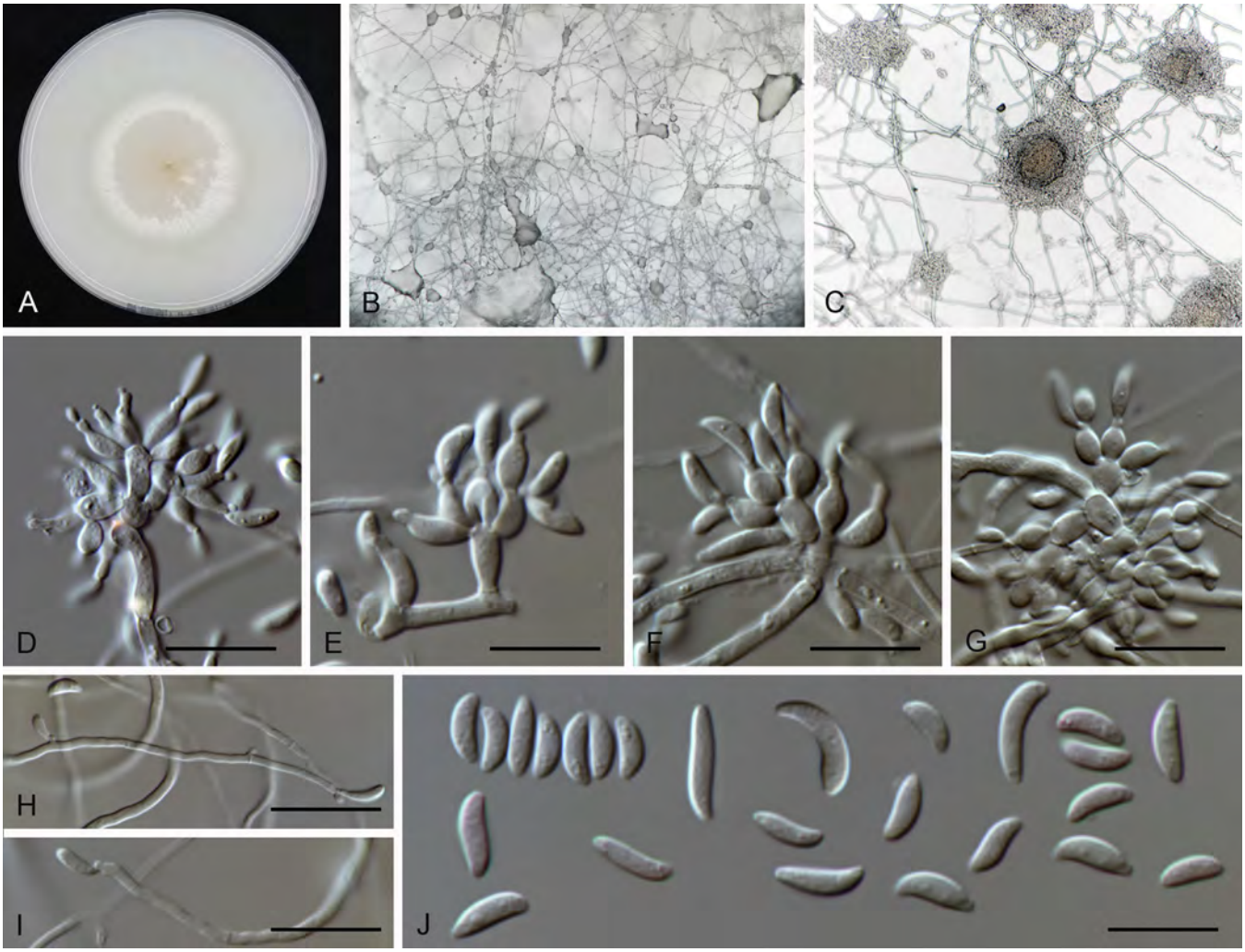

Fig. 38. *Microdochium novae-zelandiae* (ex-type CPC 29376). **A.** Colony overview. **B, C.** Sporodochium overview. **B.** From aerial mycelium. **C.** From agar surface. **D–G.** Conidiogenous cells and conidia. **H, I.** Hyphae and conidia. **J.** Conidia. Scale bars = 10 µm.

Paraphoma Morgan-Jones & J.F. White, Mycotaxon 18: 58. 1983. Fig. 41.
Synonym: *Phoma* section *Paraphoma* (Morgan-Jones & J.F. White) Boerema, Stud. Mycol. 32: 7. 1990.

Classification: *Dothideomycetes, Pleosporomycetidae, Pleosporales, Phaeosphaeriaceae.*

Type species: *Paraphoma radicina* (McAlpine) Morgan-Jones & J.F. White, basionym: *Pyrenochaeta radicina* McAlpine. Holotype: in VPRI [Australia, Shepparton, Victoria, on roots of *Prunus cerasus* (*Rosaceae*), 21 Oct 1901, Piscott, 2064.3]. Epitype and ex-epitype strain designated by de Gruyter *et al.* (2010): CBS H-16560, CBS 111.79.

DNA barcodes (genus): LSU, SSU.

DNA barcodes (species): ITS, *rpb2*, *tef1*, *tub2*. Table 13. Fig. 42.

Conidiomata pycnidial, globose to subglobose, papillate, thick-walled, pseudoparenchymatous, ostiolate, uniloculate; *conidiomatal matrix* white or buff, cream, yellow, brown or hyaline; *setae* abundant, straight or flexuous, septate, pale brown to brown, short or relatively long, stiff or hyphal-like, scattered on surface of conidiomata, or abundant around ostioles. *Micropycnidia* fertile or sterile, produced abundantly in some species of *Paraphoma*, submerged in medium. *Conidiophores* ampulliform, hyaline, mostly reduced to phialidic conidiogenous cells. *Conidiogenous cells* lageniform, monophialidic, hyaline to subhyaline. *Conidia* ellipsoidal to subglobose, hyaline, guttulate, aseptate *in vivo* and *in vitro*. *Chlamydospores* absent or present, solitary, in short or long chains or aggregated, uni- or multicellular; *multicellular chlamydospores* alternarioid, pseudosclerotioid, epicoccoid and botryoid depending on species. *Sexual morph* unknown.

Culture characteristics: Colony colour, growth and pigmentation greatly dependant on media and incubation conditions. Colonies black, brown, olivaceous, yellow, red to pink, or grey and white; slow growing; aerial mycelium flat to effuse, aerial mycelium sparsely formed, floccose to tufted, felty, woolly or compact; margins regular, smooth and sharp, or irregular, crenate and lobate.

Optimal media and cultivation conditions: CHA for colony growth and pigmentation, MEA mostly for colony pigmentation and acidified OA for both colony pigmentation and morphological identification, incubated for 1 wk in dark and 1 wk under near-ultraviolet light (13 h light, 11 h dark) at 20–22 °C to simulate colony pigmentation and sporulation.

Distribution: Temperate areas of Australia, Eurasia and North America.

Hosts: Mostly foliar pathogens of herbaceous plants, chiefly soil-borne, with wide host range including monocotyledonous plants,

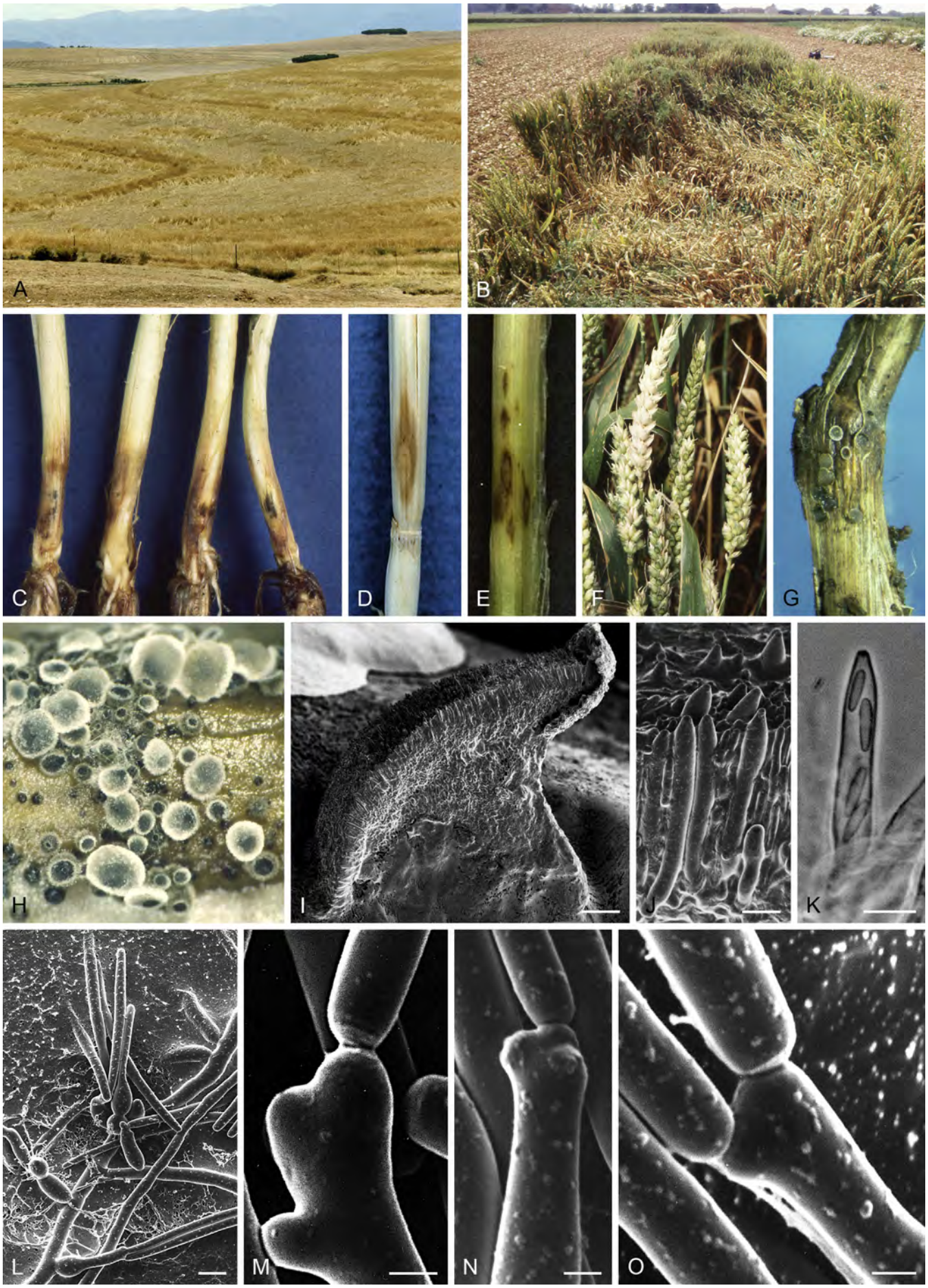

Fig. 39. *Oculimacula* spp. **A–G.** Disease symptoms. **A, B.** Eyespot lodging. **C–E.** Eyespots. **F.** Whiteheads of wheat. **G.** Apothecia of *Oculimacula gamsii* on wheat stubble. **H–K.** Sexual morphs of *Oculimacula yallundae*. **H, I.** Ascomata. **J.** Section through the ascoma showing ascal layer. **K.** Ascus and ascospores. **L–O.** Asexual morphs. **L.** Conidia and conidiogenous cells of *Oculimacula gamsii*. **M.** Conidial hila and conidiogenous cell of *Oculimacula yallundae*. **N.** Conidial hila and conidiogenous cell of *Oculimacula gamsii*. **O.** Conidial hila and conidiogenous cell of *Oculimacula anguoides*. Scale bars: I = 100 µm; J, K = 10 µm; L = 5 µm; M–O = 1 µm.

Table 12. DNA barcodes of accepted *Oculimacula* spp.

Species	Isolates[1]	GenBank accession numbers[2]		References
		ITS	*tef1*	
Oculimacula acuformis	CBS 495.80^{T}	MG934455	MG934497	Present study
O. aestiva	CBS 114730	MG934454	MG934496	Present study
O. anguioides	CBS 496.80^{T}	LT990662	LT990618	Present study
O. yallundae	CBS 110665^{NT}	MG934456	MG934498	Present study
	CBS 128.31	MG934457	MG934499	Present study
	CBS 494.80	JF412009	MG934500	Tsang (unpubl. data), present study

[1] CBS: Westerdijk Fungal Biodiversity Institute, Utrecht, the Netherlands. ^{T} and ^{NT} indicate ex-type and ex-neotype strains, respectively.
[2] ITS: internal transcribed spacers and intervening 5.8S nrDNA, *tef1*: partial translation elongation factor 1-alpha gene.

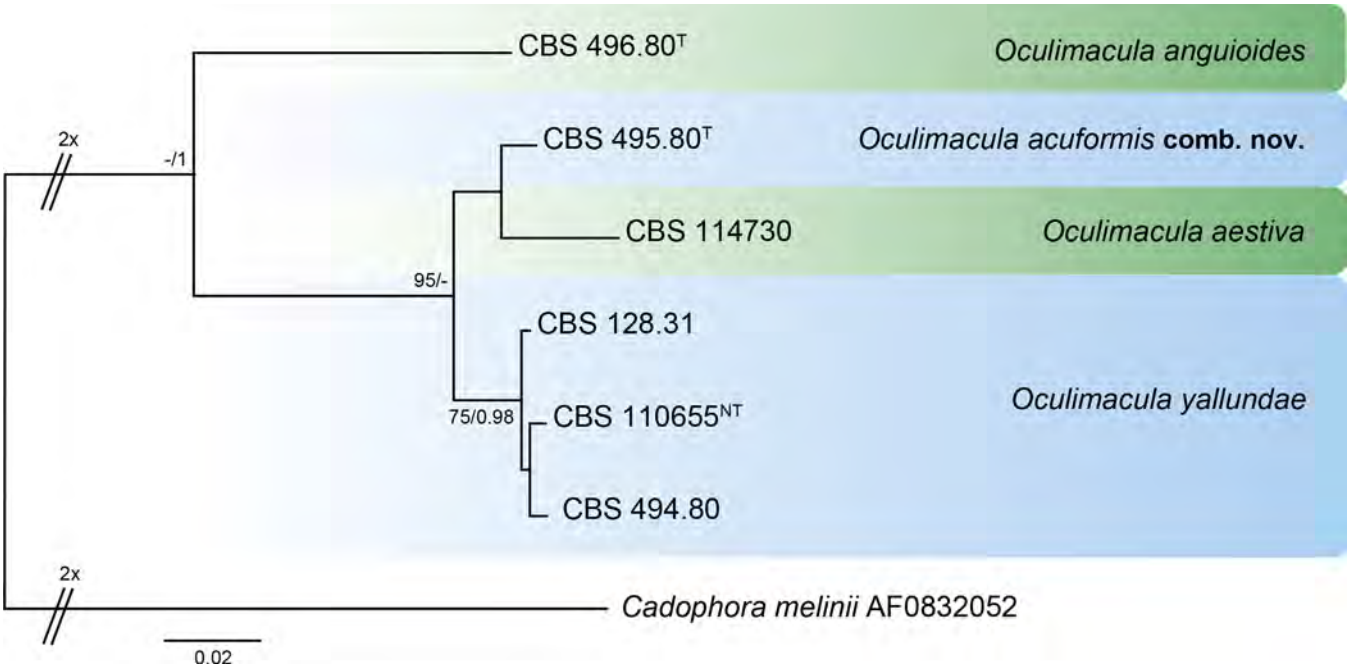

Fig. 40. RAxML phylogram obtained from the combined ITS (631 bp) and *tef1* (575 bp) sequence alignment of taxa belonging to *Oculimacula*. The tree was rooted to *Cadophora melinii*. The new combination proposed in this study is indicated in **bold**. RAxML bootstrap support (BS) values above 70 % and Bayesian posterior probability scores above 0.95 are shown at the nodes. GenBank accession numbers are indicated in Table 12. ^{T} and ^{NT} indicate ex-type and ex-neotype strains, respectively. TreeBASE: S21899.

Asteraceae, *Cupressaceae*, *Rosaceae* and *Solanaceae*, occasionally saprobic.

Disease symptoms: Crown discolouration, root rot and necrotic leaf spots.

Notes: The type species of *Paraphoma, Pa. radicina,* clustered in a separate group outside *Didymellaceae* and hence was excluded from *Phoma* (de Gruyter *et al.* 2013). In a phylogenetic analysis based on LSU and SSU, *Paraphoma radicina* clustered in the *Phaeosphaeriaceae*, although other species belonged to the *Cucurbitariaceae* and *Coniothyriaceae*. Setose pycnidial conidiomata and dictyochlamydospores, which are characteristics of species of *Paraphoma* and *Peyronellaea*, can be observed in species of other phoma-like genera, such as *Pyrenochaeta* and *Pleurophoma*. Therefore, these morphological characters are not specific to these genera. In order to delineate *Paraphoma*, phylogenetic studies based on ITS, LSU, *rpb2*, *tef1* and *tub2* have been performed (Aveskamp *et al.* 2010, Moslemi *et al.* 2016, 2018, Crous *et al.* 2017a). Using ITS and LSU in combination with protein coding genes *rpb2, tef1* and *tub2* for precise identification of species of *Paraphoma* is necessary, as LSU alone is too conservative.

References: de Gruyter & Boerema 2002, Zhang *et al.* 2009, 2012, de Gruyter *et al.* 2010, 2013 (pathogenicity, phylogeny and distribution); Boerema *et al.* 2004 (morphology, pathogenicity, media and incubation conditions); Aveskamp *et al.* 2009, 2010 (morphology, phylogeny and key of all *Paraphoma* spp.); Hay *et al.* 2015 (hosts).

Authors: A. Moslemi, P.W.J. Taylor & P.W. Crous

Phaeoacremonium W. Gams, *et al.*, Mycologia 88: 789. 1996. Fig. 43.
Synonym: *Togninia* Berl., Icon. fung. (Abellini) 3: 9. 1900.

Classification: *Sordariomycetes*, *Sordariomycetidae*, *Togniniales*, *Togniniaceae*.

Type species: *Phaeoacremonium parasiticum* (Ajello, *et al.*) W. Gams, *et al.*, basionym: *Phialophora parasitica* Ajello, *et al.* Holotype and ex-type strain: CBS H-17463, CBS 860.73.

DNA barcodes (genus): SSU, LSU.

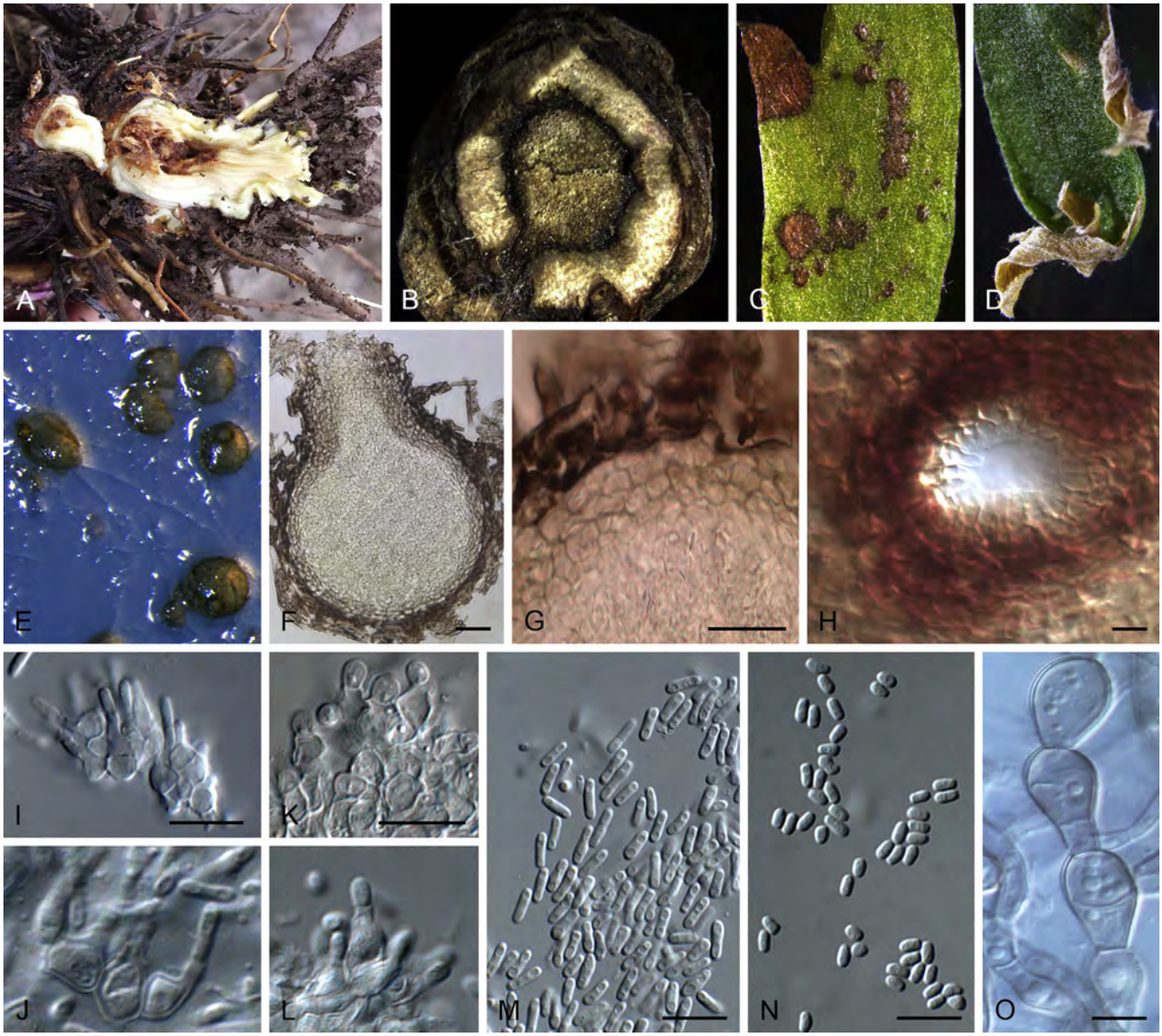

Fig. 41. *Paraphoma* spp. **A–E.** Disease symptoms. **A, B.** Crown discolouration caused by *Paraphoma vinacea* (ex-type BRIP 63684). **C.** Water-soaked and necrotic leaf lesions caused by *Paraphoma chlamydocopiosa* (ex-type BRIP 65168). **D.** Marginal leaf chlorosis caused by *Paraphoma pye* on pyrethrum leaf (ex-type BRIP 65169). **E–O.** Asexual morphs. **E.** Conidiomata on SNA of *Paraphoma fimeti* (ex-neotype CBS 170.70). **F.** Conidiomata of *Paraphoma vinacea* (ex-type BRIP 63684). **G.** Conidiomatal wall of *Paraphoma vinacea* (ex-type BRIP 63684). **H.** Ostiolar zone of *Paraphoma vinacea* (ex-type BRIP 63684). **I–L.** Condiogenous cells. **I, J.** *Paraphoma dioscoreae* (ex-type CBS 135100). **K, L.** *Paraphoma fimeti* (ex-neotype CBS 170.70). **M, N.** Conidia. **M.** *Paraphoma dioscoreae* (ex-type CBS 135100). **N.** *Paraphoma fimeti* (ex-neotype CBS 170.70). **O.** Chlamydospores of *Paraphoma vinacea* (ex-type BRIP 63684). Scale bars: F = 100 µm; G, H = 20 µm; I, K, M–O = 10 µm; I applies to I, J; K applies to K, L. Pictures B, F, G taken from Moslemi *et al.* (2016); C, D from Moslemi *et al.* (2018); I, J, M from Quaedvlieg *et al.* (2013).

DNA barcodes (species): *act*, *tub2*. Table 14. Fig. 44.

Ascomata perithecial, aggregated or solitary, superficial to immersed, non-stromatic, globose to subglobose, dark, opaque, long-necked; *necks* straight or flexuous*; ascomatal wall* fragile to leathery, comprising two layers of *textura angularis*: *outer layer* brown to dark brown, with cells smaller and more rounded than those of inner layer; *inner layer* hyaline to pale brown, cells flattened. *Paraphyses* abundant, broadly cellular, slightly constricted at septa, branching, hyaline, slightly tapering apically or thread-like towards apex. *Ascogenous hyphae* hyaline, sometimes branched in basal region, elongating during ascal formation with remnant tissue from which single asci arise. *Asci* arising in acropetal succession, appearing spicate when mature, unitunicate, 8-spored, ascal apex thickened with a nonamyloid apical ring, basally bluntly obtuse, sessile. *Ascospores* hyaline, aseptate, allantoid, reniform, cylindrical or oblong-ellipsoidal, mostly biseriate or in a single row. *Conidiophores* branched in basal region or unbranched, arising from aerial or submerged hyphae, erect, nearly cylindrical when unbranched, slightly tapering, straight or flexuous, variable in length, up to 7-septate, mostly pale brown, paler towards tip, percurrent rejuvenation observed, small warts or verruculose ornamentation mostly at base, usually with one integrated terminal phialide and one or two additional, discrete phialides at uppermost septum. *Conidiogenous cells* phialidic, discrete or integrated, terminal or lateral, mostly monophialidic, sometimes polyphialidic, sparsely warted, verruculose or smooth, pale brown to hyaline, with an inconspicuous funnel-shaped collarette. Three distinct classes of phialides (Types I–III) can be observed. *Conidia* aggregated into

Table 13. DNA barcodes of accepted *Paraphoma* spp.

Species	Isolates[1]	GenBank accession number[2]				References
		ITS	*tef1*	*tub2*	*rpb2*	
Paraphoma chlamydocopiosa	BRIP 65168^{T}	KU999072	KU999080	KU999084	–	Moslemi *et al.* (2018)
Pa. chrysanthemicola	CBS 522.66^{NT}	KF251166	KF253124	KF252661	KF252174	Quaedvlieg *et al.* (2013)
Pa. dioscoreae	CBS 135100^{T}	KF251167	KF253125	KF252662	KF252175	Quaedvlieg *et al.* (2013)
Pa. fimeti	CBS 170.70^{NT}	KF251170	KF253128	KF252665	KF252178	Quaedvlieg *et al.* (2013)
Pa. pye	BRIP 65169^{T}	KU999073	KU999081	KU999085	–	Moslemi *et al.* (2018)
Pa. radicina	CBS 111.79^{ET}	KF251172	KF253130	KF252667	KF252180	Quaedvlieg *et al.* (2013)
Pa. rhaphiolepidis	CBS 142524^{T}	KY979758	KY979896	KY979924	KY979851	Crous *et al.* (2017a)
Pa. vinacea	BRIP 63684^{T}	KU176884	KU176896	KU176892	–	Moslemi *et al.* (2016)

[1] BRIP: Queensland Plant Pathology Herbarium, Brisbane, Australia; CBS: Westerdijk Fungal Biodiversity Institute, Utrecht, The Netherlands. ^{T}, ^{ET} and ^{NT} indicate ex-type, ex-epitype and ex-neotype strains, respectively.
[2] ITS: internal transcribed spacers and intervening 5.8S nrDNA; *tef1*: partial translation elongation factor 1-alpha gene; *tub2*: partial β-tubulin gene; *rpb2*: partial RNA polymerase II second largest subunit gene.

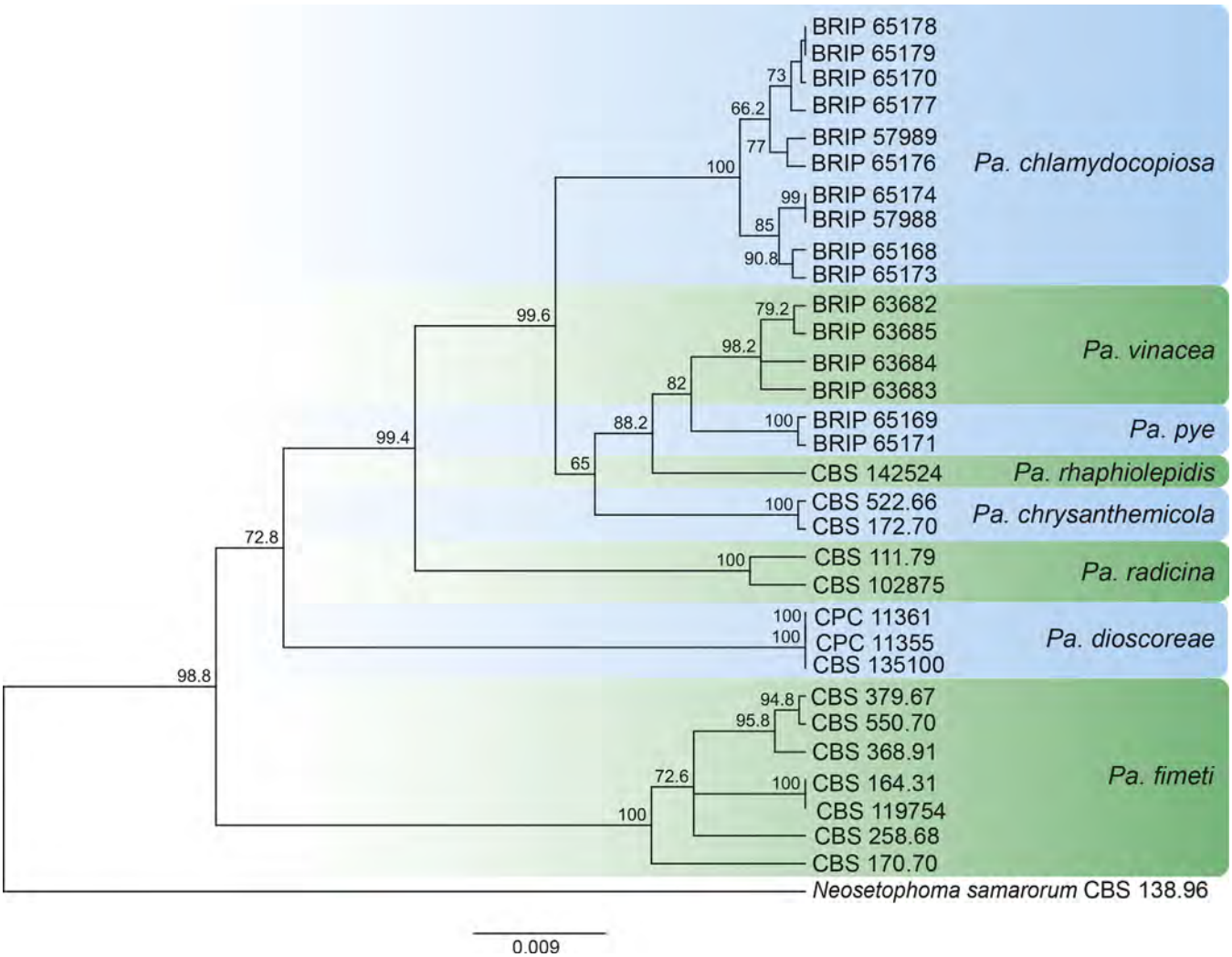

Fig. 42. Maximum likelihood PhyML combined phylogenetic tree of *Paraphoma* spp. inferred from ITS (680 bp), *tef1* (550 bp) and *tub2* (350 bp) using a GTR substitution model. Highest log likelihood -3812.4179. Bootstrap support values less than 65 % were removed. Scale bar indicated expected changes per site. The tree was rooted to *Neosetophoma samarorum* CBS 138.96. GenBank accession numbers are indicated in Table 13. TreeBASE: S22303.

round, slimy heads at apices of phialides, hyaline, aseptate, smooth-walled, oblong-ellipsoidal to obovate, cylindrical, allantoid or reniform, uncommonly fusiform-ellipsoidal or globose, becoming biguttulate with age.

Culture characteristics: Colonies on MEA flat with entire margins, mostly moderately dense, predominantly felty, and sometimes woolly; brown, olive-grey, pale yellow to beige or pink to dark pink.

Optimal media and cultivation conditions: 2 % MEA to induce sporulation of asexual morph. Cultural characters that are useful to distinguish *Phaeoacremonium* species include colour of colonies on MEA, and yellow pigment production on PDA and OA.

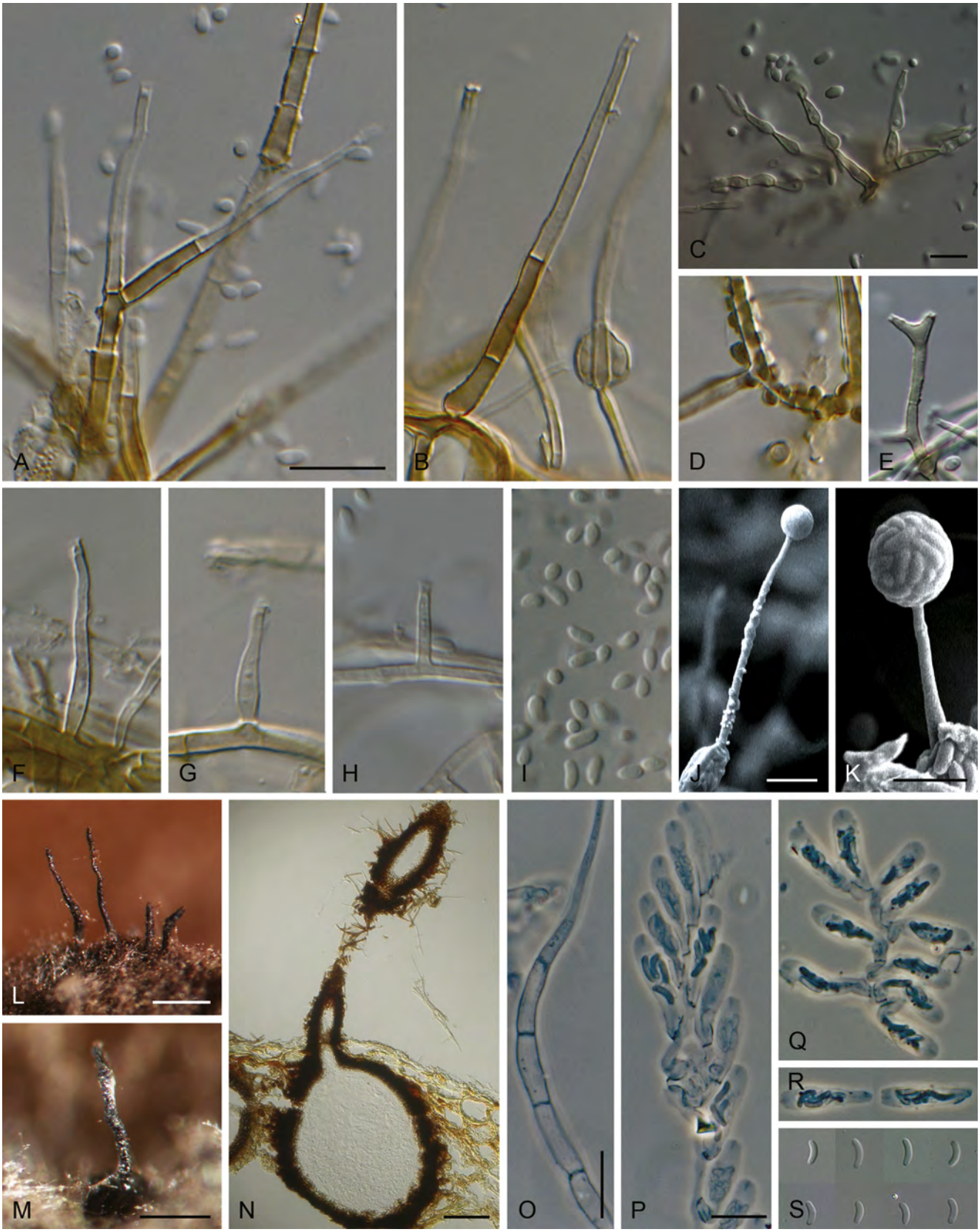

Fig. 43. Morphological structures of *Phaeoacremonium* spp. **A–K.** Asexual morphs. **A.** Conidiophores branched. **B.** Conidiophores unbranched. **C.** Percurrent rejuvenation of conidiophore. **D.** Mycelium showing prominent exudate droplets observed as warts. **E.** Conidiophore with polyphialides. **F.** Type III phialides. **G.** Type II phialide. **H.** Type I phialide. **I.** Conidia. **J.** Conidiophore. **K.** Type II phialide. **L–S.** Sexual morph. **L, M.** Ascomata on canes of *Vitis vinifera*. **N.** Longitudinal section through ascoma. **O.** One paraphyses. **P, Q.** Asci attached to ascogenous hyphae. **R.** Asci. **S.** Ascospores. **A, B, D, F, G, I.** *Phaeoacremonium parasiticum* (ex-type CBS 860.73). **C.** *Phaeoacremonium hispanicum* (ex-type CBS 123910). **E.** *Phaeoacremonium amygdalinum* (ex-type CBS 128570). **H.** *Phaeoacremonium minimum* (ex-type CBS 246.91). **L–S.** *Phaeoacremonium minimum* (holotype CBS 17463). Scale bars: A, C, J, K, O, P = 10 µm; L, M = 200 µm; N = 100 µm; A applies to A, B, D, F–I; C applies to C, E; P applies to P–S.

Table 14. DNA barcodes of accepted *Phaeoacremonium* spp.

Species	Isolates[1]	GenBank accession numbers[2]		References
		act	*tub2*	
Phaeoacremonium africanum	CBS 120863^T	EU128142	EU128100	Damm *et al.* (2008)
Pha. album	CBS 142688^T	KY906884	KY906885	Spies *et al.* (2018)
Pha. alvesii	CBS 110034^T	AY579234	AY579301	Mostert *et al.* (2005)
Pha. amstelodamense	CBS 110627^T	AY579228	AY579295	Mostert *et al.* (2005)
Pha. amygdalinum	CBS 128570^T	JN191303	JN191307	Gramaje *et al.* (2012)
Pha. angustius	CBS 114992^T	DQ173127	DQ173104	Mostert *et al.* (2006)
Pha. aquaticum	IFRDCC 3035^T	n/a[3]	n/a[3]	Hu *et al.* (2012)
Pha. argentinense	CBS 777.83^T	DQ173135	DQ173108	Mostert *et al.* (2006)
Pha. armeniacum	ICMP 17421^T	EU595463	EU596526	Graham *et al.* (2009)
Pha. aureum	CBS 142691^T	KY906656	KY906657	Spies *et al.* (2018)
Pha. australiense	CBS 113589^T	AY579229	AY579296	Mostert *et al.* (2005)
Pha. austroafricanum	CBS 112949^T	DQ173122	DQ173099	Mostert *et al.* (2006)
Pha. bibendum	CBS 142694^T	KY906758	KY906759	Spies *et al.* (2018)
Pha. canadense	PARC 327^T	KF764499	KF764651	Úrbez-Torres *et al.* (2014)
Pha. cinereum	CBS 123909^T	FJ517153	FJ517161	Gramaje *et al.* (2009)
Pha. croatiense	CBS 123037^T	EU863514	EU863482	Essakhi *et al.* (2008)
Pha. fraxinopennsylvanicum	CBS 101585^T	DQ173137	AF246809	Groenewald *et al.* (2001)
Pha. fuscum	STE-U 5969^T	EU128141	EU128098	Damm *et al.* (2008)
Pha. gamsii	CBS 142712^T	KY906740	KY906741	Spies *et al.* (2018)
Pha. geminum	CBS 142713^T	KY906648	KY906649	Spies *et al.* (2018)
Pha. globosum	ICMP 16988^T	EU595466	EU596525	Graham *et al.* (2009)
Pha. griseo-olivaceum	STE-U 5966^T	EU128139	EU128097	Damm *et al.* (2008)
Pha. griseorubrum	CBS 111657^T	AY579227	AY579294	Mostert *et al.* (2005)
Pha. hispanicum	CBS 123910^T	FJ517156	FJ517164	Gramaje *et al.* (2009)
Pha. hungaricum	CBS 123036^T	EU863515	EU863483	Essakhi *et al.* (2008)
Pha. inflatipes	CBS 391.71^T	AY579259	AF246805	Mostert *et al.* (2006)
Pha. iranianum	CBS 101357^T	DQ173120	DQ173096	Mostert *et al.* (2006)
Pha. italicum	CBS 137763^T	KJ534046	KJ534074	Raimondo *et al.* (2014)
Pha. junior	CBS 142697^T	KY906708	KY906709	Spies *et al.* (2018)
Pha. krajdenii	CBS 109479^T	AY579267	AY579330	Mostert *et al.* (2005)
Pha. leptorrhynchum	CBS 110156*	DQ173139	DQ173110	Mostert *et al.* (2006)
Pha. longicollarum	CBS 142699^T	KY906688	KY906689	Spies *et al.* (2018)
Pha. luteum	CBS 137497^T	KF835406	KF823800	Gramaje *et al.* (2014)
Pha. meliae	CBS 142710^T	KY906824	KY906825	Spies *et al.* (2018)
Pha. minimum	CBS 246.91^T	AY735497	AF246811	Mostert *et al.* (2006)
Pha. nordesticola	CMM 4312^T	KY030803	KY030807	da Silva *et al.* (2017)
Pha. occidentale	ICMP 17037^T	EU595460	EU596524	Graham *et al.* (2009)
Pha. oleae	CBS 142704^T	KY906936	KY906937	Spies *et al.* (2018)
Pha. parasiticum	CBS 860.73^T	AY579253	AF246803	Mostert *et al.* (2006)
Pha. pallidum	STE-U 6104^T	EU128144	EU128103	Damm *et al.* (2008)
Pha. paululum	CBS 142705^T	KY906880	KY906881	Spies *et al.* (2018)
Pha. pravum	CBS 142686^T	KY084248	KY084246	Present study
Pha. proliferatum	CBS 142706^T	KY906902	KY906903	Spies *et al.* (2018)
Pha. prunicola	STE-U 5967^T	EU128137	EU128095	Damm *et al.* (2008)
Pha. pseudopanacis	CBS 142101^T	KY173569	KY173609	Crous *et al.* (2016a)
Pha. roseum	PARC 273^T	KF764506	KF764658	Úrbez-Torres *et al.* (2014)
Pha. rosicola	CBS 142708^T	KY906830	KY906831	Spies *et al.* (2018)
Pha. rubrigenum	CBS 498.94^T	AY579238	AF246802	Mostert *et al.* (2006)

(*continued on next page*)

Table 14. (Continued).

Species	Isolates[1]	GenBank accession numbers[2]		References
		act	*tub2*	
Pha. santali	CBS 137498[T]	KF835403	KF823797	Gramaje *et al.* (2014)
Pha. scolyti	CBS 113597[T]	AY579224	AF246800	Mostert *et al.* (2005)
Pha. sicilianum	CBS 123034[T]	EU863520	EU863488	Essakhi *et al.* (2008)
Pha. spadicum	CBS 142711[T]	KY906838	KY906839	Spies *et al.* (2018)
Pha. sphinctrophorum	CBS 337.90[T]	DQ173142	DQ173113	Mostert *et al.* (2006)
Pha. subulatum	CBS 113584[T]	AY579231	AY579298	Mostert *et al.* (2005)
Pha. tardicrescens	CBS 110573[T]	AY579233	AY579300	Mostert *et al.* (2005)
Pha. tectonae	MFLUCC 13-0707[T]	KT285563	KT285555	Ariyawansa *et al.* (2015)
Pha. theobromatis	CBS 111586[T]	DQ173132	DQ173106	Mostert *et al.* (2006)
Pha. tuscanicum	CBS 123033[T]	EU863490	EU863458	Essakhi *et al.* (2008)
Pha. venezuelense	CBS 651.85[T]	AY579256	AY579320	Mostert *et al.* (2005)
Pha. vibratile	CBS 117115[T]	DQ649063	DQ649064	Réblová & Mostert (2007)
Pha. viticola	CBS 101738[T]	DQ173131	AF192391	Dupont *et al.* (2000)

[1] CBS: Westerdijk Fungal Biodiversity Institute, Utrecht, The Netherlands; IFRDCC: International Fungal Research and Development Center, Bailongsi, China; ICMP: International Collection of Microorganisms from Plants, Auckland, New Zealand; PARC: Pacific Agri-Food Research Centre in Summerland, British Columbia, Canada; CMM: Culture Collection of Phytopathogenic Fungi "Prof. Maria Menezes", Universidade Federal Rural de Pernambuco, Recife, Brazil; STE-U: Department of Plant Pathology, Stellenbosch University, South Africa; MFLUCC: Mae Fah Luang Culture Collection, Chiang Rai, Thailand. [T] indicates ex-type strains. *Ex-type of *Pha. novae-zealandiae*, synonymised with *Pha. leptorrhynchum* by Réblová (2011).
[2] *act*: partial actin gene; *tub2*: partial β-tubulin gene.
[3] Not available. Only ITS sequence available: NR136032.

For the sexual morph 2 % WA is used with twice-autoclaved pieces of 3–4 cm of grapevine cane at 22 °C (GWA).

Distribution: Worldwide.

Hosts: Frequently isolated from both diseased woody plants with brown wood streaking, and humans with phaeohyphomycotic infections. Other hosts include larvae of bark beetles, arthropods, and soil. Because of the involvement of members of this genus in Petri disease and esca of grapevines (*Vitis* spp.), isolates from this host have been intensively studied (Mostert *et al.* 2006, Gramaje *et al.* 2015, Spies *et al.* 2018). Even though *Phaeoacremonium* species can infect a wide range of woody hosts (more than 40 host plants), recent publications have shown the importance of *Phaeoacremonium* species in causing brown wood streaking of *Olea europaea* (*Oleaceae*) and *Prunus* spp. (*Rosaceae*) (Damm *et al.* 2008, Carlucci *et al.* 2015).

Notes: Species delimitation based on morphology alone has little value since many species have overlapping characters. Moreover, the morphology of the sexual morph cannot be used because only 15 taxa are known. The two gene regions used most frequently for phylogenetic analyses are actin (*act*) and partial beta-tubulin (*tub2*) genes (Mostert *et al.* 2006). Phylogenetic analyses combining these two regions allow for the resolution of almost all currently known *Phaeoacremonium* species with good support (≥0.97 PP, ≥96 % BS) (Fig. 44). The three exceptions to this are *Pha. griseorubrum* (paraphyletic), *Pha. roseum* (0.72 PP, 100 % BS) and *Pha. viticola* (0.87 PP, 62 % BS) (Fig. 44, also see Gramaje *et al.* 2015 and Spies *et al.* 2018). Other gene regions that have been used include the ITS, *tef1* and *cal* (Groenewald *et al.* 2001, Mostert *et al.* 2005, Úrbez-Torres *et al.* 2014). Úrbez-Torres *et al.* (2014) included ITS and *tef1* data along with *act* and *tub* in their phylogeny, which resolved all included species with more than 97 % or 96 % bootstrap support in maximum parsimony and neighbour joining analyses respectively. The ITS region is considered insufficiently variable to distinguish between several of the species and is not recommended as a barcode (Mostert *et al.* 2005); however, considering the resolution and support in the phylogeny of Úrbez-Torres *et al.* (2014), the *tef1* region is valuable in resolving issues with support and resolution in the *act-tub2* phylogeny. The *cal* region was sequenced for a limited number of species by Mostert *et al.* (2005) to resolve taxa related to *Pha. rubrigenum*. Unfortunately, sequence data for this region are available for a limited number of species and its usefulness in distinguishing between *Phaeoacremonium* species remains uncertain.

References: Crous *et al.* 1996 (taxonomy); Eskalen *et al.* 2005, Rooney-Latham *et al.* 2005 (sexual morph); Mostert *et al.* 2006, Gramaje *et al.* 2015 (taxonomy, distribution, host range, detection, identification, pathogenesis and epidemiology); Aroca & Raposo 2007, Pouzoulet *et al.* 2013, Úrbez-Torres *et al.* 2015 (detection and identification); Halleen *et al.* 2007, Damm *et al.* 2008; Aroca & Raposo 2009, Gramaje *et al.* 2010 (pathogenicity); Blanco-Ulate *et al.* 2013 (genome sequence); Moyo *et al.* 2014, Agustí-Brisach *et al.* 2015 (epidemiology); Réblová *et al.* 2015 (systematics).

Phaeoacremonium pravum C.F.J. Spies, L. Mostert & Halleen, **sp. nov.** MycoBank MB821019. Fig. 45.

Etymology: Latin, *pravum* meaning crooked, in reference to the crooked shape of some phialides.

Mycelium of branched, prominently septate, hyaline to pale brown, smooth to finely verruculose (1–)1.5–2.5 (av. 2) µm diam hyphae, forming bundles of up to 5 strands, individual strands in bundles often forming direct hyphal connections. *Conidiophores* (14.5–)16–61(–77) × 1.5–2.5 (av. 28.5 × 2) µm, smooth to finely verruculose, usually branched, hyaline, up to 9 septa. *Phialides* terminal or lateral, monophialidic, sometimes

proliferating vegetatively behind collarette, types I and II dominant, collarettes funnel-shaped, 0.5–1.5 × 0.5–2 (av. 1 × 1.5) µm, smooth, hyaline; *type I* mainly subcylindrical, sometimes elongate ampulliform, (2–)2.5–10.5(–11) × 1–2 (av. 6 × 1.5) µm; *type II* subcylindrical with tapering apex to elongate ampulliform, sometimes curved or bent especially at apex, (8–)8.5–14(–14.5) × 1.5–2(–2.5) (av. 11.5 × 2) µm; *type III* subcylindrical with tapering apex to subulate, sometimes slender navicular, (14–)14.5–26.5(–31.5) × 1.5–2 (av. 19 × 1.5) µm. *Conidia* 3–4(–4.5) × 1.5(–2) (av. 3.5 × 1.5) µm, borne in slimy heads, oblong-ovoid to ellipsoidal to allantoid.

Culture characteristics: Colonies reaching a radius of 8–10 mm after 8 d at 25 °C. Minimum temperature for growth 10 °C, optimum 20 °C, maximum 35 °C. Colonies on MEA smooth, submerged with entire edge, after 16 d white to pale buff above and in reverse. Colonies on PDA smooth, submerged, with central folds, with entire margin, after 16 d white to pale buff above and in reverse. Colonies on OA felty, folded, with submerged margins, with entire edge, after 16 d white to pale smoke grey with darker margins.

Materials examined: **South Africa**, from wood of *Vitis berlandieri* × *V. rupestris* (rootstock cv. Richter 110) (*Vitaceae*), 18 Sep. 2014, A. Vermeulen (**holotype** CBS-H 23158, culture ex-type CBS 142686 = STE-U 8363 = CSN3); ibid., on *Vitis vinifera* cv. Early Sweet cordon (*Vitaceae*), 18 Sep. 2014, A. Vermeulen, CBS 142687 = STE-U 8364 = CSN11.

Notes: There are several differences between the ex-type strain (CBS 142686) and strain CBS 142687. Strain CBS 142687 had a higher optimum and maximum temperatures for growth (25 °C and 37 °C, respectively) than strain CBS 142686 and reached a radius of 11–12 mm after 8 d at 25 °C. After 16 d, colonies of strain CBS 142687 also had pronounced pigmentation on MEA i.e. rosy vinaceous with dark purple patches with central white tufts of aerial mycelium, and on PDA i.e. livid red to dark vinaceous with white to smoke grey woolly aerial mycelium, and on OA i.e. mouse grey to olivaceous grey with white margins. The *act* sequence of strain CBS 142687 differs from that of the ex-type (CBS 142686) at six positions over a length of 210 bases, resulting in paraphyly of this species in an *act*-only phylogeny (Spies *et al.* 2018). Considering the high similarity of *tub2* sequences (598/599 identical bases), strong support for the monophyly of *Pha. pravum* in the combined *act-tub2* phylogeny, and the fact that both strains produced curved phialides, CBS 142687 is regarded as *Pha. pravum* until additional strains and data become available to indicate differently.

Authors: D. Gramaje, L. Mostert, C.F.J. Spies & F. Halleen

Phyllosticta Pers., Traité sur les Champignons Comestibles (Paris): 55. 147. 1818. Fig. 46.
Synonym: Guignardia Viala & Ravaz, Bull. Soc. mycol. Fr. 8: 63. 1892.

Classification: *Dothideomycetes*, *Dothideomycetidae*, *Botryosphaeriales*, *Phyllostictaceae*.

Type species: *Phyllosticta convallariae* Pers., nom. inval. (= *Phyllosticta cruenta* (Fr.) J. Kickx f.). Reference strain: CBS 858.71.

DNA barcode (*genus*): LSU.

DNA barcodes (*species*): ITS, *act*, *gapdh*, *tef1*. Table 15. Fig. 47.

Ascomata pseudothecial, separate to gregarious, globose to subglobose, brown to black, unilocular with a central ostiole. *Pseudoparaphyses* mostly absent at maturity, filamentous, branched, septate when present. *Asci* bitunicate, fissitunicate, clavate to subcylindrical, 8-spored, fasciculate, stipitate, with an ocular chamber. *Ascospores* bi- to triseriate, hyaline, guttulate to granular, aseptate, ellipsoid, ellipsoid-fusoid to limoniform, smooth-walled, usually with mucilaginous caps at ends, or surrounded by a mucilaginous sheath. *Conidiomata* and *spermatogonia* pycnidial, immersed, subepidermal to erumpent, unilocular, rarely multilocular, glabrous, ostiolate, dark brown to black; *ostiole* circular to oval; *conidiomatal wall* thick-walled, dark brown, *textura angularis*, with inner layers of hyaline to pale brown, thin-walled, *textura prismatica* to *angularis*. *Conidiophores* lining cavity of conidioma, reduced to conidiogenous cells, invested in mucus. *Conidiogenous cells* discrete, producing macroconidia and spermatia, also produced in separate spermatogonia, ampulliform, lageniform, doliiform to subcylindrical, hyaline, smooth, proliferating percurrently near apex, invested in a mucoid layer. *Conidia* ellipsoid-fusoid to obovoid or ovoid, rarely subcylindrical, aseptate, broadly rounded at apex, often tapering strongly toward base, unicellular, hyaline, smooth-walled, guttulate to granular, often enclosed in a persistent mucilaginous sheath, and bearing an unbranched, tapering, straight to curved, mucoid apical appendage. *Spermatogenous cells* ampulliform to lageniform or subcylindrical, hyaline, smooth, phialidic. *Spermatia* hyaline, smooth, granular, subcylindrical or dumbbell-shaped, with rounded or blunt ends (adapted from Wikee *et al.* 2013b).

Culture characteristics: Colonies on MEA, OA and PDA after 2 wk in dark at 27 °C erumpent or flat, spreading with sparse or moderate aerial mycelium; on MEA, OA and PDA surface frequently iron-grey or olivaceous grey, less frequently greenish to dark green; reverse iron-grey, olivaceous grey or black.

Optimal media and cultivation conditions: PNA, OA, PDA and SNA under near-ultraviolet light at 27 °C to induce sporulation.

Distribution: Worldwide.

Hosts: Wide range of hosts from trees to ornamentals.

Disease symptoms: Leaf spots and various fruit diseases.

Notes: *Phyllosticta* was introduced by Persoon (1818), with *Phy. convallariae* designated as type species (Donk 1968). However, this species was invalid because it lacked a description. Therefore, *Phy. cruenta*, which is a synonym of *Phy. convallariae*, was designated as type of the genus (van der Aa & Vanev 2002). There is no available type material for this species, which was described from *Polygonatum multiflorum* collected in Germany. A strain deposited in CBS previously identified as *Guignardia reticulata*, which is the sexual morph of *Phy. cruenta*, was isolated from *Polygonatum odoratum* in the Czech Republic, being a potential neotype for *Phy. cruenta*. However, this strain is sterile and we have chosen to consider it as a reference strain since we could not confirm its identification based on morphology.

Phyllosticta includes plant pathogenic species that cause diseases of significant economic importance. For example, *Phy. citricarpa* is the responsible for citrus black spot, which is considered a quarantine pest in Europe and the USA (Baayen *et al.* 2002, Glienke *et al.* 2011, Guarnaccia *et al.* 2017). Other examples include the *Phy. ampelicida* species complex that causes black rot disease on grapevines (Wicht *et al.* 2012, Carstens *et al.* 2017), and the *Phy. musarum* species complex

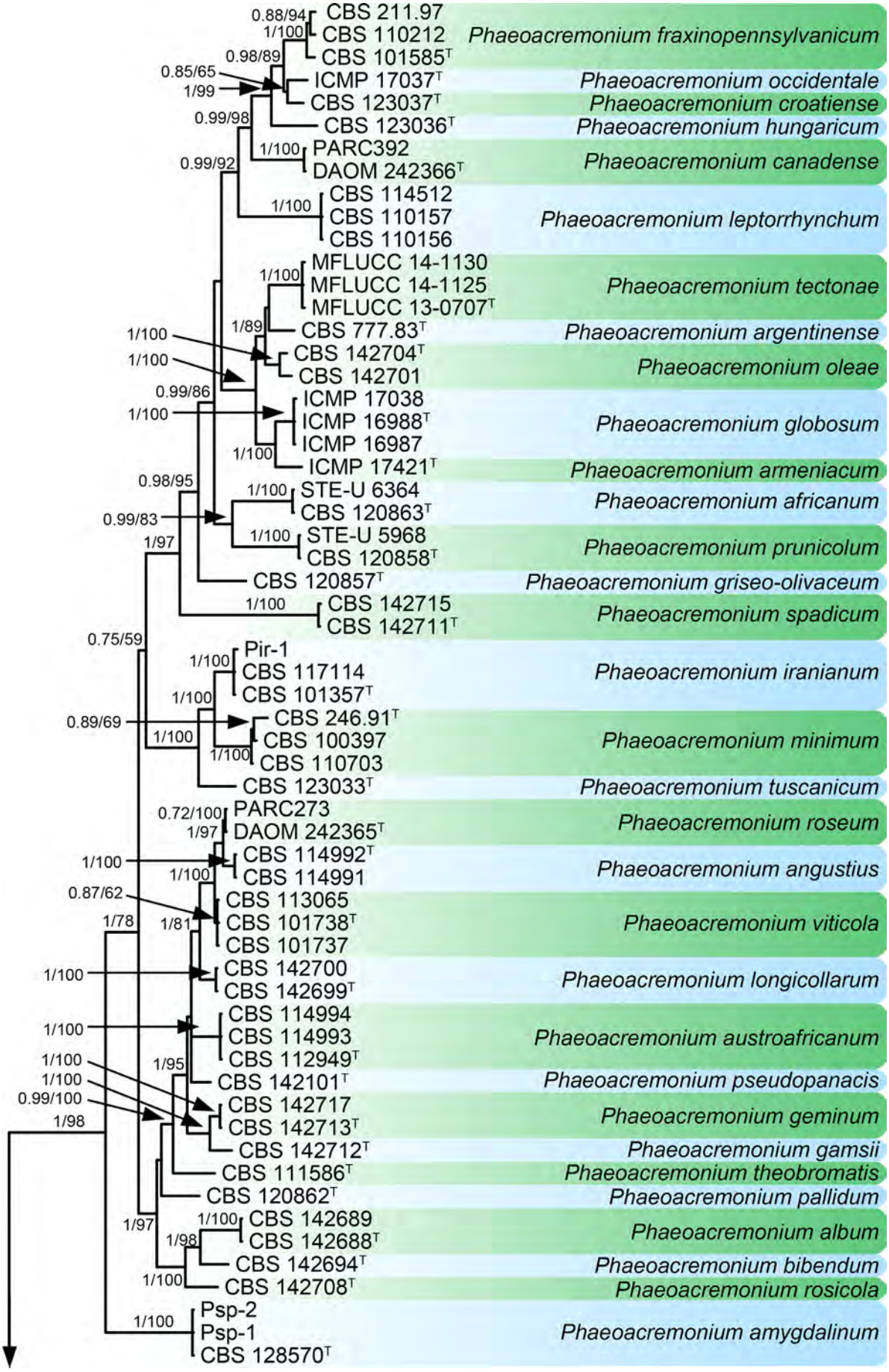

Fig. 44. Bayesian consensus tree of the genus *Phaeoacremonium* as estimated from the combined *act* (~260 bp) and *tub2* (~680 bp) regions. Bayesian posterior probability values and bootstrap support percentages are shown at the nodes. Support values of less than 0.7 posterior probability and 70 % bootstrap are not shown. *Jattaea algeriensis*, *Calosphearia africana* and *Pleurostoma richardsiae* were used as outgroups. GenBank accession numbers are listed in Spies *et al.* (2018). T indicates ex-type strains. TreeBASE: S22407.

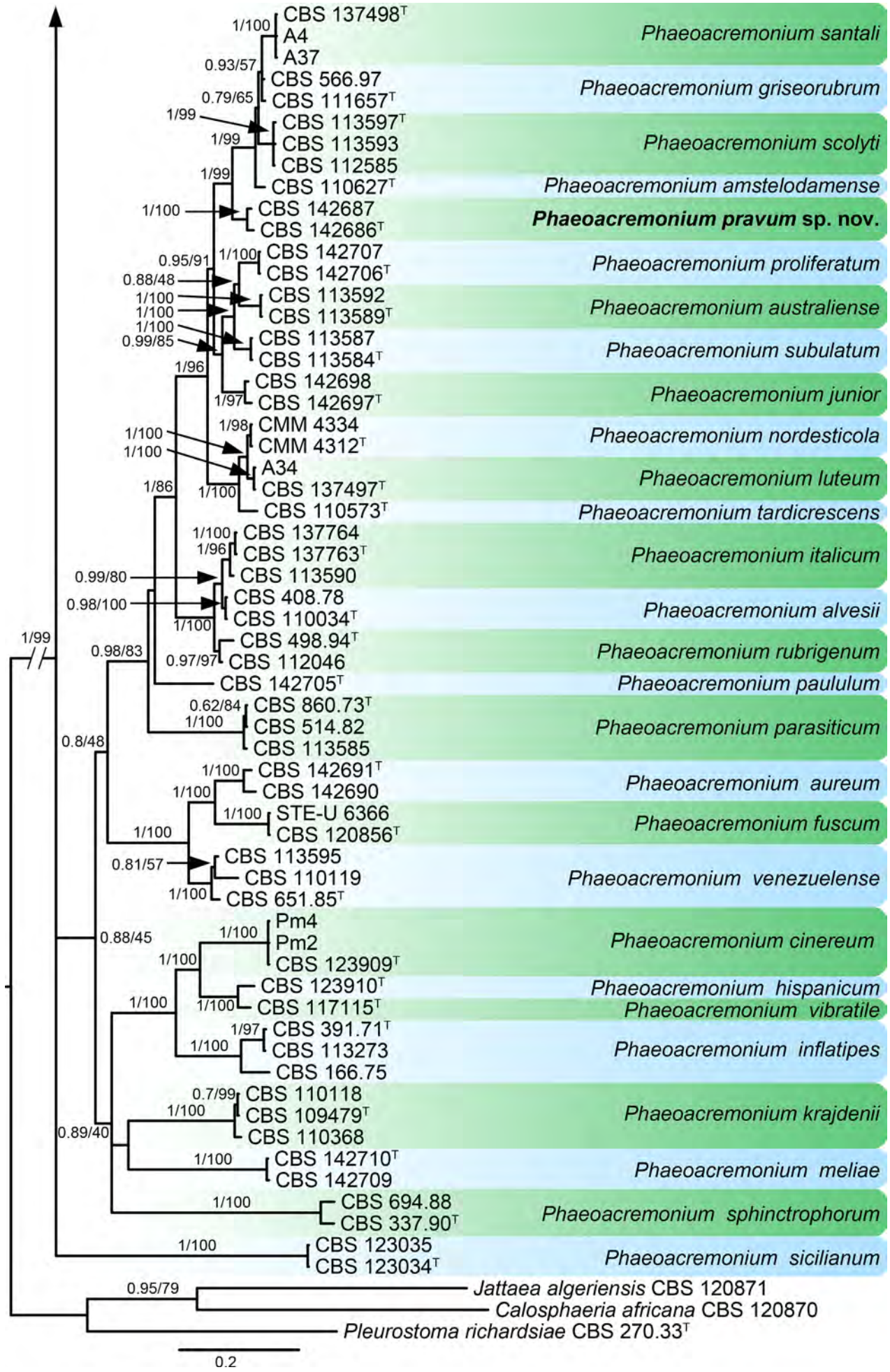

Fig. 44. (Continued).

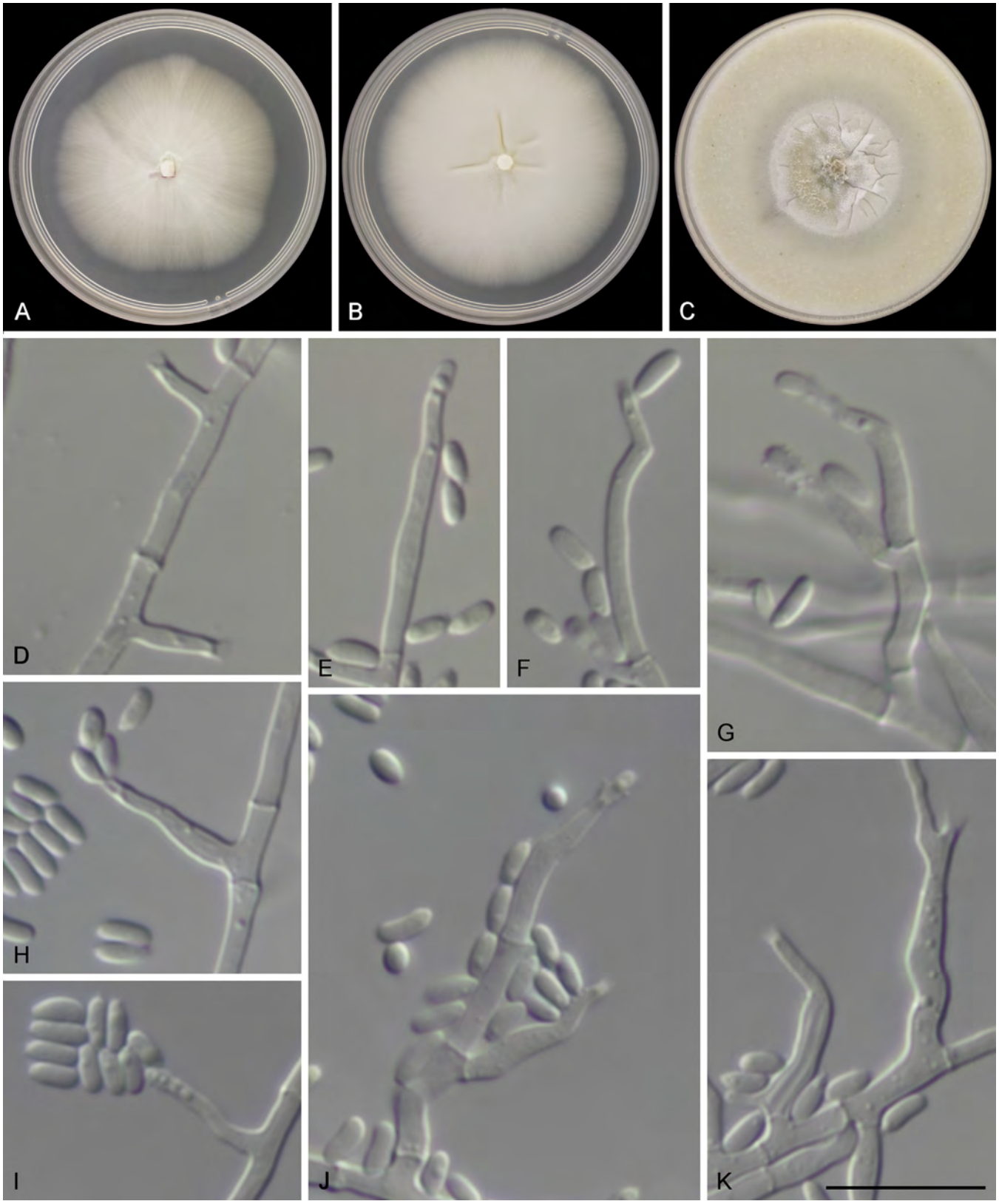

Fig. 45. *Phaeoacremonium pravum* (ex-type CBS 142686). **A–C.** Eight-d-old colonies on MEA (A), PDA (B) and OA (C). **D.** Subcylindrical type I phialides with funnel-shaped collarettes. **E, F.** Type III phialides. **G, J.** Branched conidiophores with crooked type II phialides. **H.** Elongate ampulliform type I phialide. **I.** Type I phialide with conidia borne in a slimy head. **K.** Crooked elongate ampulliform type I phialide with a funnel-shaped collarette showing lateral vegetative proliferation. Scale bar: K = 10 µm, K applies to D–K.

that is responsible for banana freckle disease (Pu *et al.* 2008, Wong *et al.* 2012).

Phoma and *Phyllosticta* have been difficult to distinguish since both genera were recognised as pycnidial fungi producing unicellular, hyaline conidia. Subsequent molecular data enabled the discrimination of both genera, as well as the fact that *Phyllosticta* was linked to its sexual morph, *Guignardia* (Glienke *et al.* 2011, Wikee *et al.* 2011, 2013b, Wong *et al.* 2012, Zhou *et al.* 2015, Guarnaccia *et al.* 2017).

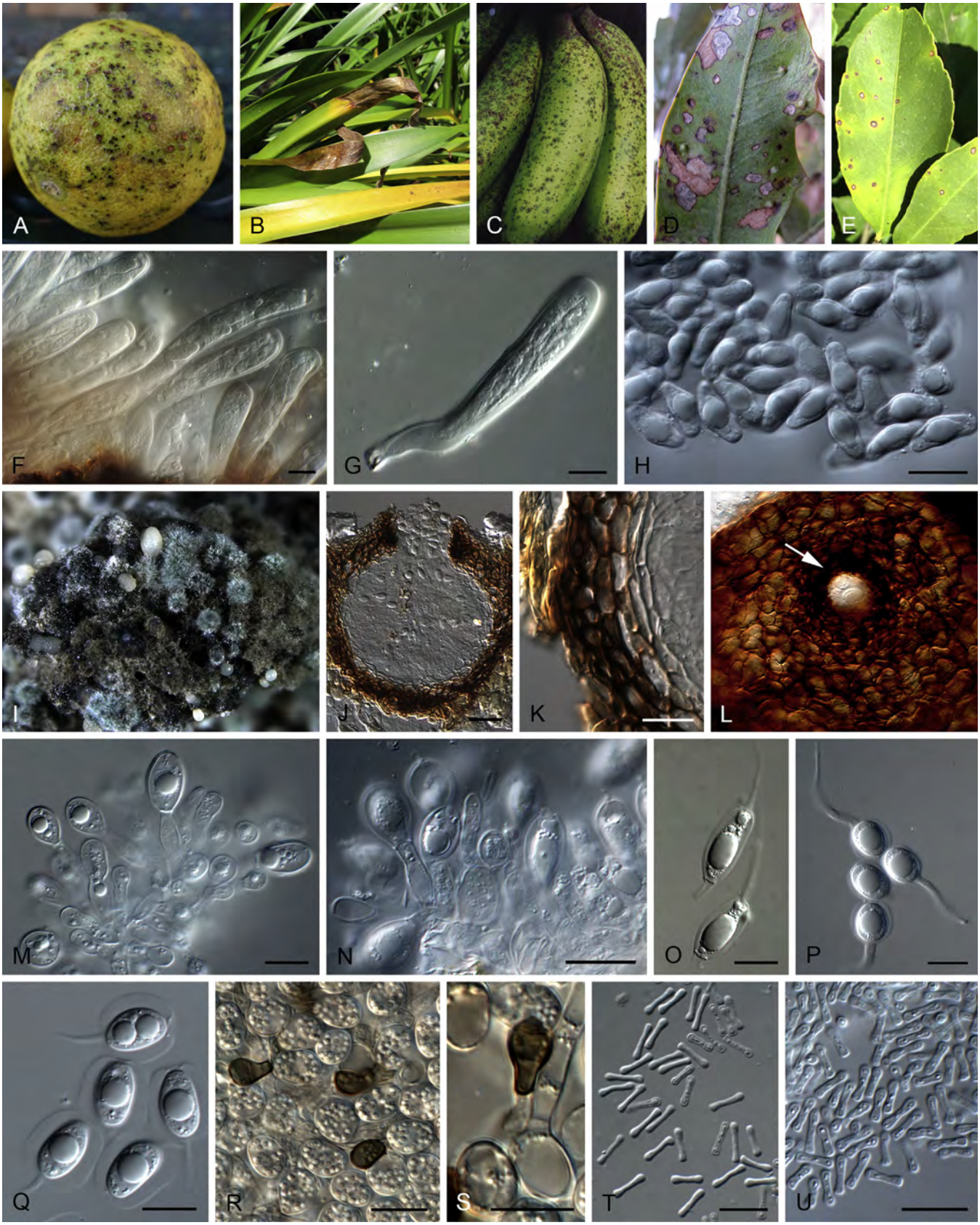

Fig. 46. *Phyllosticta* spp. **A–E.** Disease symptoms. **A.** Aloe with dead leaf tips that harbour *Phyllosticta aloeicola*. **B.** Symptoms on *Citrus maxima* caused by *Phyllosticta citrimaxima*. **C.** Water-soaked lesions on banana fruit associated with freckle disease on banana caused by *Phyllosticta* sp. **D.** Symptomatic leaf of *Cussonia* sp. caused by *Phyllosticta cussoniae*. **E.** Symptoms on lemon leaf caused by *Phyllosticta* sp. **F–H.** Sexual morphs. **F, G.** Asci and ascospores of *Phyllosticta abieticola* (ex-type CBS 112067). **H.** Ascospores of *Phyllosticta capitalensis* (ex-epitype CBS 128856). **I–U.** Asexual morphs. **I.** Conidiomata sporulating on OA of *Phyllosticta cussoniae* (ex-epitype CPC 14873). **J.** Vertical section through conidioma of *Phyllosticta rhaphiolepidis* (ex-type MUCC 432). **K.** Conidiomatal wall of *textura angularis* of *Phyllosticta rhaphiolepidis* (ex-type MUCC 432). **L.** Conidioma with ostiole (arrowed) of *Phyllosticta cordylinophila* (ex-neotype CPC 20261). **M, N.** Conidiogenous cells giving rise to conidia. **M.** *Phyllosticta foliorum* (ex-neotype CBS 447.68). **N.** *Phyllosticta capitalensis* (ex-epitype CBS 128856). **O–Q.** Conidia. **O.** *Phyllosticta aloeicola* (CPC 20677). **P.** *Phyllosticta podocarpicola* (ex-type CBS 728.79). **Q.** *Phyllosticta capitalensis* (ex-epitype CBS 128856). **R, S.** Appressoria of *Phyllosticta mangifera-indica* (ex-type CPC 20274). **T, U.** Spermatia. **T.** *Phyllosticta cussoniae* (ex-epitype CPC 14873). **U.** *Phyllosticta leucothoicola* (ex-type MUCC 553). Scale bars: I = 25 µm; others = 10 µm. Pictures A, B, D, F–M, O, P, R–U taken from Wikee *et al.* (2013b); C from Wong *et al.* (2012); N, Q from Glienke *et al.* (2011).

Table 15. DNA barcodes of accepted *Phyllosticta* spp.

Species	Isolates[1]	GenBank accession number[2]				References
		ITS	*act*	*gapdh*	*tef1*	
Phyllosticta abieticola	CBS 112067^{T}	KF170306	KF289238	–	–	Wikee *et al.* (2013b)
Phy. alliacea	MUCC 0014^{T}	AB454263	AB704207	–	–	Motohashi *et al.* (2009), Ando *et al.* (2013)
Phy. aloeicola	CBS 136058^{T}	KF154280	KF289311	KF289124	KF289193	Wikee *et al.* (2013b)
Phy. ampelicida	ATCC 200578^{NT}	KC193586	KC193581	KC193584	–	Zhang *et al.* (2013b)
Phy. ardisiicola	MUCC 0031^{T}	AB454274	AB704216	–	–	Motohashi *et al.* (2009), Ando *et al.* (2013)
Phy. aristolochiicola	BRIP 53316a^{T}	JX486129	–	–	–	Crous *et al.* (2012a)
Phy. aspidistricola	MUCC 0010^{T}	AB454260	AB704204	–	–	Motohashi *et al.* (2009), Ando *et al.* (2013)
Phy. beaumarisii	CBS 535.87^{T}	AY042927	KF306232	KF289074	KF289170	Baayen *et al.* (2002), Wikee *et al.* (2013b)
Phy. bifrenariae	CBS 128855^{T}	JF343565	JF343649	JF343744	JF343586	Glienke *et al.* (2011)
Phy. brazillianiae	CBS 129060^{T}	JF343572	JF343656	JF343758	JF343593	Glienke *et al.* (2011)
Phy. capitalensis	CBS 128856^{ET}	JF261465	JF343647	JF343776	JF261507	Glienke *et al.* (2011)
Phy. carissicola	CPC 25665^{T}	KT950849	KT950872	KT950876	KT950879	Crous *et al.* (2015e)
Phy. carochlae	CGMCC 3.17317^{T}	KJ847422	KJ847430	KJ847438	KJ847444	Zhou *et al.* (2015)
Phy. catimbauensis	URM 7672^{T}	MF466160	MF466157	–	MF466155	Crous *et al.* (2017b)
Phy. cavendishii	BRIP 55420^{IsoT}	JQ743562	–	–	–	Wong *et al.* (2012)
Phy. citriasiana	CBS 120486^{T}	FJ538360	FJ538476	JF343686	FJ538418	Wulandari *et al.* (2009), Glienke *et al.* (2011)
Phy. citribraziliensis	CBS 100098^{T}	FJ538352	FJ538468	JF343691	FJ538410	Wulandari *et al.* (2009), Glienke *et al.* (2011)
Phy. citricarpa	CBS 127454^{ET}	JF343583	JF343667	JF343771	JF343604	Glienke *et al.* (2011)
Phy. citrichinaensis	CBS 130529^{T}	JN791597	JN791526	–	JN791452	Wang *et al.* (2011)
Phy. citrimaxima	CBS 136059^{T}	KF170304	KF289300	KF289157	KF289222	Wikee *et al.* (2013b)
Phy. concentrica	CBS 937.70^{ET}	FJ538350	KF289257	JF411745	FJ538408	Wulandari *et al.* (2009), Glienke *et al.* (2011), Wikee *et al.* (2013b)
Phy. cordylinophila	CBS 136244^{NT}	KF170287	KF289295	KF289076	KF289172	Wikee *et al.* (2013b)
Phy. cornicola	CBS 111639	KF170307	KF289234	–	–	Wikee *et al.* (2013b)
Phy. cruenta	CBS 858.71	MG934458	MG934465	MG934474	MG934501	Present study
Phy. cussonia	CBS 136060^{ET}	JF343578	JF343662	JF343764	JF343599	Glienke *et al.* (2011)
Phy. elongata	CBS 126.22^{T}	FJ538353	FJ538469	KF289164	FJ538411	Wulandari *et al.* (2009), Wikee *et al.* (2013b)
Phy. ericarum	CBS 132534^{T}	KF206170	KF289291	KF289162	KF289227	Wikee *et al.* (2013b)
Phy. eugeniae	CBS 445.82	AY042926	KF289246	KF289139	KF289208	Baayen *et al.* (2002), Wikee *et al.* (2013b)
Phy. fallopiae	MUCC 0113^{T}	AB454307	AB704228	–	–	Motohashi *et al.* (2009), Ando *et al.* (2013)
Phy. foliorum	CBS 447.68^{NT}	KF170309	KF289247	KF289132	KF289201	Wikee *et al.* (2013b)
Phy. gaultheriae	CBS 447.70^{T}	JN692543	KF289248	JN692508	JN692531	Su & Cai (2012)
Phy. hamamelidis	MUCC 149	KF170289	KF289309	–	–	Wikee *et al.* (2013b)
Phy. hostae	CGMCC 3.14355^{T}	JN692535	JN692511	JN692503	JN692523	Su & Cai (2012)
Phy. hubeiensis	CGMCC 3.14986^{T}	JX025037	JX025032	JX025027	JX025042	Zhang *et al.* (2013a)
Phy. hymenocallidicola	CBS 131309^{T}	JQ044423	KF289242	KF289142	KF289211	Crous *et al.* (2011b), Wikee *et al.* (2013b)
Phy. hypoglossi	CBS 434.92^{NT}	FJ538367	FJ538483	JF343695	FJ538425	Wulandari *et al.* (2009), Glienke *et al.* (2011), Wikee *et al.* (2013b)
Phy. ilicis-aquifolii	CGMCC 3.14358^{T}	JN692538	JN692514	–	JN692526	Su & Cai (2012)
Phy. iridigena	CBS 143410^{T}	MG934459	MG934466	–	MG934502	Present study
Phy. kerriae	MUCC 0017^{T}	AB454266	AB704209	–	KC342576	Motohashi *et al.* (2009), Ando *et al.* (2013), Wikee *et al.* (2013a)

Table 15. (Continued).

Species	Isolates[1]	GenBank accession number[2]				References
		ITS	*act*	*gapdh*	*tef1*	
Phy. leucothoicola	CBS 136073^{T}	AB454370	KF289310	–	–	Motohashi *et al.* (2009), Wikee *et al.* (2013b)
Phy. ligustricola	MUCC 0024^{T}	AB454269	AB704212	–	–	Motohashi *et al.* (2009), Ando *et al.* (2013)
Phy. maculata	CBS 132581^{ET}	JQ743570	–	–	–	Wong *et al.* (2012)
Phy. mangiferae-indicae	CBS 136061^{T}	KF170305	KF289296	KF289121	KF289190	Wikee *et al.* (2013b)
Phy. mimusopisicola	CBS 138899^{T}	KP004447	–	–	–	Crous *et al.* (2014d)
Phy. minima	CBS 585.84^{NT}	KF206176	KF289249	KF289135	KF289204	Wikee *et al.* (2013b)
Phy. musarum	BRIP 55434^{IsoET}	JQ743584	–	–	–	Wong *et al.* (2012)
Phy. neopyrolae	CBS 134750^{T}	AB454318	AB704233	–	–	Motohashi *et al.* (2009), Ando *et al.* (2013)
Phy. owaniana	CBS 776.97^{ET}	FJ538368	KF289254	JF343767	FJ538426	Wulandari *et al.* (2009), Glienke *et al.* (2011), Wikee *et al.* (2013b)
Phy. pachysandricola	MUCC 124^{T}	AB454317	AB704232	–	–	Motohashi *et al.* (2009), Ando *et al.* (2013)
Phy. paracapitalensis	CBS 141353^{T}	KY855622	KY855677	KY855735	KY855951	Guarnaccia *et al.* (2017)
Phy. paracitricarpa	CBS 141357^{T}	KY855635	KY855690	KY855748	KY855964	Guarnaccia *et al.* (2017)
Phy. parthenocisii	CBS 111645	JN692542	JN692518	–	JN692530	Su & Cai (2012)
Phy. partricuspidatae	NBRC 9466^{T}	KJ847424	KJ847432	KJ847440	KJ847446	Zhou *et al.* (2015)
Phy. paxistimae	CBS 112527^{T}	KF206172	KF289239	KF289140	KF289209	Wikee *et al.* (2013b)
Phy. persooniae	CBS 143409^{T}	MG934460	MG934467	MG934475	MG934503	Present study
Phy. philoprina	CBS 587.69	KF154278	KF289250	KF289137	KF289206	Wikee *et al.* (2013b)
Phy. podocarpi	CBS 111646	AF312013	KC357670	KF289169	KC357671	Wikee *et al.* (2013b), Carroll (unpubl. data), Wikee (unpubl. data)
Phy. podocarpicola	CBS 728.79^{T}	KF206173	KF289252	KF289134	KF289203	Wikee *et al.* (2013b)
Phy. pseudotsugae	CBS 111649	KF154277	KF289236	KF289167	KF289231	Wikee *et al.* (2013b)
Phy. rhaphiolepidis	MUCC 432^{T}	DQ632660	AB704242	–	DQ632724	Andjic *et al.* (2007), Ando *et al.* (2013)
Phy. rubella	CBS 111635^{T}	KF206171	KF289233	KF289129	KF289198	Wikee *et al.* (2013b)
Phy. schimae	CGMCC 3.14354^{T}	JN692534	JN692510	JN692506	JN692522	Su & Cai (2012)
Phy. schimicola	CGMCC 3.17319^{T}	KJ847426	KJ847434	KJ854895	KJ847448	Zhou *et al.* (2015)
Phy. sphaeropsoidea	CBS 756.70	AY042934	KF289253	KF289133	KF289202	Baayen *et al.* (2002), Wikee *et al.* (2013b)
Phy. spinarum	CBS 292.90	JF343585	JF343669	JF343773	JF343606	Glienke *et al.* (2011)
Phy. styracicola	CGMCC 3.14985^{T}	JX052040	JX025035	JX025030	JX025045	Zhang *et al.* (2013a)
Phy. telopeae	CBS 777.97^{T}	KF206205	KF289255	KF289141	KF289210	Wikee *et al.* (2013b)
Phy. vaccinii	ATCC 46255^{ET}	KC193585	KC193580	KC193583	KC193582	Zhang *et al.* (2013b)
Phy. vacciniicola	CBS 136062^{T}	KF170312	KF289287	KF289165	KF289229	Wikee *et al.* (2013b)
Phy. vitis-rotundifoliae	CGMCC 3.17322^{T}	KJ847428	KJ847436	KJ847442	KJ847450	Zhou *et al.* (2015)
Phy. yuccae	CBS 117136	JN692541	JN692517	JN692507	JN692529	Su & Cai (2012)

[1] ATCC: American Type Culture Collection, Virginia, USA; BRIP: Queensland Plant Pathology Herbarium, Brisbane, Australia; CBS: Westerdijk Fungal Biodiversity Institute, Utrecht, The Netherlands; CGMCC: Chinese General Microbiological Culture Collection Center, Beijing, China; CPC: Culture collection of Pedro Crous, housed at Westerdijk Fungal Biodiversity Institute; MUCC: Murdoch University, Perth, Western Australia; NBRC: Biological Resource Center, NITE, Chiva, Japan; URM: Culture Collection Mycobank, Prof. Maria Auxiliadora Cavalcanti, Federal University of Pernambuco, Recife, Brazil. $^{T, ET, IsoT, IsoET}$ and ^{NT} indicate ex-type, ex-epitype, ex-isotype, ex-isoepitype and ex-neotype strains, respectively.

[2] ITS: internal transcribed spacers and intervening 5.8S nrDNA; *act*: partial actin gene; *gapdh*: partial glyceraldehyde-3-phosphate dehydrogenase gene; *tef1*: partial translation elongation factor 1-alpha gene.

Phyllosticta was formerly placed in the *Botryosphaeriaceae,* together with *Botryosphaeria* (Schoch *et al.* 2006). However, Wikee *et al.* (2013b) showed that it represents a different phylogenetic lineage, for which the family name *Phyllostictaceae* (Fries 1849) was resurrected.

References: van der Aa 1973 (morphology and pathogenicity); van der Aa & Vanev 2002 (synonyms, collection information and notes); Glienke *et al.* 2011, Wong *et al.* 2012, Wikee *et al.* 2013b, Zhou *et al.* 2015, Guarnaccia *et al.* 2017 (ecology, morphology and phylogeny); Wikee *et al.* 2011 (pathogenicity and phylogeny).

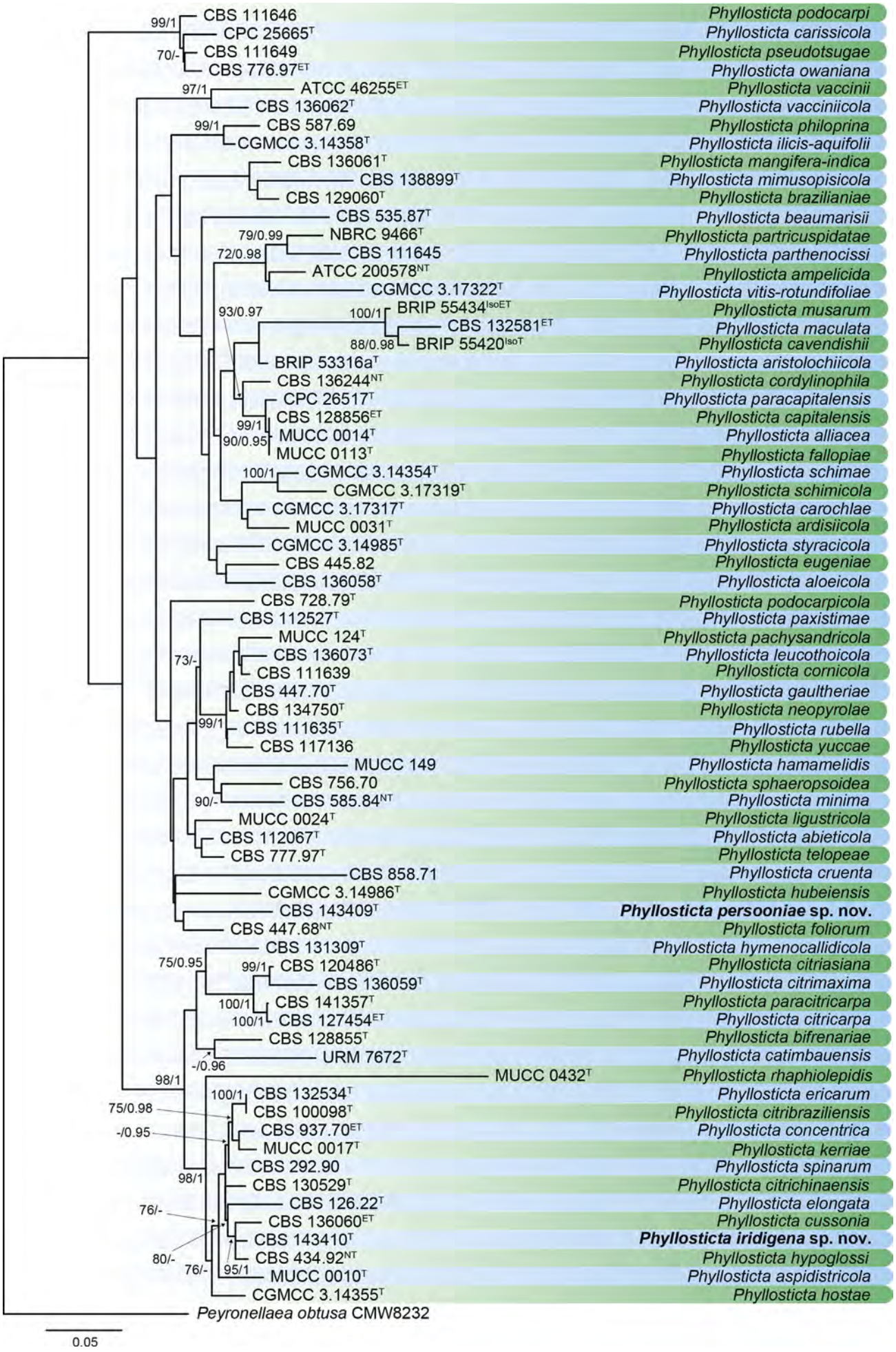

Phyllosticta iridigena Y. Marín & Crous, **sp. nov.** MycoBank MB823971. Fig. 48.

Etymology: Name reflects the host it was isolated from, *Iris*.

Conidiomata 90–200 µm diam, pycnidial, solitary, globose, dark brown, with central ostiole; *conidiomatal wall* of 3–8 layers of brown *textura angularis. Conidiophores* lining cavity, reduced to conidiogenous cells. *Conidiogenous cells* 4–7 × 4–6 µm, doliiform, hyaline, smooth, proliferating percurrently at apex. *Conidia* (10–)12–13(–15) × (7–)8(–9) µm, solitary, ellipsoid to obovoid, aseptate, smooth, hyaline, guttulate, granular; conidia encased in a mucoid sheath 2–3 µm diam, and a single apical mucoid appendage, 7–15 × 2 µm, tapering to acutely rounded apex.

Culture characteristics: Colonies flat, spreading, with moderate aerial mycelium and smooth, feathery margins, reaching 45 mm diam after 2 wk at 25 °C. On MEA surface pale olivaceous grey; reverse iron-grey. On PDA surface and reverse olivaceous grey. On OA surface pale olivaceous grey with diffuse yellow pigment in agar.

Material examined: **South Africa**, on *Iris* sp. (*Iridaceae*), 16 Jan. 2010, P.W. Crous (**holotype** CBS H-23385, culture ex-type CBS 143410 = CPC 32669).

Notes: This species clusters in a well-supported clade (95 % BS / 1 PP) with *Phy. hypoglossi* and *Phy. cussoniae*. *Phyllosticta hypoglossi* produces longer conidiogenous cells (10–15 µm) and wider conidia [(9–)10(–11) µm] than *Phy. iridigena*. Moreover, these three species are isolated from different hosts, i.e. *Phy. hypoglossi* from *Ruscus* (*Ruscaceae*), *Phy. cussoniae* from *Cussonia* (*Araliaceae*) and *Phy. iridigena* from *Iris* (*Iridaceae*). *Phyllosticta cussonia* and *Phy. iridigena* have been found in the same country, South Africa, while *Phy. hypoglossi* is an European species.

Phyllosticta persooniae Y. Marín & Crous, **sp. nov.** MycoBank MB823972. Fig. 49.

Etymology: Name reflects the host genus *Persoonia* from which it was isolated.

Conidiomata 200–300 µm diam, pycnidial, solitary, globose, dark brown, with central ostiole; *conidiomatal wall* of 3–8 layers of brown *textura angularis. Conidiophores* 10–18 × 6–7 µm, lining cavity, 0–1-septate, subcylindrical, hyaline, smooth, rarely branched. *Conidiogenous cells* 9–17 × 4–5 µm, terminal, subcylindrical, hyaline, smooth, proliferating percurrently at apex. *Conidia* (9–)10–11(–12) × (7–)8(–9) µm, solitary, ellipsoid to obovoid, aseptate, smooth, hyaline, guttulate, granular; conidia encased in a mucoid sheath that is inconspicuous and dissolves at maturity, but with a single apical mucoid appendage, 7–15 × 2–3 µm, tapering to acutely rounded apex.

Culture characteristics: Colonies flat to erumpent, spreading, with sparse to moderate aerial mycelium and feathery, lobate margins, reaching 30 mm diam after 2 wk at 25 °C. On MEA surface smoke grey; reverse olivaceous grey. On PDA surface and reverse olivaceous grey. On OA surface pale mouse grey.

Material examined: **Australia**, New South Wales, South East Forests National Park, Nunnock Swamp, on *Persoonia* sp. (*Proteaceae*), 28 Nov. 2016, P.W. Crous (**holotype** CBS H-23386, culture ex-type CBS 143409 = CPC 32603).

Notes: *Phyllosticta persooniae* is phylogenetically distant from all other species of *Phyllosticta,* the most closely related species being *Phy. foliorum*. Morphologically, these can be distinguished by the size of their conidia. *Phyllostica foliorum* is characterised by its larger conidia i.e. (12–)13–14(–15) × (9–)10(–11) ìm *vs.* (9–)10–11(–12) × (7–)8(–9) µm in *Phy. persooniae*. Moreover, *Phy. foliorum* has never been found on *Persoonia* (*Proteaceae*) or in Australia, which is the host and distribution of *Phy. persooniae* (Farr & Rossman 2017). Most species of *Phyllosticta* are host-specific.

Authors: Y. Marin-Felix & P.W. Crous

Proxipyricularia Klaubauf, *et al.*, Stud. Mycol. 79: 109. 2014. Fig. 50.

Classification: *Sordariomycetes, Sordariomycetidae, Magnaporthales, Pyriculariaceae*.

Type species: *Proxipyricularia zingiberis* (Y. Nisik.) Klaubauf, *et al.*, basionym: *Pyricularia zingiberis* Y. Nishik. Lectotype designated here: plate 4, fig. 3–8 in Nishikado Y. 1917. Ber. Ohara Inst. Landwirt. Forsch. 1: 222. Epitype and ex-epitype strain designated here: CBS H-23356, CBS 133594.

DNA barcodes (genus): LSU, ITS.

DNA barcodes (species): ITS, *act, cal*, *rpb1*. Table 16. Fig. 28.

Conidiophores solitary or in fascicles, subcylindrical, erect, olivaceous to medium brown, smooth, septate. *Conidiogenous cells* terminal and intercalary, pale brown, with denticulate conidiogenous loci and rhexolytic secession. *Conidia* solitary, formed sympodially, pyriform to obclavate, narrowed toward apex, rounded at base, 2-septate, subhyaline to pale brown, with a distinct protruding basal hilum, frequently with minute marginal frill (adapted from Klaubauf *et al.* 2014).

Culture characteristics: Colonies reaching 43–50 mm in 1 wk at 25 °C, without or with moderate aerial mycelium. On CMA surface and reverse transparent. On OA surface salmon to ochreous; reverse pale luteous to luteous. On PDA surface olivaceous to grey olivaceous with margins transparent; reverse olivaceous to grey olivaceous with margins buff.

Optimal media and cultivation conditions: On CMA and OA at 25 °C in dark, or autoclaved barley seeds placed on SNA at 25 °C under near-ultraviolet light (12 h light, 12 h dark).

Distribution: Japan.

Hosts: *Zingiber mioga* and *Z. officinale* (*Zingiberaceae*).

Disease symptoms: Leaf spots.

Notes: In a phylogenetic study of the genus *Pyricularia* based on LSU, ITS, *act*, *cal* and *rpb1*, *Pyricularia zingiberis* clustered in an independent clade distant from the type species of *Pyricularia* (Klaubauf *et al.* 2014). Therefore, the genus *Proxipyricularia* was

Fig. 47. RAxML phylogram obtained from the combined ITS (492 bp), *act* (291 bp), *gapdh* (629 bp) and *tef1* (341 bp) sequence alignment of all the accepted species of *Phyllosticta*. The tree was rooted to *Peyronellaea obtusa* CMW8232. The novelties proposed in this study are indicated in **bold**. RAxML bootstrap support (BS) values above 70 % and Bayesian posterior probability scores above 0.95 are shown at the nodes. GenBank accession numbers are indicated in Table 15. $^{T, ET, IsoT, IsoET}$ and ^{NT} indicate ex-type, ex-epitype, ex-isotype, ex-isoepitype and ex-neotype strains, respectively. TreeBASE: S21899.

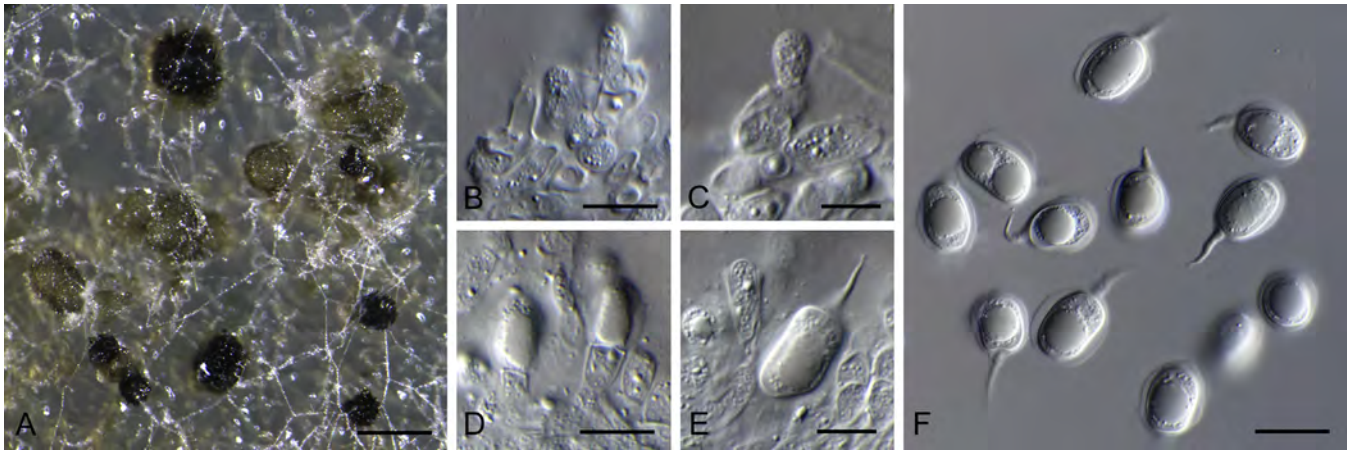

Fig. 48. *Phyllosticta iridigena* (ex-type CBS 143410). **A.** Conidiomata sporulating on SNA. **B–E.** Conidiogenous cells giving rise to conidia. **F.** Conidia. Scale bars: A = 200 µm, B–F = 10 µm.

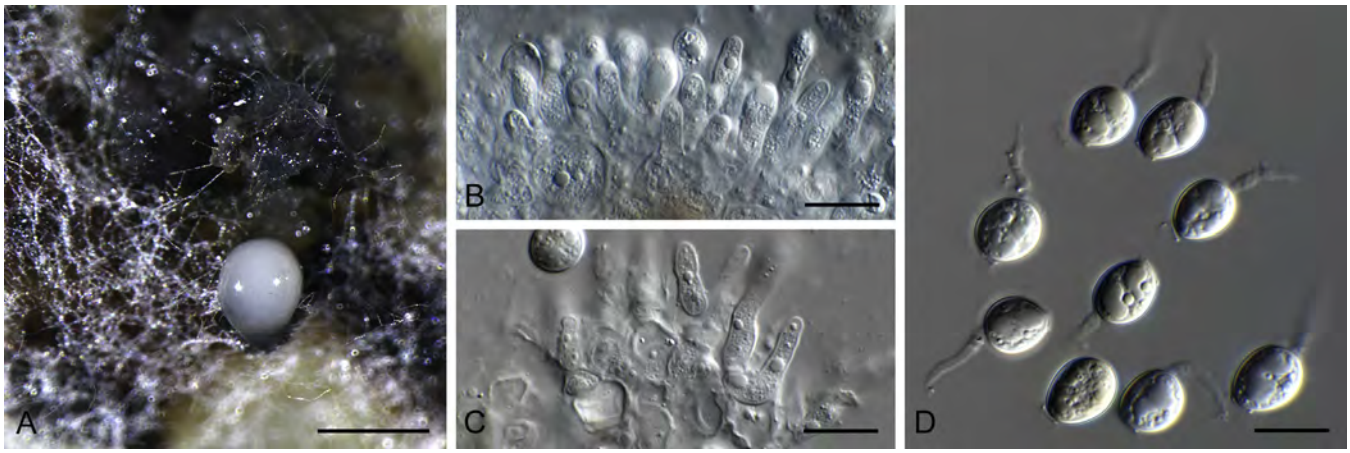

Fig. 49. *Phyllosticta persooniae* (ex-type CBS 143409). **A.** Conidiomata sporulating on OA. **B, C.** Conidiogenous cells giving rise to conidia. **D.** Conidia. Scale bars: A = 200 µm, B–D = 10 µm.

introduced to accommodate this species, which is pathogen of *Zingiber* in Japan. Morphologically, both genera are similar, being characterised by medium brown conidiophores and a terminal and intercalary denticulate rachis, and subhyaline, 2-septate, obclavate conidia (Klaubauf *et al.* 2014).

References: Nishikado 1917 (morphology and pathogenicity); Klaubauf *et al.* 2014 (morphology and phylogeny).

Proxipyricularia zingiberis (Y. Nisik.) Klaubauf, *et al.*, Stud. Mycol. 79: 109. 2014. Fig. 50.
Basionym: *Pyricularia zingiberis* Y. Nishik. (as "*Piricularia zingiberi*"), Ber. Ohara Inst. Landwirt. Forsch. 1: 216. 1917.

Description: Klaubauf *et al.* (2014).

Culture characteristics: Colonies on CMA reaching 43–50 mm after 1 wk at 25 °C, without aerial mycelium; surface and reverse transparent. On OA reaching 48–50 mm after 1 wk at 25 °C, with moderate aerial mycelium appearing slightly cottony, margins arachnoid; surface salmon to ochreous; reverse pale luteous to luteous. On PDA reaching 47–48 mm after 1 wk at 25 °C, with sparse aerial mycelium, margins fringed; surface olivaceous to grey olivaceous with margins transparent; reverse olivaceous to grey olivaceous with margins buff.

Materials examined: **Japan**, on leaves of *Zingiber officinale* (*Zingiberaceae*) (**lectotype of *Pyricularia zingiberis* designated here**, MBT379808, plate 4, fig. 3–8 in Nishikado Y. 1917. Ber. Ohara Inst. Landwirt. Forsch. 1: 222). **Japan**, Hyogo, on *Zingiber mioga* (*Zingiberaceae*), 2002, H. Kato [**epitype of *Pyricularia zingiberis* designated here** CBS H-23356, MBT379809, culture ex-epitype CBS 133594 = MAFF 240222 = HYZiM201-0-1(Z-2J)].

Notes: Type material was not designated when *Py. zingiberis* was introduced (Nishikado 1917). Therefore, we selected the drawings of Nishikado in the original description as lectotype (Ber. Ohara Inst. Landwirt. Forsch. 1: 222, plate 4, fig. 3–8). To fix the application of the generic name, an epitype for this species is designated here from the same country (Japan) and host (*Zingiber*) as that of the original specimen.

Pyriculariomyces Y. Marín, M.J. Wingf. & Crous, **gen. nov.** MycoBank MB823760. Fig. 51. Table 17.

Etymology: Named after the genus *Pyricularia*, which it resembles morphologically.

Ascomata separate, immersed, globose, brown, with central papillate neck and ostiole; *ascomatal wall* of 2–4 layers of brown cells of *textura angularis. Hamathecium* dissolving upon maturity, with some cells remaining among asci. *Asci* unitunicate, hyaline, smooth, 8-spored, subcylindrical, stipitate, apical mechanism refractive, but not staining in Meltzer's. *Ascospores* biseriate, fusoid-ellipsoid, widest in middle, tapering towards subobtusely rounded ends, slightly curved to straight, 3-septate, pale brown, guttulate. *Conidiophores* solitary, erect, straight to flexuous, unbranched, subcylindrical, brown, smooth, 1–8-septate.

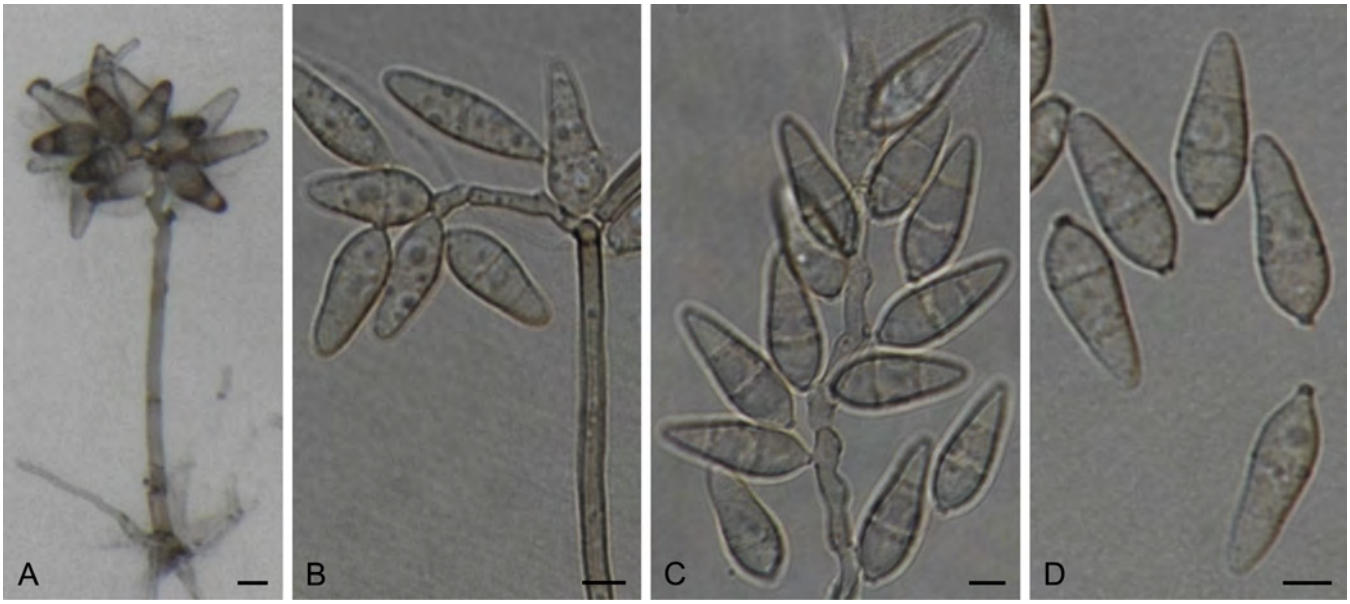

Fig. 50. *Proxipyricularia zingiberis* (ex-epitype CBS 133594). **A–C.** Conidiophores and conidia. **D.** Conidia. Scale bars = 5 µm.

Table 16. DNA barcodes of accepted *Proxipyricularia* sp.

Species	Isolates[1]	GenBank accession numbers[2]				References
		ITS	*act*	*cal*	*rpb1*	
Proxypiricularia zingiberis	CBS 133594[ET]	AB274434	AB274446	KM485246	KM485091	Hirata *et al.* (2007), Klaubauf *et al.* (2014)

[1] CBS: Westerdijk Fungal Biodiversity Institute, Utrecht, the Netherlands. [ET] indicates ex-epitype strain.
[2] ITS: internal transcribed spacers and intervening 5.8S nrDNA; *act*: partial actin gene; *cal*: partial calmodulin gene; *rpb1*: partial RNA polymerase II largest subunit gene.

Conidiogenous cells integrated, terminal, apex somewhat swollen with numerous denticle-like loci, slightly thickened and darkened. *Conidia* solitary, pyriform, brown, finely verruculose, guttulate, granular, apex subobtusely rounded, with or without mucoid cap, base truncate, hilum darkened, thickened, 2-septate.

Culture characteristics: Colonies reaching 90 mm after 2 wk at 25 °C, with moderate aerial mycelium and smooth, even margins. On MEA surface pale mouse grey with patches of dirty white; reverse isabelline with patches of pale luteous. On OA surface honey with patches of pale mouse grey. On PDA surface honey; reverse isabelline to honey.

Type species: Pyriculariomyces asari (Crous & M.J. Wingf.) Y. Marín, M.J. Wingf. & Crous. Holotype and ex-type cultures: CBS H-22625, CBS 141328 = CPC 27444.

Notes: *Pyriculariomyces* is phylogenetically closely related to *Pyricularia*. However, *Pyriculariomyces* can easily be distinguished by production of integrated terminal conidiogenous cells, while *Pyricularia* produces terminal and intercalary conidiogenous cells. In *Pyriculariaceae*, the only genera characterised by only terminal conidiogenous cells are *Barretomyces* and *Utrechtiana*. However, these genera can easily be distinguished from *Pyriculariomyces* by the septation of the conidia i.e. 4(–5)-septate in *Barretomyces* and 1–2-septate in *Utrechtiana*. Moreover, *Utrechtiana* differs in the presence of conidiogenous cells that proliferate percurrently. Moreover, *Pyriculariomyces* can be distinguished from *Pyricularia* by the production of ascomata with papillate necks with ostioles, while *Pyricularia* is characterised by ascomata with long necks.

Pyriculariomyces asari (Crous & M.J. Wingf.) Y. Marín, M.J. Wingf. & Crous, **comb. nov.** MycoBank MB823761. Fig. 51.
Basionym: *Proxipyricularia asari* Crous & M.J. Wingf., Persoonia 36: 393. 2016.

Description: Crous *et al.* (2016b).

Materials examined: **Malaysia**, Sabah, on leaves and stems of *Asarum* sp. (*Aristolochiaceae*), May 2015, M.J. Wingfield (**holotype** CBS H-22625, culture ex-type CPC 27444 = CBS 141328); ibid., CPC 27442.

Notes: *Pyriculariomyces asari* was introduced as a species of *Proxypiricularia* to accommodate two specimens collected from *Asarum* (Crous *et al.* 2016b). However, the authors at the time suggested that this species could represent another genus in the *Pyricularia* complex. The phylogenetic analysis generated here based on four different loci (Fig. 28), support this hypothesis.

Authors: Y. Marin-Felix, M.J. Wingfield & P.W. Crous

Pyricularia Sacc. Michelia 2: 20. 1880. Fig. 52.

Classification: *Sordariomycetes, Sordariomycetidae, Magnaporthales, Pyriculariaceae*.

Type species: *Pyricularia grisea* Sacc. Lectotype designated by Rossman *et al.* (1990): BPI undistributed set. Epitype and ex-epitype strain designated by Crous *et al.* (2015a): CBS H-22280, CBS 138707.

DNA barcode (genus): LSU.

DNA barcodes (species): ITS, *act, cal*, *rpb1*. Table 18. Fig. 28.

Ascomata ostiolate, solitary to gregarious, subspherical, brown to black, base immersed in host tissue, with long neck protruding above plant tissue; *ascomatal wall* consisting of several layers of

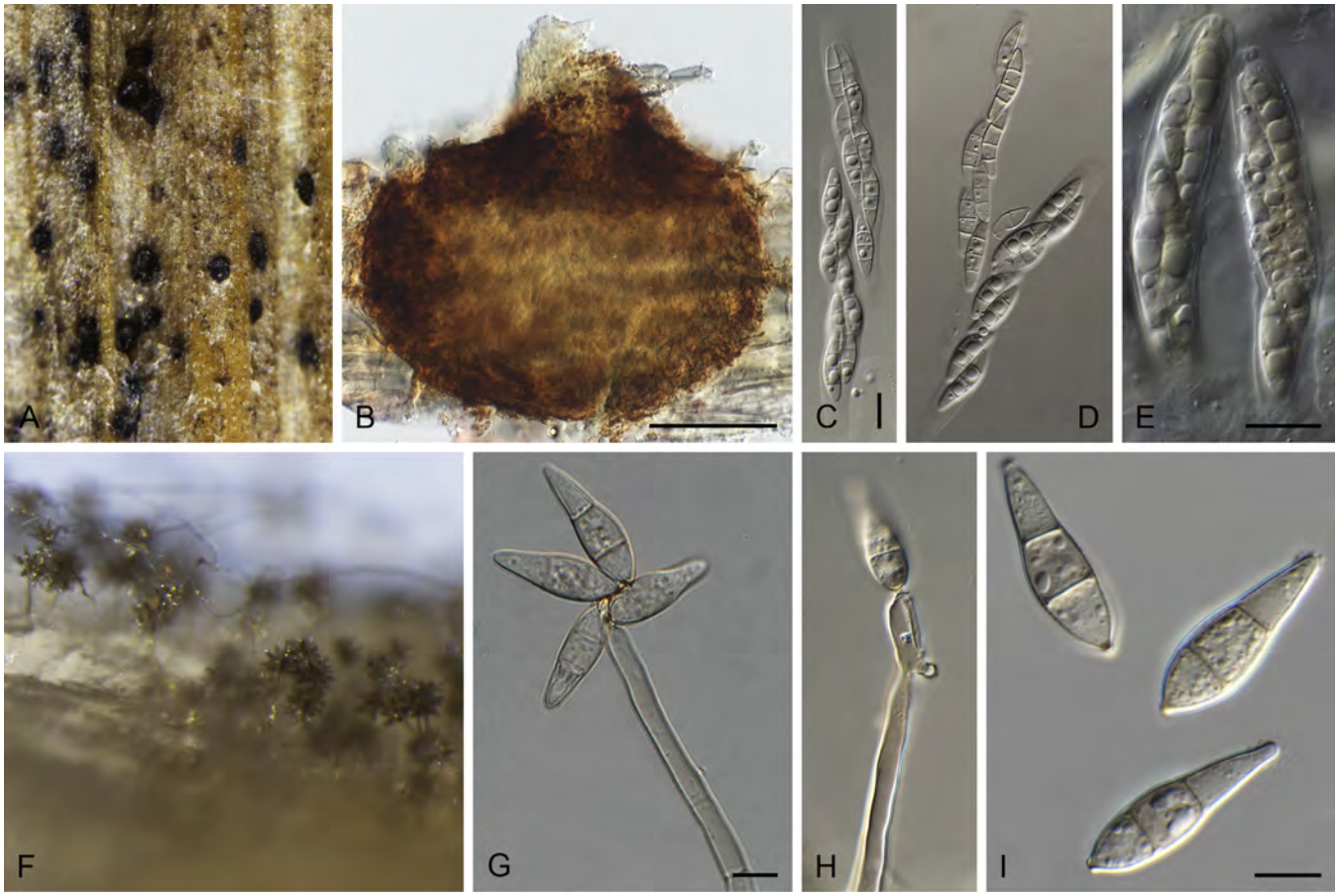

Fig. 51. *Pyriculariomyces asari* (ex-type CBS 141328). **A.** Ascomata on host tissue. **B.** Section of ascoma. **C–E.** Asci and ascospores. **F.** Conidiophores on SNA. **G, H.** Conidiophores and conidia. **I.** Conidia. Scale bars: B = 100 µm; others = 10 µm; C applies to C, D; G applies to G, I. Pictures A, B, D, E, G, H taken from Crous *et al.* (2016b).

Table 17. DNA barcodes of accepted *Pyriculariomyces* sp.

Species	Isolates[1]	GenBank accession numbers[2]				References
		ITS	*act*	*cal*	*rpb1*	
Pyriculariomyces asari	CBS 141328[T]	KX228291	KX228361	MG934541	KX228368	Crous *et al.* (2016b), present study
	CPC 27442	KX228290	KX228360	–	MG934472	Crous *et al.* (2016b), present study

[1] CBS: Westerdijk Fungal Biodiversity Institute, Utrecht, the Netherlands; CPC: Culture collection of Pedro Crous, housed at Westerdijk Fungal Biodiversity Institute. [T] indicates ex-type strain.
[2] ITS: internal transcribed spacers and intervening 5.8S nrDNA; *act*: partial actin gene; *cal*: partial calmodulin gene; *rpb1*: partial RNA polymerase II largest subunit gene.

brown cells of *textura angularis*. *Paraphyses* intermingled among asci, unbranched, septate. *Asci* 8-spored, hyaline, subcylindrical to clavate, unitunicate, short-stipitate, with prominent apical ring. *Ascospores* bi- to multiseriate in asci, hyaline, guttulate, smooth-walled, fusiform, curved with rounded ends, transversely 3-septate, slightly constricted at septa. *Conidiophores* solitary or in fascicles, subcylindrical, erect, brown, smooth, rarely branched, with sympodial proliferation. *Conidiogenous cells* terminal and intercalary, pale brown, with denticulate conidiogenous loci and rhexolytic secession. *Conidia* solitary, pyriform to obclavate, narrowed toward tip, rounded at base, 2-septate, hyaline to pale brown, with a distinct basal hilum, sometimes with marginal frill (adapted from Klaubauf *et al.* 2014).

Culture characteristics: Colonies on MEA white to vinaceous, pale olivaceous grey, smoke grey, or grey, cottony. Colonies on OA iron grey, transparent with greenish olivaceous parts, fuscous black with grey centre or hazel with smokey grey tufts.

Optimal media and cultivation conditions: On OA at 25 °C in dark, or autoclaved barley seeds placed on SNA at 25 °C under near-ultraviolet light (12 h light, 12 h dark).

Distribution: Worldwide.

Hosts: Wide range of monocot plants, including important crops of the *Poaceae* such as rice, barley, millet, oat and wheat.

Disease symptoms: Leaf spot and blast diseases.

Notes: *Pyricularia* was recently re-evaluated in a phylogenetic study based on five loci (Klaubauf *et al.* 2014). In this study, the polyphyletic nature of the genus was resolved introducing eight new genera to accommodate the species of *Pyricularia* that were not grouped with the type species *Py. grisea* and *Py. oryzae* in *Pyricularia s. str.* Moreover, the family *Pyriculariaceae* was introduced to accommodate *Pyricularia*, which was previously considered a member of *Magnaporthaceae*. *Pyriculariaceae,* as well as *Magnaporthaceae*, accommodate mainly plant

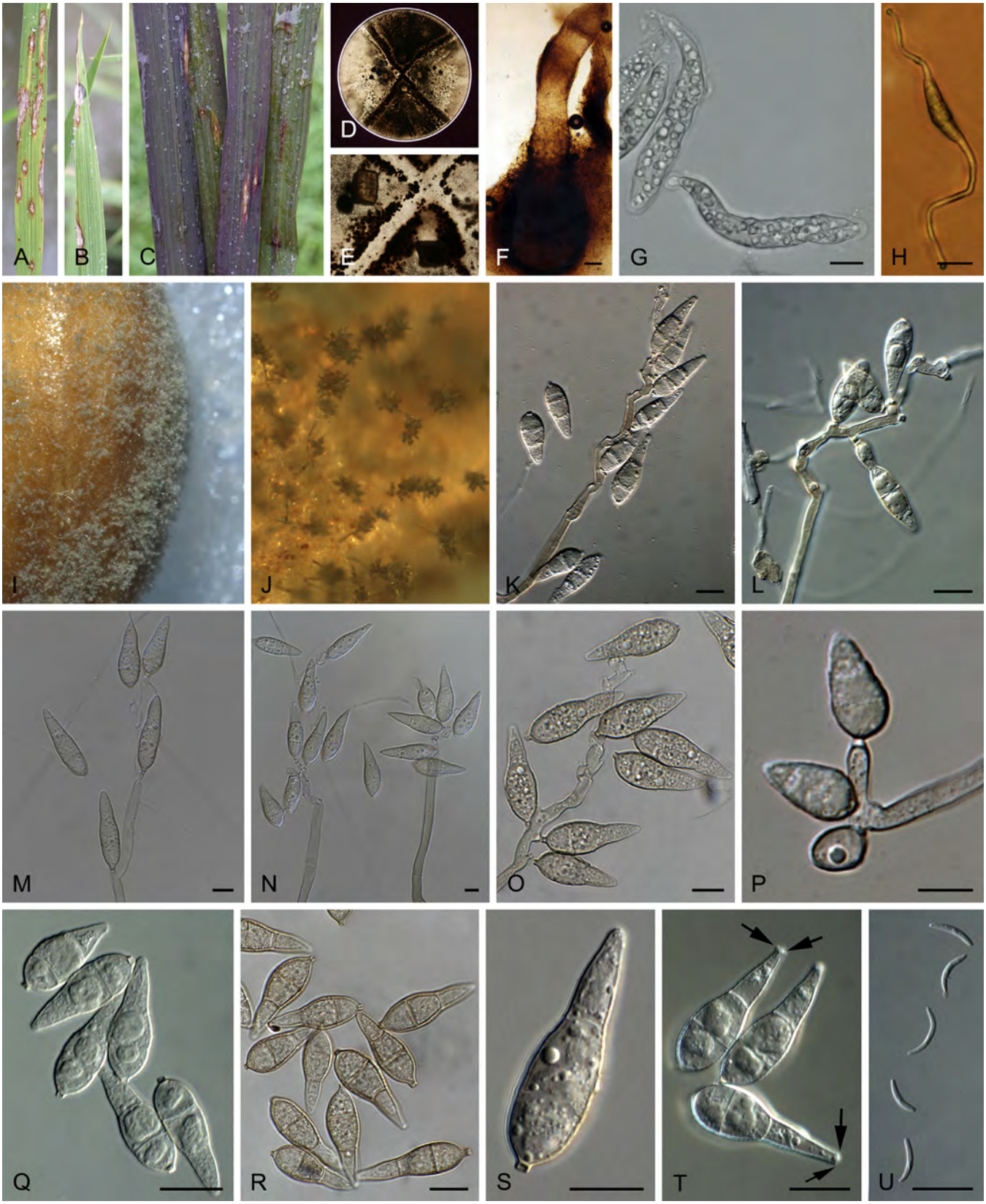

Fig. 52. *Pyricularia* spp. **A–C.** Leaf spots of rice caused by *Pyricularia oryzae*. **D–H.** Sexual morph of *Pyricularia oryzae*. **D, E.** Crossing of different strains of *Pyricularia oryzae* to produce the sexual morph. **F.** Ascoma. **G.** Asci. **H.** Germinating ascospore. **I–U.** Asexual morph. **I, J.** Sporulation on sterile barley seed on SNA. **I.** *Pyricularia grisea* (BR0029). **J.** *Pyricularia graminis-tritici* (ex-type URM7380). **K–P.** Conidiophores and conidia. **K, L.** *Pyricularia ctenantheicola* (GR0002). **M, N.** *Pyricularia graminis-tritici* (ex-type URM7380). **O.** *Pyricularia oryzae* (URM7369). **P.** *Pyricularia oryzae* (BF0028). **Q–S.** Conidia. **Q.** *Pyricularia ctenantheicola* (GR0002). **R.** *Pyricularia oryzae* (URM7369). **S.** *Pyricularia graminis-tritici* (ex-type URM7380). **T.** Macroconidia of *Pyricularia grisea* (BR0029) (arrows indicate apical marginal frill, which is a remnant of the apical mucoid cap). **U.** Microconidia of *Pyricularia grisea* (BR0029). Scale bars: F = 50 µm; others = 10 µm. Pictures D, E, G taken by Dounia Saleh, CIRAD; F, H by Didier Tharreau, CIRAD; I, K, L, P, Q, T from Klaubauf *et al.* (2014); J, M–O, R, S from Castroagudín *et al.* (2016).

Table 18. DNA barcodes of accepted *Pyricularia* spp.

Species	Isolates[1]	GenBank accession numbers[2]				References
		ITS	*act*	*cal*	*rpb1*	
Pyricularia angulata	NBRC 9625	AY265322	–	–	–	Bussaban *et al.* (2005)
Py. ctenantheicola	CBS 138601^T	KM484879	KM485183	KM485253	KM485099	Klaubauf *et al.* (2014)
Py. graminis-tritici	URM7380^T	–	KU952138	KU952892	–	Castroagudín *et al.* (2016)
Py. grisea	CBS 128304	KM484881	KM485184	KM485255	KM485101	Klaubauf *et al.* (2014)
Py. oryzae	CBS 255.38	KM484889	KM485190	KM485261	KM485109	Klaubauf *et al.* (2014)
Py. penniseticola	CBS 138603^T	KM484929	KM485220	–	KM485148	Klaubauf *et al.* (2014)
Py. pennisetigena	CBS 138604^T	KM484935	KM485225	KM485294	KM485153	Klaubauf *et al.* (2014)
Py. urashimae	CBS 142117^T	KY173437	KY173571	–	KY173578	Crous *et al.* (2016a)
Py. zingibericola	CBS 138605^T	KM484941	KM485229	KM485297	KM485157	Klaubauf *et al.* (2014)

[1] CBS: Westerdijk Fungal Biodiversity Institute, Utrecht, the Netherlands; NBRC: Biological Resource Center, NITE, Chiva, Japan; URM: Culture Collection Mycobank, Prof. Maria Auxiliadora Cavalcanti, Federal University of Pernambuco, Recife, Brazil. ^{T} indicates ex-type strains.
[2] ITS: internal transcribed spacers and intervening 5.8S nrDNA; *act*: partial actin gene; *cal*: partial calmodulin gene; *rpb1*: partial RNA polymerase II largest subunit gene.

pathogenic species, some of which are of major importance in agriculture.

Pyricularia oryzae is the causal agent of rice blast disease, which can result in up to a 30 % yield loss worldwide (Skamnioti & Gurr 2009). In a phylogenetic study based on 10 loci and 128 isolates of this species, three major clades were identified (Castroagudín *et al.* 2016). The first clade grouped the isolates associated only with rice and corresponds to the previously described rice blast pathogen *Py. oryzae* pathotype *Oryza*. The second clade accommodated isolates associated almost exclusively with wheat and corresponds to the previously described wheat blast pathogen *Py. oryzae* pathotype *Triticum*. A third clade accommodated isolates obtained from wheat as well as other *Poaceae*. This clade was distinct from *Py. oryzae* and represented a new species, *Pyricularia graminis-tritici*. This new species could not be morphologically distinguished from *Py. oryzae*, but a distinctive pathogenicity spectrum was observed (Castroagudín *et al.* 2016). However, the "*oryzae*" clade consists of various populations specific to different grass hosts that appear to be in the process of speciation. Consequently, the species in the "*oryzae*" clade are not commonly accepted, and some authors refer to them as lineages of *Py. oryzae* (Castroagudín *et al.* 2017). Further research is needed to resolve speciation within what is presently circumscribed as *Py. oryzae*.

The sexual morph has been reported only in *Py. grisea* and *Py. oryzae*, both being heterothallic species. These are indistinguishable in conidium, perithecium and ascospore morphology. However, *Py. oryzae* was described as a new species distinct from *Py. grisea* based on DNA sequence differences in three different loci (*act, cal* and *tub*) and host range, since *Py. grisea* infects only crab grass (Couch & Kohn 2002).

References: Klaubauf *et al.* 2014 (morphology and phylogeny); Castroagudín *et al.* 2016, 2017 (morphology, pathogenicity and phylogeny); Reges *et al.* 2016 (pathogenicity and phylogeny).

Authors: Y. Marin-Felix & P.W. Crous

Stenocarpella Syd. & P. Syd., Ann. Mycol. 15: 258. 1917. Fig. 53.
Synonyms: *Hendersoniopsis* Woron., Fungal and Bacterial Diseases of Agricultural Plants: 255. 1922.
Phaeostagonosporopsis Woron., La Defense des Plantes, Leningrad 2: 333. 1925.

Classification: *Sordariomycetes*, *Diaporthomycetidae*, *Diaporthales*, *Diaporthaceae*.

Type species: *Stenocarpella macrospora* (Earle) B. Sutton, basionym: *Diplodia macrospora* Earle. Isotype: IMI 12790. Ex-epitype strain designated by Crous *et al.* (2006b): CBS 117560 = MRC 8615.

DNA barcodes (genus): LSU, ITS.

DNA barcodes (species): ITS, *tef1*. Table 19.

Mycelium immersed, brown, branched, septate. *Conidiomata* pycnidial, solitary or sometimes confluent, globose or elongated, dark brown, subepidermal, unilocular; *conidiomatal wall* composed of dark brown, thick-walled cells of *textura angularis*; *neck* single, circular, papillate, protruding. *Conidiophores* usually reduced to conidiogenous cells. *Conidiogenous cells* enteroblastic, phialidic, determinate, discrete, rarely integrated on 1-septate conidiophores, cylindrical, collarette with minute channel, periclinal wall thickened, formed from inner cells of pycnidial wall. *Conidia* pale brown, 0−3-septate, continuous or constricted, cylindrical to fusiform, straight or curved, apex obtuse, base tapered and truncate, thick and smooth-walled, eguttulate. *Beta conidia* absent or present, hyaline, scolecosporous, curved. *Sexual morph* unknown (adapted from Sutton 1980).

Culture characteristics: Colonies flat, with abundant aerial mycelium giving a cottony appearance; under continuous near-ultraviolet light abundant sporulation in 1 wk. On OA surface white to rosy buff to vinaceous buff, centre isabelline; reverse vinaceous buff, centre isabelline.

Optimal media and cultivation conditions: OA and PNA at 25 °C under continuous near-ultraviolet light to promote sporulation.

Distribution: Africa, America, Asia and Europe.

Host: *Zea mays* (*Poaceae*).

Notes: The genus *Stenocarpella* was introduced by Sydow & Sydow (1917), with *S. zeae* designated as type species. Sutton (1977) synonymised *S. zeae* with *Diplodia macrospora*, transferring this latter species to *Stenocarpella,* recognising *S. macrospora* as the correct name for the type species. Two species are included in this genus i.e. *S. macrospora* and

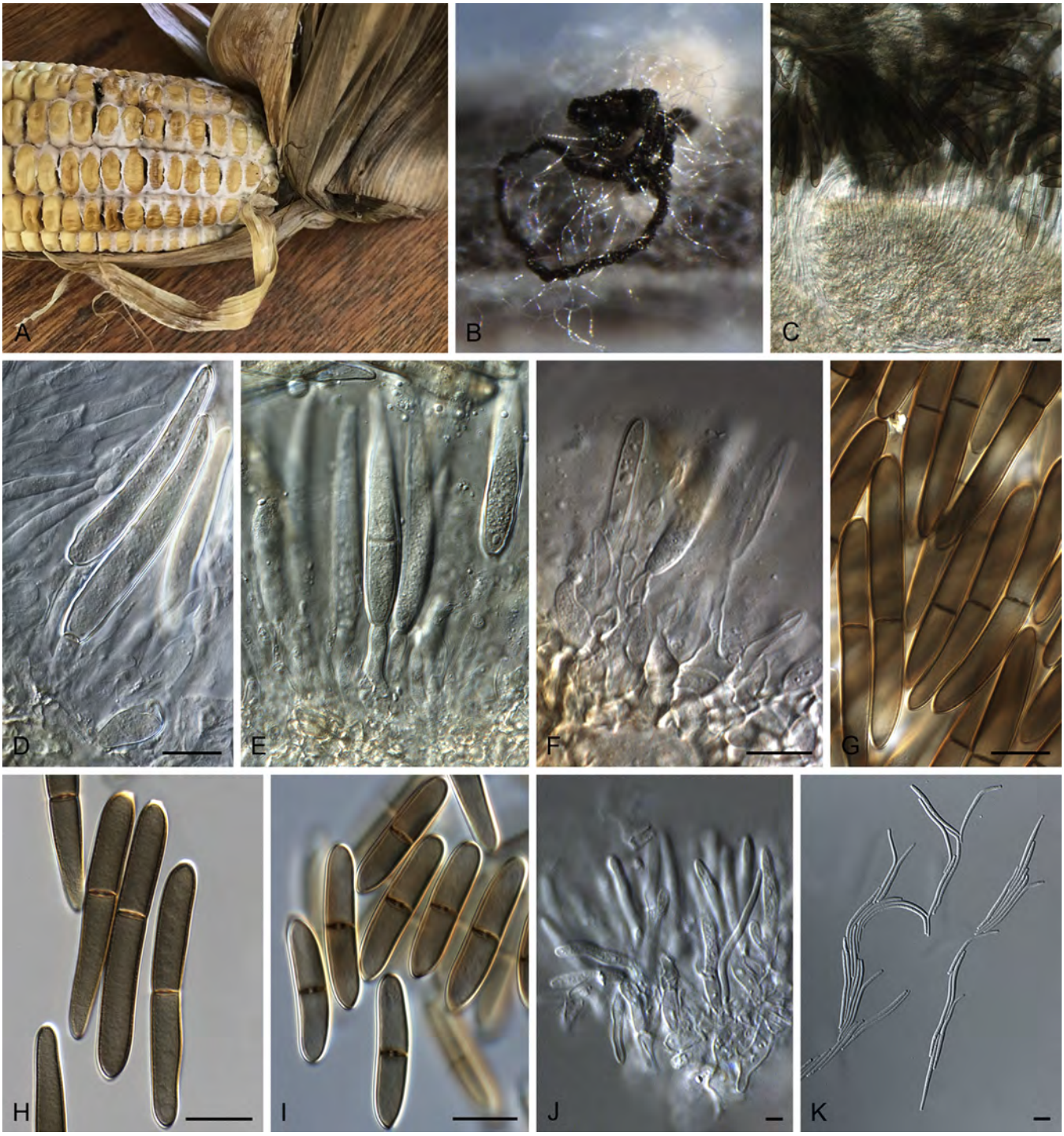

Fig. 53. *Stenocarpella* spp. **A.** *Zea mays* infected with *Stenocarpella maydis*. **B–K.** Asexual morphs. **B.** Conidiomata with exuding conidial mass on pine needle agar of *Stenocarpella maydis* (ex-epitype CBS 117559). **C.** Hyaline layer of conidiogenous cells giving rise to brown conidial mass of *Stenocarpella macrospora* (CPC 11863). **D–F.** Conidiogenous cells giving rise to conidia. **D, E.** *Stenocarpella macrospora* (CPC 11863). **F.** *Stenocarpella maydis* (ex-epitype CBS 117559). **G–I.** Conidia. **G, H.** *Stenocarpella macrospora* (CPC 11863). **I.** *Stenocarpella maydis* (ex-epitype CBS 117559). **J.** Conidiogenous cells giving rise to beta conidia of *Stenocarpella macrospora* (CPC 11863). **K.** Beta conidia of *Stenocarpella macrospora* (CPC 11863). Scale bars = 10 µm. All pictures except for A taken from Lamprecht *et al.* (2011).

Table 19. DNA barcodes of accepted *Stenocarpella* spp.

Species	Isolates[1]	GenBank accession number[2]		References
		ITS	*tef1*	
Stenocarpella macrospora	CBS 117560[ET]	FR748048	MG934504	Lamprecht *et al.* (2011), present study
S. maydis	CBS 117558[ET]	FR748051	FR748080	Lamprecht *et al.* (2011)

[1] CBS: Westerdijk Fungal Biodiversity Institute, Utrecht, The Netherlands. [ET] indicates ex-epitype strains.
[2] ITS: internal transcribed spacers and intervening 5.8S nrDNA; *tef1*: partial translation elongation factor 1-alpha gene.

S. maydis, which cause Diplodia ear rot of maize (Crous *et al.* 2006b).

Stenocarpella was initially placed in the *Botryosphaeriaceae* (*Botryosphaeriales*) because of the similarity with *Diplodia*. In a phylogenetic study based on LSU sequences, Crous *et al.* (2006b) showed that *Stenocarpella* belongs to the *Diaporthaceae* (*Diaporthales*). Subsequently, Lamprecht *et al.* (2011) confirmed this placement based on ITS and *tef1* sequences.

References: Sutton 1977, 1980 (morphology and pathogenicity); Crous *et al.* 2006b (morphology and phylogeny); Lamprecht *et al.* 2011 (morphology, pathogenicity and phylogeny).

Authors: Y. Marin-Felix & P.W. Crous

Utrechtiana Crous & Quaedvl., Persoonia 26: 153. 2011. Fig. 54.

Classification: *Sordariomycetes, Sordariomycetidae, Magnaporthales, Pyriculariaceae*.

Type species: *Utrechtiana roumeguerei* (Cavara) Videira & Crous, basionym: *Scolicotrichum roumeguerei* Cavara = *Utrechtiana cibiessia* Crous & Quaedvlieg. Holotype and ex-type strain of *Utrechtiana cibiessia*: CBS H-20594, CBS 128780.

DNA barcodes (genus): LSU, ITS.

DNA barcodes (species): ITS, *act, cal*, *rpb1*. Table 20. Fig. 28.

Mycelium internal, consisting of septate, smooth, hyaline, branched hyphae. *Conidiophores* predominantly solitary, erect, straight to flexuous, unbranched, 1-septate, medium brown to dark brown, subcylindrical with swollen basal cell. *Conidiogenous cells* integrated, terminal, cylindrical or subcylindrical, smooth or finely verruculose, thick-walled with thin-walled, clavate, bluntly rounded apex, with truncate, flattened scar, holoblastic; conidiophores rejuvenating percurrently. *Conidia* solitary, obpyriform or ellipsoid, pale brown, guttulate to granular, finely verruculose, 1–2-septate, thin-walled, apex bluntly to acutely rounded, base obtusely rounded with a flattened, darkened and thickened hilum that has a central pore. *Synasexual morph* selenosporella-like present or absent. *Microconidiophores* arranged in rosettes, branched, septate, pale brown, smooth, subcylindrical. *Microconidiogenous cells* pale brown, smooth to finely roughened, phialidic, terminal and lateral, fusoid-ellipsoid to ampulliform. *Microconidia* hyaline, smooth, aseptate, subcylindrical, straight to curved, ends obtuse.

Culture characteristics: Colonies flat, spreading, with moderate aerial mycelium and even smooth margins. On MEA surface dirty white, sometimes turning grey olivaceous when fertile; reverse luteous or olivaceous grey in centre and luteous in outer region. On OA olivaceous grey to iron-grey or dirty white.

Optimal media and cultivation conditions: On OA at 25 °C under dark, or autoclaved barley seeds placed on SNA at 25 °C under near-ultraviolet light (12 h light, 12 h dark).

Distribution: America, Asia, Australia and Europe.

Hosts: *Phragmites* spp (*Poaceae*).

Disease symptoms: Leaf spot.

Notes: The genus *Utrechtiana* was described by Crous *et al.* (2011a) to accommodate the type species named *Utrecthiana cibiessia*, which is a foliar pathogen of *Phragmites*. However, this genus was considered synonymous with *Deightoniella* by Seifert *et al.* (2011) because of the morphology of the conidiophores (solitary, brown, with percurrent rejuvenation) and conidia (brown and septate). Moreover, *U. cibiessia* was demonstrated to be a synonym of *Deightoniella roumeguerei*, which Klaubauf *et al.* (2014) showed to belong to *Pyriculariaceae*, a family containing numerous cryptic fungal genera on *Poaceae*.

However, *Deightoniella* has been shown to represent a polyphyletic genus. For example, *Deightoniella torulosa*, which is a foliar pathogen of *Musa*, proved to be a species of *Corynespora* (Crous *et al.* 2013), while a similar fungus occurring on leaf spots of *Phragmites* in South Africa was placed in *Neodeightoniella* (Crous *et al.* 2013). In a recent study, Videira *et al.* (2017) considered *Utrechtiana* and *Deightoniella* based on the type species *Deightoniella africana* to be different genera based on morphological characteristics. *Utrechtiana* lacks torsive to flexuous conidiophores with prominent conidiophore swellings, and its conidia are also pale brown, smooth to finely roughened, with prominent thickened, darkened scars. In contrast, conidia in *Deightoniella* are medium brown, verruculose, and obpyriform with prominent apical taper. In order to clarify the phylogenetic relationships between both genera, fresh material of *Deightoniella africana* is needed.

References: Constantinescu 1983 (morphology and pathogenicity); Crous *et al.* 2011a, Klaubauf *et al.* 2014, Videira *et al.* 2017 (morphology and phylogeny); Mel'nik & Shabunin 2011 (morphology).

Utrechtiana arundinacea (Corda) Crous, Quaedvl. & Y. Marín, **comb. nov.** MycoBank MB824141. Fig. 54.

Basionym: *Helminthosporium arundinaceum* Corda, as "*Helmisporium*", Icon. fung. (Prague) 3: 10, tab. 2, fig. 25. 1839.

Synonyms: *Napicladium arundinaceum* (Corda) Sacc., Syll. fung. 4: 482. 1886.

Deightoniella arundinacea (Corda) S. Hughes, Mycol. Pap. 48: 29. 1952.

Causing blight-like amphigenous lesions along leaves of *Phragmites*, medium brown with red-purple margins and yellow halo, extending across breadth of leaf, up to 7 mm diam, and along length, up to 20 cm long. *Macroconidiophores* 30–50 × 9–12 µm, amphigenous, predominantly solitary, but at times in fascicles of up to three, straight to flexuous, unbranched, 1-septate, medium brown, smooth, subcylindrical with swollen basal cell, 10–15 µm diam. *Macroconidiogenous cells* 20–35 × 7–9 µm, integrated, terminal, cylindrical, thick-walled with thin-walled apex, holoblastic; conidiophores proliferate percurrently. *Macroconidia* (22–)37–42(–45) × (17–)19–20(–21) µm, solitary, obpyriform, pale brown, guttulate, finely verruculose, (1–)2-septate, with distinct dark brown hilum, 3–4 µm. A selenosporella-like *synasexual morph* develops in culture, with microconidiophores arranged in rosettes, 15–40 × 3–6 µm, branched, 3–6-septate, pale brown, smooth, subcylindrical. *Microconidiogenous cells* 5–14 × 3–4 µm, pale brown, smooth to finely roughened, phialidic, terminal and lateral, fusoid-ellipsoid to ampulliform. *Microconidia* 7–10 × 1.5–2 µm, hyaline, smooth, aseptate, subcylindrical, straight to curved, ends obtuse. *Macroconidiophores* in culture up to 6-septate, 100 µm tall. *Macroconidia* 23–50 × 11–15 µm, slender, pyriform, prominently verrucose, medium brown.

Fig. 54. A–I. *Utrechtiana arundinacea* (ex-epitype CPC 33994). **A.** Leaf spot on *Phragmites* sp. **B–E.** Macroconidiophores bearing macroconidia. **F–H.** Microconidiophores bearing microconidia. **I.** Microconidia. **J–S.** *Utrechtiana roumeguerei* (ex-type CBS 128780). **J.** Leaf spot on *Phragmites australis*. **K.** Close-up of conidiophores on leaf surface. **L–P.** Conidiophores bearing conidia. **Q.** Germinating conidium. **R, S.** Conidia. Scale bars = 10 µm. Pictures J–S taken from Klaubauf *et al.* (2014).

Table 20. DNA barcodes of accepted *Utrechtiana* spp.

Species	Isolates[1]	GenBank accession numbers[2]				References
		ITS	*act*	*cal*	*rpb1*	
Utrechtiana arundinacea	CPC 33994^{ET}	MG934461	MG934468	MG934542	MG934473	Present study
U. roumeguerei	CBS 128780^{T}	JF951153	KM485163	KM485232	KM485047	Crous *et al.* (2011a), Klaubauf *et al.* (2014)

[1] CBS: Westerdijk Fungal Biodiversity Institute, Utrecht, the Netherlands; CPC: Personal collection of Pedro Crous housed at the Westerdijk Fungal Biodiversity Institute. ^{T} and ^{ET} indicate ex-type and ex-epitype strains, respectively.
[2] ITS: internal transcribed spacers and intervening 5.8S nrDNA; *act*: partial actin gene; *cal*: partial calmodulin gene; *rpb1*: partial RNA polymerase II largest subunit gene.

Culture characteristics: Colonies flat, spreading, with moderate aerial mycelium and even smooth margins. On MEA surface dirty white; reverse olivaceous grey in centre, luteous in outer region. On OA olivaceous grey to iron-grey.

Materials examined: **Czech Republic**, Prague, on living leaves of *Phragmites* sp. (*Poaceae*), 1838 (**holotype** in PRM missing, but slide ex-holotype**,** DAOM 19793). **The Netherlands**, on leaves of *Phragmites* sp. (*Poaceae*), 2 Jun. 2017, A. Mulder (**epitype of *Helminthosporium arundinaceum* designated here** CBS H-23402, MBT380884, culture ex-epitype CPC 33994).

Notes: *Utrechtiana arundinacea* is a commonly encountered European taxon treated in *Deightoniella* in previous studies (Constantinescu 1983, Mel'nik & Shabunin 2011, Ghosta & Abrinbana 2016). Morphologically, *U. arundinacea* and *U. constantinescui* appear to be related.

Macroconidia of *U. arundinaceum* exhibit a strange phenomenon where a third septum develops 3–5 µm from the apex. The conidium body is prominently guttulate, except for this terminal chamber, which is smooth, pale brown, and lacks any guttules. This strange conidial apex is also visible in conidia of *U. constantinescui* (Mel'nik & Shabunin 2011), and apparently plays some role in infection/attachment, probably exuding a mucoid droplet, as is also seen in some genera in the *Pyriculariaceae* (Klaubauf *et al.* 2014). Furthermore, Mel'nik & Shabunin (2011) illustrate a selenosporella-like synasexual morph in both species, which has not been seen in *U. roumeguerei*, the type species of the genus.

Utrechtiana roumeguerei was considered conspecific with *U. arundinacea* (Ellis 1957) until Constantinescu (1983) demonstrated that they are distinct species based on morphology and pathogenicity. *Utrechtiana arundinacea* often produces percurrently proliferating conidiogenous cells and obclavate 2-septate conidia, while *U. roumeguerei* is characterised by rarely percurrent conidiogenous cells and ovate to broadly ellipsoidal, 1-septate conidia. Moreover, *U. arundinacea* produces systemic infection in the host issues, whereas *U. roumeguerei* induces a local infection with limited development. In the present study, the DNA data support the placement of both taxa in the same genus (Fig. 28).

The holotype specimen of *Helminthosporium arundinaceum* could not be located in PRM, and is presumed missing. However, a slide from the original material was preserved in DAOM. Due to the lack of living culture of that species, a specimen isolated from the same host and region is here designated as epitype.

Utrechtiana constantinescui (Melnik & Shabunin) Crous & Y. Marín, **comb. nov.** MycoBank MB824142.
Basionym: *Deightoniella constantinescui* Melnik & Shabunin, Mikol. Fitopatol. 45: 257. 2011.

Notes: The new combination *U. constantinescui* is designated here based on the morphology of its macro- and microconidial morphs. Fresh material should be recollected to verify this placement. As we mentioned above, this species is morphologically related to *U. arundinacea*. Both species can be distinguished based on the shape of their macroconidia (obpyriform in *U. arundinacea vs.* barrel-shaped in *U. constantinescui*) and the position of the conidial septa in *U. constantinescui*, 7–13 µm apart.

Authors: Y. Marin-Felix, W. Quaedvlieg & P.W. Crous

Wojnowiciella Crous, *et al.*, Persoonia 34: 201. 2015. Fig. 55.

Classification: *Dothideomycetes, Pleosporomycetidae*, *Pleosporales*, *Phaeosphaeriaceae*.

Type species: *Wojnowiciella eucalypti* Crous, *et al.* Holotype and ex-type strain: CBS H-22233, CBS 139904.

DNA barcode (genus): LSU.

DNA barcodes (species): ITS, *rpb2, tef1*. Table 21. Fig. 56.

Conidiomata pycnidial, globose, brown, separate, non-papillate or papillate, with central ostiole; *conidiomatal wall* composed of 3–6 layers of brown cells, *textura angularis. Conidiophores* reduced to conidiogenous cells. *Conidiogenous cells* lining cavity, hyaline to pale brown, smooth, ampulliform to subcylindrical, appearing phialidic. *Macroconidia* subcylindrical, straight to slightly curved, apex subobtuse, base truncate, septate, at times with 1–2 oblique septa, thick-walled, verruculose, guttulate, golden brown. *Microconidia* in same or different conidiomata as macroconidia. *Microconidiophores* intermingled with macroconidiogenous cells, branched at base, septate, subcylindrical, hyaline, smooth. *Microconidiogenous cells* terminal and intercalary, hyaline, smooth, ampulliform to subcylindrical, phialidic with periclinal thickening. *Microconidia* solitary, hyaline, guttulate, smooth, subcylindrical to ellipsoid, apex obtuse to subobtuse, base truncate.

Culture characteristics: Colonies on MEA, cottony, isabelline, greenish olivaceous, mouse grey to greyish sepia, sometimes with luteous exudate; reverse greyish sepia, chestnut, fulvous. Colonies on PDA pale mouse grey, brown vinaceous or greenish olivaceous, sometimes with luteous diffusible pigment; reverse luteous and black, greyish sepia or brown vinaceous.

Optimal media and cultivation conditions: On autoclaved banana leaves placed on SNA at 25 °C under near-ultraviolet light (12 h light, 12 h dark).

Distribution: Australia, China, Colombia, Italy and South Africa.

Hosts: *Cissampelos capensis* (*Menispermaceae*), *Dactylis glomerata* (*Poaceae*), *Eucalyptus grandis* (*Myrtaceae*), *Leptocarpus* sp. (*Restionaceae*), *Lonicera* sp. and *Viburnum utile* (*Caprifoliaceae*), and *Spartium* sp. (*Fabaceae*).

Fig. 55. *Wojnowiciella* spp. **A–F.** Conidiomata overview. **A.** *Wojnowiciella leptocarpi* (ex-type CBS 116584). **B, E.** *Wojnowiciella dactylidis* (CPC 30353). **C.** *Wojnowiciella cissampeli* (ex-type CBS 141297). **D.** *Wojnowiciella eucalypti* (ex-type CBS 139904). **F.** *Wojnowiciella dactylidis* (CPC 32741). **G, H.** Hand section of the conidiomata with hyaline conidiogenous cells and dark brown conidia of *Wojnowiciella leptocarpi* (ex-type CBS 116584). **I–L.** Conidiogenous cells. **I, J.** *Wojnowiciella cissampeli* (ex-type CBS 141297). **K.** *Wojnowiciella eucalypti* (ex-type CBS 139904). **L.** *Wojnowiciella leptocarpi* (CBS 116585). **M–Q.** Macroconidia. **M, N.** *Wojnowiciella leptocarpi* (ex-type CBS 116584). **O.** *Wojnowiciella cissampeli* (ex-type CBS 141297). **P.** *Wojnowiciella dactylidis* (CPC 32741). **Q.** *Wojnowiciella dactylidis* (CPC 30353). **R.** Microconidia of *Wojnowiciella eucalypti* (ex-type CBS 139904). Scale bars: E–G = 50 µm; H = 20 µm; others = 10 µm. Pictures taken from Crous *et al.* (2015d, 2016b).

Disease symptoms: Leaf spots.

Notes: *Wojnowiciella* was established with *W. eucalypti* as type species, which differs from *Septoriella hirta* (syn. *Wojnowicia hirta*) by non-setous conidiomata, dark brown conidia and hyaline microconidia (Crous *et al.* 2015d). Although both genera belong to *Phaeosphaeriaceae*, *Wojnowicia* has been synonymised with *Septoriella* (Crous *et al.* 2015a). Currently *Wojnowiciella* comprises seven species isolated from leaf spots and twigs of different hosts (Table 21). Although they were associated with disease symptoms, their pathogenicity needs to be proven.

References: Wijayawardene *et al.* 2013 (morphology, as *Wojnowicia*); Crous *et al.* 2015d, 2016b (morphology); Li *et al.* 2015 (morphology and phylogeny, as *Wojnowicia*); Liu *et al.* 2015 (morphology and phylogeny, as *Wojnowicia*); Hernández-Restrepo *et al.* 2016c (morphology and phylogeny).

Authors: M. Hernández-Restrepo & P.W. Crous

Table 21. DNA barcodes of accepted *Wojnowiciella* spp.

Species	Isolates[1]	GenBank accession numbers[2]				References
		ITS	LSU	*rpb2*	*tef1*	
Wojnowiciella cissampeli	CBS 141297^T	KX228272	KX228323	–	LT990616	Crous *et al.* (2016b), present study
W. dactylidis	MFLUCC 13-0735^T	KP744470	KP684149	–	–	Liu *et al.* (2015)
	CPC 27468	LT990658	LT990630	LT990644	LT990611	Present study
	CPC 30353	LT990659	LT990631	–	LT990612	Present study
	CPC 32741	LT990660	LT990632	–	LT990613	Present study
	CPC 33929	LT990661	LT990633	LT990645	LT990614	Present study
W. eucalypti	CBS 139904^T	KR476741	KR476774	–	LT990617	Crous *et al.* (2015d), present study
W. leptocarpi	CBS 115684^T	KX306775	KX306800	LT990646	LT990615	Hernández-Restrepo *et al.* (2016c), present study
W. lonicerae	MFLUCC 13-0737^T	KP744471	KP684151	–	–	Liu *et al.* (2015)
W. spartii	MFLUCC 13-0402^T	KU058719	KU058729	–	–	Li *et al.* (2015)
W. viburni	MFLUCC 12-0733^T	KC594286	KC594287	–	–	Wijayawardene *et al.* (2013)

[1] CBS: Westerdijk Fungal Biodiversity Institute, Utrecht, the Netherlands; CPC: Personal collection of Pedro Crous housed at the Westerdijk Fungal Biodiversity Institute; MFLUCC: Mae Fah Luang University Culture Collection, Chiang Rai, Thailand. ^{T} indicates ex-type strain.
[2] ITS: internal transcribed spacers and intervening 5.8S nrDNA; LSU: partial large subunit RNA gene; *rpb2*: partial RNA polymerase II second largest subunit gene; *tef1*: partial translation elongation factor 1-alpha gene.

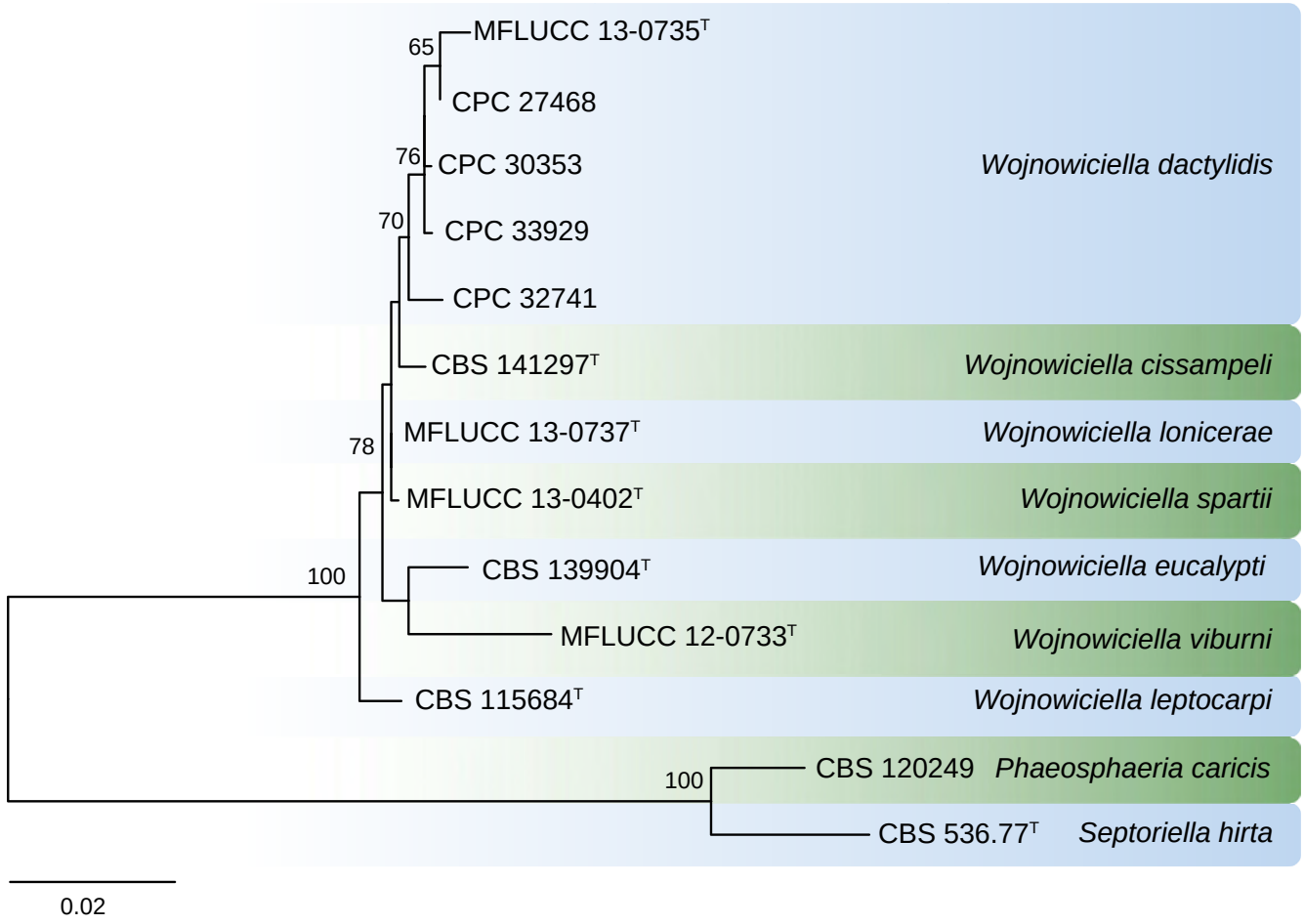

Fig. 56. RAxML phylogram obtained from the combined ITS (742 bp), LSU (885 bp), *rpb2* (1029 bp) and *tef1* (998 bp) sequence alignment of all the accepted species of *Wojnowiciella*. The tree was rooted to *Phaeosphaeria caricis* CBS 120249 and *Septoriella hirta* CBS 536.77. RAxML bootstrap support (BS) values above 70 % are shown in the nodes. GenBank accession numbers are indicated in Table 21. ^{T} indicates ex-type strains. TreeBASE: S21899.

ACKNOWLEDGEMENTS

Yasmina Marin-Felix is grateful for the financial support received from the Vice-Chancellor's postdoctoral fellowship programme from University of Pretoria, South Africa. Keith A. Seifert is thanked for making images of *Helminthosporium arundinaceum* (slide ex-holotype, DAOM 19793) available for comparison. Didier Tharreau is thanked for digital images of *Pyricularia oryzae*, and Susan Thompson for *Diaporthe gulyae*.

REFERENCES

Agustí-Brisach C, León M, García-Jiménez J, *et al.* (2015). Detection of grapevine fungal trunk pathogens on pruning shears and evaluation of their potential for spread of infection. *Plant Disease* **99**: 976–981.
Al-Subhi AM, Al-Adawi AO, Van Wyk M, *et al.* (2006). *Ceratocystis omanensis*, a new species from diseased mango trees in Oman. *Mycological Research* **110**: 237–245.

Andjic V, Hardy GE, Cortinas MN, *et al*. (2007). Multiple gene genealogies reveal important relationships between species of *Phaeophleospora* infecting *Eucalyptus* leaves. *FEMS Microbiology Letters* **268**: 22–33.

Ando Y, Masuya H, Aikawa T, *et al*. (2017). *Diaporthe toxicodendri* sp. nov., a causal fungus of the canker disease on *Toxicodendron vernicifluum* in Japan. *Mycosphere* **8**: 1157–1167.

Ando Y, Motohashi K, Yaguchi Y (2013). Taxonomic re-examination of Cryptomeria gall disease causing fungus. *Japanese Journal of Mycology* **54**: 15–26.

Ariyawansa HA, Hyde KD, Jayasiri SC, *et al*. (2015). Fungal diversity notes 111–252—taxonomic and phylogenetic contributions to fungal taxa. *Fungal Diversity* **75**: 27–274.

Aroca A, Raposo R (2007). PCR-based strategy to detect and identify species of *Phaeoacremonium* causing grapevine diseases. *Applied Environmental Microbiology* **73**: 2911–2918.

Aroca A, Raposo R (2009). Pathogenicity of *Phaeoacremonium* species on grapevines. *Journal of Phytopathology* **157**: 413–419.

Asher MJC, Shipton PJ (1981). *Biology and control of take-all*. Academic Press, London, UK.

Augustin C, Ulrich K, Ward E, *et al*. (1999). RAPD-based inter- and intravarietal classification of fungi of the *Gaeumannomyces–Phialophora* complex. *Journal of Phytopathology* **147**: 109–117.

Aveskamp MM, Verkley GJ, de Gruyter J, *et al*. (2009). DNA phylogeny reveals polyphyly of *Phoma* section *Peyronellaea* and multiple taxonomic novelties. *Mycologia* **101**: 363–382.

Aveskamp MM, de Gruyter J, Woudenberg JHC, *et al*. (2010). Highlights of the *Didymellaceae*: a polyphasic approach to characterise *Phoma* and related pleosporalean genera. *Studies in Mycology* **65**: 1–60.

Baayen RP, Bonants PJ, Verkley G, *et al*. (2002). Nonpathogenic isolates of the citrus black spot fungus, *Guignardia citricarpa*, identified as a cosmopolitan endophyte of woody plants, *G. mangiferae* (*Phyllosticta capitalensis*). *Phytopathology* **92**: 464–477.

Bateman GL, Ward E, Antoniw JF (1992). Identification of *Gaeumannomyces graminis* var. *tritici* and *G. graminis* var. *avenae* using a DNA probe and non-molecular methods. *Mycological Research* **96**: 737–742.

Baudoin ABAM (1986). First report of *Dichotomophthora indica* on common Purslane in Virginia. *Plant Disease* **70**: 352.

Blanco-Ulate B, Rolshausen P, Cantu D (2013). Draft genome sequence of the ascomycete *Phaeoacremonium aleophilum* strain UCR-PA7, a causal agent of the esca disease complex in grapevines. *Genome Announcements* **1**: e00390–e00413.

Boerema GH, de Gruyter J, Noordeloos ME, *et al*. (2004). *Phoma identification manual: differentiation of specific and infra-specific taxa in culture*. CABI Publishing, Wallingford, UK.

Boesewinkel HJ (1982). *Cylindrocladiella*, a new genus to accommodate *Cylindrocladium parvum* and other small-spored species of *Cylindrocladium*. *Canadian Journal of Botany* **60**: 2288–2294.

Braun U (1995). *A monograph of Cercosporella, Ramularia and allied genera (phytopathogenic hyphomycetes)*: **Vol. 1**. IHW Verlag, Eching, Germany.

Bussaban B, Lumyong S, Lumyong P, *et al*. (2005). Molecular and morphological characterization of *Pyricularia* and allied genera. *Mycologia* **97**: 1002–1011.

Carlucci A, Lops F, Cibelli F, *et al*. (2015). *Phaeoacremonium* species associated with olive wilt and decline in southern Italy. *European Journal of Plant Pathology* **141**: 717–729.

Carstens E, Linde CC, Slabbert R, *et al*. (2017). A global perspective on the population structure and reproductive system of *Phyllosticta citricarpa*. *Phytopathology* **107**: 758–768.

Castroagudín VL, Danelli A, Moreira SI, *et al*. (2017). The wheat blast pathogen *Pyricularia graminis-tritici* has complex origins and a disease cycle spanning multiple grass hosts. *BioRxiv*, 203455. https://doi.org/10.1101/203455.

Castroagudín VL, Moreira SI, Pereira DAS, *et al*. (2016). *Pyricularia graminis-tritici*, a new *Pyricularia* species causing wheat blast. *Persoonia* **36**: 199–216.

Chen SF, Van Wyk M, Roux J, *et al*. (2013). Taxonomy and pathogenicity of *Ceratocystis* species on *Eucalyptus* trees in South China, including *C. chinaeucensis* sp. nov. *Fungal Diversity* **58**: 267–279.

Constantinescu O (1983). *Deightoniella* on *Phragmites*. *Proceedings van de Koninklijke Nederlandse Akademie van Wetenschappen Section C* **86**: 137–141.

Couch BC, Kohn LM (2002). A multilocus gene genealogy concord-ant with host preference indicates segregation of a new species, *Magnaporthe oryzae*, from *M. grisea*. *Mycologia* **94**: 683–693.

Crous PW (2002). *Taxonomy and pathology of Cylindrocladium (Calonectria) and allied genera*. APS Press, St. Paul, Minnesota, USA.

Crous PW, Carris LM, Giraldo A, *et al*. (2015a). The Genera of Fungi – fixing the application of the type species of generic names – G 2: *Allantophomopsis, Latorua, Macrodiplodiopsis, Macrohilum, Milospium, Protostegia, Pyricularia, Robillarda, Rotula, Septoriella, Torula*, and *Wojnowicia*. *IMA Fungus* **6**: 163–198.

Crous PW, Decock C, Schoch CL (2001). *Xenocylindrocladium guianense* and *X. subverticmatum*, two new species of hyphomycetes from plant debris in the tropics. *Mycoscience* **42**: 559–566.

Crous PW, Gams W, Stalpers JA, *et al*. (2004a). MycoBank: an online initiative to launch mycology into the 21st century. *Studies in Mycology* **50**: 19–22.

Crous PW, Gams W, Wingfield MJ, *et al*. (1996). *Phaeoacremonium* gen. nov. associated with wilt and decline diseases of woody hosts and human infections. *Mycologia* **88**: 786–796.

Crous PW, Giraldo A, Hawksworth DL, *et al*. (2014a). The Genera of Fungi: fixing the application of the type species of generic names. *IMA Fungus* **5**: 141–160.

Crous PW, Groenewald JZ, Gams W (2003). Eyespot of cereals revisited: ITS phylogeny reveals new species relationships. *European Journal of Plant Pathology* **109**: 841–850.

Crous PW, Groenewald JZ, Shivas RG, *et al*. (2011a). Fungal Planet Description Sheets: 69–91. *Persoonia* **26**: 108–156.

Crous PW, Hawksworth DL, Wingfield MJ (2015b). Identifying and naming plant-pathogenic fungi: past, present, and future. *Annual Review of Phytopathology* **53**: 247–267.

Crous PW, Mohammed C, Glen M, *et al*. (2007). Eucalyptus microfungi known from culture. 3. *Eucasphaeria* and *Sympoventuria* genera nova, and new species of *Furcaspora*, *Harknessia*, *Heteroconium* and *Phacidiella*. *Fungal Diversity* **25**: 19–36.

Crous PW, Phillips AJL, Wingfield MJ (1991a). The genera *Cylindrocladium* and *Cylindrocladiella* in South Africa, with special reference to forest nurseries. *South African Journal of Forestry* **157**: 69–85.

Crous PW, Quaedvlieg W, Hansen K, *et al*. (2014b). *Phacidium* and *Ceuthospora (Phacidiaceae)* are congeneric: taxonomic and nomenclatural implications. *IMA Fungus* **5**: 173–193.

Crous PW, Schroers H-J, Groenewald JZ, *et al*. (2006a). *Metulocladosporiella* gen. nov. for the causal organism of Cladosporium speckle disease of banana. *Mycological Research* **110**: 264–275.

Crous PW, Schumacher RK, Wingfield MJ, *et al*. (2015c). Fungal Systematics and Evolution, FUSE 1. *Sydowia* **67**: 81–118.

Crous PW, Shivas RG, Quaedvlieg W, *et al*. (2014c). Fungal Planet description sheets: 214–280. *Persoonia* **32**: 184–306.

Crous PW, Schumacher RK, Wingfield MJ, *et al*. (2018). New and interesting fungi. 1. *Fungal Systematics and Evolution* **1**: 169–215.

Crous PW, Shivas RG, Wingfield MJ, *et al*. (2012a). Fungal Planet description sheets: 128–153. *Persoonia* **29**: 146–201.

Crous PW, Slippers B, Wingfield MJ, *et al*. (2006b). Phylogenetic lineages in the *Botryosphaeriaceae*. *Studies in Mycology* **55**: 235–253.

Crous PW, Summerell BA, Shivas RG, *et al*. (2011b). Fungal Planet description sheets: 92–106. *Persoonia* **27**: 130–162.

Crous PW, Summerell BA, Shivas RG, *et al*. (2012b). Fungal Planet description sheets: 107–127. *Persoonia* **28**: 138–182.

Crous PW, Summerell BA, Shivas RG, *et al*. (2012c). A re-appraisal of *Harknessia (Diaporthales)*, and the introduction of *Harknessiaceae* fam. nov. *Persoonia* **28**: 49–65.

Crous PW, Summerell BA, Swart L, *et al*. (2011c). Fungal pathogens of *Proteaceae*. *Persoonia* **27**: 20–45.

Crous PW, Verkley GJM, Groenewald JZ, *et al*. (2009). *Fungal biodiversity. CBS Laboratory Manual Series 1*. CBS-KNAW Fungal Biodiversity Centre, Utrecht, The Netherlands.

Crous PW, Wingfield MJ (1993). A re-evaluation of *Cylindrocladiella*, and a comparison with morphologically similar genera. *Mycological Research* **97**: 433–448.

Crous PW, Wingfield MJ, Burgess TI, *et al*. (2016a). Fungal Planet description sheets: 469–557. *Persoonia* **37**: 218–403.

Crous PW, Wingfield MJ, Burgess TI, *et al*. (2017a). Fungal Planet description sheets: 558–624. *Persoonia* **38**: 240–384.

Crous PW, Wingfield MJ, Burgess TI, *et al*. (2017b). Fungal Planet description sheets: 625–715. *Persoonia* **39**: 270–467.

Crous PW, Wingfield MJ, Guarro J, *et al*. (2013). Fungal Planet description sheets: 154–213. *Persoonia* **31**: 188–296.

Crous PW, Wingfield MJ, Guarro J, *et al*. (2015d). Fungal Planet description sheets: 320–370. *Persoonia* **34**: 167–266.

Crous PW, Wingfield MJ, Le Roux JJ, *et al*. (2015e). Fungal Planet description sheets: 371–399. *Persoonia* **35**: 264–327.

Crous PW, Wingfield MJ, Park RF (1991b). *Mycosphaerella nubilosa* a synonym of *M. molleriana*. *Mycological Research* **95**: 628–632.
Crous PW, Wingfield MJ, Richardson DM, *et al.* (2016b). Fungal Planet description sheets: 400–468. *Persoonia* **36**: 316–458.
Crous PW, Wingfield MJ, Schumacher RK, *et al.* (2014d). Fungal Planet description sheets: 281–319. *Persoonia* **33**: 212–289.
da Silva MA, Correia KC, Barbosa MAG, *et al.* (2017). Characterization of *Phaeoacremonium* isolates associated with Petri disease of table grape in Northeastern Brazil, with description of *Phaeoacremonium nordesticola* sp. nov. *European Journal of Plant Pathology* **149**: 695–709.
Damm U, Mostert L, Crous PW, *et al.* (2008). Novel *Phaeoacremonium* species associated with necrotic wood of *Prunus* trees. *Persoonia* **20**: 87–102.
De Beer ZW, Duong TA, Barnes I, *et al.* (2014). Redefining *Ceratocystis* and allied genera. *Studies in Mycology* **79**: 187–219.
De Beer ZW, Seifert KA, Wingfield MJ (2013a). The ophiostomatoid fungi: their dual position in the *Sordariomycetes*. In: *The ophiostomatoid fungi: expanding frontiers. CBS Biodiversity Series 12* (Seifert KA, De Beer ZW, Wingfield MJ, eds.). CBS-KNAW Fungal Biodiversity Centre, Utrecht, The Netherlands: 1–19.
De Beer ZW, Seifert KA, Wingfield MJ (2013b). A nomenclator for ophiostomatoid genera and species in the *Ophiostomatales* and *Microascales*. In: *The ophiostomatoid fungi: expanding frontiers. CBS Biodiversity Series 12* (Seifert KA, De Beer ZW, Wingfield MJ, eds.). CBS-KNAW Fungal Biodiversity Centre, Utrecht, The Netherlands: 245–322.
de Gruyter, Boerema GH (2002). Contributions towards a monograph of *Phoma* (Coelomycetes) VIII. Section *Paraphoma*: Taxa with setose pycnidia. *Persoonia* **17**: 541–561.
de Gruyter J, Woudenberg JH, Aveskamp MM, *et al.* (2010). Systematic reappraisal of species in *Phoma* section *Paraphoma, Pyrenochaeta* and *Pleurophoma*. *Mycologia* **102**: 1066–1081.
de Gruyter J, Woudenberg JHC, Aveskamp MM, *et al.* (2013). Redisposition of phoma-like anamorphs in *Pleosporales* re-evaluation. *Studies in Mycology* **75**: 1–36.
De Hoog GS, Guarro J, Gené J, *et al.* (2000). *Atlas of clinical fungi*, 2nd ed. Centraalbureau voor Schimmelcultures, Utrecht and Universitat Rovira i Virgili, Reus.
De Hoog GS, Hermanides-Nijhof EJ (1977). Survey of the black yeasts and allied fungi. *Studies in Mycology* **15**: 178–222.
De Hoog GS, van Oorschot CAN (1983). Taxonomy of the *Dactylaria* complex I: Notes on the genus *Dichotomophthora*. *Proceedings van de Koninklijke Nederlandse Akademie van Wetenschappen Section C* **86**: 55–61.
Deacon JW (1973). *Phialophora radicicola* and *Gaeumannomyces graminis* on roots of grasses and cereals. *Transactions of the British Mycological Society* **61**: 471–485.
Deacon JW (1974). Further studies on *Phialophora radicicola* and *Gaeumannomyces graminis* on roots and stem bases of grasses and cereals. *Transactions of the British Mycological Society* **63**: 307–327.
Dennis RWG (1960). *British cup fungi and their allies: An introduction to the Ascomycetes*. Ray Society, London, UK.
Dissanayake AJ, Camporesi E, Hyde KD, *et al.* (2017a). Molecular phylogenetic analysis reveals seven new *Diaporthe* species from Italy. *Mycosphere* **8**: 853–877.
Dissanayake AJ, Phillips AJL, Hyde KD, *et al.* (2017b). The current status of species in *Diaporthe*. *Mycosphere* **8**: 1106–1156.
Dissanayake AJ, Zhang W, Liu M, *et al.* (2017c). *Diaporthe* species associated with peach tree dieback in Hubei, China. *Mycosphere* **8**: 533–549.
Doilom M, Dissanayake AJ, Wanasinghe DN, *et al.* (2017). Microfungi on *Tectona grandis* (teak) in Northern Thailand. *Fungal Diversity* **82**: 107–182.
Donk MA (1968). Report of the committee for *Fungi* and *Lichen* 1964–1968. *Taxon* **17**: 578–581.
Douhan GW, Murray TD, Dyer PS (2002). Species and mating-type distribution of *Tapesia yallundae* and *T. acuformis* and occurrence of apothecia in the U.S. Pacific Northwest. *Phytopathology* **92**: 703–709.
Du Z, Fan XL, Hyde KD, *et al.* (2016). Phylogeny and morphology reveal two new species of *Diaporthe* from *Betula* spp. *China. Phytotaxa* **269**: 90–102.
Dupont J, Laloui W, Magnin S, *et al.* (2000). *Phaeoacremonium viticola*, a new species associated with esca disease of grapevine in France. *Mycologia* **92**: 499–504.
Eken C (2003). *Dichotomophthora portulacae* on *Portulaca oleracea* in Turkey. *Mycotaxon* **87**: 153–156.
Elliott ML (1991). Determination of an etiological agent of Bermuda grass decline. *Phytopathology* **81**: 1380–1384.
Elliott ML, Hagan AK, Mullen JM (1993). Association of *Gaeumannomyces graminis* var. *graminis* with a St. Augustine grass root rot disease. *Plant Disease* **77**: 206–209.
Ellis MB (1957). Some species of *Deightoniella*. *Mycological Papers* **66**: 1–12.
Ellis MB (1971). *Dematiaceous Hyphomycetes*. Commonwealth Mycological Institute, Kew, UK.
Eskalen A, Rooney-Latham S, Gubler WD (2005). Occurrence of *Togninia fraxinopennsylvanica* on esca-diseased grapevines (*Vitis vinifera*) and declining ash trees (*Fraxinus latifolia*) in California. *Plant Disease* **89**: 528.
Essakhi S, Mugnai L, Crous PW, *et al.* (2008). Molecular and phenotypic characterization of novel *Phaeoacremonium* species associated with Petri disease and esca of grapevine. *Persoonia* **21**: 119–134.
Fan XL, Hyde KD, Udayanga D, *et al.* (2015). *Diaporthe rostrata*, a novel ascomycete from *Juglans mandshurica* associated with walnut dieback. *Mycological Progress* **14**: 82.
Farr DF, Rossman AY (2017). *Fungal Databases, U.S. National Fungus Collections, ARS, USDA*. Accessed on November 2017. https://nt.ars-grin.gov/fungaldatabases/.
Freeman J, Ward E (2004). *Gaeumannomyces graminis*, the take-all fungus and its relatives. *Molecular Plant Pathology* **5**: 235–252.
Fries EM (1849). *Summa vegetabilium Scandinaviae*. Typographis Academica, Uppsala, Sweden.
Gao YH, Liu F, Cai L (2016). Unravelling *Diaporthe* species associated with *Camellia*. *Systematics and Biodiversity* **14**: 102–117.
Gao YH, Liu F, Duan W, *et al.* (2017). *Diaporthe* is paraphyletic. *IMA Fungus* **8**: 153–187.
Gao YH, Su YY, Sun W (2015). *Diaporthe* species occurring on *Lithocarpus glabra* in China, with descriptions of five new species. *Fungal Biology* **119**: 295–309.
Gao YH, Sun W, Su YY (2014). Three new species of *Phomopsis* in Gutianshan Nature Reserve in China. *Mycological Progress* **13**: 111–121.
Giraldo A, Crous PW, Schumacher RK, *et al.* (2017). The Genera of Fungi – G3: *Aleurocystis, Blastacervulus, Clypeophysalospora, Licrostroma, Neohendersonia* and *Spumatoria*. *Mycological Progress* **16**: 325–348.
Ghosta Y, Abrinbana M (2016). *Deightoniella arundinacea*, new to mycobiota of Iran. *Rostaniha* **17**: 92–94.
Glienke C, Pereira OL, Stringari D, *et al.* (2011). Endophytic and pathogenic *Phyllosticta* species, with reference to those associated with Citrus Black Spot. *Persoonia* **26**: 47–56.
Gomes RR, Glienke C, Videira SIR, *et al.* (2013). *Diaporthe*: a genus of endophytic, saprobic and plant pathogenic fungi. *Persoonia* **31**: 1–41.
Graham AB, Johnston PR, Weir BS (2009). Three new *Phaeoacremonium* species on grapevines in New Zealand. *Australasian Plant Pathology* **38**: 505–513.
Gramaje D, Agustí-Brisach C, Pérez-Sierra A, *et al.* (2012). Fungal trunk pathogens associated with wood decay of almond trees on Mallorca (Spain). *Persoonia* **28**: 1–713.
Gramaje D, Armengol J, Mohammadi H, *et al.* (2009). Novel *Phaeoacremonium* species associated with Petri disease and esca of grapevines in Iran and Spain. *Mycologia* **101**: 920–929.
Gramaje D, García-Jiménez J, Armengol J (2010). Grapevine rootstock susceptibility to fungi associated with Petri disease and esca under field conditions. *American Journal of Enology and Viticulture* **61**: 512–7520.
Gramaje D, León M, Pérez-Sierra A, *et al.* (2014). New *Phaeocremonium* species isolated from sandalwood trees in Western Australia. *IMA Fungus* **5**: 67–77.
Gramaje D, Mostert L, Groenewald JZ, *et al.* (2015). *Phaeoacremonium*: From esca disease to phaeohyphomycosis. *Fungal Biology* **119**: 759–783.
Groenewald M, Kang J-C, Crous PW, *et al.* (2001). ITS and beta-tubulin phylogeny of *Phaeoacremonium* and *Phaeomoniella* species. *Mycological Research* **105**: 651–657.
Guarnaccia V, Crous PW (2017). Emerging citrus diseases in Europe caused by *Diaporthe* spp. *IMA Fungus* **8**: 317–334.
Guarnaccia V, Groenewald JZ, Li H, *et al.* (2017). First report of *Phyllosticta citricarpa* and description of two new species, *P. paracapitalensis* and *P. paracitricarpa*, from citrus in Europe. *Studies in Mycology* **87**: 161–185.
Guarnaccia V, Groenewald JZ, Woodhall J, *et al.* (2018). *Diaporthe* diversity and pathogenicity revealed from a broad survey of grapevine diseases in Europe. *Persoonia* **40**: 135–153.
Guarnaccia V, Vitale A, Cirvilleri G, *et al.* (2016). Characterisation and pathogenicity of fungal species associated with branch cankers and stem-end rot of avocado in Italy. *European Journal of Plant Pathology* **146**: 963–976.
Halleen F, Mostert L, Crous PW (2007). Pathogenicity testing of lesser-known vascular fungi of grapevines. *Australasian Plant Pathology* **36**: 277–285.

Hay FS, Gent DH, Pilkington SJ, *et al*. (2015). Changes in distribution and frequency of fungi associated with foliar diseases complex of pyrethrum in Australia. *Plant Disease* **9**: 1227–1235.
Heath RN, Wingfield MJ, Wingfield BD, *et al*. (2009). *Ceratocystis* species on *Acacia mearnsii* and *Eucalyptus* spp. in eastern and southern Africa including six new species. *Fungal Diversity* **34**: 41–68.
Hernández-Restrepo M, Groenewald JZ, Crous PW (2016a). Taxonomic and phylogenetic re-evaluation of *Microdochium, Monographella* and *Idriella*. *Persoonia* **36**: 57–82.
Hernández-Restrepo M, Groenewald JZ, Elliott ML, *et al*. (2016b). Take-all or nothing. *Studies in Mycology* **83**: 19–48.
Hernández-Restrepo M, Schumacher RK, Wingfield MJ, *et al*. (2016c). Fungal Systematics and Evolution: FUSE 2. *Sydowia* **68**: 193–230.
Hibbett DS, Ohman A, Glotzer D, *et al*. (2011). Progress in molecular and morphological taxon discovery in *Fungi* and options for formal classification of environmental sequences. *Fungal Biology Reviews* **25**: 38–47.
Hirata K, Kusaba M, Chuma I, *et al*. (2007). Speciation in *Pyricularia* inferred from multilocus phylogenetic analysis. *Mycological Research* **111**: 799–808.
Hong SK, Kim WG, Choi HW, *et al*. (2008). Identification of *Microdochium bolleyi* associated with basal rot of creeping bent grass in Korea. *Mycobiology* **36**: 77–80.
Hu DM, Cai L, Hyde KD (2012). Three new ascomycetes from freshwater in China. *Mycologia* **104**: 1478–1489.
Huang F, Hou X, Dewdney MM, *et al*. (2013). *Diaporthe* species occurring on citrus in China. *Fungal Diversity* **61**: 237–250.
Huang F, Udayanga D, Wang X, *et al*. (2015). Endophytic *Diaporthe* associated with *Citrus*, a phylogenetic reassessment with seven new species from China. *Fungal Biology* **119**: 331–347.
Hyde KD, Hongsanan S, Jeewon R, *et al*. (2016). Fungal diversity notes 367–492, taxonomic and phylogenetic contributions to fungal taxa. *Fungal Diversity* **80**: 1–270.
Inderbitzin P, Bostock RM, Subbarao KV (2012). *Cylindrocladiella hahajimaensis*, a new species of *Cylindrocladiella* transferred from *Verticillium*. *MycoKeys* **4**: 1–8.
Jaklitsch WM, Voglmayr H (2012). Phylogenetic relationships of five genera of *Xylariales* and *Rosasphaeria* gen. nov. (*Hypocreales*). *Fungal Diversity* **52**: 75–98.
Johnston PR, Seifert KA, Stone JK, *et al*. (2014). Recommendations on generic names competing for use in *Leotiomycetes (Ascomycota)*. *IMA Fungus* **5**: 91–120.
Jones DR (2000). Fungal diseases of the foliage. In: *Diseases of Banana, Abaca and Enset* (Jones DR, ed.). CABI Publishing, Wallingford, UK: 108–111.
Kamgan NG, Jacobs K, De Beer ZW, *et al*. (2008). *Ceratocystis* and *Ophiostoma* species, including three new taxa, associated with wounds on native South African trees. *Fungal Diversity* **29**: 37–59.
Kamgan Nkuekam G, Wingfield MJ, Mohammed C, *et al*. (2012). *Ceratocystis* species, including two new species associated with nitidulid beetles, on eucalypts in Australia. *Antonie van Leeuwenhoek* **101**: 217–241.
Kamgan Nkuekam G, Wingfield MJ, Roux J (2013). *Ceratocystis* species, including two new taxa, from *Eucalyptus* trees in South Africa. *Australasian Plant Pathology* **42**: 283–311.
Kirk PM, Stalpers JA, Braun U, *et al*. (2013). A without-prejudice list of generic names of fungi for protection under the International Code of Nomenclature for algae, fungi and plants. *IMA Fungus* **4**: 381–443.
Klaubauf S, Tharreau D, Fournier E, *et al*. (2014). Resolving the polyphyletic nature of *Pyricularia (Pyriculariaceae)*. *Studies in Mycology* **79**: 85–120.
Klisiewicz JM (1985). Growth and reproduction of *Dichotomophthora portulacae* and its biological activity on purslane. *Plant Disease* **69**: 761–762.
Lamprecht SC, Crous PW, Groenewald JZ, *et al*. (2011). *Diaporthaceae* associated with root and crown rot of maize. *IMA Fungus* **2**: 13–24.
Lee S, Groenewald JZ, Crous PW (2004). Phylogenetic reassessment of the coelomycete genus *Harknessia* and its teleomorph *Wuestneia (Diaporthales)*, and the introduction of *Apoharknessia* gen. nov. *Studies in Mycology* **50**: 235–252.
Li WJ, Bhat DJ, Camporesi E, *et al*. (2015). New asexual morph taxa in *Phaeosphaeriaceae*. *Mycosphere* **6**: 681–708.
Liu JK, Hyde KD, Jones EBG, *et al*. (2015). Fungal diversity notes 1–110: taxonomic and phylogenetic contributions to fungal species. *Fungal Diversity* **72**: 1–197.
Lombard L, Cheewangkoon R, Crous PW (2017). New Cylindrocladiella spp. from Thailand soils. *Mycosphere* **8**: 1088–1104.
Lombard L, Shivas RG, To-Anun C, *et al*. (2012). Phylogeny and taxonomy of the genus *Cylindrocladiella*. *Mycological Progress* **11**: 835–868.
Lombard L, van der Merwe NA, Groenewald JZ, *et al*. (2015). Generic concepts in *Nectriaceae*. *Studies in Mycology* **80**: 189–245.
Lombard L, van Leeuwen GCM, Guarnaccia V, *et al*. (2014). *Diaporthe* species associated with *Vaccinium*, with specific reference to Europe. *Phytopathologia Mediterranea* **53**: 287–299.
Lucas JA, Dyer PS, Murray TD (2000). Pathogenicity, hostspecificity and population biology of *Tapesia* spp., causal agents of eyespot disease of cereals. *Advances in Botanical Research* **33**: 226–258.
Luo J, Walsh E, Zhang N (2014). Four new species in *Magnaporthaceae* from grass roots in New Jersey Pine Barrens. *Mycologia* **106**: 580–588.
Luo J, Zhang N (2013). *Magnaporthiopsis*, a new genus in *Magnaporthaceae*. *Mycologia* **105**: 1019–1029.
Machingambi NM, Dreyer LL, Oberlander KC, *et al*. (2015). Death of endemic *Virgilia oroboides* trees in South Africa caused by *Diaporthe virgiliae* sp nov. *Plant Pathology* **64**: 1149–1156.
Madrid H, da Cunha KC, Gené J, *et al*. (2014). Novel *Curvularia* species from clinical specimens. *Persoonia* **33**: 48–60.
Manamgoda DS, Cai L, McKenzie EHC, *et al*. (2012). A phylogenetic and taxonomic re-evaluation of the *Bipolaris – Cochliobolus – Curvularia* complex. *Fungal Diversity* **56**: 131–144.
Manamgoda DS, Rossman AY, Castlebury LA, *et al*. (2014). The genus *Bipolaris*. *Studies in Mycology* **79**: 221–288.
Marin-Felix Y, Groenewald JZ, Cai L, *et al*. (2017). Genera of phytopathogenic fungi: GOPHY 1. *Studies in Mycology* **86**: 99–216.
Mayers CG, Mcnew DL, Harrington TC, *et al*. (2015). Three genera in the *Ceratocystidaceae* are the respective symbionts of three independent lineages of ambrosia beetles with large, complex mycangia. *Fungal Biology* **119**: 1075–1092.
Mbenoun M, Wingfield MJ, Begoude Boyogueno AD, *et al*. (2014). Molecular phylogenetic analyses reveal three new *Ceratocystis* species and provide evidence for geographic differentiation of the genus in Africa. *Mycological Progress* **13**: 219–240.
McNeill J, Barrie FF, Buck WR, *et al*. (eds.) (2012). *International Code of Nomenclature for algae, fungi and plants (Melbourne Code). [Regnum Vegetabile no. 154].* A.R.G. Gantner Verlag KG.
Mehrlich FP, Fitzpatrick HM (1935). *Dichotomophthora portulacae*, a pathogen of *Portulaca oleracea*. *Mycologia* **27**: 543–550.
Mel'nik VA, Shabunin DA (2011). *Deightoniella constantinescui* sp. nov. on *Phragmites australis*. *Mikologiya i Fitopatologiya* **45**: 257–259.
Moreno-Rico O, Groenewald JZ, Crous PW (2014). Foliicolous fungi from *Arctostaphylos pungens* in Mexico. *IMA Fungus* **5**: 7–15.
Moslemi A, Ades PK, Crous PW, *et al*. (2018). *Paraphoma chlamydocopiosa* sp. nov. and *Paraphoma pye* sp. nov., two new species associated with leaf and crown infection of pyrethrum. *Plant Pathology* **67**: 124–135.
Moslemi A, Ades PK, Groom T, *et al*. (2016). Paraphoma crown rot of pyrethrum (*Tanacetum cinerariifolium*). *Plant Disease* **100**: 2363–2369.
Mostert L, Crous PW, Kang JC, *et al*. (2001). Species of *Phomopsis* and a *Libertella* sp. occurring on grapevines with specific reference to South Africa: morphological, cultural, molecular and pathological characterization. *Mycologia* **93**: 146–167.
Mostert L, Groenewald JZ, Summerbell RC, *et al*. (2005). Species of *Phaeoacremonium* associated with infections in humans and environmental reservoirs in infected woody plants. *Journal of Clinical Microbiology* **43**: 1752–1767.
Mostert L, Groenewald JZ, Summerbell RC, *et al*. (2006). Taxonomy and pathology of *Togninia (Diaporthales)* and its *Phaeoacremonium* anamorphs. *Studies in Mycology* **54**: 1–115.
Motohashi K, Inaba S, Anzai K, *et al*. (2009). Phylogenetic analyses of Japanese species of *Phyllosticta* sensu stricto. *Mycoscience* **50**: 291–302.
Moyo P, Allsopp E, Roets F, *et al*. (2014). Arthropods vector grapevine trunk disease pathogens. *Phytopathology* **104**: 1063–1069.
Müller E, Samuels GJ (1984). *Monographella maydis* sp. nov. and its connection to the tar-spot disease of *Zea mays*. *Nova Hedwigia* **40**: 112–120.
Murray TD (1996). Resistance to benzimidazole fungicides in the cereal eyespot pathogen, *Pseudocercosporella herpotrichoides*, in the Pacific Northwest 1984 to 1990. *Plant Disease* **80**: 19–23.
Nag Raj TR (1993). *Coelomycetous anamorphs with appendage-bearing conidia*. Mycologue Publications, Waterloo, Canada.
Nag Raj TR, DiCosmo F (1981). A monograph of *Harknessia* and *Mastigosporella* with notes on associated teleomorphs. *Bibliotheca Mycologica* **80**: 1–62.
Nel WJ, Duong TA, Wingfield BD, *et al*. (2018). A new genus and species for the globally important, multi-host root pathogen *Thielaviopsis basicola*. *Plant Pathology* **67**: 871–882.

Nirenberg HI (1981). Differenzierung der Erreger der Halmbruchkrankheit I. Morphologie. *Zeitschrift für Pflanzenkrankheiten und Pflanzenschutz* **88**: 241–248.
Nishikado Y (1917). Studies on the rice blast fungus. *Berichte des Ohara Instituts für landwirtschaftliche Forschungen* **1**: 171–218.
Ondřej M (1988). *Pyricularia luzulae* Ondřej sp. n. *Ceská Mykologie* **42**: 81–83.
Parkinson VO, Sivanesan A, Booth C (1981). The perfect state of the rice leaf-scald fungus and the taxonomy of both the perfect and imperfect states. *Transactions of the British Mycological Society* **76**: 59–69.
Peerally A (1991). The classification and phytopathology of *Cylindrocladium* species. *Mycotaxon* **40**: 323–366.
Persoon CH (1818). *Traité sur les champignons comestibles, contenant l'indication des espèces nuisibles; a l'histoire des champignons*. Belin-Leprieur, Paris, France.
Pfeiffer CM, Wheeler JE, Gilbertson RL (1989). First report of *Dichotomophthora indica* as a pathogen of *Myrtillocactus geometrizans* and *Gymnocalycium mihanovichii* var. *friedrichii* in Arizona. *Plant Disease* **73**: 81.
Pouzoulet J, Mailhac N, Couderc C, *et al.* (2013). A method to detect and quantify *Phaeomoniella chlamydospora* and *Phaeoacremonium aleophilum* DNA in grapevine-wood samples. *Applied Microbiology Biotechnology* **97**: 10163–10175.
Pu J, Xie Y, Zhang X, *et al.* (2008). Preinfection behaviour of *Phyllosticta musarum* on banana leaves. *Australasian Plant Pathology* **37**: 60–64.
Quaedvlieg W, Verkley GJM, Shin HD, *et al.* (2013). Sizing up *Septoria*. *Studies in Mycology* **75**: 307–390.
Rachdawong S, Cramer CL, Grabau EA, *et al.* (2002). *Gaeumannomyces graminis* vars. *avenae, graminis*, and *tritici* identified using PCR amplfication of avenacinase-like genes. *Plant Disease* **86**: 652–660.
Raimondo ML, Lops F, Carlucci A (2014). *Phaeoacremonium italicum* sp nov., a new species associated with esca of grapevine in southern Italy. *Mycologia* **106**: 1119–1126.
Rao PN (1966). A new species of *Dichotomophthora* on *Portulaca oleracea* from Hyderabad, India. *Mycopathologia et Mycologia Applicata* **28**: 137–140.
Rayner RW (1970). *A mycological colour chart*. Commonwealth Mycological Institute, Kew, UK.
Réblová M (2011). New insights into the systematics and phylogeny of the genus *Jattaea* and similar fungi of the *Calosphaeriales*. *Fungal Diversity* **49**: 167–198.
Réblová M, Mostert L (2007). *Romellia* is congeneric with *Togninia*, and description of *Conidiotheca* gen. nov. for one species of this genus with polysporous asci. *Mycological Research* **111**: 299–307.
Réblová M, Jaklitsch WM, Réblová K, *et al.* (2015). Phylogenetic reconstruction of the *Calosphaeriales* and *Togniniales* using five genes and predicted RNA secondary structures of ITS, and *Flabellascus tenuirostris* gen. et sp. nov. *PloS ONE* **10**: e0144616.
Reges JTA, Negrisoli MM, Dorigan AF, *et al.* (2016). *Pyricularia pennisetigena* and *P. zingibericola* from invasive grasses infect signal grass, barley and wheat. *Pesquisa Agropecuária Tropical, Goiânia* **46**: 206–214.
Reid J, Booth C (1989). On *Cryptosporella* and *Wuestneia*. *Canadian Journal of Botany* **67**: 879–908.
Robert V, Vu D, Amor ABH, *et al.* (2013). MycoBank gearing up for new horizons. *IMA Fungus* **4**: 371–379.
Roll-Hansen F (1992). Important pathogenic fungi on conifers in Iceland. *Acta Botanica Islandica* **11**: 9–12.
Rooney-Latham S, Eskalen A, Gubler WD (2005). Teleomorph formation of *Phaeoacremonium aleophilum*, cause of esca and grapevine decline in California. *Plant Disease* **89**: 177–184.
Rossman AY, Howard RJ, Valent B (1990). *Pyricularia grisea*, the correct name for the rice blast disease fungus. *Mycologia* **82**: 509–512.
Rossman AY, Seifert KA, Samuels GJ, *et al.* (2013). Genera in *Bionectriaceae, Hypocreaceae*, and *Nectriaceae (Hypocreales)* proposed for acceptance or rejection. *IMA Fungus* **4**: 41–51.
Routien JB (1957). Fungi isolated from soils. *Mycologia* **49**: 188–196.
Santos JM, Correia VG, Phillips AJL (2010). Primers for mating-type diagnosis in *Diaporthe* and *Phomopsis*, their use in teleomorph induction in vitro and biological species definition. *Fungal Biology* **114**: 255–270.
Santos L, Phillips AJL, Crous PW (2017). *Diaporthe* species on *Rosaceae* with descriptions of *D. pyracanthae* sp. nov. and *D. malorum* sp. nov. *Mycosphere* **8**: 485–511.
Scattolin L, Montecchio L (2007). First report of damping-off of common oak plantlets caused by *Cylindrocladiella parva* in Italy. *Plant Disease* **91**: 771.
Schoch CL, Crous PW, Wingfield MJ, *et al.* (2000). Phylogeny of *Calonectria* and selected hypocrealean genera with cylindrical macroconidia. *Studies in Mycology* **45**: 45–62.
Schoch CL, Seifert KA, Huhndorf S, *et al.* (2012). Nuclear ribosomal internal transcribed spacer (ITS) region as a universal DNA barcode marker for *Fungi*. *Proceedings of the National Academy of Sciences, USA* **109**: 6241–6246.
Schoch CL, Shoemaker RA, Seifert KA, *et al.* (2006). A multigene phylogeny of the *Dothideomycetes* using four nuclear loci. *Mycologia* **98**: 1041–1052.
Seifert K, Morgan-Jones G, Gams W, *et al.* (2011). *The genera of Hyphomycetes. CBS Biodiversity Series 9*. CBS-KNAW Fungal Biodiversity Centre, Utrecht, the Netherlands.
Senanayake IC, Crous PW, Groenewald JZ, *et al.* (2017). Families of *Diaporthales* based on morphological and phylogenetic evidence. *Studies in Mycology* **86**: 217–296.
Sivanesan A (1987). Graminicolous species of *Bipolaris, Curvularia, Drechslera, Exserohilum* and their teleomorphs. *Mycological Papers* **158**: 1–261.
Skamnioti P, Gurr SJ (2009). Against the grain: safeguarding rice from rice blast disease. *Trends in Biotechnology* **27**: 141–150.
Smith H, Wingfield MJ, Crous PW, *et al.* (1996). *Sphaeropsis sapinea* and *Botryosphaeria dothidea* endophytic in *Pinus* spp. and *Eucalyptus* spp. in South Africa. *South African Journal of Botany* **62**: 86–88.
Soares DJ, Nechet KL (2017). *Dichotomophthora* sp. causing leaf spot and foliar abscission on *Anredera cordifolia* in Brazil. *Australasian Plant Disease Notes* **12**: 51.
Speakman JB (1982). A simple, reliable method of producing perithecia of *Gaeumannomyces gramnis* var. *tritici* and its application to isolates of *Phialophora* spp. *Transactions of the British Mycological Society* **79**: 350–353.
Speakman JB (1984). Perithecia of *Gaeumannomyces graminis* var. *graminis* and *G. graminis* var. *tritici* in pure culture. *Transactions of the British Mycological Society* **82**: 720–723.
Spies CFJ, Moyo P, Halleen F, *et al.* (2018). *Phaeoacremonium* species diversity on woody hosts in the Western Cape Province of South Africa. *Persoonia* **40**: 26–62.
Sprague R (1936). Relative susceptihility of certain species of gramineae to *Cercosporella herpotrichoides*. *Journal of Agricultural Research* **53**: 659–670.
Sprague R, Fellows H (1934). Cercosporella foot rot of winter cereals. *Technical Bulletin* **428**: 1–24.
Su YY, Cai L (2012). Polyphasic characterisation of three new *Phyllosticta* spp. *Persoonia* **28**: 76–84.
Sutton BC (1977). *Coelomycetes* VI. Nomenclature of generic names proposed for *Coelomycetes*. *Mycological Papers* **141**: 1–253.
Sutton BC (1980). *The Coelomycetes. Fungi imperfecti with pycnidia, acervuli and stromata*. Commonwealth Mycological Institute, Kew, UK.
Sydow H, Sydow P (1917). Beitrag zur Kenntniss der Pilzflora der Philippinen-Inseln. *Annales Mycologici* **15**: 165–268.
Sydow H (1924). Sydow, Mycotheca germanica. Fasc. XLII-XLV (No. 2051–2250). *Annales Mycologici* **22**: 257–268.
Tan YP, Edwards J, Grice KRE, *et al.* (2013). Molecular phylogenetic analysis reveals six new *Diaporthe* species from Australia. *Fungal Diversity* **61**: 251–260.
Tanney JB, McMullin DR, Green BD, *et al.* (2016). Production of antifungal and antiinsectan metabolites by the *Picea* endophyte *Diaporthe maritima* sp. nov. *Fungal Biology* **120**: 1448–1457.
Tarigan M, Gryzenhout M, Roux J, *et al.* (2010). Three new *Ceratocystis* spp. in the *Ceratocystis moniliformis* complex from wounds on *Acacia mangium* and *A. crassicarpa*. *Mycoscience* **51**: 53–67.
Thompson SM, Tan YP, Shivas RG, *et al.* (2015). Green and brown bridges between weeds and crops reveal novel *Diaporthe* species in Australia. *Persoonia* **35**: 39–49.
Thompson SM, Tan YP, Young AJ, *et al.* (2011). Stem cankers on sunflower (*Helianthus annuus*) in Australia reveal a complex of pathogenic *Diaporthe (Phomopsis)* species. *Persoonia* **27**: 80–89.
Turner EM (1940). *Ophiobolus graminis* Sacc. var. *avenae* var. n. as the cause of take-all or white-heads in Wales. *Transactions of the British Mycological Society* **24**: 269–281.
Udayanga D, Castlebury LA, Rossman AY, *et al.* (2014a). Insights into the genus *Diaporthe*: phylogenetic species delimitation in the *D. eres* species complex. *Fungal Diversity* **67**: 203–229.
Udayanga D, Castlebury LA, Rossman AY, *et al.* (2014b). Species limits in *Diaporthe*: molecular re-assessment of *D. citri, D. cytosporella, D. foeniculina* and *D. rudis*. *Persoonia* **32**: 83–101.
Udayanga D, Castlebury LA, Rossman AY, *et al.* (2015). The *Diaporthe sojae* species complex, phylogenetic re-assessment of pathogens associated with soybean, cucurbits and other field crops. *Fungal Biology* **119**: 383–407.

Udayanga D, Liu X, McKenzie EHC, *et al*. (2011). The genus *Phomopsis*: biology, applications, species concepts and names of common phytopathogens. *Fungal Diversity* **50**: 189–225.
Udayanga D, Liu XZ, MCkenzie EHC, *et al*. (2012). Multi-locus phylogeny reveals three new species of *Diaporthe* from Thailand. *Cryptogamie Mycologie* **33**: 295–309.
Ulrich K, Augustin C, Werner A (2000). Identification and characterization of a new group of root-colonizing fungi within the *Gaeumannomyces–Phialophora* complex. *New Phytologist* **145**: 127–135.
Uotila A (1990). Infection of pruning wounds in Scots pine by *Phacidium coniferarum* and selection of pruning season. *Acta Forestalia Fennica* **215**: 1–36.
Úrbez-Torres JR, Haag P, Bowen P, *et al*. (2014). Grapevine trunk diseases in British Columbia: incidence and characterization of the fungal pathogens associated with esca and Petri diseases of grapevine. *Plant Disease* **98**: 469–482.
Úrbez-Torres JR, Haag P, Bowen P, *et al*. (2015). Development of a DNA-macroarray for the detection and identification of fungal pathogens causing decline of young grapevines. *Phytopathology* **105**: 1373–1383.
Van Coller GJ, Denman S, Groenewald JZ, *et al*. (2005). Characterisation and pathogenicity of *Cylindrocladiella* spp. associated with root and cutting rot symptoms of grapevines in nurseries. *Australasian Plant Pathology* **34**: 489–498.
van der Aa HA (1973). Studies in *Phyllosticta* I. *Studies in Mycology* **5**: 1–110.
van der Aa HA, Vanev S (2002). *A revision of the species described in Phyllosticta*. Centraalbureau voor Schimmelcultures, Utrecht, The Netherlands.
Van Niekerk JM, Groenewald JZ, Farr DF, *et al*. (2005). Reassessment of *Phomopsis* species on grapevines. *Australasian Plant Pathology* **34**: 27–39.
Van Rensburg JCJ, Lamprecht SC, Groenewald JZ, *et al*. (2006). Characterization of *Phomopsis* spp. associated with die-back of rooibos (*Aspalathus linearis*) in South Africa. *Studies in Mycology* **55**: 65–74.
Van Wyk M, Roux J, Barnes I, *et al*. (2004). *Ceratocystis bhutanensis* sp. nov., associated with the bark beetle *Ips schmutzenhoferi* on *Picea spinulosa* in Bhutan. *Studies in Mycology* **50**: 365–379.
Van Wyk M, Roux J, Barnes I, *et al*. (2006). Molecular phylogeny of the *Ceratocystis moniliformis* complex and description of *C. tribiliformis* sp. nov. *Fungal Diversity* **21**: 181–201.
Van Wyk M, Wingfield BD, Wingfield MJ (2011). Four new *Ceratocystis* spp. associated with wounds on *Eucalyptus, Schizolobium* and *Terminalia* trees in Ecuador. *Fungal Diversity* **46**: 111–131.
Videira SIR, Groenewald JZ, Nakashima C, *et al*. (2017). *Mycosphaerellaceae* – Chaos or clarity? *Studies in Mycology* **87**: 257–421.
von Arx JA (1981). Notes on *Microdochium* and *Idriella*. *Sydowia* **34**: 30–38.
von Arx JA (1984). Notes on *Monographella* and *Microdochium*. *Transactions of the British Mycological Society* **83**: 373–374.
von Arx JA, Olivier D (1952). The taxonomy of *Ophiobolus graminis* Sacc. *Transactions of the British Mycological Society* **35**: 29–33.
Walker J (1972). Type studies on *Gaeumannomyces graminis* and related fungi. *Transactions of the British Mycological Society* **58**: 427–457.
Walker J (1975). Take-all disease of *Gramineae*: A review of recent work. *Review of Plant Pathology* **54**: 113–143.
Walker J (1980). *Gaeumannomyces, Linocarpon, Ophiobolus* and several other genera of scolecospored ascomycetes and *Phialophora* conidial states, with a note on hyphopodia. *Mycotaxon* **11**: 1–129.
Walker J (1981). Taxonomy of take-all fungi and related genera and species. In: *Biology and Control of Take-all* (Asher MJC, Shipton PJ, eds.). Academic Press, London, UK: 15–84.
Wang X, Chen G, Huang F, *et al*. (2011). *Phyllosticta* species associated with citrus diseases in China. *Fungal Diversity* **52**: 209–224.
Ward E, Bateman GL (1999). Comparison of *Gaeumannomyces*- and *Phialophora*-like fungal pathogens from maize and other plants using DNA methods. *New Phytologist* **141**: 323–331.
Wicht B, Petrini O, Jermini M, *et al*. (2012). Molecular, proteomic and morphological characterization of the ascomycete *Guignardia bidwellii*, agent of grape black rot: a polyphasic approach to fungal identification. *Mycologia* **104**: 1036–1045.
Wijayawardene N, Song Y, Bhat DJ, *et al*. (2013). *Wojnowicia viburni*, sp. nov., from China and its phylogenetic placement. *Sydowia* **65**: 129–138.
Wikee S, Lombard L, Crous PW, *et al*. (2013a). *Phyllosticta capitalensis*, a widespread endophyte of plants. *Fungal Diversity* **60**: 91–105.
Wikee S, Lombard L, Nakashima C, *et al*. (2013b). A phylogenetic re-evaluation of *Phyllosticta* (*Botryosphaeriales*). *Studies in Mycology* **76**: 1–29.
Wikee S, Udayanga D, Crous PW, *et al*. (2011). *Phyllosticta* – an overview of current status of species recognition. *Fungal Diversity* **51**: 43–61.
Wilson M (1920). A new disease of the Douglas fir in Scotland. *Transactions of the Royal Scottish Arboricultural Society* **34**: 145–149.
Wilson AM, Godlonton T, van der Nest MA, *et al*. (2015). Unisexual reproduction in *Huntiella moniliformis*. *Fungal Genetics and Biology* **80**: 1–9.
Wingfield BD, Van Wyk M, Roos H, *et al*. (2013). *Ceratocystis*: emerging evidence for discrete generic boundaries. In: *The ophiostomatoid fungi: Expanding frontiers. CBS biodiversity series 12* (Seifert KA, De Beer ZW, Wingfield MJ, eds.). CBS-KNAW Fungal Biodiversity Centre, Utrecht, The Netherlands: 57–64.
Wong MH, Crous PW, Henderson J, *et al*. (2012). *Phyllosticta* species associated with freckle disease of banana. *Fungal Diversity* **56**: 173–187.
Wong PTW (2002). *Gaeumannomyces wongoonoo* sp. nov., the cause of a patch disease of buffalo grass (St Augustine grass). *Mycological Research* **106**: 857–862.
Wong PTW, Walker J (1975). Germinating phialidic conidia of *Gaeumannomyces graminis* and phialophora-like fungi from *Gramineae*. *Transactions of the British Mycological Society* **65**: 41–47.
Wulandari NF, To-anun C, Hyde KD, *et al*. (2009). *Phyllosticta citriasiana* sp. nov., the cause of Citrus tan spot of *Citrus maxima* in Asia. *Fungal Diversity* **34**: 23–39.
Yang Q, Du Z, Tian CM (2018). Phylogeny and morphology reveal two new species of *Diaporthe* from Traditional Chinese Medicine in Northeast China. *Phytotaxa* **336**: 159–170.
Yang Q, Fan XL, Du Z, *et al*. (2017a). *Diaporthe juglandicola* sp. nov. (*Diaporthales*, *Ascomycetes*) evidenced by morphological characters and phylogenetic analysis. *Mycosphere* **8**: 817–826.
Yang Q, Fan XL, Du Z, *et al*. (2017b). *Diaporthe* species occurring on *Senna bicapsularis* in southern China, with descriptions of two new species. *Phytotaxa* **302**: 145–155.
Yang Q, Fan XL, Du Z, *et al*. (2017c). *Diaporthe camptothecicola* sp. nov. on *Camptotheca acuminata* in China. *Mycotaxon* **132**: 591–601.
Yao JM, Wang YC, Zhu YG (1992). A new variety of the pathogen of maize take-all. *Acta Mycologica Sinica* **11**: 99–104.
Yuan Z-Q, Mohammed C (2002). *Ceratocystis moniliformopsis* sp. nov., an early coloniser of *Eucalyptus obliqua* logs in Tasmania, Australia. *Australian Systematic Botany* **15**: 125–133.
Zhang K, Su YY, Cai L (2013a). Morphological and phylogenetic characterization of two new species of *Phyllosticta* from China. *Mycological Progress* **12**: 547–556.
Zhang K, Zhang N, Cai L (2013b). Typification and phylogenetic study of *Phyllosticta ampelicida* and *P. vaccinii*. *Mycologia* **105**: 1030–1042.
Zhang W, Nan Z, Tian P, *et al*. (2015). *Microdochium paspali*, a new species causing seashore paspalum disease in southern China. *Mycologia* **107**: 80–89.
Zhang Y, Crous PW, Schoch CL, *et al*. (2012). *Pleosporales*. *Fungal Diversity* **53**: 1–221.
Zhang Y, Schoch CL, Fournier J, *et al*. (2009). Multi-locus phylogeny of *Pleosporales*: a taxonomic, ecological and evolutionary re-evaluation. *Studies in Mycology* **64**: 85–102.
Zhang ZF, Liu F, Zhou X, *et al*. (2017). Culturable mycobiota from Karst caves in China, with descriptions of 20 new species. *Persoonia* **39**: 1–31.
Zhou N, Chen Q, Carroll G, *et al*. (2015). Polyphasic characterization of four new plant pathogenic *Phyllosticta* species from China, Japan and the United States. *Fungal Biology* **119**: 433–446.

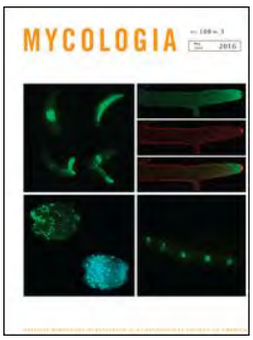

Mycologia

ISSN: 0027-5514 (Print) 1557-2536 (Online) Journal homepage: http://www.tandfonline.com/loi/umyc20

Nine novel species of *Huntiella* from southern China with three distinct mating strategies and variable levels of pathogenicity

FeiFei Liu, GuoQing Li, Jolanda Roux, Irene Barnes, Andrea M. Wilson, Michael J. Wingfield & ShuaiFei Chen

To cite this article: FeiFei Liu, GuoQing Li, Jolanda Roux, Irene Barnes, Andrea M. Wilson, Michael J. Wingfield & ShuaiFei Chen (2018): Nine novel species of *Huntiella* from southern China with three distinct mating strategies and variable levels of pathogenicity, Mycologia, DOI: 10.1080/00275514.2018.1515450

To link to this article: https://doi.org/10.1080/00275514.2018.1515450

MYCOLOGIA
https://doi.org/10.1080/00275514.2018.1515450

Taylor & Francis
Taylor & Francis Group

Nine novel species of *Huntiella* from southern China with three distinct mating strategies and variable levels of pathogenicity

FeiFei Liu[a], GuoQing Li[b], Jolanda Roux [a], Irene Barnes [a], Andrea M. Wilson [a], Michael J. Wingfield[a], and ShuaiFei Chen [b]

[a]Department of Biochemistry, Genetics and Microbiology, Forestry and Agricultural Biotechnology Institute, University of Pretoria, Pretoria 0028, South Africa; [b]China Eucalypt Research Centre, Chinese Academy of Forestry, Zhanjiang 524022, Guangdong Province, China

ABSTRACT

The ascomycete genus *Huntiella* (Microascales) has a cosmopolitan distribution and occurs on a wide range of woody plants. Little is known regarding the identity, diversity, origin, or impact of these fungi in China. Recently, isolates of *Huntiella* spp. were collected from stumps of freshly felled trees or wounds on plantation-grown *Eucalyptus* in Guangdong, Guangxi, Fujian, and Hainan provinces of southern China. Additional isolates were obtained from stumps of *Acacia confusa* near *Eucalyptus* plantations in Hainan Province. The aim of this study was to identify these *Huntiella* species and to test their pathogenicity on *Eucalyptus* seedlings. Morphology and multigene phylogenies of the nuclear rDNA internal transcribed spacer (ITS1-5.8S-ITS2 = ITS) region and partial β-tubulin (*BT1*) and translation elongation factor 1α (*TEF1α*) genes revealed nine previously unknown *Huntiella* species, eight from *Eucalyptus* and one from *A. confusa*. The mating types of these species were determined, showing that seven are heterothallic, one is homothallic, and one is unisexual (*MAT1-2-1* gene). Pathogenicity tests showed that the nine *Huntiella* species can produce lesions on *Eucalyptus* seedlings, larger than wounds caused by controls on these plants. This study provides a basic understanding of the distribution, diversity, and pathogenicity of *Huntiella* species in southern China.

ARTICLE HISTORY
Received 3 March 2018
Accepted 21 August 2018

KEYWORDS
Ceratocystidaceae; *Ceratocystis moniliformis* complex; phylogeny; plantation forestry; 9 new taxa

INTRODUCTION

The genus *Huntiella* belongs to the family Ceratocystidaceae (Microascales, Ascomycetes) as defined by De Beer et al. (2014). Other genera in the family include *Ambrosiella, Berkeleyomyces, Bretziella, Ceratocystis, Chalaropsis, Davidsoniella, Endoconidiophora, Meredithiella, Phialophoropsis*, and *Thielaviopsis* (De Beer et al. 2014, 2017; Mayers et al. 2015; Nel et al. 2017). The Ceratocystidaceae includes many important fungal pathogens of trees and agents of blue stain of timber globally (Wingfield et al. 1993; Roux and Wingfield 2009; De Beer et al. 2014). These fungi infect their hosts through wounds and are most commonly spread by insects, including bark beetles, nitidulid beetles, flies, and mites (Hayslett et al. 2008; Heath et al. 2009; Seifert et al. 2013; Mbenoun et al. 2016; Wingfield et al. 2017). Most species of Ceratocystidaceae share similar morphological characters, having dark, globoid ascomata and elongated necks that exude sticky ascospore masses at their tips. These characters reflect a general adaptation to insect dispersal (Upadhyay 1981; Wingfield et al. 1993; Seifert et al. 2013).

Until relatively recently, species of *Huntiella* were treated in *Ceratocystis* and commonly referred to as the *C. moniliformis* complex (Wingfield et al. 2013; De Beer et al. 2014). *Huntiella* species are distinguished from other genera in the Ceratocystidaceae based on their ecology, morphological characters, and phylogenetic relationships inferred from DNA sequence data (De Beer et al. 2014). Species of *Huntiella* are similar to those of *Ceratocystis*, having "hat-shaped" ascospores, but they differ in that *Huntiella* species have ascomata with "thick collar plates" connecting the ascomatal necks and bases. The ascomatal bases of *Huntiella* are rough-walled and ornamented with spines, whereas those of *Ceratocystis* are generally smooth-walled (Hedgcock 1906; De Beer et al. 2014). In addition, it is rare to find aleurioconidia in *Huntiella* species, whereas these are commonly produced by most *Ceratocystis* species (Hedgcock 1906; Seifert et al. 2013).

Huntiella includes at least 20 species on a broad range of hosts, with a cosmopolitan distribution (Van Wyk et al. 2006; De Beer et al. 2014; De Errasti et al. 2015; Mbenoun et al. 2016). For example, *H. moniliformis* is reported worldwide, including Africa (Luc 1952; Heath et al. 2009; Kamgan Nkuekam et al. 2012), Asia (Kitajima

CONTACT ShuaiFei Chen shuaifei.chen@gmail.com
Supplemental data for this article can be accessed on the publisher's Web site.

Published online 15 Nov 2018

1936; Roldan 1962), Europe (Bakshi 1951; Kowalski and Butin 1989), North America (Hedgcock 1906; Davidson 1935), and South America (Cristobal and Hansen 1962; Van Wyk et al. 2011). *Huntiella* species are commonly encountered on tree wounds and generally regarded as nonpathogenic (Davidson 1935; Van Wyk et al. 2006; De Errasti et al. 2015; Mbenoun et al. 2016). Some species produce lesions in artificial inoculation experiments (Tarigan et al. 2010; Chen et al. 2013; De Errasti et al. 2015; Mbenoun et al. 2016), raising concern that under certain situations, they could be more important than has generally been assumed.

Species boundaries in *Huntiella* are not easily defined. Most have similar morphologies, and as new species are described it has become increasingly difficult to delimit them based on morphological characters alone (Van Wyk et al. 2006; Kamgan Nkuekam et al. 2008; Mbenoun et al. 2016). It is possible to distinguish between species based on DNA sequence comparisons and phylogenetic inference. Unfortunately, nuclear rDNA internal transcribed spacer (ITS1-5.8S-ITS2 = ITS) region, selected as the barcoding region for fungal species identification (Schoch et al. 2012), is of limited use in delineating *Huntiella* species (Van Wyk et al. 2004, 2006, 2011; Mbenoun et al. 2014). In contrast, partial β-tubulin (*BT1*) and translation elongation factor 1α (*TEF1α*) gene sequences provide better resolution among species, despite examples of incongruency between these regions (Kamgan Nkuekam et al. 2008; Mbenoun et al. 2014).

In surveys of potential fungal pathogens of plantation-grown forest tree species in southern China, several isolates resembling species of *Huntiella* were obtained from fresh stumps and wounds on *Eucalyptus* and *Acacia* trees. The aim of this study was to identify these isolates based on morphology and multigene phylogenies of the ITS, *BT1*, and *TEF1α* sequences.

MATERIALS AND METHODS

Fungal isolates.—Wood chips with structures resembling those of *Huntiella* species were collected from wounds of fallen trees and recently harvested stems (up to 1 mo old) of *Eucalyptus* species (FIG. 1A–B) and other tree species in the vicinity of *Eucalyptus* plantations. These samples were collected within the Guangdong, Guangxi, Fujian, and Hainan provinces of southern China between Sep 2013 and Apr 2014. Cultures were isolated by transferring ascospore masses from ascomata growing on the surfaces of the wood chips to 2% malt extract agar medium (MEA; 20 g/L malt extract [Biolab, Midrand, South Africa], 20 g/L agar [Difco, Maryland, USA]), and incubated at 25 C for 1 wk. Isolates were regularly inspected under a dissecting microscope and purified by isolating single hyphal tips onto 2% MEA.

Cultures of *Huntiella* isolates were deposited in the culture collection of the China Eucalypt Research Centre (CERC), Chinese Academy of Forestry (CAF), Zhanjiang, China. Duplicate cultures have also been preserved in the culture collection (CMW) of the Forestry and Agricultural Biotechnology Institute (FABI), University of Pretoria, South Africa. Furthermore, representative isolates of novel species were deposited at the culture collection (CBS) of the Westerdijk Fungal Biodiversity Institute, Utrecht, the Netherlands. Dried specimens were also deposited at the National Collection of Fungi (PREM), Pretoria, South Africa.

DNA extraction, PCR, and sequencing.—Isolates obtained during this study were used for DNA sequence–based characterization. DNA was extracted from the mycelium of single hyphal tip isolates grown on 2% MEA for 2–3 wk at 25 C, using the protocol developed by Möller et al. (1992). Final DNA concentrations of ~100 ng/μL were prepared for polymerase chain reaction (PCR) amplification using a Thermo Scientific NanoDrop ND-1000 spectrophotometer (Nano Drop Technologies, Wilmington, Delaware).

Three markers were amplified for sequencing and phylogenetic analysis. The ITS was amplified with the primers ITS1 and ITS4 (White et al. 1990). A partial fragment of the *BT1* was amplified with the primers Bt1a and Bt1b (Glass and Donaldson 1995), and a partial fragment of *TEF1α* was amplified with the primers TEF1F and TEF2R (Jacobs et al. 2004).

Standard PCR reactions of 25 μL were conducted for each gene region. These reactions contained 50 ng of DNA template, 1 μM of each primer, 5 μL MyTaq PCR buffer (Bioline, London, UK), and 1 unit of MyTaq DNA polymerase (Bioline). The amplification reactions were conducted on a Veriti 96-well thermal cycler (Applied Biosystems, Foster City, California). The thermocycling protocol for all three gene regions was as follows: an initial denaturation step at 95 C for 5 min, followed by 35 cycles of 30 s at 95 C, 45 s at 56 C, and 60 s at 72 C. The reaction was completed with a final extension at 72 C for 10 min.

PCR products were purified using ExoSap-IT PCR Product Clean-up Reagent (Thermo Fisher Scientific, Waltham, Massachusetts) to remove excess primers and dNTPs. Purified products were sequenced using the BigDye Terminator 3.1 cycle sequencing premix kit (Applied Biosystems), employing the same forward and reverse primers as used for PCR. The sequencing protocol consisted of 25 cycles of 10 s at 96 C, 5 s at

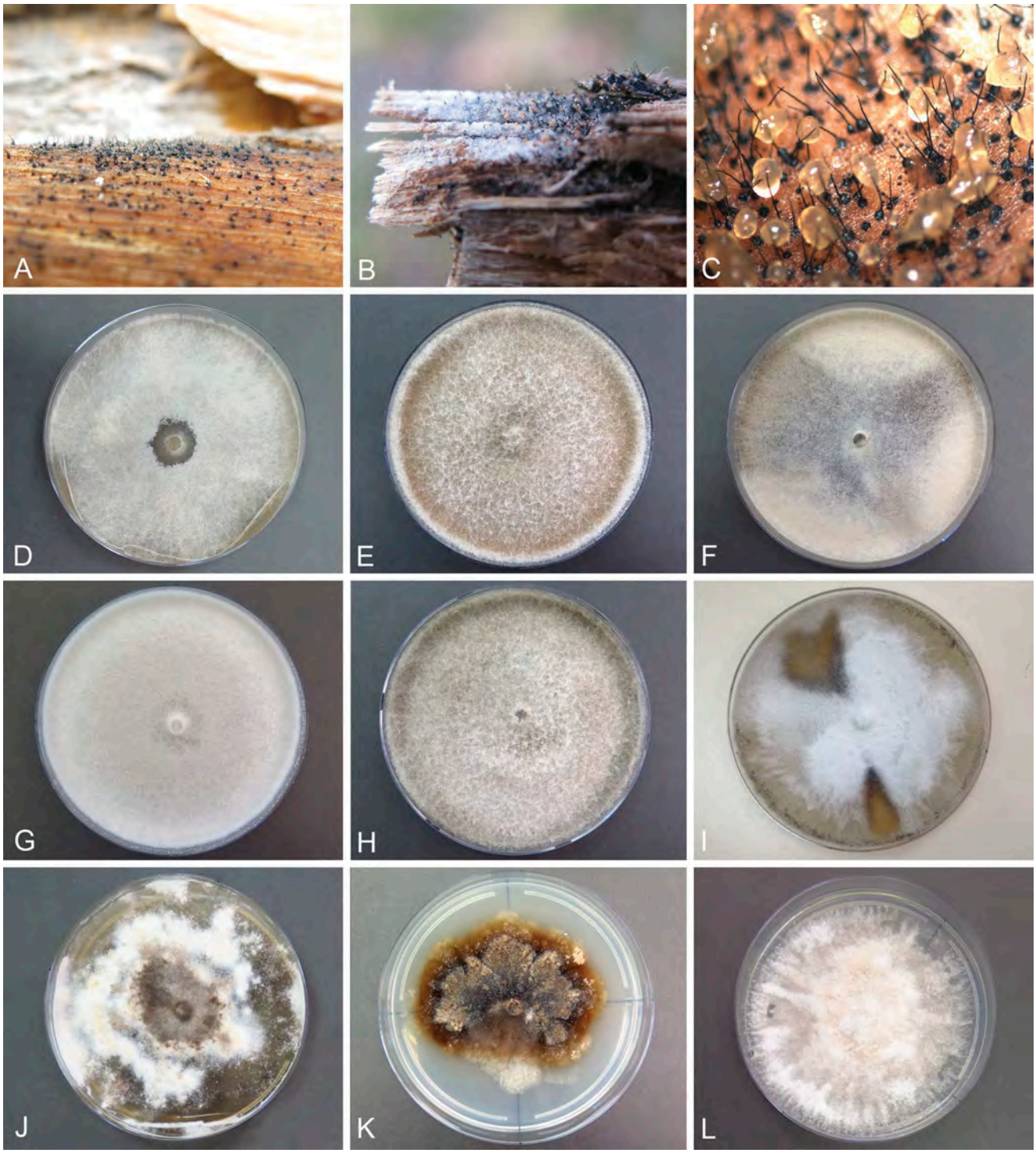

Figure 1. Structures of *Huntiella* on wood in the field and colony morphology on agar medium. A. Abundant *Huntiella* structures produced on a *Eucalyptus* stump. B. Ascomata on *Eucalyptus* stump producing ascospore masses in cold weather. C. *Huntiella fecunda* producing abundant ascomata and ascospores on the surface of 2% MEA. D–L. Colony morphologies of different *Huntiella* species on 90-mm Petri dishes containing 2% MEA after 2 wk. D. *H. ani*. E. *H. bellula*. F. *H. confusa*. G. *H. eucalypti*. H. *H. fabiensis*. I. *H. fecunda*. J. *H. glaber*. K. *H. inaequabilis*. L. *H. meiensis*.

56 C, and 4 min at 60 C. An ABI PRISM 3100 autosequencer (Applied Biosystems) was used for sequencing.

Phylogenetic analyses.—Sequence data for the representative type isolates of all published *Huntiella* species were downloaded from GenBank. Sequences

produced in this study and those from GenBank were checked manually in MEGA 7 and Geneious 7.0 was used to analyze the consensus sequences. All sequences were aligned using MAFFT 7 (http://align.bmr.kyushuu.ac.jp/mafft/on-line/server; Katoh et al. 2002) and then confirmed manually. Sequence alignments for all data sets were deposited in TreeBASE (study no. 22889), and sequences for the novel species were deposited in GenBank (TABLE 1).

Maximum parsimony (MP) phylogenetic analyses of single-gene data sets for the ITS, *BT1*, and *TEF1α* gene regions and the combined sequence data sets based on parsimony were carried out using PAUP 4.0b10 (Swofford 2003). The heuristic tree search algorithm was selected to generate phylograms, with the following options: sequence randomization (reps = 1000), tree bisection reconnection (TBR) branch swapping, and gaps treated as a fifth character. To determine the confidence intervals of the branch nodes, 1000 bootstrap replicates were conducted with the full heuristic search option. The parameters estimated for the most parsimonious trees included the tree length (TL), retention index (RI), consistency index (CI), and rescaled consistency index (RC). A partition homogeneity test (PHT; Swofford 2003) was run to verify that data for the three gene regions could be combined in the analyses.

Maximum likelihood (ML) analysis was carried out using PhyML 3.1 (Guindon and Gascuel 2003) on the data sets for the individual gene regions and the combined data set. Substitution models were selected for each data set with the Akaike information criterion (AIC) in jModeltest 2.1.5 (Posada 2008). Confidence levels for nodes were estimated using 1000 replicate bootstrap analyses. For both MP and ML analyses, *Ceratocystis cercfabiensis* (CMW 43029; Liu et al. 2015) was used as the outgroup taxon.

Morphological and growth studies.—For each of the putative new species identified in the phylogenetic analyses, growth and morphological studies were conducted. Cultures were grown on 2% MEA for 1–2 wk at 25 C. Descriptions of colony morphology and color (upper and reverse surfaces) were based on the mycological color charts of Rayner (1970). The morphology of fruiting structures was studied using 1–2-wk-old cultures on 2% MEA, which were incubated at 25 C. Microscope slides were prepared by placing each structure in 80% lactic acid, and these were examined using a Nikon H550L microscope (Nikon, Yokohama, Japan). Fifty measurements of characteristic morphological structures were made for each isolate. All measurements were computed and presented as (minimum–)(mean − SD)–(mean + SD)(–maximum).

To determine the optimal growth temperature for the putative new species, two or three isolates of each species were used for growth studies at temperatures ranging from 5 to 35 C, at 5-degree intervals. Five replicate plates were prepared for each isolate at each temperature, by transferring a 4-mm plug to the centers of 90-mm Petri dishes containing 2% MEA. Plates were incubated at the test temperatures for 4 d. Measurements were taken along two perpendicular axes, centered on the plugs and at right angles to each other for each colony, and the averages of diameter measurements at each temperature were computed.

Mating tests.—The mating type of each isolate of the new species was determined by positive amplification using specific mating type primers developed by Wilson et al. (2015). Primers Oman_111_F and Oman_111_R amplify a 335-bp fragment of the *MAT1-1-1* gene, and primers Om_Mo_121_F and Om_Mo_121_R amplify a 572-bp fragment of the *MAT1-2-1* gene. The same PCR protocol described above was used, with the exception that the annealing temperature was 53 C (Wilson et al. 2015).

Isolates of opposite mating type of the same species were crossed with each other in all possible combinations in an attempt to induce the production of ascomata. Mycelium-covered agar blocks were placed next to each other ca. 2 cm apart on a single plate. These pairings were done on 90-mm Petri dishes containing 2% MEA and incubated in the dark for 1–2 mo at 20 C. Crosses were inspected once per wk for the presence of ascomata.

Pathogenicity tests.—Seventeen isolates representing the nine *Huntiella* species were selected for pathogenicity trials to inoculate on *Eucalyptus* clone CEPT-11 (*Eucalyptus urophylla* × *E. grandis*) in a glasshouse. Isolates were grown on 2% MEA at 25 C for 7 d before inoculation. The seedlings were 2 m in height and had an average diameter at the root collar of 2 cm.

Inoculations were conducted using the same method described by Liu et al. (2018). Fifteen seedlings were inoculated for each of the 17 isolates, and 15 additional seedlings were inoculated with sterile MEA plugs to serve as negative controls. The inoculated seedlings were arranged in a randomized design in the glasshouse. The inoculated plants were evaluated after 6 wk by measuring lesion lengths in the

Table 1. List of *Huntiella* and *Ceratocystis* species included in this study.

Species[a]	CMW no.[b]	Other no.[b]	GenBank accession no.[c]			Host (or substrate)	Origin	Latitude and longitude	Reference
			ITS	*BT1*	*TEF1a*				
Ceratocystis cercfabiensis	CMW 43029	CERC 2170; CBS 139654	KP727592	KP727618	KP727643	*Eucalyptus* sp.	Hainan, China		Liu et al. 2015
Huntiella ani	**CMW 44684**[d,e]	**CERC 2827; CBS 143283**	**MH118602**	**MH118635**	**MH118668**	*Eucalyptus* sp.	Guangxi, China	23°26′34″N, 108°14′40″E	Present study
H. ani	**CMW 44686**[d,e]	**CERC 2829 CBS 143282**	**MH118603**	**MH118636**	**MH118669**	*Eucalyptus* sp.	Guangxi, China	23°26′34″N, 108°14′40″E	Present study
H. ani	**CMW 44687**	**CERC 2830**	**MH118604**	**MH118637**	**MH118670**	*Eucalyptus* sp.	Guangxi, China	23°26′34″N, 108°14′40″E	Present study
H. ani	**CMW 49315**[d]	**CERC 2871; CBS 143284**	**MH118611**	**MH118644**	**MH118677**	*Eucalyptus* sp.	Guangxi, China	24°28′2″N, 109°45′50″E	Present study
H. bellula	**CMW 49312**[d,e]	**CERC 2854; CBS 143286**	**MH118607**	**MH118640**	**MH118673**	*Eucalyptus* sp.	Guangxi, China	24°28′2″N, 109°45′50″E	Present study
H. bellula	**CMW 44702**	**CERC 2859**	**MH118608**	**MH118641**	**MH118674**	*Eucalyptus* sp.	Guangxi, China	24°28′2″N, 109°45′50″E	Present study
H. bellula	**CMW 49313**	**CERC 2861**	**MH118609**	**MH118642**	**MH118675**	*Eucalyptus* sp.	Guangxi, China	24°28′2″N, 109°45′50″E	Present study
H. bellula	**CMW 49314**[d,e]	**CERC 2862; CBS 143285**	**MH118610**	**MH118643**	**MH118676**	*Eucalyptus* sp.	Guangxi, China	24°28′2″N, 109°45′50″E	Present study
H. bellula	**CMW 49316**[d]	**CERC 2880; CBS 143287**	**MH118612**	**MH118645**	**MH118678**	*Eucalyptus* sp.	Guangxi, China	24°20′33″N, 110°4′59″E	Present study
H. bhutanensis	CMW 8242	CBS 112907	AY528951	AY528956	AY528961	*Picea spinulosa*	Jelekha, Bhutan		Van Wyk et al. 2004
H. bhutanensis	CMW 8217	CBS 114289	AY528957	AY528962	AY528952	*Picea spinulosa*	Jelekha, Bhutan		Van Wyk et al. 2004
H. ceramica	CMW 15245	CBS 122299	EU245022	EU244994	EU244926	*Eucalyptus grandis*	Malawi		Heath et al. 2009
H. ceramica	CMW 15248	CBS 122300	EU245024	EU244996	EU244928	*Eucalyptus grandis*	Malawi		Heath et al. 2009
H. chinaeucensis	CMW 24658	CBS 127185	JQ862729	JQ862717	JQ862741	*Eucalyptus* sp.	Guangdong, China		Chen et al. 2013
H. chinaeucensis	CMW 24661	CBS 127186	JQ862731	JQ862719	JQ862743	*Eucalyptus* sp.	Guangdong, China		Chen et al. 2013
H. chlamydoformis	CMW 36932	CBS 131674	KF769087	KF769109	KF769098	*Theobroma cacao*	Cameroon		Mbenoun et al. 2016
H. chlamydoformis	CMW 37102	CBS 131675	KF769088	KF769110	KF769099	*Terminalia superba*	Cameroon		Mbenoun et al. 2016
H. confusa	**CMW 49300**[d,e]	**CERC 2141; CBS 143289**	**MH118582**	**MH118615**	**MH118648**	*Acacia confusa*	Hainan, China	19°42′57″N, 109°37′3″E	Present study
H. confusa	**CMW 43452**[d]	**CERC 2158; CBS 143577**	**MH118583**	**MH118616**	**MH118649**	*Acacia confusa*	Hainan, China	19°42′57″N, 109°37′3″E	Present study
H. confusa	**CMW 43453**[d,e]	**CERC 2162; CBS 143288**	**MH118584**	**MH118617**	**MH118650**	*Acacia confusa*	Hainan, China	19°42′57″N, 109°37′3″E	Present study
H. cryptoformis	CMW 36826	CBS 131277	KC691462	KC691486	KC691510	*Terminalia sericea*	South Africa		Mbenoun et al. 2014
H. cryptoformis	CMW 36828	CBS 131279	KC691464	KC691488	KC691512	*Ziziphus mucronata*	South Africa		Mbenoun et al. 2014
H. decipiens	CMW 25918	CBS 129735	HQ203218	HQ203235	HQ236437	*Eucalyptus cloeziana*	South Africa		Kamgan Nkuekam et al. 2013
H. decipiens	CMW 25914	CBS 129737	HQ203219	HQ203236	HQ236438	*Eucalyptus maculata*	South Africa		Kamgan Nkuekam et al. 2013
H. eucalypti	**CMW 44692**[d,e]	**CERC 2840; CBS 143291**	**MH118605**	**MH118638**	**MH118671**	*Eucalyptus* sp.	Guangxi, China	24°40′38″N, 108°20′16″E	Present study
H. eucalypti	**CMW 44693**[d,e]	**CERC 2841; CBS 143290**	**MH118606**	**MH118639**	**MH118672**	*Eucalyptus* sp.	Guangxi, China	24°40′38″N, 108°20′16″E	Present study
H. fabiensis	**CMW 44370**[d,e]	**CERC 2736; CBS 143293**	**MH118589**	**MH118622**	**MH118655**	*Eucalyptus* sp.	Guangdong, China	24°44′3″N, 116°22′39″E	Present study
H. fabiensis	**CMW 49307**[d]	**CERC 2753; CBS 143294**	**MH118596**	**MH118629**	**MH118662**	*Eucalyptus* sp.	Guangdong, China	24°44′3″N, 116°22′39″E	Present study
H. fabiensis	**CMW 49308**	**CERC 2755**	**MH118597**	**MH118630**	**MH118663**	*Eucalyptus* sp.	Guangdong, China	24°44′3″N, 116°22′39″E	Present study
H. fabiensis	**CMW 44382**	**CERC 2762**	**MH118598**	**MH118631**	**MH118664**	*Eucalyptus* sp.	Guangdong, China	24°44′3″N, 116°22′39″E	Present study
H. fabiensis	**CMW 49309**[d,e]	**CERC 2763; CBS 143292**	**MH118599**	**MH118632**	**MH118665**	*Eucalyptus* sp.	Guangdong, China	24°44′3″N, 116°22′39″E	Present study
H. fabiensis	**CMW 49310**	**CERC 2764**	**MH118600**	**MH118633**	**MH118666**	*Eucalyptus* sp.	Guangdong, China	24°44′3″N, 116°22′39″E	Present study
H. fabiensis	**CMW 49311**	**CERC 2765**	**MH118601**	**MH118634**	**MH118667**	*Eucalyptus* sp.	Guangdong, China	24°44′3″N, 116°22′39″E	Present study
H. fecunda	**CMW 49301**[d,e]	**CERC 2446; CBS 143304**	**MH118585**	**MH118618**	**MH118651**	*Eucalyptus* sp.	Fujian, China	24°44′36″N, 117°50′5″E	Present study

(*Continued*)

Table 1. (Continued).

Species[a]	CMW no.[b]	Other no.[b]	GenBank accession no.[c] ITS	*BT1*	*TEF1a*	Host (or substrate)	Origin	Latitude and longitude	Reference
H. fecunda	**CMW 49302**[d]	**CERC 2449; CBS 143296**	**MH118586**	**MH118619**	**MH118652**	*Eucalyptus* sp.	Fujian, China	24°44′36″N, 117°50′5″E	Present study
H. fecunda	**CMW 49303**[d,e]	**CERC 2451a; CBS 143295**	**MH118587**	**MH118620**	**MH118653**	*Eucalyptus* sp.	Fujian, China	24°44′36″N, 117°50′5″E	Present study
H. fecunda	**CMW 49304**	**CERC 2451f**	**MH118588**	**MH118621**	**MH118654**	*Eucalyptus* sp.	Fujian, China	24°44′36″N, 117°50′5″E	Present study
H. glaber	**CMW 43436**[d,e]	**CERC 2132; CBS 143298**	**MH118580**	**MH118613**	**MH118646**	*Eucalyptus exserta*	Hainan, China	19°2′14″N, 110°30′32″E	Present study
H. glaber	**CMW 49299**[d]	**CERC 2133; CBS 143297**	**MH118581**	**MH118614**	**MH118647**	*Eucalyptus exserta*	Hainan, China	19°2′14″N, 110°30′32″E	Present study
H. inaequabilis	**CMW 44372**[d,e]	**CERC 2740; CBS 143300**	**MH118590**	**MH118623**	**MH118656**	*Eucalyptus* sp.	Guangdong, China	24°44′3″N, 116°22′39″E	Present study
H. inaequabilis	**CMW 49306**[d,e]	**CERC 2749; CBS 143299**	**MH118595**	**MH118628**	**MH118661**	*Eucalyptus* sp.	Guangdong, China	24°44′3″N, 116°22′39″E	Present study
H. inquinana	CMW 21106		EU588587	EU588666	EU588674	*Acacia mangium*	Indonesia		Tarigan et al. 2010
H. inquinana	CMW 21107	CBS 124009	EU588588	EU588667	EU588675	*Acacia mangium*	Indonesia		Tarigan et al. 2010
H. meiensis	**CMW 44374**[d,e]	**CERC 2742; CBS 143302**	**MH118591**	**MH118624**	**MH118657**	*Eucalyptus* sp.	Guangdong, China	24°44′3″N, 116°22′39″E	Present study
H. meiensis	**CMW 44375**	**CERC 2743**	**MH118592**	**MH118625**	**MH118658**	*Eucalyptus* sp.	Guangdong, China	24°44′3″N, 116°22′39″E	Present study
H. meiensis	**CMW 49305**[d]	**CERC 2744; CBS 143303**	**MH118593**	**MH118626**	**MH118659**	*Eucalyptus* sp.	Guangdong, China	24°44′3″N, 116°22′39″E	Present study
H. meiensis	**CMW 44376**[d,e]	**CERC 2746; CBS 143301**	**MH118594**	**MH118627**	**MH118660**	*Eucalyptus* sp.	Guangdong, China	24°44′3″N, 116°22′39″E	Present study
H. microbasis	CMW 21117	CBS 124013	EU588593	EU588672	EU588680	*Acacia mangium*	Indonesia		Tarigan et al. 2010
H. microbasis	CMW 21115	CBS 124015	EU588592	EU588671	EU588679	*Acacia mangium*	Indonesia		Tarigan et al. 2010
H. moniliformis	CMW 9590	CBS 116452	AY431101	AY528985	AY529006	*Eucalyptus grandis*	South Africa		Van Wyk et al. 2006
H. moniliformis	CMW 4114	CBS 118151	AY528997	AY528986	AY529007	*Shizolobium parahyba*	Ecuador		Van Wyk et al. 2006
H. moniliformopsis	CMW 9986	CBS 109441	AY528998	AY528987	AY529008	*Eucalyptus obliqua*	Australia		Yuan and Mohammed 2002
H. moniliformopsis	CMW 10214	CBS 115792	AY528999	AY528988	AY529009	*Eucalyptus sieberi*	Australia		Yuan and Mohammed 2002
H. oblonga	CMW 23803	CBS 122291	EU245019	EU244991	EU244951	*Acacia mearnsii*	South Africa		Heath et al. 2009
H. oblonga	CMW 23802		EU245020	EU244992	EU244952	*Acacia mearnsii*	South Africa		Heath et al. 2009
H. omanensis	CMW 11048	CBS 115787	DQ074742	DQ074732	DQ074737	*Mangifera indica*	Oman		Al-Subhi et al. 2006
H. omanensis	CMW 3800	CBS 117839	DQ074743	DQ074733	DQ074738	*Mangifera indica*	Oman		Al-Subhi et al. 2006
H. pycnanthi	CMW 36916	CBS 131672	KF769096	KF769118	KF769107	*Theobroma cacao*	Cameroon		Mbenoun et al. 2016
H. pycnanthi	CMW 36910		KF769095	KF769117	KF769106	*Theobroma cacao*	Cameroon		Mbenoun et al. 2016
H. salinaria	CMW 25911	CBS 129733	HQ203213	HQ203230	HQ236432	*Eucalyptus maculata*	South Africa		Kamgan Nkuekam et al. 2013
H. salinaria	CMW 30703	CBS 129734	HQ203214	HQ203231	HQ236433	*Eucalyptus saligna*	South Africa		Kamgan Nkuekam et al. 2013
H. savannae	CMW 17300	CBS 121151	EF408551	EF408565	EF408572	*Acacia nigrescens*	South Africa		Kamgan Nkuekam et al. 2008
H. savannae	CMW 17297		EF408552	EF408566	EF408573	*Combretum zeyheri*	South Africa		Kamgan Nkuekam et al. 2008
H. sublaevis	CMW 22449	CBS 122517	FJ151431	FJ151465	FJ151487	*Terminalia ivorensis*	Ecuador		Van Wyk et al. 2011
H. sublaevis	CMW 22444	CBS 122518	FJ151430	FJ151464	FJ151486	*Terminalia ivorensis*	Ecuador		Van Wyk et al. 2011
H. sumatrana	CMW 21109	CBS 124011	EU588589	EU588668	EU588676	*Acacia mangium*	Indonesia		Tarigan et al. 2010
H. sumatrana	CMW 21111	CBS 124012	EU588590	EU588669	EU588677	*Acacia mangium*	Indonesia		Tarigan et al. 2010
H. tribiliformis	CMW 13011	CBS 115867	AY528991	AY529001	AY529012	*Pinus merkusii*	Indonesia		Van Wyk et al. 2006
H. tribiliformis	CMW 13012	CBS 118242	AY528992	AY529002	AY529013	*Pinus merkusii*	Indonesia		Van Wyk et al. 2006
H. tyalla	CMW 28917		HM071899	HM071909	HQ236448	*Eucalyptus grandis*	Australia		Kamgan Nkuekam et al. 2012
H. tyalla	CMW 28920		HM071896	HM071910	HQ236449	*Eucalyptus grandis*	Australia		Kamgan Nkuekam et al. 2012

[a]Species indicated in bold are newly described in this study.
[b]CMW = culture collection of the Forestry and Agricultural Biotechnology Institute (FABI), University of Pretoria, Pretoria, South Africa; CERC = culture collection of China Eucalypt Research Centre (CERC), Chinese Academy of Forestry (CAF), Zhanjiang, Guangdong Province, China; CBS = Westerdijk Fungal Biodiversity Institute, Utrecht, the Netherlands.
[c]GenBank accession numbers indicated in bold were generated in this study.
[d]Isolates used for the growth study.
[e]Isolates used for the pathogenicity study.

cambium. The inoculated fungi were reisolated by cutting small pieces of wood from the edges of the lesions/wounds and cultivating them in 2% MEA at 25 C. Reisolations were made from five randomly selected seedlings per test isolate and all seedlings that served as negative controls. The data were analyzed using one-way analyses of variance (ANOVAs) using SAS 9.3 (SAS Institute Inc. 2011).

RESULTS

Fungal isolates.—Collectively, 33 isolates with morphology typical of species in *Huntiella* were obtained (FIG. 1C–L). Of these, 30 were from *Eucalyptus* species and included 13 from Guangdong Province, 11 from Guangxi Province, 4 from Fujian Province, and two from Hainan Province (TABLE 1; FIG. 2). The remaining three were obtained from *Acacia confusa* in Hainan Province. All isolates were fast growing on MEA, produced dark ascomata with conical spines ornamenting their bases, had long necks, and produced hat-shaped ascospores. Additionally, all cultures also produced both sexual and asexual structures in culture, typically within 1 wk. However, the ability to produce these structures diminished over time. All of these characters are typical of species in *Huntiella* (Van Wyk et al. 2004; De Beer et al. 2014). Isolates obtained from this study have been preserved in the three culture collections described above (TABLE 1).

Sequencing and phylogenetic analyses.—PCR products and sequence data were generated for all 33 isolates, which were approximately 540 bp for ITS, 530 bp for *BT1*, and 830 bp for *TEF1α*. All sequences obtained for the 33 *Huntiella* isolates in this study were deposited in GenBank (TABLE 1).

Four data sets were used in the phylogenetic analyses, namely, the ITS (72 taxa, 612 characters), *BT1* (72 taxa, 564 characters), *TEF1α* (72 taxa, 844 characters), and a combined data set (72 taxa, 2020 characters). The aligned sequences for the data sets were deposited in TreeBASE (no. 22889). Statistical values for the parameters used in the phylogenetic trees for the MP analyses and the best fit substitution models of ML are provided in TABLE 2. Partition homogeneity tests (PHTs) with 1000 replicates for the three gene regions produced a $P = 0.045$, indicating that the data sets could be combined (Cunningham 1997).

Data for 19 previously described species of *Huntiella* were included in the analyses, which also included the 33 isolates from China. Topologies of the trees resulting from the MP and ML analyses were concordant, showing similar phylogenetic relationships among the species for all data sets (FIG. 3; SUPPLEMENTARY FIGS. 1, 2, and 3). Furthermore, the isolates from China formed nine well-resolved and unique phylogenetic groups based on three of the data sets, excluding ITS (SUPPLEMENTARY FIG. 1). Phylogenetic groups 1–6 were composed of isolates from China, were most closely related to *H. bhutanensis*, and formed subclade 1 of the Asian Clade (FIG. 3). Groups 7 and 8 were phylogenetically close to *H. chinaeucensis, H. inquinans, H. microbasis, H. omanensis*, and *H. sumatrana* in subclade 2 of the Asian Clade (FIG. 3). Phylogenetic group 9 was most closely related to *H. moniliformis, H. sublaevis*, and *H. tyalla* of the Indo-Pacific Clade (FIG. 3).

Morphological and growth studies.—The isolates representing the nine new phylogenetic groups all had morphological characteristics typical of *Huntiella* species. They produced hat-shaped ascospores and had short conical spines on their ascomatal bases. Colonies of isolates for the nine phylogenetic groups grew rapidly on MEA, covering the surfaces of 90-mm Petri dishes in 4–5 d (FIG. 1C–L) and had optimal growth at temperatures between 25 and 30 C. Mycelium was white when young and turned darker with age (FIG. 1C–L). Morphological differences were observed between isolates representing each phylogenetic group and their closest phylogenetic neighbor, especially in the sizes of ascomatal bases and conidia. Furthermore, there were also cases of growth rate differences.

Mating tests.—All isolates in phylogenetic group 8 (*H. glaber*) had both the *MAT1-1-1* and *MAT1-2-1* genes in a single isolate, were able to sexually reproduce in isolation, and are thus homothallic. Isolates in group 9 (*H. fecunda*) had only the *MAT1-2-1* gene but were able to sexually reproduce in isolation and are thus unisexual. Isolates in the seven other groups were heterothallic, having either a *MAT1-1-1* gene or a *MAT1-2-1* gene. In the case of these groups, isolates of opposite mating type were crossed and produced sexual structures in culture. This confirmed their heterothallic nature.

Pathogenicity tests.—All 17 *Huntiella* isolates tested for pathogenicity on the *Eucalyptus* seedlings produced localized lesions on the cambium after 6 wk. The negative controls produced only a wound response or callus around the inoculation sites (FIGS. 13 and 14). Results of ANOVA tests showed that the

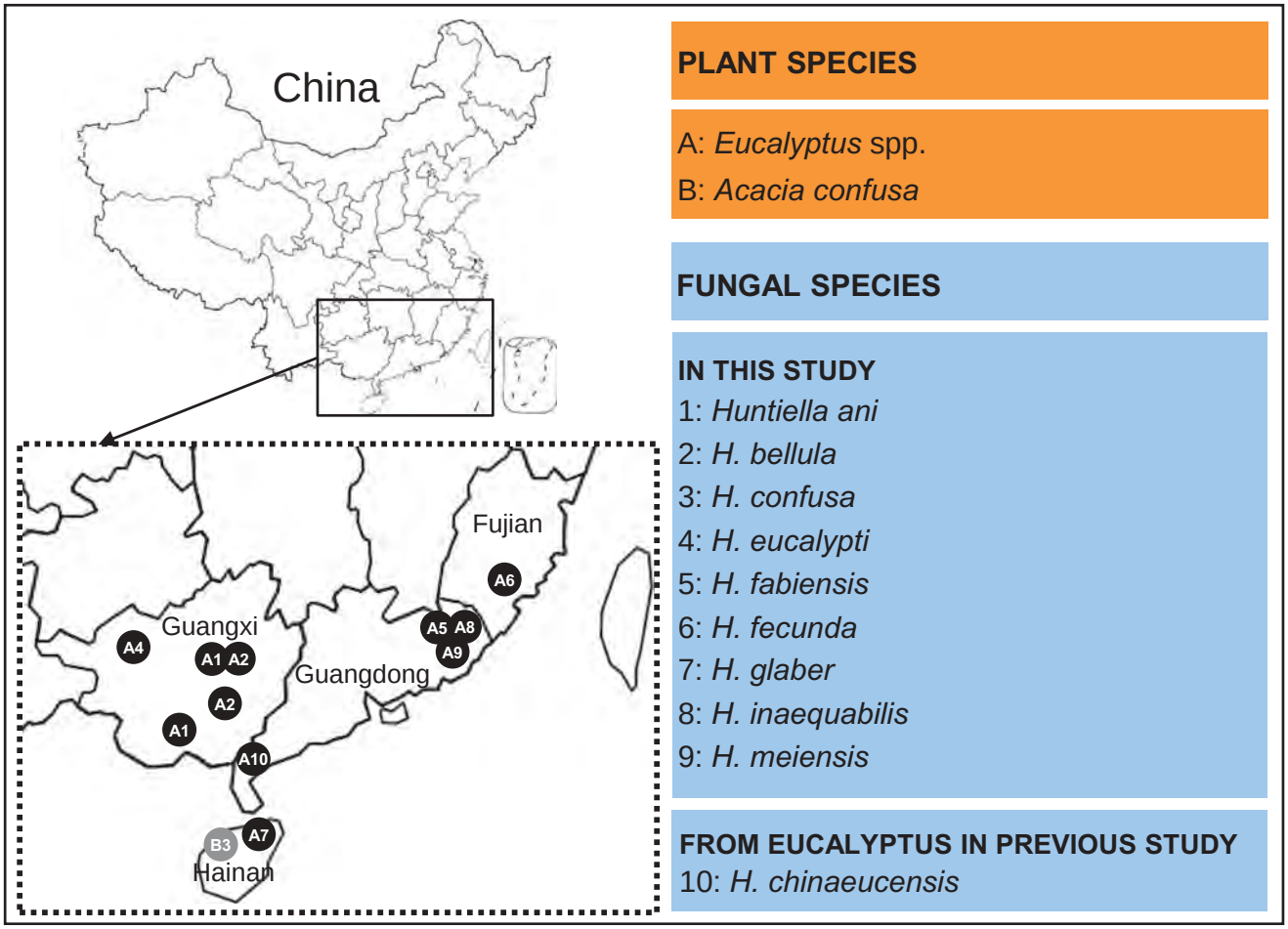

Figure 2. Map showing the nine species of *Huntiella* detected from different regions and plant hosts in China. The different *Huntiella* species are indicated as numbers 1 to 9, and the plant hosts are shown as letters A to B. A1, for example, indicates *H. ani* isolated from *Eucalyptus* spp. in Guangxi Province.

Table 2. Parameters used in phylogenetic analyses in this study.

Analysis	Parameter	ITS	*BT1*	*TEF1a*	Combined
MP	No. of taxa	72	72	72	72
	No. of bp	612	564	844	2020
	PIC	16	67	202	285
	Number trees	3000	42	3000	128
	Tree length	29	130	454	626
	CI	0.69	0.738	0.782	0.752
	RI	0.919	0.933	0.945	0.936
	HI	0.31	0.262	0.218	0.248
ML	Subst. model	TPM2uf+I	TrN+I+G	TPM2uf+G	TIM2+I+G
	NST	6	6	6	6
	P-inv	0.468	0.513	—	0.474
	Gamma	—	0.658	0.271	0.589

Note. bp = base pairs; PIC = number of parsimony informative characters; CI = consistency index; RI = retention index; HI = homoplasy index; Subst. model = best-fit substitution model; NST = number of substitution rate categories.

lesions produced by *H. bellula* (CMW 49312 and CMW 49314), *H. eucalypti* (CMW 44693), *H. fabiensis* (CMW 44370), *H. fecunda* (CMW 49301 and CMW 49303), *H. glaber* (CMW 43436), and *H. meiensis* (CMW 44376) were significantly longer than the wounds produced by negative controls ($P < 0.05$) (FIG. 13). Isolate CMW 44370 (*H. fabiensis*) was the most aggressive and produced significantly longer lesions. In contrast, isolates CMW 44684 and CMW 44686 (*H. ani*) had the lowest level of aggressiveness (FIG. 13). Significantly different lesion lengths were associated with different isolates of some species,

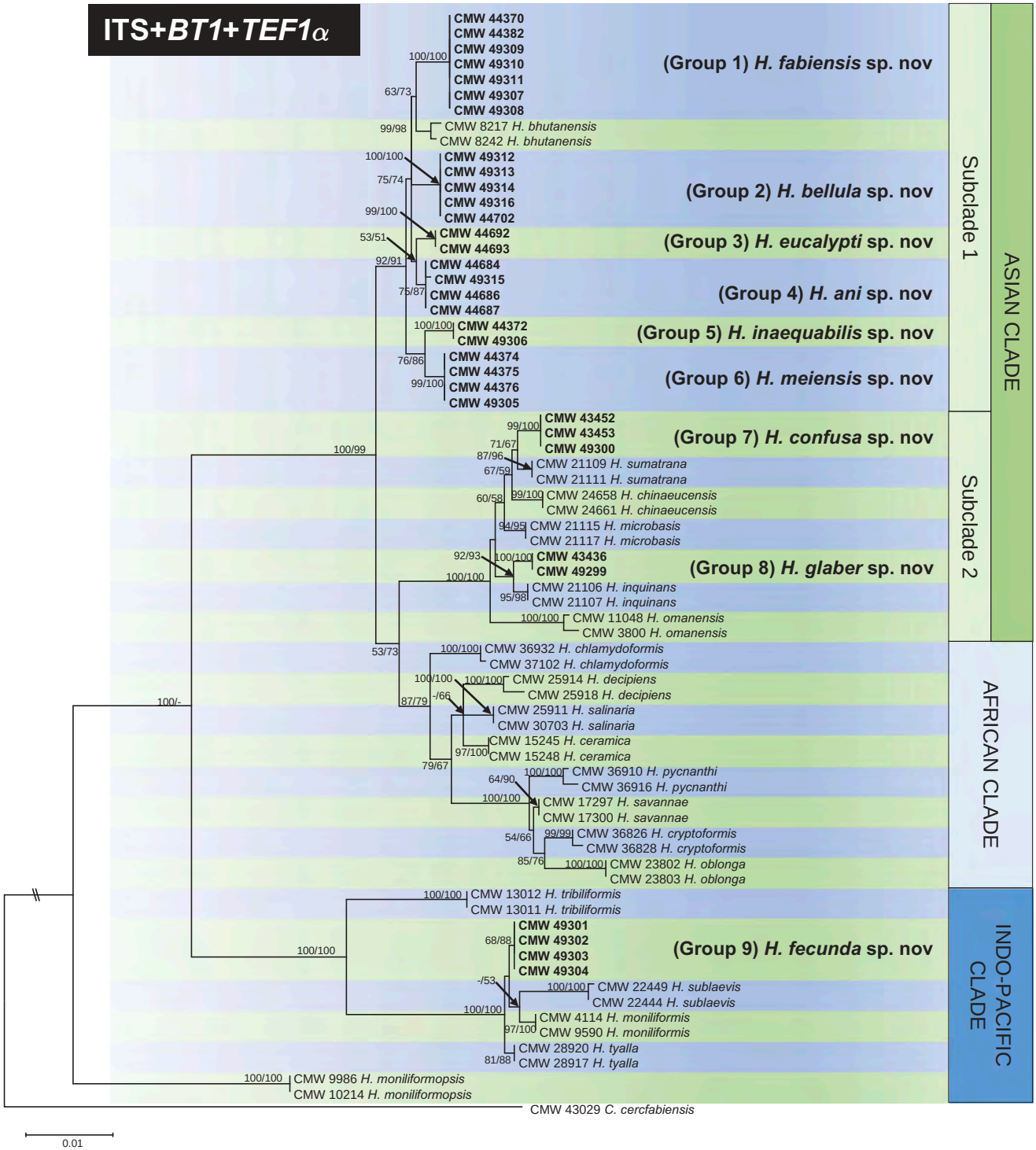

Figure 3. Phylogenetic trees based on maximum likelihood (ML) analysis of a combined data set of ITS, *BT1*, and *TEF1α* gene sequences for *Huntiella* species. Isolates in bold were obtained and sequenced in this study. Bootstrap values >50% for maximum parsimony (MP) and ML are presented above branches as MP/ML. Bootstrap values lower than 50% are marked with *. Nodes lacking bootstrap support are marked with -. *Ceratocystis cercfabiensis* (CMW 43029) represents the outgroup.

such as *H. fabiensis* and *H. meiensis* (FIG. 13). The inoculated fungi were easily reisolated from lesions on inoculated seedlings, but not from the negative controls, thus fulfilling Koch's postulates.

TAXONOMY

Based on phylogenetic analyses, growth, and morphological studies, the 33 *Huntiella* isolates from *Eucalyptus* and *Acacia* in China represent nine novel

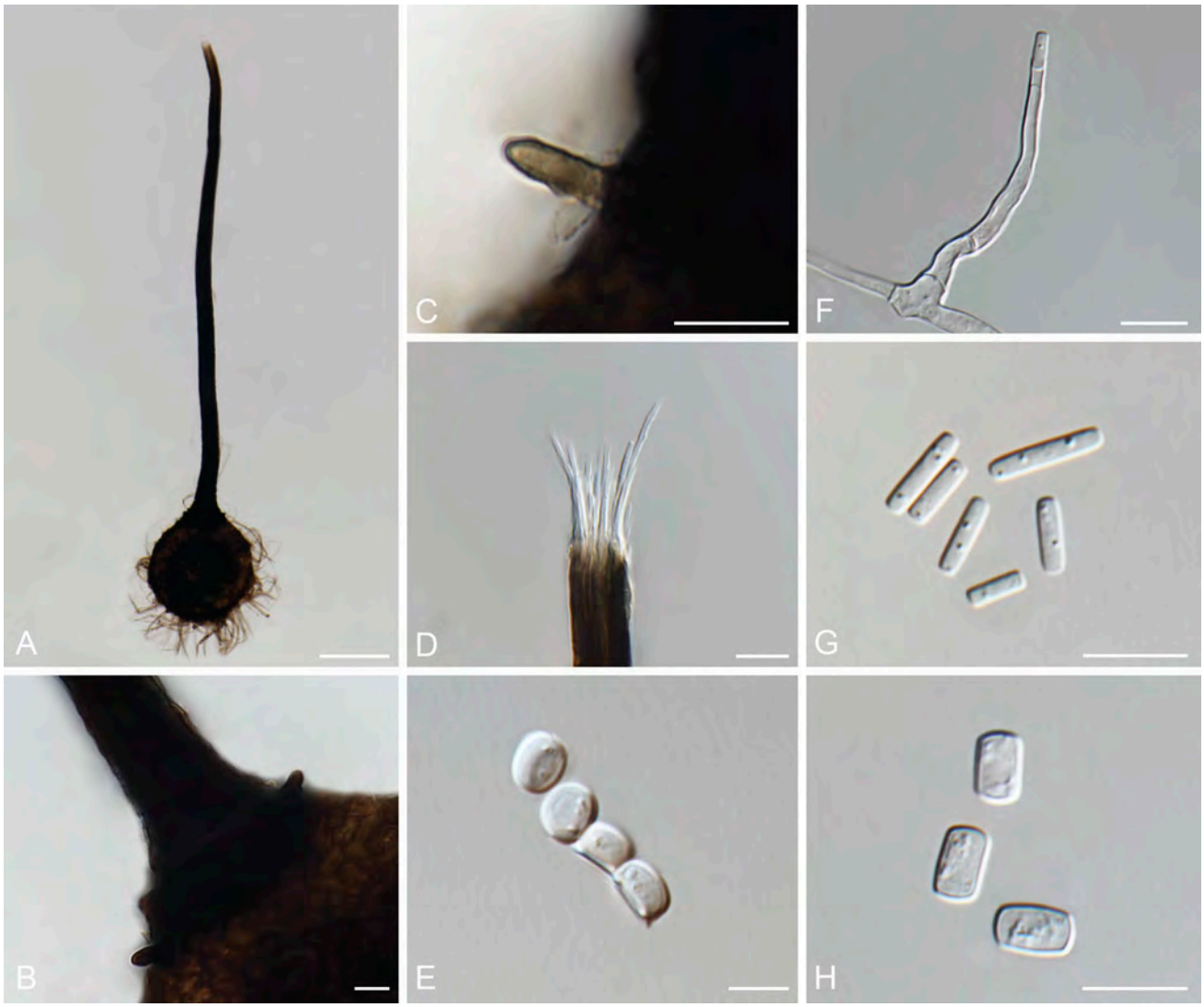

Figure 4. Morphological characters of *Huntiella ani*. A. Ascoma with obpyriform base and extended neck. B–C. Conical spines on the surface of ascomatal base. D. Tip of ascomatal neck with divergent ostiolar hyphae. E. Hat-shaped ascospore in top view and side view. F. Flask-shaped conidiophore. G. Various sizes of bacilliform conidia. H. Barrel-shaped conidia. Bars: A = 100 µm; B–D, F–H = 10 µm; E = 5 µm.

species. The following descriptions for these species are provided.

Huntiella ani F.F. Liu & S.F. Chen, sp. nov. FIG. 4
MycoBank MB826735

Typification: CHINA. GUANGXI PROVINCE: Nanning region, *Eucalyptus* plantation (23°26′34″N, 108°14′40″E), isolated from recently harvested tree stump, Jan 2014, *S.F. Chen, F.F. Liu* & *G.Q. Li* (**holotype** PREM 62020). Ex-holotype culture: CMW 44686 = CBS 143282 = CERC 2829.

Etymology: The name refers to the Chinese name "An" for the host *Eucalyptus*, from which it was collected.

Mating strategy: Heterothallic with isolates having either a *MAT1-1-1* gene or a *MAT1-2-1* gene.

Sexual state: Ascomata superficial, scattered near center of colony. Ascomatal bases dark brown, globose to obpyriform, (104.5–)124–167(–224) µm long and (117.5–)128.5–173(–232) µm wide, ornamented with conical, thick-walled, dark brown spines, (6–)8.5–15.5(–21) µm long. Ascomatal necks dark, erect, slender, (493–)520–667(–845) µm long, (9.5–)10.5–12.5(–14) µm wide at apex and (29.5–)33–44.5(–54) µm wide at base. Ostiolar hyphae present, hyaline, divergent, (14.5–)19.5–28.5(–33) µm long. Asci not observed. Ascospores hat-shaped, invested in sheath, aseptate, (4.5–)4.5–5.5(–6) µm long and (1.5–)2.5–3(–3.5) µm wide with sheath in side view. Ascospores accumulating in creamy to yellow droplets at tip of ascomatal neck.

Asexual state: Conidiophores arising laterally from vegetative hyphae, scattered or arising in clusters, multiseptate, hyaline, consisting of 2–3 cylindrical cells terminating in a phialide. Conidiogenous cells phialidic, cylindrical, (18.5–)27–45.5(–59) µm long, (1.5–)1.5–2.5(–3) µm wide at apex and (2–)3–4.5(–5.5) µm wide at base. Conidia of two forms: (i) bacilliform conidia hyaline, aseptate, cylindrical, (4–)5–8.5(–12.5) µm long and (1.5–)1.5–2.5(–3) µm wide; and (ii) barrel-shaped conidia hyaline, aseptate, in chains, (4–)5–7.5(–9) µm long and (2.5–)3–4(–5) µm wide. Chlamydospores not observed.

Culture characters: Colonies on MEA fast growing, optimal temperature for growth 25 C, no growth at 5, 30, and 35 C. After 4 d, colonies grew 7.1 mm at 10 C, 32.2 mm at 15 C, 51.7 mm at 20 C, and 66.4 mm at 25 C. Colonies round with even margins. Mycelium fluffy, smooth, dense on MEA, initially hyaline to white, turning to grayish sepia (15"") after 2–3 wk, reverse honey (19") turning chaetura drab (17""k) when older. Colony surfaces scattered with dark brown to black ascomata.

Habitat: Stumps of recently cut *Eucalyptus* trees.

Distribution: Guangxi Province, China.

Other specimens examined: CHINA. GUANGXI PROVINCE: Nanning region, *Eucalyptus* plantation (23°26′34″N, 108°14′40″E), isolated from recently harvested tree stump, Jan 2014, *S.F. Chen, F.F. Liu* & *G.Q. Li*, PREM 62021, culture CMW 44684 = CBS 143283 = CERC 2827. GUANGXI PROVINCE: Liuzhou region, *Eucalyptus* plantation (24°28′2″N, 109°45′50″E). Isolated from recently harvested tree stump, Jan 2014, *S.F. Chen, F.F. Liu* & *G.Q. Li*, PREM 62022, culture CMW 49315 = CBS 143284 = CERC 2871.

Notes: Huntiella ani is closely related to *H. eucalypti*. The asexual structures of the two species are similar. *Huntiella ani* can be distinguished from *H. eucalypti* based on its optimal temperature for growth in culture. *Huntiella ani* did not grow at 5 C, but *H. eucalypti* grew 10.5 mm at 5 C after 4 d. It also differed from *H. eucalypti* in five bases in the *TEF1α* gene and one base in the *BT1* gene.

Huntiella bellula F.F. Liu & S.F. Chen, sp. nov. FIG. 5
MycoBank MB826738

Typification: CHINA. GUANGXI PROVINCE: Liuzhou region, *Eucalyptus* plantation (24°28′2″N, 109°45′50″E), isolated from recently harvested tree stump, Jan 2014, *S.F. Chen, F.F. Liu* & *G.Q. Li* (**holotype** PREM 62023). Ex-holotype culture: CMW 49314 = CBS 143285 = CERC 2862.

Etymology: "*bellus*" (Latin) = beauty, referring to the beauty of the fungal structures of this species.

Mating strategy: Heterothallic with isolates having either a *MAT1-1-1* gene or a *MAT1-2-1* gene.

Sexual state: Ascomata superficial, scattered near center of colony. Ascomatal bases black, globose to subglobose, (172.5–)179–228.5(–250.5) µm long and (184–)195–230.5(–244) µm wide, ornamented with conical, thick-walled, dark brown spines, (5–)7.5–16.0(–20) µm long. Ascomatal necks dark brown to black, erect, slender, forming an obvious bulbous collar at junction with ascomatal base, (395–)450–631(–707.5) µm long, (10.5–)11.5–13.5(–14.5) µm wide at apex and (42.5–)45–59.5(–69) µm wide at base. Ostiolar hyphae present, hyaline, divergent, (18–)20–29.5(–32.5) µm long. Asci not observed. Ascospores hat-shaped, invested in sheath, aseptate, (5–)5.5–6.5(–6.5) µm long and (2.5–)2.5–3(–4) µm wide with sheath in side view. Ascospores accumulating in creamy to yellow droplets at tip of ascomatal neck.

Asexual state: Conidiophores arising laterally from vegetative hyphae, scattered or arising in clusters, multiseptate, hyaline, consisting of 2–3 cylindrical cells terminating in a phialide. Conidiogenous cells phialidic, cylindrical, (21.5–)26.5–38.5(–50) µm long, (1–)1.5–2(–2.5) µm wide at apex and (2–)2.5–4(–6) µm wide at base. Conidia of two forms: (i) bacilliform conidia hyaline, aseptate, cylindrical, (5.5–)6.5–9(–12) µm long and (1.5–)1.5–2(–2) µm wide; and (ii) barrel-shaped conidia not observed. Chlamydospores not observed.

Culture characters: Colonies on MEA fast growing, optimal temperature for growth 25 C, no growth at 35 C. After 4 d, colonies grew 5.3 mm at 5 C, 10.5 mm at 10 C, 33.6 mm at 15 C, 54.4 mm at 20 C, 75.5 mm at 25 C, and 5.7 mm at 30 C. Colonies were round and smooth with even margins. Aerial mycelium fluffy, extensive on MEA, initially white, turning to grayish sepia (15"") after 2–3 wk, reverse chamois (19"b) turning fuscous black (7""k) when older. Colony surfaces scattered with dark brown to black ascomata.

Habitat: Stumps of recently cut *Eucalyptus* trees.

Distribution: Guangxi Province, China.

Other specimens examined: CHINA. GUANGXI PROVINCE: Liuzhou region, *Eucalyptus* plantation (24°28′2″N, 109°45″50″E), isolated from recently harvested tree stump, Jan 2014, *S.F. Chen, F.F. Liu* & *G.Q. Li*, PREM 62024, culture CMW 49312 = CBS 143286 = CERC 2854. GUANGXI PROVINCE: Laibin region, *Eucalyptus* plantation (24°20′33″N, 110°4′59″E). Isolated from recently harvested tree stump, Jan 2014, *S.F. Chen, F.F. Liu* & *G.Q. Li*, PREM 62025, culture CMW 49316 = CBS 143287 = CERC 2880.

Notes: Huntiella bellula is closely related to *H. fabiensis* and *H. bhutanensis* (Van Wyk et al. 2004). However, *H. bellula* can be distinguished from these

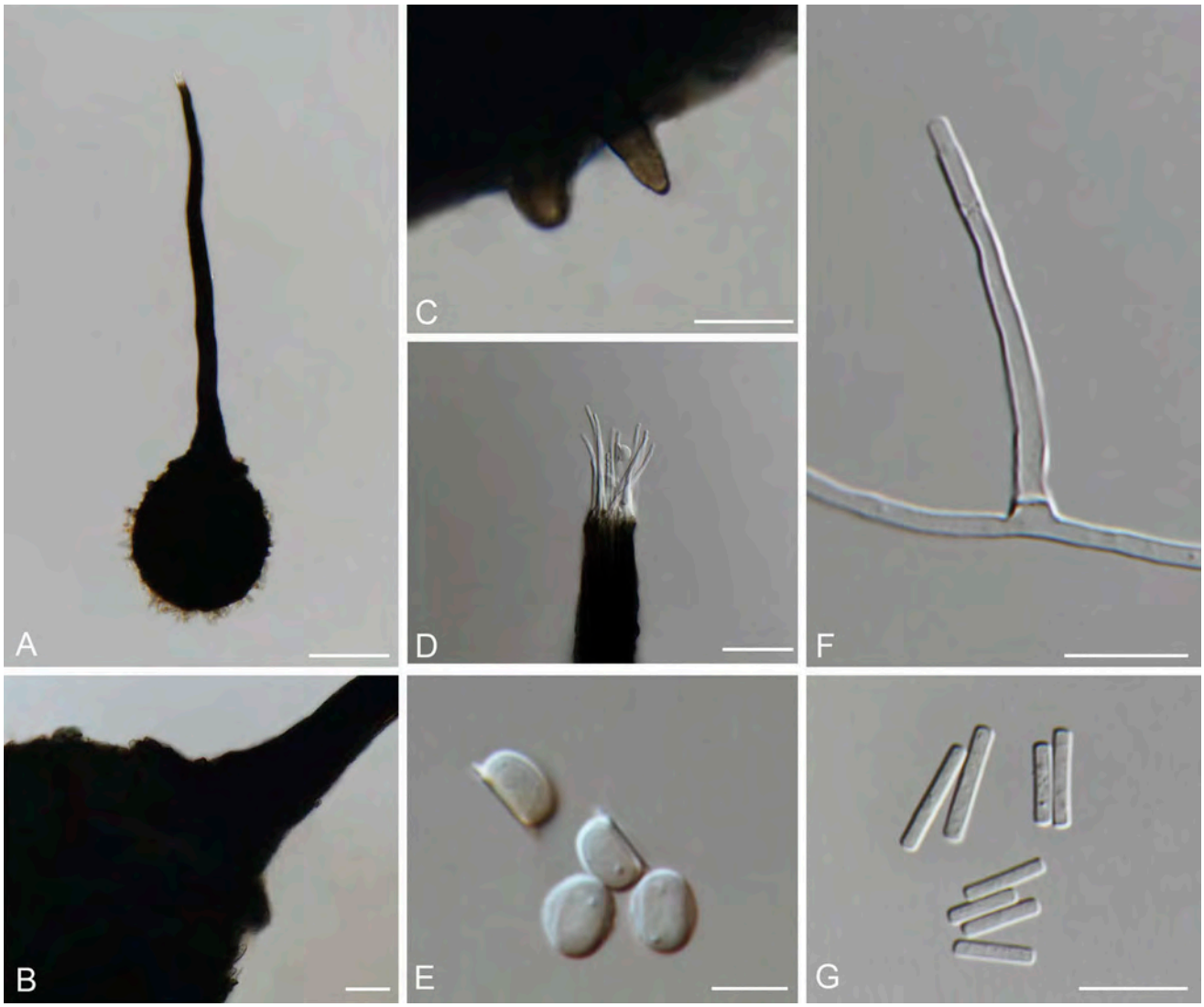

Figure 5. Morphological characters of *Huntiella bellula*. A. Ascoma with subglobose base and extended neck. B. Ascomatal base showing bulbous collar structure at neck base. C. Conical spines on the surface of ascomatal base. D. Tip of ascomatal neck with divergent ostiolar hyphae. E. Hat-shaped ascospore in top view and side view. F. Flask-shaped conidiophore. G. Various sizes of bacilliform conidia. Bars: A = 100 µm; B, D = 20 µm; C, F–G = 10 µm; E = 5 µm.

two species by the sizes of the ascomatal bases and necks, ascospores, and bacilliform conidia (TABLE 3). Ascomatal bases of *H. bellula* (average 203.5 × 212.5 µm) are larger than those of *H. bhutanensis* (average 158 × 158 µm). Ascomatal necks of *H. bellula* (average 540.5 µm) are longer than those of *H. bhutanensis* (average 486 µm) and *H. fabiensis* (average 373.5 µm). Ascospores of *H. bellula* (average 6 µm) are longer than those of *H. bhutanensis* (average 5 µm) and shorter than those of *H. fabiensis* (average 6.5 µm). Bacilliform conidia of *H. bellula* (average 7.5 × 1.5 µm) are smaller than those of *H. bhutanensis* (average 8 × 2 µm) and *H. fabiensis* (average 8 × 2 µm). Barrel-shaped conidia are present in *H. fabiensis* and *H. bhutanensis*, but not observed in *H. bellula*. Based on DNA sequence data, *H. bellula* differs from *H. fabiensis* in seven bases in the *TEF1α* gene and seven bases in the *BT1* gene, and from *H. bhutanensis* in five bases in the *TEF1α* gene, five bases in the *BT1* gene, and one base in the ITS region.

Huntiella confusa F.F. Liu & S.F. Chen, sp. nov. FIG. 6
MycoBank MB826740

Typification: CHINA. HAINAN PROVINCE: LinGao County, *Acacia confusa* tree (19°42′57″N, 109° 37′3″E), isolated from the fresh stump of a fallen tree, Sep 2013, *S.F. Chen, F.F. Liu, T. Huang & B. Liu* (**holotype** PREM 62026). Ex-holotype culture: CMW 43453 = CBS 143288 = CERC 2162.

Table 3. Morphological comparisons of closely related *Huntiella* species.

Specie[a]	Ascomatal base length[b]	Ascomatal base width	Ascomatal neck length	Ostiolar hyphae length	Ascospore height	Ascospore width	Bacilliform conidia length	Bacilliform conidia width	Barrel-shaped conidia length	Barrel-shaped conidia width
Huntiella ani	(104.5–)124–167(–224) (av. 145.5)	(117.5–)128.5–173 (–232) (av. 150.5)	(493–)520–667(–845) (av. 593.5)	(14.5–)19.5–28.5(–33) (av. 24)	(1.5–)2.5–3(–3.5) (av. 3)	(4.5–)4.5–5.5(–6) (av. 5)	(4–)5–8.5(–12.5) (av. 7)	(1.5–)1.5–2.5(–3) (av. 2)	(4–)5–7.5(–9) (av. 6)	(2.5–)3–4(–5) (av. 3.5)
H. bellula	(172.5–)179–228.5 (–250.5) (av. 203.5)	(184–)195–230.5(–244) (av. 212.5)	(395–)450–631(–707.5) (av. 540.5)	(18–)20–29.5(–32.5) (av. 25)	(2.5–)2.5–3(–4) (av. 3)	(5–)5.5–6.5(–6.5) (av. 6)	(5.5–)6.5–9(–12) (av. 7.5)	(1.5–)1.5–2(–2) (av. 1.5)	NA[c]	NA
H. bhutanensis	(112–)138–178(–206) (av. 158)	(112–)138–178(–206) (av. 158)	(450–)453–519 (av. 486)	(13–)18–26(–34) (av. 22)	2–5 (av. 3.5)	4–6 (av. 5)	6–7–9(–10) (av. 8)	1–3 (av. 2)	3–5 (av. 4)	(1.5–)2–3(–3.5) (av. 2.5)
H. confusa	NA	NA	NA	NA	NA	NA	(4.5–)5.5–7.5(–10) (av. 6.5)	(1.5–)1.5–2(–3) (av. 2)	NA	NA
H. chinaeucensis	(166–)212–271(–315) (av. 241.5)	(196–)232–304(–355) (av. 268)	(333–)410–551(–629) (av. 480.5)	(20–)24–37(–47) (av. 30.5)	3–4 (av. 3.5)	6–8(–9) (av. 7)	(5–)6–8(–9) (av. 7)	1–3 (av. 2)		
H. sumatrana	(148–)168–218(–293) (av. 193)	(158–)187–235(–296) (av. 211)	(323–)390–574(–687) (av. 482)	(21–)24–32(–35) (av. 28)	3–4 (av. 3.5)	5–7 (av. 6)	5–7(–8) (av. 6)	2–4(–5) (av. 3)	(4–)5–7(–8) (av. 6)	1–3 (av. 2)
H. eucalypti	NA	NA	NA	NA	NA	NA	(4–)6–8.5(–11) (av. 7)	(1.5–)1.5–2(–2.5) (av. 2)	NA	NA
H. fabiensis	(146.5–)163.5–219.5 (–244.5) (av. 191.5)	(158.5–)163–222.5 (–259.5) (av. 192.5)	(254.5–)316–431.5 (–470.5) (av. 373.5)	(12.5–)16.5–27.5(–28.5) (av. 22)	(2–)3–3.5(–4) (av. 3.5)	(5.5–)6–7(–8) (av. 6.5)	(4–)6–10(–13.5) (av. 8)	(1.5–)1.5–2(–2.5) (av. 2)	(3–)5–8(–10.5) (av. 6.5)	(2.5–)3–5(–7) (av. 4)
H. fecunda	(92.5–)106–173(–234) (av. 139.5)	(111–)118.5–184(–253) (av. 151.5)	(365.5–)521–828 (–1052.5) (av. 674.5)	(15–)18–23.5(–25.5) (av. 20.5)	(2–)2–2.5(–3) (av. 2.5)	(4.5–)5–5.5(–5.5) (av. 5.5)	(4–)5–7(–8.5) (av. 6)	(1.5–)1.5–2(–3) (av. 2)	NA	NA
H. tyalla	143.0–175.5(–195.5) (av. 159.25)	(116.5–)136.0–167.0 (–177.5) (av. 201.5)	(428.5–)466.5–607.5 (–772.5) (av. 537)	(14.5–)18.0–24.5(–28.5) (av. 21.25)	(2.0–)2.0–2.5(–3.0) (av. 2.25)	(3.5–)4.0–4.5(–5.0) (av. 4.45)	(8.5–)9.0–11.0 (–12.0) (av. 10)	(1.5–)2.0–2.5 (–3.5) (av. 2.25)	(5.0–)6.5–8.5(–9.5) (av. 7.5)	(1.5–)2.0–2.5(–3.0) (av. 2.25)
H. sublaevis	(98–)131–173(–187) (av. 152)	(102–)144–192(–231) (av. 168)	(522–)598–802(–990) (av. 700)	(15–)18–24(–25) (av. 21)	2–4 (av. 3)	4–6 (av. 5)	5–8 (av. 6.5)	1–3 (av. 2)	3–6 (av. 4.5)	2–3 (av. 2.5)
H. glaber	(133–)152.5–210.5(–237) (av. 181.5)	(128.5–)146.5–207.5 (–228) (av. 177)	(259.5–)328–548.5 (–722.5) (av. 438.5)	NA	(2–)2.5–3(–3.5) (av. 3)	(4.5–)5.5–6.5(–7) (av. 6)	(7–)8.5–12(–15.5) (av. 10)	(1.5–)2–3(–3) (av. 2.5)	NA	NA
H. microbasis	(65–)82–122(–162) (av. 101)	(82–)100–146(–185) (av. 246)	(185–)301–499(–574) (av. 400)	(9–)14–22(–25) (av. 18)	2–4 (av. 3)	5–7 (av. 6)	(3–)4–6(–11) (av. 5)	1–3 (av. 2)	NA	NA
H. inquinans	(116–)149–205(–236) (av. 177)	(130–)161–217(–270) (av. 189)	(347–)393–575(–687) (av. 484)	(20–)24–34(–38) (av. 29)	2–4 (av. 3)	5–7 (av. 6)	(5–)6–8(–11) (av. 7)	(2–)3–5(–7) (av. 4)	(4–)5–7(–8) (av. 6)	1–3 (av. 2)
H. omanensis	(154–)206–254(–279) (av. 230)	(154–)206–254(–279) (av. 230)	(385–)443–819(–1097) (av. 631)	(10–)18–36(–50) (av. 27)	2–4 (av. 3)	5–7 (av. 6)	6–8(–9) (av. 7)	2–3 (av. 2.5)	(5–)6–8(–10) (av. 7)	3–5
H. inaequabilis	NA	NA	NA	NA	NA	NA	(4–)4.5–9(–17.5) (av. 6.5)	(1.5–)1.5–2(–2) (av. 2)	(4.5–)5.5–7.5(–9.5) (av. 6.5)	(3.5–)3.5–5(–6) (av. 4)
H. meiensis	(119.5–)139–195(–219.5) (av. 167)	(129.5–)145–194.5 (–220) (av. 169.5)	(290–)299.5–347.5 (–416.5) (av. 323.5)	(9)12–18.5(–22.5) (av. 15.5)	(2–)2.5–3.5(–4) (av. 3)	(4.5–)5.5–6.5(–7) (av. 6)	(4–)5–7.5(–10.5) (av. 6.5)	(1.5–)1.5–2.5 (–3.5) (av. 2)	(5.5–)6–8.5(–11) (av. 7.5)	(3.5–)4–5.5(–6.5) (av. 5)

[a]Species indicated in bold are newly described in this study.
[b]Measurements are in micrometres.
[c]NA: not observed.

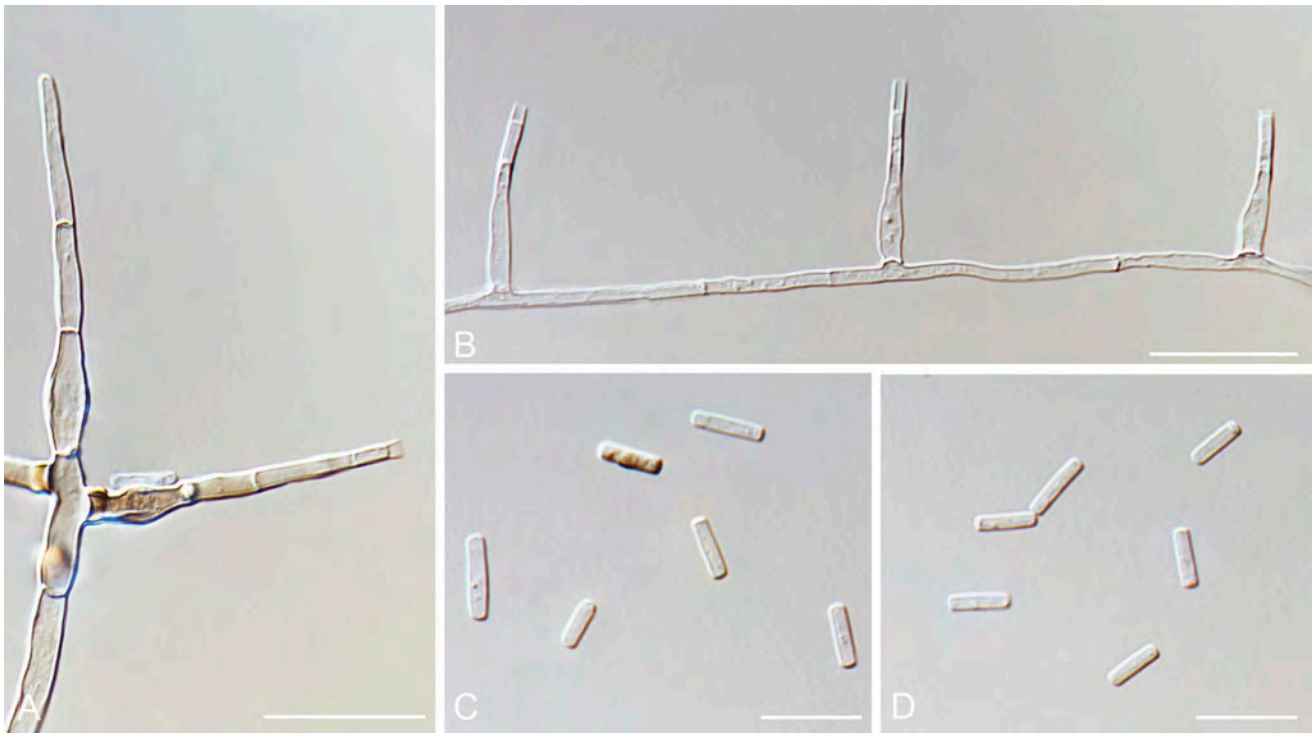

Figure 6. Morphological characters of *Huntiella confusa*. A–B. Flask-shaped conidiophore. C–D. Various sizes of bacilliform conidia. Bars: A–B = 20 µm; C–D = 10 µm.

Etymology: The name refers to the species epithet of the host *Acacia confusa*, from which it was collected.

Mating strategy: Heterothallic with isolates having either a *MAT1-1-1* gene or a *MAT1-2-1* gene.

Sexual state: Not observed.

Asexual state: Conidiophores arising laterally from vegetative hyphae, scattered or arising in clusters, multiseptate, hyaline, consisting of 2–3 cylindrical cells terminating in a phialide. Conidiogenous cells phialidic, cylindrical, (17–)20–33(–48) µm long, (1.5–)1.5–2(–3) µm wide at apex and (2–)2.5–4.5(–6.5) µm wide at base. Conidia of two forms: (i) bacilliform conidia hyaline, aseptate, cylindrical, (4.5–)5.5–7.5(–10) µm long and (1.5–)1.5–2(–3) µm wide; and (ii) barrel-shaped conidia not observed. Chlamydospores not observed.

Culture characters: Colonies on MEA fast growing, optimal temperature for growth 30 C, no growth at 5 C. After 4 d, colonies grew 2.3 mm at 10 C, 19.0 mm at 15 C, 40.5 mm at 20 C, 59.5 mm at 25 C, 69.3 mm at 30 C, and 30.4 mm at 35 C. Colonies round with even margins. Mycelium fluffy, dense on MEA, initially white, turning to dark brick (7”k) after 2–3 wk, reverse buff (19”f) to sepia (13”k) when older.

Habitat: Wounds on fallen *Acacia confusa* trees.

Distribution: Hainan Province, China.

Other specimens examined: CHINA. HAINAN PROVINCE: LinGao County, *Acacia confusa* tree (19°42′57″N, 109°37′3″E), isolated from stump of a fallen tree, Sep 2013, *S.F. Chen, F.F. Liu, T. Huang & B. Liu*, PREM 62027, culture CMW 49300 = CBS 143289 = CERC 2141; PREM 62028, culture CMW 43452 = CBS 143577 = CERC 2158.

Notes: Huntiella confusa is closely related to *H. chinaeucensis* (Chen et al. 2013) and *H. sumatrana* (Tarigan et al. 2010) but can be distinguished by the size of its bacilliform conidia (TABLE 3). Bacilliform conidia of *H. confusa* (average 6.5 × 2 µm) are longer than those of *H. sumatrana* (average 6 × 3 µm) and shorter than those of *H. chinaeucensis* (average 7 × 2 µm). In addition, barrel-shaped conidia are not observed in *H. confusa* and *H. chinaeucensis* but are present in *H. sumatrana*. *Huntiella confusa* differs from *H. chinaeucensis* in nine bases in the *TEF1α* gene and two bases in the *BT1* gene, and from *H. sumatrana* in three bases in the *TEF1α* gene and three bases in the *BT1* gene.

Huntiella eucalypti F.F. Liu & S.F. Chen, sp. nov. FIG. 7

MycoBank MB826741

Typification: CHINA. GUANGXI PROVINCE: Hechi region, *Eucalyptus* plantation (24°40′38″N, 108°20′16″E), isolated from recently harvested tree stump, Jan 2014, *S.F. Chen, F.F. Liu & G.Q. Li* (**holotype** PREM 62029). Ex-holotype culture: CMW 44693 = CBS 143290 = CERC 2841.

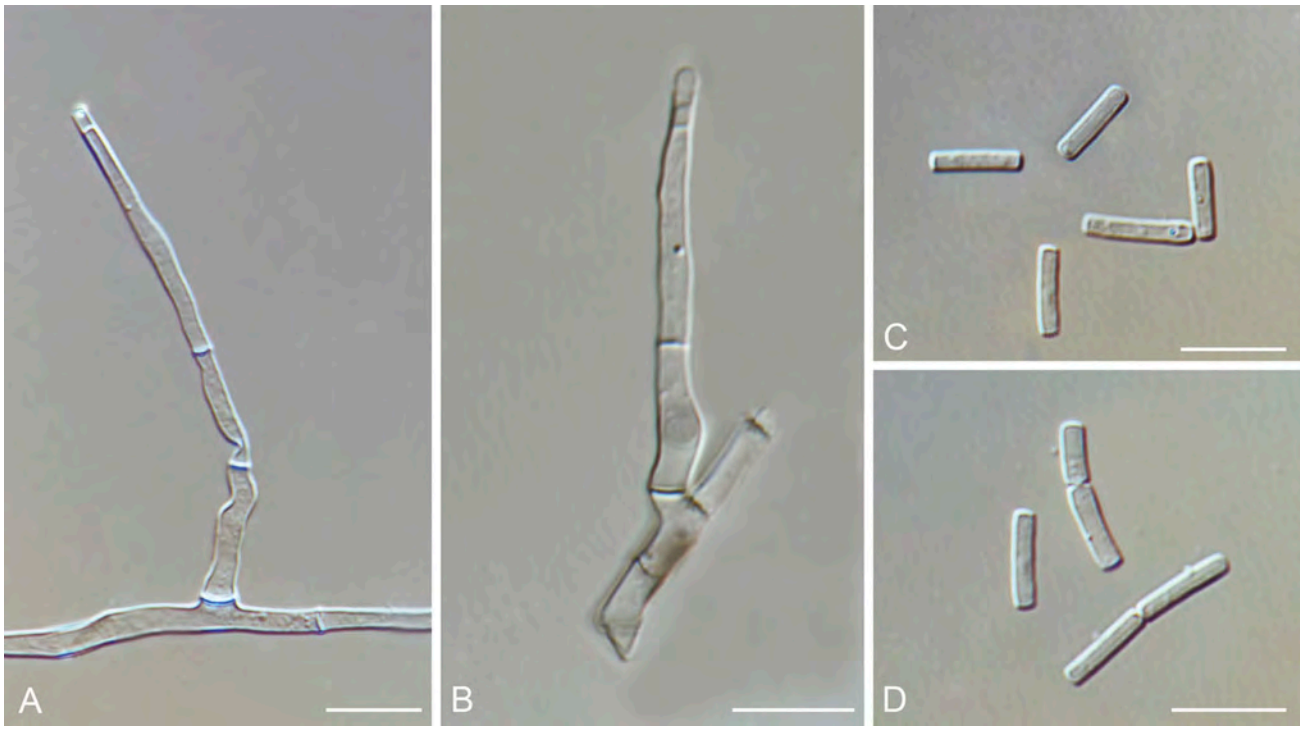

Figure 7. Morphological characters of *Huntiella eucalypti*. A–B. Flask-shaped conidiophore. C–D. Various sizes of bacilliform conidia Bars: A–D = 10 µm.

Etymology: The name refers to *Eucalyptus*, the host from which it was collected.

Mating strategy: Heterothallic with isolates having either a *MAT1-1-1* gene or a *MAT1-2-1* gene.

Sexual state: Not observed.

Asexual state: Conidiophores arising laterally from vegetative hyphae, scattered or arising in clusters, multiseptate, hyaline, consisting of 2–3 cylindrical cells terminating in a phialide. Conidiogenous cells phialidic, cylindrical, (24.5–)27–44.5(–56) µm long, (1.5–)1.5–2(–2) µm wide at apex and (2.5–)2.5–3.5(–4.5) µm wide at base. Conidia of two forms: (i) bacilliform conidia hyaline, aseptate, cylindrical, (4–)6–8.5(–11) µm long and (1.5–)1.5–2(–2.5) µm wide; and (ii) barrel-shaped conidia not observed. Chlamydospores not observed.

Culture characters: Colonies on MEA fast growing, optimal temperature for growth 25 C, no growth at 35 C. After 4 d, colonies grew 10.5 mm at 5 C, 14.4 mm at 10 C, 32.9 mm at 15 C, 53.2 mm at 20 C, 67.5 mm at 25 C, and 4.5 mm at 30 C. Colonies round with even margins. Aerial mycelium white, fluffy, extensive on MEA, reverse white to mikado brown (13"i) after 2–3 wk.

Habitat: Stumps of recently cut *Eucalyptus* trees.

Distribution: Guangxi Province, China.

Other specimens examined: CHINA. GUANGXI PROVINCE: Hechi region, *Eucalyptus* plantation (24° 40′38″N, 108°20′16″E), isolated from recently harvested tree stump, Jan 2014, *S.F. Chen, F.F. Liu* & *G.Q. Li*, PREM 62030, culture CMW 44692 = CBS 143291 = CERC 2840.

Huntiella fabiensis F.F. Liu & S.F. Chen, sp. nov. FIG. 8

MycoBank MB826743

Typification: CHINA. GUANGDONG PROVINCE: Meizhou region, *Eucalyptus* plantation (24°44′3″N, 116°22′39″E), isolated from recently harvested tree stump, Jan 2014, *S.F. Chen, J.N. Li* & *C. Chen* (**holotype** PREM 62031). Ex-holotype culture: CMW 49309 = CBS 143292 = CERC 2763.

Etymology: The name refers to the Forestry and Agricultural Biotechnology Institute (FABI) at the University of Pretoria in South Africa, where this work was conducted.

Mating strategy: Heterothallic with isolates having either a *MAT1-1-1* gene or a *MAT1-2-1* gene.

Sexual state: Ascomata superficial, scattered near center of colony. Ascomatal bases black, globose, (146.5–)163.5–219.5(–244.5) µm long and (158.5–)163–222.5(–259.5) µm wide, ornamented with conical, thick-walled, dark brown spines, (7–)8.0–15.5(–18) µm long. Ascomatal necks dark brown to black, erect, slender, (254.5–)316–431.5(–470.5) µm long, (10.5–)11.5–15(–17.5) µm wide at apex and (34–)

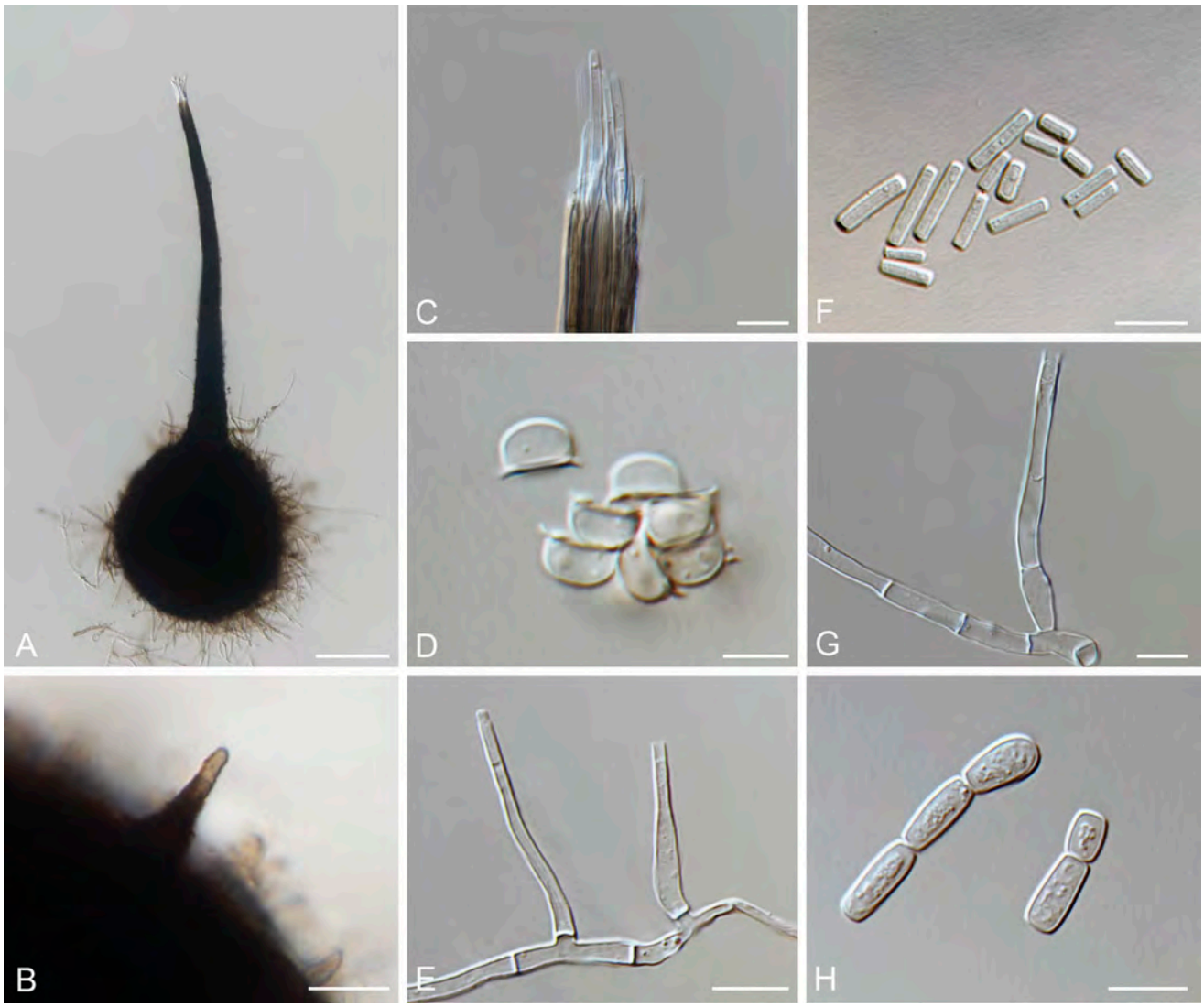

Figure 8. Morphological characters of *Huntiella fabiensis*. A. Ascoma with globose base and extended neck. B. Conical spines on the surface of ascomatal base. C. Tip of ascomatal neck with convergent ostiolar hyphae. D. Hat-shaped ascospore in side view. E. Flask-shaped conidiophores. F. Various sizes of bacilliform conidia. G. Secondary conidiophores with emerging barrel-shaped conidia. H. Barrel-shaped conidia in chains. Bars: A = 100 µm; B–C, E–H = 10 µm; D = 5 µm.

37.5–57.5(–71) µm wide at base. Ostiolar hyphae present, hyaline, convergent, (12.5–)16.5–27.5(–28.5) µm long. Asci not observed. Ascospores hat-shaped, invested in sheath, aseptate, (5.5–)6–7(–8) µm long and (2–)3–3.5(–4) µm wide with sheath in side view. Ascospores accumulating in creamy to yellow droplets at tip of ascomatal neck.

Asexual state: Conidiophores arising laterally from vegetative hyphae, scattered or arising in clusters, multiseptate, hyaline, consisting of 2–3 cylindrical cells terminating in a phialide. Conidiogenous cells phialidic, cylindrical, (19–)24.5–52(–75.5) µm long, (1.5–)1.5–3(–4) µm wide at apex and (2.5–)3–4(–5.5) µm wide at base. Conidia of two forms: (i) bacilliform conidia hyaline, aseptate, cylindrical, (4–)6–10(–13.5) µm long and (1.5–)1.5–2(–2.5) µm wide; and (ii) barrel-shaped conidia hyaline, aseptate, in chains, (3–)5–8(–10.5) µm long and (2.5–)3–5(–7) µm wide. Chlamydospores not observed.

Culture characters: Colonies on MEA fast growing, optimal temperature for growth 25 C, no growth at 35 C. After 4 d, colonies grew 7.7 mm at 5 C, 16.7 mm at 10 C, 35.5 mm at 15 C, 59.6 mm at 20 C, 70.9 mm at 25 C, and 3.4 mm at 30 C. Colonies round with even margins. Mycelium fluffy, smooth on MEA, initially hyaline to white, turning to smoke gray (21’’’’f) after 2–3 wk, reverse buff (19’’f) turning fuscous black (3’’’’k) when older. Colony surfaces scattered with dark brown to black ascomata.

Habitat: Stumps of recently cut *Eucalyptus* trees.

Distribution: Guangdong Province, China.

Other specimens examined: CHINA. GUANGDONG PROVINCE: Meizhou region, *Eucalyptus* plantation (24°44′3″N, 116°22′39″E), isolated from recently harvested tree stump, Jan 2014, *S.F. Chen, J.N. Li & C. Chen*, PREM 62032, culture CMW 44370 = CBS 143293 = CERC 2736; PREM 62033, culture CMW 49307 = CBS 143294 = CERC 2753.

Notes: Huntiella fabiensis is closely related to *H. bhutanensis* (Van Wyk et al. 2004). However, *H. fabiensis* can be distinguished from *H. bhutanensis* by the sizes of the ascomatal bases, ascospores, and barrel-shaped conidia (TABLE 3). Ascomatal bases of *H. fabiensis* (average 191.5 × 192.5 µm) are larger than those of *H. bhutanensis* (average 158 × 158 µm). Ascospores of *H. fabiensis* (average 3.5 × 6.5 µm) are wider than those of *H. bhutanensis* (average 3.5 × 5 µm). Barrel-shaped conidia of *H. fabiensis* (average 6.5 × 4 µm) are larger than those of *H. bhutanensis* (average 4 × 2.5 µm). The optimal growth temperature for *H. fabiensis* is 25 C, but that of *H. bhutanensis* is 20 to 25 C (Van Wyk et al. 2004). Based on DNA sequence data, *H. fabiensis* differs from *H. bhutanensis* by four bases in the *TEF1α* gene, six bases in the *BT1* gene, and one base in the ITS region.

Huntiella fecunda F.F. Liu & S.F. Chen, sp. nov. FIG. 9
MycoBank MB826744

Typification: CHINA. FUJIAN PROVINCE: Zhangzhou region, *Eucalyptus* plantation (24°44′36″N, 117°50′5″E), isolated from recently harvested tree

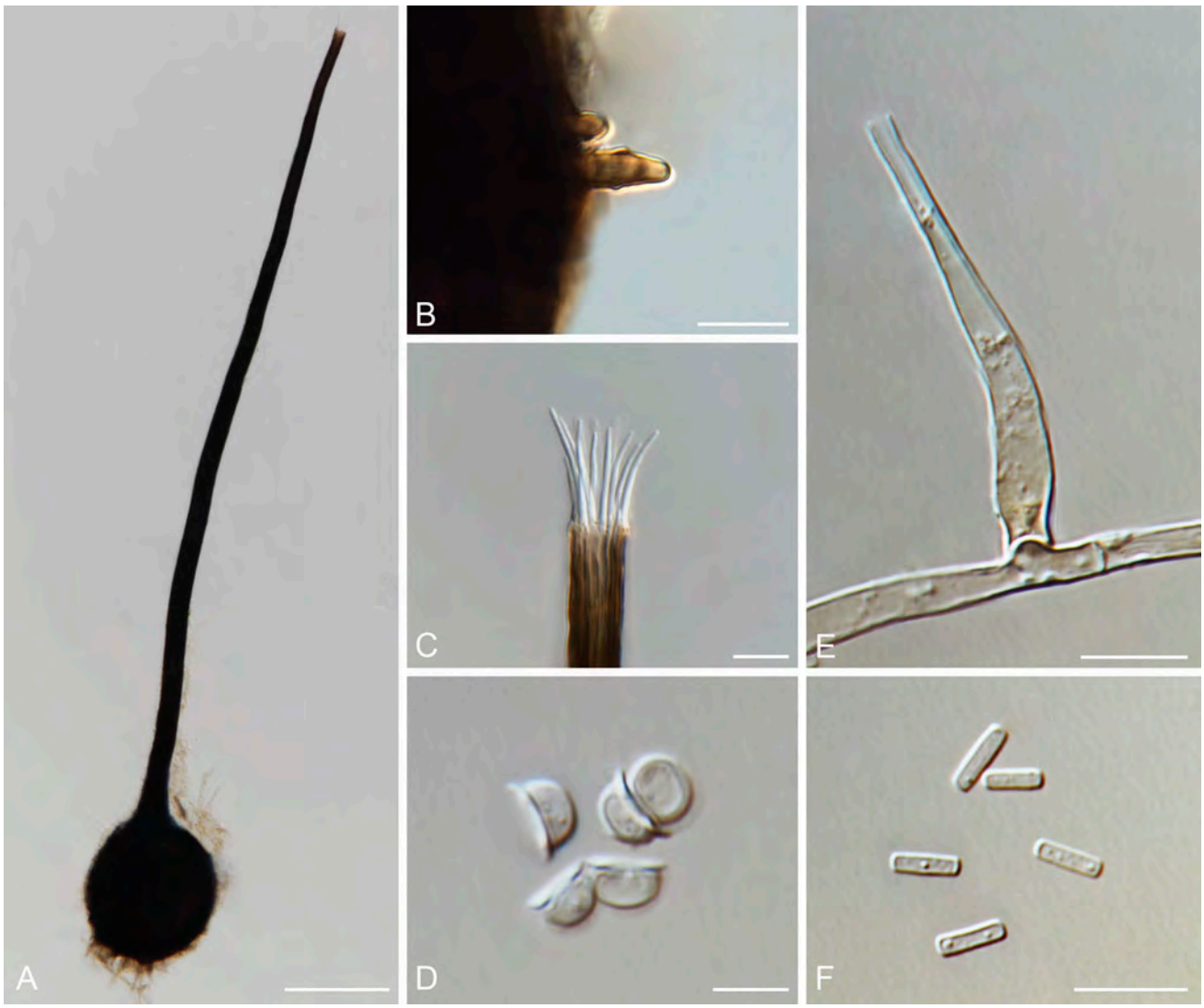

Figure 9. Morphological characters of *Huntiella fecunda*. A. Ascoma with subglobose base and extended neck. B. Conical spines on the surface of ascomatal base. C. Tip of ascomatal neck with divergent ostiolar hyphae. D. Hat-shaped ascospore in top view and side view. E. Flask-shaped conidiophore. F. Various sizes of bacilliform conidia. Bars: A = 100 µm; B–C, E–F = 10 µm; D = 5 µm.

stump, Oct 2013, *S.F. Chen, F.F. Liu* & *G.Q, Li* (**holotype** PREM 62034). Ex-holotype culture: CMW 49303 = CBS 143295 = CERC 2451a.

Etymology: "*fecundus*" (Latin) = fecund, referring to the prolific production of ascomata in culture.

Mating strategy: Unisexual, sexually reproducing isolates possess only the *MAT1-2-1* gene.

Sexual state: Ascomata superficial, scattered near center of colony. Ascomatal bases dark brown to black, globose or obpyriform, (92.5–)106–173(–234) µm long and (111–)118.5–184(–253) µm wide, ornamented with conical, thick-walled, dark brown spines, (5–)7.0–18.5(–23) µm long. Ascomatal necks dark brown to black, erect, slender, forming a bulbous collar at junction with ascomatal base, (365.5–)521–828(–1052.5) µm long, (9.5–)10–12(–13.5) µm wide at apex and (23.5–)29.5–47.5(–66.5) µm wide at base. Ostiolar hyphae present, hyaline, divergent, (15–)18–23.5(–25.5) µm long. Asci not observed. Ascospores hat-shaped, invested in sheath, aseptate, (4.5–)5–5.5(–5.5) µm long and (2–)2–2.5(–3) µm wide with sheath in side view. Ascospores accumulating in creamy to yellow droplets at tip of ascomatal neck.

Asexual state: Conidiophores arising laterally from vegetative hyphae, scattered or arising in clusters, multiseptate, hyaline, consisting of 2–3 cylindrical cells terminating in a phialide. Conidiogenous cells phialidic, cylindrical, (16–)18.5–32.5(–53) µm long, (1.5–)1.5–2(–2.5) µm wide at apex and (2–)2.5–3.5(–5.5) µm wide at base. Conidia of two forms: (i) bacilliform conidia hyaline, aseptate, cylindrical, (4–)5–7(–8.5) µm long and (1.5–)1.5–2(–3) µm wide; and (ii) barrel-shaped conidia not observed. Chlamydospores not observed.

Culture characters: Colonies on MEA fast growing, optimal temperature for growth 25 to 30 C, no growth at 5 and 35 C. After 4 d, colonies grew 4.8 mm at 10 C, 29.2 mm at 15 C, 45.6 mm at 20 C, 61.0 mm at 25 C, and 63.7 mm at 30 C. Colonies round with even margins. Aerial mycelium fluffy, smooth, extensive on MEA, initially white, turning to dark brown after 7–10 d, especially under areas where ascomata produced, reverse white turning fuscous black (7""k) when older. Colony surfaces scattered with abundant dark brown to black ascomata.

Habitat: Stumps of recently cut *Eucalyptus* trees.

Distribution: Fujian Province, China.

Other specimens examined: CHINA. FUJIAN PROVINCE: Zhangzhou region, *Eucalyptus* plantation (24°44′36″N, 117°50′5″E), isolated from recently harvested tree stump, Oct 2013, *S.F. Chen, F.F. Liu* & *G.Q. Li*, PREM 62035, culture CMW 49301 = CBS 143304 = CERC 2446; PREM 62036, culture CMW 49302 = CBS 143296 = CERC 2449.

Notes: Huntiella fecunda is closely related to *H. moniliformis* (Van Wyk et al. 2006), *H. sublaevis* (Van Wyk et al. 2011), and *H. tyalla* (Kamgan Nkuekam et al. 2012). *Huntiella fecunda* and *H. moniliformis* can be distinguished based on growth characters, with *H. moniliformis* rarely growing below 20 C (Van Wyk et al. 2006), whereas *H. fecunda* grows well at 15 C and has reduced growth at 10 C. *Huntiella fecunda* can be distinguished from *H. sublaevis* and *H. tyalla* by the sizes of the ascomatal bases and bacilliform conidia (TABLE 3). Ascomatal bases of *H. fecunda* (average 139.5 × 151.5 µm) are smaller than those of *H. sublaevis* (average 152 × 168 µm) and *H. tyalla* (average 159.25 × 201.5 µm). Bacilliform conidia of *H. fecunda* (average 6 × 2 µm) are shorter than those of *H. sublaevis* (average 6.5 × 2 µm) and *H. tyalla* (average 10 × 2.25 µm). Barrel-shaped conidia are present in *H. sublaevis* and *H. tyalla* but were not observed in *H. fecunda*. *Huntiella fecunda* can also be distinguished from *H. sublaevis* and *H. tyalla* based on growth at different temperatures. *Huntiella sublaevis* does not grow below 15 C, but *H. fecunda* grows at this temperature. *Huntiella fecunda* does not grow at 35 C, but *H. tyalla* grows 34 mm at 35 C in 3 d on MEA.

Based on DNA sequence data, *H. fecunda* differs from *H. moniliformis* in three bases in the *TEF1α* gene and one base in the *BT1* gene. *Huntiella fecunda* differs from *H. sublaevis* in 15 bases in the *TEF1α* gene and two bases in the *BT1* gene, and from *H. tyalla* in one base in the *TEF1α* gene, two bases in the *BT1* gene, and one base in the ITS region.

Huntiella glaber F.F. Liu & S.F. Chen, sp. nov. FIG. 10
MycoBank MB826745

Typification: CHINA. HAINAN PROVINCE: Chengmai County, *Eucalyptus exserta* plantation (19° 2′14″N, 110°30′32″E), isolated from exposed wood of fallen tree, Sep 2013, *S.F. Chen, F.F. Liu, T. Huang* & *B. Liu* (**holotype** PREM 62037). Ex-holotype culture: CMW 49299 = CBS 143297 = CERC 2133.

Etymology: "*glaber*" (Latin) = hairless or bald, referring to the absence of ostiolar hyphae at the apices of the ascomata.

Mating strategy: Homothallic, with sexually competent isolates having both the *MAT1-1-1* and *MAT1-2-1* genes.

Sexual state: Ascomata superficial, scattered near center of colony. Ascomatal bases black, globose, (133–)152.5–210.5(–237) µm long and (128.5–)146.5–207.5(–228) µm wide, ornamented with conical, thick-walled, dark brown spines, (8.0–)8.0–17.5(–26) µm long. Ascomatal necks dark brown to black, erect, slender, forming a bulbous collar at junction with ascomatal base, (259.5–)328–548.5(–722.5) µm long, (8.5–)10–

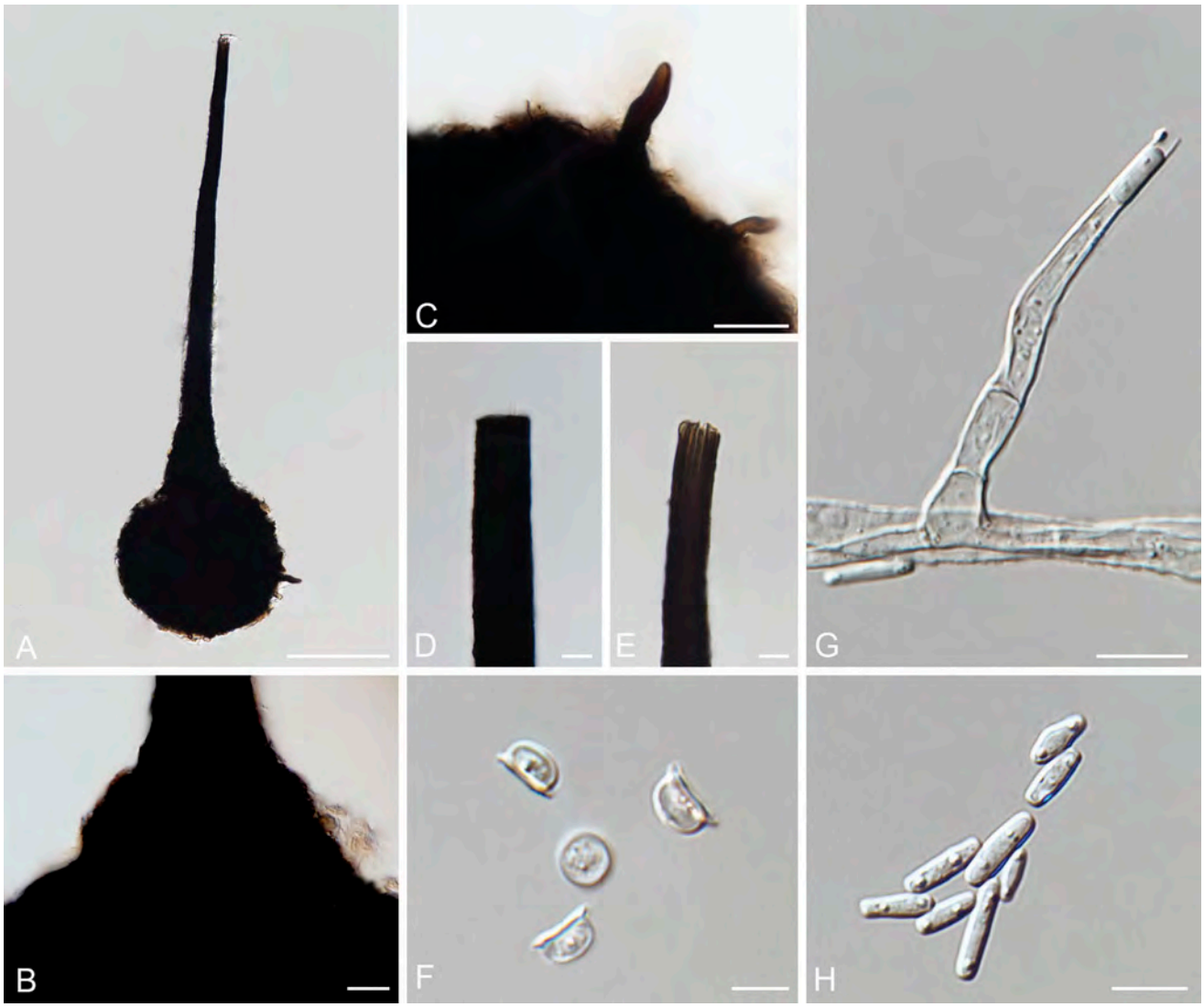

Figure 10. Morphological characters of *Huntiella glaber*. A. Ascoma with globose base and extended neck. B. Ascomatal base showing bulbous collar structure at neck base. C. Conical spines on the surface of ascomatal base. D–E. Tip of ascomatal neck without ostiolar hyphae. F. Hat-shaped ascospore in top view and side view. G. Flask-shaped conidiophore. H. Various sizes of bacilliform conidia. Bars: A = 100 µm; B–C = 20 µm; D–E, G–H = 10 µm; F = 5 µm.

15(–23) µm wide at apex and (42–)49–67.5(–78.5) µm wide at base. Ostiolar hyphae very few or absent. Asci not observed. Ascospores hat-shaped, invested in sheath, aseptate, (4.5–)5.5–6.5(–7) µm long and (2–)2.5–3(–3.5) µm wide with sheath in side view. Ascospores accumulating in creamy to yellow droplets at tip of ascomatal neck.

Asexual state: Conidiophores arising laterally from vegetative hyphae, scattered or arising in clusters, multiseptate, hyaline, consisting of 2–3 cylindrical cells terminating in a phialide. Conidiogenous cells phialidic, cylindrical, (19–)25–45.5(–79) µm long, (1.5–)2–2.5(–3) µm wide at apex and (2.5–)3.5–4.5(–6) µm wide at base. Conidia of two forms: (i) bacilliform conidia hyaline, aseptate, cylindrical, (7–)8.5–12(–15.5) µm long and (1.5–)2–3(–3) µm wide; and (ii) barrel-shaped conidia not observed. Chlamydospores not observed.

Culture characters: Colonies on MEA fast growing, optimal temperature for growth 30 C, no growth at 5 C. After 4 d, colonies grew 5.7 mm at 10 C, 26.4 mm at 15 C, 56.0 mm at 20 C, 79.6 mm at 25 C, 86.0 mm at 30 C, and 42.3 mm at 35 C. Colonies round with even margins. Aerial mycelium fluffy, extensive on MEA, initially white, turning to grayish sepia (15"") after 2–3 wk, reverse white turning brown vinaceous (5"m) when older. Colony surfaces scattered with dark brown to black ascomata.

Habitat: Exposed wood of fallen *Eucalyptus exserta* trees.

Distribution: Hainan Province, China.

Other specimens examined: CHINA. HAINAN PROVINCE: Chengmai County, *Eucalyptus exserta* plantation (19°2′14″N, 110°30′32″E), isolated from exposed wood of fallen tree, Sep 2013, *S.F. Chen, F.F. Liu, T. Huang & B. Liu*, PREM 62038, culture CMW 43436 = CBS 143298 = CERC 2132.

Notes: Huntiella glaber is closely related to *H. inquinans* (Tarigan et al. 2010), *H. microbasis* (Tarigan et al. 2010), and *H. omanensis* (Al-Subhi et al. 2006). *Huntiella glaber* can be distinguished by the sizes of the bacilliform conidia and number of ostiolar hyphae (TABLE 3). Bacilliform conidia of *H. glaber* (average 10 × 2.5 µm) are longer than those of *H. inquinans* (average 7 × 4 µm), *H. microbasis* (average 5 × 2 µm), and *H. omanensis* (average 7 × 2.5 µm). In addition, ostiolar hyphae are very few or absent in *H. glaber*, but present in *H. inquinans* (Tarigan et al. 2010), *H. microbasis* (Tarigan et al. 2010), and *H. omanensis* (Al-Subhi et al. 2006). Based on DNA sequence data, *H. glaber* differs from *H. inquinans* in seven bases in the *TEF1α* gene and one base in the *BT1* gene; *H. glaber* differs from *H. microbasis* in five bases in the *TEF1α* gene and seven bases in the *BT1* gene; and from *H. omanensis* in 16 bases in the *TEF1α* gene, five bases in the *BT1* gene, and three bases in the ITS region.

Huntiella inaequabilis F.F. Liu & S.F. Chen, sp. nov. FIG. 11

MycoBank MB826746

Typification: CHINA. GUANGDONG PROVINCE: Meizhou region, *Eucalyptus* plantation (24°44′3″N, 116°22′39″E), isolated from recently harvested tree stump, Jan 2014, *S.F. Chen, J.N. Li & C. Chen* (**holotype** PREM 62039). Ex-holotype culture: CMW 49306 = CBS 143299 = CERC 2749.

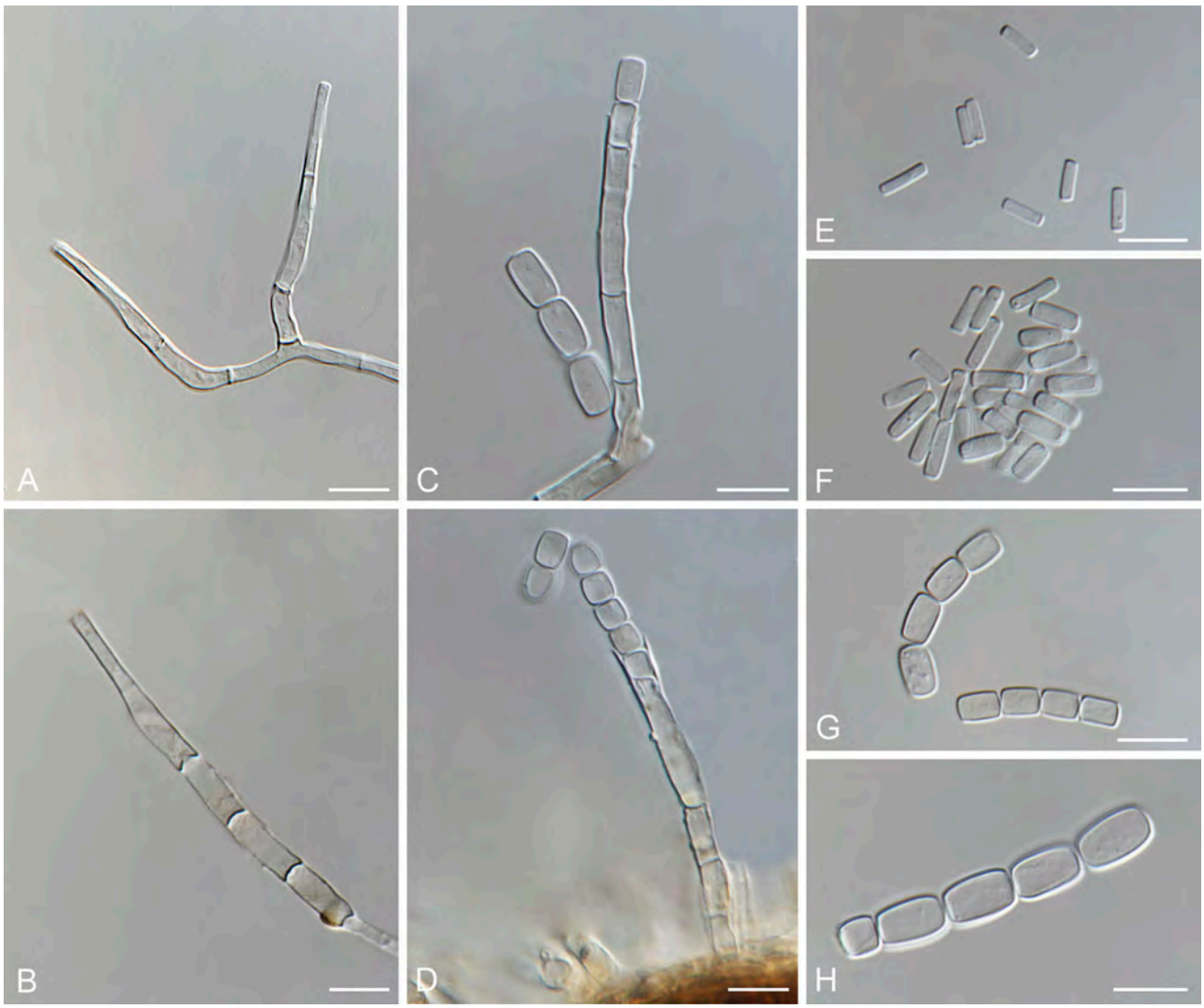

Figure 11. Morphological characters of *Huntiella inaequabilis*. A–B. Flask-shaped conidiophores. C–D. Secondary conidiophores with emerging barrel-shaped conidia. E–F. Bacilliform conidia. G–H. Barrel-shaped conidia in chains. Bars: A–H = 10 µm.

Etymology: "*inaequabilis*" (Latin) = unequal and irregular, referring to the shape of the culture colony, distinguishing *H. inaequabilis* from other *Huntiella* species.

Mating strategy: Heterothallic with isolates having either a *MAT1-1-1* gene or a *MAT1-2-1* gene.

Sexual state: Not observed.

Asexual state: Conidiophores arising laterally from vegetative hyphae, scattered or arising in clusters, multiseptate, hyaline, consisting of 2–3 cylindrical cells terminating in a phialide. Conidiogenous cells phialidic, cylindrical, (27.5–)35–56(–72) µm long, (1.5–)1.5–2(–2.5) µm wide at apex and (2.5–)2.5–4(–7) µm wide at base. Conidia of two forms: (i) bacilliform conidia hyaline, aseptate, cylindrical, (4–)4.5–9(–17.5) µm long and (1.5–)1.5–2(–2) µm wide; and (ii) barrel-shaped conidia hyaline, aseptate, in chains, (4.5–)5.5–7.5(–9.5) µm long and (3.5–)3.5–5(–6) µm wide. Chlamydospores not observed.

Culture characters: Colonies on MEA slow growing, optimal temperature for growth 25 C, no growth at 35 C. After 4 d, colonies grew 4.3 mm at 5 C, 9.1 mm at 10 C, 19.1 mm at 15 C, 26.5 mm at 20 C, 31.6 mm at 25 C, and 14.6 mm at 30 C. Colony margins unequal and irregular. Mycelium cottony, dense on MEA, initially white, turning to chaetura drab (17""k) after 7–10 d, reverse buff (19"f) to mars brown (13'm) when getting older.

Habitat: Stumps of recently cut *Eucalyptus* trees.

Distribution: Guangdong Province, China.

Other specimens examined: CHINA. GUANGDONG PROVINCE: Meizhou region, *Eucalyptus* plantation (24°44′3″N, 116°22′39″E), isolated from recently harvested tree stump, Jan 2014, *S.F. Chen, J.N. Li* & *C. Chen*, PREM 62040, culture CMW 44372 = CBS 143300 = CERC 2740.

Notes: Huntiella inaequabilis is closely related to *H. meiensis*. Because sexual structures for *H. inaequabilis* could not be induced in vitro, it can only be distinguished from other *Huntiella* species based on the morphology of the asexual state. The barrel-shaped conidia of *H. inaequabilis* (average 6.5 × 4 µm) are smaller than those of *H. meiensis* (average 7.5 × 5 µm). In addition, the colonies of *H. inaequabilis* on MEA at 25 C are small and irregular in outline, whereas those of *H. meiensis* are have smooth round margins. Growth of *H. inaequabilis* at 25 C is slower (average 31.6 mm) than for *H. meiensis* (average 71.5 mm). Based on DNA sequence data, *H. inaequabilis* differs from *H. meiensis* by six bases in the *TEF1α* gene and four bases in the *BT1* gene.

Huntiella meiensis F.F. Liu & S.F. Chen, sp. nov. FIG. 12

MycoBank MB826747

Typification: CHINA. GUANGDONG PROVINCE: Meizhou region, *Eucalyptus* plantation (24°44′3″N, 116°22′39″E), isolated from recently harvested tree stump, Jan 2014, *S.F. Chen, J.N. Li* & *C. Chen* (**holotype** PREM 62041). Ex-holotype culture: CMW 44376 = CBS 143301= CERC 2746.

Etymology: The name refers to the Meizhou, Guandong Province of China, where this fungus was collected.

Mating strategy: Heterothallic with isolates having either a *MAT1-1-1* gene or a *MAT1-2-1* gene.

Sexual state: Ascomata superficial, scattered near center of colony. Ascomatal bases black, globose to oval, (119.5–)139–195(–219.5) µm long and (129.5–)145–194.5(–220) µm wide, ornamented with many conical, thick-walled, dark brown spines, (6–)8.0–17.0(–28) µm long. Ascomatal necks dark brown to black, erect, slender, (290–)299.5–347.5(–416.5) µm long, (10–)11–13(–14.5) µm wide at apex and (33–)40–59(–77.5) µm wide at base. Ostiolar hyphae present, hyaline, convergent, (9)12–18.5(–22.5) µm long. Asci not observed. Ascospores hat-shaped, invested in sheath, aseptate, (4.5–)5.5–6.5(–7) µm long and (2–)2.5–3.5(–4) µm wide with sheath in side view. Ascospores accumulating in creamy to yellow droplets at tip of ascomatal neck.

Asexual state: Conidiophores arising laterally from vegetative hyphae, scattered or arising in clusters, multiseptate, hyaline, consisting of 2–3 cylindrical cells terminating in a phialide. Conidiogenous cells phialidic, cylindrical, (28–)31.5–52(–73) µm long, (1.5–)1.5–2.5(–2.5) µm wide at apex and (3–)3.5–4.5(–6) µm wide at base. Conidia of two forms: (i) bacilliform conidia hyaline, aseptate, cylindrical, (4–)5–7.5(–10.5) µm long and (1.5–)1.5–2.5(–3.5) µm wide; and (ii) barrel-shaped conidia hyaline, aseptate, in chains, (5.5–)6–8.5(–11) µm long and (3.5–)4–5.5(–6.5) µm wide. Chlamydospores not observed.

Culture characters: Colonies on MEA fast growing, optimal temperature for growth 25 C, no growth at 5 and 35 C. After 4 d colonies grew 12.7 mm at 10 C, 38.4 mm at 15 C, 60.2 mm at 20 C, 71.5 mm at 25 C, and 5.8 mm at 30 C. Colonies round with even margins. Mycelium flocky, dense on MEA, initially white, turning to mouse gray (13"") after 2–3 wk, reverse white turning dark brick (7"k) when older. Colony surfaces scattered with dark brown to black ascomata.

Habitat: Stumps of recently cut *Eucalyptus* trees.

Distribution: Guangdong Province, China.

Other specimens examined: CHINA. GUANGDONG PROVINCE: Meizhou region, *Eucalyptus* plantation (24°44′3″N, 116°22′39″E), isolated from recently harvested tree stump, Jan 2014, *S.F. Chen, J.N. Li* & *C. Chen*, PREM 62042, culture CMW 44374 = CBS 143302 = CERC 2742; PREM 62043, culture CMW 49305 = CBS 143303 = CERC 2744.

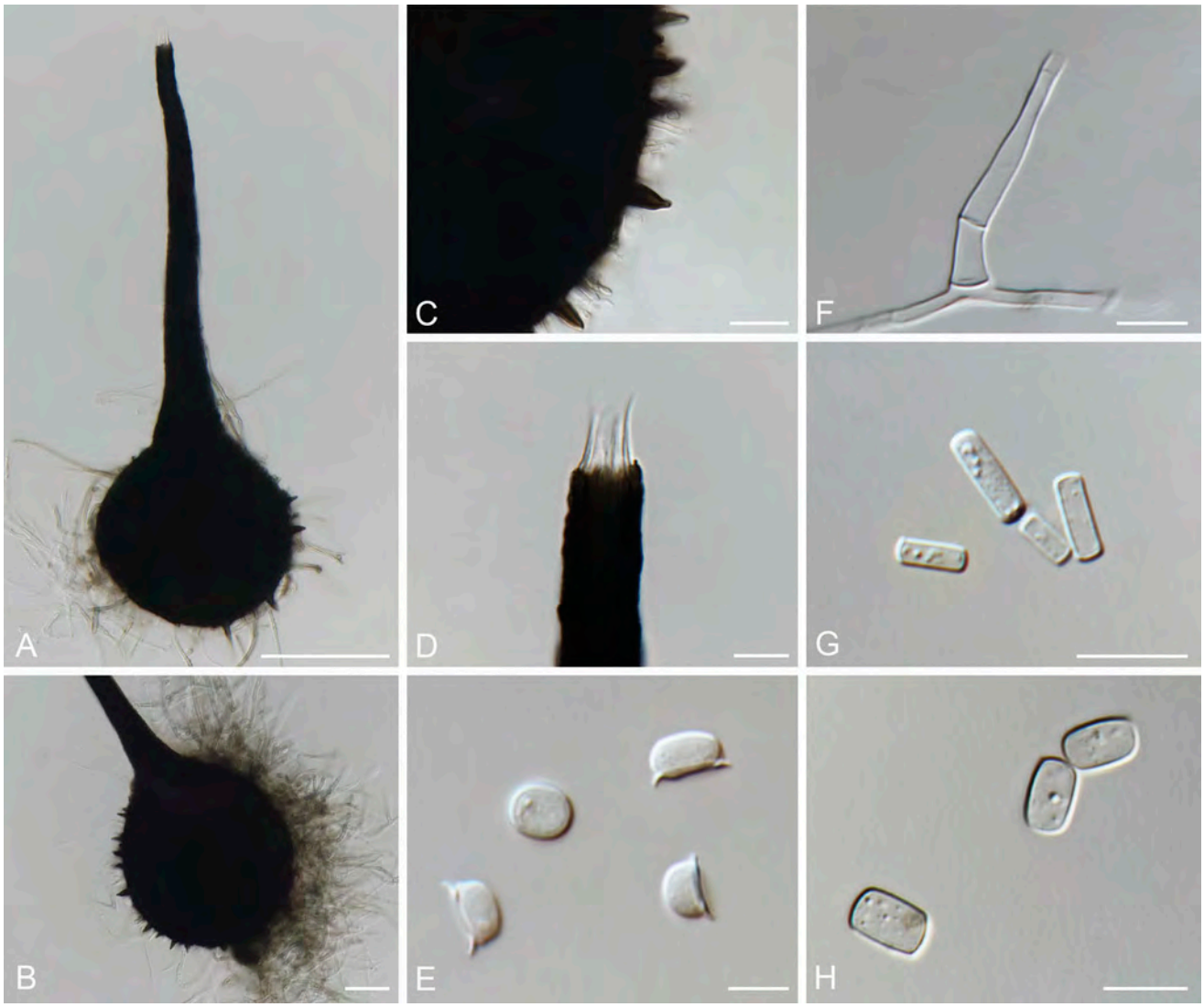

Figure 12. Morphological characters of *Huntiella meiensis*. A. Ascoma with globose base and extended neck. B–C. Conical spines on the surface of ascomatal base. D. Tip of ascomatal neck with convergent ostiolar hyphae. E. Hat-shaped ascospore in top view and side view. F. Flask-shaped conidiophore. G. Bacilliform conidia. H. Barrel-shaped conidia. Bars: A = 100 µm; B = 50 µm; C = 20 µm; D, F–H = 10 µm; E = 5 µm.

DISCUSSION

Huntiella moniliformis, the type species of the genus, was first isolated from sweet-gum wood (*Liquidambar styraciflua*) in Texas (Von Schrenk 1903). Subsequently, the taxonomy of the species related to *H. moniliformis* presented considerable challenges, especially before the advent of DNA sequence data to resolve species boundaries. *Huntiella moniliformis* was first described as *Ceratostomella moniliformis* by Hedgcock (1906) and later was reduced to synonymy with the genus *Ceratocystis* (Moreau 1952). Several descriptions of *H. moniliformis* were subsequently presented (Davidson 1935; Kitajima 1936; Bakshi 1951; Luc 1952; Hunt 1956; Roldan 1962; Upadhyay 1981), although it became increasingly clear (Wingfield et al. 2013) that these fungi were not closely related to the morphological similar *Ceratocystis* spp. De Beer et al. (2014) presented the first conclusive evidence that *Huntiella* represents a discrete genus, clearly separated from *Ceratocystis*, using robust DNA sequence-based phylogenetic inference, morphology, and ecological characters.

Subsequent to the discovery of *H. moniliformis* in the USA more than 100 years ago (Von Schrenk 1903), species in this genus have been reported from many different parts of the world, including Africa, Australasia, and South America (Van Wyk et al. 2006; Heath et al. 2009; Kamgan Nkuekam et al. 2012; De Beer et al. 2014). As is true for other genera in Ceratocystidaceae (De Beer et al. 2014), many *Huntiella* species rely on insects for their dispersal

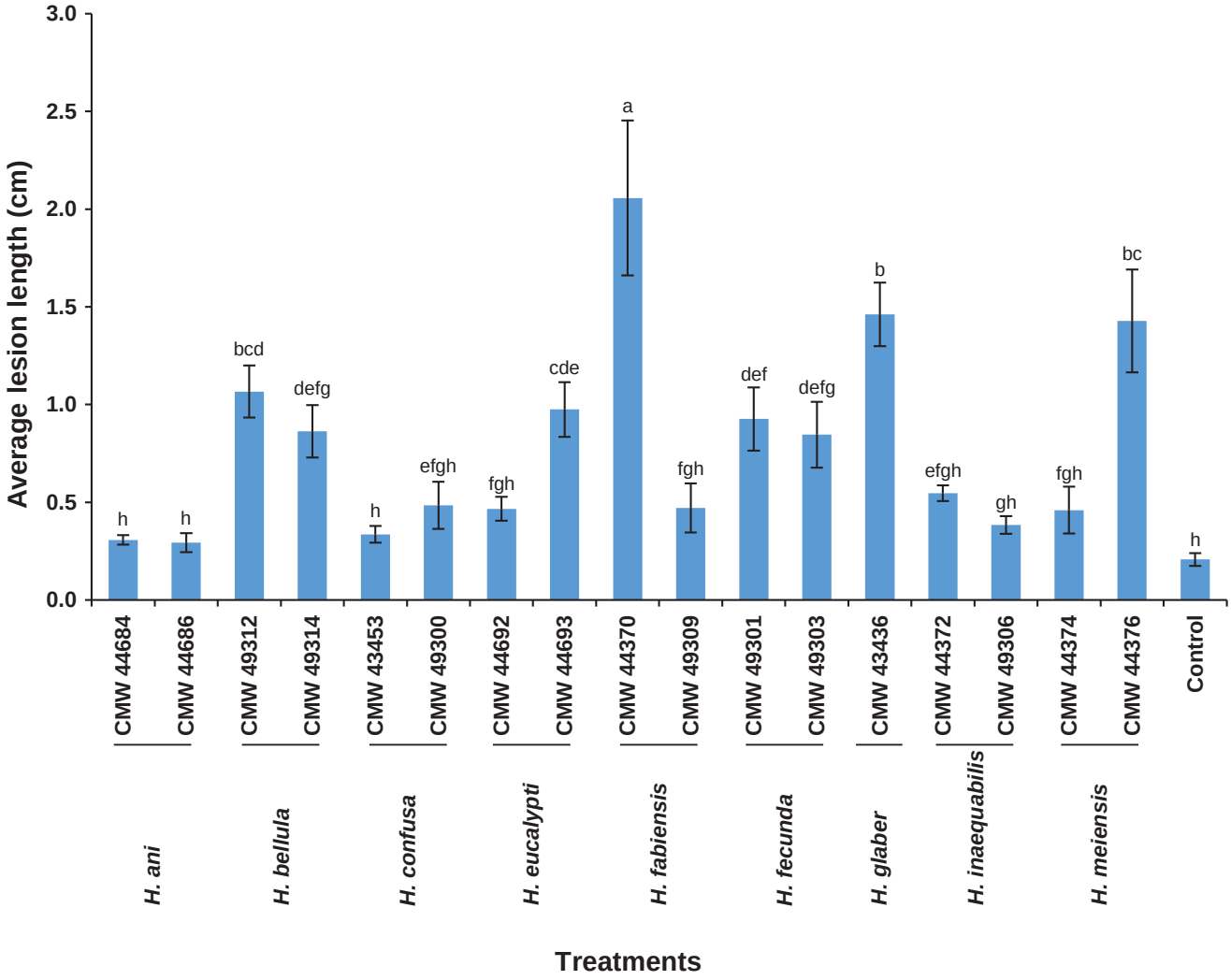

Figure 13. Histogram indicating the average lesion length (in cm) resulting from inoculation trials of *Eucalyptus* seedlings inoculated with 17 isolates of nine *Huntiella* species and the negative controls. Vertical bars represent standard error of means. Different letters above the bars indicate treatments that were statistically different (P = 0.05).

and fertilization (Kamgan Nkuekam et al. 2012; De Errasti et al. 2015). This has probably led to their being introduced accidentally into new areas, although very little is known regarding their pathways of spread.

In this study of *Huntiella* in southern China, a surprising number of new species were discovered, although only two host genera were examined. All of the newly described species, except for *H. confusa*, were obtained from freshly wounded *Eucalyptus* tissues in plantations across four provinces. *Huntiella confusa* was from an *Acacia confusa* tree in Hainan Province. All species were identified based on comparisons of ITS, *BT1*, and *TEF1α* sequence data and supported by morphological characters.

Different clades reflecting geographic origins were characterized within *Huntiella* (Mbenoun et al. 2014) based on analyses of the combined gene regions. Our isolates grouped in the two larger clades referred to as the Indo-Pacific Clade and Asian Clade. Only *H. fecunda* belonged to the Indo-Pacific Clade, the only species collected from Fujian Province, our northernmost sampling site. The remaining eight species grouped in two subclades (subclades 1 and 2) within the Asian Clade. *Huntiella confusa* and *H. glaber* grouped in subclade 2, including the previously described species *H. chinaeucensis, H. inquinans, H. microbasis*, and *H. sumatrana*. These two newly described species can be distinguished from their closest relatives by their morphological characters and phylogenetic inference. *Huntiella chinaeucensis* was described from *Eucalyptus* in Guangdong Province of China (Chen et al. 2013), whereas *H. sumatrana, H. microbasis*, and *H. inquinans* were

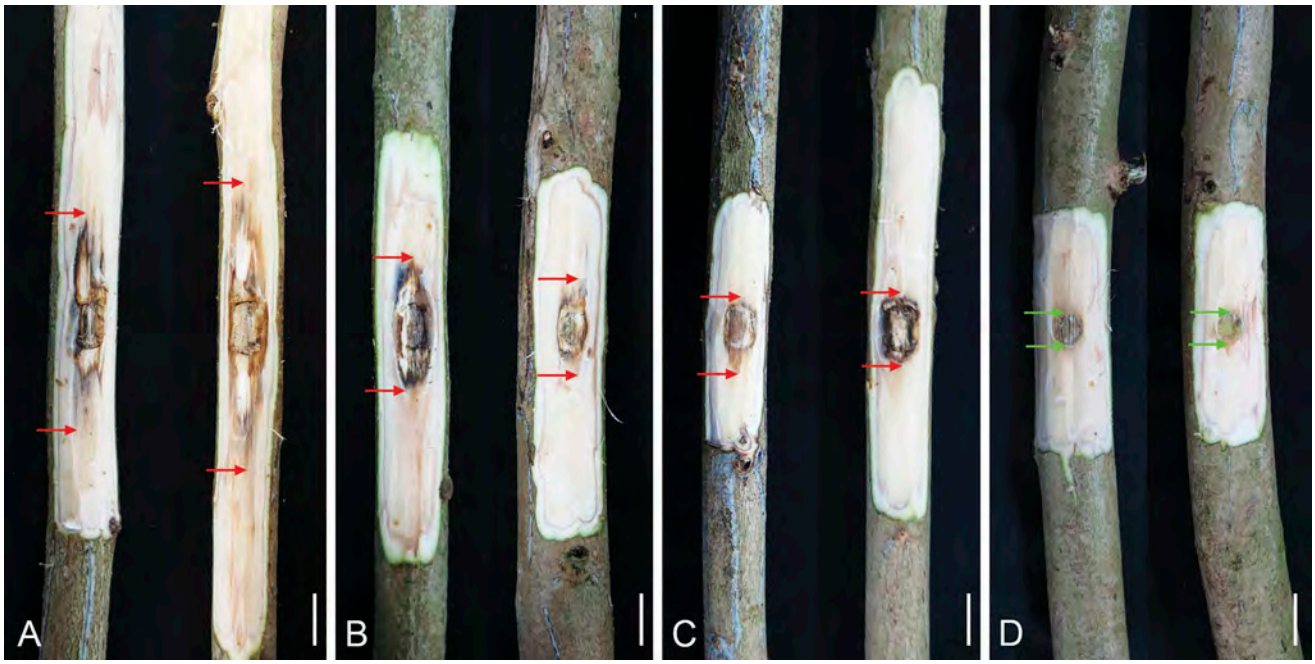

Figure 14. Lesions resulting from inoculations of *Huntiella* species onto *Eucalyptus* seedlings and wound responses on the negative controls. A–C. Lesions produced by *H. fabiensis* (CMW 44370), *H. fecunda* (CMW 49303), and *H. ani* (CMW 44684), respectively. D. Negative controls showing absence of lesion but only wound development; arrows indicate the terminal ends of the lesions (red arrows) and wounds (green arrows). Scale bars: A–D = 10 mm.

from *Acacia mangium* in Indonesia (Tarigan et al. 2010). All are known only from wounds on their hosts and have not been associated with diseases of these trees. *Huntiella confusa* and *H. glaber* were both collected only from Hainan Province, which is the southernmost province of China.

Six of the newly described *Huntiella* species (*H. ani, H. bellula, H. eucalypti, H. fabiensis, H. inaequabilis*, and *H. meiensis*), together with the previously described *H. bhutanensis*, formed subclade 1 of the Asian Clade of *Huntiella*. These six species could be recognized with confidence based on phylogenetic analyses of the *BT1* and *TEF1α* gene sequences. In addition, morphological and growth differences in culture can also be used to distinguish among them. The six species were collected from fresh wounds on recently cut *Eucalyptus* trees in Guangdong and Guangxi provinces, which are adjacent provinces with similar environments. It is relevant that all species obtained in these two provinces grouped in the same species complex, suggesting that the environmental conditions may play an important role in species adaptation.

Huntiella species are well known to lose their ability to produce sexual structures with successive transfers on artificial media (Van Wyk et al. 2004; De Beer et al. 2014). This was also true for the species described here. This prompted an effort to define the mating strategies of the species and to attempt to induce sporulation by pairing cultures of opposite mating type in culture. The majority of the newly described species were heterothallic, based on the genetic analysis of their mating genes. It was thus possible to induce the production of sexual structures in pairing tests with four of the seven species. Our results showed that mating strategies of *Huntiella* species differ in each of two subclades of the larger Asian Clade.

It was interesting that *H. fecunda* undergoes unisexual reproduction. This makes it one of only six species known to exhibit this sexual strategy (Glass and Smith 1994; Lin et al. 2005; Alby et al. 2009; Wilson et al. 2015; Schuerg et al. 2017). Unisexuality is a unique form of homothallism, recently recognized in *H. moniliformis* by Wilson et al. (2015). In this situation, only the *MAT1-2-1* gene is present in sexually reproducing cultures (Wilson et al. 2015).

Species of *Huntiella* are generally considered saprobes (Van Wyk et al. 2006; De Beer et al. 2014) that infect freshly cut wounds on trees. Several reports show that some species can cause lesions on the stems of artificially inoculated trees (Tarigan et al. 2010; Chen et al. 2013; De Errasti et al. 2015; Mbenoun et al. 2016). This is consistent with our pathogenicity tests, where all of the *Huntiella* species tested showed the capacity to

cause distinct lesions in sapwood when inoculated on healthy seedlings. Although we do not consider these fungi to be primary pathogens, they may contribute to tree mortality (De Errasti et al. 2015).

Prior to this study, only one *Huntiella* species, *H. chinaeucensis*, was known from China, where it was isolated from *Eucalyptus* trees in Guangdong Province (Chen et al. 2013). Application of multigene phylogenetic analysis has made it possible to identify nine novel species of *Huntiella* from China, bringing the total number of known *Huntiella* species to 30. The relatively large number of new species found in this study conducted in a fairly limited area suggests that many more novel species of *Huntiella* await discovery in China.

Until recently, the Ceratocystidaceae have been relatively poorly known in China. Although *Huntiella* spp. are not considered important agents of plant disease, numerous *Ceratocystis* have been described from China in contemporary studies. Other than *C. fimbriata* sensu stricto, which was isolated from *Ipomoea batatas* (Sy 1956), these include *C. cercfabiensis* from recently harvested *Eucalyptus* stumps in South China (Liu et al. 2015), *C. changhui*, the causal agent of black rot on *Colocasia esculenta* (Liu et al. 2018), *C. collisensis* from *Cunninghamia lanceolata* in Fujian Province (Liu et al. 2015), and *C. manginecans*, also from stumps of *Eucalyptus* in Guangdong Province (Chen et al. 2013). Our results, and recent reports of new species of *Ceratocystis*, suggest that a relatively high diversity of Ceratocystidaceae occur in this geographic region. Their ecological importance, especially as plant pathogens and agents of wood degradation, deserves further study.

ACKNOWLEDGMENTS

We thank the University of Pretoria and China Eucalypt Research Centre (CERC) for facilities and equipment to undertake this work.

FUNDING

This study was supported by the National Natural Science Foundation of China (NSFC) (project no. 31622019), the National Key R&D Program of China (project no. 2016YFD0600505), and the International Science & Technology Cooperation Program of China (project no. 2012DFG31830). We acknowledge members of the Tree Protection Cooperative Programme (TPCP) and the National Research Foundation (NRF), South Africa, for financial support.

ORCID

Jolanda Roux http://orcid.org/0000-0003-4155-5718
Irene Barnes http://orcid.org/0000-0002-4349-3402
Andrea M. Wilson http://orcid.org/0000-0002-3239-0045
ShuaiFei Chen http://orcid.org/0000-0002-3920-9982

LITERATURE CITED

Alby K, Schaefer D, Bennett RJ. 2009. Homothallic and heterothallic mating in the opportunistic pathogen *Candida albicans*. Nature 460:890–893.

Al-Subhi AM, Al-Adawi AO, Van Wyk M, Deadman ML, Wingfield MJ. 2006. *Ceratocystis omanensis*, a new species from diseased mango trees in Oman. Mycological Research 110:237–245.

Bakshi BK. 1951. Studies on four species of *Ceratocystis*, with a discussion of fungi causing sap-stain in Britain. Mycological Papers 35:1–16.

Chen SF, Van Wyk M, Roux J, Wingfield MJ, Xie YJ, Zhou XD. 2013. Taxonomy and pathogenicity of *Ceratocystis* species on *Eucalyptus* trees in South China, including *C. chinaeucensis* sp. nov. Fungal Diversity 58:267–279.

Cristobal BD, Hansen AJ. 1962. Un hongo semjante a *Ceratocystis moniliformis* en cacao en Costa Rica. Turrialba 12:46–47.

Cunningham CW. 1997. Can three incongruence tests predict when data should be combined. Molecular Biology and Evolution 14:733–740.

Davidson RW. 1935. Fungi causing stain in logs and lumber in the southern states, including five new species. Journal of Agricultural Research 50:789–807.

De Beer ZW, Duong TA, Barnes I, Wingfield BD, Wingfield MJ. 2014. Redefining *Ceratocystis* and allied genera. Studies in Mycology 79:187–219.

De Beer ZW, Marincowitz S, Duong TA, Wingfield MJ. 2017. *Bretziella*, a new genus to accommodate the oak wilt fungus, *Ceratocystis fagacearum* (Microascales, Ascomycota). MycoKeys 27:1–19.

De Errasti A, De Beer ZW, Rajchenberg M, Coetzee MPA, Wingfield MJ, Roux J. 2015. *Huntiella decorticans* sp. nov. (Ceratocystidaceae) associated with dying *Nothofagus* in Patagonia. Mycologia 107:512–521.

Glass NL, Donaldson GC. 1995. Development of primer sets designed for use with the PCR to amplify conserved genes from filamentous Ascomycetes. Applied and Environmental Microbiology 61:1323–1330.

Glass NL, Smith ML. 1994. Structure and function of a mating-type gene from the homothallic species *Neurospora africana*. Molecular and General Genetics 244:401–409.

Guindon S, Gascuel O. 2003. A simple, fast, and accurate algorithm to estimate large phylogenies by maximum likelihood. Systematic Biology 52:696–704.

Hayslett M, Juzwik J, Moltzan B. 2008. Three *Colopterus* beetle species carry the oak wilt fungus to fresh wounds on red oak in Missouri. Plant Disease 92:270–275.

Heath RN, Wingfield MJ, Wingfield BD, Meke G, Mbaga A, Roux J. 2009. *Ceratocystis* species on *Acacia mearnsii* and *Eucalyptus* spp. in eastern and southern Africa including six new species. Fungal Diversity 34:41–68.

Hedgcock GG. 1906. Studies upon some chromogenic fungi which discolor wood. Missouri Botanical Garden Annual Report 17:59–124.

Hunt J. 1956. Taxonomy of the genus *Ceratocystis*. Lloydia 19:1–58.

Jacobs K, Bergdahl DR, Wingfield MJ, Halik S, Seifert KA, Bright DE, Wingfield BD. 2004. *Leptographium wingfieldii* introduced into North America and found associated with exotic *Tomicus piniperda* and native bark beetles. Mycological Research 108:411–418.

Kamgan Nkuekam G, Jacobs K, De Beer ZW, Wingfield MJ, Roux J. 2008. *Ceratocystis* and *Ophiostoma* species including three new taxa, associated with wounds on native South African trees. Fungal Diversity 29:37–59.

Kamgan Nkuekam G, Wingfield MJ, Mohammed C, Carnegie AJ, Pegg GS, Roux J. 2012. *Ceratocystis* species, including two new species associated with nitidulid beetles, on eucalypts in Australia. Antonie van Leeuwenhoek 101:217–241.

Kamgan Nkuekam G, Wingfield MJ, Roux J. 2013. *Ceratocystis* species, including two new taxa, from *Eucalyptus* trees in South Africa. Australasian Plant Pathology 42:283–311.

Katoh K, Misawa K, Kuma K, Miyata T. 2002. MAFFT: a novel method for rapid multiple sequence alignment based on fast Fourier transform. Nucleic Acids Research 30:3059–3066.

Kitajima K. 1936. Researches on the discolourations of logs of *Fagus crenata* Blume caused by *Endoconidiophora Bunae*, n. sp. and on its preventive method. Bulletin of Imperial Forest Experiments Station, Meguro 35:1–134.

Kowalski T, Butin H. 1989. Taxonomie bekannter und neuer *Ceratocystis*-Arten an Eiche (*Quercus robur* L.). Phytopathology 124:236–248.

Lin X, Hull CM, Heitman J. 2005. Sexual reproduction between partners of the same mating type in *Cryptococcus neoformans*. Nature 434:1017–1021.

Liu FF, Barnes I, Roux J, Wingfield MJ, Chen SF. 2018. Molecular phylogenetics and microsatellite analysis reveal a new pathogenic *Ceratocystis* species in the Asian-Australian Clade. Plant Pathology 67:1097–1113.

Liu FF, Mbenoun M, Barnes I, Roux J, Wingfield MJ, Li GQ, Li JQ, Chen SF. 2015. New *Ceratocystis* species from *Eucalyptus* and *Cunninghamia* in South China. Antonie van Leeuwenhoek 107: 1451–1473.

Luc M. 1952. *Ophiostoma moniliforme* (Hedgc.) H. et P. Syd. and its various forms. Reviews in Mycology 17:10–16.

Mayers CG, McNew DL, Harrington TC, Roeper RA, Fraedrich SW, Biedermann PH, Castrillo LA, Reed SE. 2015. Three genera in the Ceratocystidaceae are the respective symbionts of three independent lineages of ambrosia beetles with large, complex mycangia. Fungal Biology 119: 1075–1092.

Mbenoun M, Wingfield MJ, Begoude Boyogueno AD, Nsouga Amougou F, Petchayo Tigang, S, ten Hoopen GM, Mfegue CV, Dibog L, Nyassé S, Wingfield BD, Roux J. 2016. Diversity and pathogenicity of the Ceratocystidaceae associated with cacao agroforests in Cameroon. Plant Pathology 65:64–78.

Mbenoun M, Wingfield MJ, Begoude Boyogueno AD, Wingfield BD, Roux J. 2014. Molecular phylogenetic analyses reveal three new *Ceratocystis* species and provide evidence for geographic differentiation of the genus in Africa. Mycological Progress 13:219–240.

Möller EM, Bahnweg G, Sandermann H, Geiger HH. 1992. A simple and efficient protocol for isolation of high molecular weight DNA from filamentous fungi, fruit bodies, and infected plant tissues. Nucleic Acids Research 20:6115–6116.

Moreau C. 1952. Coexistence des formes *Thielaviopsis* et Graphium chez une souche de *Ceratocystis major* (van Beyma) nov. comb. Remarques sur les variations des *Ceratocystis*. Revue de Mycologie (Supplément Colonial No. 1) 12:17–25.

Nel WJ, Duong TA, Wingfield BD, Wingfield MJ, De Beer ZW. 2017. A new genus and species for the globally important, multi-host root pathogen *Thielaviopsis basicola*. Plant Pathology 67:871–882.

Posada D. 2008. jModelTest: phylogenetic model averaging. Molecular Biology and Evolution 25:1253–1256.

Rayner RW. 1970. A mycological colour chart. Kew, UK: Commonwealth Mycological Institute and British Mycological Society.

Roldan EF. 1962. Species of *Ceratocystis* (*Ceratostomella*) causing stain in rattan. The Philippine Journal of Science 91:415–423.

Roux J, Wingfield MJ. 2009. *Ceratocystis* species: emerging pathogens of non–native plantation *Eucalyptus* and *Acacia* species. Southern Forests 71:115–120.

SAS Institute Inc. 2011. SAS® 9.3 System options: reference. 2nd ed. Cary, North Carolina.

Schoch CL, Seifert KA, Huhndorf S, Robert V, Spouge JL, Levesque CA, Chen W, Bolchacova E, Voigt K, Crous PW, Miller AN. 2012. Nuclear ribosomal internal transcribed spacer (ITS) region as a universal DNA barcode marker for Fungi. Proceedings of the National Academy of Sciences of the United States of America 109:6241–6246.

Schuerg T, Gabriel R, Baecker N, E Baker S, W Singer S. 2017. *Thermoascus aurantiacus* is an intriguing host for the industrial production of cellulases. Current Biotechnology 6:89–97.

Seifert KA, De Beer ZW, Wingfield MJ. 2013. The ophiostomatoid fungi: expanding frontiers. CBS Biodiversity Series No. 12. Utrecht, The Netherlands: CBS-KNAW Fungal Biodiversity Centre. p. 191–200.

Swofford DL. 2003. PAUP*. Phylogenetic Analysis Using Parsimony (*and other methods). Version 4. Sunderland, Massachusetts: Sinauer Associates.

Sy CM. 1956. Studies on the control of black rot (*Ophiostoma fimbriatum*) of sweet potato. Acta Phytopathologica Sinica 2:81–95.

Tarigan M, Van Wyk M, Roux J, Tjahjono B, Wingfield MJ. 2010. Three new *Ceratocystis* spp. in the *Ceratocystis moniliformis* complex from wounds on *Acacia mangium* and *A. crassicarpa*. Mycoscience 51:53–67.

Upadhyay HP. 1981. A monograph of *Ceratocystis* and *Ceratocystiopsis*. Athens, Georgia: University of Georgia Press. p. 176.

Van Wyk M, Roux J, Barnes I, Wingfield BD, Chhetri DB, Kirisits T, Wingfield MJ. 2004. *Ceratocystis bhutanensis* sp. nov., associated with the bark beetle *Ips schmutzenhoferi* on *Picea spinulosa* in Bhutan. Studies in Mycology 50:365–379.

Van Wyk M, Roux J, Barnes I, Wingfield BD, Wingfield MJ. 2006. Molecular phylogeny of the *Ceratocystis moniliformis* complex and description of *C. tribilliformis* sp. nov. Fungal Diversity 21:181–201.

Van Wyk M, Wingfield BD, Wingfield MJ. 2011. Four new *Ceratocystis* spp. associated with wounds on *Eucalyptus*, *Schizolobium* and *Terminalia* trees in Ecuador. Fungal Diversity 46:111–131.

Von Schrenk H. 1903. The "bluing" and the "red-hot" of the western yellow pine, with special reference to the Black Hills Forest Reserve. U.S. Department of Agriculture. Bureau of Plant Industry Bulletin 36:1–46.

White TJ, Bruns T, Lee S, Taylor JW. 1990. Amplification and direct sequencing of fungal ribosomal RNA genes for phylogenetics. In: Innis MA, Gelfand DH, Sninsky JJ, White TJ, eds. PCR protocols: a guide to the methods and applications. New York: Academic Press. p. 315–322.

Wilson AM, Godlonton T, Van der Nest MA, Wilken PM, Wingfield MJ, Wingfield BD. 2015. Unisexual reproduction in *Huntiella moniliformis*. Fungal Genetics and Biology 80:1–9.

Wingfield BD, Van Wyk M, Roos H, Wingfield MJ. 2013. *Ceratocystis*: emerging evidence for discrete generic boundaries. In: Seifert KA, De Beer ZW, Wingfield MJ, eds. The ophiostomatoid fungi: expanding frontiers. Utrecht, The Netherlands: CBS-KNAW Fungal Biodiversity Centre. p. 57–64.

Wingfield MJ, Barnes I, De Beer ZW, Roux J, Wingfield BD, Taerum SJ. 2017. Novel associations between ophiostomatoid fungi, insects and tree hosts: current status—future prospects. Biological Invasions 19:3215–3228.

Wingfield MJ, Seifert KA, Webber JEF. 1993. *Ceratocystis* and *Ophiostoma*: taxonomy, ecology and pathogenicity. St Paul, Minnesota: American Phytopathological Society Press. p. 7–13.

Yuan ZQ, Mohammed C. 2002. *Ceratocystis moniliformopsis* sp. nov., an early colonizer of *Eucalyptus obliqua* logs in Tasmania, Australia. Australian Systematic Botany 15:125–133.